Petrographic and geochemical characterisation of the Breaksea Orthogneiss, Fiordland, New Zealand.

Watton, J.W., BSc
40967824

Presented to the Department of Earth and Planetary Sciences,
Division of Environmental and Life Sciences
in Partial Fulfilment fo the Requirements for the Degree of

Honours, Bsc
Macquarie University
November 2009

Statement of Originality

All the work submitted in this thesis is the original work of the author except where otherwise acknowledged. No part of this thesis has been previously submitted to any other university or institution

_____ _____

Signed – James Watton Date

Abstract

Characterisation of the Breaksea Orthogneiss shows four distinct lithologies: Breaksea Omphacite Granulite (BOG) is the dominant country rock; Breaksea Eclogite (BE); layered garnetite – pyroxenite and hornblende peridotite occur as inclusionary rafts within the main body. The BOG shows chemical characteristics similar to the Western Fiordland Orthogneiss, from a source at a depth below that at which plagioclase is stable. Hornblende peridotite sampled is chemically analogous to the hornblende peridotite of the Hawes Head Ultramafics unit found at Charles Sound, Fiordland.

Preservation of primary igneous textures and crsytallisation of garnet + Tschermak's diopside is observed in the layered garnetite – pyroxenite rock. Retrograde thermal re-equilibration results in a phase transition from Tschermak's diopside to diopside, and in the presence of Na, diopside to omphacite. Re-equilibration is observed on a mineral scale and proposed on an outcrop scale.

Outcrop scale re-equilibration causing Na to diffuse from the BOG into inclusionary rafts facilitates the diopside – omphacite change in Na poor rocks, accounting for the garnet – omphacite BE unit and omphacite present in the garnetite unit. Further evidence of retrograde metamorphic activity can be observed in symplectite development in the BOG, BE and hornblene peridotite.

Table of Contents

Chapter 1 – Introduction
- 1.1 Exposed roots of magmatic arcs 1-1
- 1.2 Experimental crystallisation of garnet and high Ts diopside on liquidus 1-2
- 1.3 Aims 1-2

Chapter 2 – Regional Geology
- 2.1 Regional Setting 2-1
- 2.2 Fiordland, New Zealand 2-1
- 2.3 Western Fiordland Orthogneiss 2-5
- 2.4 Tectonic History 2-10
- 2.5 Tectonic Models 2-11

Chapter 3 – Fieldwork
- 3.1 Introduction and Aims 3-1
- 3.2 Methods and Logistics 3-2
- 3.3 Results 3-4
- 3.4 Discussion 3-12

Chapter 4 – Petrography
- 4.1 Introduction 4-1
- 4.2 Results 4-2

Chapter 5 – Whole Rock Geochemistry
- 5.1 Methods 5-1
  - 5.1.1 Major and Trace element analysis by XRF and ICP-MS 5-1
  - 5.1.2 Whole rock isotope analysis by TIMS 5-9
- 5.2 Results 5-11

Chapter 6 – Mineral Geochemistry
- 6.1 Methods 6-1
  - 6.1.1 Mineral major element analysis by EMP 6-1
  - 6.1.2 Mineral trace element analysis by LA-ICP-MS 6-3
  - 6.1.3 Mineral and symplectite element mapping by EMP 6-7
- 6.2 Results 6-13
  - 6.2.1 EMP 6-13
  - 6.2.2 LA-ICP-MS 6-32
  - 6.2.3 Element mapping 6-44

Chapter 7 – Discussion 7-1

Chapter 8 – Conclusion 8-1

References

Appendix for chapter 5
- WFO database A5.A

Appendix for chapter 6
- LA-ICP-MS LLD and error A6.A/B
- Element mapping MATLAB scripts A6.C
- EMP data A6.D
- LA-ICP-MS data A6.E

List of Figures

Fig. 2.01 Geological map of New Zealand 2-3
- 2.02 South Island, New Zealand 2-4
- 2.03 Fiordland, New Zealand 2-9
- 3.01 Breaksea Orthogneiss 3-3

3.02 Breaksea Omphacite Granulite (BOG) outcrop photo 3-5
3.03 BOG outcrop photo 3-5
3.04 Breaksea Eclogite (BE) outcrop photo 3-7
3.05 BE outcrop photo 3-7
3.06 Layered Garnetite – Pyroxenite outcrop photo 3-9
3.07 Layered Garnetite – Pyroxenite outcrop photo 3-9
3.08 Hornblende Peridotite outcrop photo 3-11
3.09 Hornblende Peridotite outcrop photo 3-11
3.10 Large scale outcrop photo 3-13
4.01 0905B thin section 4-5
4.02 0905B thin section 4-6
4.03 0905B thin section 4-7
4.04 0905B thin section 4-8
4.05 0905B thin section 4-9
4.06 0905B thin section 4-9
4.07 0905B thin section 4-10
4.08 0905B thin section 4-11
4.09 0905B thin section 4-12
4.10 0905C thin section 4-13
4.11 0905C thin section 4-13
4.12 0905C thin section 4-14
4.13 0904C thin section 4-17
4.14 0904C thin section 4-18
4.15 0904C thin section 4-19
4.16 0910B thin section 4-21
4.17 0906B thin section 4-22
4.18 0906A thin section 4-25
4.19 0906A thin section 4-26
4.20 0903B thin section 4-28
4.21 0903B thin section 4-28
5.01 Harker diagram SiO2 vs. Al2O3 5-17
5.02 Harker diagram SiO2 vs. MgO 5-17
5.03 Harker diagram SiO2 vs. Na2O 5-18
5.04 Harker diagram SiO2 vs. Sr 5-18
5.05 Harker diagram SiO2 vs. Y 5-19
5.06 Harker diagram SO2 vs. MnO 5-19
5.07 TAS diagram 5-20
5.08 BOG spider plot 5-21
5.09 BOG REE plot 5-21
5.10 BE spider plot 5-24
5.11 BE REE plot 5-24
5.12 Garnetite spider plot 5-27
5.13 Garnetite REE plot 5-27
5.14 Pyroxenite spider plot 5-29
5.15 Pyroxenite REE plot 5-29
5.16 Hornblende peridotite spider plot 5-31
5.17 Hornblende peridotite REE plot 5-31
5.18 TIMS isotopic data 5-32
6.01 BOG garnet traverse 6-15
6.02 BOG garnet traverse 6-16
6.03 BOG garnet variation 6-16
6.04 BOQ Q-J diagram 6-17
6.05 BOG Quad diagram 6-18

6.06 BOG Ca-Na diagram 6-18
6.07 BOG plagioclase zoning 6-19
6.08 BOG plagioclase variation 6-19
6.09 Amphibole classification 6-20
6.10 BE garnet zoning 6-22
6.11 BE garnet variation 6-22
6.12 BE Q-J diagram 6-23
6.13 BE Ca-Na diagram 6-23
6.14 Garnetite garnet variation 6-25
6.15 Pyroxenite garnet variation 6-25
6.16 Garnetite Q-J diagram 6-26
6.17 Pyroxenite Q-J diagram 6-26
6.18 Garnetite Quad diagram 6-27
6.19 Pyroxenite Quad diagram 6-27
6.20 Garnetite Ca-Na diagram 6-28
6.21 Garnetite Ca-Na diagram 6-28
6.22 Hornblende peridotite garnet variation 6-30
6.23 hornblende peridotite Q-J diagram 6-31
6.24 hornblende peridotite Quad diagram 6-31
6.25 BOG laser data spider plot 6-34
6.26 BOG laser data REE plot 6-34
6.27 Inclusionary rafts of BOG and BE in laser data spider plot 6-35
6.28 Inclusionary rafts of BOG and BE in laser data REE plot 6-35
6.29 BE laser data spider plot 6-37
6.30 BE laser data REE plot 6-37
6.31 Garnetite laser data spider plot 6-40
6.32 Garnetite laser data REE plot 6-40
6.33 Pyroxenite laser data spider plot 6-41
6.34 Pyroxenite laser data REE plot 6-41
6.35 Hornblende peridotite laser data spider plot 6-43
6.36 Hornblende peridotite laser data REE plot 6-43
6.37 0905B element map 6-46
6.38 0905B element map 6-46
6.39 0905B element map 6-47
6.40 0905B element map 6-47
6.41 0909 thin section photo of element mapping area 6-48
6.42 0909 element map 6-48
6.43 0909 element map 6-49
6.44 0909 element map 6-49
6.45 0909 element map 6-50
6.46 0909 element map 6-50
6.47 0905C thin section photo of element mapping area 6-51
6.48 0905C element map 6-51
6.49 0905C element map 6-52
6.50 0905C element map 6-52
6.51 0905C element map 6-53
6.52 0905C element map 6-53
6.53 0904C thin section photo of element mapping area 6-55
6.54 0904C element map 6-56
6.55 0904C element map 6-56
6.56 0904C element map 6-57
6.57 0904C element map 6-57
6.58 0906B element map 6-58

6.59 0906B element map 6-58
6.60 0906B element map 6-59
6.61 0903B thin section photo of element mapping area 6-62
6.62 0903B element map 6-62
6.63 0903B element map 6-63
6.64 0903B element map 6-63
7.01 Harker diagram SiO2 vs. Al2O3 7-5
7.02 Harker diagram SiO2 vs. MgO 7-5
7.03 Harker diagram SiO2 vs. Na2O 7-6
7.04 Harker diagram SiO2 vs. Sr 7-6
7.05 Harker diagram SiO2 vs. Y 7-7
7.06 Harker diagram SiO2 vs. MnO 7-7
7.07 TAS plot 7-8
7.08 Misty Pluton spider plot 7-14
7.09 Misty Pluton REE plot 7-14
7.10 BOG whole rock and laser comparison spider plot 7-15
7.11 BOG whole rock and laser comparison REE plot 7-15
7.12 BE whole rock and laser comparison spider plot 7-16
7.13 BE whole rock and laser comparison spider plot 7-16
7.14 Garnetite whole rock and laser comparison spider plot 7-17
7.15 Garnetite whole rock and laser comparison REE plot 7-17
7.16 Pyroxenite whole rock and laser comparison spider plot 7-18
7.17 Pyroxenite whole rock and laser comparison REE plot 7-18
7.18 Hornblende peridotite whole rock and laser comparison spider plot 7-19
7.19 Hornblende peridotite whole rock and laser comparison REE plot 7-19
7.20 0906B element map 7-26
7.21 0904C element map 7-33

List of Tables

Table 5.01 LLD for XRF 5-1
5.02 LOI for samples 5-1
5.03 ICP-MS operating conditions 5-3
5.04 Comparison of ICP-MS reference materials 5-6/7
5.05 BCR-2 calibration 5-8
5.06 TIMS reference materials 5-10
5.07 EMP major element data 5-13
5.08 CIPW Norms 5-14
5.09 ICP-MS trace element data 5-15/16
6.01 EMP standard data 6-2
6.02 LLD for EMP 6-2
6.03 operating conditions for LA-ICP-MS 6-3
6.04 LA-ICP-MS reference materials 6-5/6
6.05 Element mapping crystals used 6-7
6.06 Element map sizes 6-7
6.07A Love and Scott alpha factors 6-9
6.07B Kato alpha factors 6-10
6.07C Transposed Kato alpha factors 6-11
6.08 Element mapping comparison to PAP values 6-12

1. Introduction

1.1 Exposed roots of magmatic arcs

There are various localities throughout the world that show the exposed root of a magmatic arc; Fiordland, New Zealand, where this study is based is one such example. Other exposed roots of magmatic arcs include the Jurassic Talkeetna Island arc in South Central Alaska; Cretaceous Ladakh-Kohistan arc in Northern Pakistan and the Cretaceous Palaeogene Coast Plutonic Complex in South Eastern Alaska.

The base of the Talkeetna Island arc is comprised of 2km of ultramafic cumulates; dunite harzburgite and pyroxenites (DeBari & Coleman, 1989; DeBari & Sleep, 2009) overlain by 200m of garnet bearing gabbro. This is overlain by 2km of gabbroic rocks with plagioclase-orthopyroxene-clinopyroxene ± spinel mineral assemblages (DeBari & Coleman, 1989; DeBari & Sleep, 2009), with amphibole increasing in abundance from <2% in ultramafic cumulate rocks to 100% in some amphibolite pods (DeBari & Sleep, 2009), corresponding to a decrease in pressure, temperature and depth. The Talkeetna arc is interpreted to be the remains of a magma chamber that crystallized at the base of an intra oceanic arc (DeBari & Coleman, 1989).

The Ladakh-Kohistan arc was initiated as an intra oceanic arc before accreting onto continental crust before subsequently being underplated by other continental crust (Petterson & Treloar, 2004). The deepest exposure of the Ladakh-Kohistan arc is the Jijal complex, and ultramafics sequence below a garnet rich granulite facies meta-gabbro. The ultramafics consist of peridotites, pyroxenites, websterites and dunites, with the contact between the garnet rich granulite and ultramafics being interpreted as the petrological Moho (Heuberger, 2004). The meta-gabbro has been dated as coinciding with the collision of the Ladakh-Kohistan arc and the Karakoram microplate (Petterson & Windley, 1985; Treloar et al., 1996).

The Central Belt of the Coast Plutonic Complex consists of biotite-hornblende-plagioclase-quartz gneiss metamorphosed at T=620-730°C and pressures of up to

8kbar, equivalent to burial up to 30km (Crawford et al., 1987) and is the result of two sections of continental crust accreting to one another (Crawford et al., 1987; Wood et al., 2009).

Magmatic arcs show a wide degree of variation in setting and tectonic history, though all show progressively mafic to ultramafics mineral assemblages at greater depths, including the crystallization of garnet bearing phases.

1.2 Experimental crystallization of garnet and high Ts diopside on liquidus

Alonso-Perez et al., (2009) conduct experiments with synthetic andesite to determine the effects of changing pressure and H_2O content on garnet fractionation in island arc roots. Alonso-Perex et al., (2009) found that at P=12kbar and T>930℃ garnet and high-Tschermak's diopside will crystallise from a liquid, at T between 930℃ and 850℃ garnet, high-Tschermak's diopside and plagioclase (with orthopyroxene and ilmenite accessory minerals) will crystallise. Cooling, decreasing pressure or increasing H_2O content all have the effect of crystallising amphibole in preference to diopside. Increased amphibole in the Talkeetna arc corresponds with a decrease in depth that in turn results in a decreased temperature and pressure.

1.3 Aims

Aims of this study are to:

Characterise the Breaksea Orthogneiss, between Breaskea Sound and Coal River, in terms of geochemistry and mineralogy

Compare the Breaksea Orthogneiss to the Western Fiordland Orthogneiss constituent plutons and to the Hawes Head Ultramafic units

Using the exposed root of a magmatic arc to gain insights into high-pressure magmatic processes and thus infer an origin for the Breaksea Orthogneiss.

2. Regional Geology

2.1 Regional Setting

New Zealand is divided geographically into the North and South Islands and geologically into ten separate terranes, the Northland and East Coast Allochthons and two regional batholiths that intrude into these terranes, along with three main metamorphic zones (Fig. 2.01) (Mortimer, 2004).

2.2 Fiordland, New Zealand

Eastern and Western Provinces

Fiordland, in the South Island of New Zealand involves three of the aforementioned terranes, which are divided into Eastern and Western Provinces and intruded by the Median Batholith (Fig. 2.01). The westernmost part of the Eastern Province equates to the Brook Street Terrane of Fig. 2.01, while the Buller and Takaka Terranes constitute the Western Province. The division of Fiordland into these areas is done on the basis of chronological and geochemical constraints.

Median Batholith

What is now known as the Median Batholith has undergone a number of nomenclature changes and modifications to its definition and constituent rock units; Landis & Coombs (1967) introduced the term Median Tectonic Line, a fault separating components of a paired metamorphic belt (Fig 2.02). Bishop et al., (1985) modified this definition to a 'major terrane boundary' between the Eastern and Western Provinces. This MTL nomenclature and interpretation was superseded by the Median Tectonic Zone (Fig. 2.02), which purported that the MTZ was a zone of deformed crustal fragments and

magmatic arc rocks that is 5000km^2 in size (Frost & Coombs, 1989; Bradshaw, 1993; Kimbrough et al., 1993). Following this, Mortimer (1999) states that 4600km^2 (92%) of the MTZ is made up of as many as 70 discrete plutonic units, with the remaining 400km^2 made up of volcanic or sedimentary rocks. To emphasise the dominantly plutonic nature of the MTZ, Mortimer (1999) proposed the term Median Batholith (Fig. 2.02) as a regional designation of the plutonic rocks of the MTZ as well as plutonic rocks that intrude the Western Province.

The Median Batholith has experienced two main phases of magmatic activity; from 345 – 195Ma and from 168 – 114Ma (Bradshaw, 1993; Muir et al., 1998) which are representative of episodic subduction at the Gondwana margin. Klepeis & Clarke (2004) state that the earlier magmatic phase of the Median Batholith is the outboard part of the Mesozoic magmatic arc that formed during Early Triassic – Early Cretaceous subduction related magmatism (discussed further below).

The Darran Suite rocks constitute part of the earlier magmatic phase, while the Western Fiordland Orthogneiss, Seperation Point Suite and Arthur River Complex were emplaced during the later stage of magmatic activity in the Median Batholith (Klepeis & Clarke, 2004). These plutons form parts of the Median Batholith that intrude the Western Province.

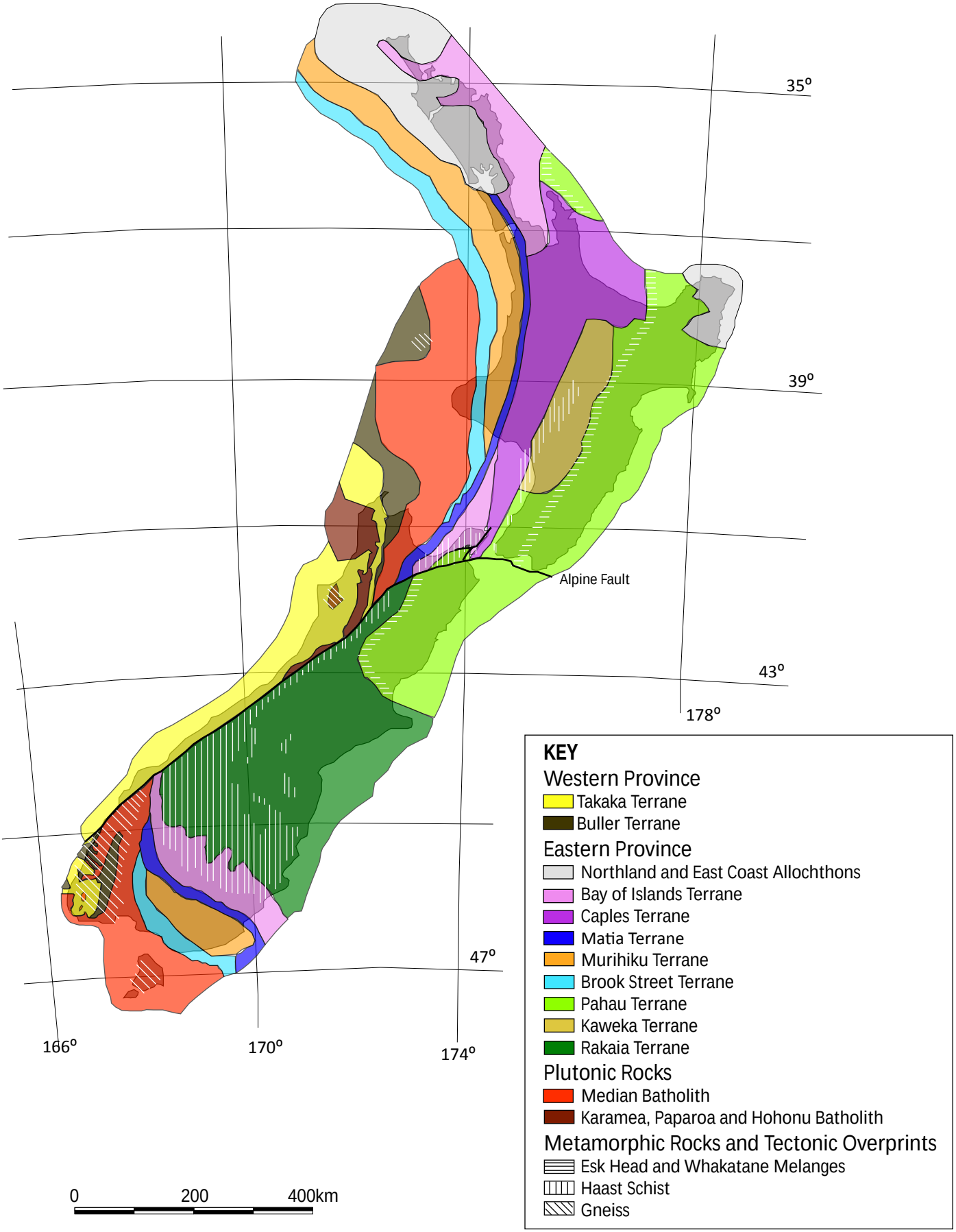

Fig 2.01 Geological map of New Zealand showing divisions from Mortimer (2004).

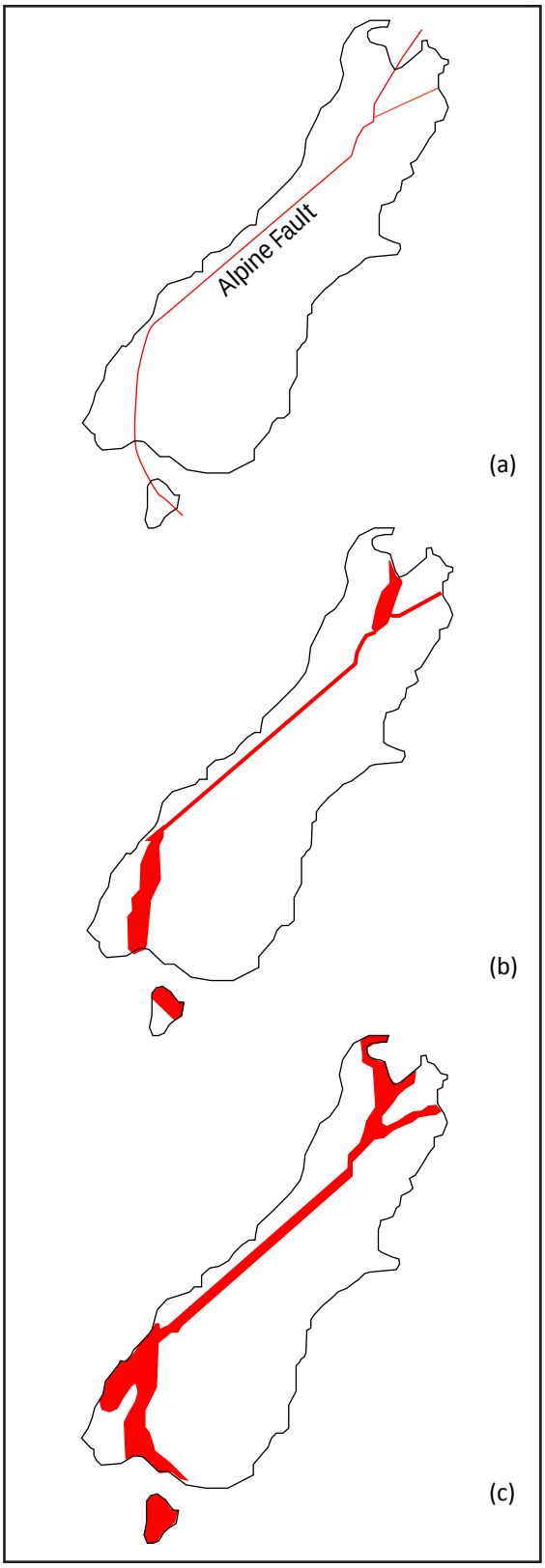

Fig 2.02 South Island, New Zealand showing the evolution from the Median Tectonic Line (a) to Median Tectonic Zone (b) to the current Median Batholith (c). Modified from Mortimer et al., (1999).

2.3 Western Fiordland Orthogneiss

The parts of Fiordland made up by the Western Province and Median Batholith, particularly the Western Fiordland Orthogneiss suite are the subject of this study and are of particular interest.

The Western Fiordland Orthogneiss is part of the later Median Batholith tectonic activity, and is a suite including felsic diorites, monzodiorites and minor gabbros (Allibone et al., 2009; Scott & Cooper, 2006) comprised of the Worsley Pluton, Mckerr Intrusives, Lake Wade Diorite, Misty Pluton (north of study area), Malaspina Pluton (north and south of the study area), Breaksea Orthogneiss (within the study area, composed of omphacite granulite and eclogite) and Resolution Orthogneiss (Allibone et al 2009) (Fig. 2.03).

Geochronology

The tectonic history of Fiordland relevant to this study is essentially the examination of the evolution of an early Mesozoic magmatic arc along the ancient Gondwana Margin (Kelpeis & Clarke, 2004) and can be broken down into four main tectonic and time constrained phases;

Formation of part of the arc in a location outboard to the Gondwana Margin during the early Triassic (247 – 131Ma) which resulted in the production of magmas with a low Sr/Y ratio, indicative of a source region at depths where residual plagioclase is stable. This phase of magmatism resulted in the emplacement of rocks such as the Darran Suite, based on geochemical correlations (Klepeis & Clarke, 2004).

During the Cretaceous (130-105Ma) the MTZ accreted onto the Gondwana Margin, manifested in the form of contractional deformation, crustal thickening and associated

magmatism along the eastern edge of the Gondwana margin Dating of mafic dykes in the Arthur River Complex suggests that accretion began as early as 136Ma and probably by 129Ma (Klepeis & Clarke 2004). Associated magmatism from this period is marked by magmas with a high Sr/Y ratio (>50) which indicates a source region at a depth below that at which residual plagioclase is stable. (Klepeis & Clarke, 2004). Based on dating and geochemical analysis by Muir et al., (1998) it is known that during this period of tectonic activity the SPS and WFO where emplaced (Klepeis & Clarke, 2004; Bradshaw, 1989; Kimbrough et al., 1984).

From 105-83Ma Fiordland was undergoing extension, evident in the Doubtful Sound (DSSZ) and Anita Shear Zones (Fig. 2.03) and associated cross cutting relationships (DSSZ cuts the WFO). This is viewed as representing the divergence of New Zealand from Gondwana (Klepeis & Clarke, 2004; McCulloch et al., 1987).

Finally, from 83-52Ma seafloor spreading took place in the Tasman Sea (Klepeis & Clarke, 2004)

Geochemistry

The 'characteristc' geochemical signatures indicative of the Western Fiordland Orthogneiss are integral in comparing samples collected and categorising variations from this 'norm'. The Western Firodland Orthogneiss are characterised by Muir et al., (1998) as having moderate (54-57 wt%) SiO2, high Al2O3 (17-23 wt%), high total alkalis (Na2O+K2O=6-9 wt% with Na2O/K2O=1.5-2.0), high Sr (800-1850ppm) and low Y (<17ppm). This depletion in yttrium is seen as an indicator by Allibone et al., (2009); McCulloch et al., (1987); Muir et al., 1998) of a magma source region within the garnet stability field (resulting in a HREE depletion) which is inferred to amount to a thickened crust (>40km) at the time of emplacement (Muir et al., 1998). Muir et al., (1998) also note that while chondrite normalised REE patterns are similar to those of the Separation

Point Suite (SPS), total REE concentrations are higher in the Western Fiordland Orthogneiss (WFO) and from Muir et al., (1995) and Ireland & Gibson (1998) the conclusion is drawn that the WFO is the deep crustal equivalent of the SPS. Allibone et al., (2009), note that new geochemical data separates the SPS and WFO and chemically different, with high Sr/y ratios simply reflected both the SPS and WFO being emplaced at comparable depths.

Muir et al., (1998) attempted to resolve a protolith for the Western Fiordland Orthogneiss by conducting modal and non-modal batch melting models of the Darran Suite. All models concluded that a residue with ~10% grt and ~30% partial meltin are required, resulting in an acceptable fit. Batch melting models conducted by Muir et al., (1998) concluded that the Western Fiordland Orthogneiss could represent a 30% partial melt of the Darran Suite (part of the MTZ), from a garnet amphibolite source with 5% plagioclase, 11% garnet, 15% amphibole and 63%. The Separation Point Suite, with its lower total REE concentrations, could reflect either lower degrees of partial melting (<20%) or a greater amount of residual garnet (>10%), in the source region (Muir et al., 1998), although this relationship is challenged by Allibone et al., (2009).

Metamorphic Studies

Mineral assemblages observed in the WFO are typically clinopyroxene-orthopyroxene-horblende-plagioclase which yield peak metamorphic pressures of <10kbar and temperatures >750°C (Dacxko & Halpin, 2009). Less common mineral assemblages observed show garnet-omphacite-plagioclase, with hornblende, plagioclase and potassium feldspar occasionally observed as retrograde symplectites, with quartz and rutile present as accessory minerals (Klepeis & Clarke, 2004; Daczko et al., 2002; Gibson et al., 1988). These mineral assemblages have yielded peak metamorphic pressures of ~12 kbar for garnet reaction zones and ~18kbar for the Breaksea Orthogneiss (Daczko & Halpin, 2009) and temperatures > 750°C (Daczko & Halpin, 2009; Daczko et al., 2002)

however, Daczko & Halpin (2009) suggest that peak metamorphic pressure may be as low as 11kbar, due to metastability.

The age of the WFO has been determined by U-Pb SID and ion probe dating on zircon grains as well as whole rock Rb-Sr to yield an average age of 123.2 ± 5.4Ma (Mattinson et al., 1986; McCulloch et al., 1987; Gibson & Ireland, 1995; Muir et al., 1998). U-Pb ion probe dating of zircon grains by Gibson & Ireland (1995) yield a metamorphic age of 107.5 ± 2.8 Ma. Extension and exhumation ages of 92.1 ± 1.6Ma were calculated based on U-Pb SID dating of apatite and K-Ar dating of hornblende (Mattinson et al., 1986, Gibson et al., 1988).

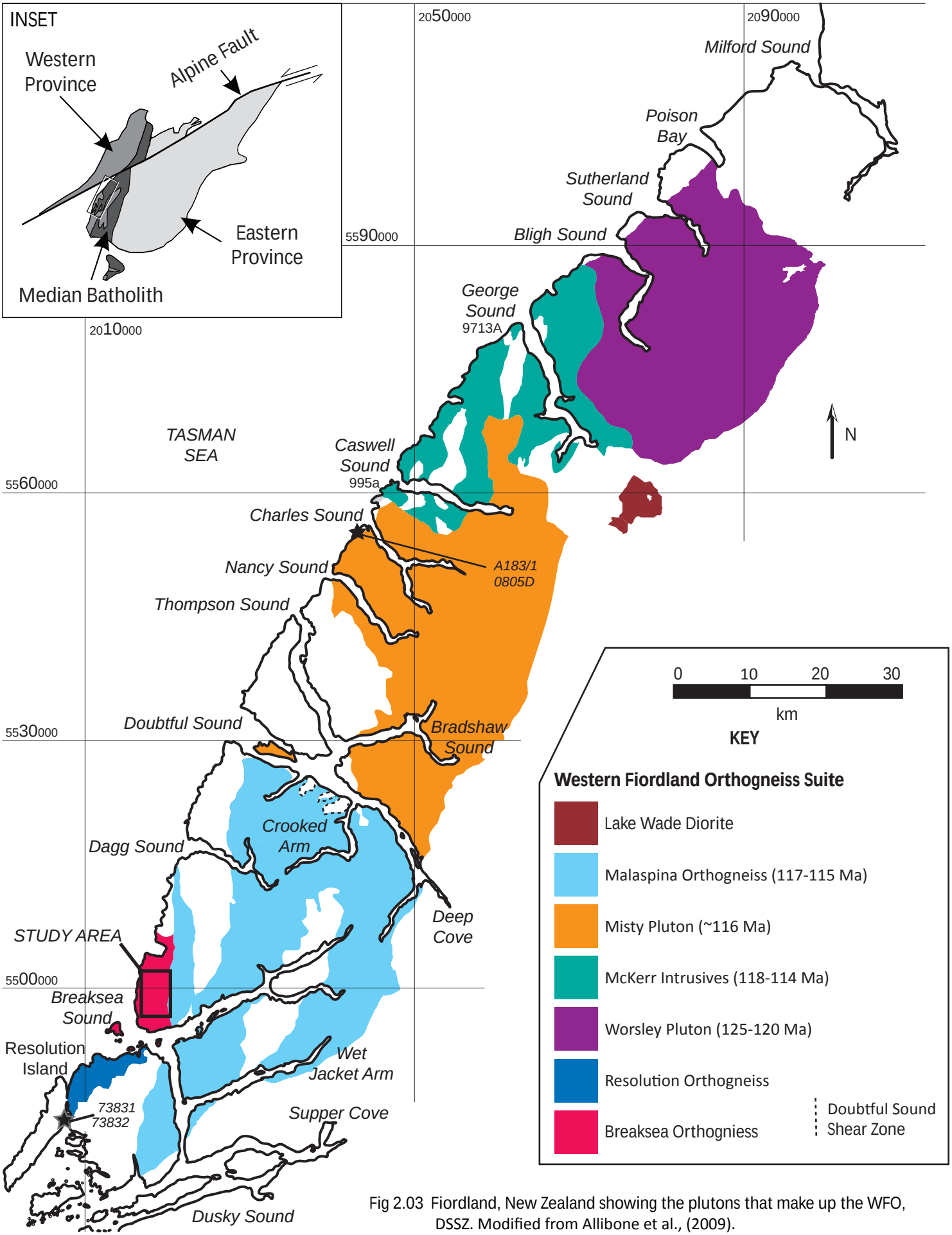

Fig 2.03 Fiordland, New Zealand showing the plutons that make up the WFO, DSSZ. Modified from Allibone et al., (2009).

2.4 Tectonic History

The period of tectonic activity during the Cretaceous (130-105Ma) is of extreme significance to this study as it concerns the rocks involved in the study, but also has broader implications in terms of resolving a protolith to the WFO; the review of postulated theories for contractional deformation and crustal thickening and comparison to field observations and geochemical data has lead to the evolution of various tectonic models for WFO timing, source and emplacement as broader studies and databases have been developed.

As stated previously, part of the Gondwana margin underwent convergence at c. 130Ma resulting in crustal thickening and the production of unique HiSY and high Na wt% magmas (SPS and WFO). Muir et al's (1998) batch melting experiments concluded that acceptable chemical signatures for the SPS and WFO are produced by remelting the Darran Suite (part of the Median Batholith), emplaced prior to convergence.

Contractional deformation observed during the same time period has been attributed to either the accretion of MTZ onto the Gondwana margin or the collision of a basaltic plateau with the active subduction zone on the outboard side of the Gondwana margin arc (Klepeis & Clarke 2004).

Extension between 105 – 83Ma could be the result of the collision of the ontong java plateau the subduction zone or subduction rollback along the Gondwana margin (Klepeis & Clarke, 2004)

2.5 Tectonic Models

Gibson et al., (1988) produced one of the first tectonic models for the emplacement of the WFO; stating that the WFO was part of a metamorphic core complex and was emplaced at 12kbar during extension at 108Ma, with exhumation following (Gibson et al., 1988, 1989; Gibson & Ireland, 1995; Hill, 1995). It is important to note that research that lead to these theories was conducted mainly north of the study area in the Malaspina Pluton (Fig. 2.03) and therefore did not appreciate the WFO as the collection of multiple intrusions that it is, rather interpreting the WFO as one massive batholith. This model emphasises the importance that sheared contacts between the WFO and older adjacent rocks hold in relation to tectonic history (Allibone et al., 2009). Intensely deformed intrusive contacts between the northern WFO and surrounding rocks indicate that the WFO is not the lower part of a metamorphic core complex separated from adjacent older rocks by a ductile shear zone and that WFO and WFO intruded rocks share similar post emplacement P-T-t paths (Bradshaw, 1990; Daczko et al., 2002; Clarke et al., 2009; Allibone et al., 2009).

Bradshaw (1989, 1990), working in the Worsely Pluton (Fig. 2.03) north of the study area, proposed that the WFO pluton was emplaced at 6kbar, on the basis of contact metamorphic assemblages and intrusive contacts observed which subsequently underwent thickening due to tectonic loading, increasing to the peak pressure of 12kbar. Daczko et al., (2001) and Clarke et al., (2001) follow the Bradshaw (1989, 1990) model, stating WFO emplacement at c. 125Ma, reasoning that tectonic loading was the result of thrust faults seen in Caswell Sound (McKerr Intrusives) and the Pembroke Valley (Arthur River Complex). Brown (1996) used Bradshaw's (1989, 1990) model of tectonic loading but stated that crustal thickening was the result of magma emplacement rather than tectonic loading.

The present adaption on fitting a tectonic history for the WFO to recorded observations is one based on intensive mapping of WFO-country rock contacts by Allibone et al., (2009) in which previous theories are combined to a certain degree. Allibone et al., (2009) argue that the Worsely Pluton, Arthur River Complex, and McKerr Intrusives where emplaced into the mid crust at P = 6 - 11kbar c. 125Ma, followed by a period of crustal thickening ensuing from thrust faulting and magmatic loading after which the Malaspina Pluton was emplaced at 116 ± 2Ma into deep crust, but prior to the onset of extension marked by the development of the Doubtful Sound Shear Zone. This is based on the observations that the Malaspina Pluton does not show evidence of post emplacement loading and leads to the conclusion that tectonic loading occurred between 120 – 116Ma (Allibone et al., 2009), emphasizing the fact that the WFO must be treated as the multiple intrusions.

Allibone et al., (2009) also point towards an autochthonous intrusive relationship between the Malaspina Pluton and the Deep Cove Gneiss on the basis of dating, P-T-t calculations and mineral assemblages, relegating extensional ductile shear zones (which originally gave rise to Gibson et al's., (1988) core complex model) to discontinuous features that mark the contact between hot coarse grained dioritic intrusions and cooler finer grained country rock as opposed to being part of a metamorphic core complex.

3. Fieldwork

3.1 Introduction and aims

The Western Fiordland Orthogneiss suite (WFO) is comprised of multiple litholigical units delineated during recent mapping by Geological and Nuclear Sciences (GNS) of New Zealand; these are the Worsley Pluton, Mckerr Intrusives, Lake Wade Diorite, Misty Pluton (north of study area), Malaspina Pluton (north and south of the study area), Breaksea Orthogneiss (within the study area, composed of omphacite granulite and eclogite) and Resolution Orthogneiss (Allibone et al 2009) (Fig. 2.03).

The Breaksea Orthogneiss, which lies between Breaksea Sound and Coal River is heterogeneous in nature; made up of a main meta-diorite body (labeled Breaksea Omphacite Granulite, BOG) and multiple inclusions of eclogite (labeled Breaksea Eclogite, BE) as well as other inclusions of interlayered garnetite-pyroxenite and a single inclusion of hornblende peridotite (Fig. 3.10). The area north of Breaksea Sound amd south of Coal River selected is an ideal fieldwork location as it possessed a known camp site with helicopter access (GPS 2020743, 5501256) and allowed for the easiest access to visible inclusions of hornblende peridotite as well as multiple outcrops of BE and other rock units within the main BOG and thus provided an excellent opportunity for in situ observations of rock fabrics and relationships and the best overall sampling of the lithologies that make up the Breaksea Orthogneiss.

The purpose of fieldwork was to collect samples for petrographic and geochemical analysis of all rock types encountered. Specific aims included: characterising the Breaksea Orthogneiss between Breaksea Sound and Coal River; observing field relationships between BOG, BE and other units within the Breaksea Orthogneiss for comparison to WFO database (Allidone et al., 2009; DePaoli et al., 2009) (Appendix 5.A) to gain insights into protolith and relationships between protoliths; building knowledge

about source composition and depth and using field relationships to infer information about processes that occur at a deep crustal level in order to further investigate the effects of high pressure magmatic processes.

Locations were recorded using a Garmin 72 GPS, set to New Zealand map grid and Geodetic Datum 1949 with an accuracy of 10m. Sample locations are shown on Fig. 3.01. Structural data was measured using a Brunton compass, set to 8° declination.

3.2 Method and logistics

Fieldwork was conducted in Western Fiordland, about 3km south of Coal River (Fig. 3.01), from the 13th – 18th January 2009. Transport from Te Anau to Fiordland was by helicopter. Fieldwork was funded by Macquarie University Safety Net Grant. All field locations were reached on foot along ridgelines that surrounded the field party's campsite (Fig. 3.10); the field party camped in a grassy saddle at GPS location 2020743, 5501256. Nathan Daczko, Geoff Clarke and Matthew De Paoli provided field assistance.

111 samples from the GNS PETLAB database (http://pet.gns.cri.nz/) collected from the various plutons that make up the WFO have been used as a comparison which are shown on Fig. 3.01.

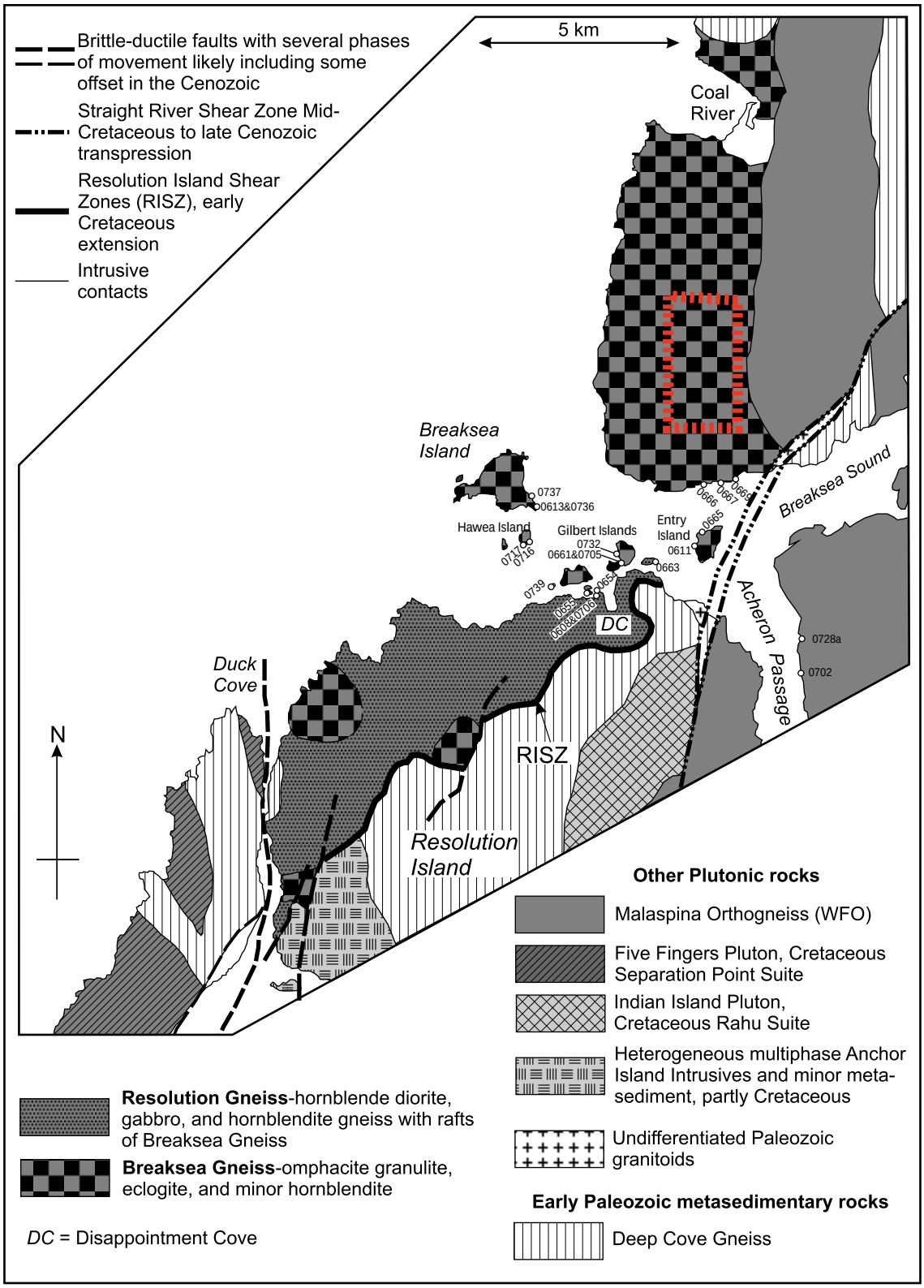

Fig 3.01 map showing Breaksea Orthogneiss and study location (red). From DePaoli et al., 2009

3.3 Results

Breaksea Orthogneiss

The Breaksea Orthogneiss can be broken up into four lithologies on the basis of mineral composition and field relations: The main meta-diorite named the Breaksea Omphacite Granulite (Figs. 3.02 & 3.03) and three different inclusion types: (I) eclogite named the Breaksea Eclogite (Figs. 3.04 & 3.05), (II) inclusions of layered garnetite-pyroxenite (Figs. 3.06 & 3.07) and (III) hornblende peridotite (Figs 3.08 & 3.09).

Breaksea Omphacite Granulite

The dominant unit of the Breaksea Orthogneiss, the BOG is typically ameta-dioritic granulite gneiss with a omphacite, plagioclase ± garnet composition with illmenite, kyanite, apatite and rutile present as accessory minerals. A BOG variant (sample 0905C) containing enstatite (15%)and no garnet was also observed. A typical sample contains 50% plagioclase, 25-45% omphacite and 5-25% garnet. Pyroxene and garnet modal variations are generally not well defined and can vary over tens of metres although in some instances fine and coarse garnet domains are observed (Fig. 3.02) on a centimeter scale. Grains are typically coarse, ranging from 2-5mm in hand sample with some garnet porphyroblasts measuring up to 30mm across (Fig. 3.03). Garnet shows textural variation in its occurrence, appearing as coronas surrounding omphacite grains as well as in separate leucosomes (Fig. 3.02) which correspond to fine and coarse garnet domains. The BOG has a well defined gneissocity that is commonly oblique to compositional banding (Fig. 3.02) and defined by plagioclase and omphacite, with an average measurement of 129°/71°/NE The unit outcrops regularly throughout the field area.

Fig 3.02 Breaksea Omphacite Granulite showing compositional banding (orange) dividing finer garnet (coronas around pyroxene) and coarse garnet (surrounded by leucosomes) as well as the main foliation (green) which is oblique to compositional banding. Lens cap is 60mm diameter.

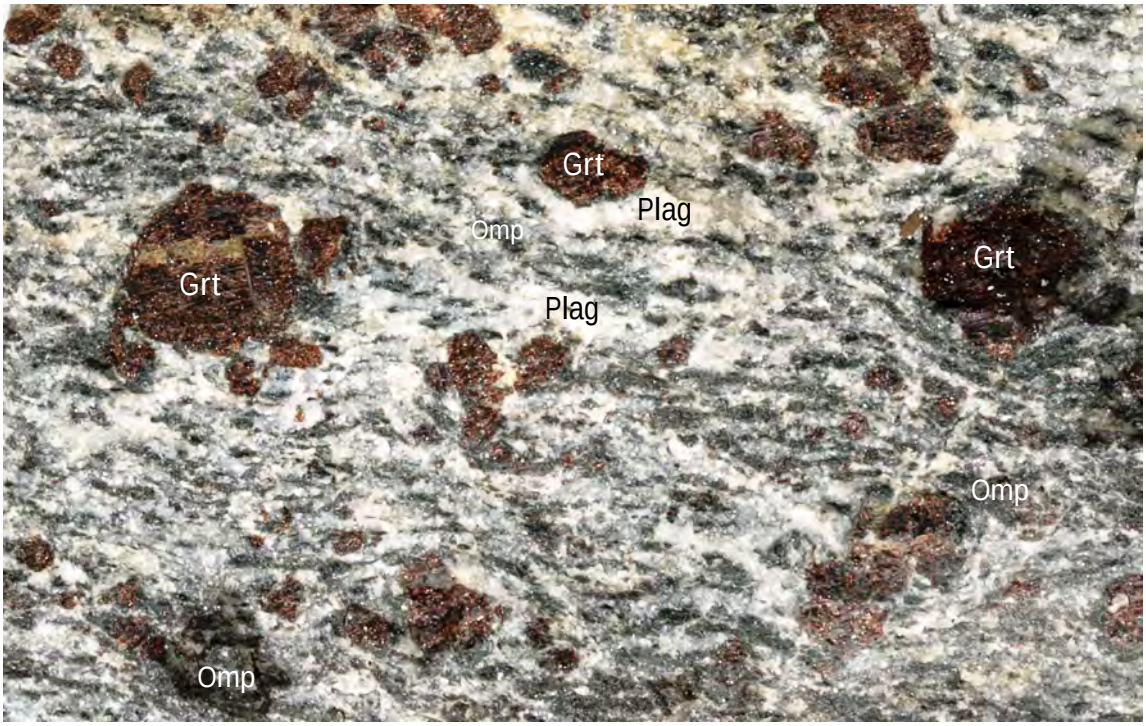

Fig 3.03 Breaksea Omphacite Granulite showing large garnet porphyroblasts. Base of photo is 100mm.

Breaksea Eclogite

Within the BOG, there are multiple inclusions of BE which are essentially large xenoliths completely enveloped by the surrounding BOG. These xenoliths occur on a cm (Fig. 3.04) to tens of metres scale with one such xenolith measuring 5-20 x ~50m. The Breaksea Eclogite typically consists of 45-50% garnet and 45-50% omphacite present with 0-10% pargasite, plagioclase, minor biotite and opaque minerals present as interstitial symplectites. Not all BE sample locations display symplectite development (0901B and 0904C show symplectite development). The BE is typically medium to coarse grained with grainsize ranging from 1-3mm in hand sample. The eclogite is massive in appearance, lacking a defined foliation similar to the BOG encountered, which can be observed in (Fig. 3.05), however the xenolith pictured in Fig. 3.04 shows extensional stretching along a slightly oblique direction to the BOG foliation (elongate along 000°). The BE was encountered at four different locations in the field (Sites 1, 2, 4 and 10).

The BE xenoliths encountered were always podiform or lenticular in shape, elongated at approximately a 1:4 ratio (Fig. 3.04). The scale of such xenoliths varied; the smallest being 5 x 20cm (Fig. 3.04) and the largest being ~5-20 x 50m (Fig. 3.10). The xenoliths were completely surrounded on all sides by BOG with their elongation direction sub parallel to the main BOG foliation direction.

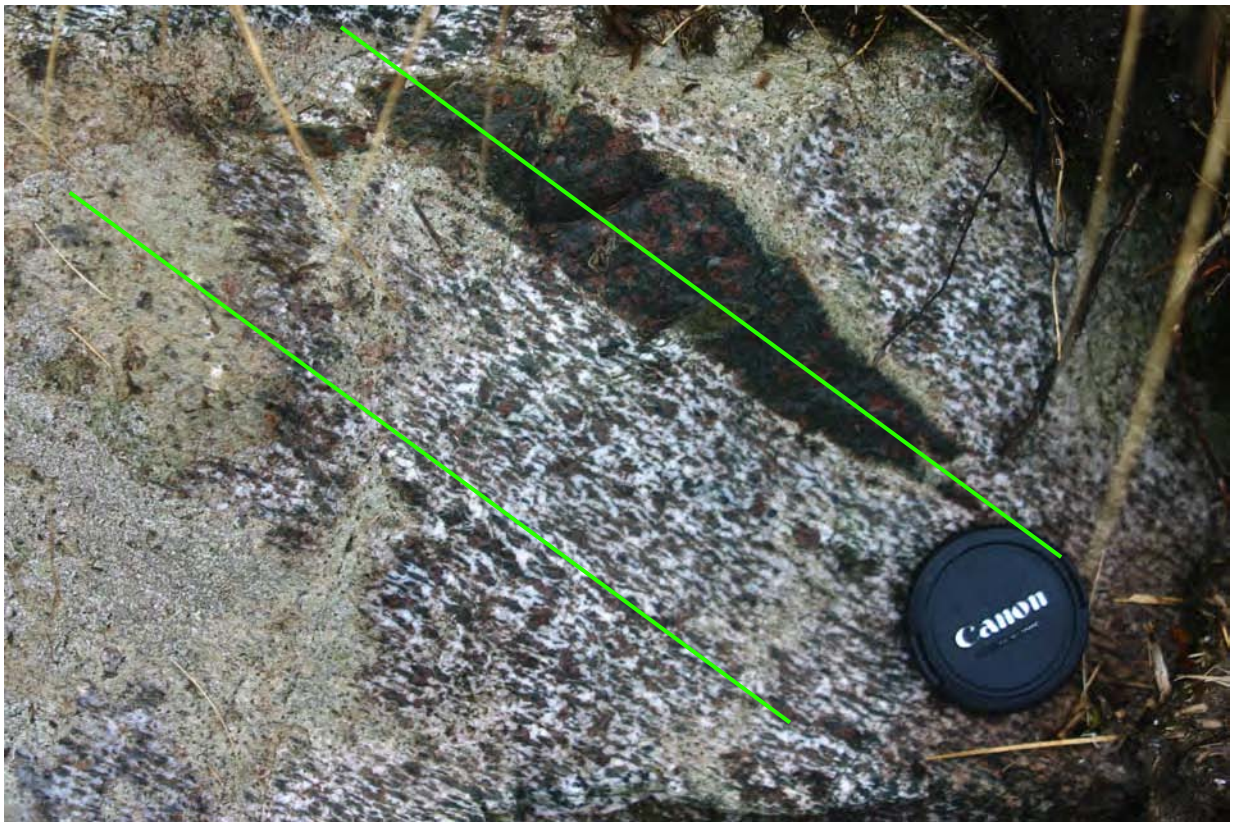

Fig 3.04 Cognate inclusion of Breaksea Eclogite within BOG. Note that elongation of the inclusion is sub parallel to main BOG foliation. Lens cap is 60mm diameter.

Fig 3.05 Breaksea Eclogite. Note the lack of a well defined folitaion as seen in the BOG. Red mineral is garnet, dark green mineral is omphacite. Lens cap is 60mm diameter.

Layered Garnetite – Pyroxenite

At two site locations (Site 6 & 10) (Figs 3.06 & 3.07) interlayered garnetite and pyroxenite rocks were sampled (fig xx). This rock unit occurs as inclusions within the BOG at two site locations and measured ≈ 50m x 50m at each. Individual layers were commonly 6-10cm thick, with some layers as thin as 2cm and some up to 30cm. The rock exhibits a unique weathering feature where the garnetite layers have a lower relief than the pyroxenite layers (Fig. 3.06)). The garnetite layers typically consist of 80-85% garnet, 5-20% diopside whilst the pyroxenites layers consist of 95% diopside and 5% garnet. Grainsize in the garnetite layers varies from 1-4mm, with garnet and pyroxene being of similar grainsize and 1-5mm in the pyroxenite layers, with garnet grains generally being no larger than 1mm (all measurements taken from hand sample). There is no foliation evident in this rock as there was in the previous rock types encountered. The individual layers of garnetite and pyroxenite show irregular and gradational boundaries over 3-5m (Fig. 3.07).

Fig 3.06 Interlayered garnetite and pyroxenite unit. Note that the garnetite is subordinate to the pyroxenite. Lens cap is 60mm diameter.

Fig 3.07 Indications of mixing within interlayered garnetite and pyroxenite. Dotted line shows that layer boundaries are not straight contacts. Lens cap is 60mm diameter.

Hornblende Peridotite

At one site location (Site 3) a hornblende peridotite was sampled (Fig. 3.08), occurring as a metre (~30x10m) scale podiform inclusion within the BOG. The hornblende peridotite consisted of 40% hornblende, 35% olivine, 15% diopside, 5% enstatite and 5% opaque minerals with spinel present as an accessory phase. The sample was medium grained with grainsize typically 1-3mm in hand sample, with minor hornblende prophyroblasts up to 12mm across. The olivine and hornblende show a very well defined foliation trending 194°/59°/SE (Fig. 3.08) although some of the outcrop showed enough magnetism to deflect a compass needle substantially. Within this hornblende peridotite inclusion there were minor bands of hornblendite (Fig. 3.09).

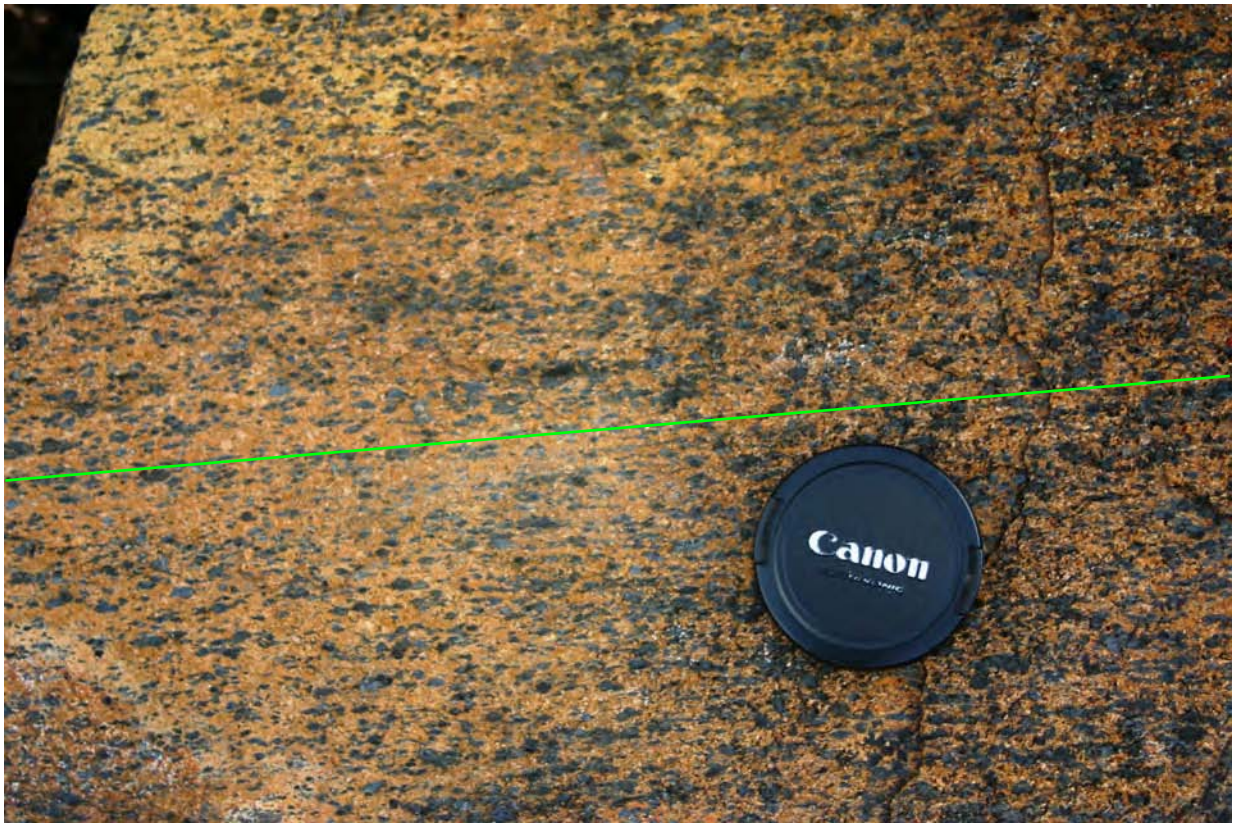

Fig 3.08 Hornblende Peridotite. Green line marks main foliation. Darker mineral is hornblende and lighter, yellow/brown minerals are olivine and orthopyroxene. Lens cap is 60mm diameter.

Fig 3.09 Rare hornblendite band within hornblende peridotite. Lens cap is 60mm diameter.

3.4 Discussion

Textural properties of the inclusions observed lead to inferences regarding their emplacement; for all lithologies, the podiform shape, preferential elongation sub parallel to the main foliation direction suggest ductile deformation during metamorphism which in turn suggests a depth in the ductile range of deformation during metamorphism. It also implies that the podiform shape is a product of metamorphism and that these inclusions were present prior to this metamorphic event.

The interlayered garnetite-pyroxenite of sites 0906 and 0910 is of great significance as the compositional banding observed appears to be consistent with the primary igneous texture of magmatic layering.

The interaction of garnetite and pyroxenite layers observed (Figs 3.06 & 3.07) is further evidence in support of the fact that this banding depicts how these liquids settled and interacted with each other within their host magma chamber as opposed to this layering being a form of metamorphic foliation or partial remelting feature.

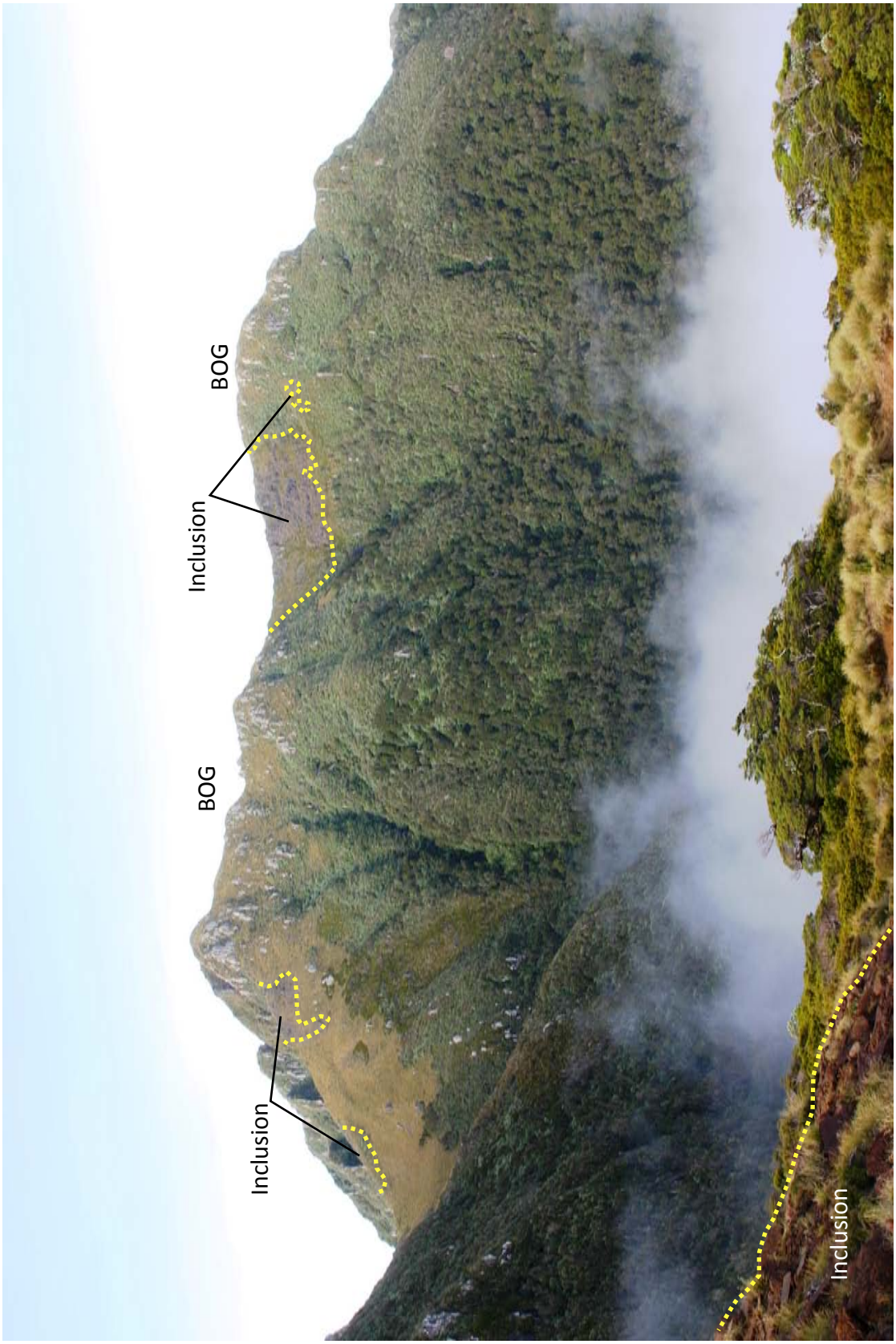

Fig 3.10 Long range view of cognate inclusion shape and relationship to surroundinf BOG. Large marked inclusion in background is ~50m across. Taken from site 3.

4. Petrography

4.1 Introduction

24 petrographic samples were cut to size, mounted, ground to 30µm thickness and polished on 46 x 26mm glass slides. The samples were examined using a Nikon Eclipse E400 Pol binocular petrographic microscope. Samples were grouped according to litholigies determined during fieldwork, with representative and atypical thin sections being photographed using a Canon EOS 300 digital SLR camera.

22 of the samples were collected by James Watton, Nathan Daczko, Geoff Clarke and Matthew De Paoli, while two of the samples were supplied by Luke (73831 and 73832). Of these, 19 are Western Fiordland Orthogneiss samples, with 9 being samples of Breaksea Omphacite Granulite (BOG); 10 of Breaksea Eclogite (BE); 4 of interlayered garnetite and pyroxenite and 1 of hornblende peridotite.

4.2 Results

Breaksea Orthogneiss

As defined during fieldwork, the Breaksea Orthogneiss has been subdivided into the Breaksea Omphacite Granulite and Breaksea Eclogite.

Breaksea Omphacite Granulite

Mineral modes have been estimated by visual inspection of thin sections. The BOG is comprised of plagioclase feldspar (50%); omphacite (25 - 45%); garnet (4 - 25%). Accessory minerals include rutile, kyanite, orthoclase and apatite as well as minor biotite, pargasite, ilmenite and zircon. One sample (0905C) also contained orthopyroxene (5-10%). Fig 4.01 shows a typical BOG composition.

Plagioclase grains range from 0.20 – 0.50mm and are xenoblastic (Figs. 4.01 - 4.02); although some plagioclase grains in contact with garnet show straight crystal faces (Fig. 4.02). Plagioclase also occurs as inclusions within garnet (Fig. 4.03 and 4.04). Omphacite ranges from 0.10 – 0.45mm and are mainly xenoblastic (Figs. 4.01 – 4.02), also occurring as inclusions within garnet (Fig. 4.03). Garnet generally ranges in size from 0.50 – 1.50mm within the main foliation (Figs. 4.01 – 4.02) with porphyroblasts up to 3.5mm across (Figs. 4.03 – 4.04).

Rutile measures 0.08 – 0.55mm long and are subidioblastic to idioblastic (Figs. 4.02, 4.04 – 4.06) and also appear as exsolutions in omphacite and garnet along three different crystallographic axes (Fig. 4.07). Rutile can be seen in association with plagioclase (Figs. 4.02 and 4.05), omphacite (Fig. 4.02) and garnet (Figs. 4.04 and 4.06). Rutile shows inclined extinction indicative of a higher pressure at formation (El Goresy et al., 2001; Withers et al., 2003; Wu et al., .2005). Hematite can be seen as a small replacement texture in Fig 4.04.

Apatite is xenoblastic and ranges in size from 0.20 – 0.42mm. It can be seen in association with plagioclase, omphacite and garnet (Figs. 4.03 – 4.04, 4.07). Kyanite is acicular and is usually 0.20 – 0.75 mm long (Fig. 4.08). It occurs in association with plagioclase and is commonly rimmed by anorthite (Fig. 4.08).

Minor biotite ranges is size from 0.13 – 0.22mm and it seen as a symplectite material indicative of mineral replacement (Figs. 4.06 and 4.08). Minor pargasite (Fig. 4.07) is also present as a plagioclase – pargasite symplectite of very fine grain size (<0.05mm).

The BOG shows limited evidence of retrogression by the development of symplectites along some grain boundaries. These symplectites are very fine grained (<0.05mm) and have varying compositions; biotite – plagioclase (Figs. 4.04, 4.06, 4.08); clinopyroxene – plagioclase (Figs. 4.06 and 4.08) and pargasite – clinopyroxene – plagioclase (Fig. 4.07). Due to their very fine grain size these symplectites were marked for examination in greater detail by element mapping (Chapter 6).

The major textural feature observed for the BOG is the well developed gneissocity visible in Fig. 4.01, observed through the elongation of plagioclase, omphacite and small garnet grains along the foliation direction.

Garnet in the BOG occurs in two different textural settings as shown in Fig. 4.03; as foliated coarse intergrowths with omphacite, showing idioblastic grain boundaries and growing into the plagioclase domains; and as porphyroblasts, retaining the idioblastic grain boundaries with plagioclase and containing inclusions of plagioclase, omphacite, apatite and rutile. The outside edges of the inclusions are idioblastic, as are grain boundaries still in contact with this outside edge (apatite and omphacite in Figs. 4.04 and 4.07) while the plagioclase – omphacite boundary within the inclusion is commonly xenoblastic (Figs. 4.04 and 4.07). Furthermore, symplectite development can be seen within garnet in Fig. 4.07. Normally forming as a post peak metamorphic reaction, this is seen as an indicator that these inclusions initially contained less plagioclase and more omphacite and that during metamorphism plagioclase has replaced some of the omphacite present.

Omphacite is seen in direct contact with plagioclase in many samples (Figs. 4.01 – 4.03 and 4.05) with no evidence of symplectite development; evidence that omphacite and plagioclase were in equilibrium with one another. The fact that some samples (Figs. 4.04, 4.06 – 4.08) show symplectite development is viewed as a retrograde metamorphic feature. Symplectites are also seen solely in omphacite (Fig. 4.06) and also in the Breaksea Eclogite (Figs 4.13 – 4.15) between omphacite and garnet.

Epidote filled veins cut the main foliation (Fig. 4.09), and are attributed to recent brittle movement. This is only seen in one BOG sample (0909B).

Variation from the common BOG described above was seen in sample 0905C (Figs. 4.10 – 4.12); this sample is a two pyroxene plagioclase gneiss that lacks garnet. Modal composition is plagioclase (50%), omphacite (35-40%), enstatite (5-10%) with

accessory minerals apatite, kyanite, ilmenite, orthoclase and biotite. Mineral textures follow those found in the main BOG. There is a larger amount of symplectite development seen in this sample compared to the common BOG (Figs. 4.10 and 4.12)

Fig 4.01 0905B (a) PPL (b) XPL Base of photo: 7mm - Representative micrograph of the Breaksea Omphacite Granulite.

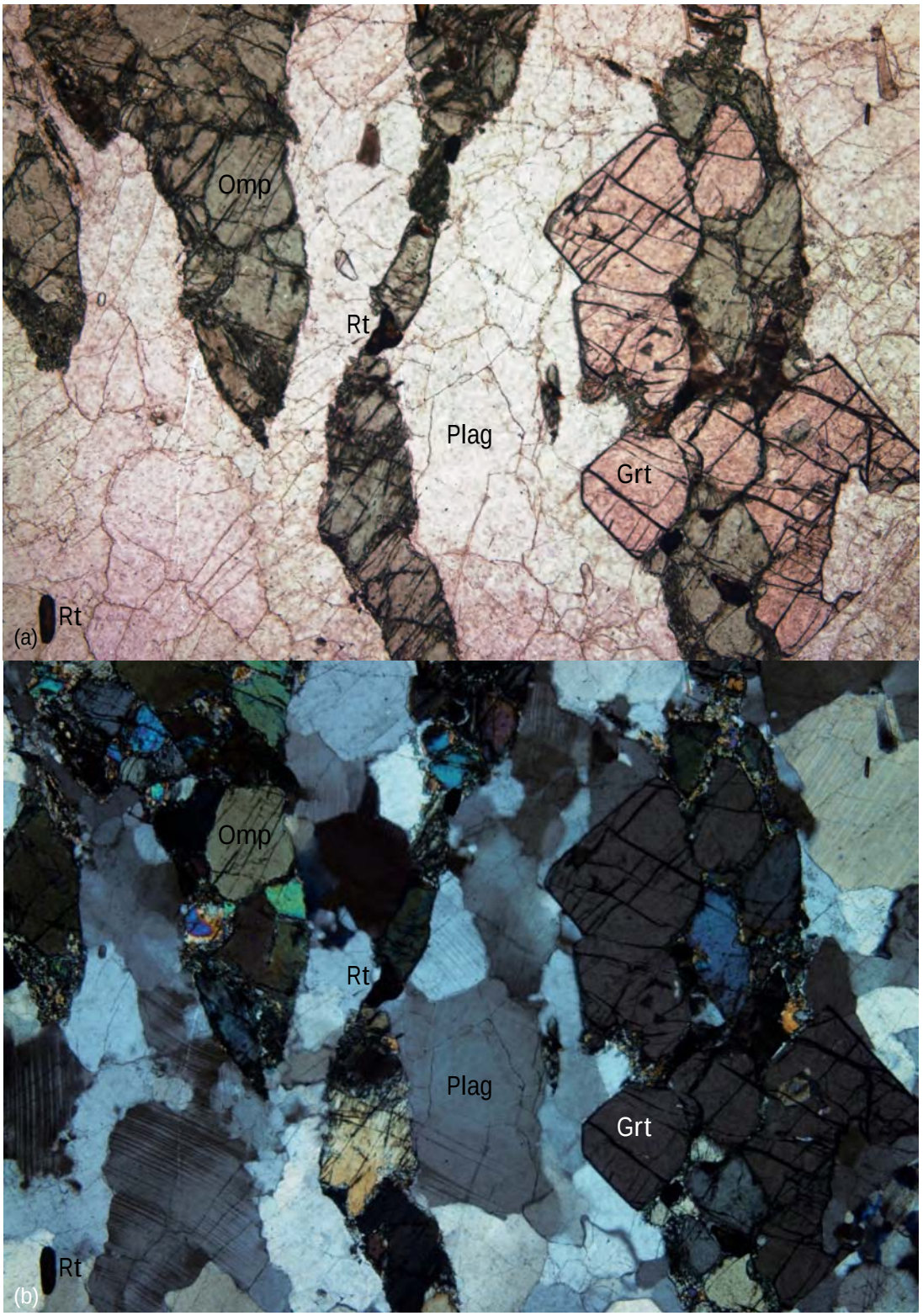

Fig 4.02 0905B (a) PPL (b) XPL Base of photo: 2.5mm - Plagioclase and garnet exhibiting idioblastic grain boundaries; rutile in association with omphacite and plagioclase.

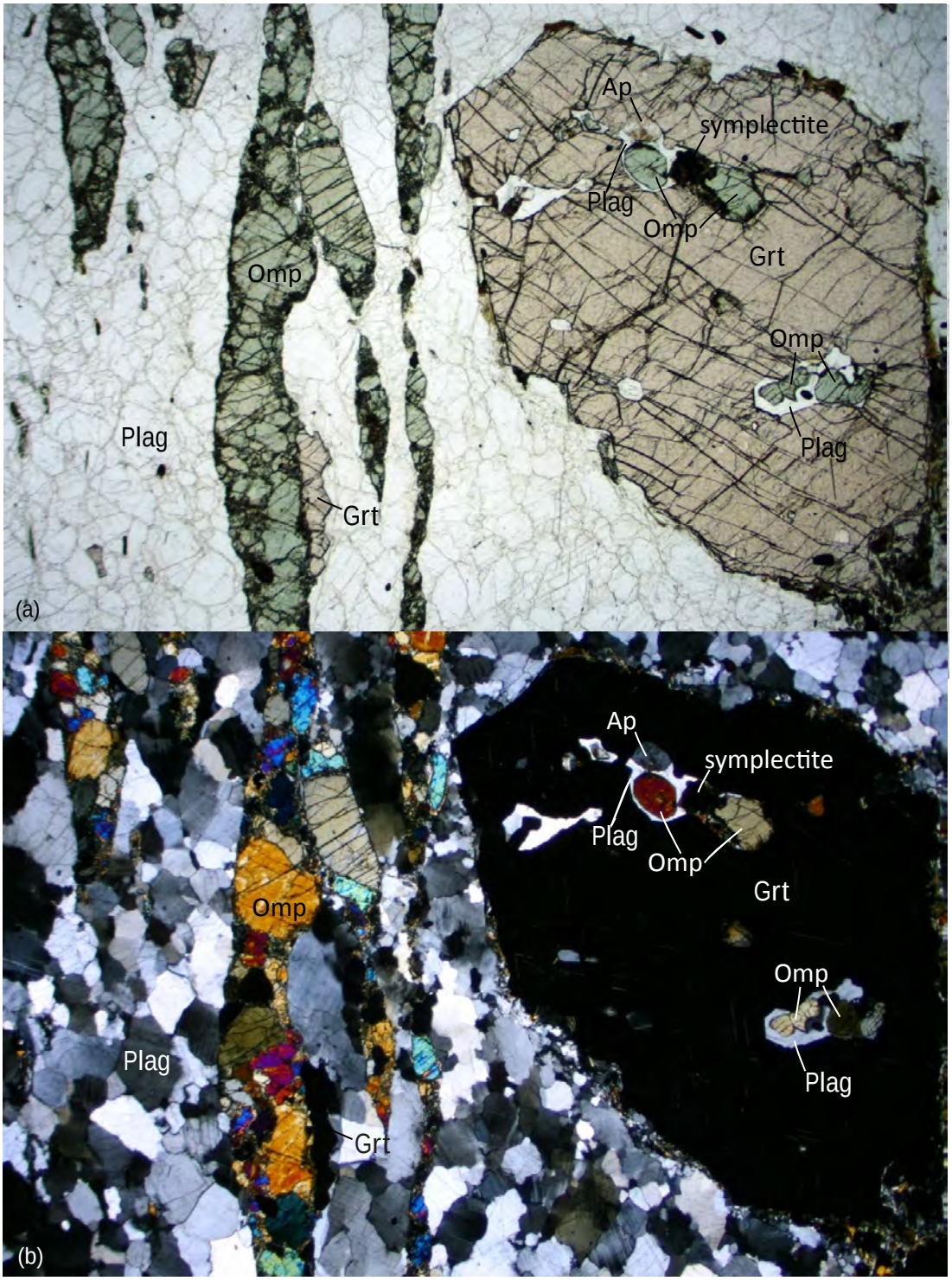

Fig 4.03 0905B (a) PPL (b) XPL Base of photo: 9.25mm - Photomicrograph showing the two textural settings of garnet growth; intergrown with omphacite and as porphyroblasts. Omphacite rimmed by plagioclase can be seen as inclusions within garnet. Apatite is also visible as an inclusion.

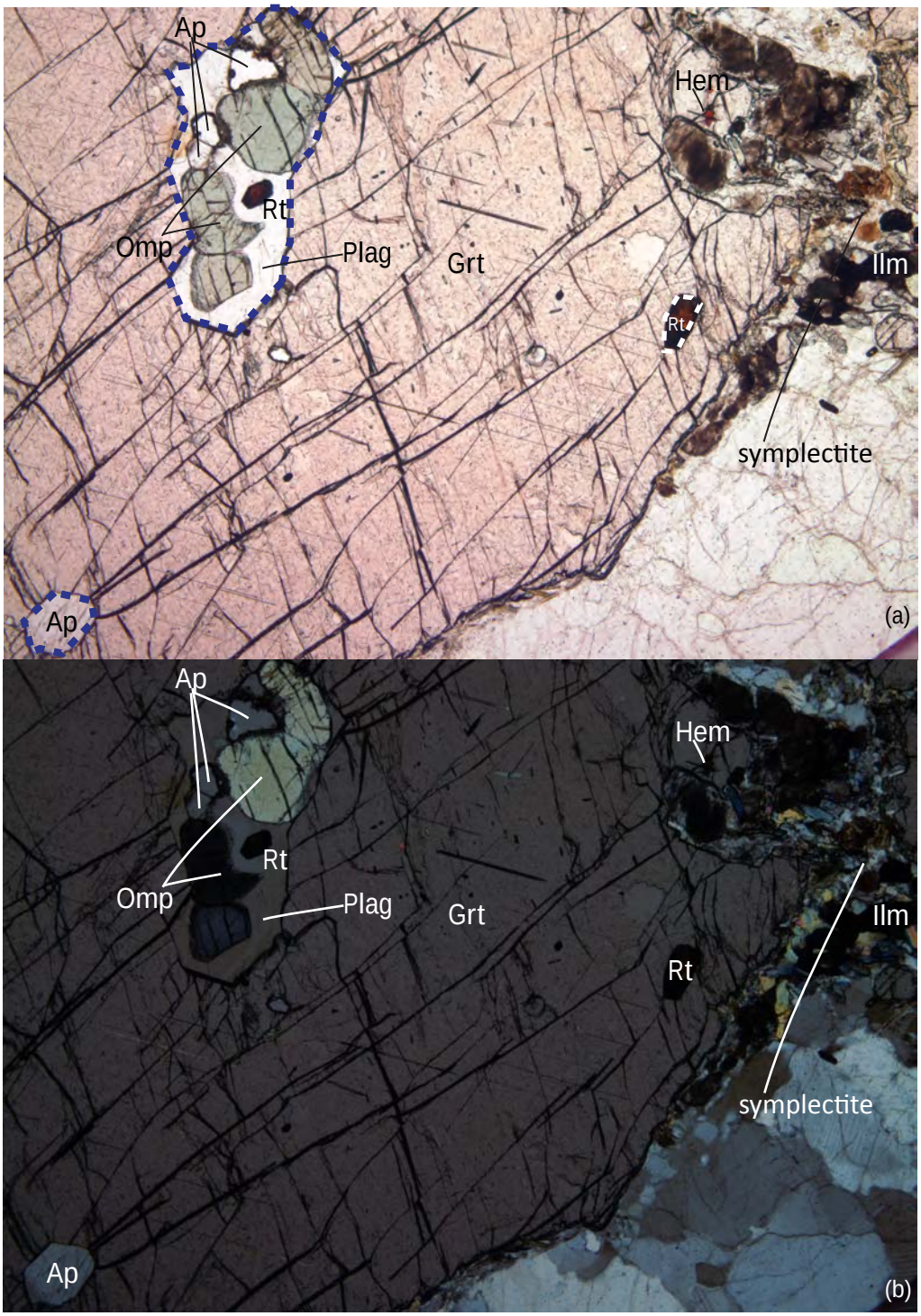

Fig 4.04 0905B (a) PPL (b) XPL Base of photo: 2.3mm - Garnet poprhyroblast; omphacite rimmed by plagioclase, apatite and rutile inclusions within garnet; hematite replacement texture and illmenite. Biotite - Plagioclase symplectite development is marked. Note the idioblastic outside edge of the main inclusion within garnet, while grain boundaries inside the inclusion are xenoblastic.

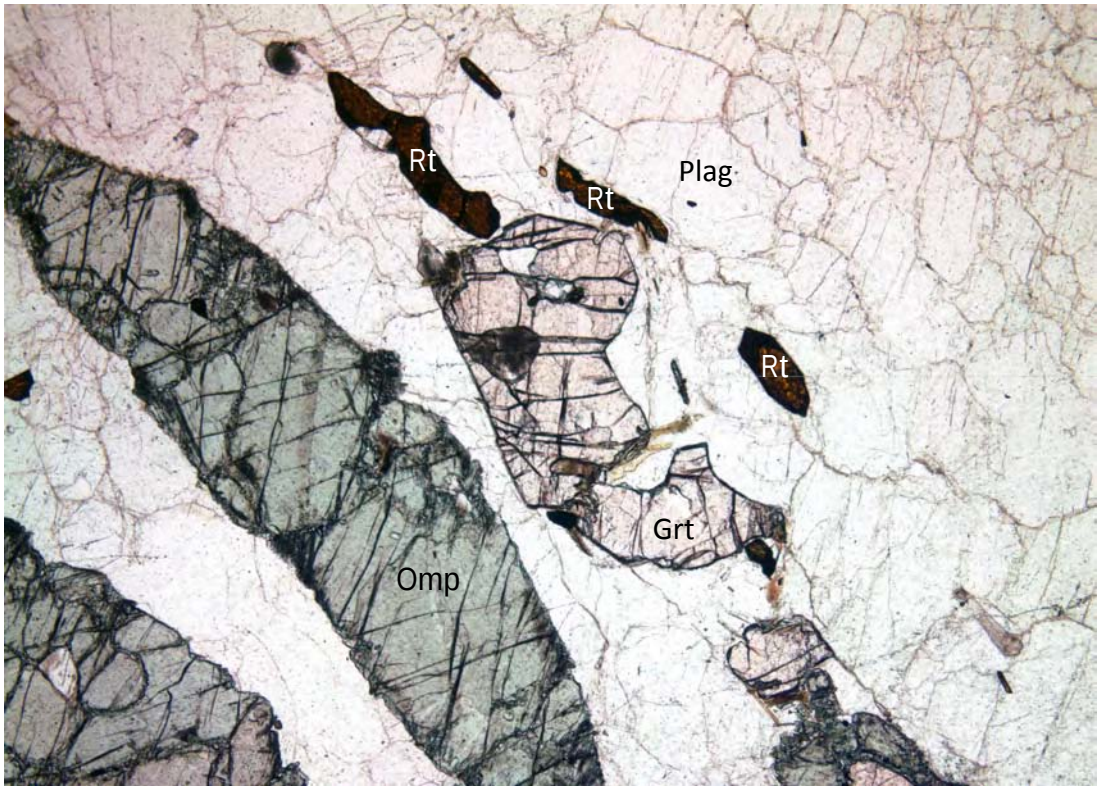

Fig 4.05 0905B (a) PPL Base of photo: 2.5mm - Rutile in association with plagioclase.

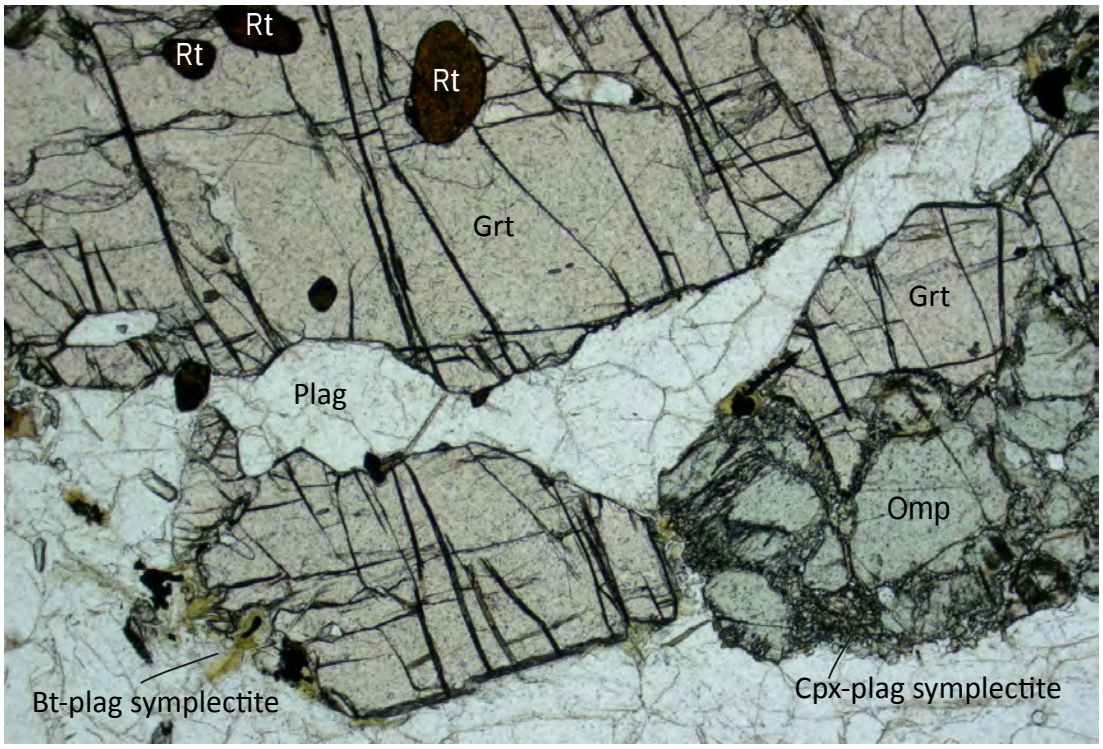

Fig 4.06 0905B (a) PPL Base of photo: 2.5mm - Rutile in association with garnet. Biotite - plagioclase and clinopyroxene - plagioclase symplectites are visible.

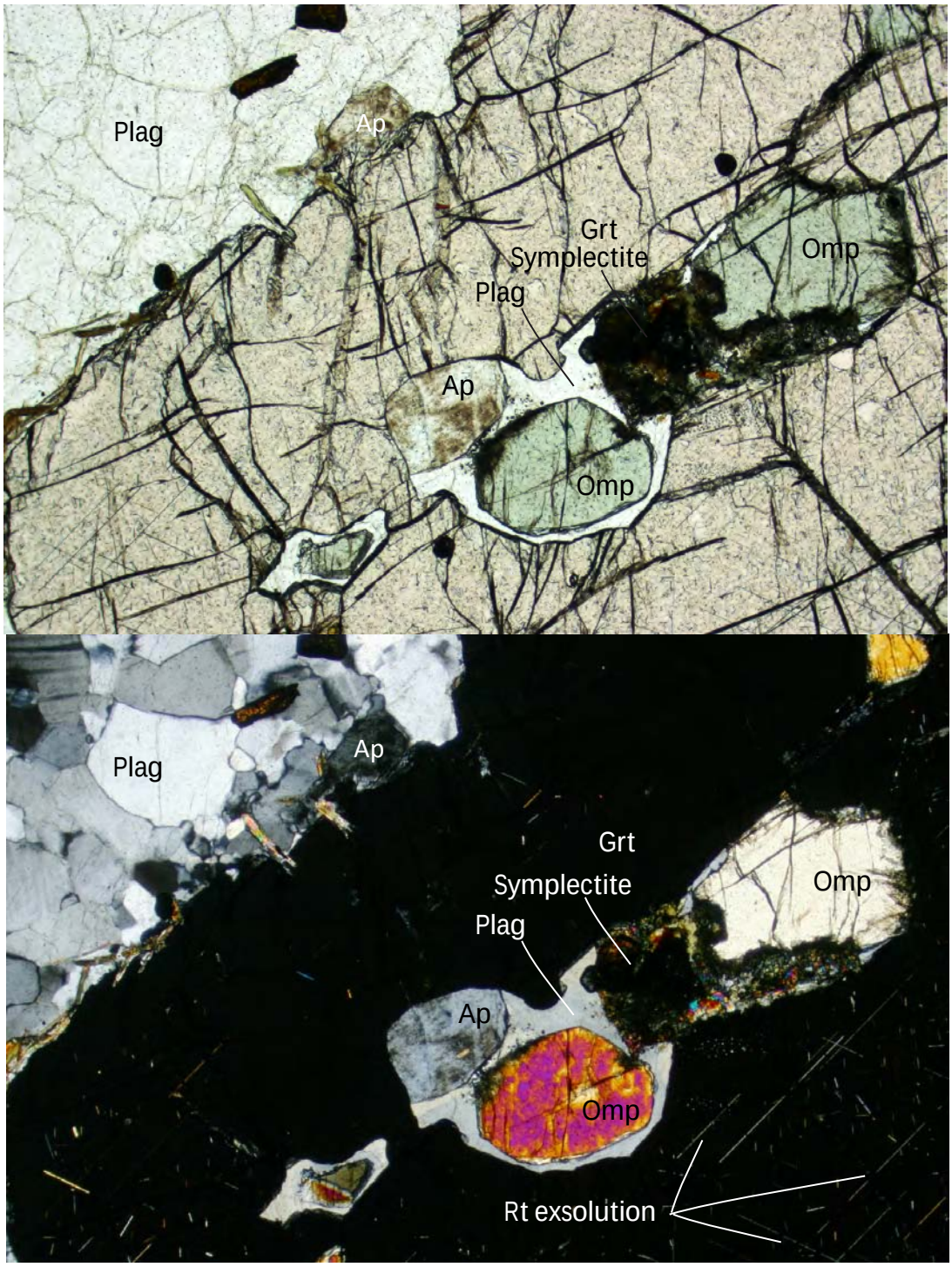

Fig 4.07 0905B (a) PPL (b) XPL Base of photo: 2.5mm - Garnet poprhyroblast; omphacite, plagioclase and apatite inclusions within garnet. Apatite can also be seen adjacent to plagioclase. Rutile exsolutions are visible in (b). Symplectite development is marked. Note the idioblastic outside edge of the main inclusion within garnet, while grain boundaries inside the inclusion are subidioblastic to xenoblastic.

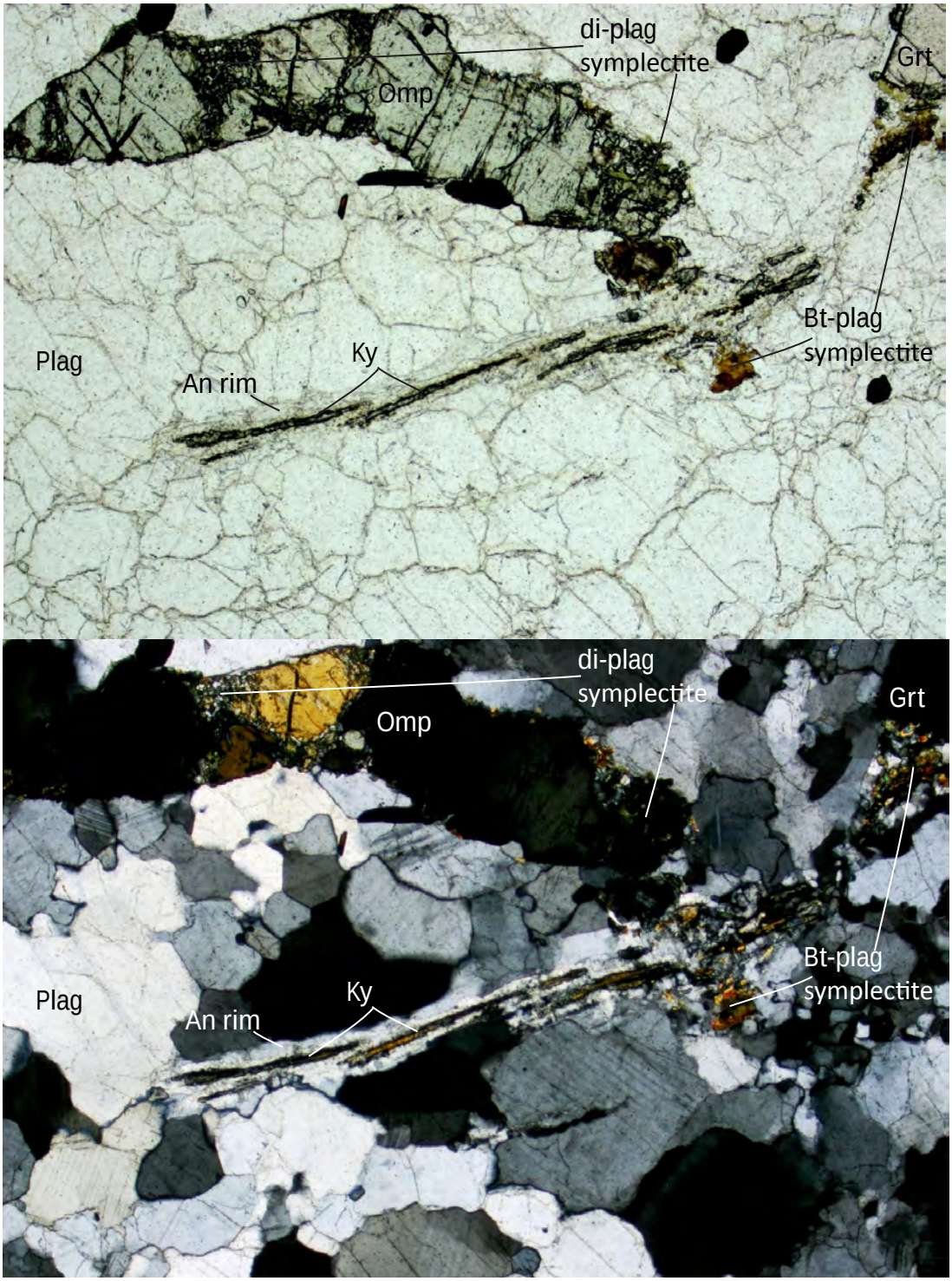

Fig 4.08 0905B (a) PPL (b) XPL Base of photo: 2.5mm - Acicular kyanite with anorthite rim (best viewed in (b)). Biotite - plagioclase and diopside- plagioclase symplectites are visible.

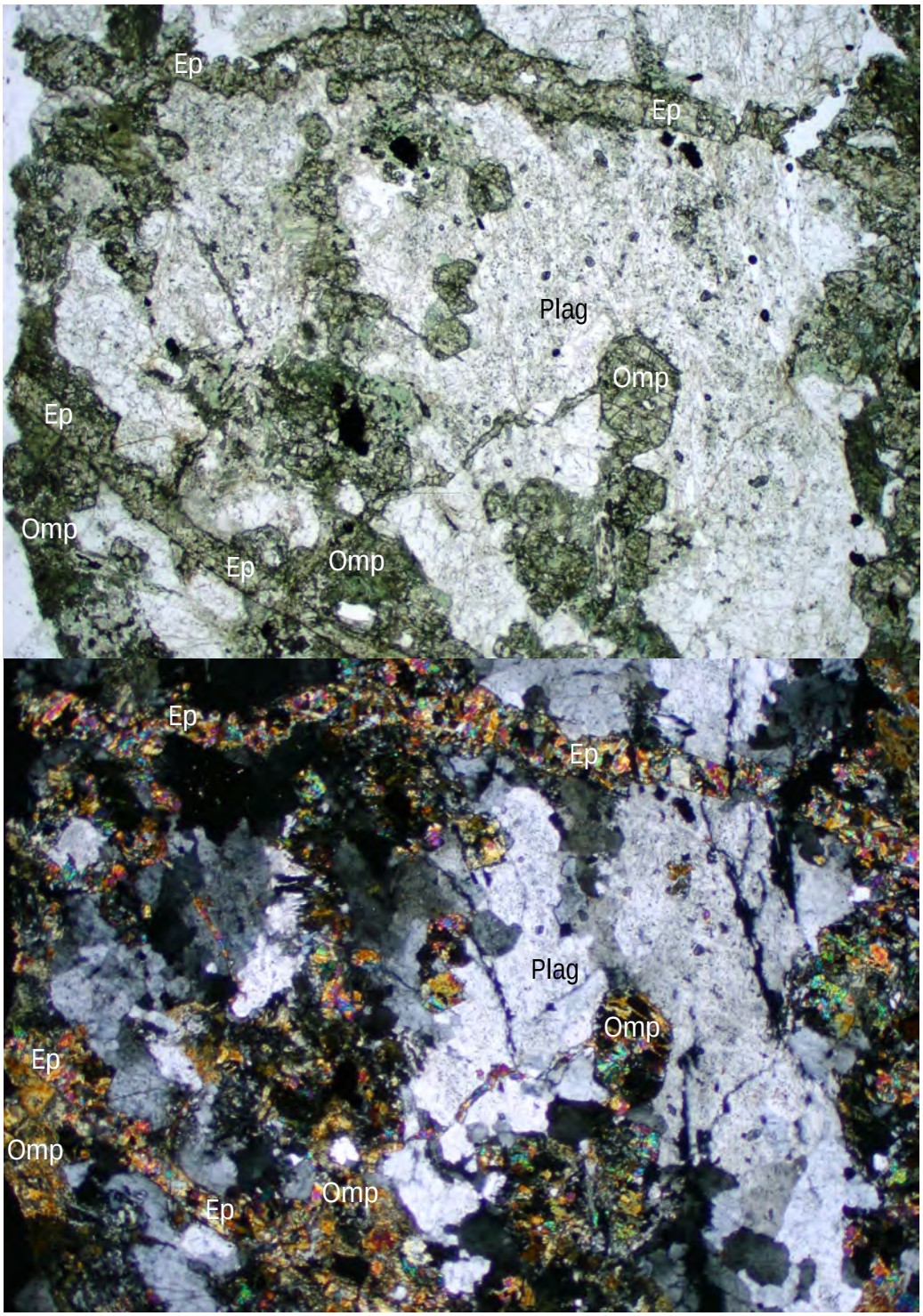

Fig 4.09 0908B (a) PPL (b) XPL Base of photo: 7mm - Epidote veins cutting across omphacite - plagioclase defined foliation.

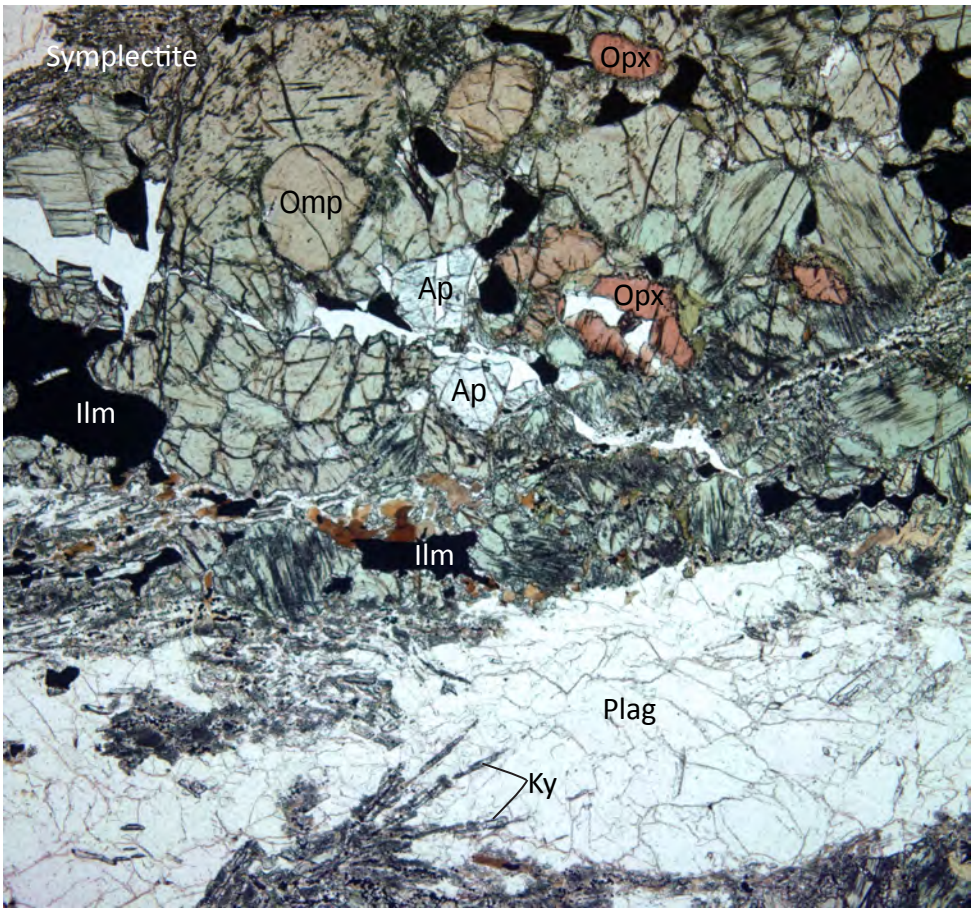

Fig 4.10 0905C (a) PPL Base of photo: 2.14mm - Two pyroxene gneiss, shown with illmenite and apatite. Minor acicular kyanite and symplectite development also visible.

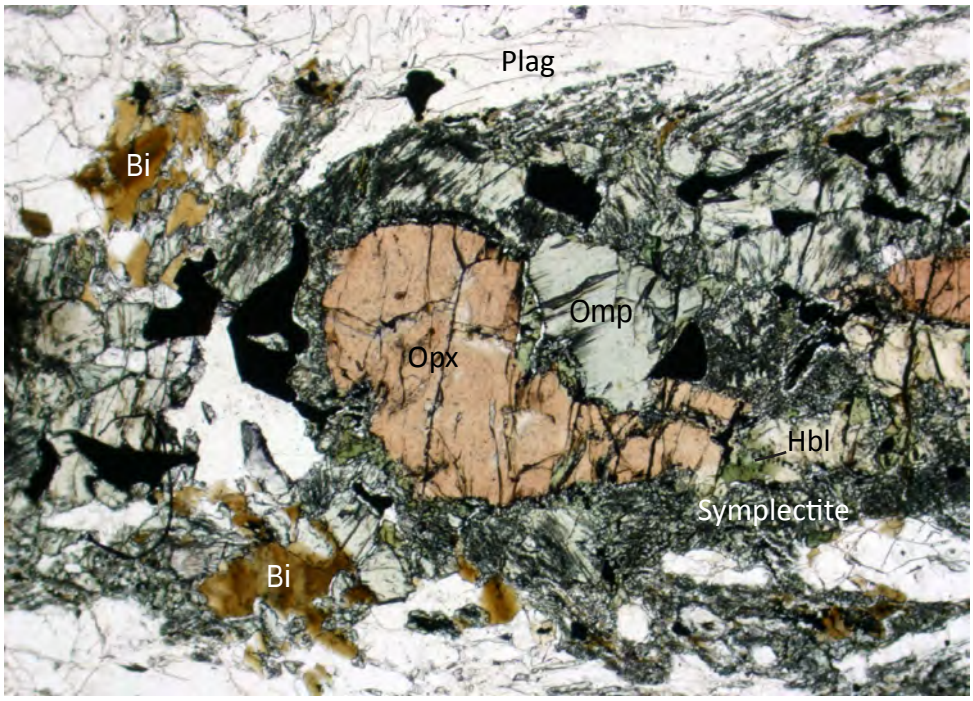

Fig 4.11 0905C (a) PPL Base of photo: 2.34mm - Biotite replacing orthopyroxene. Symplectite development and minor hornblende also visible.

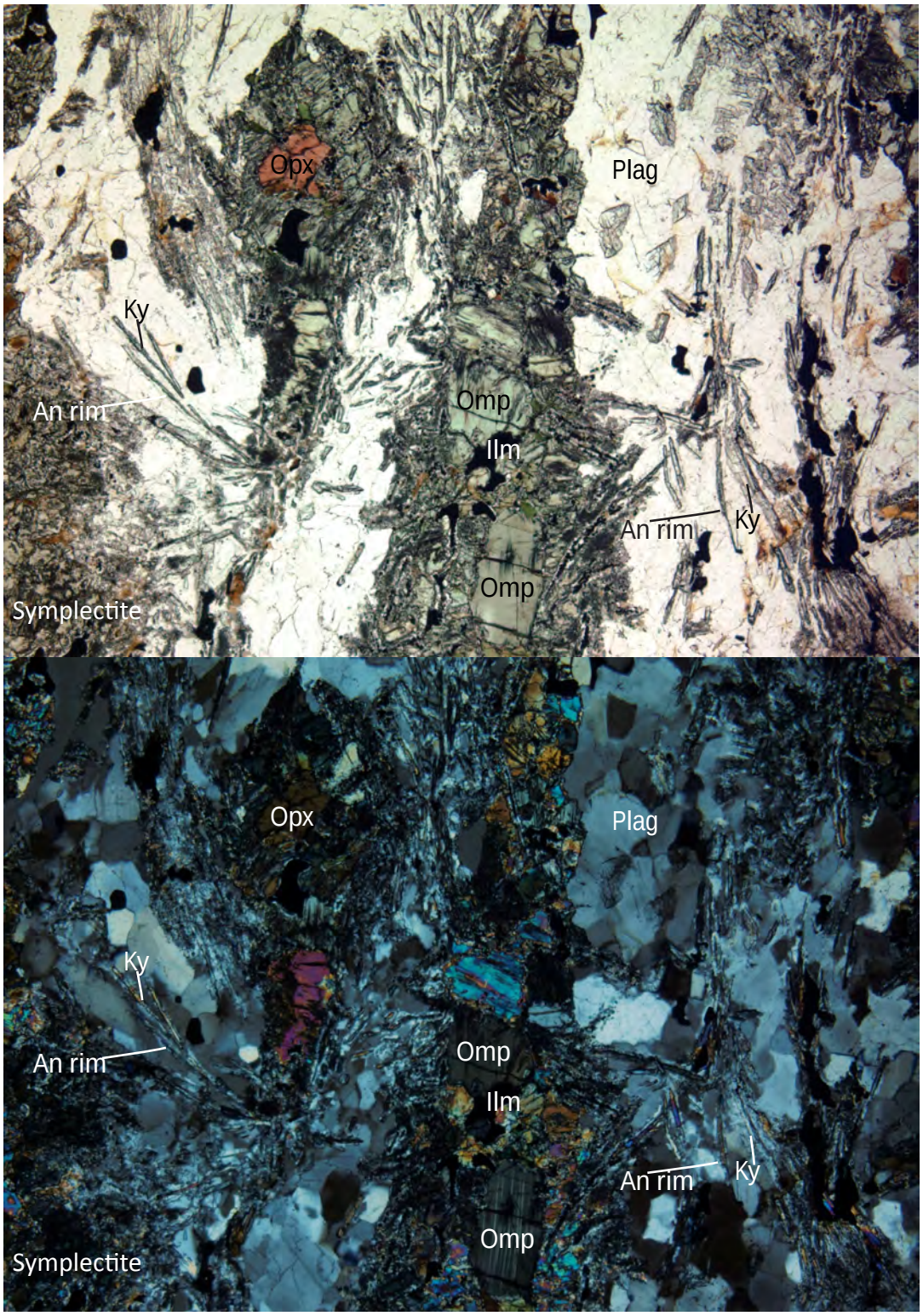

Fig 4.12 0905C (a) PPL (b) XPL Base of photo: 2.26mm - Acicular kyanite with anorthite rim. Plagioclase, omphacite, orthopyroxene, illmenite and symplectite also present.

Breaksea Eclogite

The BE is comprised of garnet (40-45%) and omphacite (50%). Accessory minerals include rutile and ilmenite as well as minor pargasite, biotite and plagioclase commonly present as symplectites. Fig. 4.13 shows a typical BE composition.

Garnet ranges in size from 0.18 – 0.84mm and forms equant xenoblastic crystals (Figs. 4.13 – 4.15). Omphacite ranges from 0.16 – 1.78mm and also forms equant xenoblastic crystals (Figs. 4.13 – 4.15); although some of the larger omphacite grains (Fig. 4.13) are elongate at approximately a 2:1 ratio.

Rutile occurs in two distinct textural settings; as idioblastic grains 0.09 – 0.26mm across that share boundaries with omphacite and garnet (Figs. 4.13 – 4.15) and as highly idioblastic inclusions within omphacite (Fig. 4.15) and garnet (Fig. 4.14) at a much finer grain size (0.02 – 0.14mm). Ilmenite is xenoblastic, with grain size 0.18 – 0.34mm and can be seen within the biotite – pargasite – plagioclase symplectite in Fig. 4.15.

Accessory minerals pargasite, biotite and plagioclase occur along some grain boundaries in the form of symplectite development; pargasite – plagioclase can be seen in Fig. 4.14 and biotite – pargasite – plagioclase can be seen in Fig. 4.15. These symplectites have a very fine grain size (<0.05mm) and will be examined in greater detail by element mapping (Chapter 6).

Like the BOG, the BE shows minor evidence for retrograde metamorphic activity marked by the presence of symplectite development at grain boundaries (Figs. 4.13 – 4.15). The textural location (i.e. grain boundary replacement) of the symplectites and hydrous nature of the minerals present suggests their formation is likely post peak metamorphic pressure and temperature. The growth of ilmenite within these areas of symplectite development suggests that it too is a later mineral growth.

Rutile however does not occur as symplectite material but rather as idioblastic inclusions in garnet and omphacite (Figs. 4.14 and 4.15) and as standalone grains adjacent to garnet and omphacite (Fig. 4.13). This indicates that rutile growth was coeval to garnet and omphacite growth.

The xenoblastic nature of the main mineral constituents' garnet and omphacite and rounded nature of inclusions suggests that the growth of these minerals has been influenced heavily by solid state adjustment during metamorphism and any primary igneous textures are no longer preserved in this rock.

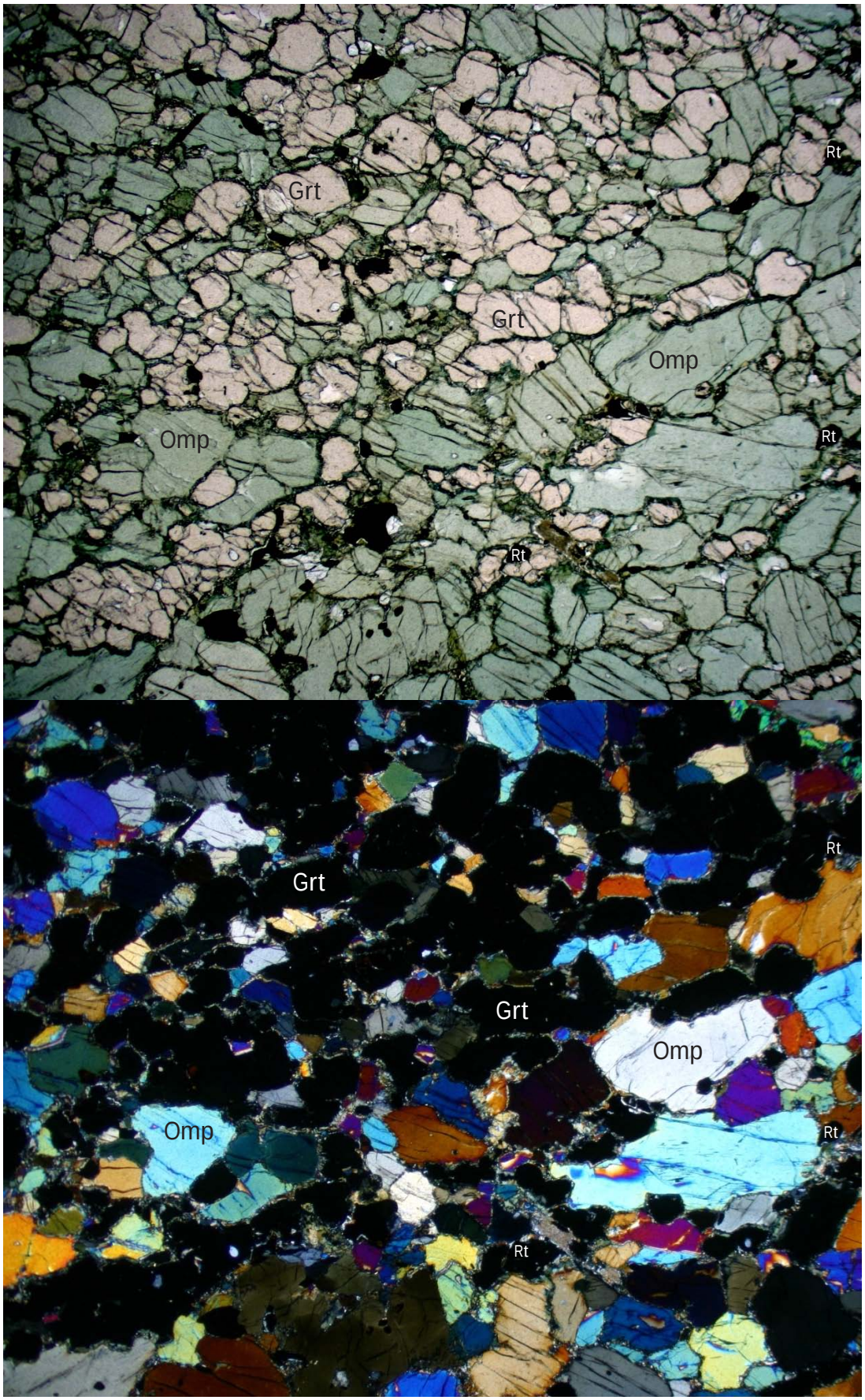

Fig 4.13 0904C (a) PPL (b) XPL Base of photo: 8.61mm - Representative micrograph of the Breaksea Eclogite. Hornblende - biotite - plagioclase symplectite development can be observed at grain boundaries. Rutile can be seen in contact with both garnet and omphacite.

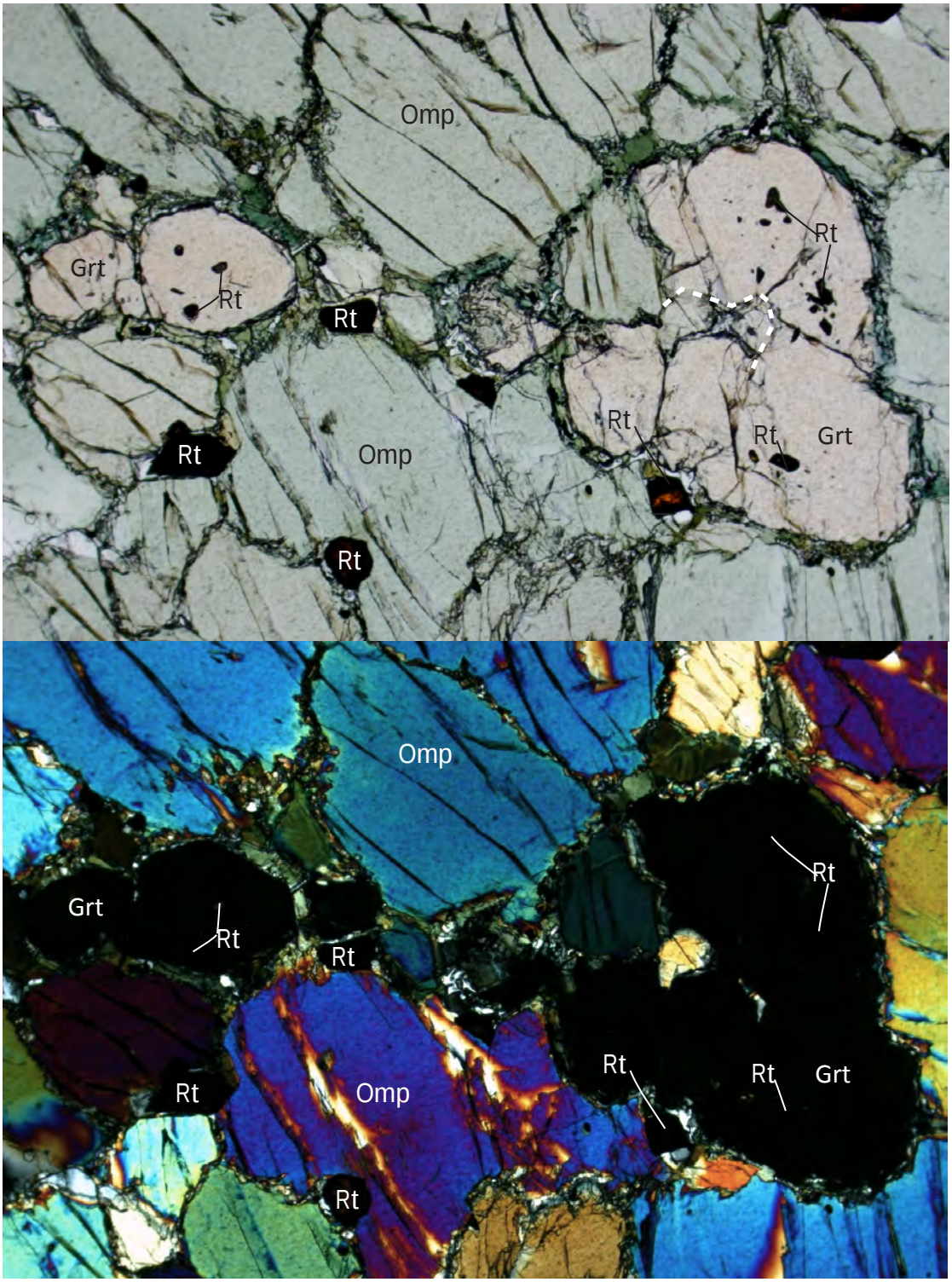

Fig 4.14 0904C (a) PPL (b) XPL Base of photo: 2.48mm - Idioblastic rutile included within garnet and next to omphacite. Minor hornblende - plagioclase symplectite development can be observed at grain boundaries. Some grain boundaries are Euhedral (marked)

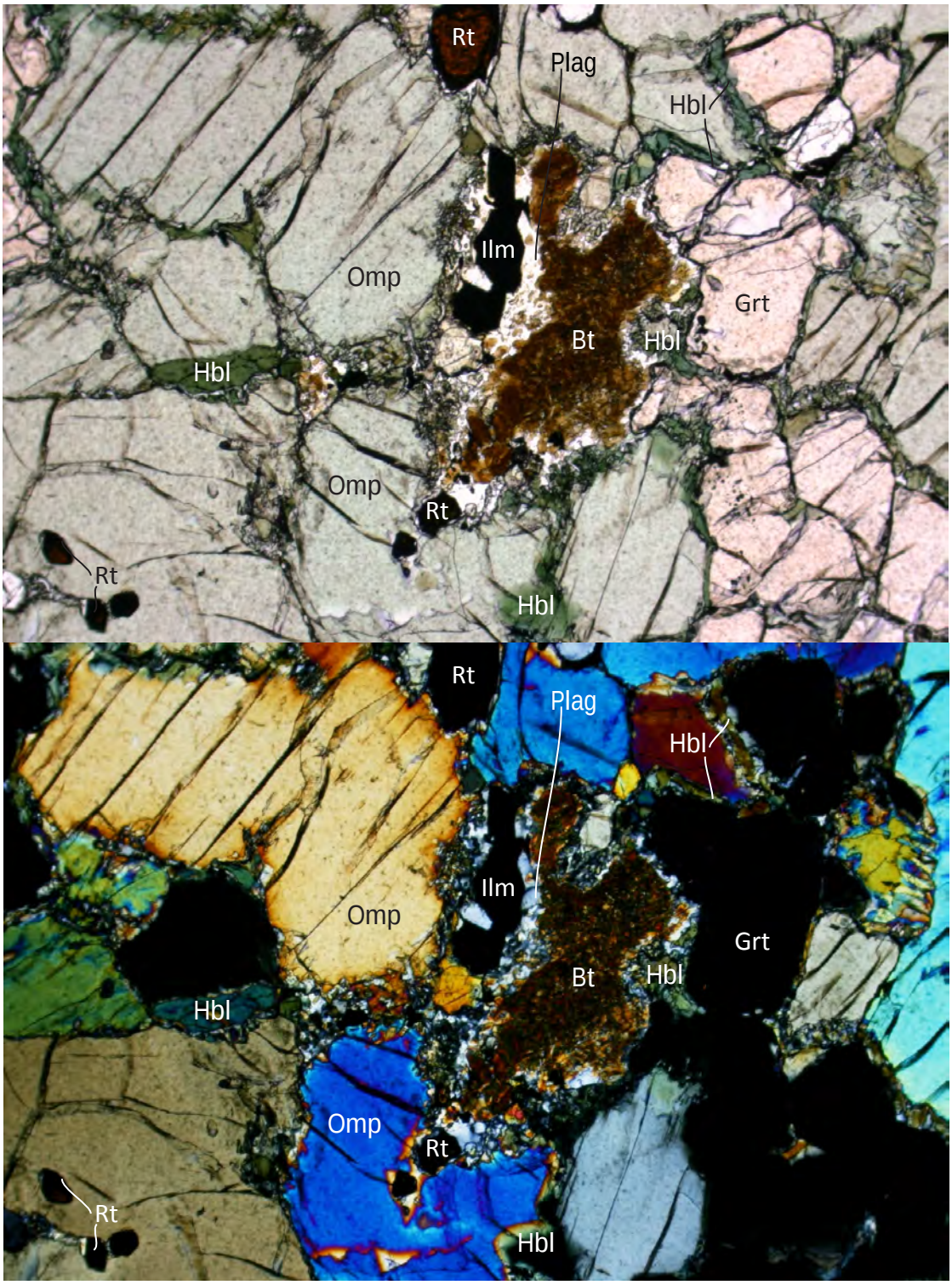

Fig 4.15 0904C (a) PPL (b) XPL Base of photo: 2.48mm - Symplectite showing Illmentite, hornblende, biotite and plagioclase. Rutile as individual grains and as inclusions within omphacite can be seen.

Interlayered Garnetite – Pyroxenite

The interlayered units of garnetite and pyroxenite will each be treated separately for rock descriptions but due to their spatial relationship (interlayering, Figs. 3.06 and 3.07) the implications of thin section examination will be discussed as a single unit.

Garnetite layers are comprised of garnet (80-85%) and diopside (15-20%) with accessory rutile and minor pargasite. There is very little symplectite development. Fig. 4.16 shows a typical garnetite layer composition.

Garnet exhibits equant crystal shapes with sub-idioblastic edges (Figs. 4.16 and 4.17). Grain size is between 0.42 – 1.70mm. Diopside ranges from 0.34 – 1.70mm and also forms equant sub-idioblastic crystals (Figs. 4.16 and 4.17).

Rutile occurs as finer grained (0.20 – 0.42mm) idioblastic grains which share boundaries with both garnet and diopside (Fig. 4.17). This implies that rutile growth was coeval to garnet and diopside growth, similar to the BE.

Pargasite measures between 0.42 – 0.85mm in length and has an 'interstitial' appearance to its growth – highly xenoblastic, it forms along grain boundaries and appears to have not been in equilibrium with clinopyroxene and garnet; leading to the inference that pargasite is present as a later, retrograde mineral replacement (Fig. 4.17). This retrograde action, in the absence of symplectites, will be examined in greater detail using element mapping (Chapter 6); should retrograde processes have affected the garnetite, it would be reasonable to expect that diopside will show a narrow zoning at its rim where mineral re-equilibration has taken place.

Garnetite layers are similar in crystal habit and size to the BE, the three deviations from BE that result in it being classified as a different rock unit are the much higher garnet modal percentage, less symplectite development and interlayering with the pyroxenite unit mentioned in chapter 3 and below.

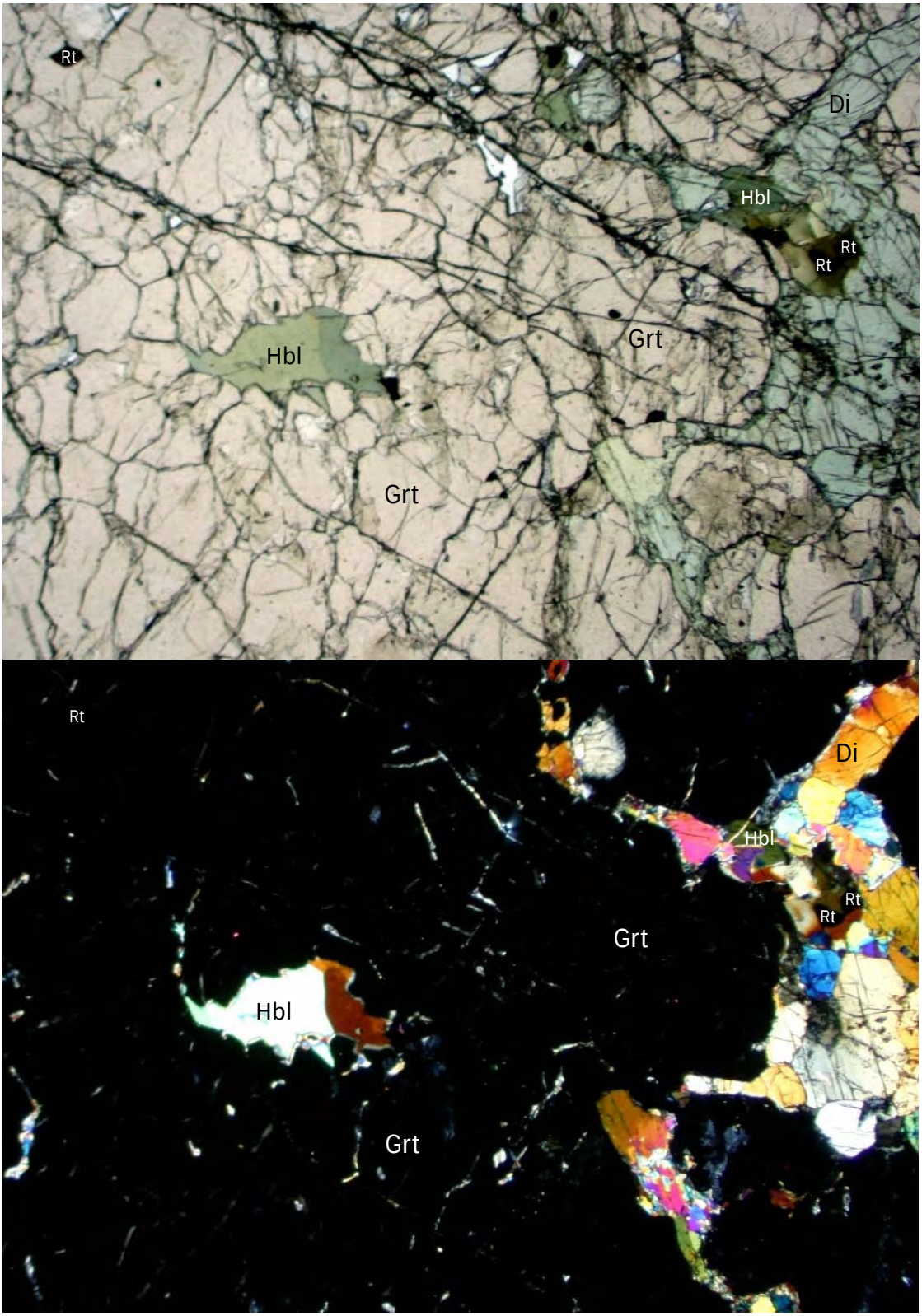

Fig 4.16 0910B (a) PPL (b) XPL Base of photo: 6.93mm - Garnetite layer, showing high modal proportion of garnet; diopside, rutile and hornblende.

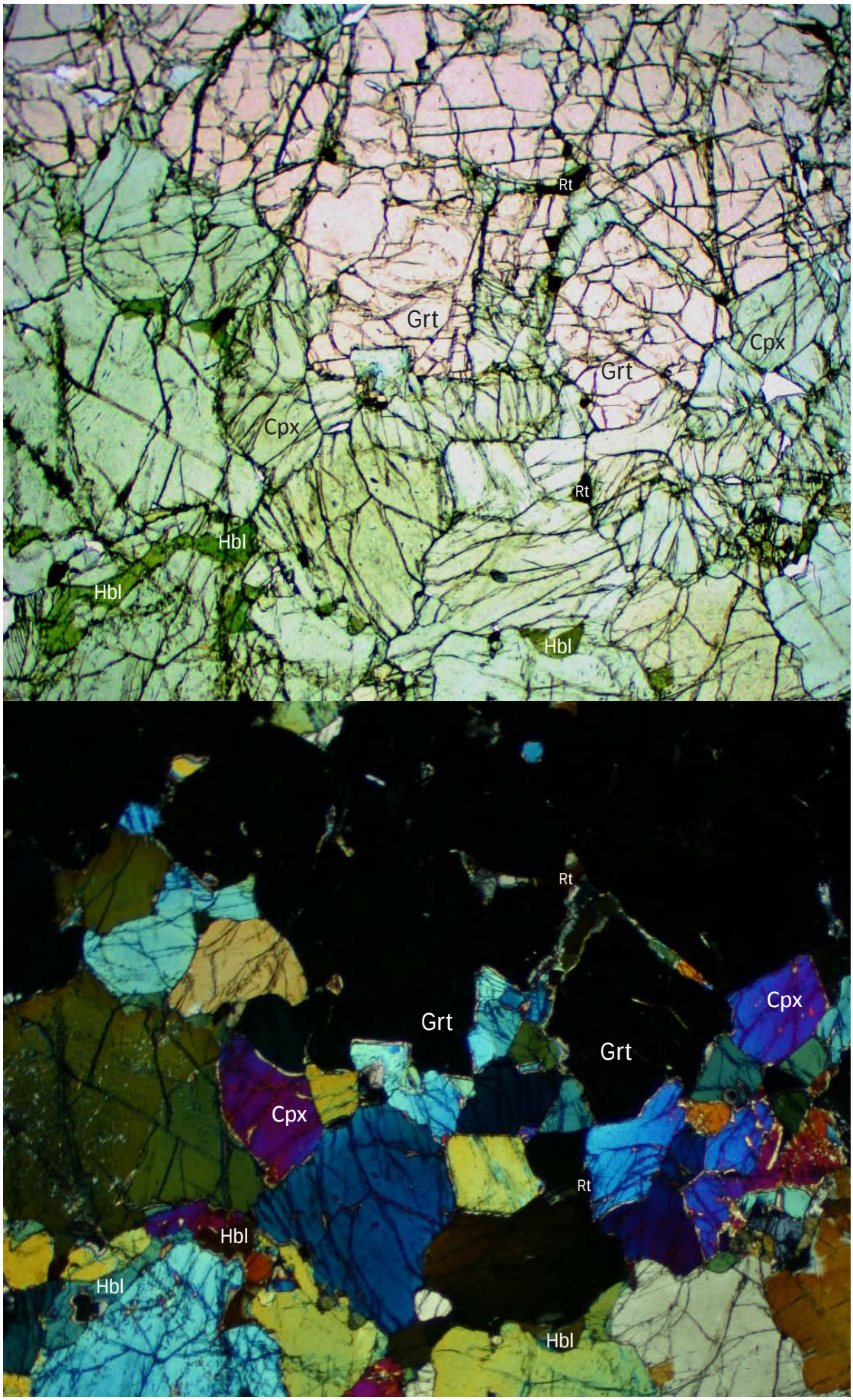

Fig 4.17 0906B (a) PPL (b) XPL Base of photo: 7.00mm - Garnet, diopside (light green), hornblende (dark green) and rutile in garnetite layer. Note that hornblende is found mostly along grain boundaries and that rutile shares boundaries with both grt and cpx.

Pyroxenite layers are comprised of 95% clinopyroxene and 5% garnet with accessory rutile with no symplectite development evident. Fig. 4.18 shows the typical pyroxenite layer composition.

Diopside is equant, with sub-idioblastic grain boundaries and ranges in size from 0.19 – 2.00mm (Figs. 4.18 and 4.19). Garnet occurs in two textural settings; as 'interstitial' material with xenoblastic grains that are commonly highly fractured measuring 0.06 – 0.12mm long (Figs. 4.18 and 4.19) and as idioblastic inclusions that are elongate at approximately a 2:1 ratio and measure between 0.06 – 0.20mm long (Figs. 4.18 and 4.19). Rutile also occurs in two different textural settings; as subhedral grains in contact with clinopyroxene (Figs. 4.18 and 4.19) measuring 0.06 – 0.10mm long and as an exsolution feature in clinopyroxene (Fig. 4.19) measuring 0.03 – 0.25mm long and oriented along three different crystallographic axes; two are perpendicular to each other and the third bisects these unequally at 30° - 60° (Fig. 4.19). Rutile exsolutions exhibit an inclined extinction, identical to that of the BOG, indicative of higher pressure formation (El Goresy et al., 2001; Withers et al., 2003; Wu et al., .2005). The subhedral nature of rutile grains suggests, similar to the garnetite, BE and BOG units already discussed, that rutile growth was coeval to that of clinopyroxene. The inclined extinction and subsequent higher pressure consequences lead to the assumption that rutile has formed in a single growth event rather than a higher pressure event (forming the sub-idioblastic grains) followed by a cooling event (forming the rutile exsolution).

The two garnet textures observed are paramount to resolving the origins of garnet in this sample i.e. whether it is a metamorphic growth (as it appears to be in the BE) or a preserved igneous texture as proposed in chapter 3 using field relationships, taking with it the implication that garnet has crystallised in an igneous system.

Garnet is seen forming at grain boundaries as fractured, xenoblastic grains (Figs. 4.18 and 4.19). This is indicative of a garnet growth phase during metamorphism or as an interstitial phase in a cumulate phase.

Garnet is also seen as euhedral inclusions within clinopyroxene grains (Figs. 4.18 and 4.19). The growth of these garnet grains is along crystallographic axes and is parallel to rutile exsolution. The major implication of this is that garnet was crystallising concurrently with clinopyroxene as opposed to a metamorphic replacement as seen at grain boundaries; rendering this a preserved igneous texture within this metamorphosed rock and adding further argument to the observation made in chapter 3 that these garnetite and pyroxenite layers are preserved primary igneous layers.

After viewing the garnetite and pyroxenite in context with spatial relationships and mineral relationships especially within the pyroxenite layer, it becomes apparent that these interlayered units are very distinct from the BE; if not in mineral composition (for garnetite) then definitely in modal percentages and inferences stemming from their microstructures; that these units retain primary igneous textures as opposed to largely metamorphic textures observed in the BE.

NB: due to the deduction that igneous textures have been retained by these units, textural terms with igneous connotations were used e.g. interstitial.

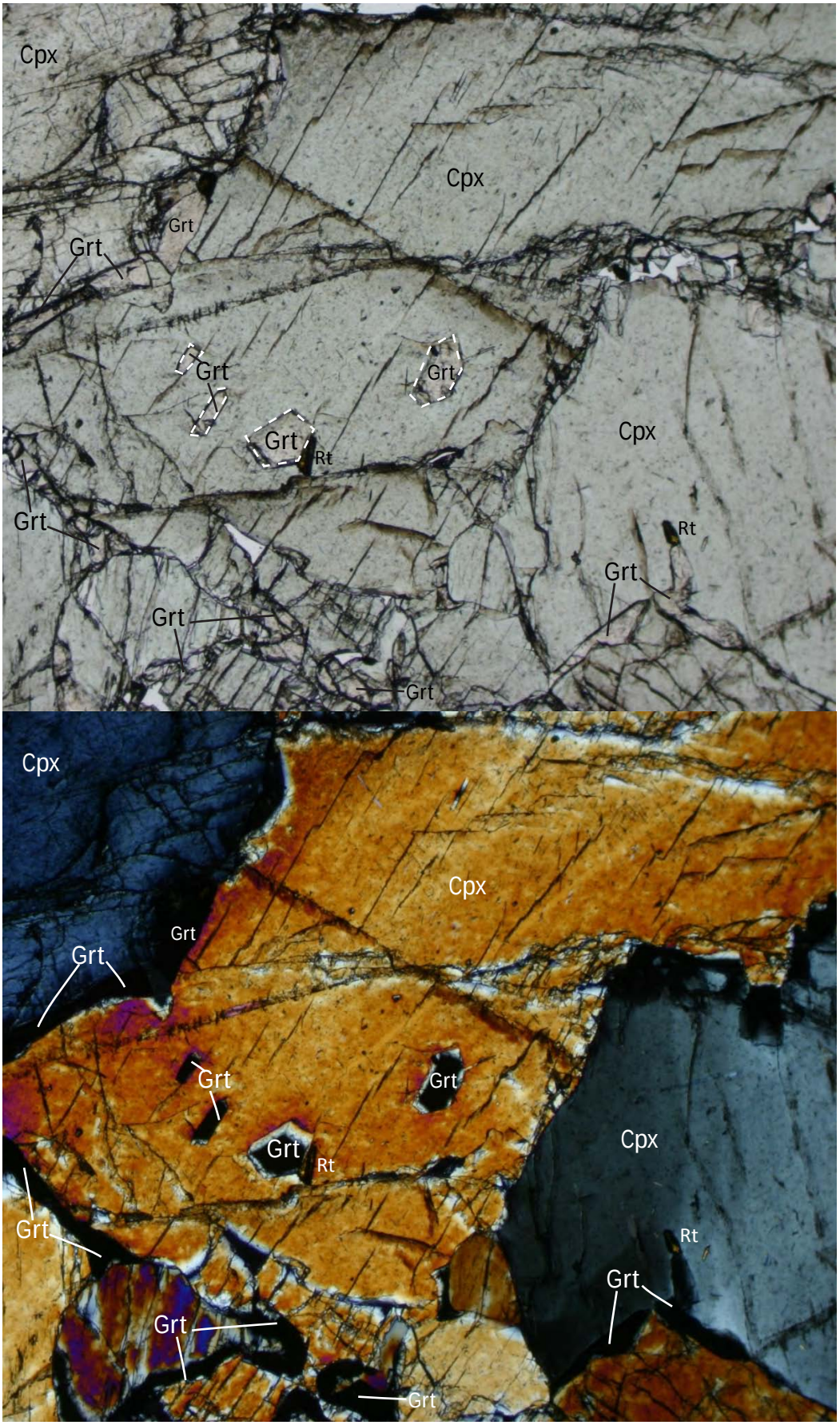

Fig 4.18 0906A (a) PPL (b) XPL Base of photo: 1.96mm - Pyroxenite layer showing two textural phases of garnet; interstitial grain boundary growth and idioblastic, crystallographically alligned inclusions in clinopyroxene. Rutile grains are also visible.

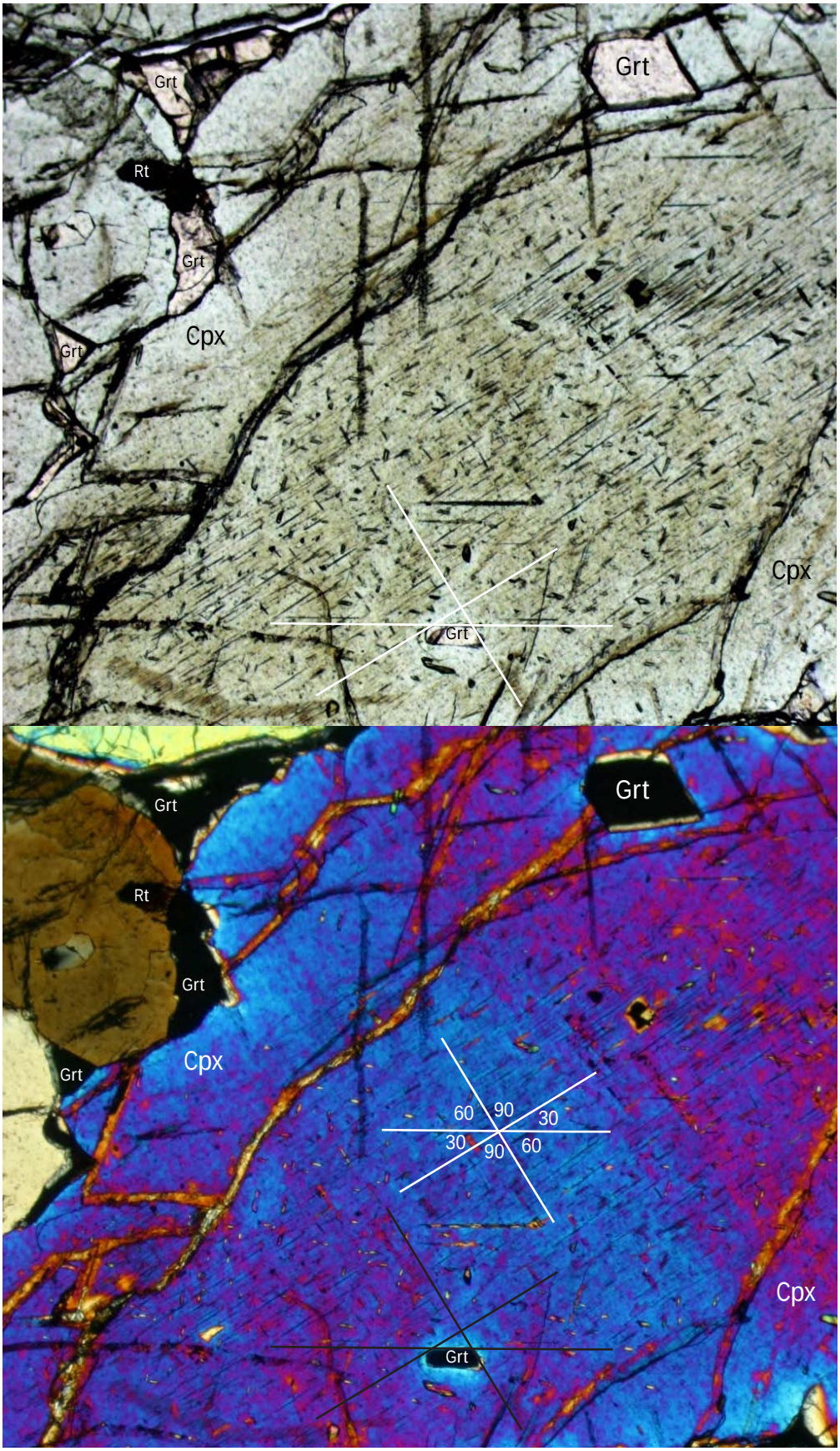

Fig 4.19 0906A (a) PPL (b) XPL Base of photo: 1.68mm - Pyroxenite layer showing two textural phases of garnet; interstitial grain boundary growth and idioblastic inclusions in clinopyroxene. Two textural phases of rutile are also shown; sub-idioblastic grains and exsolution along three different axes. Extrapolation of grt inclusion grain boundaries shows they are crystallographically aligned along identical axes to rt exsolution.

Hornblende Peridotite

Hornblende peridotite is comprised of pargasite (40%), olivine (35%), diopside (10-15%) enstatite (5%), with accessory ilmenite, spinel and garnet. Fig. 4.20 shows a typical hornblende peridotite composition.

Pargasite grainsize ranges between 0.1 – 2mm, are sub-idioblastic and show ilmenite exsolution (determined by EMP, Chapter 6) along one main crystallographic axis (Fig. 4.20). Olivine grains vary in size from 0.5 – 1.4mm and are typically sub-idioblastic. Enstatite is seen primarily in symplectite development and as such forms very small grain sizes <0.05mm and is examined further by element mapping (Chapter 6). Diopside forms grains that range in size from 0.3 – 1mm and are xenoblastic.

Ilmenite is seen in two textural settings; as an exsolution feature in pargasite and as xenoblastic mineral growths along cracks and grain boundaries, giving the appearance that it is 'interstitial', or was not in equilibrium with pargasite, olivine and orthopyroxene during growth (Fig. 4.20 and 4.21). Ilmenite exsolution measures between 0.14 – 0.93mm while interstitial ilmenite shows a range of grain sizes from 0.08 – 1.50mm. Spinel is always seen in association with interstitial ilmenite (Fig. 4.21) and forms xenoblastic grains measuring from 0.08 – 0.16mm

Garnet is seen as inclusions within pargasite, but mainly along grain boundaries (Fig. 4.21), forming xenoblastic grains, it measures between 0.1 – 0.3mm. The growth of garnet mainly along grain boundary areas suggests a metamorphic texture.

There is some symplectite development in the hornblende peridotite (Fig. 4.21) along pargasite and diopside grain boundaries, which will be further examined by element mapping (Chapter 6) along with symplectites from other rock units.

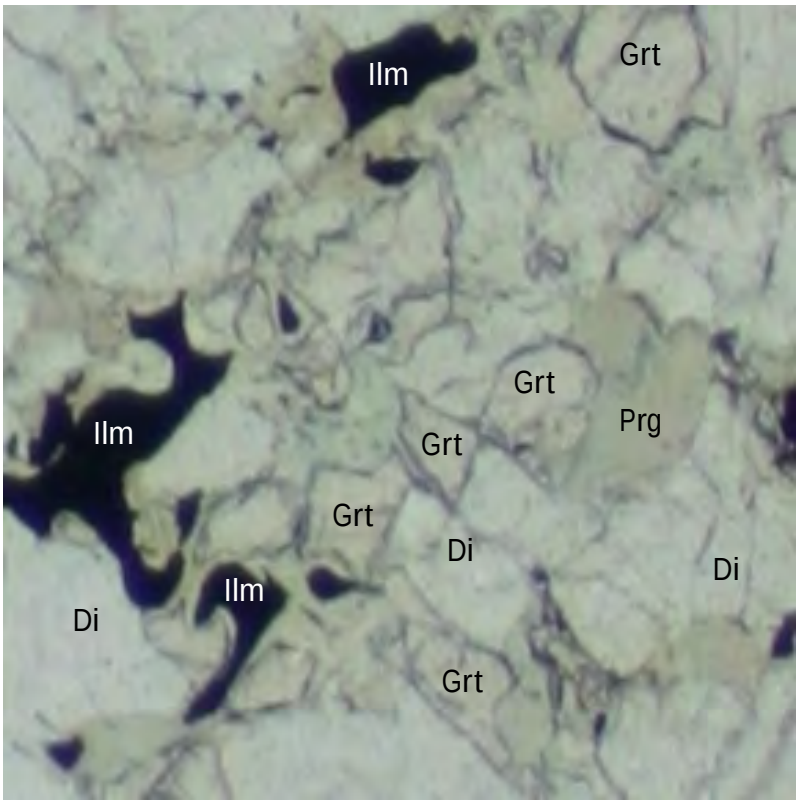

Fig 4.20 0903B (a) PPL Base of photo: 1.0.24mm - Hornblende peridotite showing pargasite, diopside, ilmenite and garnet.

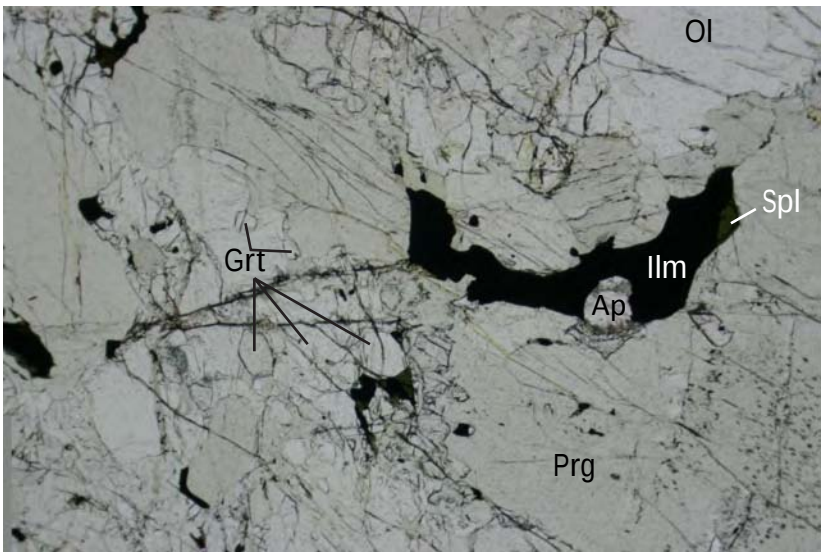

Fig 4.21 0903B (a) PPL Base of photo: 2.5mm - Hornblende peridotite showing ilmenite with spinel in association. Apatite , olivine and garnet also visible.

5. Whole Rock Geochemistry

5.1 Methods

5.1.1 Major and trace element analysis by XRF and ICP-MS

Eleven samples were analysed for major and trace elements by X-ray fluorescence (XRF). Fifteen samples were selected for trace element analyses by inductively coupled plasma mass spectrometry (ICP-MS) including five samples from this study and ten samples from previously published data of the WFO. WFO suite geochemical data is provided in Appendix 5.A.

XRF sample preparation was undertaken post fieldwork at Geological and Nuclear Science Laboratories in Dunedin, New Zealand. Selected rock samples were cut using a circular rock saw to remove weathering and altered material, ensuring the selection of representative portions. Samples were transported to SpectraChem Laboratory and crushed in a hydraulic press with tungsten carbide plates and powdered in a TEMA tungsten carbide mill. The press and mill were thoroughly cleaned with MQ water and 100% ethanol between samples. ICP-MS powders were derived through identical processes (five samples used rock powders prepared at GNS Labs), with ten powers being provided by Matthew De Paoli (The University of Sydney), having had XRF analyses run in years prior by identical laboratories (see below).

Further preparation from fine rock powder to an analysis ready sample is detailed in the specific analysis technique methodology below.

XRF analyses were conducted in Wellington, New Zealand at the SpectraChem Laboratory using a Siemens SRS 3000 sequential XRF spectrometer, to ensure parity with other WFO data analyses conducted at the same laboratory. For major element analysis a glass disc was prepared using; 1.50g borate glass, 0.2g sodium nitrate and 0.28g sample material giving a sample/flux ratio of 1:5.42 heated to 1100°C. For

trace element analysis a pressed pellet comprising 10% w/ w wax with boric acid backing was used. See Norrish & Hutton (1969) for full details of sample preparation. Lower limits of detection are given in Table 5.01. Loss on ignition (LOI) was determined by heating the samples to 1000°C for one hour and is given in Table 5.02.

Major Element	wt % oxide	Trace Element	ppm
SiO_2	0.01	Sc	2
TiO_2	0.01	V	1
Al_2O_3	0.01	Cr	1
Fe_2O_3	0.01	Ni	1
MnO	0.01	Cu	1
MgO	0.01	Zn	1
CaO	0.01	Ga	1
Na_2O	0.01	As	1
K_2O	0.01	Rb	1
P_2O_5	0.01	Sr	1
		Y	1
		Zr	1
		Nb	1
		Ba	5
		La	5
		Ce	5
		Pb	1
		Th	1
		U	1

Table 5.01 Lower Limits of Detection (LLD) for major and trace elements analysed by XRF.

Sample	LOI (wt% oxide)
0902D	0.10
0903A	-0.30
0904C	-0.25
0907	0.07
0906A	0.04
0906B	-0.46
0910C	0.25
0910B	-0.53
0901A	0.06
0901C	0.02
0902A	0.10

Table 5.02 LOI for 11 samples analysed by XRF

Trace element analysis using ICP-MS were conducted in the Geochemical Analysis Unit (GAU) located in the Australian Research Council (ARC) National Key Centre for Geochemical Evolution and Metallogeny of Continents (GEMOC), based in the Department of Earth and Planetary Sciences at Macquarie University, Sydney, using an Agilent 7500cs ICP-MS.

Samples were weighed to ~0.1g and digested in Teflon bombs using HNO_3 (2mL; Ajax) and HF (2mL; Merck suprapur grade) by Peter Wieland (GAU) and James Watton, dried down, ultrasonicated and redigested before being diluted with HNO_3 ready for analysis.

Operating conditions are listed in Table 5.03. Analyses were run by Justin Payne (GAU).

Variable	Parameter
IC-MPS type	Octopole Reaction System
Make & Model	Agilent 7500cs
Nebuliser type	Self aspirating concentric
Make & Model	Agilent micro flow
Nebuliser Gas	Ar
Nebuliser gas flow rate	100mL/min
Nebuliser pump	0.1 rps
RF power	1550W
RF matching	1.66V
Sample depth	5.5 - 7mm
Torch H	-0.2mm
Torch V	0.5mm
Carrier Gas	Ar
Carrier gas flow rate	1.13 L/min
Collision cell gas	He
Make up gas flow rate	0.23 L/min
External standard	BCR-2A
Reference samples (for accuracy)	BHVO-2 BIR-1
Internal standard	15µL spike of Li, As, Rh, In, Tm, Bi in 2% HNO_3
Count time	3 x 70s repetition

Dwell time	300ms
Lower Limits of Detection	$<10^{-3}$

Table 5.03 ICP-MS operating conditions

Analyses were conducted in one run of eight samples and one run of seven samples, using the following run and measurement order, once for samples at 1/1000 dilution and once for samples at 1/5000 dilution;

1. 2% HNO_3 rinse x3.
2. Internal standard.
3. Method blank.
4. 2% HNO_3 rinse.
5. BCR-2 in 1/1000, 1/2000 and 1/5000 dilutions (First Group Table 5.05).
6. 2% HNO_3 rinse.
7. BIR-1 in 1/1000, 1/2000 and 1/5000 dilutions.
8. 2% HNO_3 rinse x2.
9. BHVO-2 in 1/1000, 1/2000 and 1/5000 dilutions.
10. 2% HNO_3 rinse x3.
11. Samples x8 (1x each sample).
12. 2% HNO_3 rinse x2.
13. BCR-2 in 1/1000, 1/2000 and 1/5000 dilutions (Second Group Table 5.05).
14. 2% HNO_3 rinse.
15. BIR-1 in 1/1000 dilution.
16. 2% HNO_3 rinse x2.
17. BHVO-2 in 1/1000 dilution.
18. 2% HNO_3 rinse x3.
19. Samples x7 (1x each sample).
20. 2% HNO_3 rinse x2.
21. BCR-2 in 1/1000, 1/2000 and 1/5000 dilutions (Third Group Table 5.05).
22. 2% HNO_3 rinse.
23. BIR-1 in 1/1000, 1/2000 and 1/5000 dilutions.
24. 2% HNO_3 rinse x2.
25. BHVO-2 in 1/1000, 1/2000 and 1/5000 dilutions.
26. 2% HNO_3 rinse.

The initial 2% HNO_3 rinse is measured three times and averaged as a background reading. The running of a method blank ensures zero contamination in sample preparation chemistry and as a measure of precision. The internal standard is

measured individually and added to all samples to apply drift and matrix affect corrections. Data is corrected to BCR-2 to measure instrument sensitivity and drift. BHVO-2 and BIR-1 reference samples are used for accuracy to real values and reproducibility of results.

Tungsten readings are omitted from results as a tungsten mill was used in sample crushing. Zirconium values are taken from XRF as zircon is difficult to dissolve fully. Arsenic is taken from XRF and lithium, rhodium, indium, thulium and bismuth are omitted due to their use in the internal standard solution.

Measured and expected concentrations for reference materials BHVO-2 and BIR-1 are shown in Table 5.04, BCR-2 variation over time from expected results are shown in Table 5.05.

Element	BHVO-2 expected conc. (ppm)	2σ (ppm)	BHVO-2 measured conc. (ppm) Ave (n=7)	2σ (ppm)	BIR-1 expected conc. (ppm)	2σ (ppm)	BIR-1 measured conc. (ppm) Ave (n=7)	2σ (ppm)
Li	4.8	0.4	4.16	0.56	3.2	0.4	3.2	0.38
Be	1	0.2	1.34	0.31	0.12	0.02	0.15	0.04
Sc	32	2	35	3.25	43	4	48.8	1.93
Ti	16300	4000	17440	984	5600	1000	6340	107
V	317	22	321	20.9	319	36	338	5.52
Cr	280	38	280	15.8	391	30	305	11.9
Mn	1317	77	1365	92.0	1394	124	1453	34.0
Co	45	6	45	3.20	52	6	55.8	1.18
Ni	119	14	132	10.4	166	14	202	6.99
Cu	127	14	172	11.0	119	16	167	5.62
Zn	103	12	100	13.1	72	36	74.9	11.8
Ga	21.7	1.8	20.9	1.07	15.3	1.6	15.8	0.531
Rb	9.8	2.0	9.0	0.25	0.2	0.02	0.19	0.015
Sr	389	46	390	22.6	109	4	109	8.66
Y	26	4	28	1.50	15.6	1.8	17.0	1.09
Zr	172	22	179	5.16	14	0.2	15.0	0.431
Nb	18.1	2	19.1	1.05	0.55	0.1	0.54	0.022
Mo	4	0.4	4	0.093	0.07		0.08	0.007
Cd	0.06	0.012	0.08	0.023	0.097		0.07	0.033
Cs	0.1	0.02	0.1	0.013	0.007	0.006	0.01	0.001
Ba	130	26	135	19.7	7.14		6.14	0.420

La	15	2	16	2.29	0.615	0.042	0.58	0.036
Ce	38	4	39	5.56	1.92	0.16	1.75	0.142
Pr	5.35	0.34	5.45	0.727	0.37	0.04	0.36	0.026
Nd	25	3.6	25	3.36	2.38	0.02	2.26	0.167
Sm	6.2	0.8	6.3	0.814	1.12	0.04	1.06	0.079
Eu	2.07	0.04	2.10	0.254	0.53		0.49	0.038
Tb	0.9	0.06	1.0	0.123	0.36	0.06	0.34	0.031
Gd	6.3	0.4	6.3	0.864	1.87	0.08	1.84	0.169
Dy	5.31	0.04	5.39	0.689	2.51		2.40	0.214
Ho	1.04	0.08	1.03	0.134	0.56	0.1	0.55	0.050
Er	2.54	0.02	2.63	0.328	1.66		1.62	0.156
Yb	0.28	0.02	0.28	0.037	1.65		1.53	0.164
Lu	4.1	0.6	4.5	0.583	0.25	0.04	0.23	0.024
Hf	1.4	0.12	1.2	0.156	0.582	0.008	0.53	0.057
Ta	0.21	0.22	2.03	33.1	0.0357	0.0008	0.04	0.006
Pb	1.6	0.6	1.6	0.243	3.1	0.6	2.74	0.392
Th	1.2	0.6	1.3	0.233	0.032	0.008	0.03	0.007
U	0.403	0.002	0.440	0.085	0.01	0.002	0.01	0.003
$^{87}Sr/^{86}Sr$ (n=2)	0.703487	19	0.703467	8				
$^{143}Nd/^{144}Nd$ (n=1)	0.512981	10	0.512974	6				

Table 5.04 Expected and measured concentrations and errors for BHVO-2 and BIR-1 reference materials. Isotope 2σ error is $x10^{-6}$

USGS values; BHVO-2 (Wilson, 1997; Gao et al., 2002; Weis et al., 2005); BIR-1 (Flanagan, 1984; Gladney & Roelands, 1988; Govindaraju, 1994). Also available at GeoRem database

Element	BCR-2 calib. value	First Group ave	% Relative deviation	Second Group ave	% Relative deviation	Third Group ave	% Relative deviation
Li	7.9	9.0	1.14	8.7	1.11	7.9	1.00
Be	2.66	3.14	1.18	2.96	1.11	2.44	0.92
Sc	33.86	33.83	1.00	35.46	1.05	33.53	0.99
Ti	13595.45	13798.31	1.01	14075.25	1.04	13550.62	1.00
V	396.47	407.55	1.03	411.82	1.04	391.68	0.99
Cr	16.69	17.25	1.03	17.89	1.07	16.32	0.98
Mn	1520	1528	1.01	1570	1.03	1475	0.97
Co	36.45	37.54	1.03	37.64	1.03	34.69	0.95
Ni	13.46	14.28	1.06	14.25	1.06	13.23	0.98
Cu	27.23	27.53	1.01	28.10	1.03	27.59	1.01
Zn	125.43	136.43	1.09	134.14	1.07	125.54	1.00
Ga	21.15	21.26	1.01	21.49	1.02	20.52	0.97
Rb	46.42	45.28	0.98	46.58	1.00	45.98	0.99
Sr	329.13	322.18	0.98	331.15	1.01	322.66	0.98
Y	38	38	1.00	38	1.00	38	0.99
Zr	192.39	193.93	1.01	195.84	1.02	189.92	0.99
Nb	12.64	11.96	0.95	12.32	0.97	12.64	1.00
Mo	251.74	248.90	0.99	251.67	1.00	253.57	1.01
Cd	0.38	0.39	1.02	0.37	0.96	0.37	1.00
Sn	2.69	2.99	1.11	2.61	0.97	2.76	1.28
Sb	0.28	0.28	0.99	0.27	0.98	0.29	1.02
Cs	1.19	1.14	0.95	1.17	0.98	1.28	1.03
Ba	658.68	636.42	0.97	652.17	0.99	717.06	1.07
La	24.76	23.73	0.96	24.29	0.98	27.02	1.09
Ce	51.73	50.57	0.98	51.28	0.99	55.86	1.09
Pr	6.83	6.45	0.94	6.60	0.97	7.39	1.08
Nd	28.32	27.05	0.96	27.6	0.98	30.7	1.08
Sm	6.59	6.29	0.95	6.43	0.98	7.13	1.08
Eu	2.04	1.94	0.95	1.98	0.97	2.23	1.08
Gd	6.8	6.45	0.95	6.6	0.97	7.6	1.09
Tb	1.07	1.02	0.95	1.04	0.97	1.18	1.11
Dy	6.28	6.01	0.96	6.10	0.97	6.95	1.11
Ho	1.31	1.26	0.96	1.27	0.97	1.45	1.11
Er	3.66	3.52	0.96	3.56	0.97	4.07	1.11
Yb	3.28	3.12	0.95	3.21	0.98	3.71	1.13
Lu	0.49	0.47	0.96	0.48	0.98	0.55	1.12
Hf	4.76	4.54	0.95	4.63	0.97	5.38	1.13
Ta	0.75	0.71	0.95	0.73	0.97	0.85	1.13
W	0.94	0.77	0.81	0.87	0.92	1.05	1.14
Pb	10.32	9.84	0.95	10.21	0.99	12.23	1.11
Th	6.1	5.6	0.92	6.0	0.98	7.6	1.25
U	1.67	1.53	0.91	1.64	0.98	2.08	1.25

Table 5.05 BCR-2 Calibration value and Drift throughout run

5.1.2 Whole rock isotope ratio analysis by TIMS

The same fifteen samples were analysed for Sr and Nd isotope ratios, with analysis being conducted in the Geochemical Analysis Unit (GAU) located in the Australian Research Council (ARC) National Key Centre for Geochemical Evolution and Metallogeny of Continents (GEMOC), based in the Department of Earth and Planetary Sciences at Macquarie University, Sydney, using a Thermo Finnigan Triton Thermal Ionisation Mass Spectrometer (TIMS). Sample preparation and analyses were conducted by Peter Wieland (GAU) and James Watton.

Samples were digested by the same initial process used for ICP-MS (i.e. Teflon bomb HNO_3 and HF mix), dried, mixed with $HClO_4$, HCl (6N) and H_2O_2. The samples were re-dissolved in HCl (6N), dried, had HCL and HF added and were centrifuged in Teflon vials. The samples were then eluted through chromatographic columns containing a wet powder resin by way of HCl addition in known quantities as outlined in Pin & Bassin (1992) to remove Sr. The remaining sample was eluted through a second LN.Spec column to remove Nd as outline in Pin et al., (1997).

Both the Sr and Nd separates were then dried down once more and loaded onto rhenium wire filaments. This was done by redissolving the separates, heating the filament with ~2A of current, adding and drying 1µL of an activator solution, 1µL of separate and another 1µL of activator solution using variations and procedures outlined in the Thermo FInnigan TIMS operational handbook.

For Sr, samples produced between 1.5 – 6 volts of signal at single filament temperatures between 1390 – 1460°C produced by currents of ~2700mA (evaporation). For Nd, samples produced between 2 – 10 volts of signal at double filament currents of 4500mA (ionisation) and 1200 – 1800mA (evaporation). Samples were heated at slower rates approaching known optimum currents to avoid flooding detector cups.

BHVO-2 and SRM (Sr) and JMC (Nd) standards were also run. BHVO-2 expected and measured isotope ratios are shown in Table 5.04.

Corrections to data were automatically applied by the TIMS software to account for isobaric interference between Rb/Sr and Sm/Nd.

Error for all samples measured for Sr showed an absolute standard error <10^{-5} for $^{87}Sr/^{86}Sr$ and for Nd showed an absolute standard error <10^{-5} for $^{143}Nd/^{144}Nd$ (I.e. errors were always 0.000009 or better). Samples which did not show constant or strong signal for the entire run method (200 readings) were re-run (if enough sample remained on the filament and filament was undamaged) or were re loaded and run at subsequent times.

Table 5.06 shows comparison between Sr and Nd reference material and published data.

	SRM987 published	**2σ**	**SRM987 measured**	**2σ**
$^{87}Sr/^{86}Sr$	0.710234	18	0.710238	6
	JMC-Nd published	**2σ**	**JMC-Nd measured**	**2σ**
$^{143}Nd/^{144}Nd$	0.511107	2	0.511115	8

Table 5.06 Sr and Nd reference material isotope data

SRM987 data from Stein et al., (2007); Balcaen et al., (2005). GeoReM ID 3593.

JMC-Nd data from Zhang et al., (2001). GeoReM ID 1599.

5.2 Results – XRF, ICP-MS & TIMS

Breaksea Omphacite Granulite

The BOG possesses moderate SiO_2 (52.82 – 53.63 wt% oxide), high Al_2O_3 (17.85 – 18.42 wt% oxide), low MgO (4.39 – 4.63 wt% oxide), moderate to high total alkalis ($Na_2O + K_2O$ = 5.41 – 6.16 wt% oxide with Na_2O/K_2O = 3.44 – 4.26), high Sr (992 – 1254ppm) and low Y (13.9 – 21.1ppm) (data from Table 5.07 & 5.09) (Figs. 5.01 – 5.05 and 5.07). The BOG also shows low MnO (0.11 – 0.13 wt% oxide) (Fig. 5.06) and Mg# between 31 and 33 (Mg# = molar (Mg/[Mg + Fe_T])*100) (Table 5.07). BOG samples from this study plot on the boundary of gabbro and into compositions not realised by natural magmas on a TAS diagram (Fig. 5.07).

Anhydrous CIPW norm calculations show mostly concordant idealised mineral modes for the BOG samples 0901A, 0902A and 0907 (Table 5.08), showing an average plagioclase mode of 64.11wt%; hypersthene equal to 9.27wt%; hematite equal to 8.39wt%; orthoclase equal to 7.14wt%; diopside equal to 4.39wt%; titanite equal to 2.9wt%; quartz equal to 2wt%; apatite equal to 1.05wt% with ilmenite making up 0.26wt%, totalling 99.51%.

Hydrous CIPW norm calculations also show concordant idealised mineral modes between samples of the BOG (Table 5.08), showing an average plagioclase mode of 64.11wt%; biotite equal to 10.24wt%; hematite equal to 8.39wt%; quartz equal to 6.20wt%; hornblende equal to 5.67wt% wollastonite equal to 2.42wt%; apatite equal to 1.05wt% and ilmenite making up 0.26wt%, totalling to 98.34%.

Multi element spider diagrams and REE plots normalised to primitive mantle values of Sun & McDonough (1989) [spider diagram] and McDonough et al., (1991) [REE plots] show that the BOG plots with only a small amount of variation in values between samples (Figs. 5.08 & 5.09). The BOG has an average ΣREE = 150.0 (Table 5.09). The Spider plot shows trace elements at an undulating pattern 1 – 200 times primitive mantle values, with variable results for Cs and Rb; positive anomalies at Ba, Pb and Sr and negative anomalies at Nb, Zr and a weak negative anomaly at Ti.

Overall, the BOG shows a descending pattern from Nd onwards to Lu (excluding anomalies). The REE plot shows enrichment of ~40 x PM in the LREE, following an evenly descending pattern to ~4 x PM in the HREE, with three samples (0709A, 0737B and 0907) showing weakly positive Eu anomalies, one sample (B47/8/428) showing a weakly negative Eu anomaly while two samples (0611A and 0669) show no anomaly. The BOG has an average Sr/Y ratio of 66.74 (Table 5.09).

BOG spider and REE plots are given as a grey background on plots of other units to use as a comparative tool during discussion.

The BOG shows a range of values in the Rb-Sr isotopic system; $^{87}Sr/^{86}Sr$ ratios vary from 0.703994 – 0.704887 (TIMS), $^{87}Rb/^{86}Sr$ ratios from 0.018069 – 0.058343 (ICP-MS), calculated Sr_i at 120Ma from 0.703792 – 0.704209. The BOG shows a more limited range of values in the Sm-Nd isotopic system; $^{143}Nd/^{144}Nd$ from 0.512631 – 0.512712 (TIMS), $^{147}Sm/^{144}Nd$ from 0.121319 – 0.137691 (ICP-MS) and calculated εNd at 120Ma from 0.89 – 2.60 (Table 5.09). Graphical comparison of isotope data to the SPS and Darran suites can be seen in Fig 5.18.

	Breaksea Omphacite Granulite			Breaksea Eclogite			Garnetite		Pyroxenite		Hornblende Peridotite
						(+ qtz & plag)					
Major element (wt% oxide)	0901A	0902A	0907	0902D	0904C	0901C	0906B	0910B	0906A	0910C	0903A
SiO2	53.63	52.82	53.21	43.13	42.18	49.39	42.16	40.09	48.63	48.85	39.64
TiO2	1.37	1.39	1.18	2.39	1.88	1.92	0.59	0.45	1.00	0.84	0.68
Al2O3	17.85	17.90	18.42	13.14	16.97	13.27	17.19	19.83	9.05	8.36	3.52
Fe2O3	8.14	8.41	8.63	13.74	15.42	13.20	17.15	19.21	9.10	9.29	18.25
MnO	0.12	0.11	0.13	0.15	0.31	0.20	0.39	0.44	0.11	0.12	0.22
MgO	4.59	4.39	4.63	10.65	8.44	7.50	10.52	10.33	10.99	11.30	32.86
CaO	7.26	7.71	7.75	13.34	12.39	8.86	11.23	9.50	18.79	18.82	3.96
Na2O	4.78	4.83	4.30	2.47	1.89	3.23	0.94	0.44	2.24	1.95	0.67
K2O	1.39	1.13	1.10	0.52	0.02	1.27	0.02	0.02	0.00	0.03	0.18
P2O5	0.44	0.54	0.37	0.05	0.42	0.61	0.03	0.04	0.00	0.00	0.03
LOI (%)	0.06	0.10	0.07	0.10	-0.25	0.02	-0.46	-0.53	0.04	0.25	-0.30
Total	99.63	99.34	99.79	99.67	99.66	99.47	99.75	99.82	99.96	99.80	99.72
Mg#	32.72	31.06	31.64	40.06	32.05	32.88	34.60	31.68	51.01	51.18	60.82
Na2O/K2O	3.44	4.26	3.90	4.73	82.96	2.55	49.89	17.52	562.25	70.21	3.74
Na2O+K2O	6.16	5.97	5.41	2.99	1.92	4.50	0.96	0.46	2.24	1.98	0.85

Table 5.07 Major element data from XRF.

CIPW Normative Mode (wt%)											
Mineral	0901A	0902A	0907	0902D	0904C	0901C	0906B	0910B	0906A	0910C	0903A
Quartz	1.53	1.18	3.29	0	0	2.03	0	1.8	0	0	0
Corundum	0	0	0	0	0	0	0	1.9	0	0	0
Orthoclase	8.2	6.7	6.52	3.08	0.13	7.48	0.11	0.15	0.02	0.16	1.06
Albite	40.41	40.88	36.41	15.44	16.02	27.36	7.98	3.69	11.58	12.2	5.65
Anorthite	23.17	23.81	27.67	23.24	37.74	17.95	42.61	46.89	14.64	13.96	6.09
Nepheline	0	0	0	2.94	0	0	0	0	3.98	2.33	0
Diopside	4.41	5.08	3.69	27.15	12.19	12.57	9.64	0	58.76	59.88	9.24
Hypersthene	9.4	8.59	9.83	0	7.57	12.86	20.83	25.73	0	0	12.62
Olivine	0	0	0	9.76	5.46	0	0.64	0	0.09	0.26	45.52
Magnetite	0	0	0	0	0	0	0	0.13	0	0	0
Ilmenite	0.26	0.23	0.28	0.32	0.66	0.43	0.83	0.85	0.23	0.25	0.47
Hematite	8.14	8.41	8.63	13.74	15.42	13.2	17.15	19.12	9.1	9.29	18.25
Titanite	3.04	3.11	2.55	0	3.75	4.16	0.37	0	0	0	1.06
Perovskite	0	0	0	3.78	0	0	0	0	1.5	1.21	0
Apatite	1.04	1.27	0.87	0.12	0.99	1.44	0.07	0.09	0	0	0.07
Total	99.59	99.28	99.74	99.57	99.94	99.48	100.22	100.36	99.92	99.56	100.03
CIPW Normative Mode w Hornblende (wt%)											
Quartz	6.53	5.08	6.98	0	0	5.61	0	1.9	0	0	0
Corundum	0	0	0	0	0	0	0	1.9	0	0	0
Albite	40.4	40.88	36.41	10.94	11.1	27.36	6.24	3.69	10.93	10.12	0
Anorthite	23.17	23.81	27.67	23.24	37.74	17.95	42.6	46.89	14.64	13.96	6.09
Wollastonite	2.98	2.86	1.41	7.06	0	4.31	0	0	20.15	20.21	0
Magnetite	0	0	0	0	0	0	0	0.13	0	0	0
Ilmenite	0.26	0.23	0.28	0.32	0.66	0.43	0.83	0.85	0.23	0.25	0.47
Hematite	8.14	8.41	8.63	13.74	15.42	13.2	17.15	19.12	9.1	9.29	18.25
Apatite	1.04	1.27	0.87	0.12	0.99	1.44	0.07	0.09	0	0	0.07
Biotite	11.76	9.61	9.36	4.42	0.19	10.73	0.16	0.21	0.03	0.24	1.51
Hornblende	4.07	5.84	7.1	37.51	30.37	16.75	18.57	0	43.95	44.78	19.56
Total	98.35	98	98.7	97.35	96.47	97.79	85.62	74.79	99.04	98.85	45.96

Table 5.08 CIPW norms based on XRF data from GDCKit (Janousek et al., 2008).

	Breaksea Omphacite Granulite						Misty Pluton		Breaksea Eclogite			Garnetite	Pyroxenite	Hornblende Peridotite	Discarded		
Element	0709A	B47/8/428	0737B	0611A	0669	0907	A183/8	0805D	0725	0664	0904C	0906B	0906A	0903A	0771	0705	0709B
Li	9.4	8.7	7.1	9.4	11.1	9	9.9	5.5	5	5.7	7.8	3.6	5.8	3.6	5.5	3.3	2.7
Be	1.39	1.08	1.42	1	1.36	1.13	1.36	1.08	0.52	0.61	0.59	0.36	0.68	0.13	1.55	0.13	0.87
Sc	14.4	21	17.2	23.1	16.4	17.6	12.5	14.5	38.5	37.3	38	61.6	47.3	21.6	33.8	49.8	42.2
Ti	6951	6866	7380	5074	5597	6325	5918.3	5713	9925	8349	9637	2661	6350	4183	12294	2723	19943
V	164	209	181	228	159	161	133.9	159.4	399	390	264	286	434	114	369	280	363
Cr	64	65	60	88	40	38	0	0	107	100	119	109	314	352	114	3358	75
Mn	844	1165	789	1134	844	952	874.5	769.4	2139	1954	2356	3138	870	1740	1659	1243	2136
Co	53	103	93	74	39	78	61.5	56.7	93	89	111	118	84	161	93	98	77
Ni	38	45	35	57	37	25	17.9	25.2	80	86	40	56	137	710	95	384	54
Cu	68	139	26	168	51	69	32.7	13.7	198	16	17	8	11	28	275	18	155
Zn	84	99	82	95	77	81	84.9	88.3	103	127	96	84	65	120	151	43	146
Ga	20	18.7	20	18.6	19.9	19.4	22	21.8	16	19.1	18.7	15.5	18.2	4.3	20.3	9.1	19.6
As	1	2	<1	1	< 0.3	<1	<1	<1	<1	0.3	<1	<1	<1	<1		<1	<1
Rb	19.72	6.96	8.47	7.76	20.88	9.86	7.19	0.9	0.43	0.33	0.33	0.31	0.1	0.72	1.27	0.11	1.1
Sr	1001	1035	1254	1050	1010	992	1205.9	1448.9	242	178	123	66	161	144	432	92	627
Y	13.9	21.1	14	16.9	17.2	14.5	13.7	13.5	30.3	27.9	39.6	56.9	9.2	5.3	26	9.8	46.2
Zr	91	50	54	42	61	45	44	10	37	46	54	38	42	19		45	99
Nb	5.57	2.14	4.99	1.02	3.49	3.53	5.32	1.51	1.81	2.81	7.72	0.18	0.06	1.04	4.93	0.19	16.82
Mo	0.49	0.37	0.4	0.23	0.46	0.36	0.46	0.04	0.17	0.24	0.22	0.12	0.05	0.08	0.47	0.16	0.31
Cd	0.05	0.07	0.06	0.05	0.04	0.05	0.08	0.09	0.08	0.07	0.09	0.08	0.08	0.02	0.08	0.06	0.09
Cs	0.35	0.07	0.12	0.09	0.5	0.27	0	0.01	0.03	0.02	0.01	0.02	0.01	0.01	0.03	0.01	0.03
Ba	767	470	672	403	578	514	715.3	263.2	28	8	25	3	1	48	24	8	76
La	25.2	20.5	22.8	16.9	21.5	17.2	21.1	12.9	6.1	6.1	5.3	1.4	2	1.5	25.8	1.2	66.9
Ce	52.5	47	48	38.5	45.6	36.4	43.4	31	20	20.1	15.9	5.3	9.3	5.1	61.4	4.5	142
Pr	6.75	6.52	6.2	5.28	5.93	4.71	5.68	4.63	3.46	3.54	2.62	1.09	2.03	0.95	8.67	0.96	18.5
Nd	27.6	29.2	26	23.8	24.8	20	23.1	21	18.8	18.9	14.3	6.94	12.69	5.3	38.2	5.85	78.8
Sm	5.32	6.34	5.03	5.21	5.06	4.13	4.39	4.38	5.38	5.38	4.87	3.49	3.95	1.53	7.97	2.01	15.4
Eu	1.85	1.81	1.68	1.64	1.65	1.53	1.62	1.54	1.63	1.56	1.9	1.3	1.22	0.49	1.98	0.67	5.08

	Breaksea Omphacite Granulite						Misty Pluton		Breaksea Eclogite			Garnetite	Pyroxenite	Hornblende Peridotite	Discarded		
Element	0709A	B47/8/428	0737B	0611A	0669	0907	A183/8	0805D	0725	0664	0904C	0906B	0906A	0903A	0771	0705	0709B
Tb	0.58	0.81	0.56	0.65	0.61	0.51	0.49	0.48	0.91	0.79	1.04	1.08	0.45	0.21	0.94	0.34	1.74
Gd	4.29	5.74	4.1	4.64	4.28	3.61	3.81	3.62	5.95	5.33	6.34	5.87	3.48	1.5	6.71	2.26	12.7
Dy	2.86	4.31	2.83	3.43	3.15	2.65	2.49	2.39	5.22	4.16	6.6	7.43	2.14	1.14	4.89	1.97	8.87
Ho	0.53	0.83	0.53	0.66	0.62	0.52	0.47	0.44	1.03	0.79	1.47	1.78	0.35	0.22	0.94	0.39	1.68
Er	1.36	2.2	1.4	1.74	1.64	1.38	1.27	1.17	2.64	1.97	4.24	5.47	0.76	0.54	2.45	1.02	4.39
Yb	1.1	1.85	1.18	1.41	1.41	1.19	1.06	0.91	2.09	1.54	4.06	5.76	0.45	0.4	2.01	0.81	3.69
Lu	0.16	0.27	0.17	0.21	0.21	0.18	0.15	0.13	0.3	0.22	0.63	0.91	0.06	0.06	0.29	0.11	0.55
Hf	1.79	1.54	1.57	1.36	1.56	1.29	0.69	0.59	1.02	1.06	1.39	0.72	1.5	0.48	1.14	0.65	1.01
Ta	1.07	1.94	1.43	1.02	0.56	0.24	0.26	0.07	0.81	0.62	0.51	0.03	0.02	0.06	1.15	1.35	1.67
Pb	12.9	9.99	12.39	7.58	10.9	7.49	8.51	3.35	0.6	0.45	0.33	0.17	0.23	0.31	1.65	0.61	1.57
Th	1.97	1.02	1.28	1.45	1.86	1.05	0.26	0.08	0.11	0.14	0.17	0.02	0.02	0.05	1.37	0.02	3.16
U	0.42	0.24	0.27	0.25	0.37	0.26	0.07	0.03	0.04	0.07	0.08	0.01	0.01	0.01	0.45	0.01	0.88
Sr/Y	72.23	49.02	89.92	61.98	58.66	68.63	88.17	106.98	7.99	6.38	3.1	1.15	17.59	27.11	16.6	9.41	13.58
ΣREE	158.4	169.5	151.6	144.2	150.1	126.1	135.2	112.5	142.3	135.6	146.9	166.2	95.3	45.9	222.1	81.6	448.4
Age	120	120	120	120	120	120			120	120	120	120	120	120	120	120	120
$^{87}Sr/^{86}Sr$	0.704887	0.7041	0.703994	0.704036	0.704078	0.704258			0.704006		0.704077	0.70404	0.704287	0.704303	0.704035	0.703953	0.704067
2σ	4	6	8	12	10	12			8		10	10	94	6	10	12	6
$^{87}Rb/^{86}Sr$	0.055622	0.018969	0.019056	0.020863	0.058343	0.028039			0.004985	0.005190	0.007505	0.013437	0.001791	0.014192	0.008297	0.003350	0.004971
Sr_i	0.703792	0.704058	0.703961	0.704001	0.703978	0.704209			0.703998		0.704064	0.704019	0.704325	0.704279	0.704011	0.703945	0.704059
$^{143}Nd/^{144}Nd$	0.512712	0.512668	0.512680	0.512691	0.512674	0.512631			0.512725	0.512729	0.512714	0.512792	0.512720	0.512661	0.512692	0.512766	0.512685
2σ	6	10	8	8	4	6			6	4	10	8	8	12	4	6	4
$^{147}Sm/^{144}Nd$	0.121319	0.136725	0.121969	0.137691	0.128498	0.129944			0.179987	0.179271	0.214248	0.316871	0.196031	0.181306	0.131301	0.216462	0.122884
εNd	2.6	1.5	1.97	1.94	1.76	0.89			1.96	2.05	1.21	1.16	1.61	0.69	2.05	2.19	2.05

Table 5.09 Trace element data from ICP-MS. Misty Pluton data from Emami (2008). Values in red from XRF. ^{87}Rb (27.83%), ^{86}Sr (9.86%), ^{147}Sm (14.99%) and ^{144}Nd (23.8%) calculated from ICP-MS and elemental abundances

Isotope 2σ error given is $x10^{-6}$

$Sr_i = {}^{87}Sr/^{86}Sr_{SAMPLE} - {}^{87}Rb/^{86}{}_{SAMPLE}\ (e^{\lambda T}-1)$ where $\lambda=1.42\text{-}^{11}$ (McCulloch et al., 1987; Davis et al., 1977)

$\varepsilon Nd=[(^{143}Nd/^{144}Nd^{T}{}_{INIT}/(^{143}Nd/^{144}Nd)^{T}{}_{CHUR}-1]10^{4}$ where $(^{143}Nd/^{144}Nd)^{T}{}_{INIT}$ are initial ratios at T=120MA and $(^{143}Nd/^{144}Nd)^{T}{}_{CHUR} = 0.512638 - 0.1966(e^{\lambda T} - 1)$ where $\lambda=6.54^{-12}$ (McCulloch et al., 1987; Lugmair & Marti, 1978).

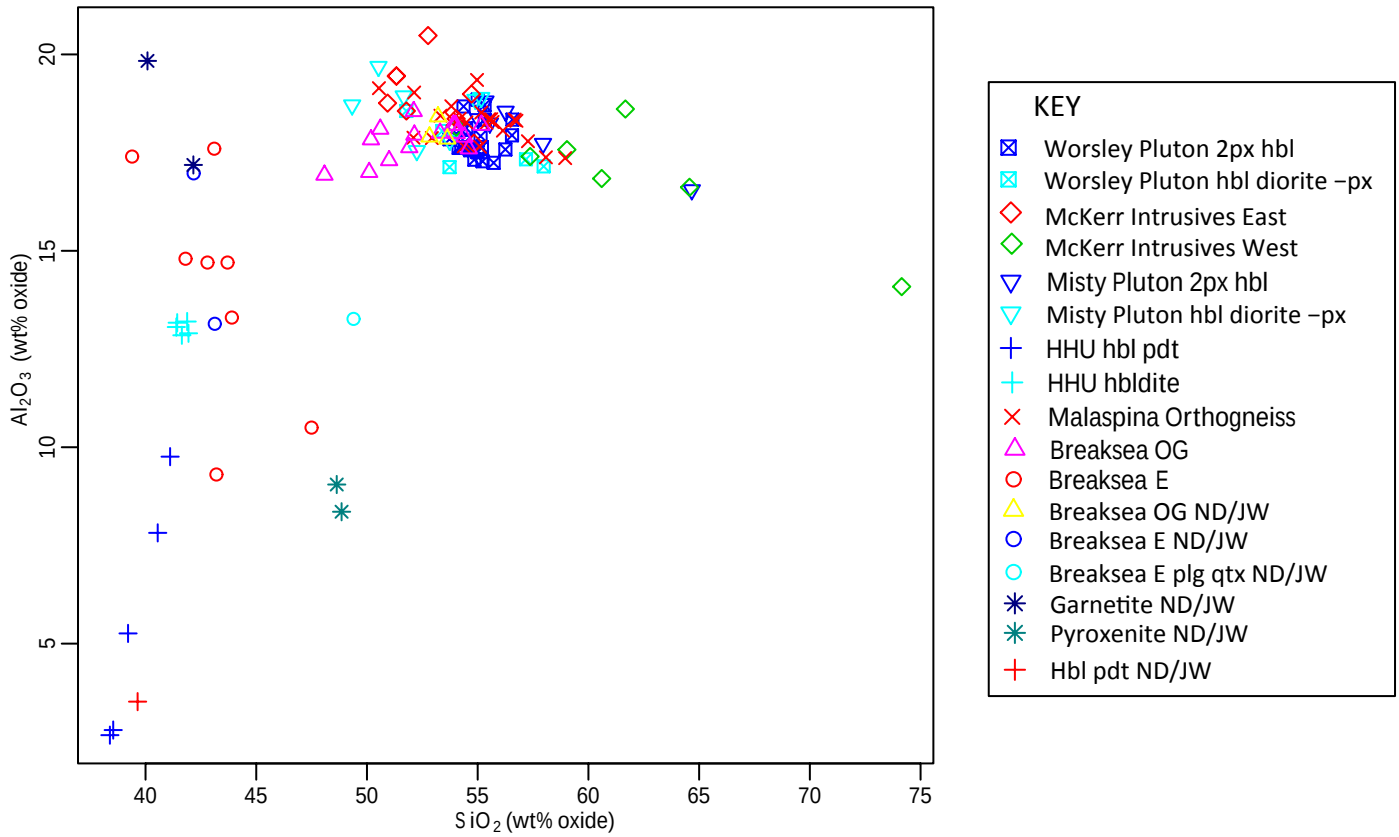

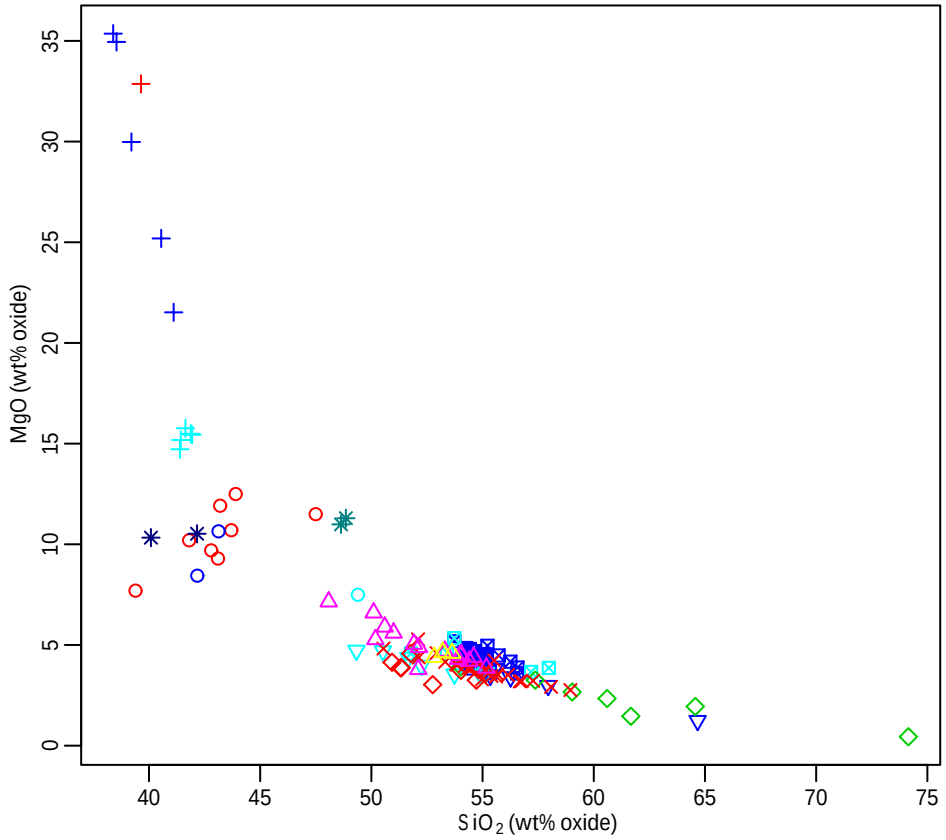

Fig 5.01 SiO_2 vs Al_2O_3
Fig 5.02 SiO_2 vs MgO

Amounts are wt% oxide. Samples with suffix ND/JW correspond to sample groups in row one of Table 5.07. Other data is listed North to South from WFO database given in Appendix 5.A.

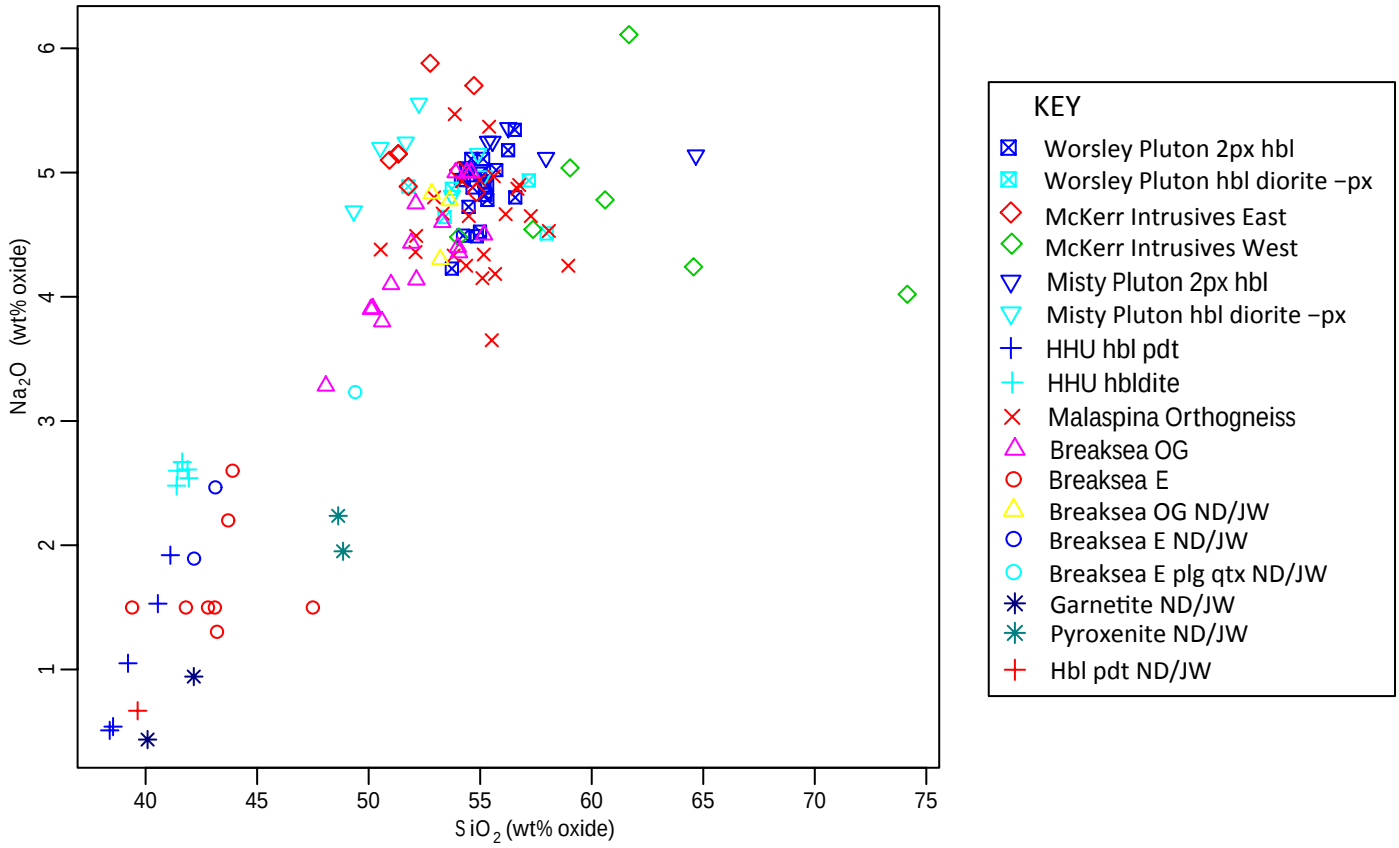

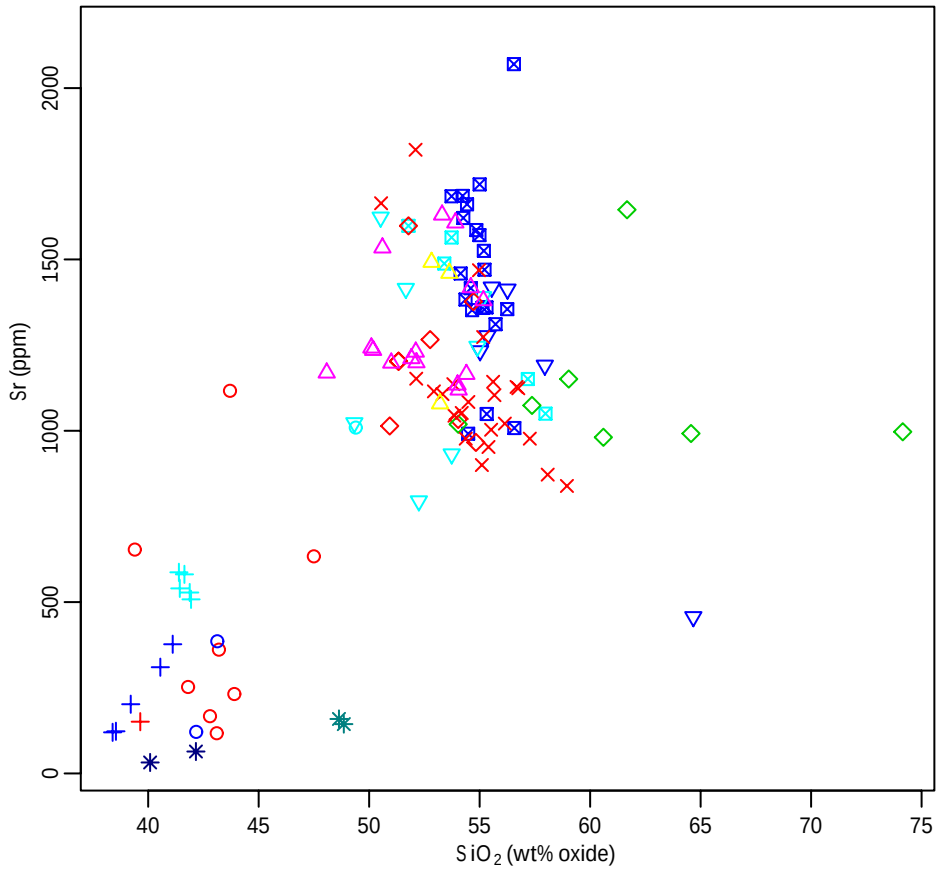

Fig 5.03 SiO_2 vs Na_2O
Fig 5.04 SiO_2 vs Sr

Amounts are wt% oxide (Na_2O, SiO_2) and ppm (Sr). Samples with suffix ND/JW correspond to sample groups in row one of Table 5.07. Other data is listed North to South from WFO database given in Appendix 5.A.

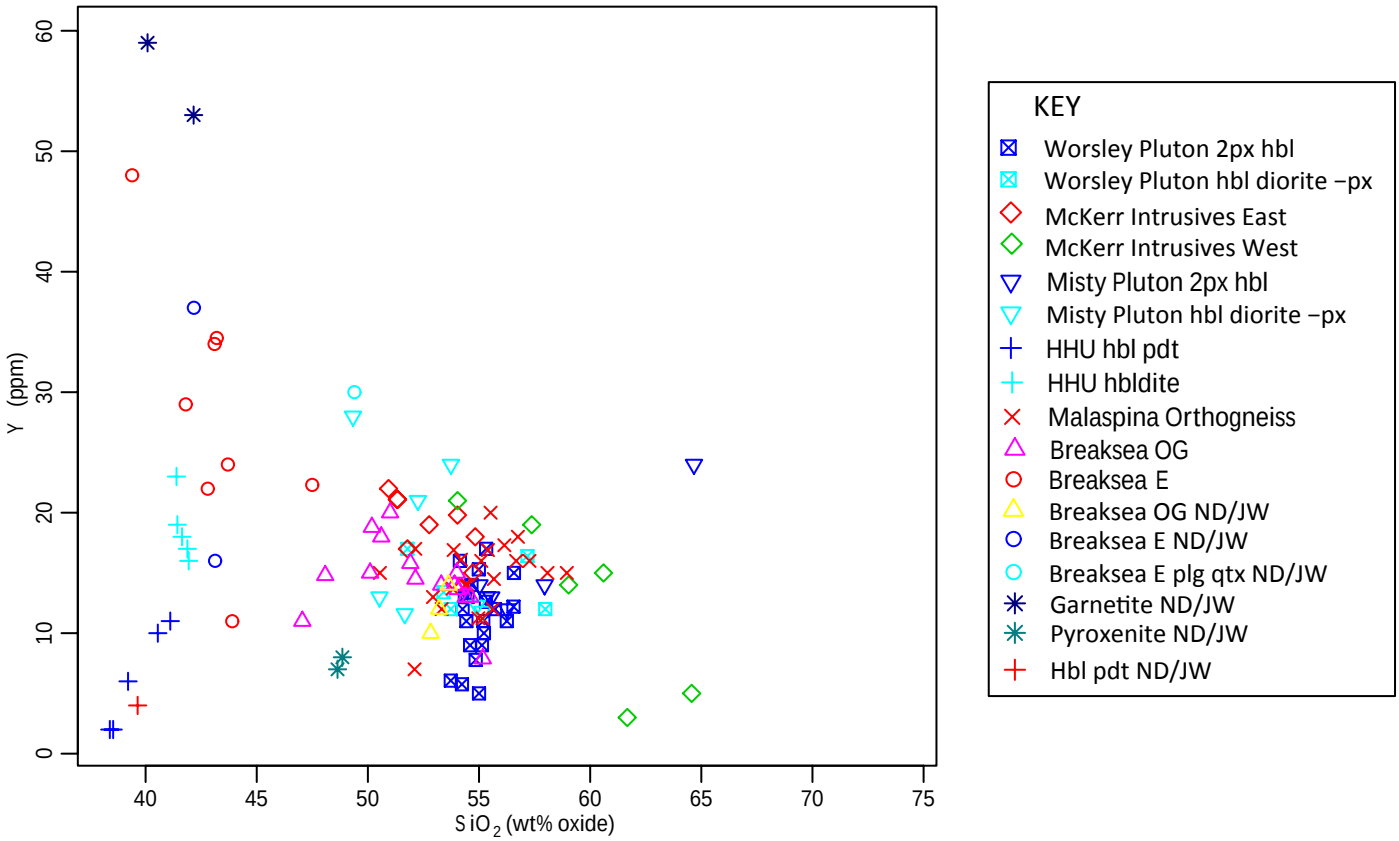

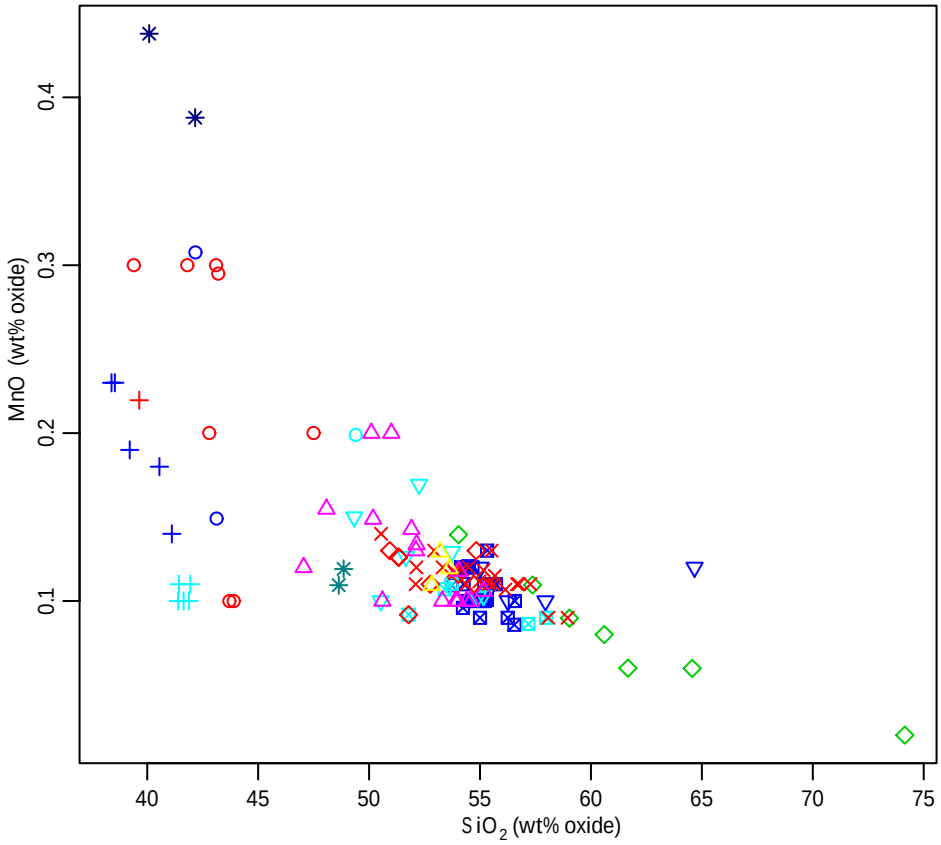

Fig 5.03 SiO_2 vs Y

Fig 5.04 SiO_2 vs MnO

Amounts are wt% oxide (MnO, SiO_2) and ppm (Y). Samples with suffix ND/JW correspond to sample groups in row one of Table 5.07. Other data is listed North to South from WFO database given in Appendix 5.A.

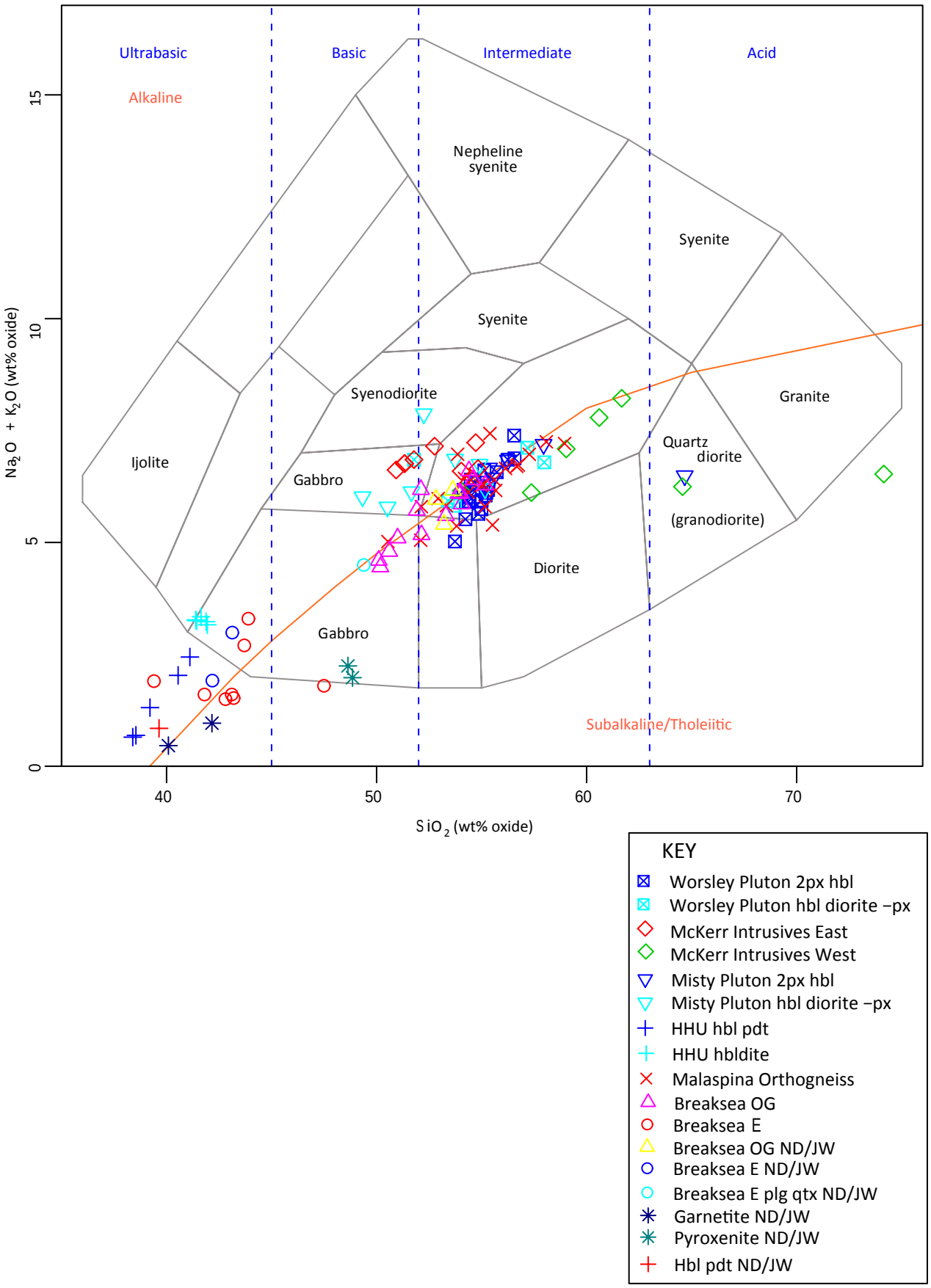

Fig 5.07 TAS diagram after Cox et al., (1979).
Amounts are wt% oxide. Samples with suffix ND/JW correspond to sample groups in row one of Table 5.07. Other data is listed North to South from WFO database given in Appendix 5.A.

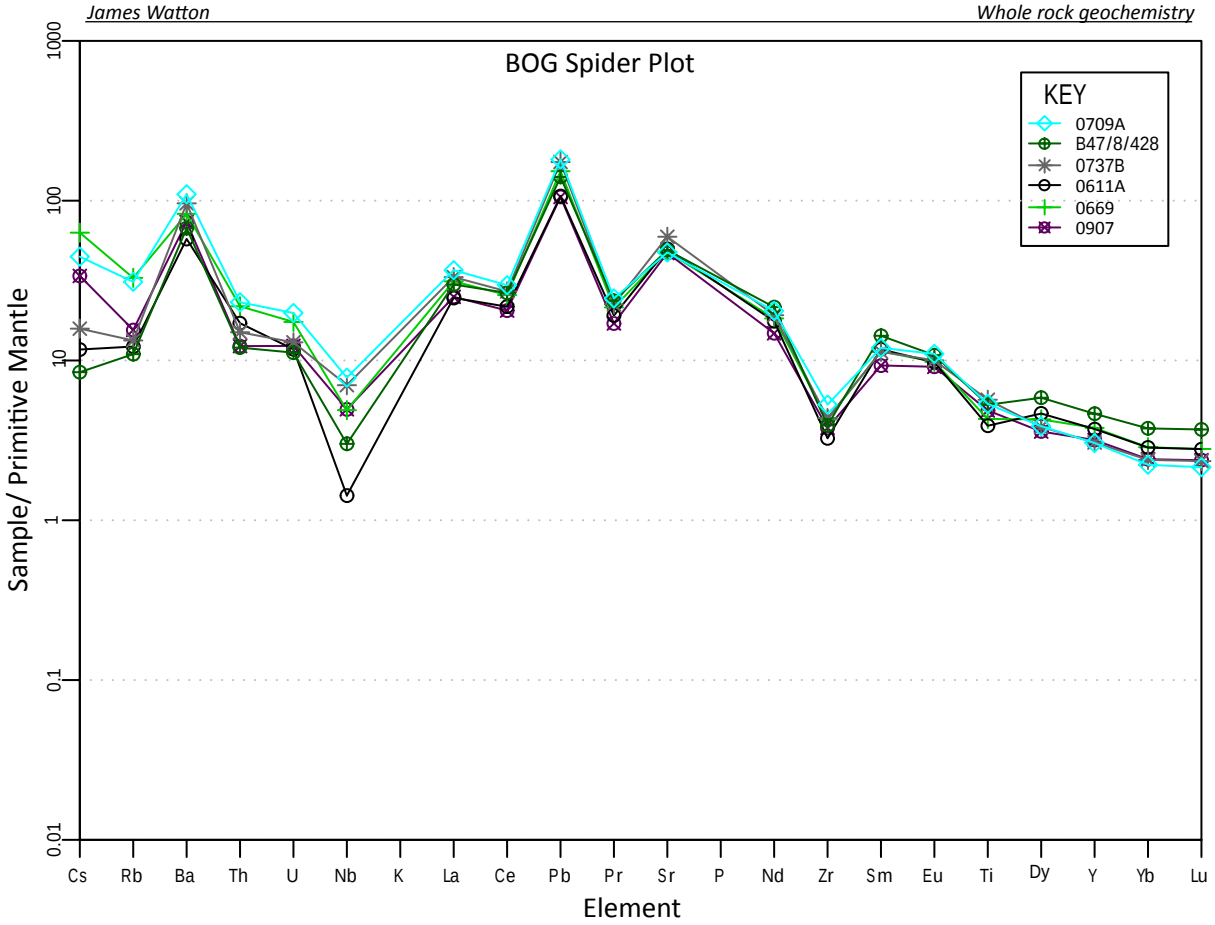

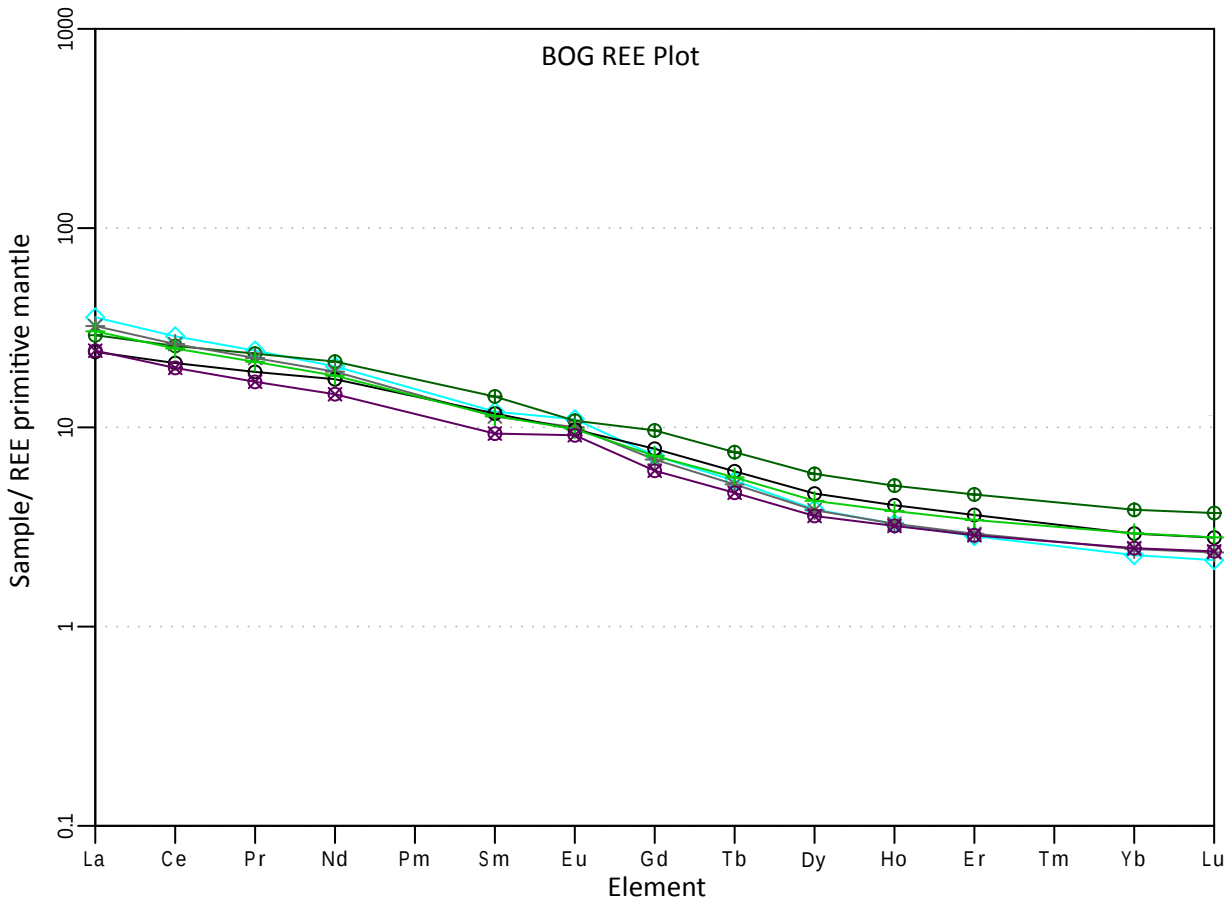

Fig 5.08 Spider diagram of BOG normalised to primitive mantle values of Sun & McDonough (1989).
Fig 5.09 REE plot of BOG normalised to primitive mantle values of McDonough et al., (1991).

Breaksea Eclogite

The BE possesses very low SiO_2 (42.18 – 43.13 wt% oxide), moderate Al_2O_3 (13.14 – 16.97 wt% oxide), moderate to high MgO (8.44 – 10.65 wt% oxide), low total alkalis ($Na_2O + K_2O$ = 1.92 – 2.99 wt% oxide with Na_2O/K_2O = 4.73 – 82.96), low Sr (178 – 242ppm) and high Y (27.9 – 30.3ppm) (data from Table 5.07 & 5.09) (Figs. 5.01 – 5.05 and 5.07). The BE shows variable MnO (0.15 – 0.31 wt% oxide) (Fig. 5.06) and Mg# between 32 and 40 (Mg# = molar (Mg/[Mg + Fe_T])*100) (Table 5.07). There is also a BE sample with plagioclase and quartz which displays different chemical signatures as a result (SiO_2 = 49.39 wt% oxide; Al_2O_3 = 13.27 wt% oxide; MgO = 7.50 wt% oxide; $Na_2O + K_2O$ = 4.50 wt% oxide; Na_2O/K_2O = 2.55; Sr = 123ppm; Y = 39.6ppm; MnO = 0.20 wt% oxide; Mg# = 0.33) and as such is plotted separately to other BE samples. BE rocks from this study plot in or below (lower SiO_2 and total alkalis) the gabbro field, with the plagioclase and quartz bearing sample plotting in the gabbro field on a TAS diagram (Fig. 5.07).

Anhydrous CIPW norm calculations show variable results in the two normal BE samples and as such ranges are given rather than averages. Individual results are shown in Table 5.08. Plagioclase varies from 38.88 – 53.75wt%; diopside varies from 12.19 – 27.15wt%; hematite ranges from 13.74 – 15.42wt%; olivine from 5.46 – 9.76wt%; hypersthene varies from 0 – 7.57wt%; perovskite from 0 – 3.78wt%; titanite from 0 – 3.75wt%; orthoclase ranges from 0.13 – 3.08wt%; nepheline varies from 0 – 2.94wt%; ilmenite from 0.32 – 0.66wt%; apatite from 0.12 – 0.99wt%; quartz is calculated at 0.00wt% for normal BE and 2.03wt% for the plagioclase and quartz bearing sample (0901C). Sample 0901C also has a higher calculated orthoclase (7.48wt%) and albite (27.36wt%) content, while having a lower anorthite content (17.95wt%). Totals are within 0.43wt% of 100% for normal samples and within 0.52wt% of 100% for sample 0901C.

Hydrous CIPW norm calculations show similar information (Table 5.08); anorthite, ilmenite, quartz, apatite and hematite amounts are identical to anhydrous CIPW norm calculations while albite amounts are lower (10.94 – 11.1wt%); wollastonite ranges from 0 – 7.06wt%; biotite ranges from 0.19 – 4.42wt% and hornblende from

30.37 – 37.51wt%. Sample 0901C shows higher quartz (5.61wt%); wollastonite equal to 4.31wt%; biotite equal to 10.76wt% and hornblende totalling 16.75wt%. Totals are lower; as low as 96.47wt% for BE and 97.79wt% for sample 0901C.

Multi element spider diagrams and REE plots show that the BE has only small amounts of variation in the LREE and MREE, with sample 0904C showing some elevation in HREE over samples 0725 and 0664 (Figs. 5.10 & 5.11). The BE has an average ΣREE = 141.6 (Table 5.09). Spider plots show a generally increasing pattern from Cs to P, and a decreasing pattern from P onwards to Lu, values between 0.8 – 12 times primitive mantle values (Sun & McDonough, 1989) (Fig. 5.10), with spread results for Ba, Nb, Yb and Lu, no positive anomalies, with negative anomalies at Rb, Pb, Sr, Zn and a weak negative anomaly at Eu. REE plots show LREE depletion relative to the BOG (~10 x PM), in a weakly ascending hump pattern which has a downward slope from Gd onwards, samples 0725 and 0664 show a HREE pattern matching the BOG (Fig. 5.11). Sample 0904C shows a downward slope, but is much less pronounced that in samples 0725 and 0664. The weak negative Eu anomaly is also visible in samples 0715 and 0664 (Fig. 5.11). The BE has an average Sr/Y ratio of 5.82 (Table 5.09).

The BE shows a limited range in the Rb-Sr isotopic system; $^{87}Sr/^{86}Sr$ ratios from 0.704006 – 0.704077 (TIMS), $^{87}Rb/^{86}Sr$ ratios from 0.004985 – 0.007505 (ICP-MS), calculated Sr_i at 120Ma from 0.703998 – 0.704064. The BE also shows a constrained range of values in the Sm-Nd isotopic system; $^{143}Nd/^{144}Nd$ from 0.512714 – 0.512729 (TIMS), $^{147}Sm/^{144}Nd$ from 0.179271 – 0.214248 (ICP-MS) and calculated εNd at 120Ma from 1.21 – 2.05 (Table 5.09). Graphical comparison of isotope data to the SPS and Darran suites can be seen in Fig 5.18.

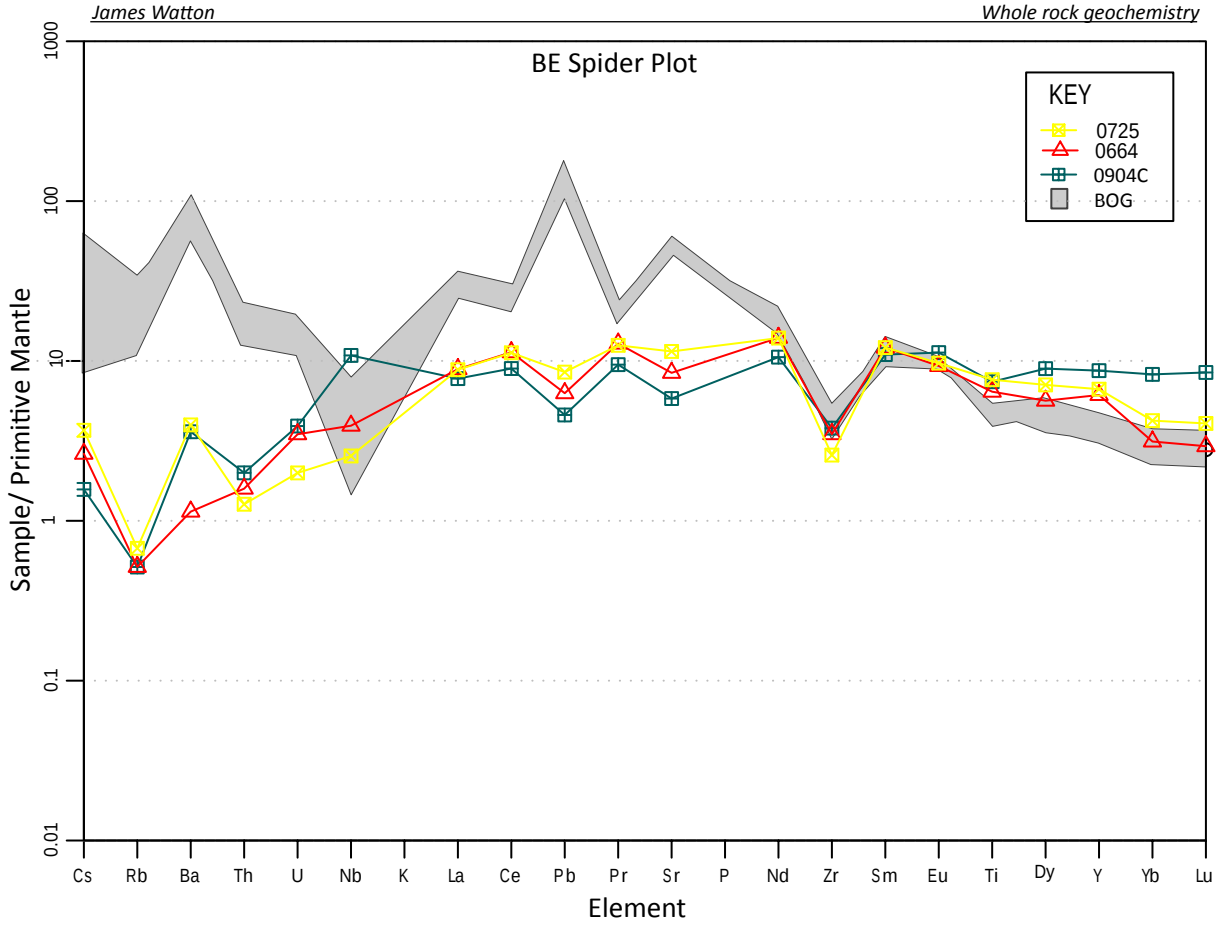

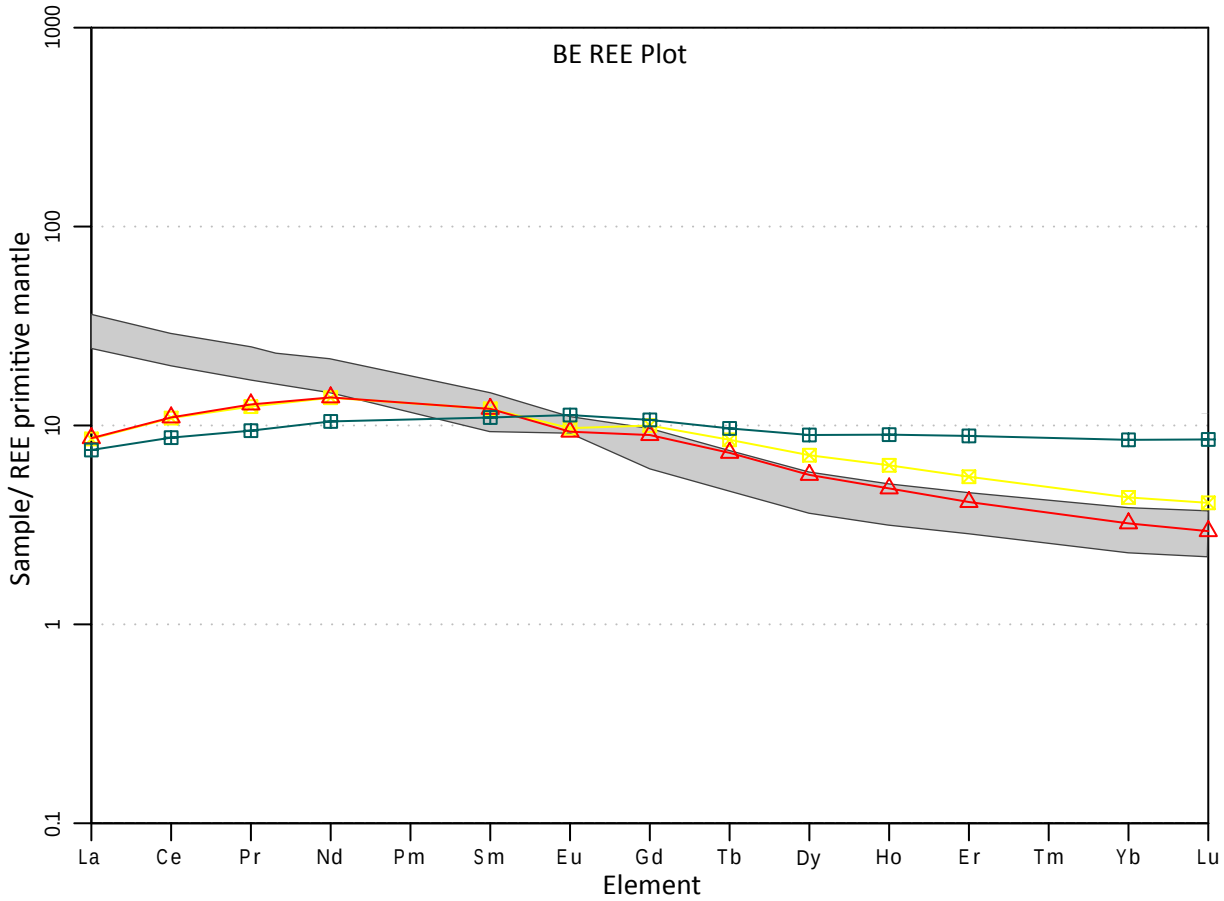

Fig 5.10 Spider diagram of BE normalised to primitive mantle values of Sun & McDonough (1989).
Fig 5.11 REE plot of BE normalised to primitive mantle values of McDonough et al., (1991). Shown in grey is the Spider and REE pattern for BOG.

Layered Garnetite – Pyroxenite

Garnetite has the lowest measured SiO_2 (40.09 – 42.16 wt% oxide), high Al_2O_3 (17.19 – 19.83 wt% oxide), moderate to high MgO (10.33 – 10.52 wt% oxide) very low total alkalis ($Na_2O + K_2O$ = 0.46 – 0.96 wt% oxide with Na_2O/K_2O = 17.52 – 49.89), lowest Sr (66ppm) and highest Y (56.9ppm) (data from Table 5.07 & 5.09) (Figs. 5.01 – 5.05 and 5.07). Garnetite also shows the highest MnO (0.39 – 0.44 wt% oxide) (Fig. 5.06) and highest Fe_2O_3 (17.15 – 19.21 wt% oxide, along with hornblende peridotite) and Mg# between 32 – 05 (Mg# = molar (Mg/[Mg +Fe_T])*100) (Table 5.07). Garnetite plots outside the fields of natural magmas on a TAS diagram (Fig. 5.07).

Anhydrous CIPW norms for garnetite show that the two samples 0906B and 0910B are comparable in terms of idealised mineral modes (Table 5.08), with plagioclase totalling to 50.58wt% for both samples, hypersthene ranging between 20.83 – 25.73wt%; hematite ranging between 17.15 – 19.12wt%; diopside varies from 0.00wt% (0910B) to 9.64wt% (0906B); samples show similar ilmenite (0.83 – 0.85wt%); orthoclase (0.11 – 0.15wt%) and apatite (0.07 – 0.09wt%); sample 0906B has 0.37wt% calculated titanite (0910B has 0.00wt%) and 0.64wt% olivine (0910B has 0.00wt%) while sample 0910B has quartz (1.8wt%); corundum (1.9wt%) and magnetite (0.13wt%) where 0906B has none. Totals are within 0.36wt% for both samples.

Hydrous CIPW norms show similar amounts for all included minerals (Table 5.08) except albite in sample 0906B (6.24wt% compared to 7.98wt% anhydrous). Both samples have concordant calculated biotite (0.16wt% and 0.21wt%) while sample 0906B has 18.57wt% hornblende whereas 0910B has 0.00wt%. Totals for hydrous CIPW norms are low, 85.62wt% for 0906B and 74.79wt% for 0910B.

Garnetite has ΣREE = 166.2 and multi element spider plots show a continuously ascending pattern from Cs to Lu, with negative anomalies at Th, Nb, Zr, Ti, Pb and Sr and positive anomalies at Cs and Y. REE plots show a continuously ascending pattern from 2 x PM depleted LREE to 12 x PM enriched HREE with a weak negative Eu anomaly (Figs. 5.12 & 5.13). Garnetite has a Sr/Y ratio of 1.15 (Table 5.09).

Garnetite shows an $^{87}Sr/^{86}Sr$ ratio of 0.704040 (TIMS), $^{87}Rb/^{86}Sr$ ratio of 0.013437 (ICP-MS), calculated Sr_i at 120Ma of 0.704019. The garnetite sample shows an $^{143}Nd/^{144}Nd$ ratio of 0.512792 (TIMS), $^{147}Sm/^{144}Nd$ of 0.316871 (ICP-MS) and calculated εNd at 120Ma of 1.16 (Table 5.09). Graphical comparison of isotope data to the SPS and Darran suites can be seen in Fig 5.18.

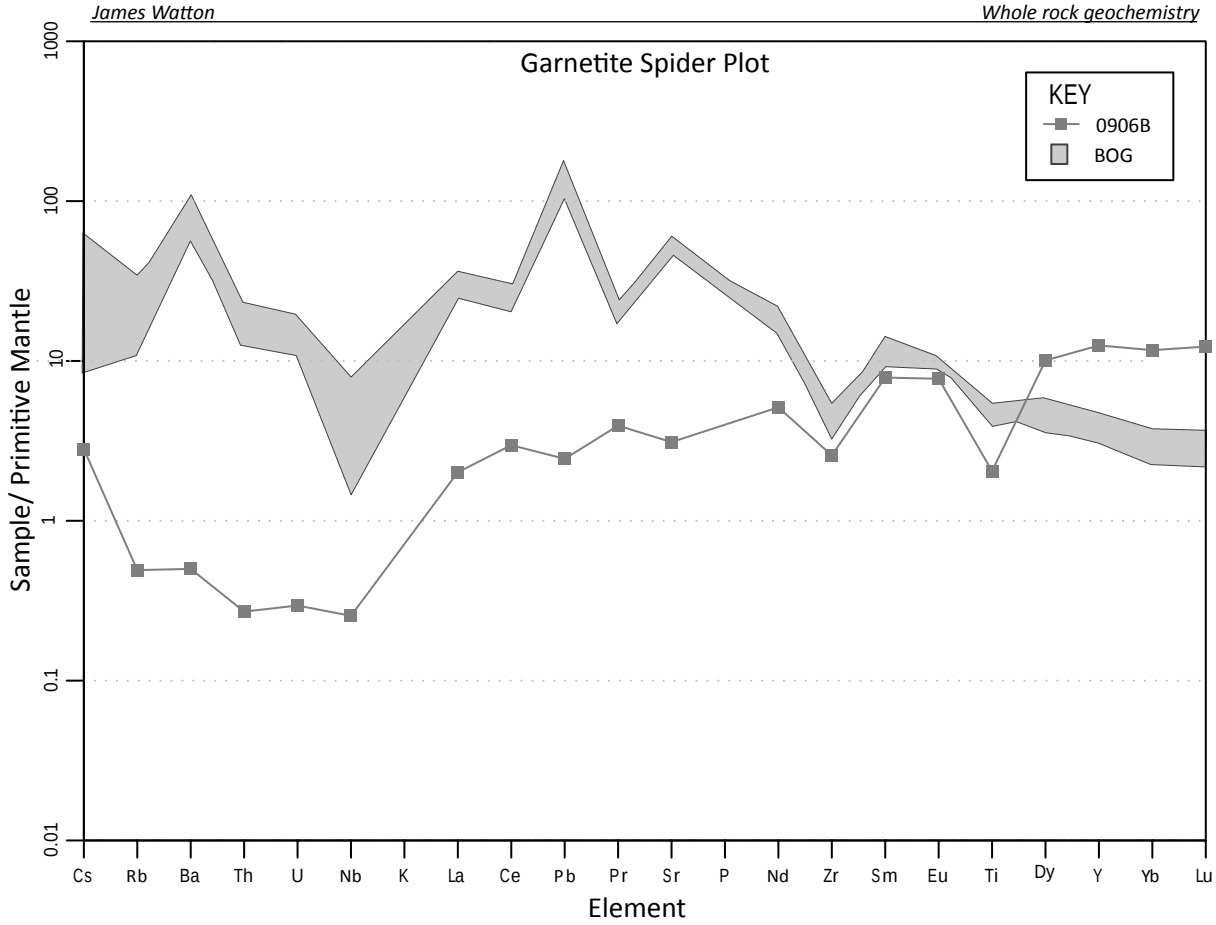

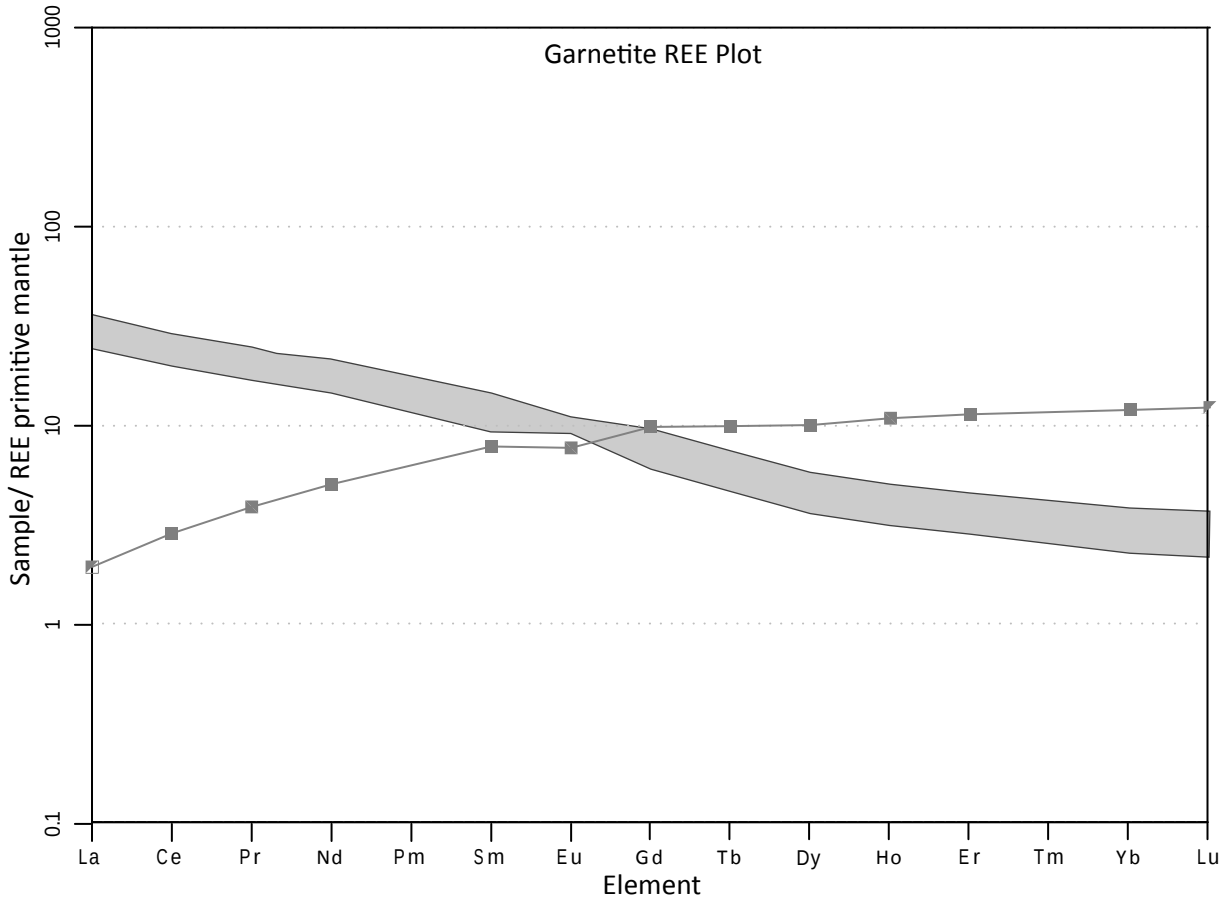

Fig 5.12 Spider diagram of garnetite normalised to primitive mantle values of Sun & McDonough (1989).
Fig 5.13 REE plot of garnetite normalised to primitive mantle values of McDonough et al., (1991).
Shown in grey is the Spider and REE pattern for BOG.

Pyroxenite shows a moderate to low SiO_2 content (48.85 – 48.63 wt% oxide), low Al_2O_3 (8.36 – 9.05 wt% oxide), moderate to high MgO (10.99 – 11.30 wt% oxide), low total alkalis ($Na_2O + K_2O$ = 1.98 – 2.24 wt% oxide with Na_2O/K_2O = 70.21 – 562.25), low Sr (161ppm) and low Y (9.2ppm) (data from Table 5.07 & 5.09) (Figs. 5.01 – 5.05 and 5.07). Also of note is that the pyroxenite has the highest CaO content of all rocks (18.79 – 18.82 wt% oxide) compared to the BOG which has 7.26 – 7.75 wt% oxide. Pyroxenite also shows the low MnO (0.11 – 0.12 wt% oxide) (Fig. 5.06) and Mg# equal to 51 (Mg# = molar (Mg/[Mg +Fe_T])*100) (Table 5.07). Pyroxenite, with higher bulk SiO_2 and Na_2O content than garnetite plots slightly up and to the right of garnetite on a TAS diagram – in the gabbro field (Fig. 5.07).

Anhydrous CIPW norms for pyroxenite samples 0906A and 0910B show near identical calculated idealised mineral modes (Table5.08), with an average diopside calculation of 59.32wt%; plagioclase averaging 26.19wt%; hematite 9.20wt%; nepheline 3.16wt%; perovskite 1.36wt%; ilmenite 0.24wt%; olivine 0.18wt% and orthoclase 0.09wt%. Calculated totals average 99.74wt%. Hydrous CIPW norms again show very similar calculated compositions for the two samples (Table 5.08), with hornblende averaging 44.37wt%; plagioclase 24.83wt%; wollastonite 20.18wt%; hematite and ilmenite identical at 9.20wt% and 0.24wt% respectively. Biotite is calculated at 0.16 wt%. Average total is 98.95wt%.

The pyroxenite sample has ΣREE = 95.3 and a Sr/Y ratio of 17.59 (Table 5.09). The multi element spider plot shows a humped pattern, ascending from Rb to Sm and descending from Eu to Lu, with negative anomalies at Nb, Pb and Zr and a positive anomaly at Cs. The REE plot shows a humped pattern ascending in the LREE to Sm and descending from Sm through to the HREE, varying from ~0.9 x PM to ~9 x PM (Figs. 5.14 & 5.15).

Pyroxenite shows a $^{87}Sr/^{86}Sr$ ratio of 0.704287 (TIMS), $^{87}Rb/^{86}Sr$ ratio of 0.001791 (ICP-MS), calculated Sr_i at 120Ma of 0.704325. The pyroxenite sample shows an $^{143}Nd/^{144}Nd$ ratio of 0.512720 (TIMS), $^{147}Sm/^{144}Nd$ of 0.196031 (ICP-MS) and calculated εNd at 120Ma of 1.61 (Table 5.09). Graphical comparison of isotope data to the SPS and Darran suites can be seen in Fig 5.18.

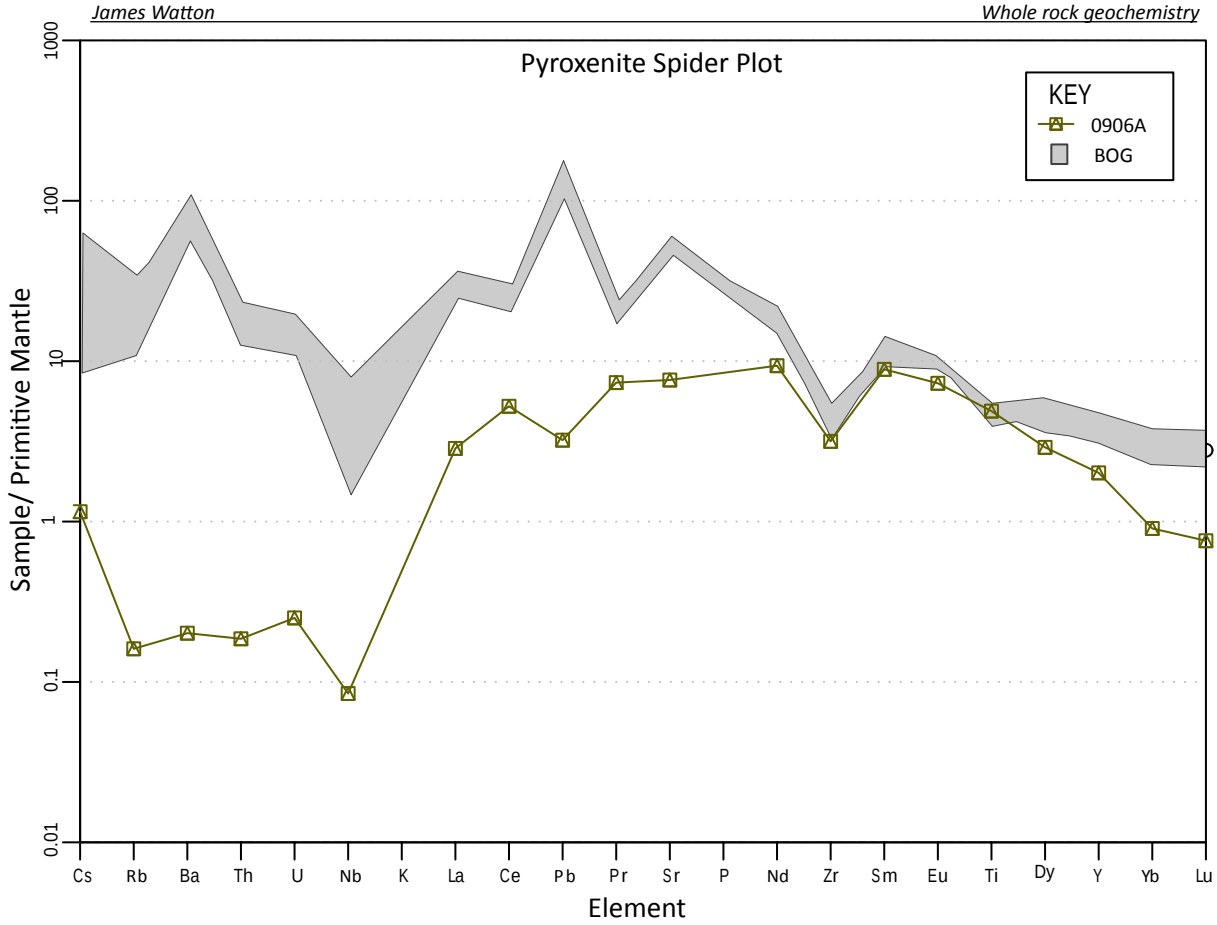

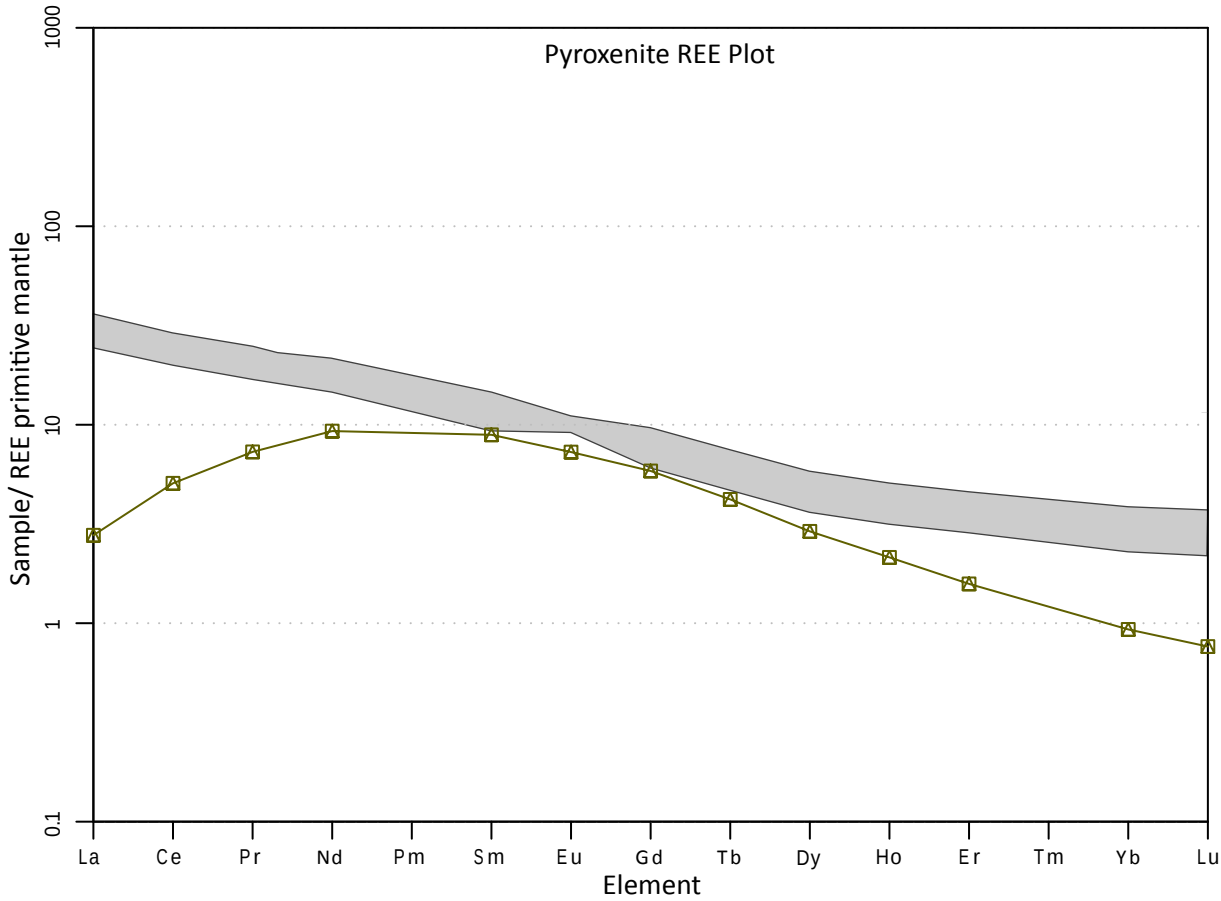

Fig 5.14 Spider diagram of pyroxenite normalised to primitive mantle values of Sun & McDonough (1989).
Fig 5.15 REE plot of pyroxenite normalised to primitive mantle values of McDonough et al., (1991).
Shown in grey is the Spider and REE pattern for BOG.

Hornblende Peridotite

Hornblende Peridotite has the lowest SiO_2 content (39.64 wt% oxide), lowest Al_2O_3 (3.52 wt% oxide), highest MgO (32.86 wt% oxide), very low total alkalis ($Na_2O + K_2O$ = 0.85 wt% oxide with Na_2O/K_2O = 3.74), low Sr (144ppm) and the lowest Y (5.3ppm) (data from Table 5.07 & 5.09) (Figs. 5.01 – 5.05 and 5.07). The hornblende peridotite also has the highest Fe_2O_3 content (18.25 wt% oxide, along with garnetite), has moderate MnO (0.22 wt% oxide) (Fig. 5.06) and the highest Mg# of 61 (Mg# = molar $(Mg/[Mg + Fe_T])*100$) (Table 5.07). Hornblende peridotite plots outside the composition of natural magmas on a TAS diagram (Fig. 5.07).

Anhydrous CIPW norms calculate an idealised mineral mode for olivine equal to 45.52wt%; hematite 18.25wt%; hypersthene 12.62wt%; plagioclase 11.74wt%; diopside 9.24wt%; orthoclase and titanate 1.06wt%; ilmenite 0.47wt% and apatite 0.07wt%. The calculated total is 100.03wt%.

The hydrous CIPW norm calculation is very poor – totalling 45.96wt%. is shows 19.56wt% hornblende, identical hematite at 18.25wt%; anorthite of 6.09%; biotite equal to 1.51wt% and identical ilmenite and apatite (0.47 and 0.07wt% respectively).

The hornblende peridotite sample has ΣREE = 45.9 and a Sr/Y ratio of 27.11 (Table 5.09). A primitive mantle (Sun & McDonough, 1989) normalised multi element spider plot shows a humped pattern, ascending until Sr and descending from Sr onto Lu, with negative anomalies at Th, U, Pr, Zr and Eu and positive anomalies at Ba, Nb, Pb, Sr and Ti. The REE plot shows a humped pattern ranging from ~0.8 x PM to 4 x PM, indicating an overall depletion in the REE. LREE's show an ascending pattern from La to Nd and decrease from Nd to Lu with no anomalies (Figs. 5.16 & 5.17).

Hornblende peridotite shows an $^{87}Sr/^{86}Sr$ ratio of 0.704303 (TIMS), $^{87}Rb/^{86}Sr$ ratio of 0.014192 (ICP-MS), calculated Sr_i at 120Ma of 0.704279. The hornblende peridotite sample shows an $^{143}Nd/^{144}Nd$ ratio of 0.512661 (TIMS), $^{147}Sm/^{144}Nd$ of 0.181306 (ICP-MS) and calculated εNd at 120Ma of 0.69 (Table 5.09). Graphical comparison of isotope data to the SPS and Darran suites can be seen in Fig 5.18.

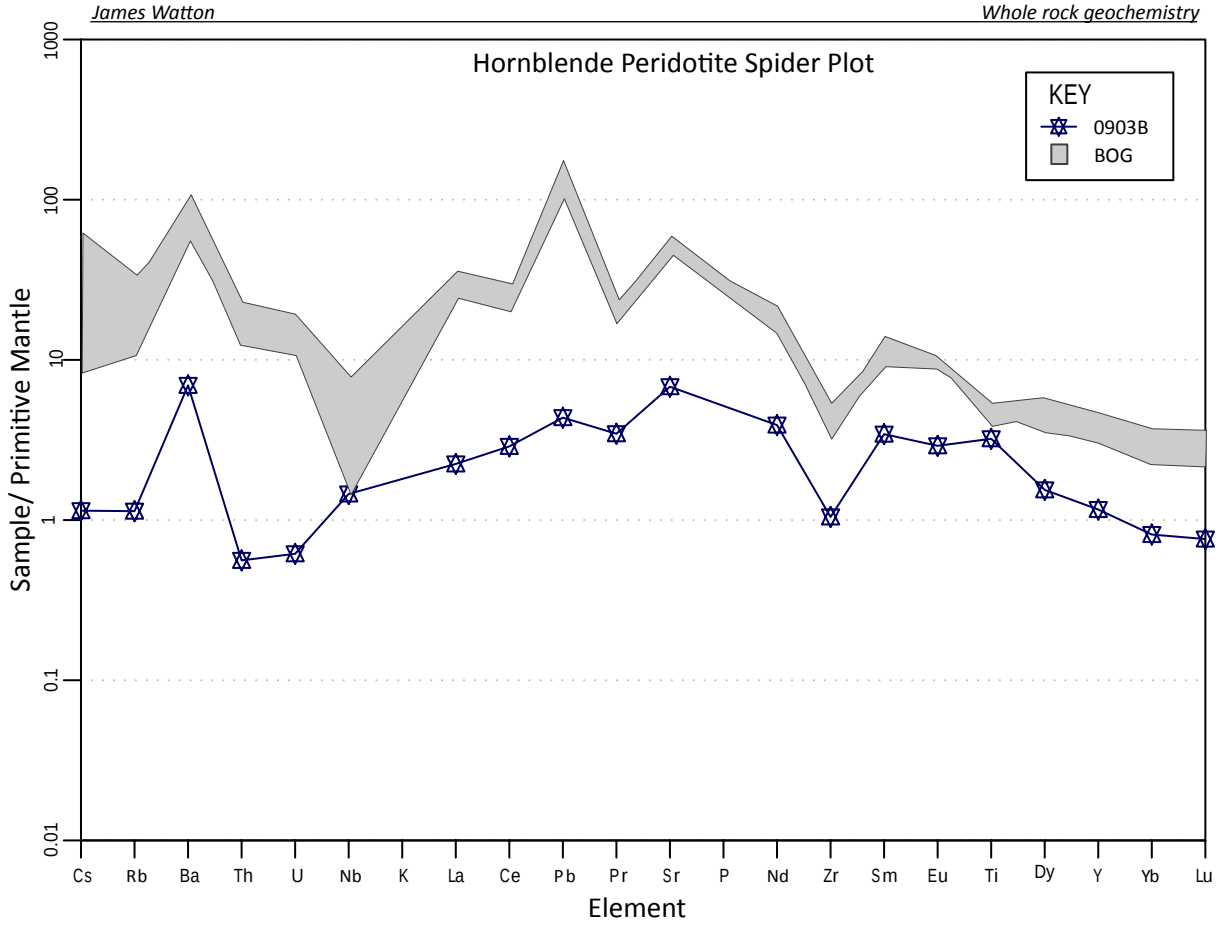

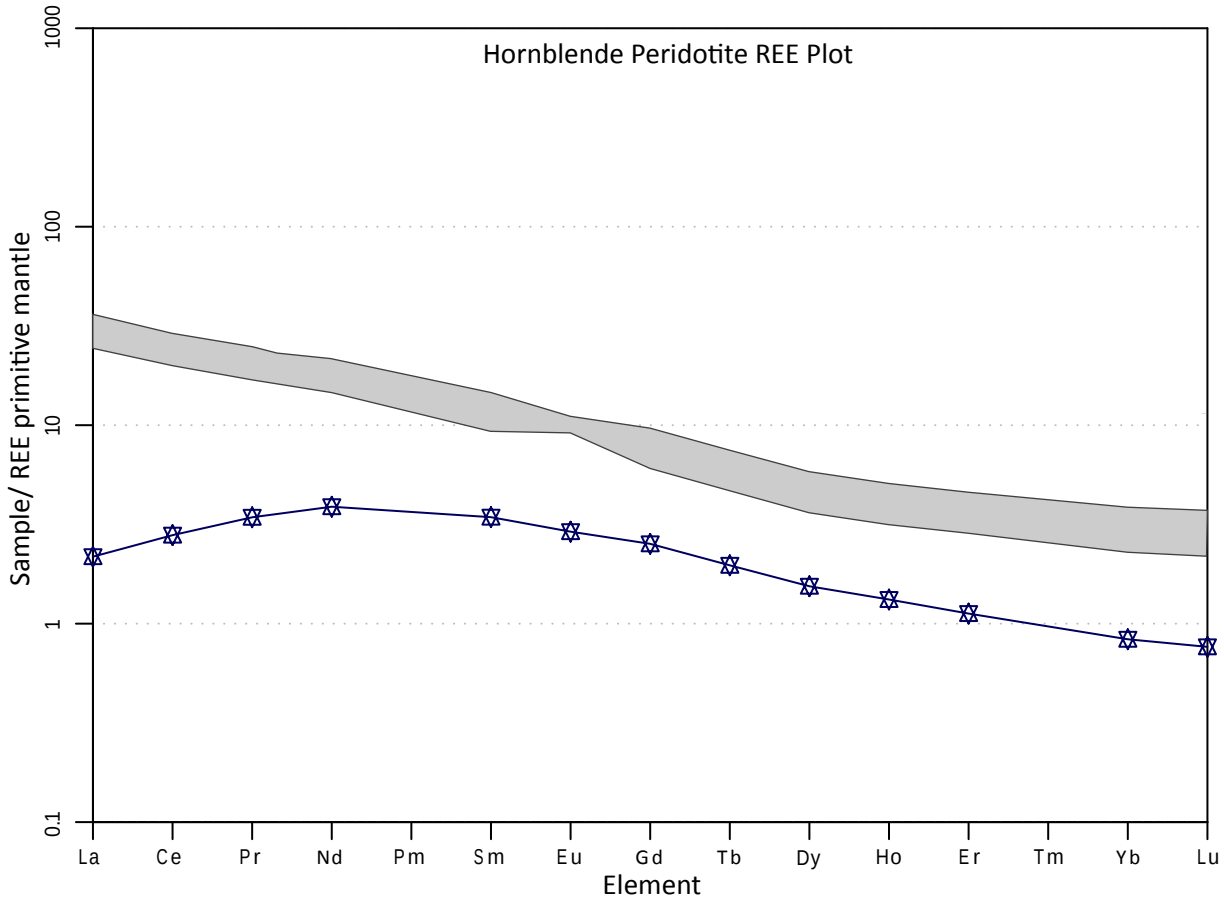

Fig 5.16 Spider diagram of hornblende peridotite normalised to primitive mantle values of Sun & McDonough (1989).
Fig 5.17 REE plot of hornblende peridotite normalised to primitive mantle values of McDonough et al., (1991). Shown in grey is the Spider and REE pattern for BOG.

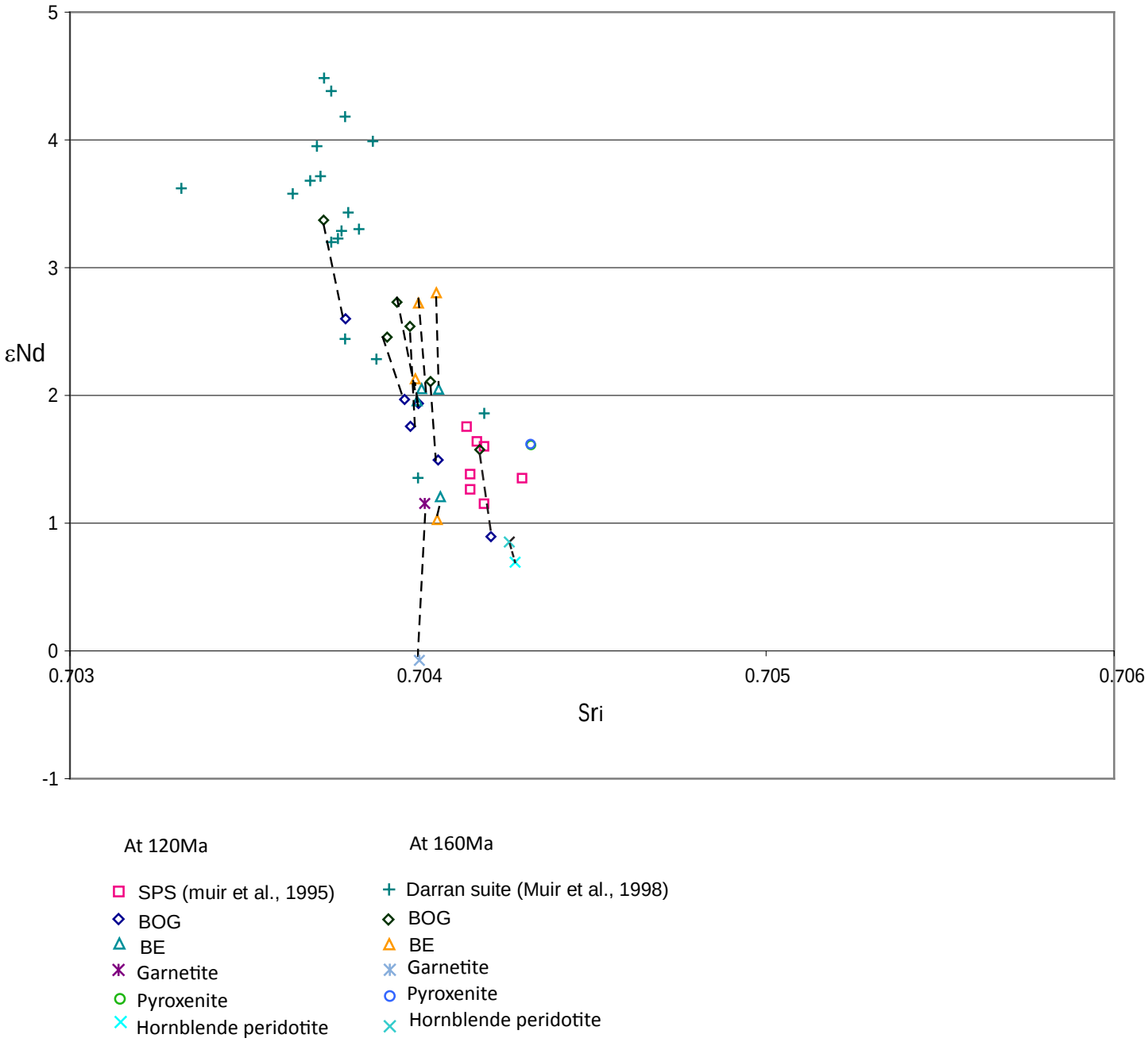

Fig 5.18 Sr_i vs. εNd for BOG, BE, garnetite, pyroxenite and hornblende peridotite. Data for SPS and Darran Suite is from McCulloch et al., (1987). dashed lines represent trend as Sr_i and εNd age is altered by +20Ma at each point. SPS data should be compared to the initial datapoint for samples from this study i.e. comparing both at 120Ma, while Darran suite data should be compared to the end point at each trendline.

6. Mineral Geochemistry

6.1 Methods

6.1.1 Mineral major element analysis by EMP

Polished thin sections of 30μm were petrographically examined and eight representative samples were selected for analysis by Electron Microprobe (EMP). Thin sections were prepared by Steve Craven and Manal Bebbington with assistance from James Watton. Analysis was undertaken in the Geochemical Analysis Unit (GAU) located in the Australian Research Council (ARC) National Key Centre for Geochemical Evolution and Metallogeny of Continents (GEMOC), based in the Department of Earth and Planetary Sciences at Macquarie University, Sydney, using a CAMECA SX100 EMP.

Thin sections were coated in carbon and kept free of oils and dirt to provide an evenly conductive surface. Operating conditions used were a 15keV accelerating voltage and 20nA beam current, with count times of 10s (peak and bkg). The EMP is fitted with five wavelength dispersive spectrometers and one energy dispersive spectrometer. LTAP (Al, Na), TAP (Si, Mg), LLIF (Fe, Mn, Ni, Cr) and LPET (Ti, Ca, K) crystals used. Standards used for calibration are shown in Table 6.01. Lower limits of detection (LLD) and %relative standard deviation (%rsd) are shown in Table 6.02. For Cr and Ni, Chromite and Nickel are used as the standard and so are 100 wt% oxides each. Analysis was undertaken by Norm Pearson, Nathan Daczko and James Watton.

	Standard used (wt% oxide)							
Major element	**Albite**	**Fe_2O_3**	**Kyanite**	**Olivine**	**Spessartine**	**Orthoclase**	**Wollastonite**	**Rutile**
SiO_2	68.13	0.00	37.01	41.16	36.05	64.65	51.72	0.00
TiO_2	0.00	0.00	0.00	0.00	0.03	0.00	0.00	100.04
Al_2O_3	19.76	0.00	62.70	0.00	20.63	17.04	0.00	0.00
FeO	0.01	89.99	0.17	7.62	1.66	1.69	0.00	0.00
MnO	0.00	0.00	0.00	0.10	40.87	0.00	0.00	0.00
MgO	0.00	0.00	0.02	50.77	0.00	0.00	0.00	0.00
CaO	0.38	0.00	0.00	0.00	0.46	0.00	48.28	0.00
Na_2O	11.46	0.00	0.00	0.00	0.00	0.94	0.00	0.00
K_2O	0.23	0.00	0.00	0.00	0.00	15.41	0.00	0.00

Table 6.01 Standards used for EMP calibration. Uderlined numbers are standard values used for respective major elements

Major element	LLD (wt%)	% rsd
SiO_2	0.03	0.27
TiO_2	0.02	0.19
Al_2O_3	0.01	0.18
Cr_2O_3	0.04	0.56
FeO	0.03	0.34
MnO	0.03	0.55
MgO	0.03	0.22
CaO	0.02	0.27
Na_2O	0.02	0.56
K_2O	0.01	0.49
NiO	0.03	0.30
P_2O_5	0.01	0.65
Cl	0.01	0.82

Table 6.02 LLD and %rsd for CAMECA SX100

PAP matrix corrections are automatically applied by CAMECA software. Data from EMP major element wt% oxide data, was converted to cations, balanced to relevant oxygen atoms (mineral dependant), had FeO converted to Fe_2O_3 (to achieve correct total cations) and checked for poor analyses (low totals, elements present but not analysed, hydrous minerals). This processed EMP data was then used for interpretation.

6.1.2 Mineral trace element analysis by LA-ICP-MS

Following petrographic examination, seven polished thick sections of ~200µm were prepared for analysis by laser ablation inductively coupled plasma mass spectrometry (LA-ICP-MS). Thick sections were prepared by Steve Craven and Manal Bebbington. Analysis was undertaken in the Geochemical Analysis Unit (GAU) located in the Australian Research Council (ARC) National Key Centre for Geochemical Evolution and Metallogeny of Continents (GEMOC), based in the Department of Earth and Planetary Sciences at Macquarie University, Sydney, using an Agilent 7500s LA-ICP-MS.

Operating conditions are listed in Table 6.03. Analyses were conducted by James Watton.

Variable	Parameter
ICP-MS type	Quadrupole
Make and Model	Agilent 7500s
Laser type	Nd:YAG
Make and Model	New Wave UP213
Beam Diameter	20 - 60µm
Carrier Gas	He in cell Ar added before plasma
Gas flow rate	0.8L/min
Laser pulse rate	5Hz
External Standard	NIST610
Reference Sample (for accuracy)	BCR-2G
Data processing and reduction software	GLITTER v4.4 rev. 525
Background count time	60s
Signal count time	120s
dwell time	30ms per isotope

Table 6.03 Operating conditions for LA-ICP-MS

Analyses were conducted in small runs varying from 5 – 12 samples in between standard measurements in the following order:

1. NIST610 x2
2. BCR-2 x1
3. Samples (5-12)
4. NIST610 x2

Single runs are kept to no longer than ~40min before NIST610 standard is measured. Data is corrected to NIST610 to account for instrument sensitivity and drift. BCR-2G reference sample is used for accuracy to real values and reproducibility of results. Measurements are conducted under operator supervision and are not commenced until background counts reach normal levels. After opening the laser cell (for sample changes), 30min is allowed to elapse to achieve nominal background counts and the NIST610 standard is measured twice, followed by the BDR-2 reference, before a new run can commence. Calcium from EMP analysis is used as an internal standard and the garnet run method is used.

Measured and expected concentrations for BCR-2G and NIST610 are listed in Table 6.04.

LLD's (for 99% confidence) and 1σ error are calculated on a single analysis basis and are given in Appendix 6.A and 6.B. Data is checked and optimum background and signal ranges are selected using the GLITTER software, poor analyses (laser ablating through one mineral into another, poor signal quality, high background) are rejected, data are then exported giving LLD filtered data (Appendix 6.E).

Element	NIST610 expected conc. (ppm)	1σ (ppm)	NIST610 measured conc. (ppm) Ave (n=32)	1σ (ppm)	%RSD	Measured/ expected	BCR-2G expected conc. (ppm)	1σ (ppm)	BCR-2G measured conc. (ppm) Ave (n=7)	1σ (ppm)	%RSD	Measured/ expected
Li			481.93	4.7	0.98				9.54	0.39	4.12	
Be			458.02	16.7	3.65				1.92	0.14	7.03	
Sc	450	3	449.76	4.0	0.88	1.00	33	0.8	30.53	1.04	3.42	0.93
Ti			476.13	4.7	0.98		13700	300	14455.50	269.44	1.86	1.06
V	444	7	445.44	8.7	1.94	1.00	414	8	421.16	10.29	2.44	1.02
Cr	388	6	388.68	4.8	1.24	1.00	35.8	1.3	35.72	0.93	2.60	1.00
Mn												
Co												
Ni	415	4	415.57	5.8	1.40	1.00	10.8	0.7	10.71	0.34	3.15	0.99
Cu												
Zn												
Ga	431	5	429.55	9.3	2.16	1.00	22.7	0.9	21.06	0.70	3.34	0.93
Rb	430	7	429.44	5.6	1.29	1.00	49	2	48.44	1.43	2.96	0.99
Sr	525	5	523.72	10.0	1.90	1.00	342	6	343.99	3.08	0.90	1.01
Y	490	4	488.66	9.9	2.03	1.00	35.3	0.7	30.92	1.01	3.28	0.88
Zr	490	4	488.63	9.8	2.01	1.00	194	4	175.11	5.58	3.19	0.90
Nb	512	6	511.48	5.3	1.03	1.00	12.8	0.4	13.59	0.39	2.87	1.06
Mo												
Cd												
Cs	361	8	360.04	7.2	1.99	1.00	1.13	0.08	1.08	0.05	4.25	0.96
Ba	446	4	444.31	10.6	2.38	1.00	660	19	693.15	8.40	1.21	1.05

Element	NIST610 expected conc. (ppm)	1σ (ppm)	NIST610 measured conc. (ppm) Ave (n=32)	1σ (ppm)	%RSD	Measured/ expected	BCR-2G expected conc. (ppm)	1σ (ppm)	BCR-2G measured conc. (ppm) Ave (n=7)	1σ (ppm)	%RSD	Measured/ expected
La	440	3	438.30	11.0	2.51	1.00	25	0.7	23.99	0.60	2.49	0.96
Ce	446	3	444.40	10.6	2.39	1.00	50.5	1.6	53.04	0.88	1.66	1.05
Pr	468	3	466.02	12.4	2.66	1.00	6.8	0.3	6.84	0.18	2.67	1.01
Nd	454	3	451.88	13.6	3.02	1.00	29	1	28.95	0.62	2.15	1.00
Sm	463	3	460.53	15.2	3.30	0.99	6.6	0.4	6.37	0.20	3.14	0.96
Eu	452	3	449.75	13.9	3.09	1.00	1.92	0.12	1.92	0.10	5.01	1.00
Tb												
Gd	450	5	447.55	15.3	3.42	0.99	6.5	0.4	5.89	0.24	4.10	0.91
Dy	453	4	450.58	15.4	3.42	0.99	6.5	0.4	5.78	0.30	5.26	0.89
Ho	475	3	472.25	17.7	3.75	0.99	1.3	0.08	1.11	0.10	8.92	0.85
Er	463	3	460.27	17.9	3.88	0.99	3.6	0.2	3.14	0.18	5.86	0.87
Yb	479	4	476.21	17.7	3.73	0.99	3.5	0.2	3.11	0.13	4.03	0.89
Lu	467	4	464.16	18.3	3.94	0.99	0.51	0.03	0.40	0.05	13.45	0.79
Hf	458	6	455.31	17.0	3.74	0.99	5	0.3	4.52	0.19	4.14	0.90
Ta	490	6	488.16	16.4	3.36	1.00	0.8	0.05	0.70	0.07	10.68	0.87
Pb			416.26	19.2	4.61		11.5	0.6	9.17	0.45	4.88	0.80
Th	481	3	477.49	22.8	4.77	0.99	6.1	0.3	5.75	0.17	3.03	0.94
U	487	3	484.06	18.5	3.81	0.99	1.73	0.09	1.78	0.11	6.33	1.03

Table 6.04 NIST610 and BCR-2G expected vs measured values. NIST610 values from Norman et al., (1996); BCR-2G values from Norman et al., (1998)

6.1.3 Mineral and symplectite examination using Element Mapping by EMP

Following petrographic examination, six polished thin sections (PTS) were selected for element mapping by Electron Microprobe (EMP). Polished thin sections were prepared by Steve Craven and Manal Bebbington with assistance from James Watton. Analysis was undertaken in the Geochemical Analysis Unit (GAU) located in the Australian Research Council (ARC) National Key Centre for Geochemical Evolution and Metallogeny of Continents (GEMOC), based in the Department of Earth and Planetary Sciences at Macquarie University, Sydney, using a CAMECA SX100 EMP.

PTS were coated in carbon and kept free of oils and dirt to provide an evenly conductive surface. Operating conditions used were a 15keV accelerating voltage and 100nA beam current, with count times of 150µs (peak, no background) and a 4µm step size between readings, map sizes included 512 x 512 and 256 x 256 pixels. Element mapping was conducted in two consecutive sessions, measuring nine major elements (Table 6.05). As each crystal can only measure one element oxide at a time, one element map actually consists of two mapping runs for each sample (Table 6.05). Table 6.06 shows which PTS were mapped in which session and at what size.

		Major element and crystal used								
		SiO_2	TiO_2	Al_2O_3	FeO	MnO	MgO	CaO	Na_2O	K_2O
Session 1	map run 1	TAP	LLIF	LTAP	LIF			LPET		
	map run 2					LLIF	TAP		LTAP	LPET
Session 2	map run 1	TAP	LIF	LTAP	LLIF			LPET		
	map run 2					LLIF	TAP		LTAP	LPET

Table 6.05 Session and run specific crystals used for element mapping

	Polished thin section					
	0906B	0905B	0909	0905C	0904C	0903B
session	1	1	2	2	2	2
map size (µm)	512x512	512x512	512x512	512x512	256x256	256x256

Table 6.06 Session order and map size used in element mapping

The main difference between sessions 1 and 2 was switching the analysing crystals for TiO_2 and FeO. This was done to aid matrix effect correction simplicity (outlined below) during processing. EMP calibration is performed as per methods and standards in section 6.1.1.

Element mapping data reduction was done according to the following procedure:

1. Export element maps to ASCII using EMP software – one file per element.
2. Change filenames to reflect PTS name and element suffix eg. *jww0904CSi.txt*
3. Delete header information
4. Run *elmap_incl_Ti.m* script using MATLAB eg. *elmap_inl_Ti(256,512,'jww0905B');*(Appendix 6.C)
   User must type *save fname fname* to save the processed data to a file.
   At this point, data is in a single matrix, prepared for Bence Albee matrix corrections (from cps to wt% oxide)
5. At this point in testing background correction scripts were run using MATLAB (see discussion); *BackgroundCorrection_cpx.m* and *BackgroundCorrection_grt.m* (Appendix 6.C)
6. Run *BenceAlbee_Love_Scott.m* or *BenceAlbee_Kato_Transposed.m* scripts using MATLAB to perform Bence Albee matrix corrections according to the alpha factors and resultant beta factors from Love & Scott (1984) or Kato (2005) (Appendix 6.C)
   User must select *fname.mat*, enter count time (150µs) and iterations (3)
   File saved as *fnameba_LS.mat* or *fnameba_K_Tr.mat*
7. At this point during testing, garnet, clinpyroxene and plagioclase masking scripts were run using MATLAB (see discussion); *filter0906B.m* and *filter0905B.m* (Appendix 6.C)
8. Run *ELMAPGUI.m* script using MATLAB to explore the processed wt% oxide data in a Graphical User Interface (Appendix 6.C)
   User must select either the *fnameba_LS.mat* or *fnameba_k_Tr.mat* file
   Adjust wt% oxide cutoffs for individual elements and export element mapping screenshots.

Scripts used are modified from scripts written by Daczko, N. (2001) to include Ti and updated alpha and beta factors, as well as new scripts made for background removal and data masking. Scripts modified and written by Nathan Daczko and James Watton.

Alpha and beta factors for Love & Scott (1984) and Kato (2005) are given in Table 6.07 and comparison between PAP matrix correction and Bence-Albee matrix corrections for background corrected and uncorrected data are shown in Table 6.08.

	Love & Scott α-factors (Armstrong, 1984 Microbeam Analysis)									
	Emitter									
Absorber	Si	Ti	Al	Fe	Mn	Mg	Ca	Na	K	
SiO_2	1.000	1.111	0.999	1.148	1.161	1.086	1.091	1.352	1.144	Si
TiO_2	1.083	1.000	1.220	1.087	1.113	1.440	0.863	2.021	0.935	Ti
Al_2O_3	1.494	1.089	1.000	1.128	1.140	1.009	1.068	1.242	1.118	Al
FeO	1.279	0.894	1.556	1.000	1.014	2.013	0.932	3.066	0.987	Fe
MnO	1.211	0.846	1.451	0.987	1.000	1.846	0.902	2.778	0.959	Mn
MgO	1.431	1.099	1.756	1.141	1.153	1.000	1.073	1.130	1.120	Mg
CaO	1.048	1.161	1.149	1.124	1.149	1.302	1.000	1.741	0.858	Ca
Na_2O	1.356	1.071	1.645	1.114	1.125	2.134	1.044	1.000	1.088	Na
K_2O	0.987	1.132	1.072	1.093	1.117	1.196	1.197	1.564	1.000	K
	standards used									
Albite	0.68	0.00	0.20	0.00	0.00	0.00	0.00	0.11	0.00	
Fe2O3	0.00	0.00	0.00	0.90	0.00	0.00	0.00	0.00	0.00	
Kyanite	0.37	0.00	0.63	0.00	0.00	0.00	0.00	0.00	0.00	
Olivine	0.41	0.00	0.00	0.08	0.00	0.51	0.00	0.00	0.00	
MnGarnet	0.36	0.00	0.21	0.02	0.41	0.00	0.00	0.00	0.00	
Orthoclase	0.65	0.00	0.17	0.02	0.00	0.00	0.00	0.01	0.15	
CaSiO3	0.52	0.00	0.00	0.00	0.00	0.00	0.48	0.00	0.00	
TiO2	0.00	1.00	0.00	0.00	0.00	0.00	0.00	0.00	0.00	
	β-factors									
	Si	Ti	Al	Fe	Mn	Mg	Ca	Na	K	
	1.023153047	1.000439969	0.999554086	1.128935799	1.084905728	1.109841781	1.047044051	1.29164622	1.111077012	

Table 6.07A Bence-Albee Calculation of Wt% conc. of oxides from x-ray counts. Love & Scott (1984).

	Kato α-factors (2005)									
	Emitter									
Absorber	Si	Ti	Al	Fe	Mn	Mg	Ca	Na	K	
SiO_2	1	1.127	1.028	1.173	1.186	1.113	1.114	1.416	1.175	Si
TiO_2	1.055	1.000	1.18	1.102	1.127	1.368	0.877	1.889	0.948	Ti
Al_2O_3	1.448	1.103	1.000	1.151	1.164	1.035	1.087	1.294	1.144	Al
FeO	1.202	0.880	1.417	1.000	0.979	1.745	0.919	2.541	0.978	Fe
MnO	1.138	0.836	1.325	0.988	1.000	1.606	0.888	2.313	0.949	Mn
MgO	1.45	1.114	1.741	1.165	1.177	1.000	1.096	1.182	1.152	Mg
CaO	1.032	1.171	1.136	1.140	1.166	1.283	1.000	1.724	0.900	Ca
Na_2O	1.357	1.083	1.618	1.136	1.148	2.044	1.062	1.000	1.112	Na
K_2O	0.969	1.14	1.054	1.104	1.130	1.177	1.218	1.548	1.000	K
	standards used									
Albite	0.68	0.00	0.20	0.00	0.00	0.00	0.00	0.11	0.00	
Fe2O3	0.00	0.00	0.00	0.90	0.00	0.00	0.00	0.00	0.00	
Kyanite	0.37	0.00	0.63	0.00	0.00	0.00	0.00	0.00	0.00	
Olivine	0.41	0.00	0.00	0.08	0.00	0.51	0.00	0.00	0.00	
MnGarnet	0.36	0.00	0.21	0.02	0.41	0.00	0.00	0.00	0.00	
Orthoclase	0.65	0.00	0.17	0.02	0.00	0.00	0.00	0.01	0.15	
CaSiO3	0.52	0.00	0.00	0.00	0.00	0.00	0.48	0.00	0.00	
TiO2	0.00	1.00	0.00	0.00	0.00	0.00	0.00	0.00	0.00	
	β-factors									
	Si	Ti	Al	Fe	Mn	Mg	Ca	Na	K	
	1.015428486	1.000439969	1.010051387	1.151411269	1.098371433	1.100303146	1.058939521	1.345380807	1.135623436	

Table 6.07B Bence-Albee Calculation of Wt% conc. of oxides from x-ray counts. Kato (2005).

	Kato Transposed α-factors (2005)									
	Emitter									
Absorber	Si	Ti	Al	Fe	Mn	Mg	Ca	Na	K	
SiO_2	1	1.055	1.448	1.202	1.138	1.45	1.032	1.357	0.969	Si
TiO_2	1.127	1.000	1.103	0.880	0.836	1.114	1.171	1.083	1.14	Ti
Al_2O_3	1.028	1.18	1.000	1.417	1.325	1.741	1.136	1.618	1.054	Al
FeO	1.173	1.102	1.151	1.000	0.988	1.165	1.140	1.136	1.104	Fe
MnO	1.186	1.127	1.164	0.979	1.000	1.177	1.166	1.148	1.130	Mn
MgO	1.113	1.368	1.035	1.745	1.606	1.000	1.283	2.044	1.177	Mg
CaO	1.114	0.877	1.087	0.919	0.888	1.096	1.000	1.062	1.218	Ca
Na_2O	1.416	1.889	1.294	2.541	2.313	1.182	1.724	1.000	1.548	Na
K_2O	1.175	0.948	1.144	0.978	0.949	1.152	0.900	1.112	1.000	K
	standards used									
Albite	0.68	0.00	0.20	0.00	0.00	0.00	0.00	0.11	0.00	
Fe2O3	0.00	0.00	0.00	0.90	0.00	0.00	0.00	0.00	0.00	
Kyanite	0.37	0.00	0.63	0.00	0.00	0.00	0.00	0.00	0.00	
Olivine	0.41	0.00	0.00	0.08	0.00	0.51	0.00	0.00	0.00	
MnGarnet	0.36	0.00	0.21	0.02	0.41	0.00	0.00	0.00	0.00	
Orthoclase	0.65	0.00	0.17	0.02	0.00	0.00	0.00	0.01	0.15	
CaSiO3	0.52	0.00	0.00	0.00	0.00	0.00	0.48	0.00	0.00	
TiO2	0.00	1.00	0.00	0.00	0.00	0.00	0.00	0.00	0.00	
	β-factors									
	Si	Ti	Al	Fe	Mn	Mg	Ca	Na	K	
	1.055016858	1.000439969	1.164922395	1.457809148	1.113058804	1.194402014	1.016529585	1.365594366	0.993350837	

Table 6.07C Bence-Albee Calculation of Wt% conc. of oxides from x-ray counts. Kato (2005).

PTS no. used for testing	Known PAP corr. From probe	Pk-Bgd Bence-Albee correction of raw EMP data (Love & Scott)		Pk-Bgd Bence-Albee correction of raw EMP data (Kato)		Map total 0906B (Love & Scott)				Map total 0906B (Kato)			
		t=1s Iterations=10	%Relative Deviation	t=.995s Iterations=10	%Relative Deviation	t=0.133s Iterations=3	%Relative Deviation	t=0.125s Iterations=3	%Relative Deviation	t=0.132s Iterations=3	%Relative Deviation	t=0.125s Iterations=3	%Relative Deviation
0906B grt core						No corr.		Bkg corr. t=0.150s		No corr.		Bkg corr. t=0.150s	
SiO2	39.43	40.30	2.21	35.90	8.95	39.30	0.33	41.49	5.23	35.15	10.85	36.79	6.69
TiO2	0.04	0.04	2.20	0.04	2.20	0.03	26.65	0.00	97.56	0.04	2.20	0.00	100.00
Al2O3	22.25	22.52	1.20	22.61	1.60	21.48	3.48	22.35	0.43	21.20	4.74	22.19	0.29
Cr2O3	0.02	-		-		-		-		-		-	
Fe2O3	0.00	-		-		-		-		-		-	
FeO	19.96	18.58	6.91	20.49	2.66	21.03	5.36	19.37	2.96	23.26	16.53	21.31	6.76
MnO	0.58	0.59	1.10	0.61	4.52	0.77	31.94	0.30	48.59	0.80	37.08	0.31	46.88
MgO	10.12	10.16	0.44	11.28	11.52	11.21	10.82	11.49	13.59	12.13	19.92	12.64	24.96
CaO	8.18	8.13	0.62	8.54	4.39	8.21	0.36	8.66	5.86	8.65	5.74	9.05	10.63
Na2O	0.03	0.03	7.14	0.02	28.57	0.13	364.29	0.02	28.57	0.10	257.14	0.02	28.57
K2O	0.00	0.00	0.00	0.00	0.00	0.10	100.00	0.00	0.00	0.10	100.00	0.00	0.00
NiO2	0.02	-		-		-		-		-		-	
Total	100.61	100.35	0.26	99.49	1.11	102.26	1.64	103.68	3.05	101.43	0.81	102.31	1.69
FeO	19.96	18.58	6.91	20.49	2.66								
omp core													
SiO2	50.71	51.64	1.84	49.40	2.57	48.07	5.20	50.83	0.25	45.95	9.38	48.25	4.84
TiO2	0.67	0.66	1.11	0.66	1.11	0.11	83.52	0.00	100.00	0.11	83.52	0.00	100.00
Al2O3	7.87	7.95	1.00	8.52	8.24	8.54	8.50	8.67	10.15	9.04	14.85	9.30	18.15
Cr2O3	0.01	-		-		-				-			
Fe2O3	0.00	-		-		-				-			
FeO	7.65	7.12	6.93	7.75	1.31	7.79	1.83	6.38	16.60	8.57	12.03	6.94	9.28
MnO	0.04	0.04	7.41	0.04	7.41	0.19	339.81	0.00	100.00	0.20	362.96	0.00	100.00
MgO	10.74	10.76	0.16	11.87	10.49	10.81	0.62	11.22	4.44	11.82	10.03	12.36	15.05
CaO	19.34	19.23	0.55	19.77	2.24	19.70	1.88	20.99	8.55	20.38	5.40	21.43	10.83
Na2O	3.09	3.14	1.67	2.76	10.63	3.35	8.47	3.24	4.91	2.92	5.45	2.90	6.10
K2O	0.00	0.00	0.00	0.00	0.00	0.09	4900.00	0.00	0.00	0.09	4900.00	0.00	0.00
NiO2	0.02	-											
Total	100.13	100.54	0.41	100.77	0.64	98.65	1.48	101.33	1.20	99.08	1.05	101.18	1.05
FeO	7.65	7.12	6.95	7.75	1.28								

Table 6.08 Comparative matrix correction results on PTS 0906B. %Relative Deviation = ABS[{1-(result/PAP value)}*100].
grt core bkg corrections are based on average garnet bkg counts. omp core bkg corrections are based on average omphacite bkg counts. See in text (Chapter 7) for explanation of colours.

6.2 Results

Complete EMP data is available in Appendix 6.D and LA-ICP-MS data is available in Appendix 6.E. Grey fields showing mineral major (EMP) and trace element (LA-ICP-MS) compositions/concentrations have been included in plots of other lithologies to allow for ease of comparison to the main BOG unit, excluding outliers (from symplectites) except for the calcic amphibole classification plot (Fig. 6.09), which shows pargasite from the Hawes Head Ultramafics study of Emami (2008) as a grey field, for comparison to the hornblende peridotite. Fields are contoured to represent data density, when needed (indicated on figures).

6.2.1 Electron Microprobe (EMP)

Breaksea Omphacite Granulite

Garnet in the BOG ranges from an average composition of $Alm_{43}Pyp_{38}Grs_{18}Sps_{1}$ at mineral grain cores to $Alm_{46}Pyp_{28}Grs_{23}Sps_{3}$ at mineral grain rims (Figs. 6.01 & 6.02) (Alm = almandine, Pyp = pyrope, Grs = grossular and Sps = Spessartine),
showing a general downward trend in the pyrope end member and an upward trend in the grossular (strong) and almandine (weaker) end members, moving from the garnet core to rim (Figs. 6.01 – 6.03). Garnet variation occurs within 150µm of the grain boundary. The BOG variant 0905C contains no garnet.

Both Quad and Ca-Na group pyroxenes (Morimoto et al., 1988) are present in the BOG with the majority of pyroxene grains being Ca-Na group pyroxenes (Fig. 4.04). Quad group pyroxenes in the BOG were only found within symplectites and are classified as diopside (Fig 6.05). Ca-Na group pyroxenes present are all classified as omphacite, concurring with petrographic examination (Fig. 6.06). The BOG variant 0905C contains Quad and Ca-Na group pyroxenes, with diopside within symplectites and orthopyroxene observed in thin section present as enstatite (Fig. 6.05), omphacite is the only Ca-Na pyroxene in sample 0905C (Fig. 6.06).

Plagioclase shows weak zoning (Fig. 6.07), varying from core values of an average $Ab_{73}An_{25}Or_2$ to rim values of an average $Ab_{82}An_{16}Or_2$, indicating an increase in albite and decrease in anorthite end members from core to rim (Fig 6.08) (Ab = albite, An = anorthite and Or = orthoclase). Symplectites from sample 0909 contain plagioclase with an andesine to labradorite composition ($Ab_{48-60}An_{50-48}Or_2$) (Fig. 6.08). There is some potassium feldspar in both BOG samples (Fig. 6.08). A traverse across a plagioclase grain in the BOG variant 0905C shows similar zoning to the main BOG (Fig. 6.07).

Hornblende is present in sample 0905B of the BOG as the calcic amphibole pargasite (Leake et al., 1997) (Fig. 6.09). Element mapping will further examine chemical zoning in the BOG (this chapter).

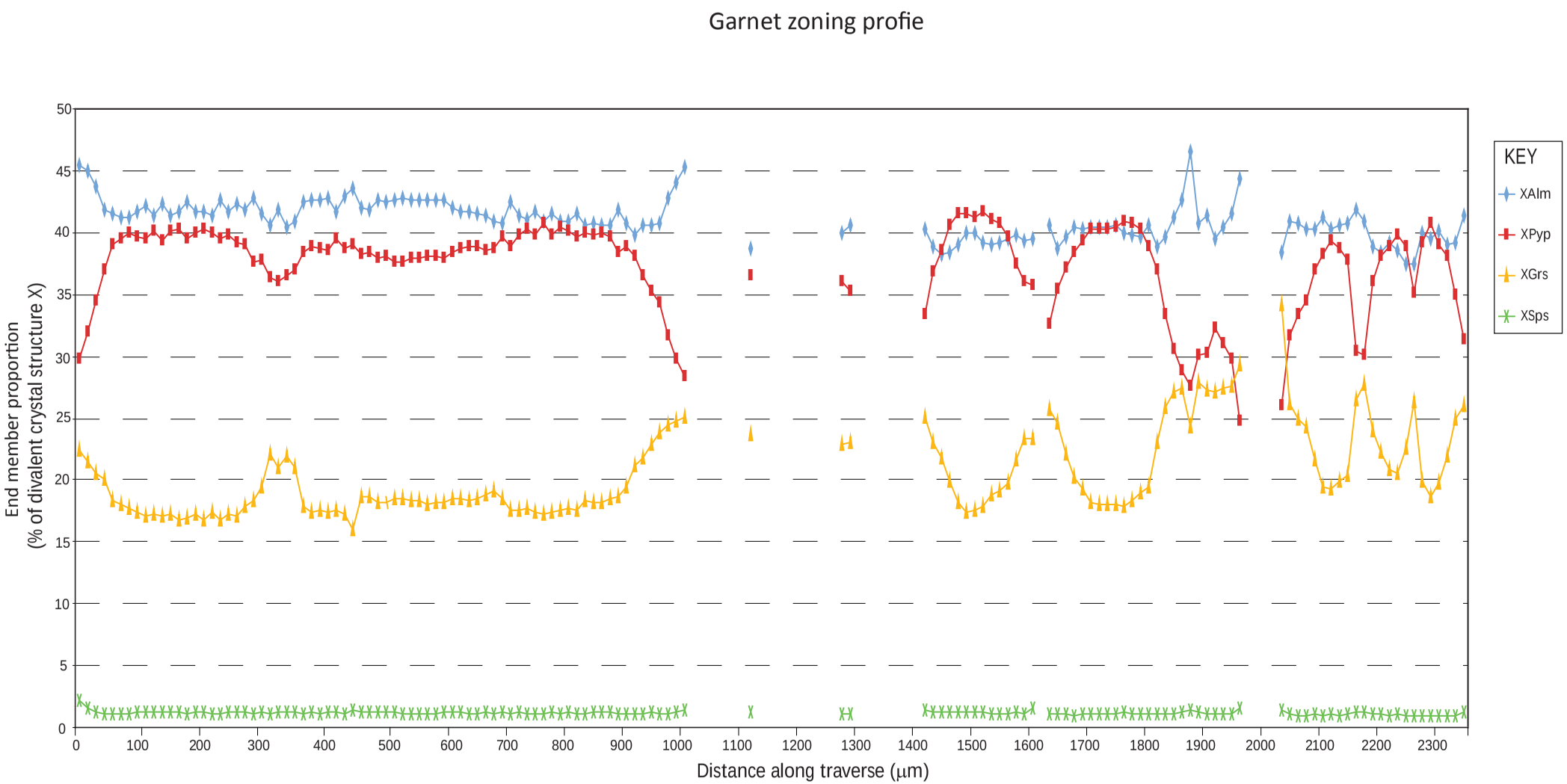

Fig 6.01 Garnet zoning in BOG (0909). Structure used is $X_3Y_2Si_3O_{12}$

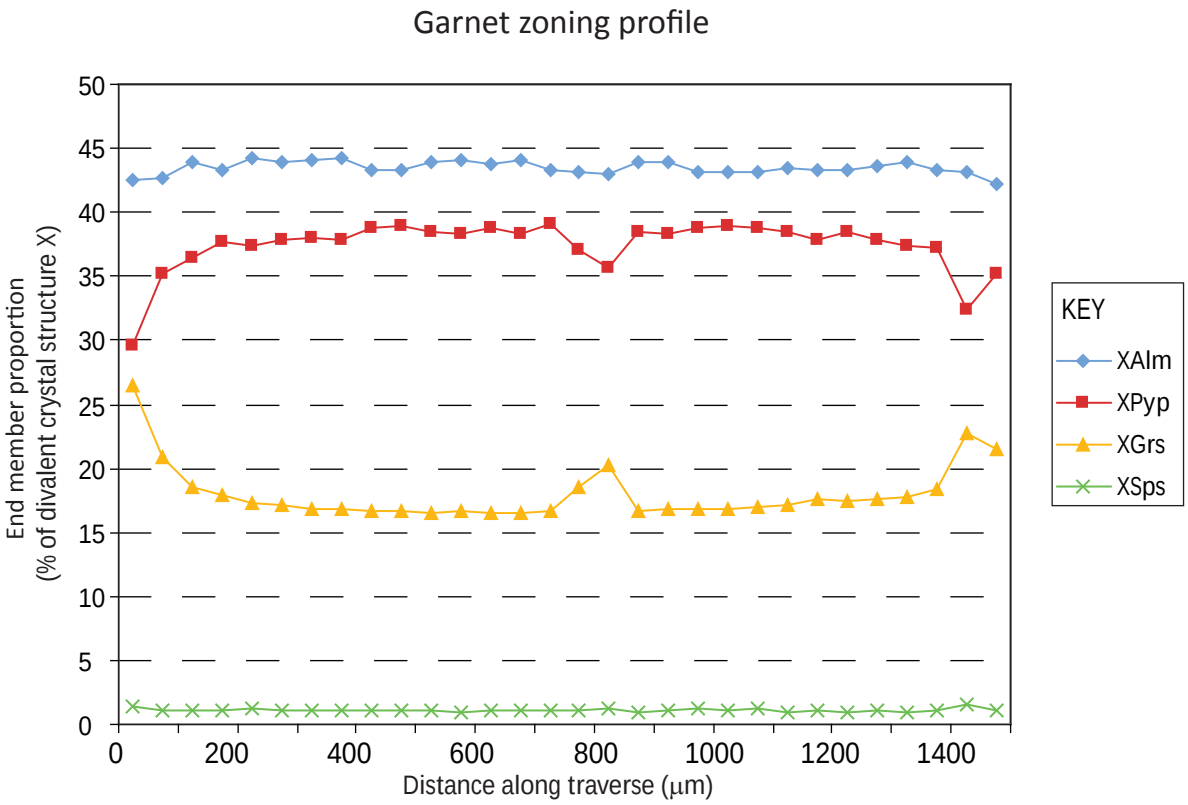

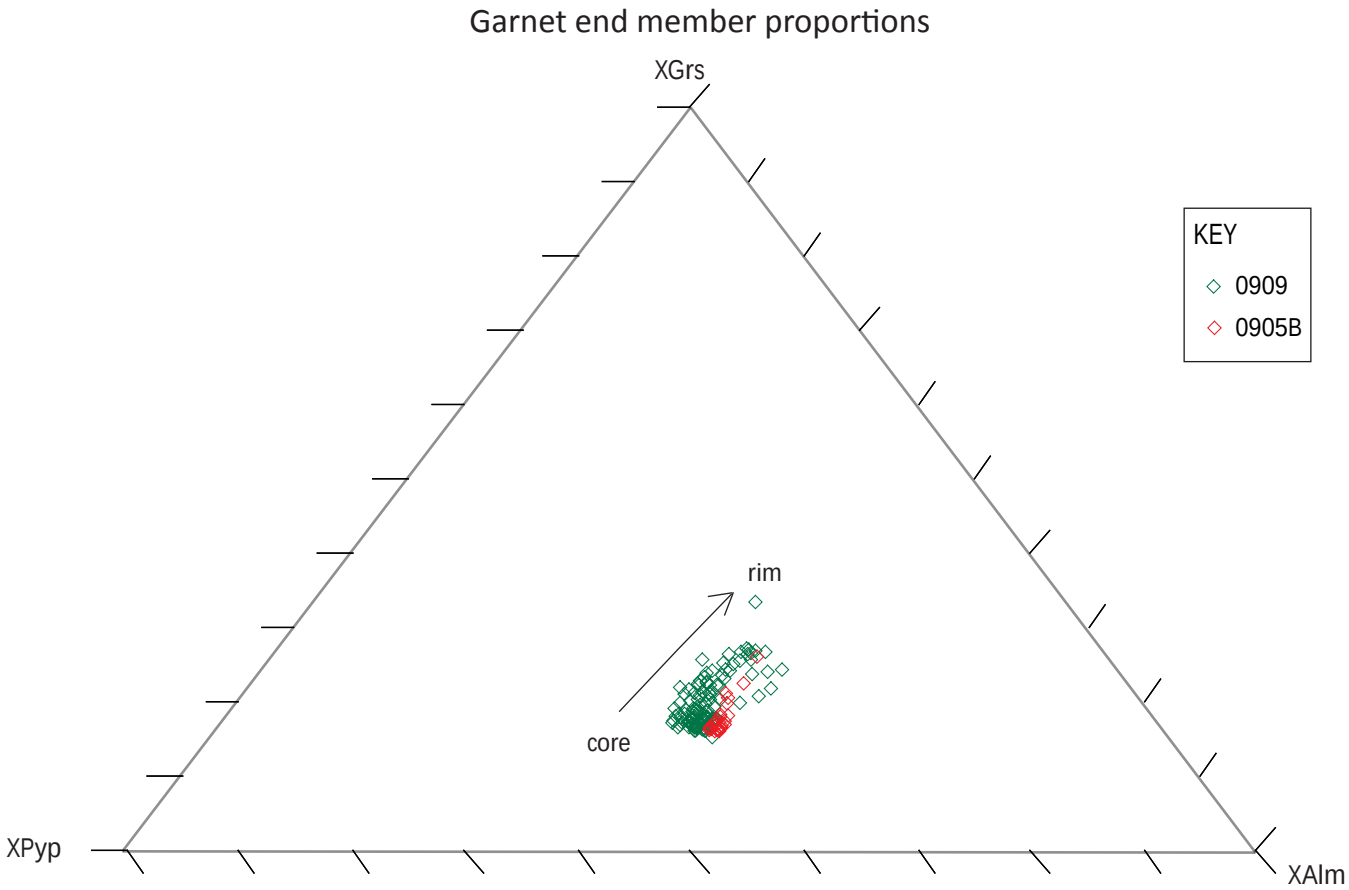

Fig 6.02 Garnet zoning in BOG (0905B). Structure used is $X_3Y_2Si_3O_{12}$
Fig 6.03 Ternary plot showing BOG core/rim variation in garnet end member proportions.

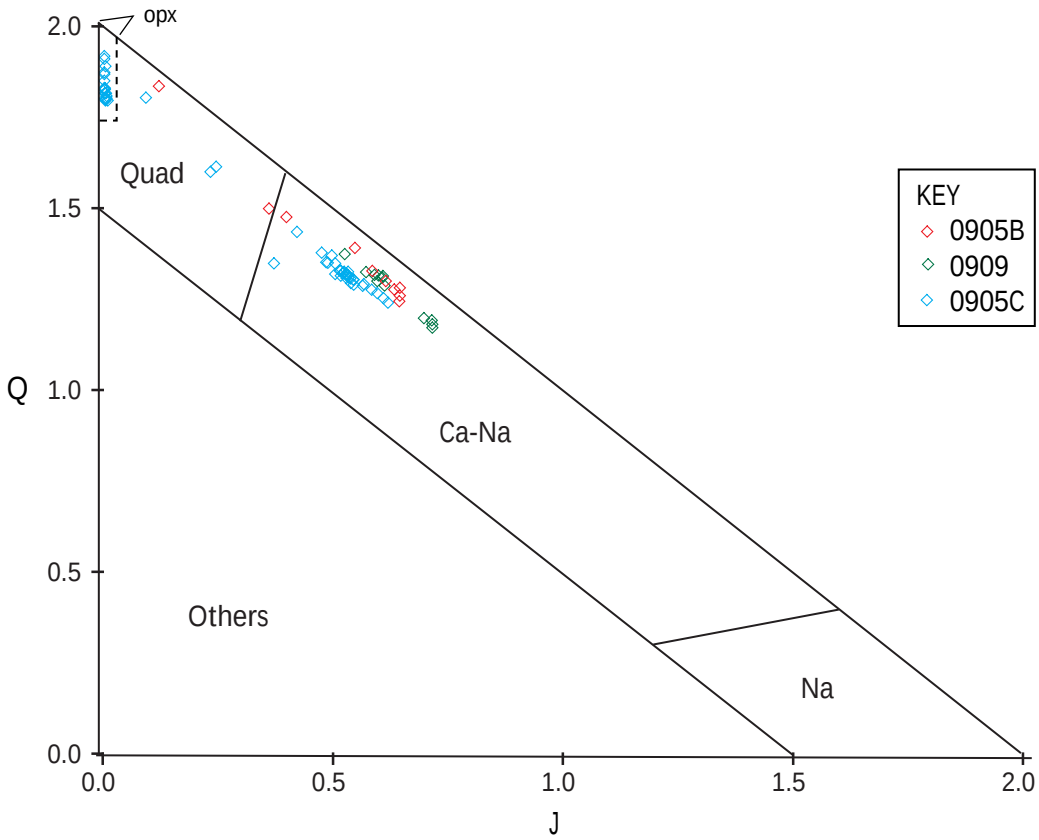

Fig 6.04 Q-J classification diagram (Morimoto et al., 1988) for BOG (0905B & 0909) and BOG variant (0905C) $Q=Ca^{2+}+Mg^{2+}+Fe^{2+}$(molar); $J=2xNa^{+}$(molar).

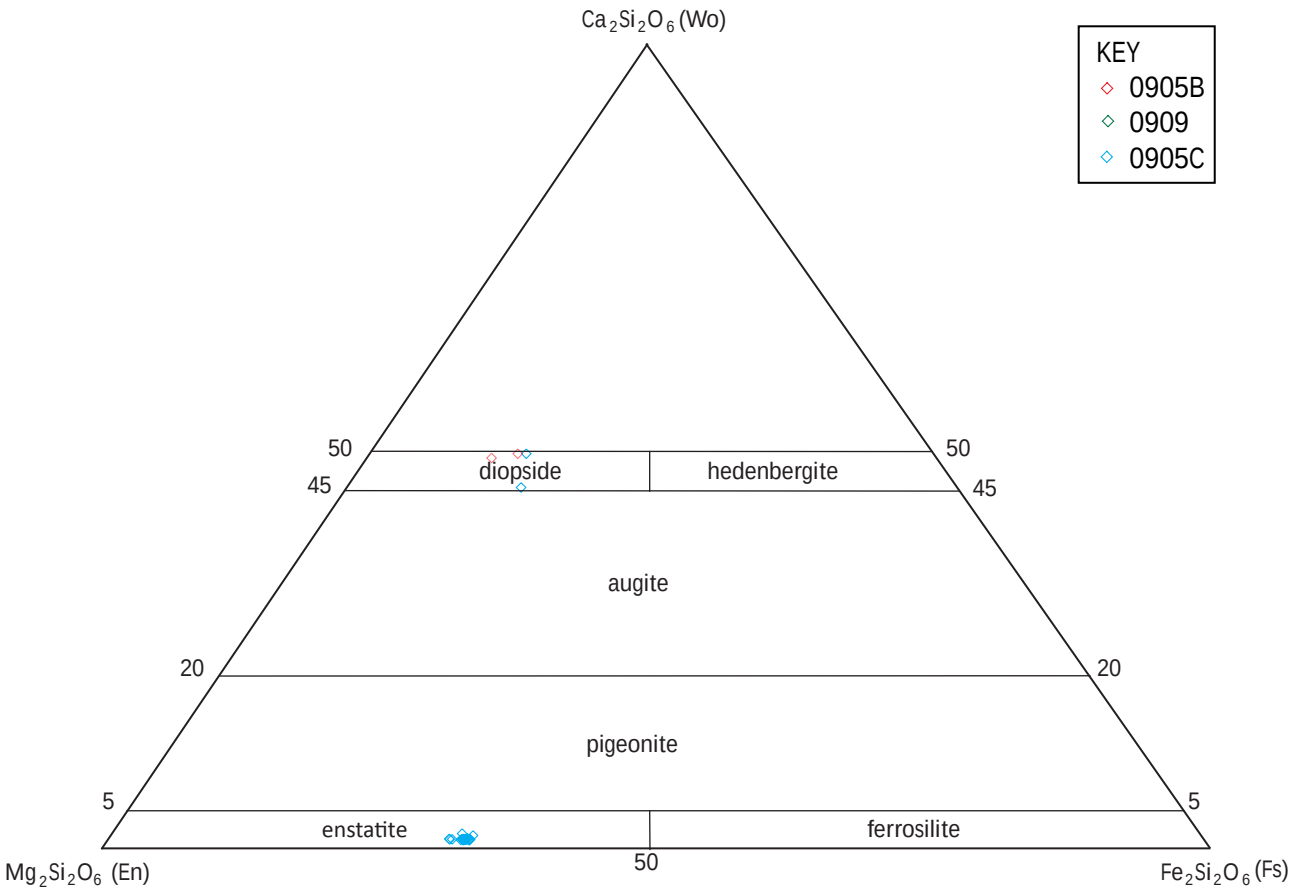

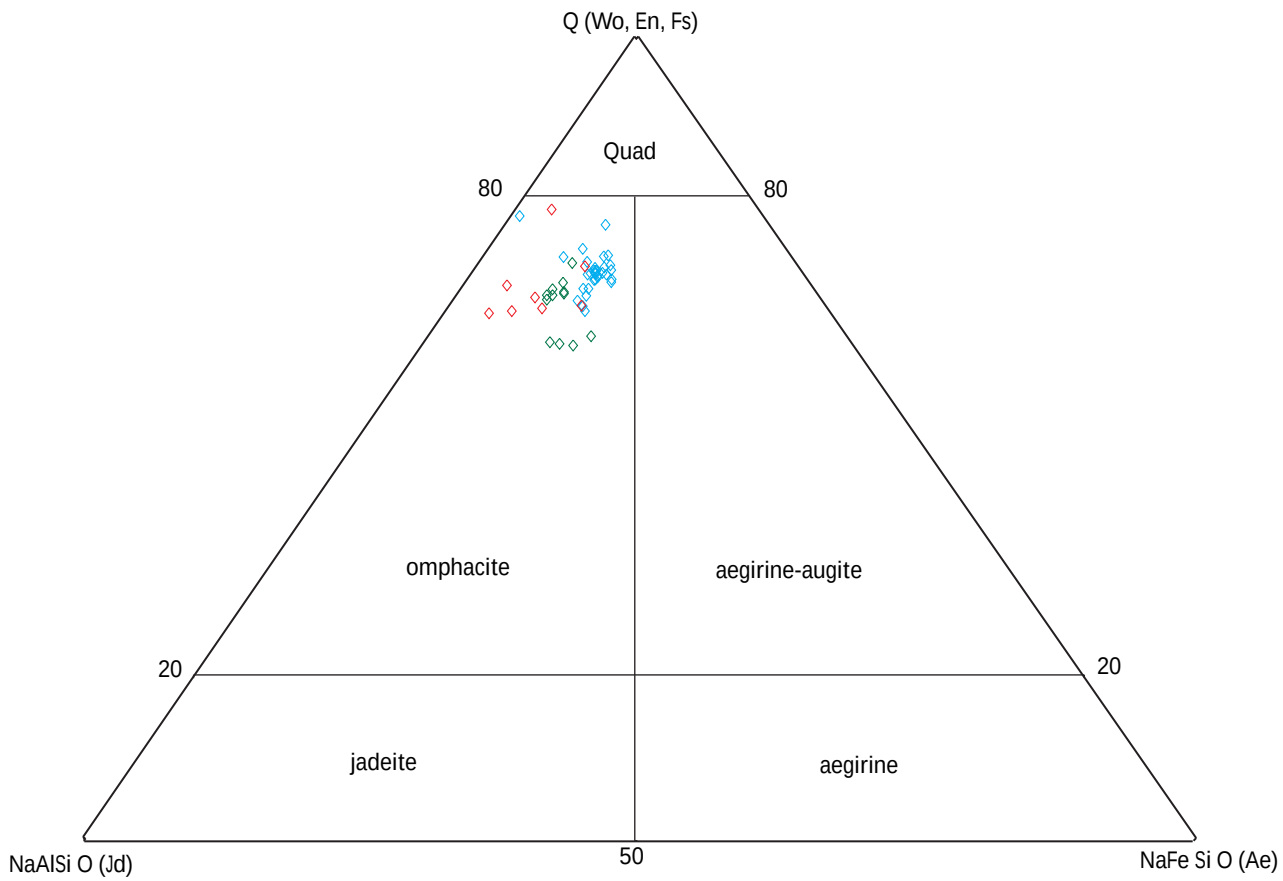

Fig 6.05 classification diagram for Ca pyroxenes (Morimoto et al., 1988) for BOG (0905B & 0909) and BOG variant (0905C)
Fig 6.06 classification diagram for Ca-Na pyroxenes (Morimoto et al., 1988) for BOG (0905B & 0909) and BOG variant (0905C)

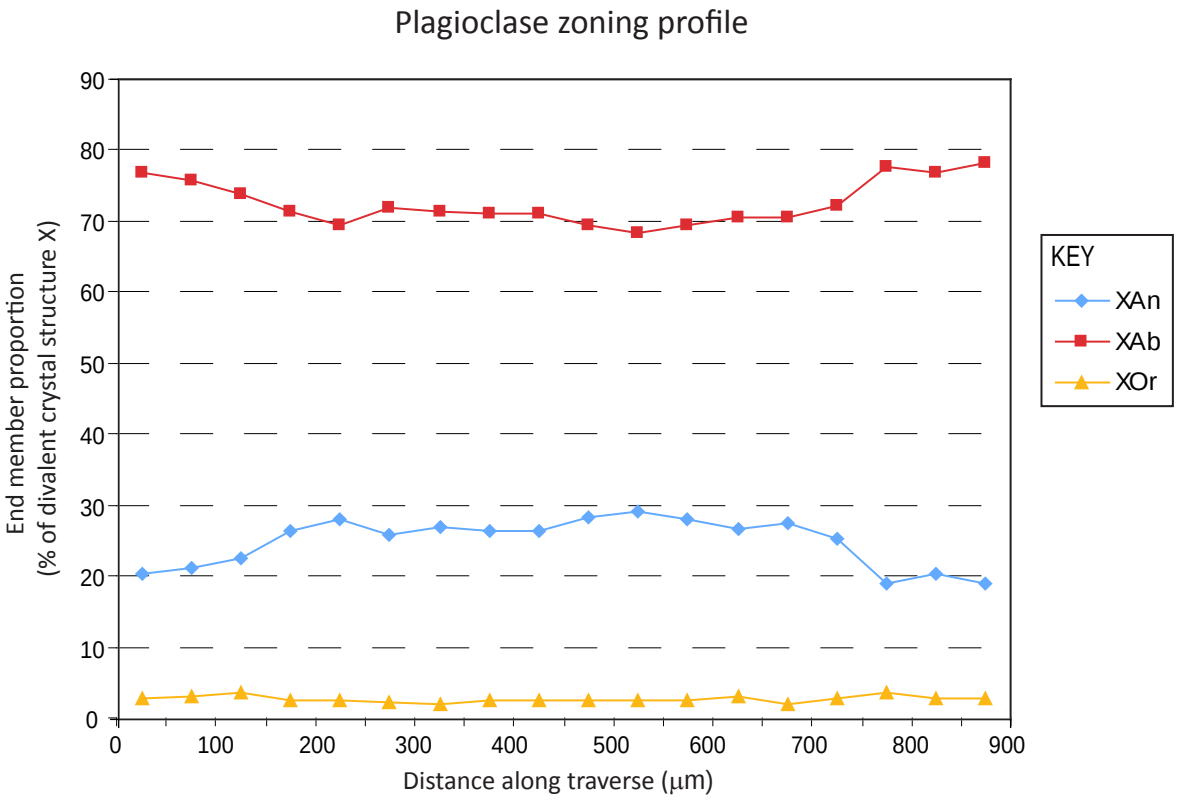

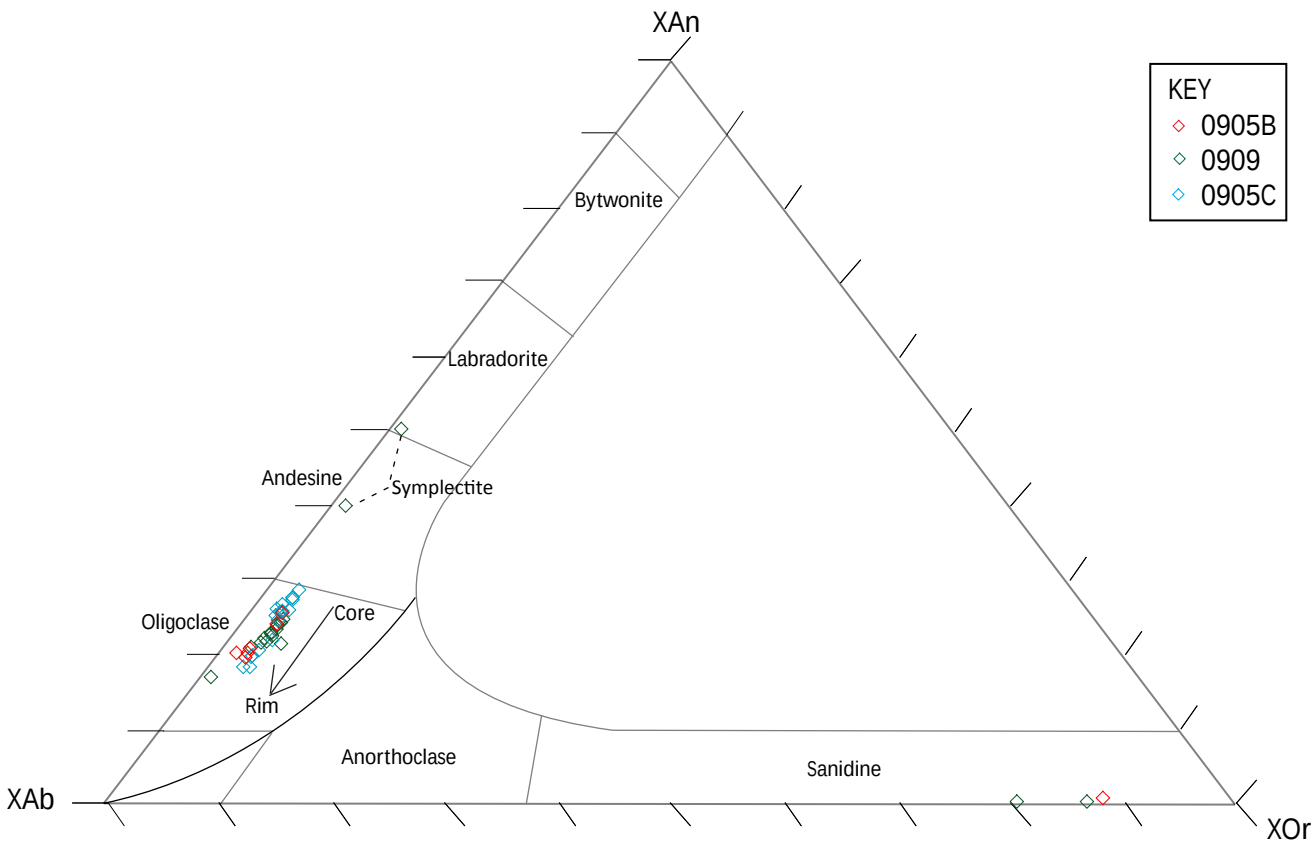

Fig 6.07 Plagioclase zoning in BOG variant (0905C).
Plagioclase structure is $XAlSi_3O_8$ where X=K,$^+$Na$^+$, Ca^{2+}(NB when X=Ca^{2+}, Si=Si_2 and Al=Al_2).

Fig 6.08 Ternary plot showing BOG (0905B & 0909) and BOG variant (0905C) core/rim variation in plagioclase end member proportions. Feldspar ternary boundaries from Deer et al., 1966)

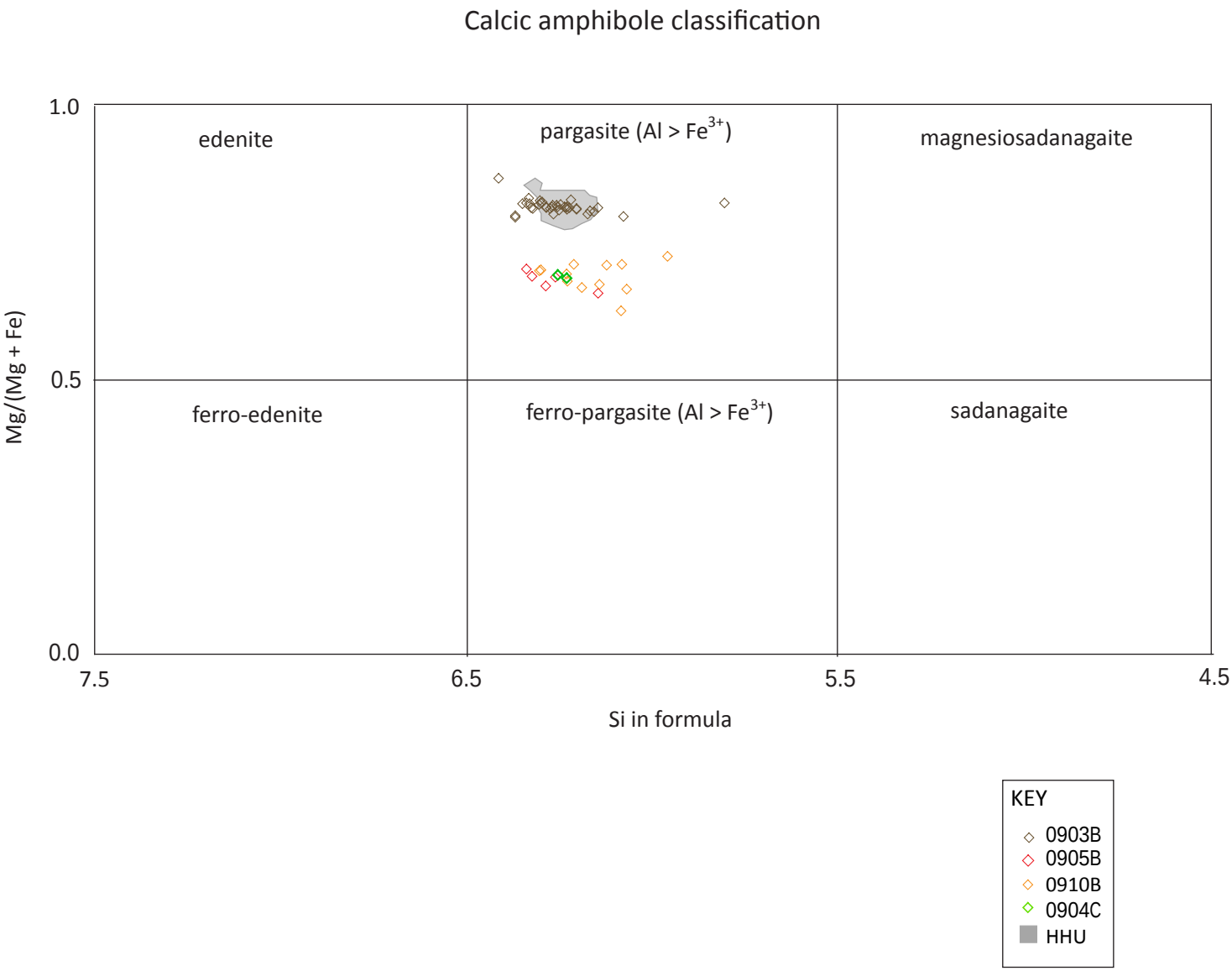

Fig 6.09 Calcic amphibole classification (Leake et al., 1997) of all amphibole grains. HHU values from Emami (2008)

Breaksea Eclogite

Garnet composition of the BE ranges from $Alm_{38}Pyp_{34}Grs_{26}Sps_{1}$ at mineral cores to $Alm_{44}Pyp_{27}Grs_{27}Sps_{2}$ at mineral rims, indicating an upward trend in almandine and downward trend in pyrope end members from core to rim (Figs. 6.10 & 6.11). Garnet variation occurs within 200µm of grain boundaries, as the garnet mineral traverse indicates (Fig. 6.10).

The BE contains only Ca-Na group pyroxenes (Morimoto et al., 1988) (Fig. 6.12) which are classified as both omphacite and aegerine-augite (Fig. 6.13). Element mapping (this chapter) will further determine the nature of pyroxene and plagioclase within symplectites in the BE. Hornblende present in BE symplectites is the calcic amphibole pargasite (Leake et al., 1997) (Fig. 6.09).

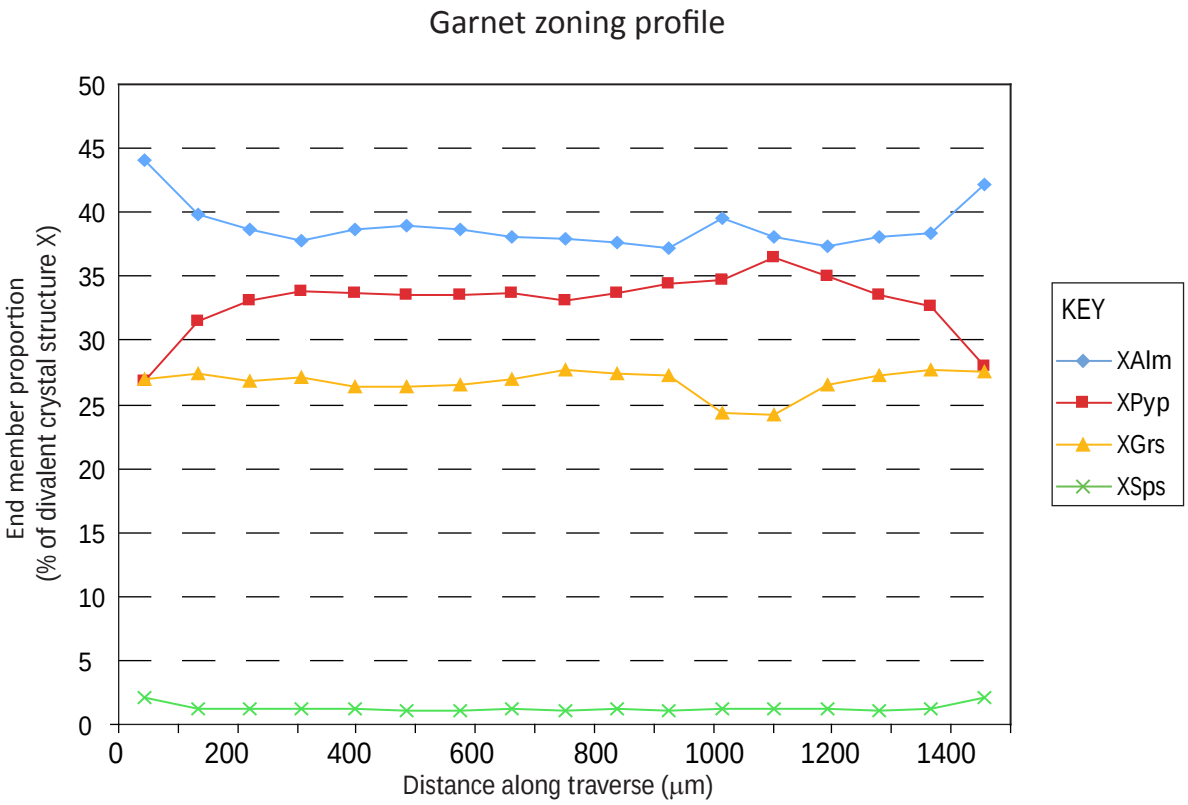

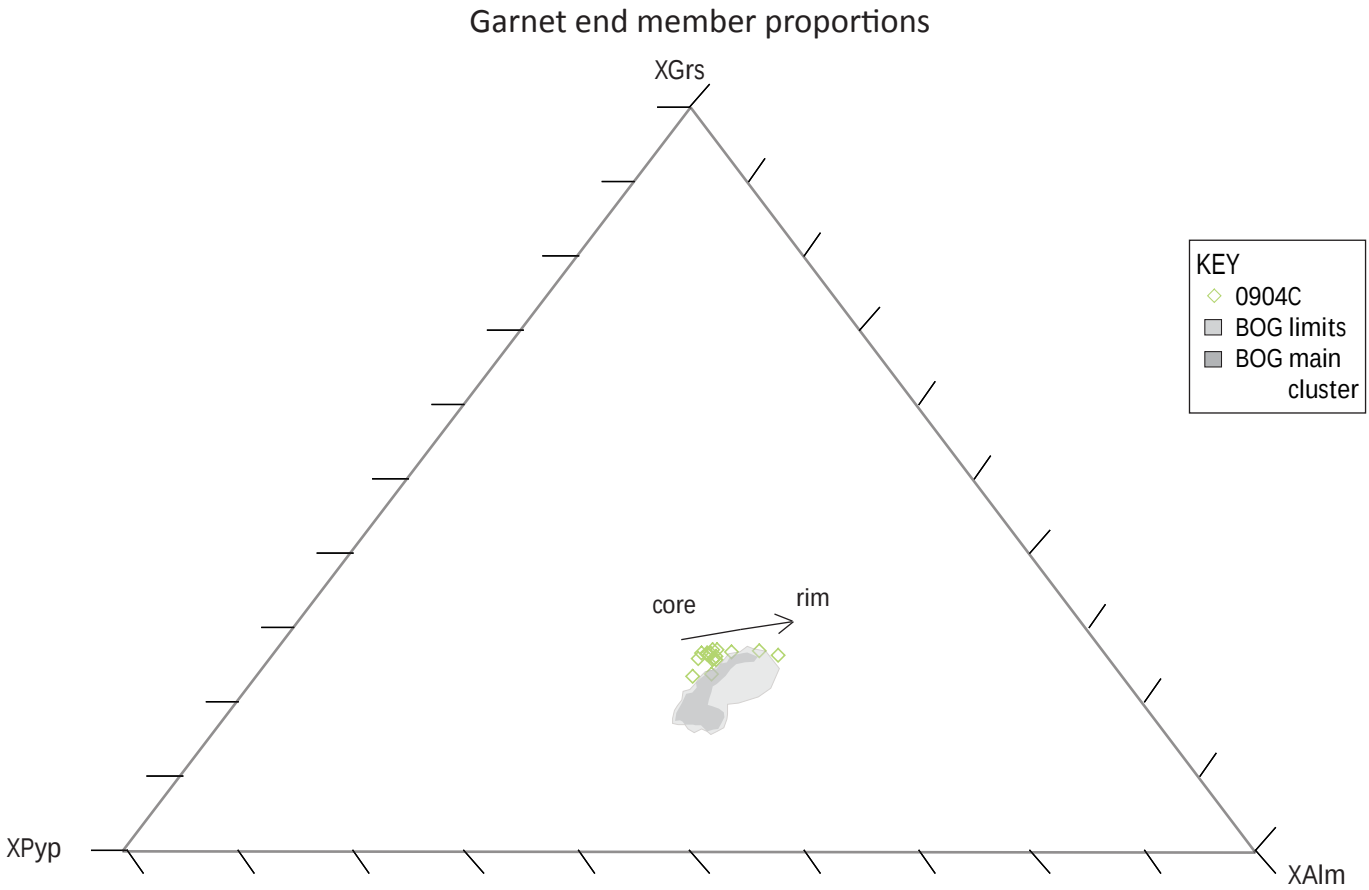

Fig 6.10 Garnet zoning in BE (0904C). Structure used is $X_3Y_2Si_3O_{12}$
Fig 6.11 Ternary plot showing BE core/rim variation in garnet end member proportions.

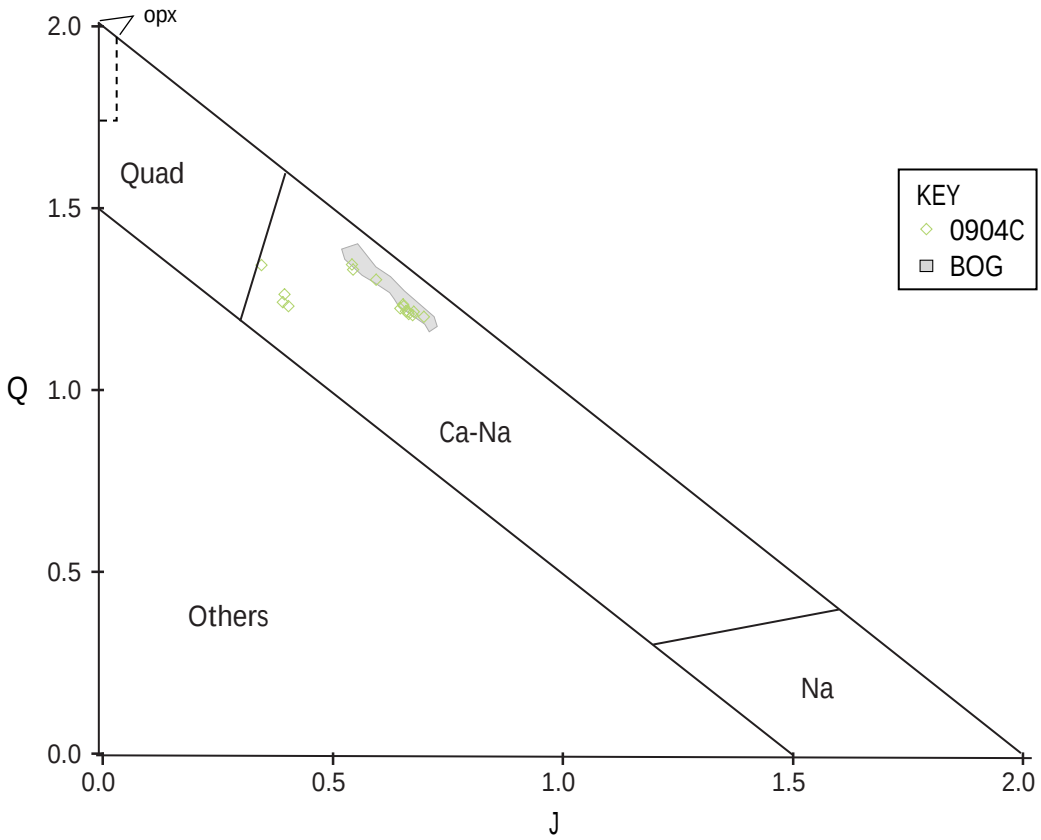

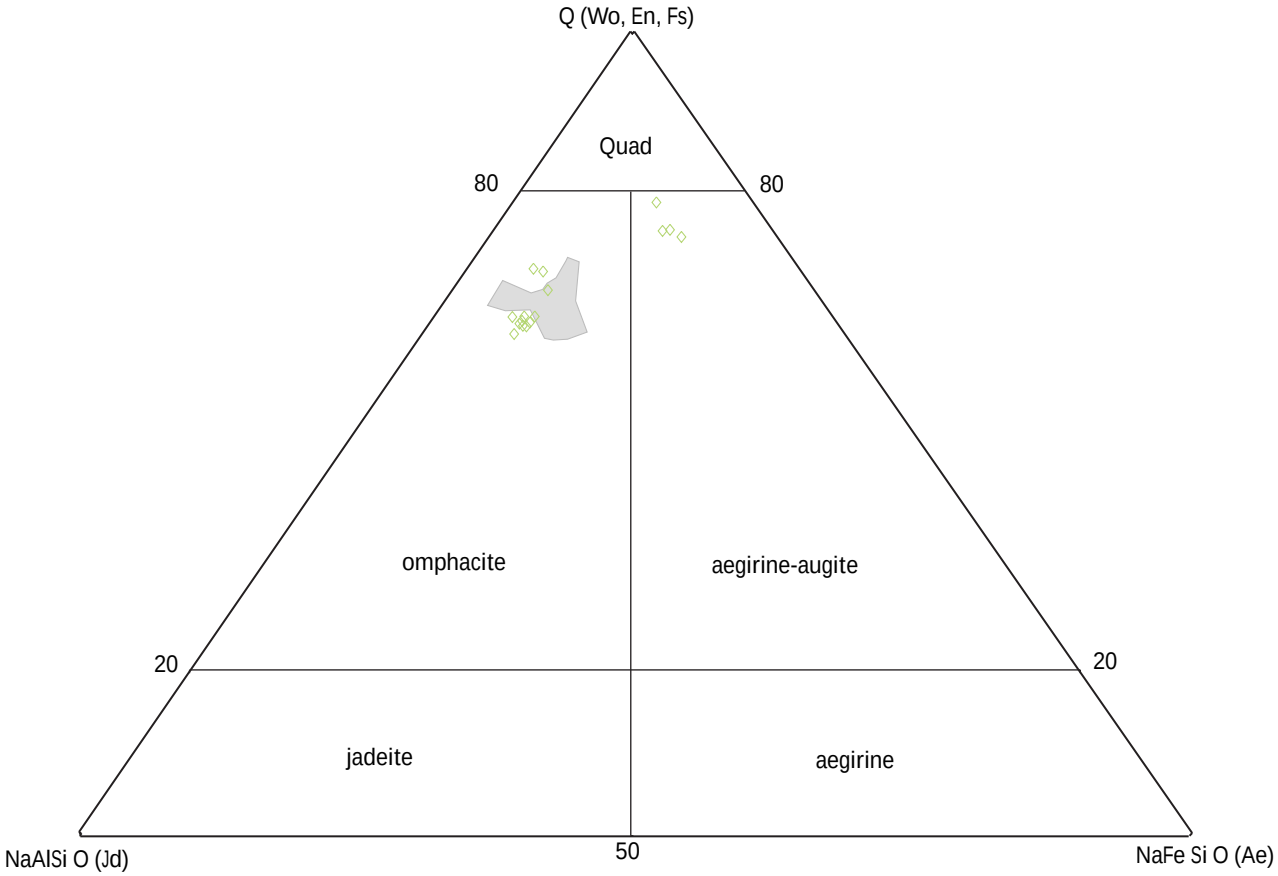

Fig 6.12 Q-J classification diagram (Morimoto et al., 1988) for BE (0904C). BOG shown in grey.
$Q=Ca^{2+}+Mg^{2+}+Fe^{2+}$(molar); $J=2xNa^{+}$(molar).

Fig 6.13 Ca-Na pyroxene classification diagram (Morimoto et al., 1988) for BE. BOG shown in grey.

Layered Garnetite – Pyroxenite

Garnet within the garnetite layer (samples 0906B & 0910B) ranges from $Alm_{36}Pyp_{43}Grs_{20}Sps_{1}$ at mineral cores to $Alm_{43}Pyp_{31}Grs_{24}Sps_{1}$ at mineral rims indicating an upward trend in almandine (stronger) and grossular (weaker) end members with a downward trend in pyrope from mineral core to rim (Fig. 6.14).

Both Quad and Ca-Na group pyroxenes (Morimoto et al., 1988) (Fig. 6.16) are present in the garnetite layer as diopside, omphacite and aegirine-augite (Figs. 6.18 & 6.20). Diopside content of pyroxene grains decreases as grains become more augite (Mg rich) rich towards mineral grain rims (Fig. 6.18). Omphacite and aegirine-augite plot as a cluster (Fig. 6.20) and show little evidence of a compositional (zoning) trends within grains. Sample 0906B and 0910B show different garnet and pyroxene compositions even though they occur in the same textural environment.

Interstitial hornblende observed in thin section (Fig. 4.17) is the calcic amphibole pargasite (Leake et al., 1997) (Fig. 6.09).

Garnet within the pyroxenite later (sample 0906A) varies from core values of$Alm_{38}Pyp_{38}Grs_{18}Sps_{1}$ to $Alm_{45}Pyp_{31}Grs_{24}Sps_{2}$ at rims (Fig. 6.15), indicating and upward trend in almandine and grossular end members and a downward trend in pyrope from core to rim.

Quad and Ca-Na pyroxenes (Morimoto et al., 1988) are represented in the pyroxenite sample in the form of diopside, augite and omphacite (Figs. 6.19 & 6.21). Quad pyroxenes become Mg poor (augite rich) towards grain rims (Fig. 6.19), while the few omphacite grains analysed by EMP show little compositional variation. 0906A also shows different compositions of garnet and pyroxene, even though it is found directly adjacent to 0906B.

Symplectite composition and width of zoning within pyroxenes will be assessed by element maps (this chapter).

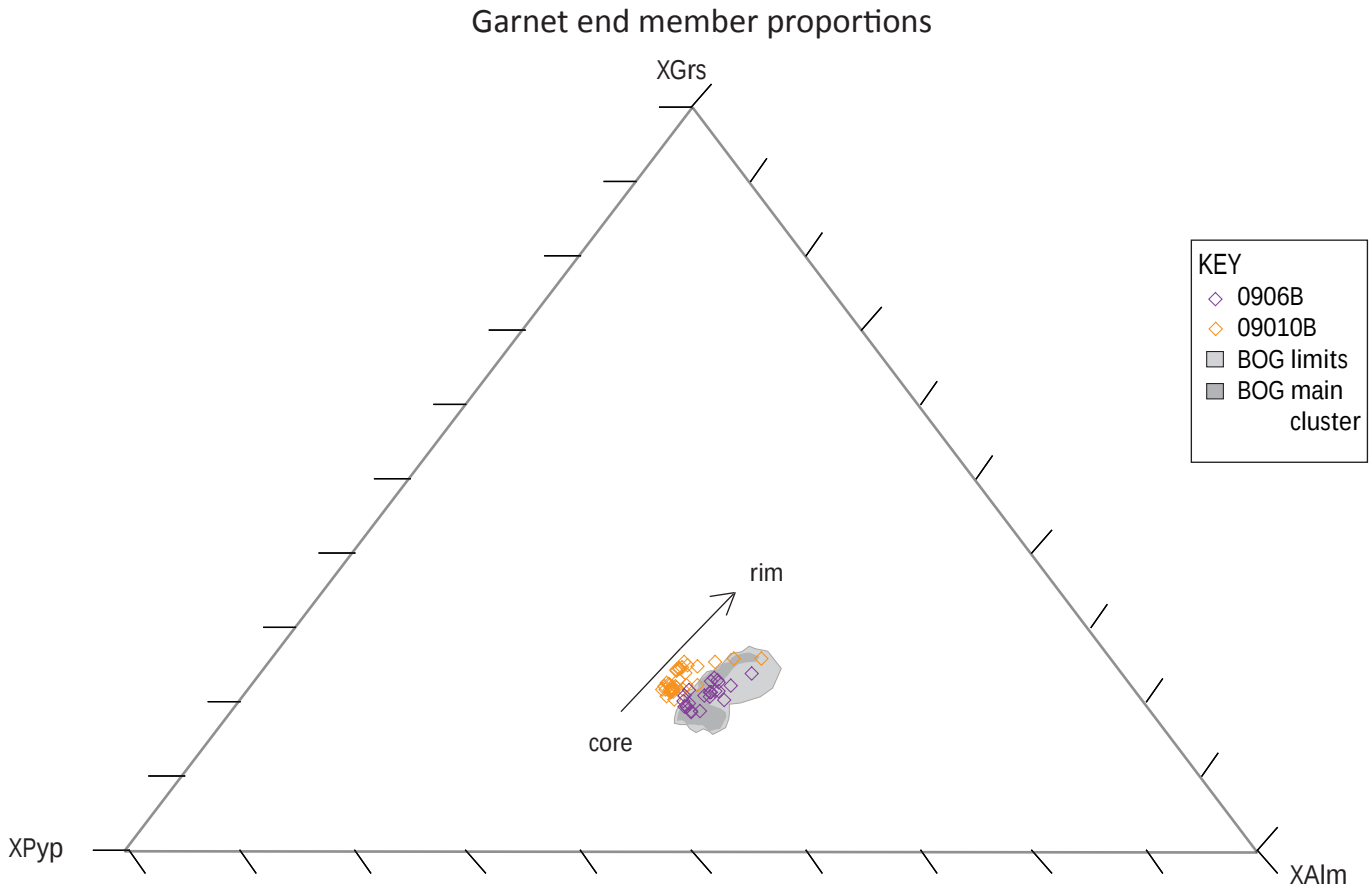

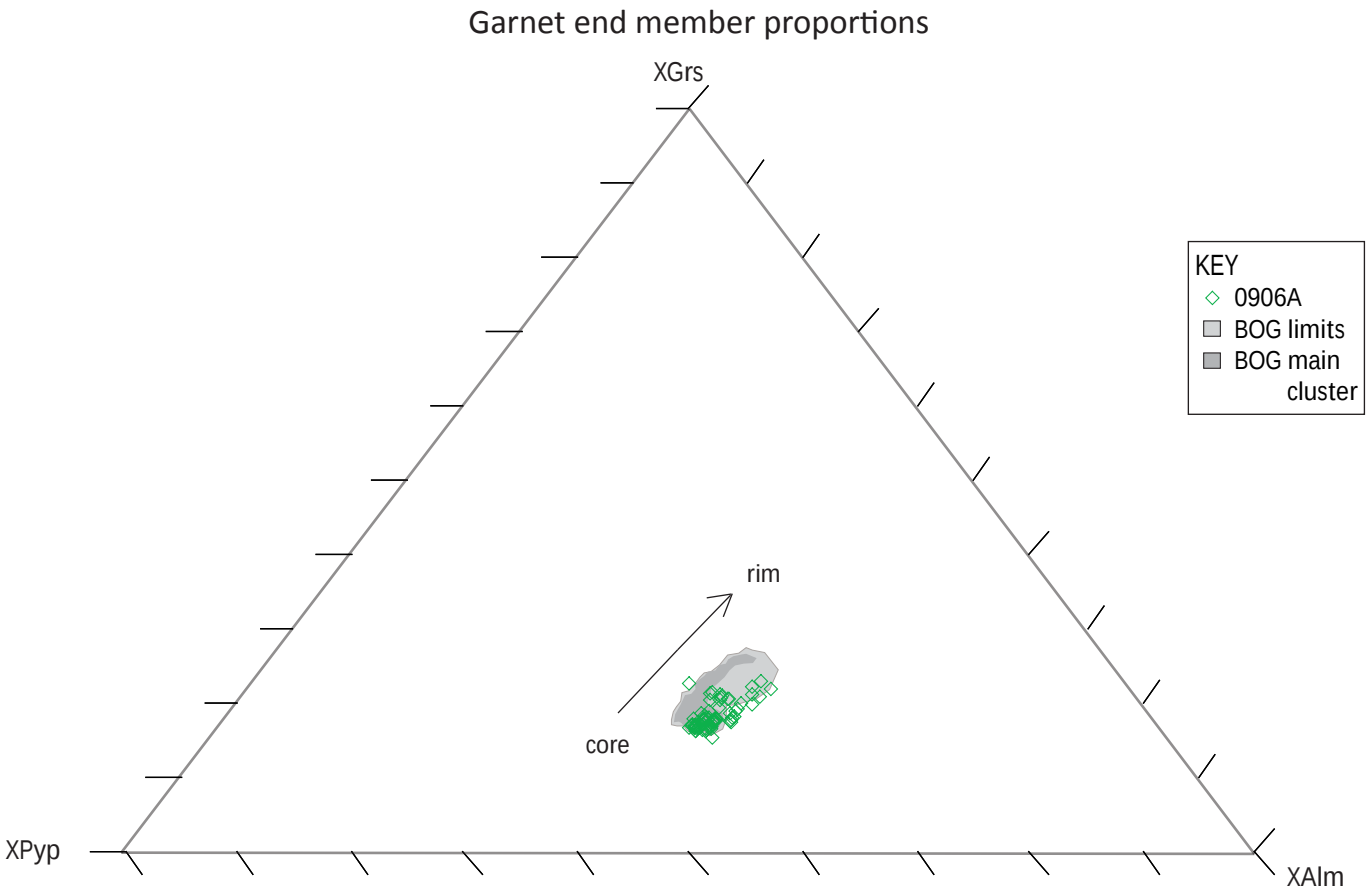

Fig 6.14 Ternary plot showing garnetite core/rim variation in garnet end member proportions.
Fig 6.15 Ternary plot showing pyroxente core/rim variation in garnet end member proportions.

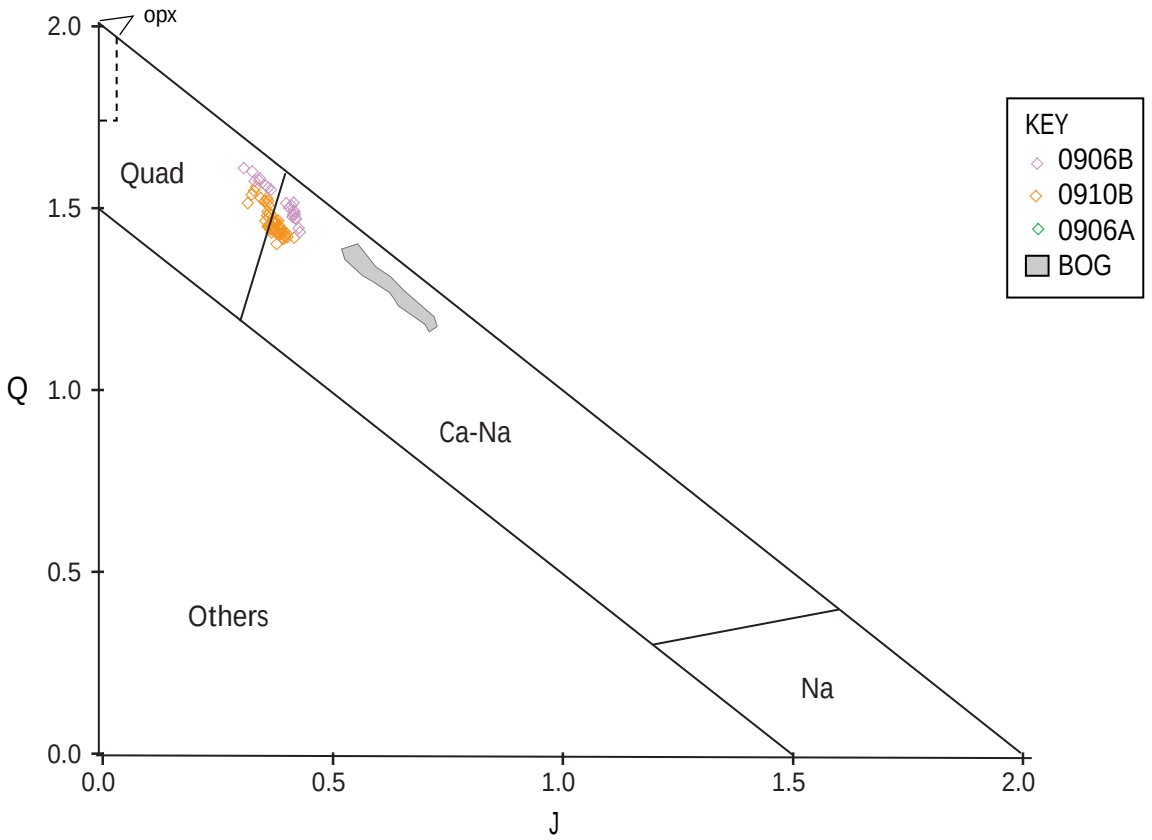

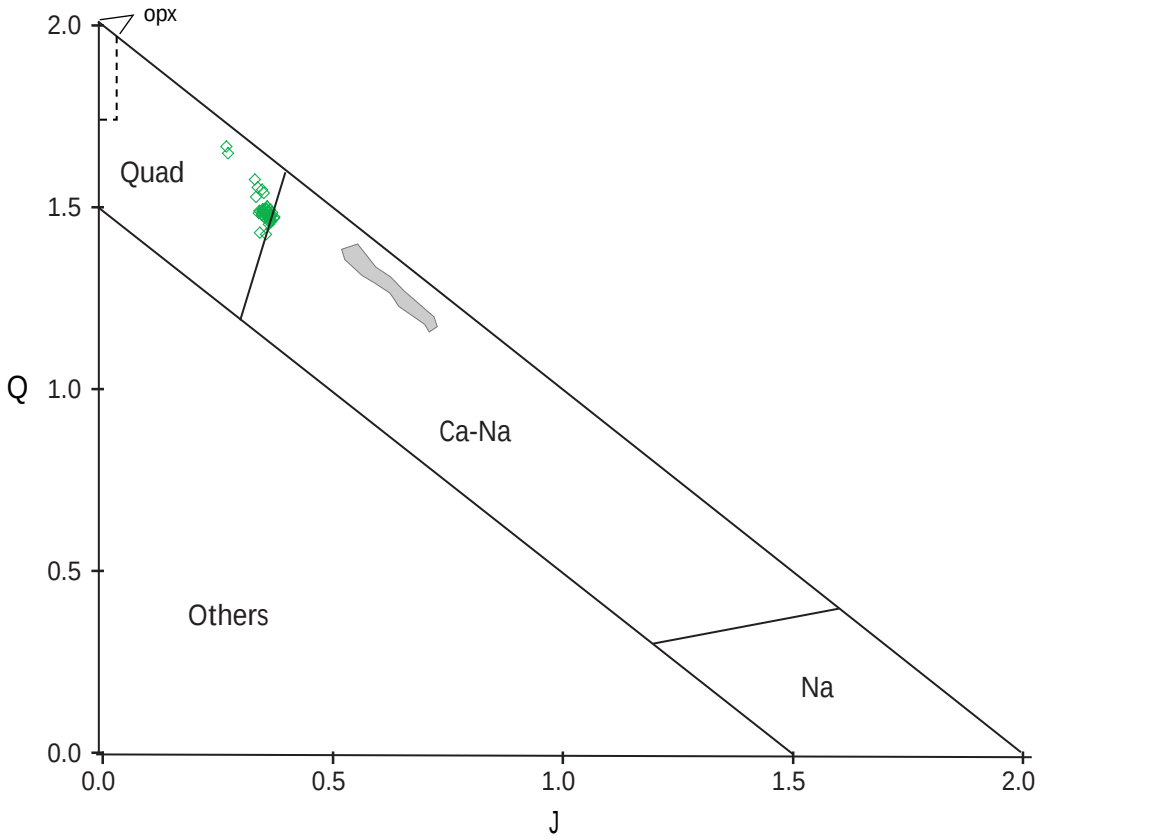

Fig 6.16 Q-J classification diagram (Morimoto et al., 1988) for garnetite (0906B & 09010B) $Q=Ca^{2+}+Mg^{2+}+Fe^{2+}$ (molar); $J=2xNa^{+}$ (molar). BOG is shown in grey.

Fig 6.17 Q-J classification diagram (Morimoto et al., 1988) for pyroxenite (0906A) $Q=Ca^{2+}+Mg^{2+}+Fe^{2+}$ (molar); $J=2xNa^{+}$ (molar). BOG is shown in grey.

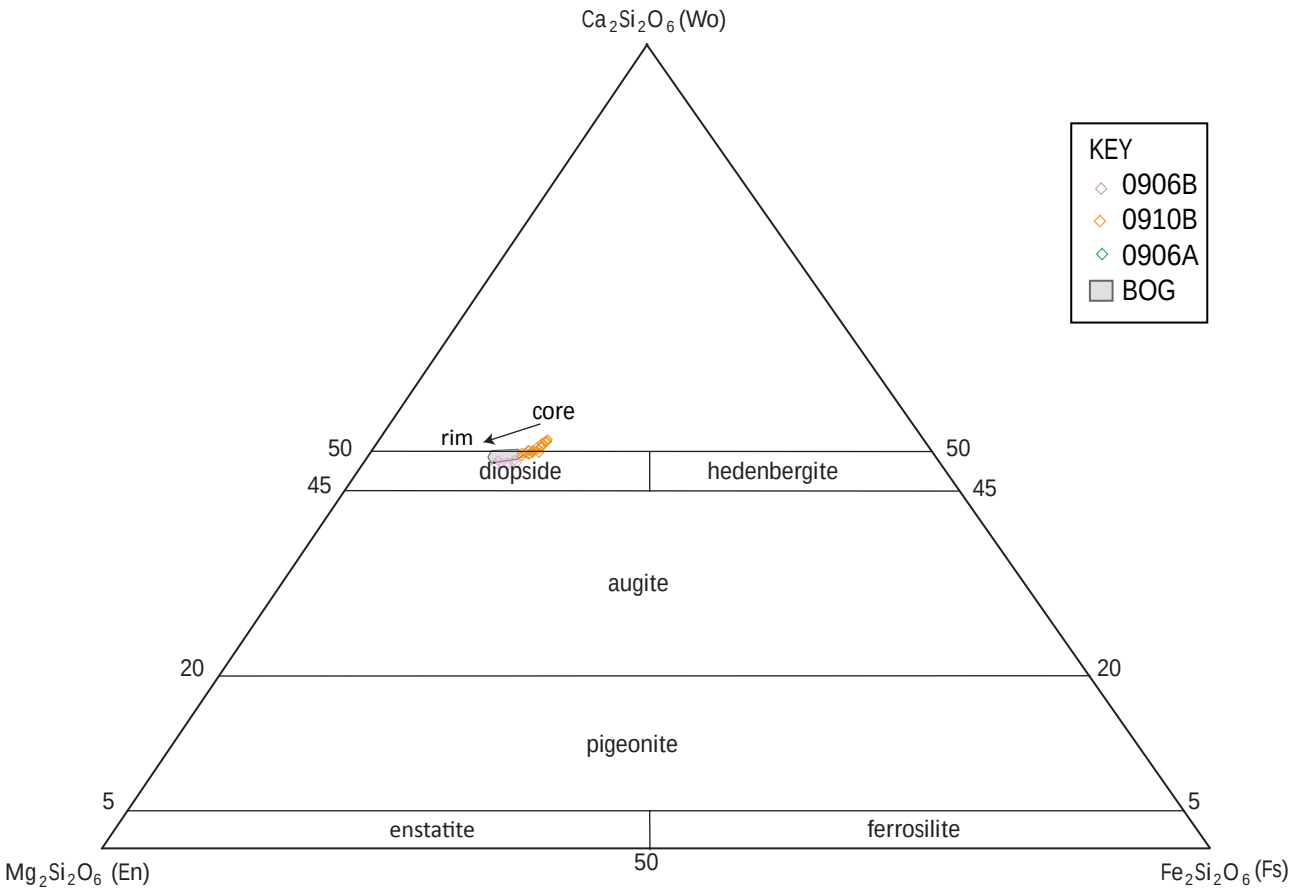

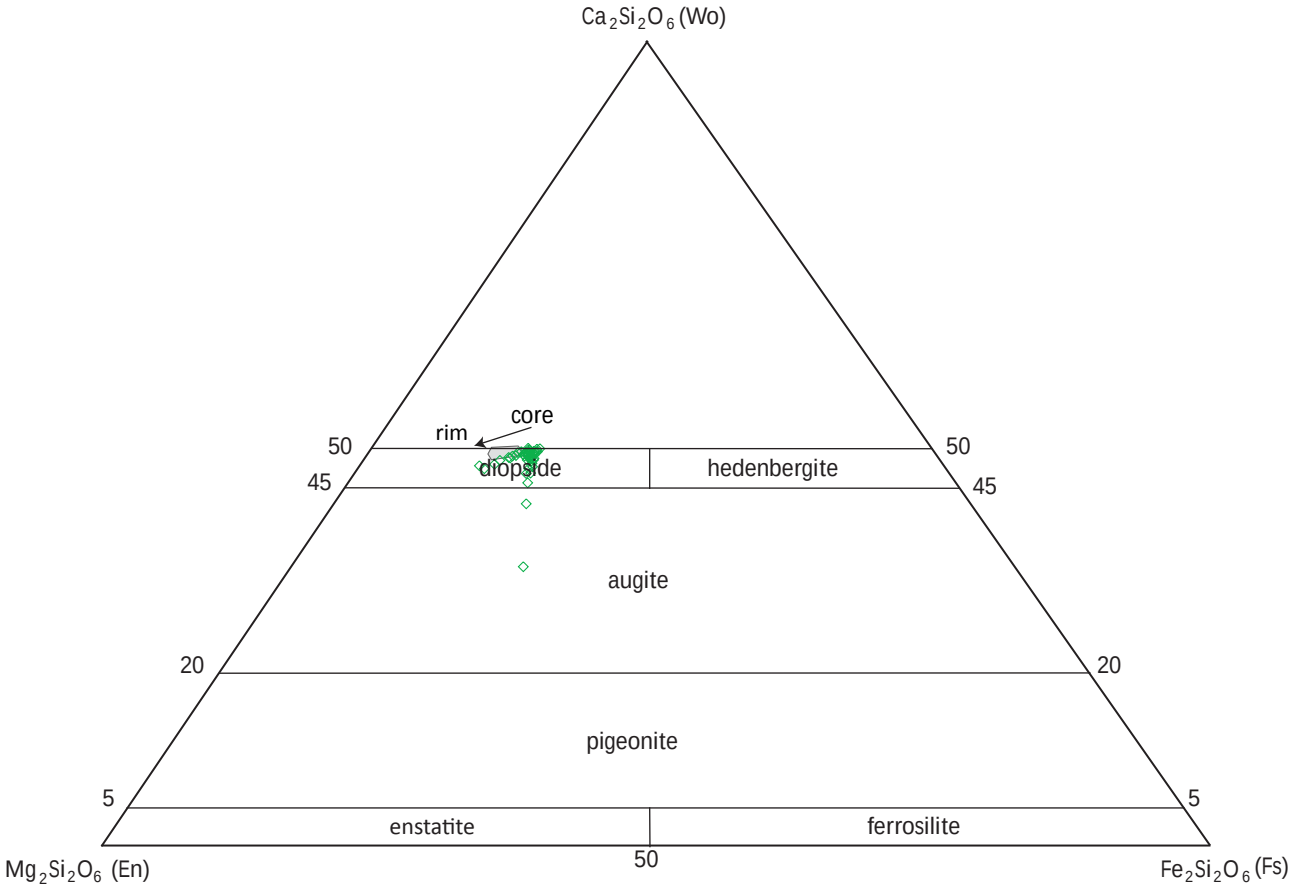

Fig 6.18 classification diagram for Ca pyroxenes (Morimoto et al., 1988) for garnetite (0906B & 0910B). BOG shown in grey.
Fig 6.19 classification diagram for Ca pyroxenes (Morimoto et al., 1988) for pyroxenite (0906A) . BOG shown in grey.

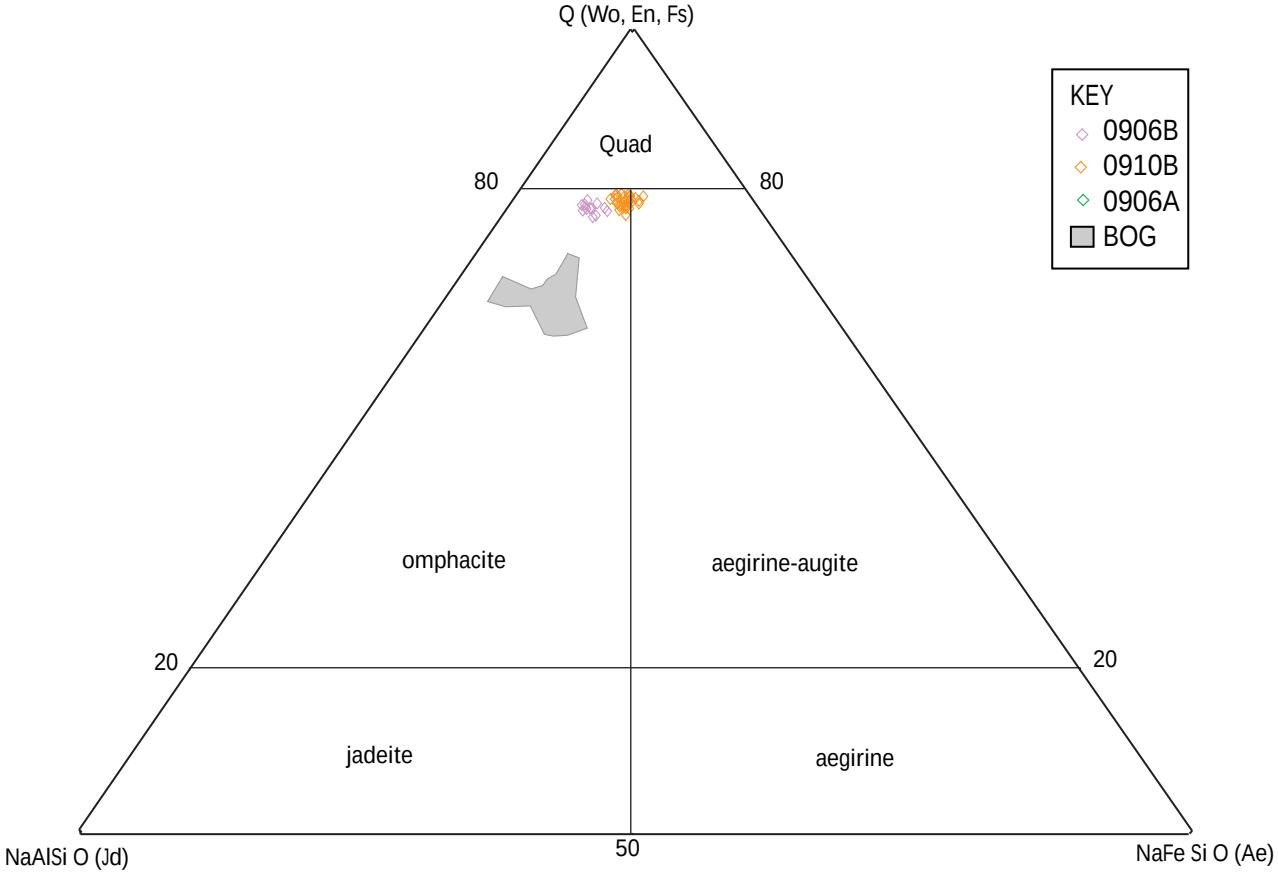

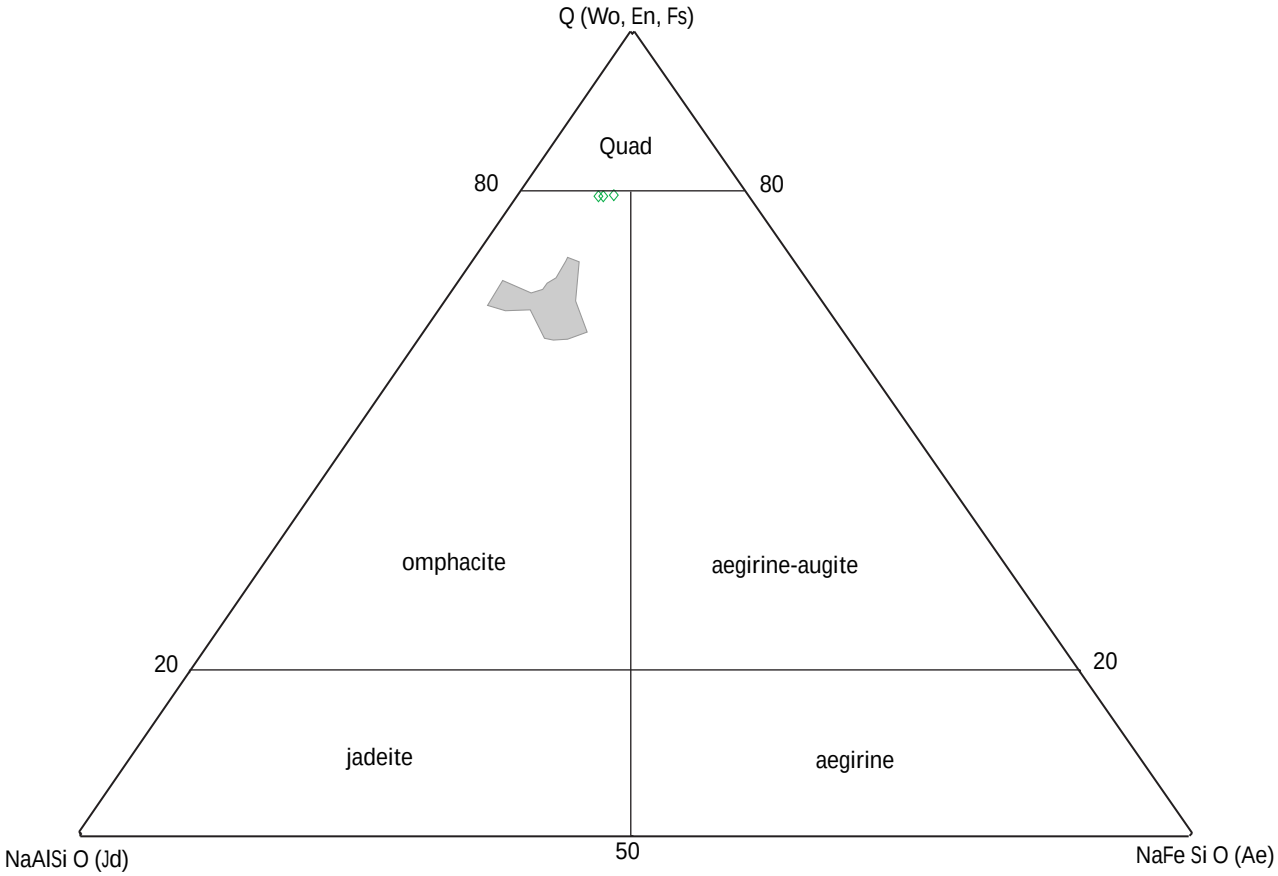

Fig 6.20 classification diagram for Ca-Na pyroxenes (Morimoto et al., 1988) for garnetite (0906B & 0910B). BOG shown in grey.
Fig 6.21 classification diagram for Ca-Na pyroxenes (Morimoto et al., 1988) for pyroxenite (0906A). BOG shown in grey.

Hornblende Peridotite

Garnet in the hornblende peridotite sample varies from $Alm_{38}Pyp_{44}Grs_{16}Sps_{2}$ at mineral cores to $Alm_{42}Pyp_{40}Grs_{16}Sps_{2}$ at mineral rims (Fig. 6.22). Variation is controlled only by the Fe and Mg end members (almandine and pyrope) and is evident through an increase in almandine and a decrease in pyrope from core to rim (Fig. 6.22).

Quad group pyroxenes (Morimoto et al., 1988) (Fig. 6.23) are the only pyroxene group represented in the hornblende peridotite, of diopside and enstatite compositions (Fig. 6.24).

Hornblende in the hornblende peridotite is the calcic amphibole pargasite (Leake et al., 1997) (Fig 6.09). Element mapping will resolve compositional make up and variation in opaque and symplectite minerals (this chapter). Olivine in the hornblende peridotite sample has the composition $Fo_{75}Fa_{25}$ (Fo = forsterite, Fa = fayalite).

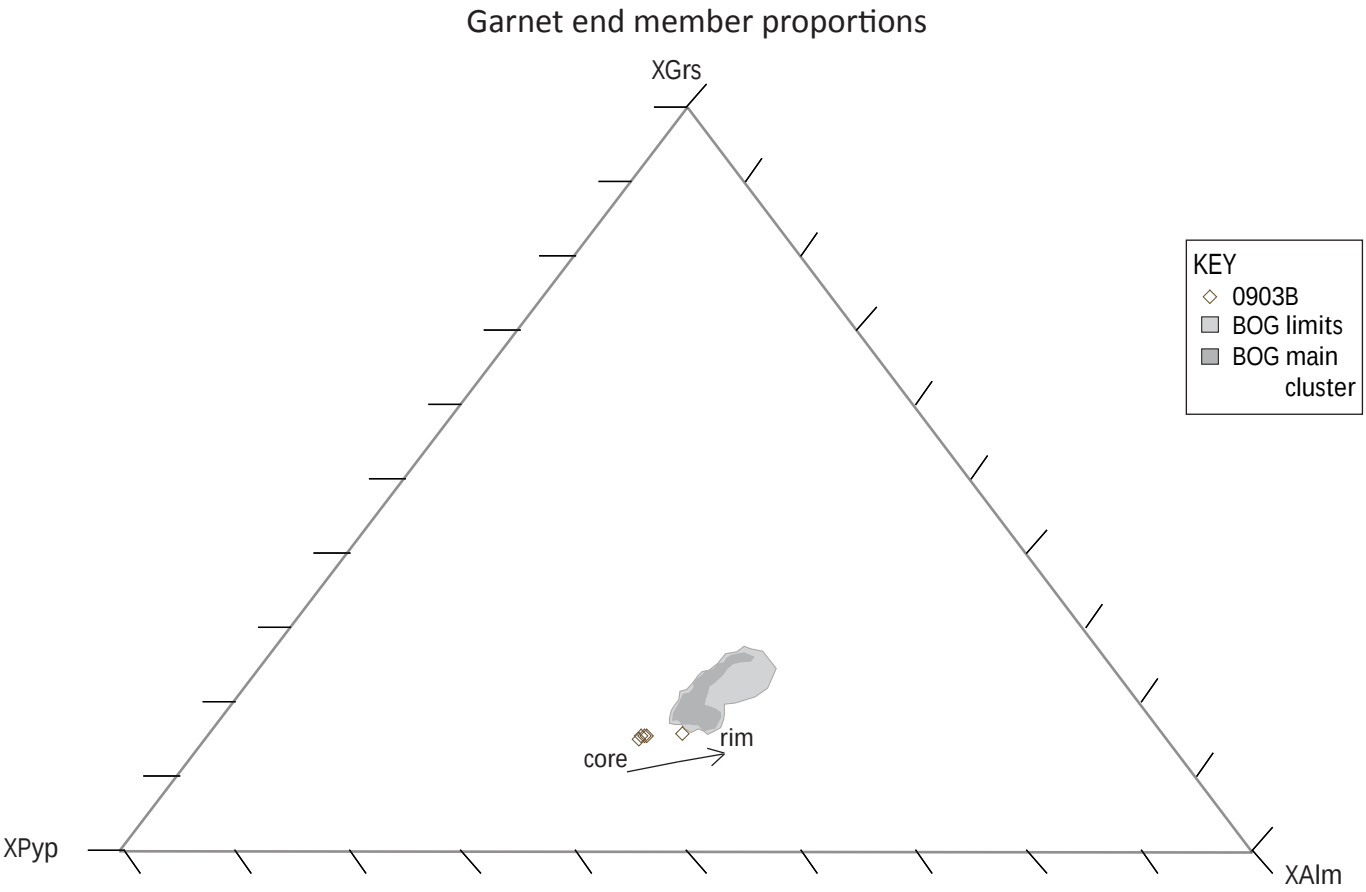

Fig 6.22 Ternary plot showing horblende peridotite core/rim variation in garnet end member proportions.

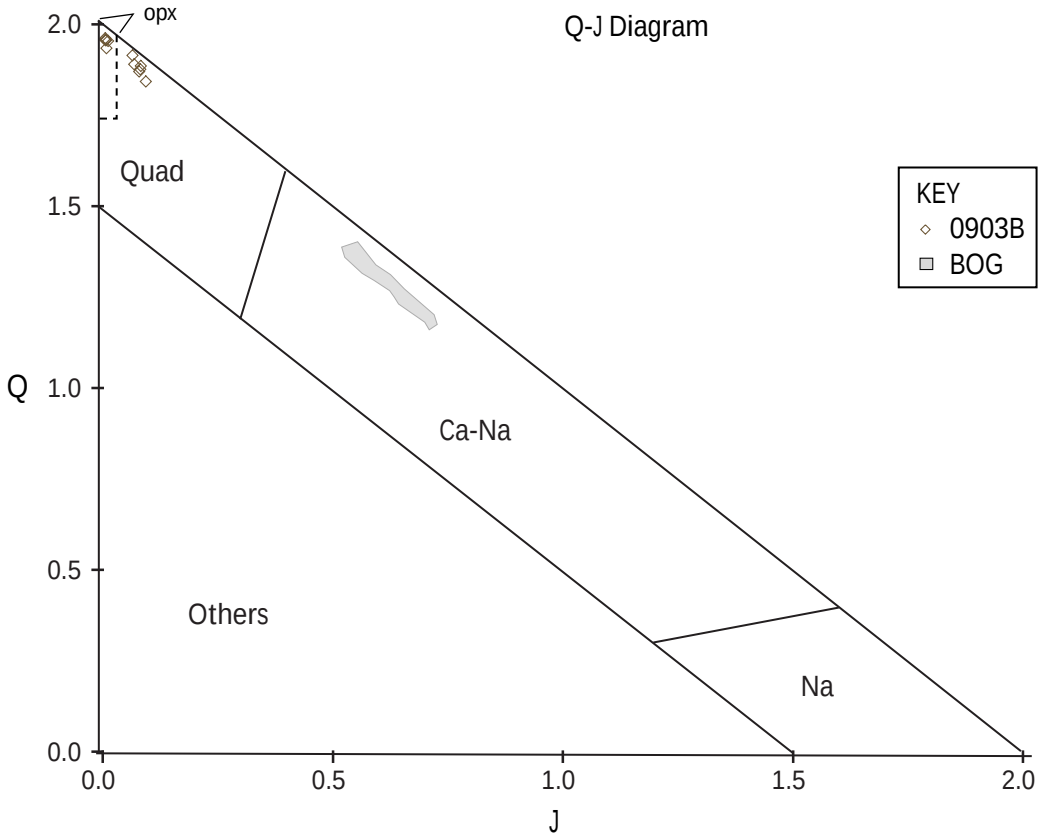

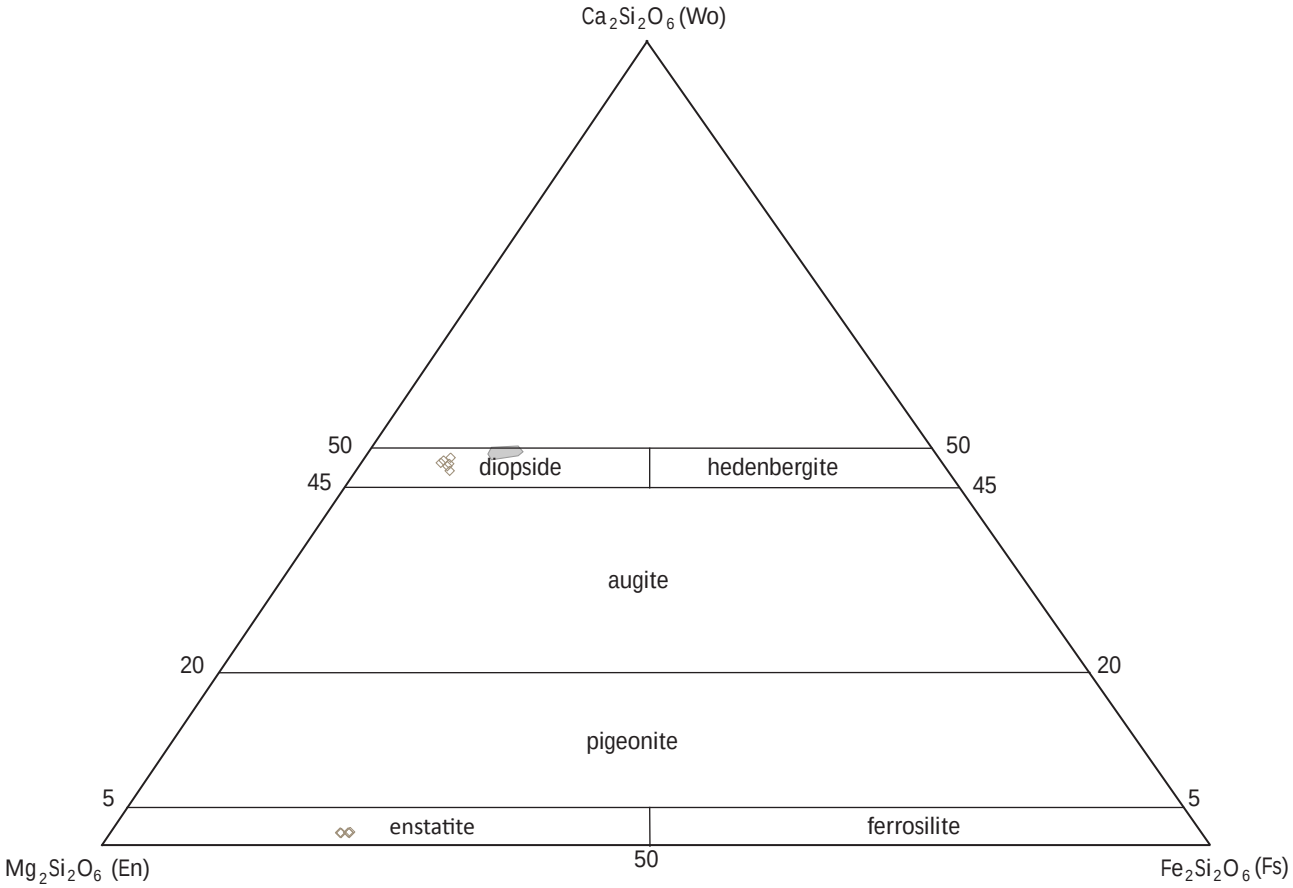

Fig 6.23 Q-J classification diagram (Morimoto et al., 1988) for hornblende peridotite (0903B). BOG shown in grey. $Q=Ca^{2+}+Mg^{2+}+Fe^{2+}$ (molar); $J=2xNa^{+}$ (molar).

Fig 6.24 Quad pyroxene classification diagram (Morimoto et al., 1988) for hornblende peridotite (0903B). BOG shown in grey.

6.2.2 Laser ablation inductively coupled plasma mass spectrometry (LA-ICP-MS)

Breaksea Omphacite Granulite

Laser ablation was conducted on 22 mineral grains of BOG (sample 0905B) and is shown in Appendix 6.E. Multi element spider plots and REE plots normalised to primitive mantle values of Sun & McDonough (1989) [spider plots] and McDonough et al., (1991) [REE plots] show the trace element patterns for garnet, omphacite and plagioclase (Figs. 6.25 & 6.26). 3 samples were discarded as the ablation drove through multiple minerals (thus lowering the signal count time on the desired mineral and raising error).

Garnet shows varied patterns from Cs to Ce, due to many of these elements being <LLD (Appendix 6.A) in garnet and are as such not plotted. From Pb to Dy garnet shows a steeply ascending pattern and from Dy to Lu shows a slightly descending pattern. There are large negative anomalies at Sr and Ti, and moderate negative anomalies at Pr, Nd and Zr (Fig. 6.25). The REE plot for garnet shows the same steeply ascending pattern from La to Eu, flattening at Gd and descending from Dy to Lu (Fig. 6.26).

Spider plots of BOG omphacite show a generally humped pattern (Fig. 6.25); ascending from Cs to Pr and decreasing from Nd to Lu, with negative anomalies at Sr, P and Zr. The REE plot for omphacite also shows the same humped pattern, ascending from La to Nd and descending from Nd to Er, with intermittent results for the HREE's (Fig. 6.26).

Plagioclase spider plots show a generally descending pattern, with strong positive anomalies at Ba, Pb and Sr as well as a moderate positive anomaly at Eu, with negative anomalies at Rb and Ti (Fig. 6.25). The REE plot for plagioclase shows the same descending pattern; from La to Sm with a strong positive anomaly at Eu, and no recorded data from Eu onwards to the HREE's (<LLD) (Fig. 6.26).

Laser ablation was also conducted on 6 garnet grains from a raft of BOG within the Resolution Orthogneiss (sample 73831) (Appendix 6.E) (Figs. 2.03 & 3.01). Garnet follows the same spider and REE patterns, although shows normalised concentrations on average 4-10 times higher than the BOG (Figs 6.27 &6.28). Garnet follows a steeply ascending spider plot pattern from Ce to Dy and a flat to very slightly descending pattern from Dy to Yb, descending to Lu. The spider plot shows strong negative anomalies at Sr and Ti with a moderate negative anomaly at Nd. There are positive anomalies at Pb (two grains) and Zr. From Cs to La patterns are varied due to the lower concentrations of these elements in garnet (Fig. 6.27). The REE plot shows the same information, with a steeply ascending slope from La to Gd, which flattens from Gd to Dy and is weakly decreasing from Dy to Lu (Fig. 6.28). There is no noticeable Eu anomaly in these grains. Values from Cs to Ce are not indicative of overall patterns as elements are not plotted due to being <LLD (Appendix 6.E).

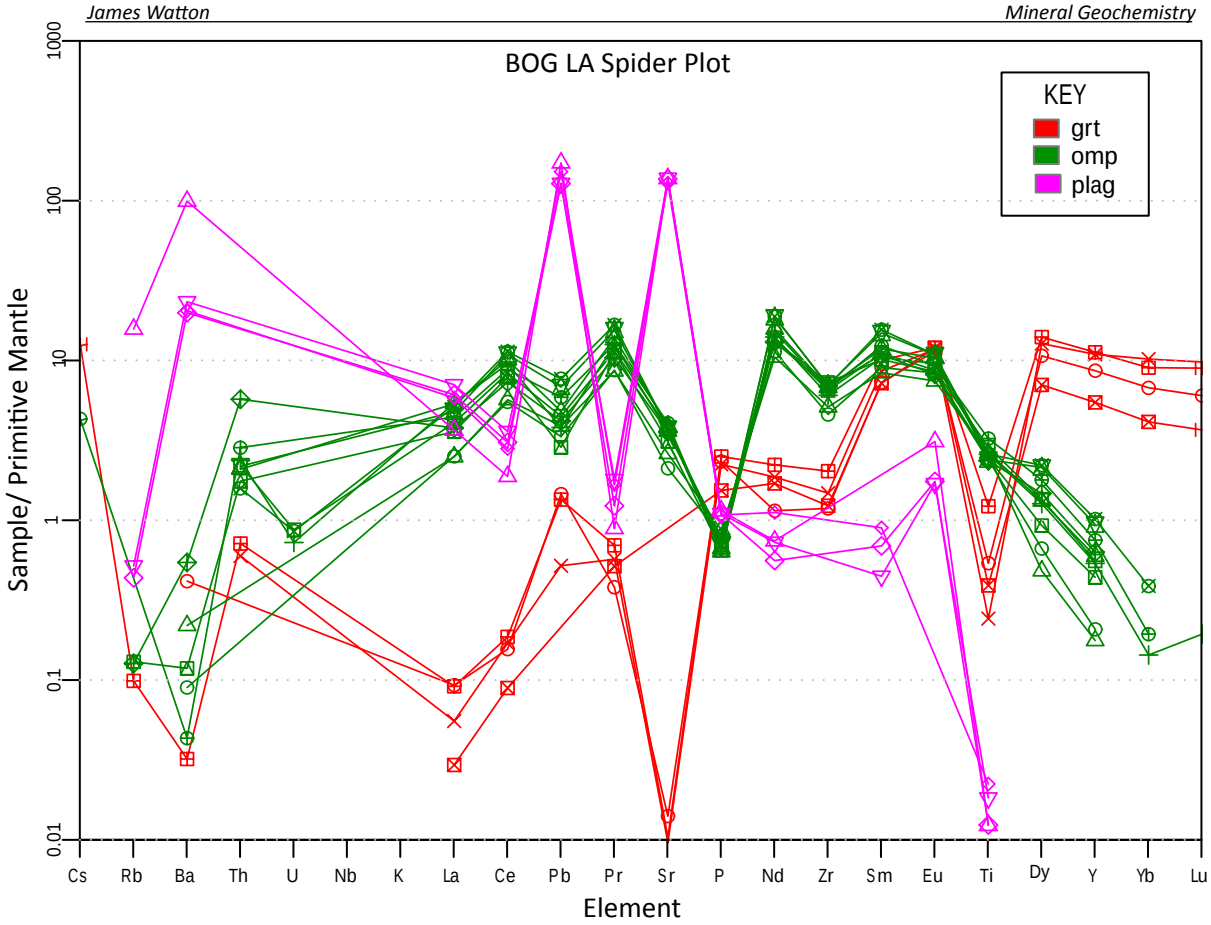

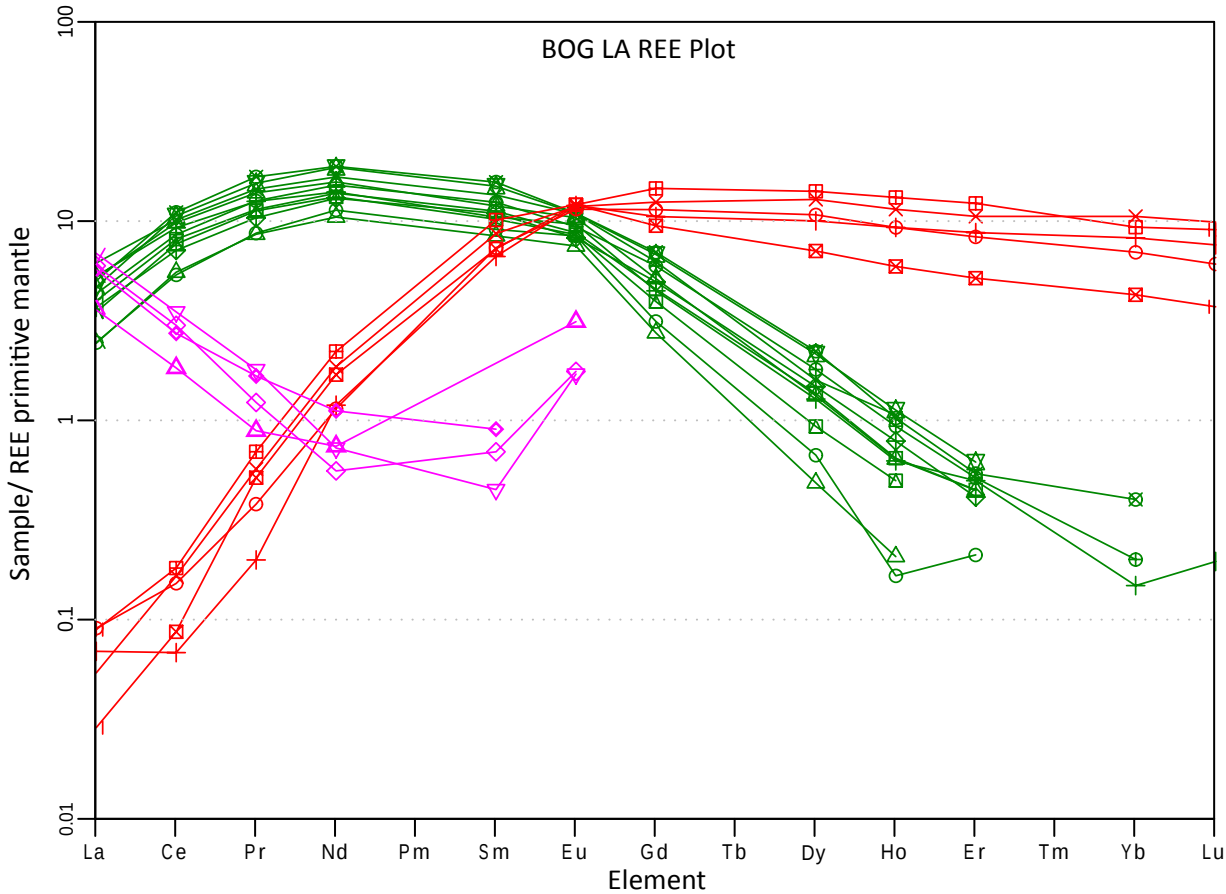

Fig 6.25 Spider diagram of LA mineral grains from BOG normalised to primitive mantle values of Sun & McDonough (1989).

Fig 6.26 REE plot of LA mineral grains from BOG normalised to primitive mantle values of McDonough et al., (1991).

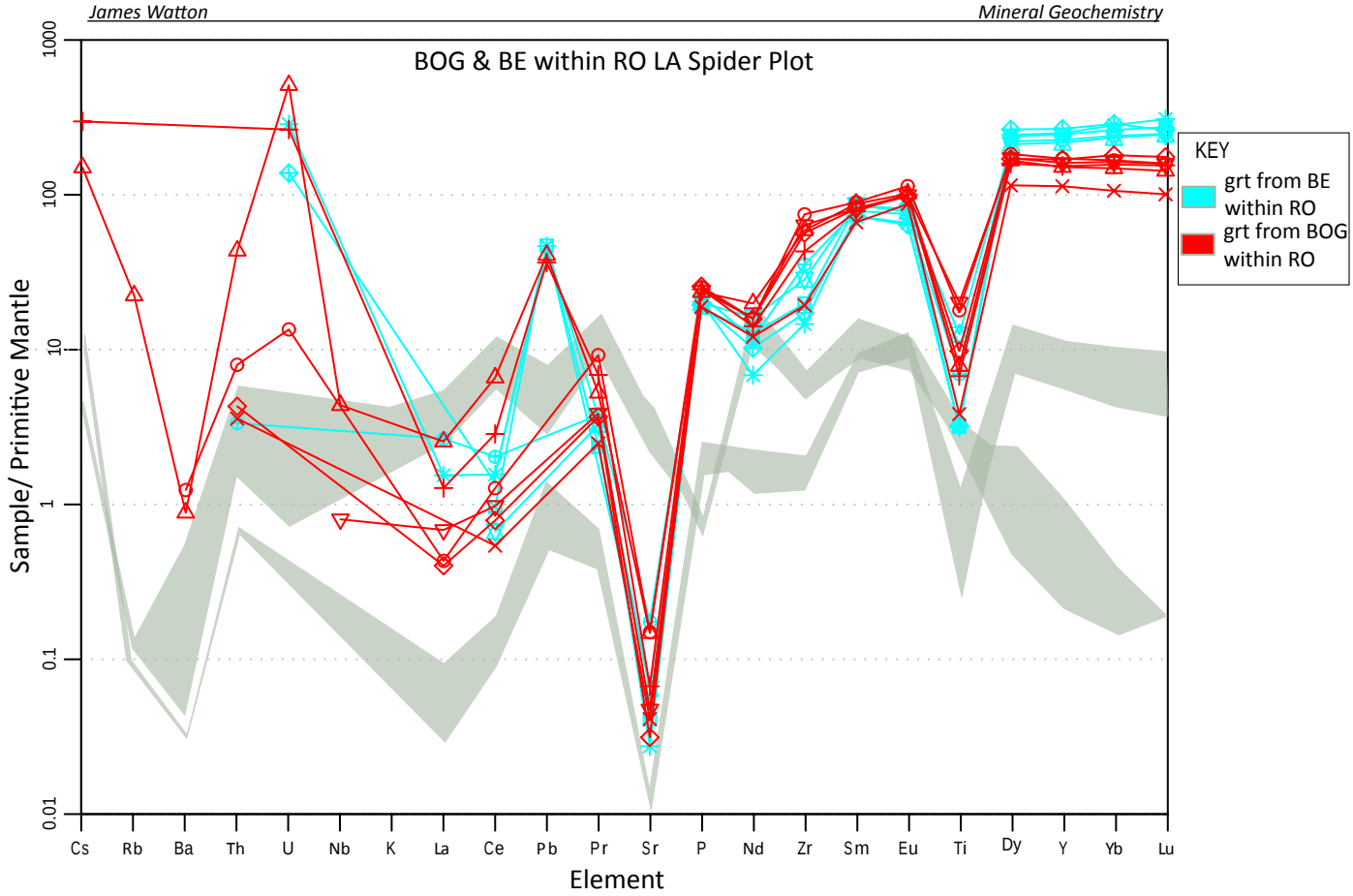

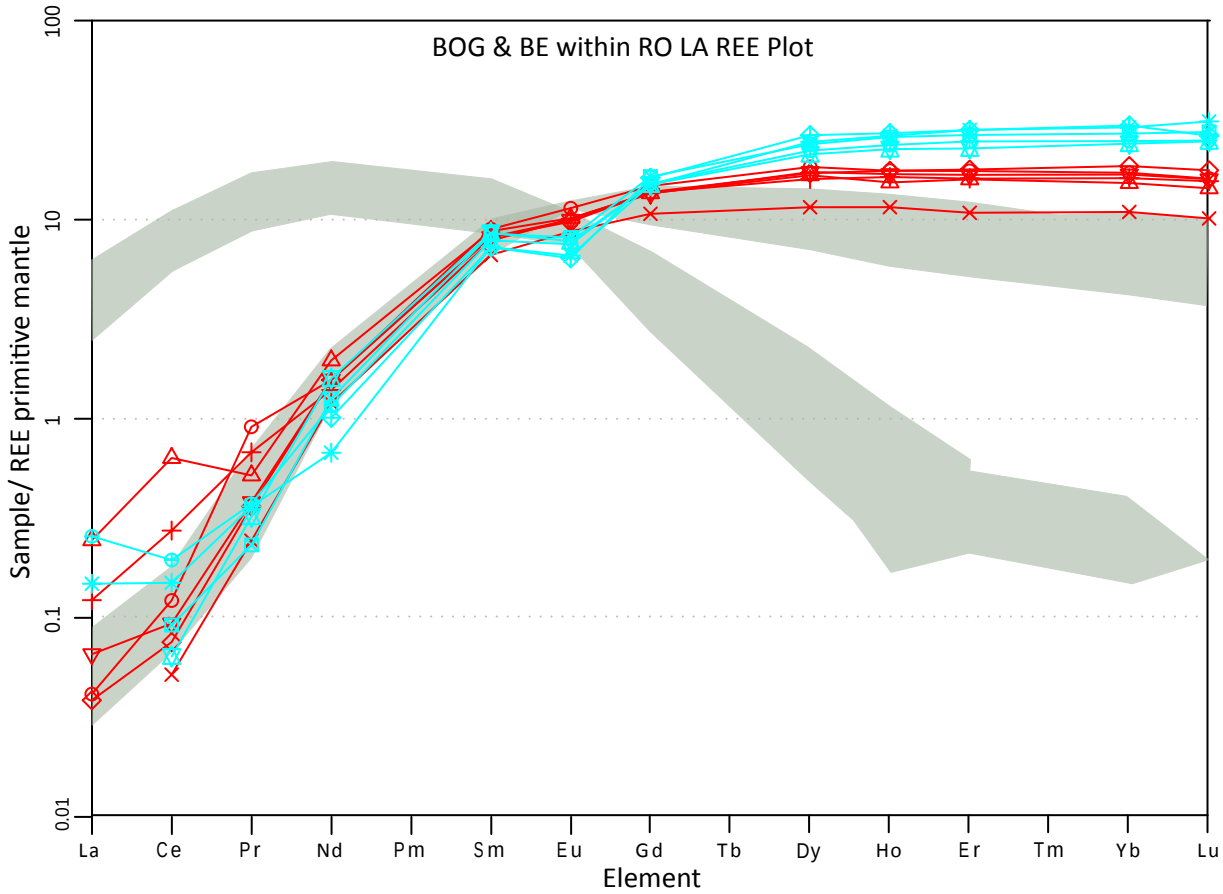

Fig 6.27 Spider diagram of LA mineral grains from BOG & BE cognate inclusions in Resolution Orthogneiss normalised to primitive mantle values of Sun & McDonough (1989).

Fig 6.28 REE plot of of LA mineral grains from BOG & BE cognate inclusions in Resolution Orthogneiss normalised to primitive mantle values of McDonough et al., (1991). Grey shows BOG LAM data.

Breaksea Eclogite

Laser ablation was conducted on 9 mineral grains of BE (sample 0904C) (Appendix 6.E). Multi element spider plots and REE plots normalised to primitive mantle values of Sun & McDonough (1989) [spider plots] and McDonough et al., (1991) [REE plots] show trace element patterns for garnet and omphacite (Figs. 6.29 and 6.30).

Garnet shows a spider plot similar to the BOG, steeply ascending from Ce to Eu and descending slightly from Dy to Lu (Fig. 6.29). Strong negative anomalies can be seen at Sr and Ti with moderate negative anomalies at Nd and Zr. The REE plot shows a similar trend; ascending from La to Gd and decreasing from Dy to Ly (Fig. 6.30), with no anomalous concentrations.

Omphacite spider and REE plots show a similar, though slightly more depleted pattern than the BOG (Figs. 6.29 & 6.30), with a humped shape, ascending from La to Nd and decreasing from Sm to Yb (Fig. 6.29), with a strong negative anomaly at P and moderate negative anomalies at Pb and Zr. The REE plot shows the same humped pattern (Fig. 6.30), ascending from La until Nd and descending from Nd to Lu.

Laser ablation was also conducted on 5 garnet grains from a sample of BE present as a raft within the Resolution Orthogneiss (sample 73832) (Appendix 6.E) (Figs. 2.03 & 3.01). Garnet follows a similar pattern to the BE and BOG, although are enriched by an order of 4-10x BOG. (Figs. 6.27 & 6.28). The spider plot shows a steeply increasing pattern from Ce to Eu, and a slightly increasing pattern from Dy to Lu, with a positive anomaly at Pb and negative anomalies at Sr, Nd, Eu and Ti (Fig. 6.27). The REE plot shows the same steeply increasing pattern from La to Eu, with a slightly increasing pattern from Dy to Lu. Visible on the REE plot is a negative Eu anomaly (Fig. 6.28). The HREE's are more enriched than both the BOG and the raft of BOG from the Resolution Orthogneiss.

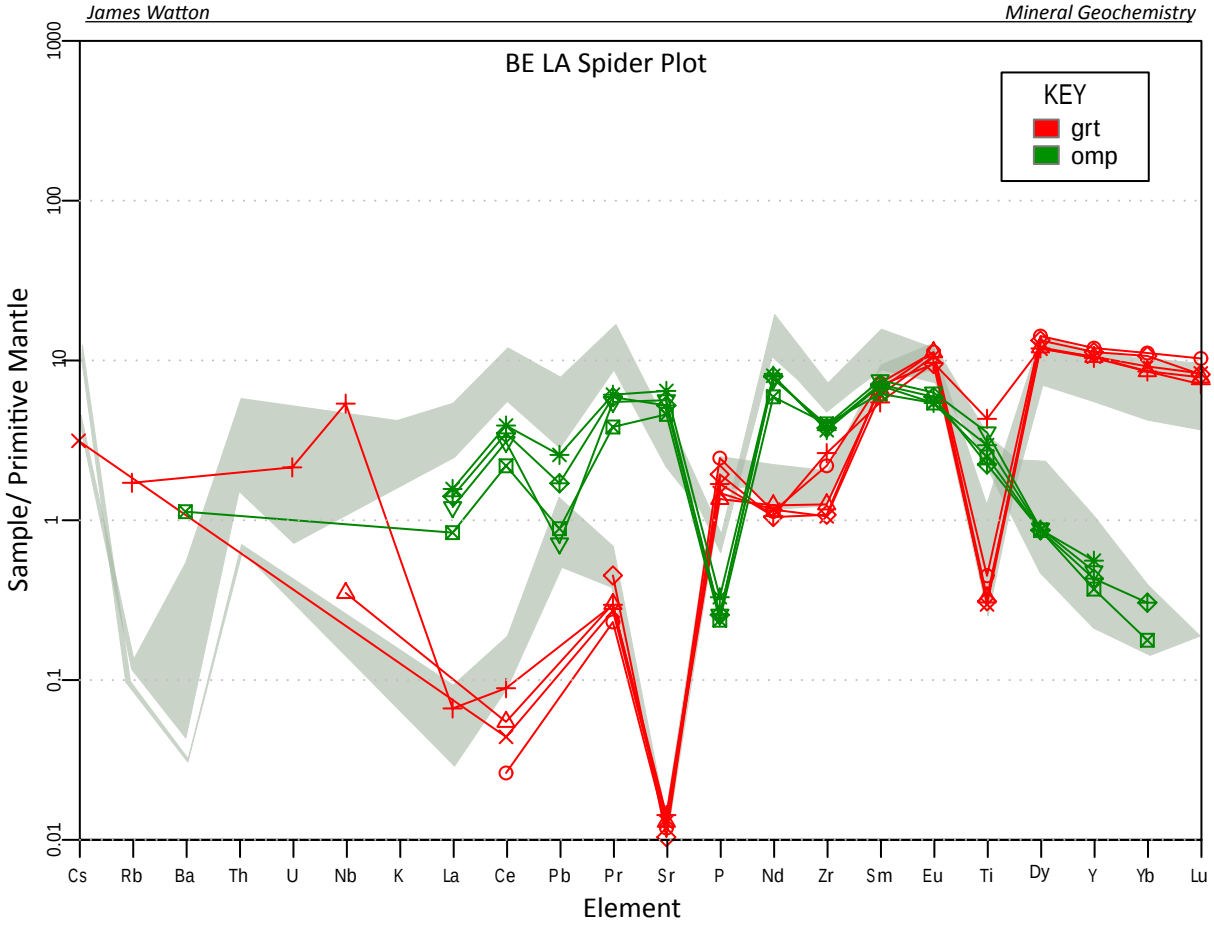

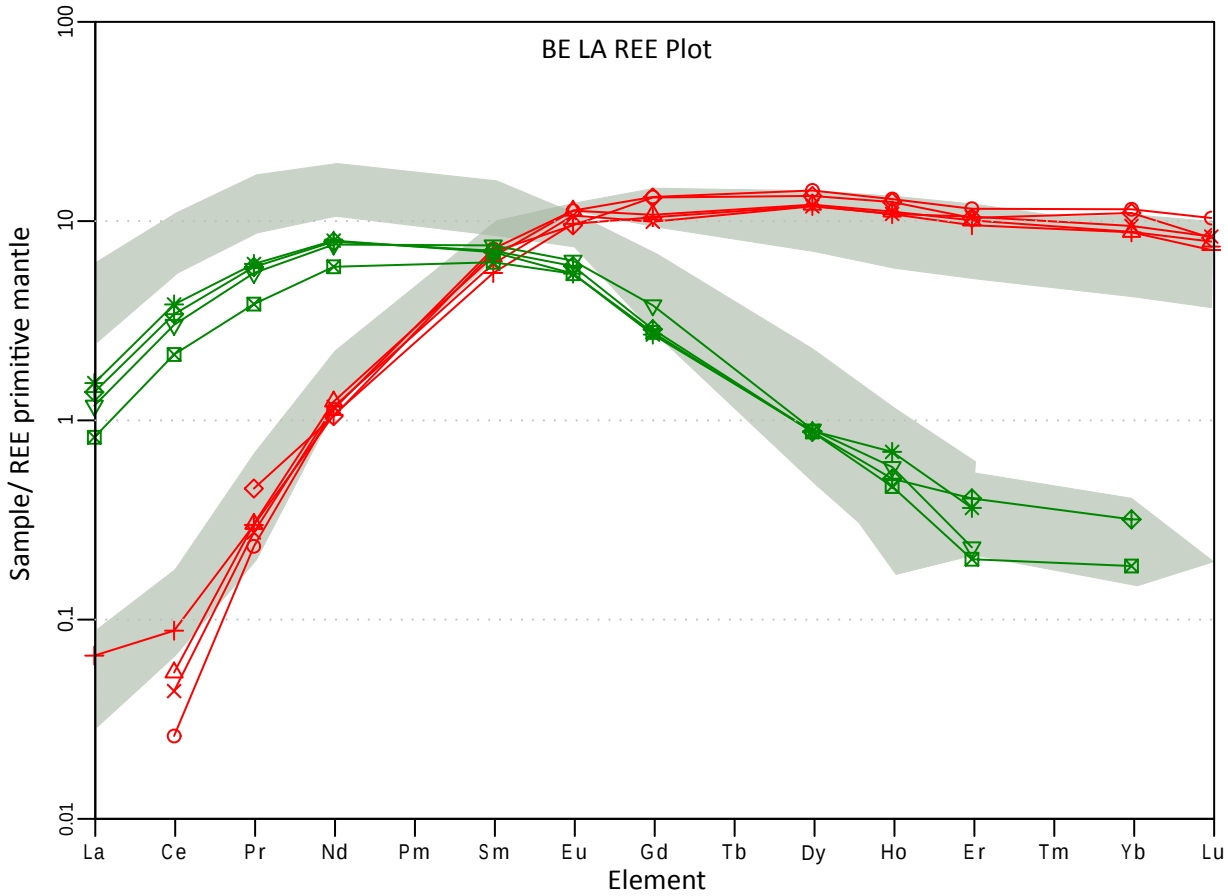

Fig 6.29 Spider diagram of LA mineral grains from BE normalised to primitive mantle values of Sun & McDonough (1989).

Fig 6.30 REE plot of LA mineral grains from BE normalised to primitive mantle values of McDonough et al., (1991). Grey shows BOG LA data.

Layered Garnetite – Pyroxenite

Laser ablation was conducted on 10 mineral grains in the garnetite sample 0906B and 7 mineral grains from pyroxenite sample 0906A (Appendix 6.E). Multi element spider plots and REE plots normalised to primitive mantle values of Sun & McDonough (1989) [spider plots] and McDonough et al., (1991) [REE plots] show trace element patterns for garnet, omphacite and diopside (Figs. 6.31 – 6.34). Garnet has been separated into core and rim readings as they produced different results, omphacite has also been differentiated from diopside.

Garnet in the garnetite layer shows an identical, even slightly depleted, spider plot pattern relative to the BOG from Ce to Dy, with the absence of Pb. Garnet cores have concentrations <LLD for all elements from Cs to Ce, except Ba while garnet rims have concentrations <LLD for all elements from Cs to Ce, including Ba (Fig. 6.31). From Dy to Lu deviation from BOG samples is visible, as the garnetite core and rim values continue to increase through the HREE's up to Lu (Fig. 6.31). This pattern is better emphasised in the REE plot, showing the now typical steep increase in REE's from Ce to Dy, with the absence of La and a slightly lower Eu value than the BOG. From Dy to Ly the deviation from BOG garnet grain values is again clear, with the HREE's for garnetite continuing to increase (Fig. 6.32). Variation in core and rim values for garnet occurs in the HREE's, where the garnet core shows a slightly higher concentration that the garnet rims, though both follow the same pattern (Figs. 6.31 and 6.32).

Omphacite in the garnetite layer shows a near identical spider and REE pattern to the BOG; a hump pattern ascending from Th to Nd and descending from Sm to Yb, with Cs, Rb, Ba and Lu being absent, along with a weak positive Sr anomaly and without the negative Ti anomaly seen in the BOG (Fig. 6.31). The REE plot shows omphacite following a humped pattern within the values obtained for the BOG (Fig. 6.32).

Garnet grains in the pyroxenite layer show a steeply increasing spider plot pattern from Ce to Dy, with negative anomalies at Sr, Nd, Zr and Ti (Fig. 6.33). Garnet core and rim values are comparable up until Dy, where garnet rim values show a slightly descending pattern, falling within the BOG field, while the garnet core values stay on a slightly ascending pattern from Dy to Lu (Fig 6.33). This pattern is emphasised in the REE plot, which shows comparable REE plots for core and rim values up until Er where rim concentrations decrease, identical to the BOG field, while core values continue to increase through the HREE's (Fig 6.34). Both the core and rim values are below BOG values from Pr to Dy. Core and Rim values are largely absent from Cs to Ce.

Diopside within the pyroxenite sample shows a pattern similar to omphacite in the BOG from La to Eu, but shows a positive Sr anomaly and a stronger negative Zr anomaly than the BOG. From Ti to Lu diopside shows elevated concentrations relative to the BOG (Fig. 6.33). The REE plot accentuates these differences; from La to Eu the diopside plots along the lower edge of the BOG field (slightly more depleted LREE's), while from Dy to Lu plots on the upper edge to above the BOG field (slightly enriched HREE's) (Fig. 6.34), creating a flatter overall pattern while still retaining the humped shape.

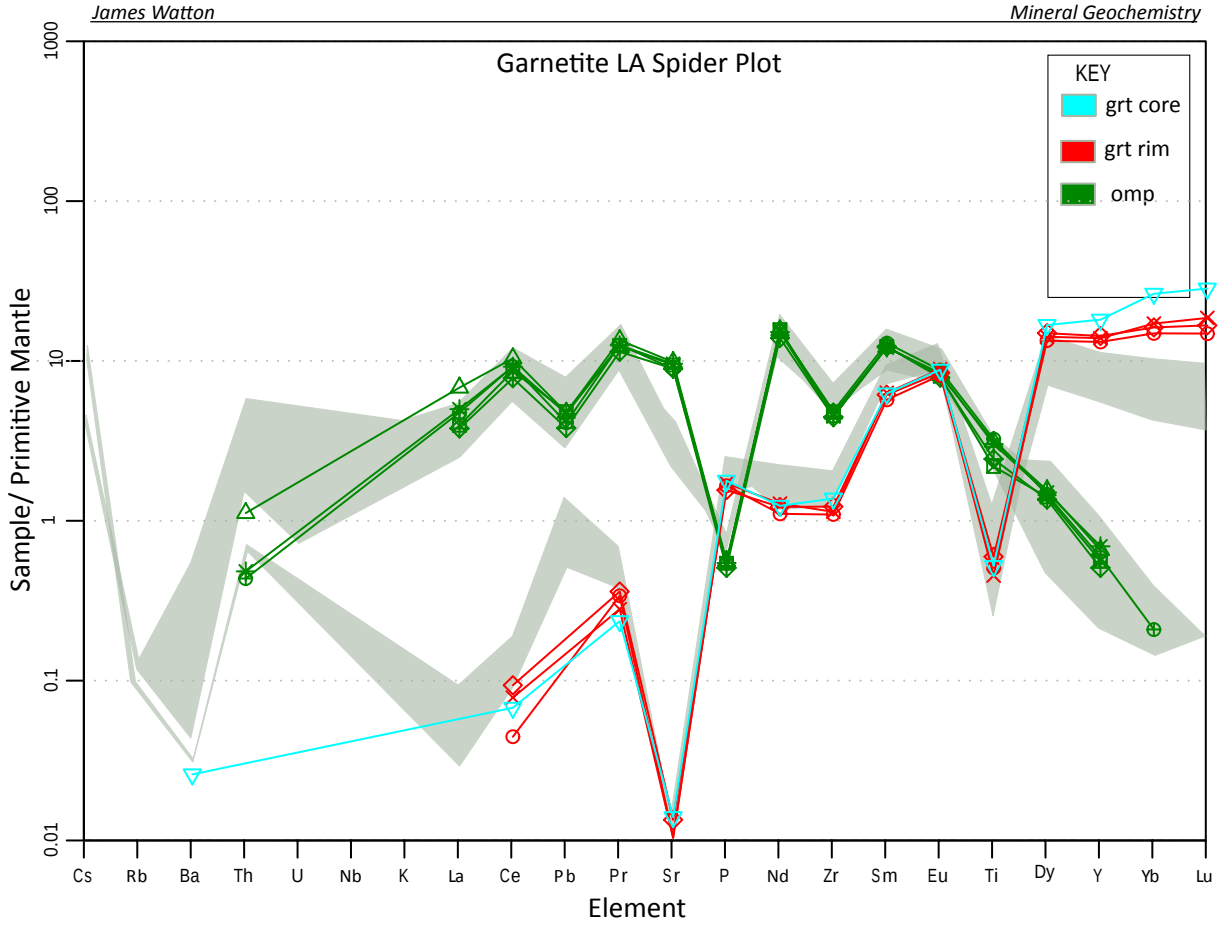

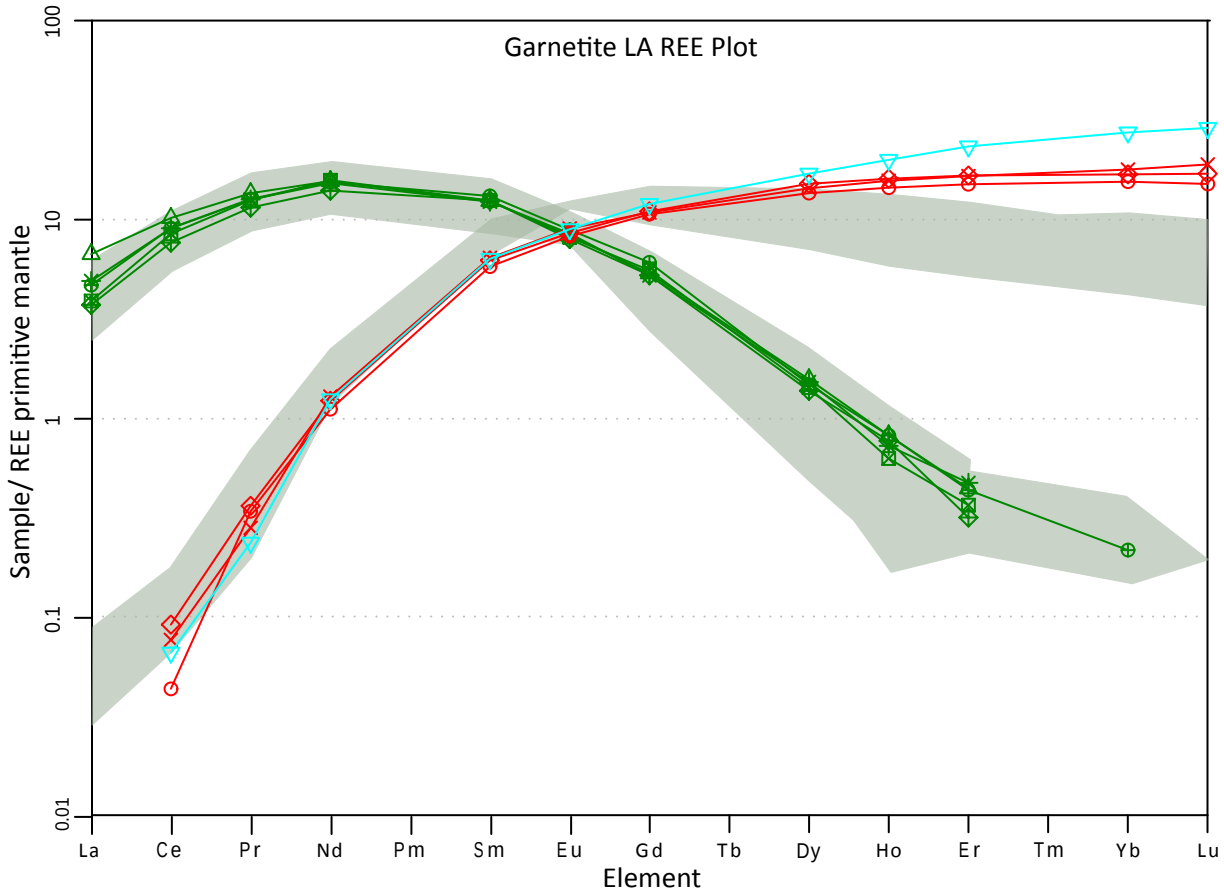

Fig 6.31 Spider diagram of LA mineral grains from garnetite normalised to primitive mantle values of Sun & McDonough (1989).

Fig 6.32 REE plot of of LA mineral grains from garnetite normalised to primitive mantle values of McDonough et al., (1991). Grey shows BOG LA data.

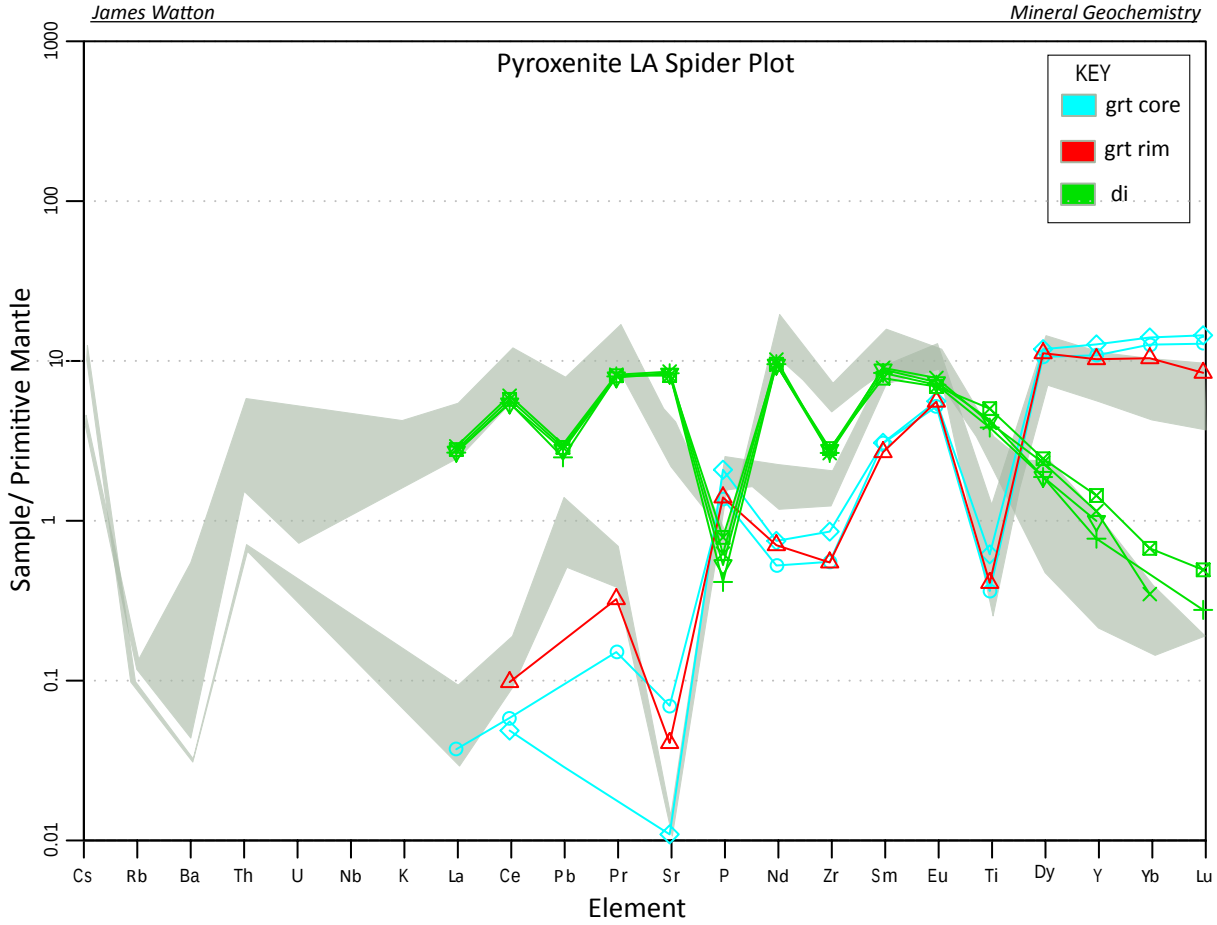

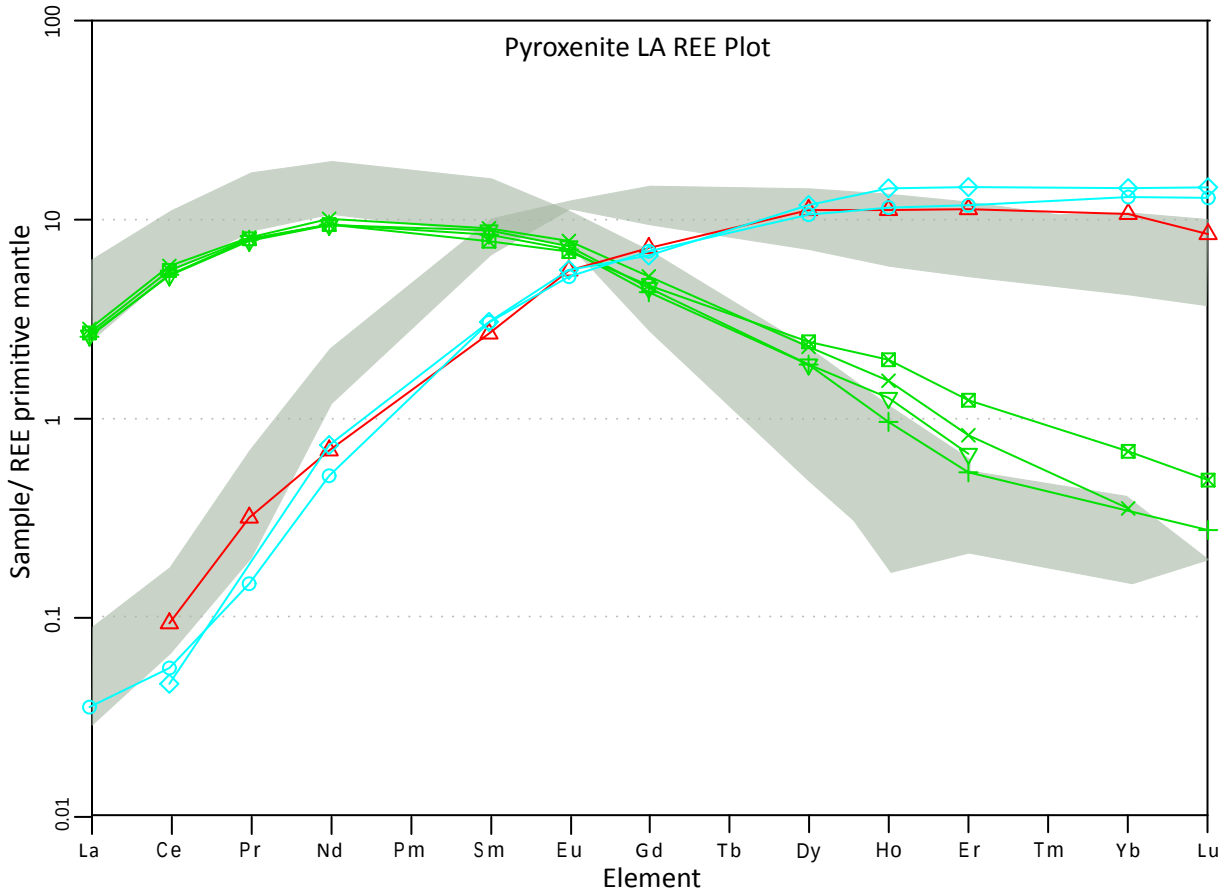

Fig 6.33 Spider diagram of LA mineral grains from pyroxenite normalised to primitive mantle values of Sun & McDonough (1989).

Fig 6.34 REE plot of of LA mineral grains from garnetite normalised to primitive mantle values of McDonough et al., (1991). Grey shows BOG LA data.

Hornblende Peridotite

Laser ablation was conducted on 10 mineral grains within the hornblende peridotite sample 0903B (Appendix 6.E). Multi element spider plots and REE plots normalised to primitive mantle values of Sun & McDonough (1989) [spider plots] and McDonough et al., (1991) [REE plots] show trace element patterns for garnet, pargasite and enstatite (Figs. 6.35 & 6.36).

Garnet within the hornblende peridotite sample shows a marked difference from garnet patterns found in the BOG (Figs. 6.35 & 6.36); showing an increasing pattern from La to Dy that is not as steep as that of the BOG, with a positive anomaly at La and negative anomalies at Sr, Nd and Ti (Fig. 6.35). From Dy to Lu garnet shows flat or ascending concentrations, unlike the BOG which decreases. The REE plot also shows the differences between the garnet in sample 0903B and the BOG, with elevated La and increasing HREE's, but with depleted Nd, Sm and Eu relative to the BOG (Fig. 6.36).

Enstatite grains from the hornblende peridotite sample show an overall humped pattern, though at abundances much lower than those seen in omphacite and diopside (Fig. 6.35), ascending from Rb to Sr and descending from Nd to Y, with negative anomalies at Pb, P, Zr and Ti. The REE plot for enstatite shows a humped pattern, ascending from La to Nd and decreasing from Sm to Er, at much lower abundances than the BOG omphacite (Fig. 6.36).

Pargasite data from the hornblende peridotite sample also shows a humped pattern, though at greatly increased abundances (Figs. 6.35 & 6.36), the spider plot shows an ascending pattern from Cs to Sr and a descending pattern from Nd to Lu, with positive anomalies at Cs, Rb and Ba and negative anomalies at Pb, P, Zr and Ti (Fig. 6.35). The REE pattern for pargasite shows a humped pattern ascending from La to Nd and descending from Sm to Lu, with abundances becoming more varied in the HREE's (Fig. 6.36).

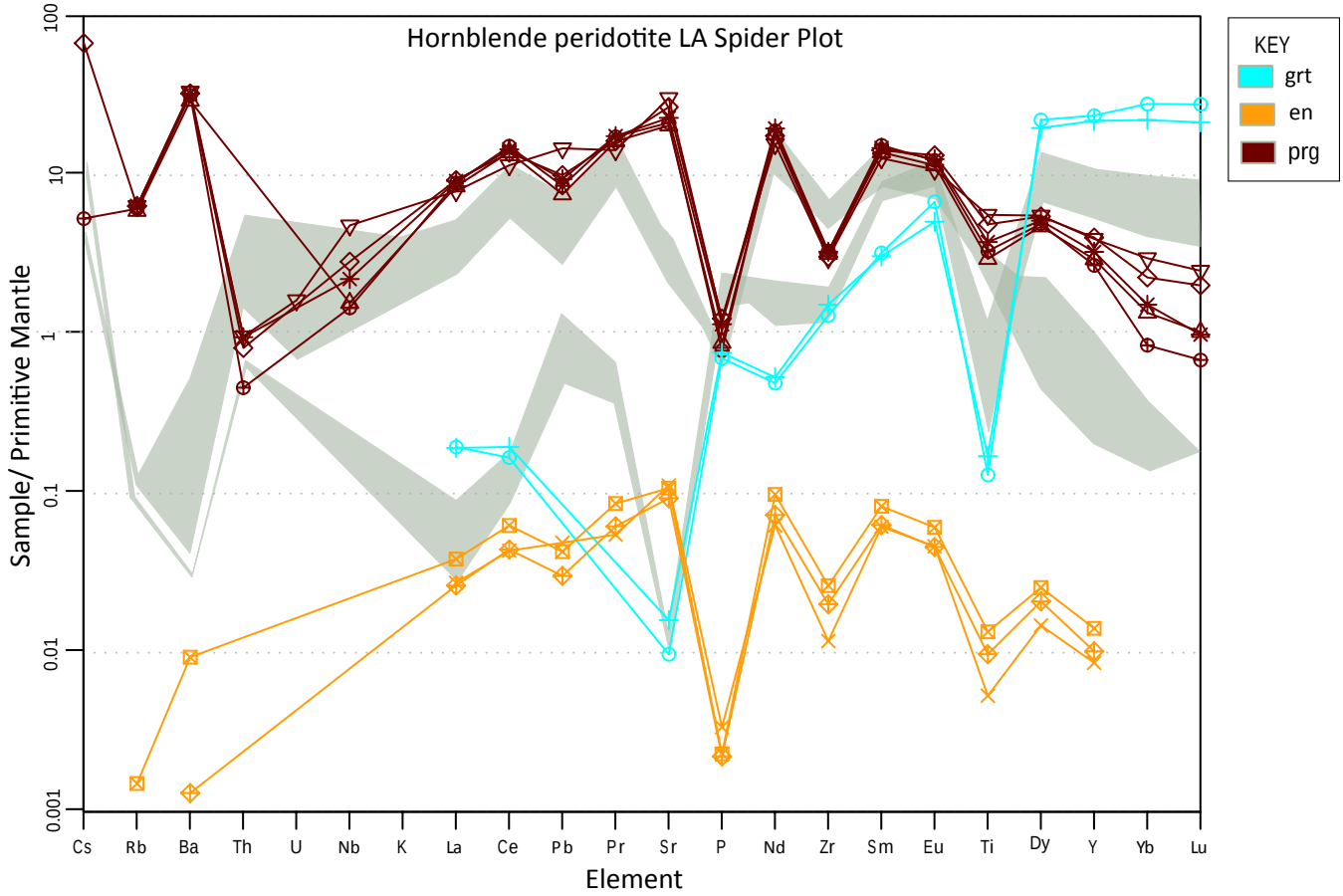

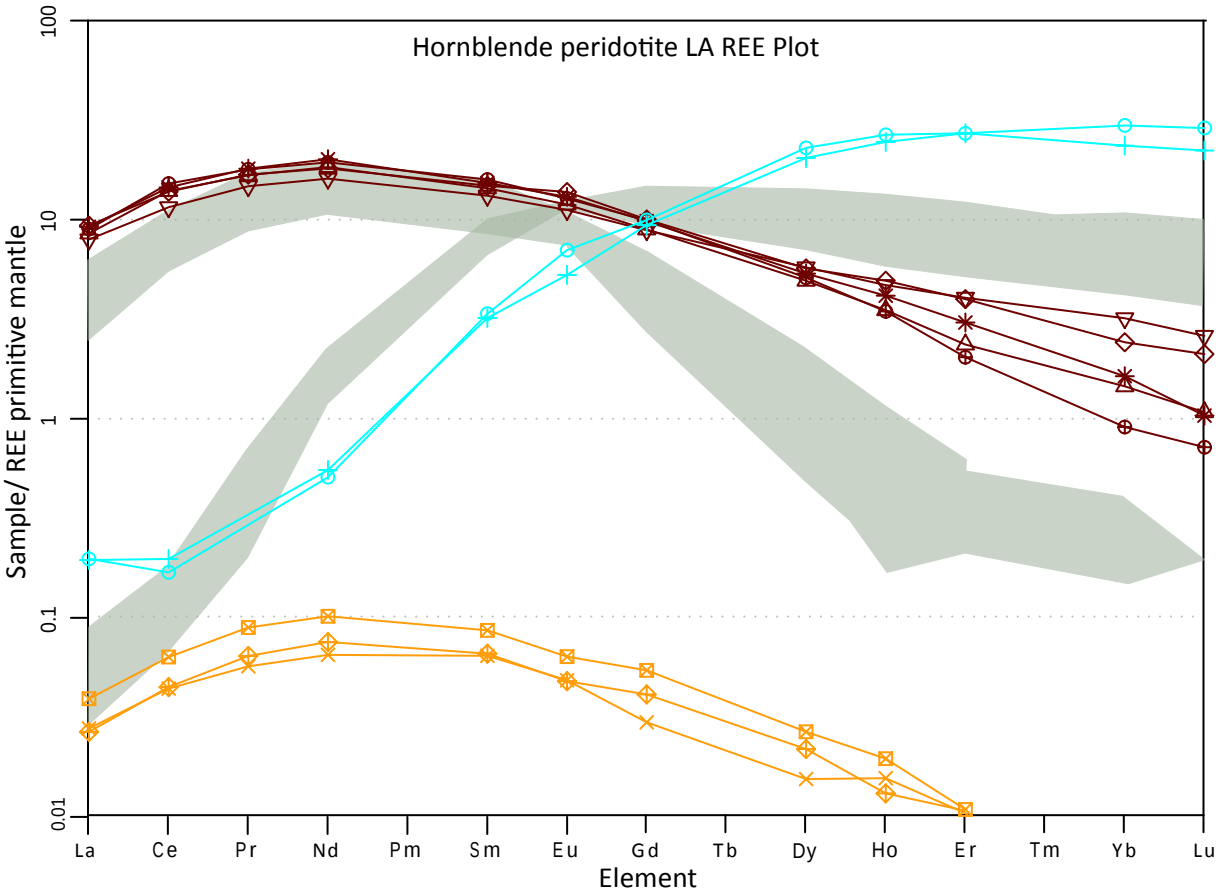

Fig 6.35 Spider diagram of LA mineral grains from hornblende peridotite normalised to primitive mantle values of Sun & McDonough (1989).

Fig 6.36 REE plot of of LA mineral grains from hornblende peridotite normalised to primitive mantle values of McDonough et al., (1991). Grey shows BOG LA data.

6.2.3 Mineral and symplectite examination using Element Mapping

Element mapping using MATLAB was performed on 6 polished thin sections of representative lithologies, to aid in mineral identification, zoning and symplectite composition. Slides analysed were 0905B, 0909 (BOG), 0905C (BOG variant), 0904C (BE) 0906B (garnetite) and 0903B (hornblende peridotite). Wt% cutoffs for the graphical display are adjusted for indicator elements to highlight different minerals and zoning within minerals. Element maps are shown with thin section photographs of mapped areas where available. Maps for samples 0905B, 0905C, 0906B and 0909 are 512 x 512 steps (step size 4μm = map size 2.048mm across) while maps for samples 0904C and 0903B are 256 x 256 steps (1.024mm across).

Breaksea Omphacite Granulite

Element mapping focussed on garnet and pyroxene zoning (0905B) and symplectite composition (0909 and 0905B)

Mapping sample 0905B, by displaying Mg from 0 – 15wt% (Fig. 6.37) shows pargasite development in symplectite and the extent of pyrope zoning in garnet. Pargasite is also visible within an inclusion in garnet. Showing Al from 0 – 19wt% (Fig. 6.38) highlights the extent of zoning in omphacite and shows plagioclase in symplectite and unzoned orthoclase grains. Viewing Ca from 0 – 30wt% (Fig. 6.39) shows apatite in omphacite, plagioclase and garnet and also highlights pargasite within the garnet inclusion and in symplectite, while viewing Ca from 7 – 14wt% allows the extent of grossular zoning in garnet to be easily observed (Fig. 6.40).

Sample 0909 in PPL can be viewed in Fig. 6.41. Displaying Mg from 0 – 0.15wt% (Fig. 6.42) shows pargasite in symplectite development at garnet and omphacite grain boundaries; biotite in symplectite and zoning in both omphacite and garnet. Viewing Al from 5 – 28wt% delineates the breakdown of omphacite into symplectite being replaced by plagioclase (Fig. 6.43). Also visible are small amounts of andesine – labradorite plagioclase in symplectite. Ca from 6 – 22wt% shows apatite, the extent

of zoning in omphacite and garnet as well as showing pargasite in symplectite development (Fig. 6.44). Fe (0 – 45wt%) (Fig. 6.45) used in conjuction with Ti (0 – 45wt%) (Fig. 6.46) shows that opaque minerals are rutile, ilmenite and hematite, with hematite and ilmenite present within the symplectite.

The BOG variant 0905C mapped area can be viewed in PPL (Fig. 6.47). Displaying Mg from 0 – 20wt% shows enstatite as well as the breakdown of omphacite into biotite and pargasite within a symplectite(Fig. 6.48). Na from 0 – 12wt% shows orthoclase (not complete orthoclase end member), Na zoning in plagioclase and omphacite (Fig. 6.49). Al from 0 – 40wt% shows bladed and interstitial kyanite grains (Fig. 6.50). Ca from 0 – 18wt% shows apatite and confirms the petrographic observation of anorthite rims around kyanite blades (Fig. 6.51), as well as showing the higher anorthite content in plagioclase cores compared to rims. Fe from 0 – 50wt% effectively highlights interstitial ilmenite present within the symplectite (Fig. 6.52).

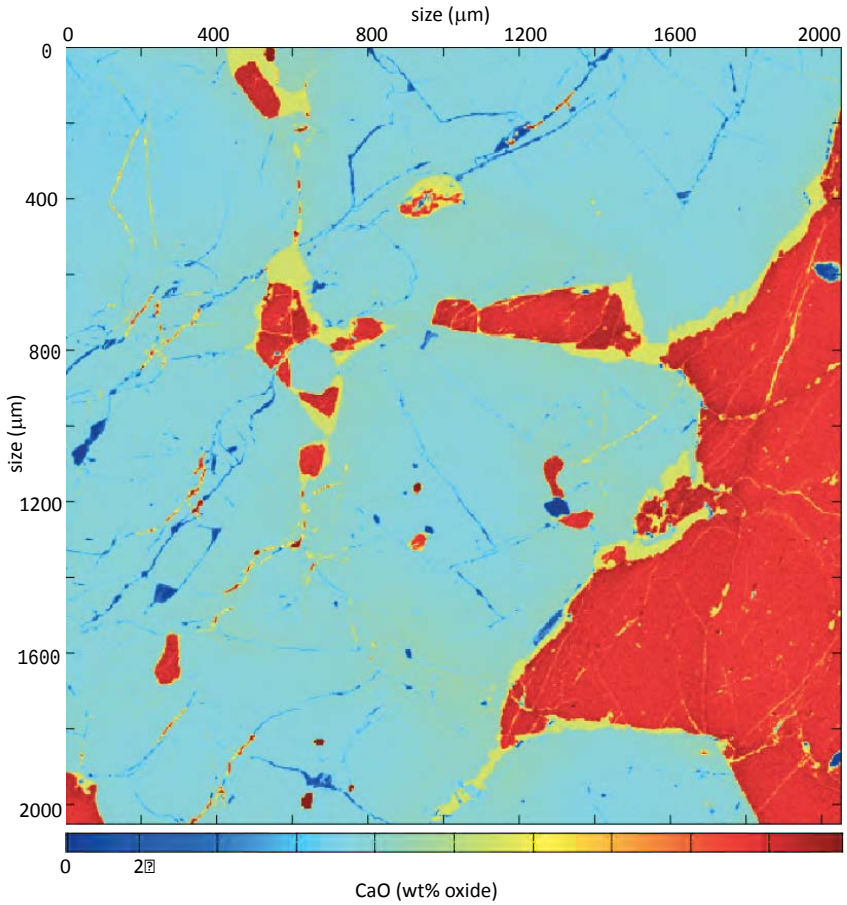

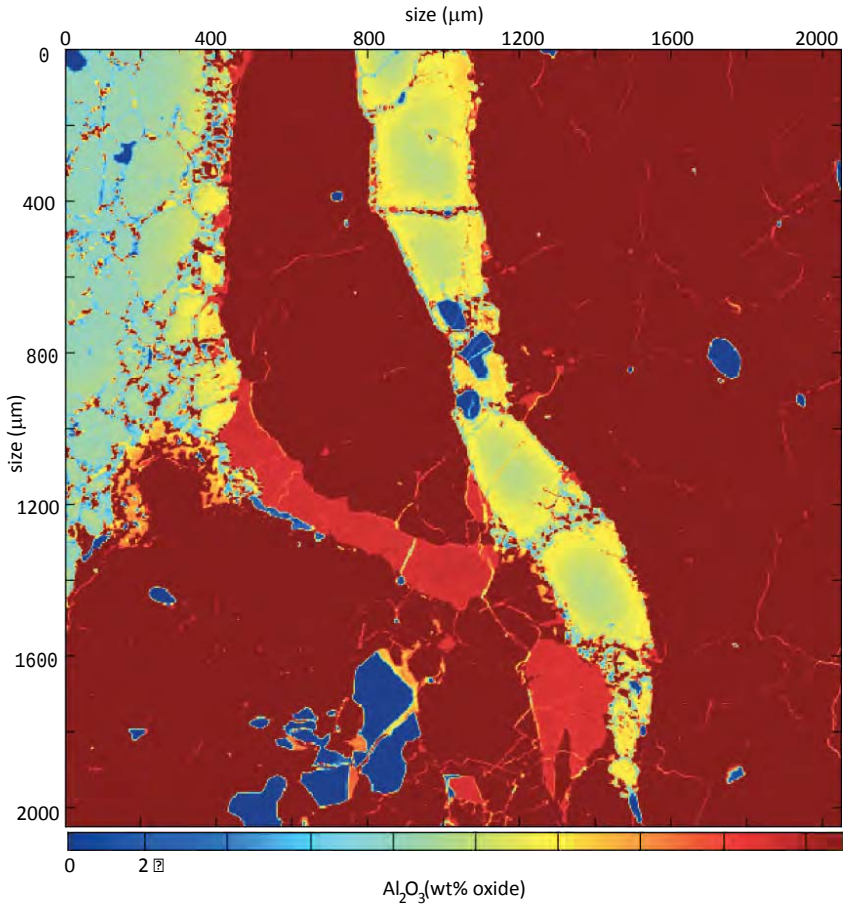

Fig 6.37 0905B. Element mapping image showing MgO concentration. Pargasite in symplectite and inclusions within garnet, omphacite and garnet and extent of zoning are visible.

Fig 6.38 0905B. Element mapping image showing Al_2O_3concentration. Omphacite zoning, plagioclase in symplectite and plagioclase grains and omphacite Both images are 2.048mm across

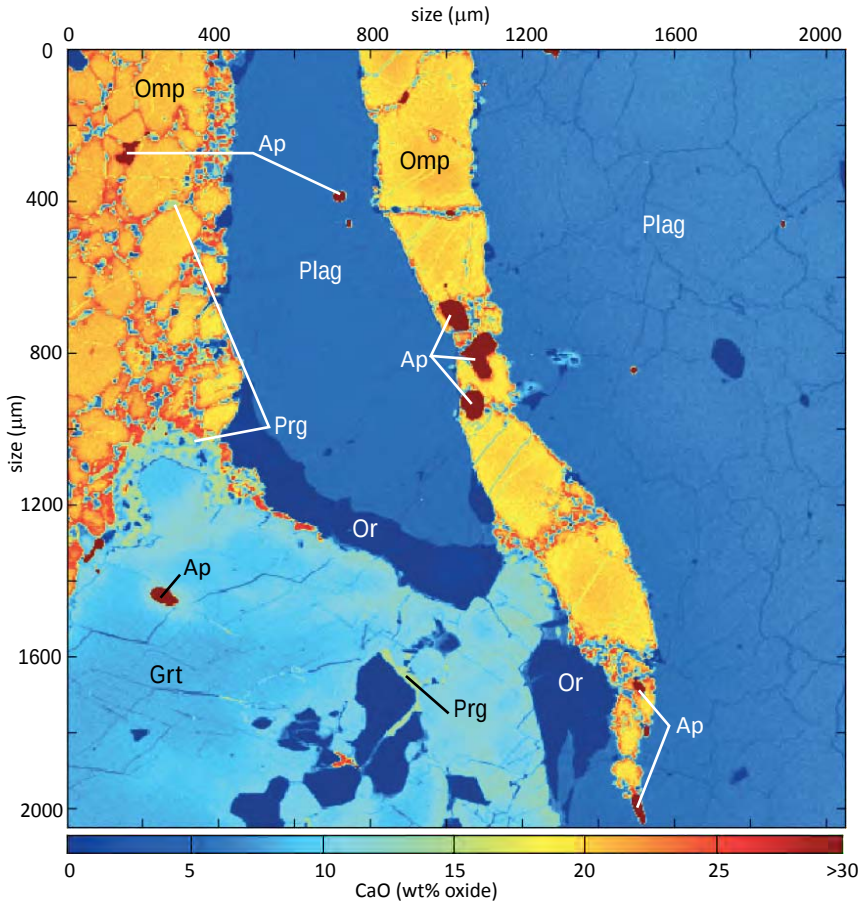

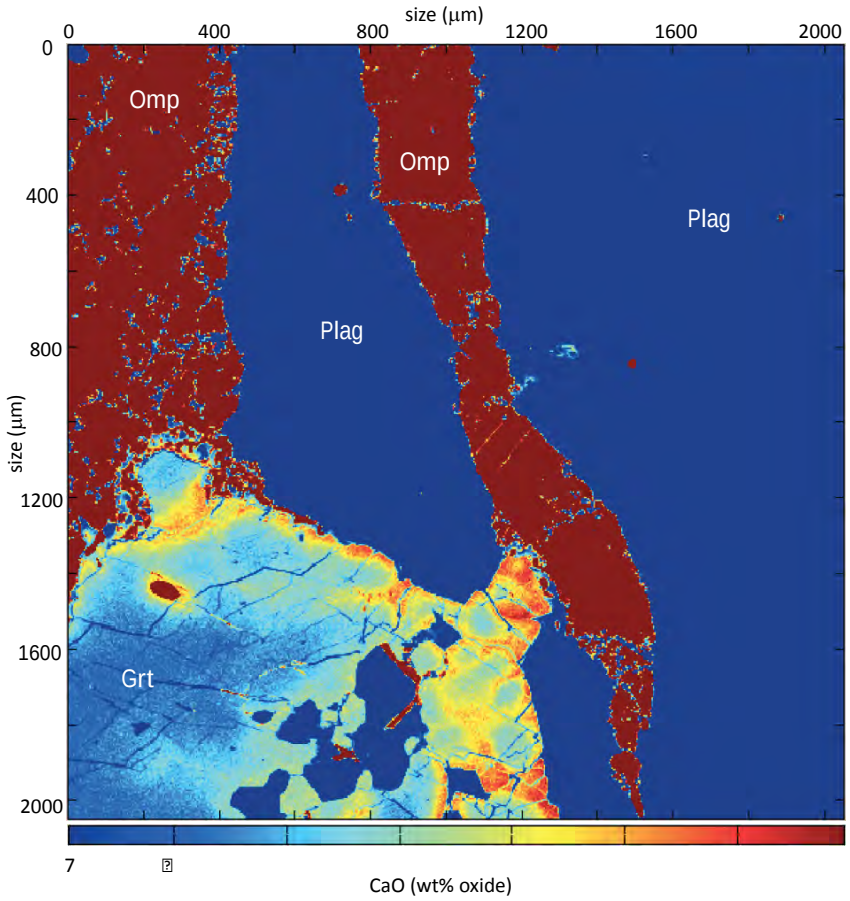

Fig 6.39 0905B. Element mapping image showing CaO concentration. Apatite is visible in omphacite, garnet and plagioclase.

Fig 6.40 0905B. Element mapping image showing CaO concentration. Extent of grossular zoning in garnet is visible. Both images are 2.048mm across.

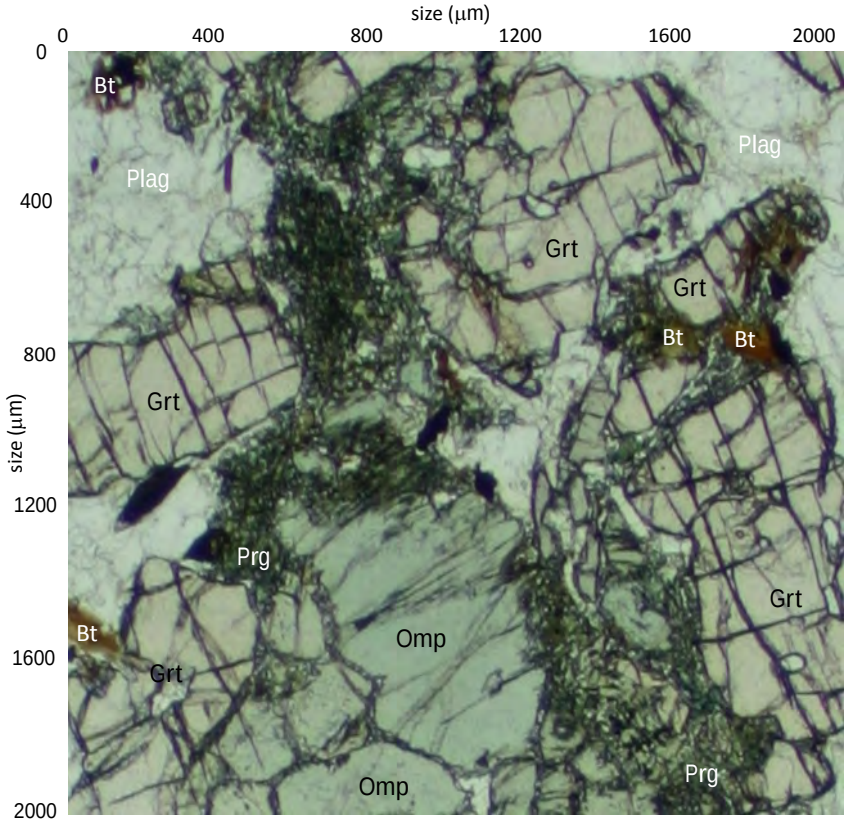

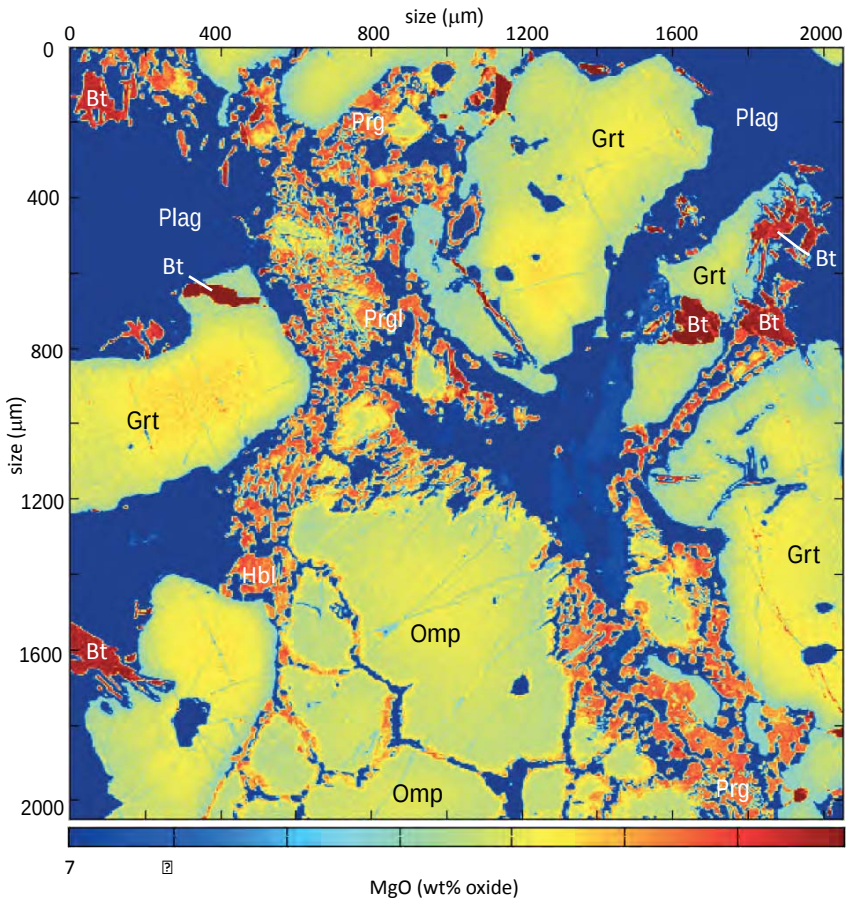

Fig 6.41 0909. PPL photomicrograph of element mapping area.

Fig 6.42 0909. Element mapping image showing MgO concentration. Pargasite and biotite at garnet and omphacite grain boundaries is visible. Extent of pyrope zoning in garnet and zoning in omphacite is also visible. Both images are 2.048mm across.

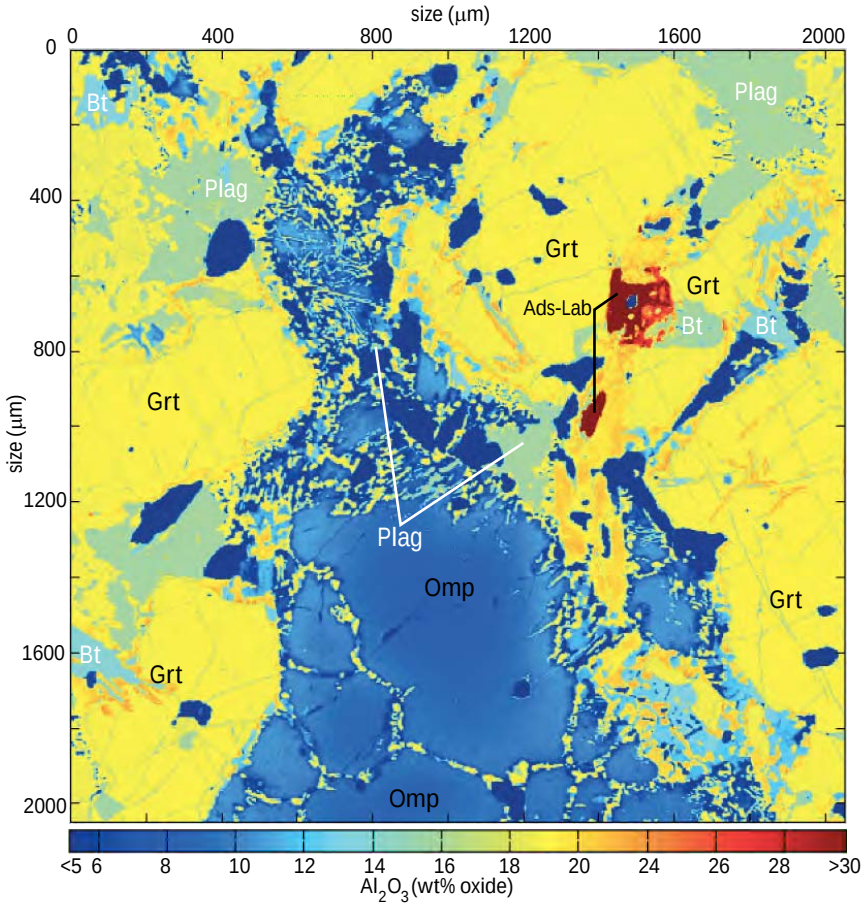

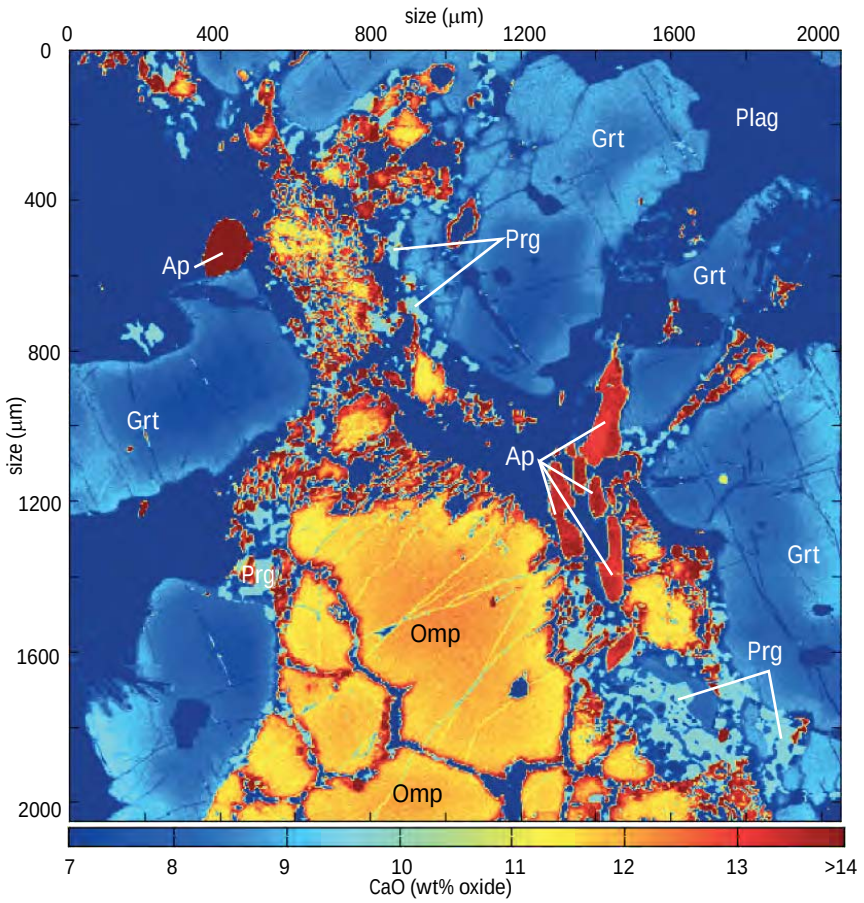

Fig 6.43 0909. Element mapping image showing Al_2O_3 concentration. Plagioclase grains and omphacite breakdown to plagioclase in symplectite visible. Andesine - labradorite plagioclase also visible.

Fig 6.44 0909. Element mapping image showing CaO concentration. Shows apatite, pargasite development in symplectite, extent of grossular zoning in garnet and zoning in omphacite. Both images are 2.048mm across.

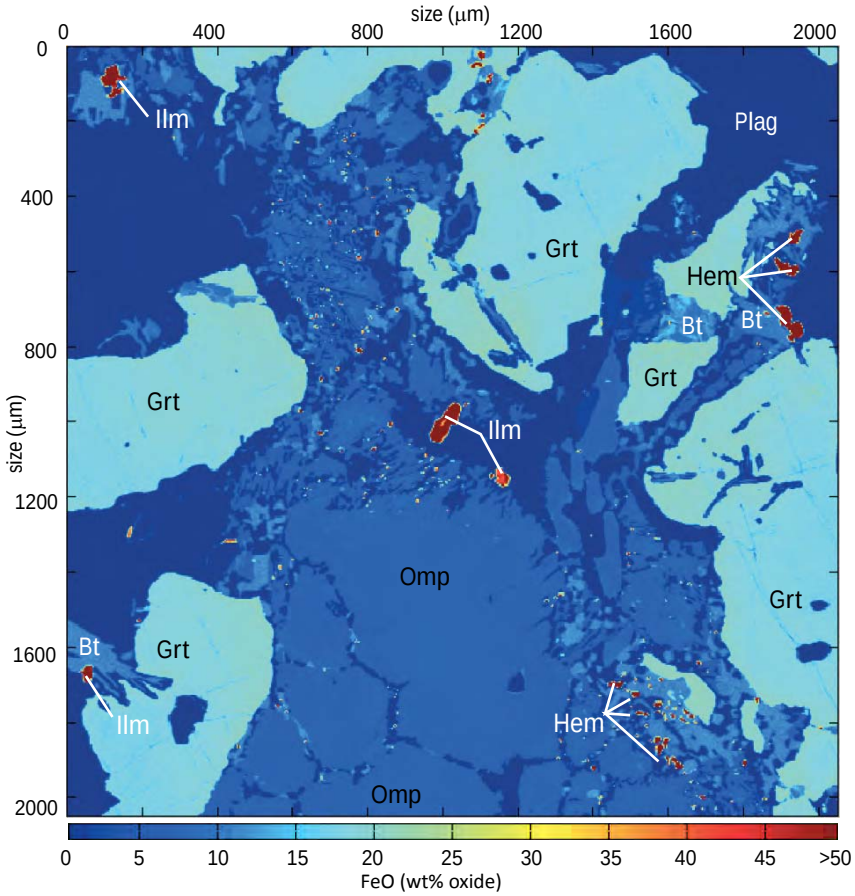

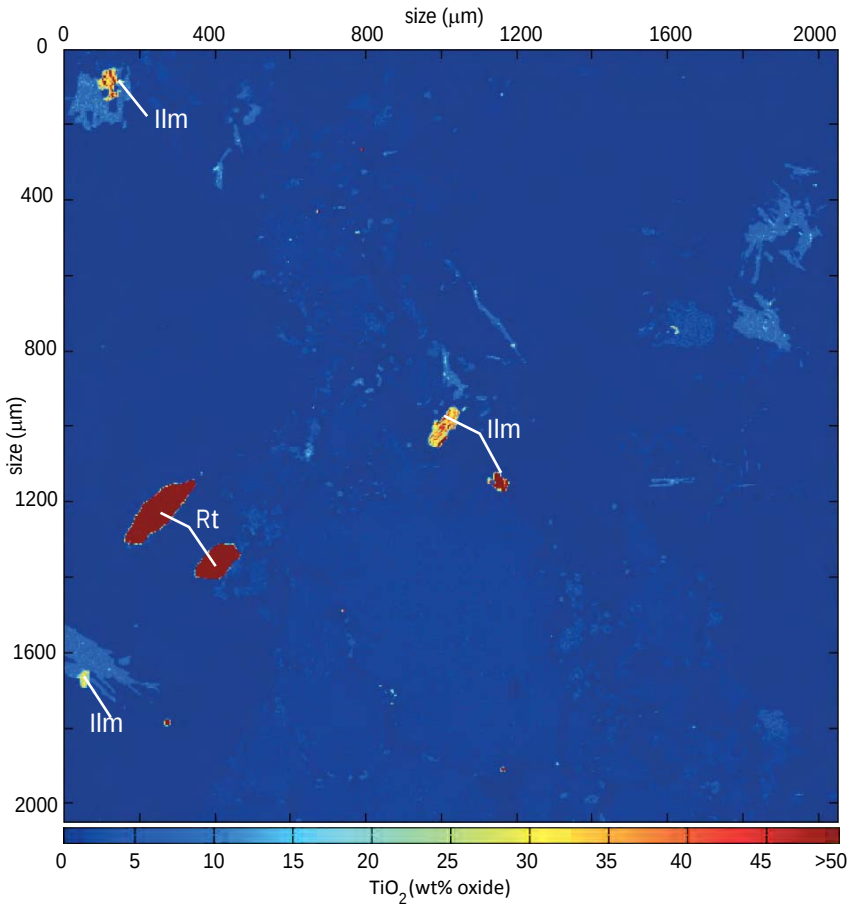

Fig 6.45 0909. Element mapping image showing FeO concentration. Shows ilmenite and hematite within symplectite.
Fig 6.46 0909. Element mapping image showing TiO_2 concentration. Shows rutile and ilmenite within symplectite.
Both images are 2.048mm across.

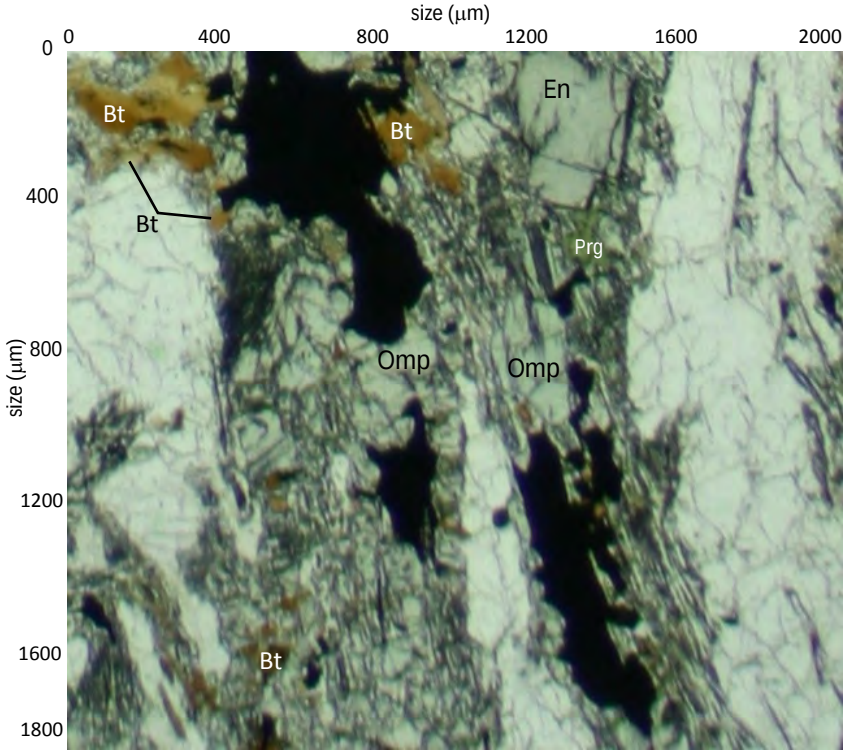

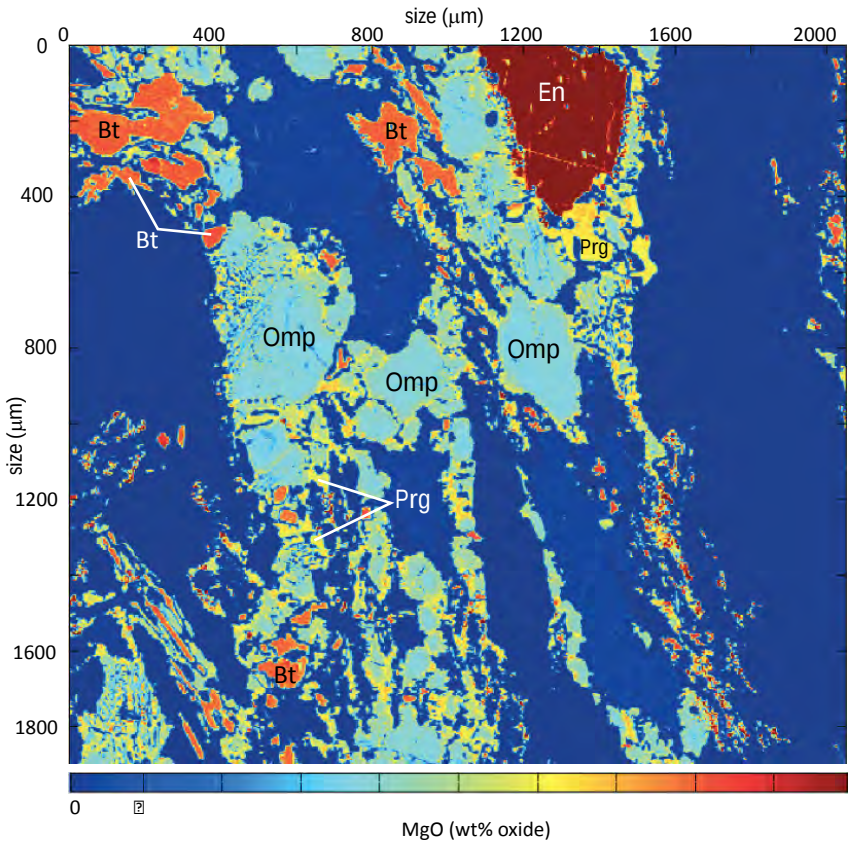

Fig 6.47 0905C. PPL photomicrograph of element mapping area.

Fig 6.48 0905C. Element mapping image showing MgO concentration. Enstatite is visible, as is the breakdown of omphacite into pargasite and biotite in symplectite. Both images are 2.048mm across.

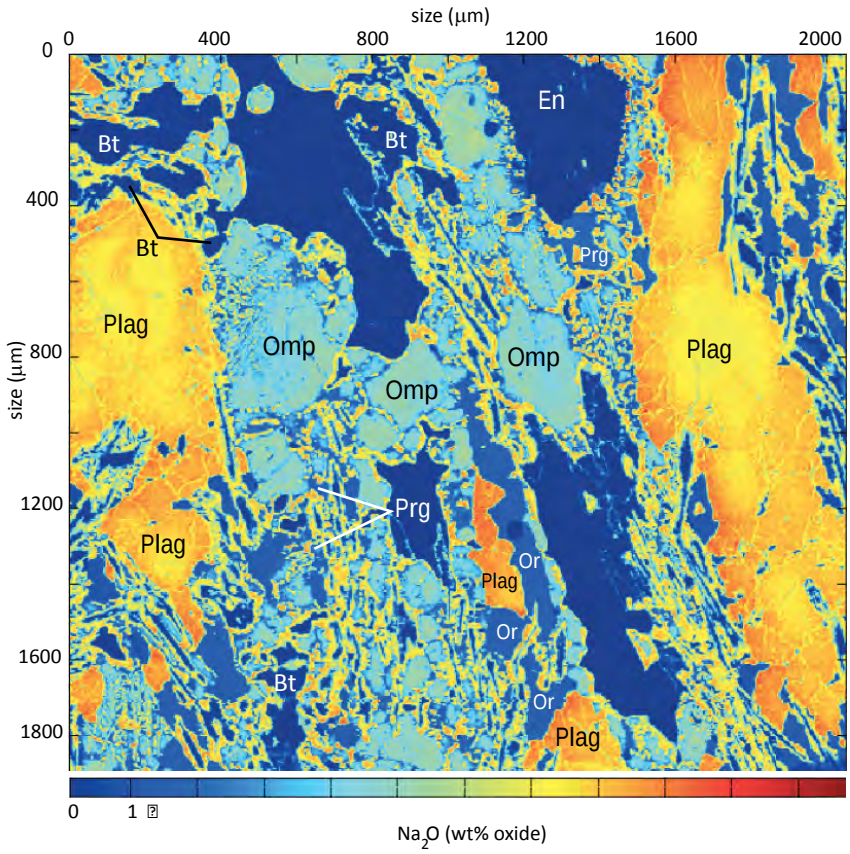

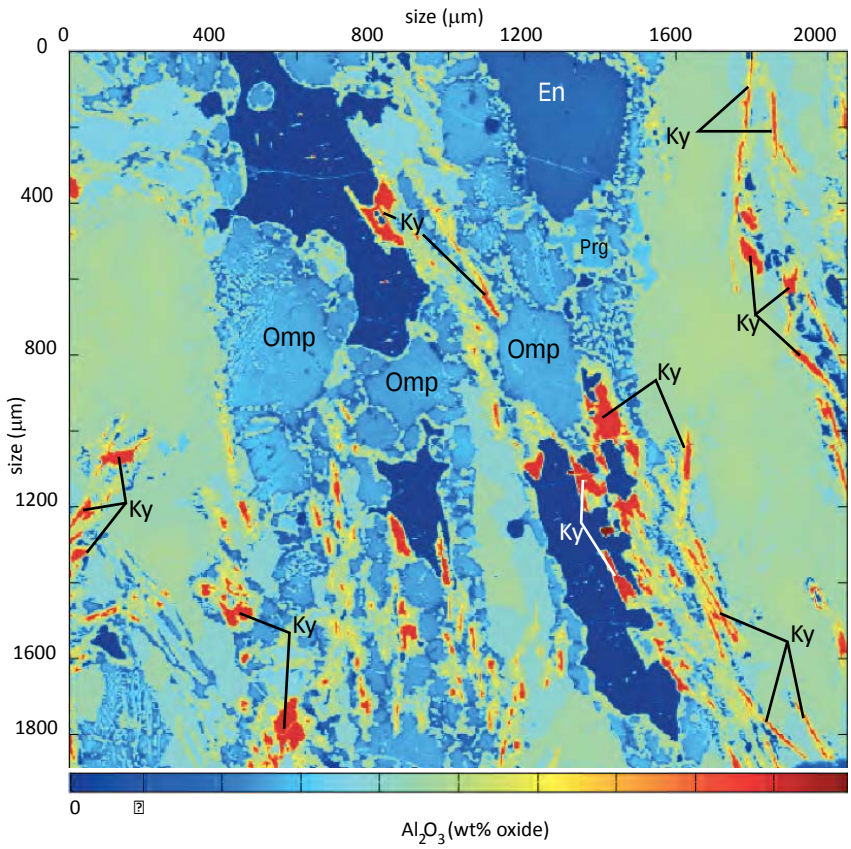

Fig 6.49 0905C. Element mapping image showing Na_2O concentration. Alkali feldpsar (Or) and Na zoning in plagioclase (strong) and omphacite (weak) can be observed.

Fig 6.50 0905C. Element mapping image showing Al_2O_3 concentration. Both bladed and interstitial kyanite are visible. Both images are 2.048mm across.

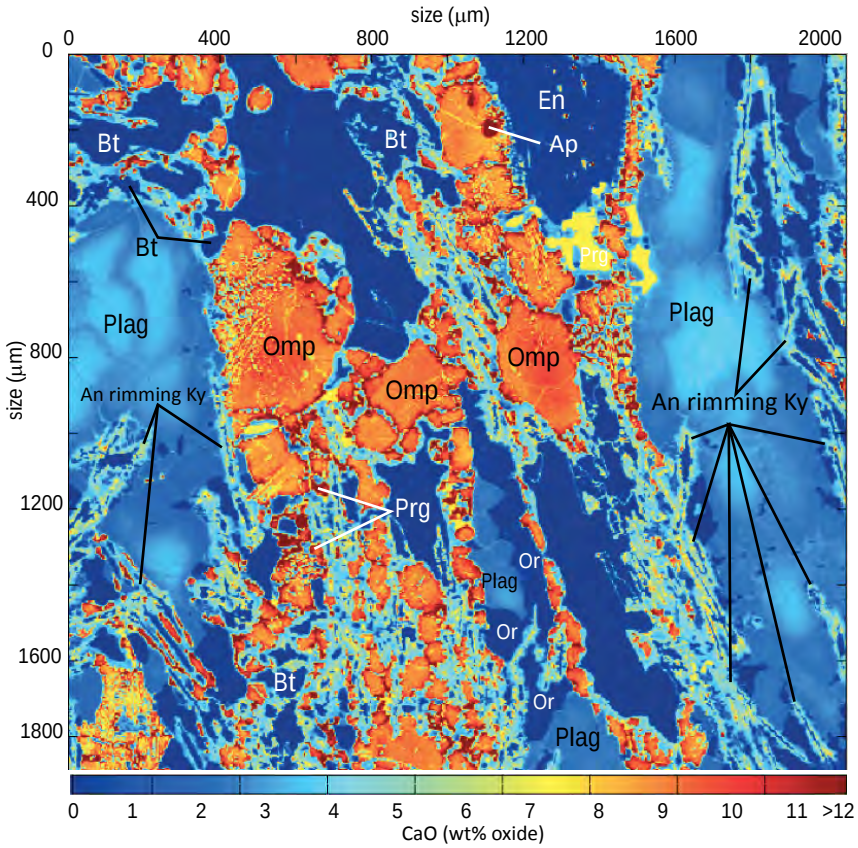

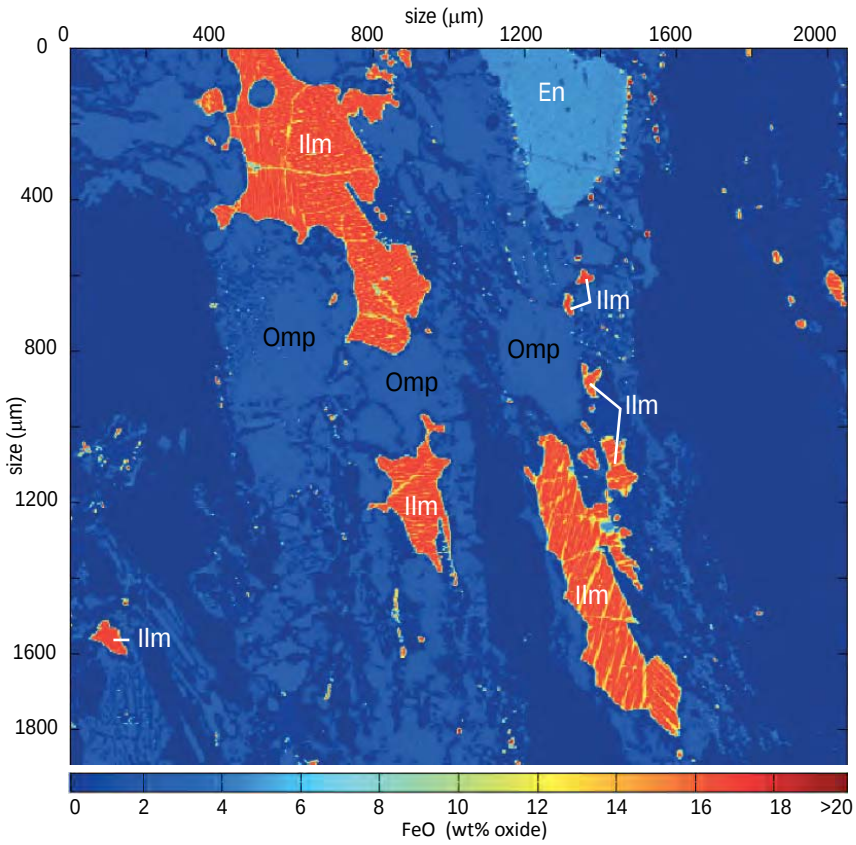

Fig 6.51 0905C. Element mapping image showing CaO concentration. Apatite, and anorthite rims around kyanite blades are visible. Higher anorthite content of plagioclase cores can also be observed.

Fig 6.52 0905C. Element mapping image showing FeO concentration, allows the viewing of ilmenite. Both images are 2.048mm across.

Breaksea Eclogite

BE sample 0904C can be seen in PPL and XPL in Fig. 6.53. Mg from 0-15wt% shows omphacite breakdown into biotite and pargasite symplectite (Fig. 6.54). Al from 8 – 25wt% shows plagioclase development in symplectite (Fig. 6.55). Ti from 0 – 100wt% shows ilmenite – rutile exsolution (Fig 6.56). Ca from 0 – 25wt% shows the extent of zoning in omphacite and also shows pargasite and biotite in symplectite (Fig. 6.57). Ca from 0 – 25wt% also shows epidote within the symplectite (Fig. 6.57).

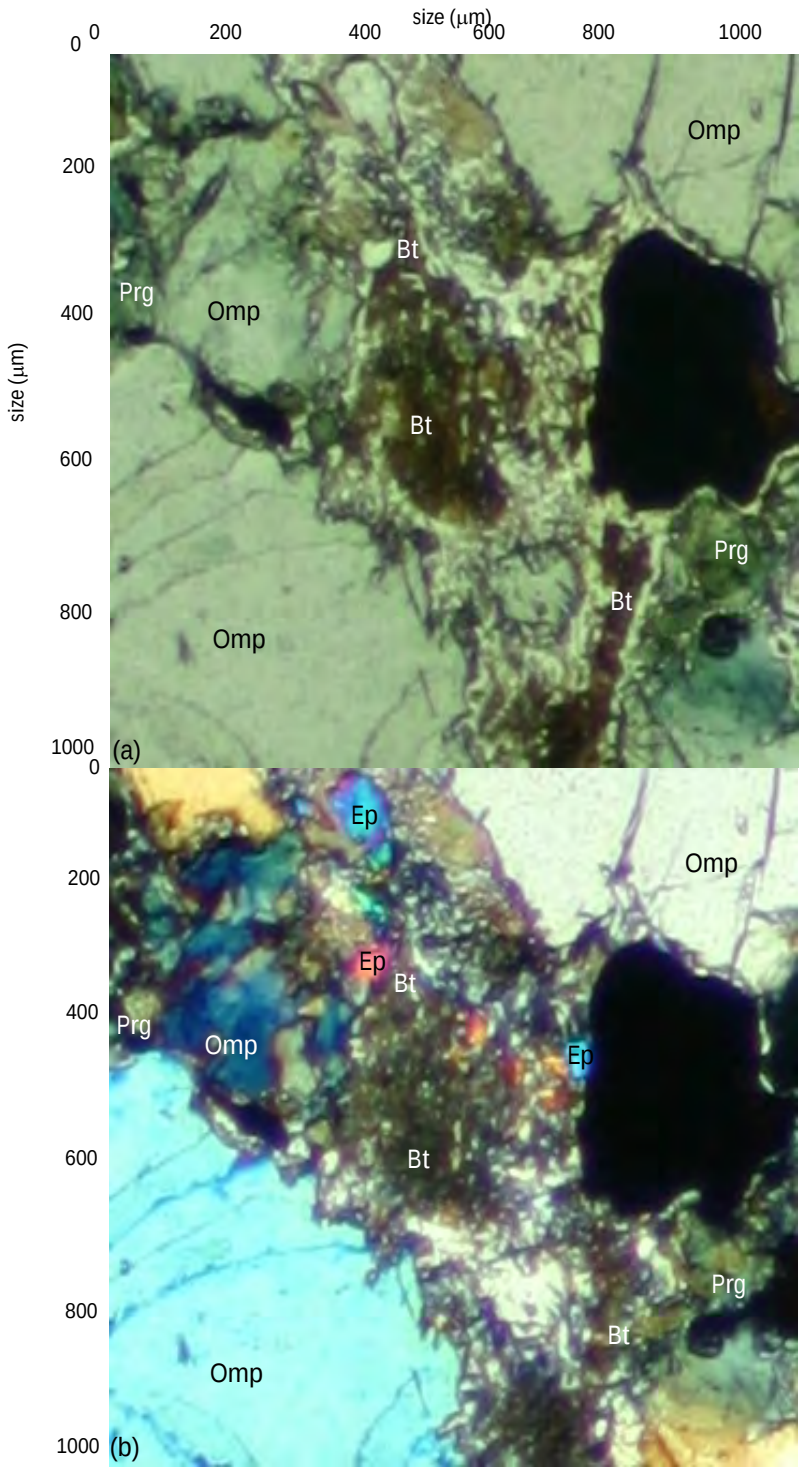

Fig 6.53 0904C (a) PPL (b) XPL Base of photo: 1.024mm Photomicrograph of 0904C element mapping area.

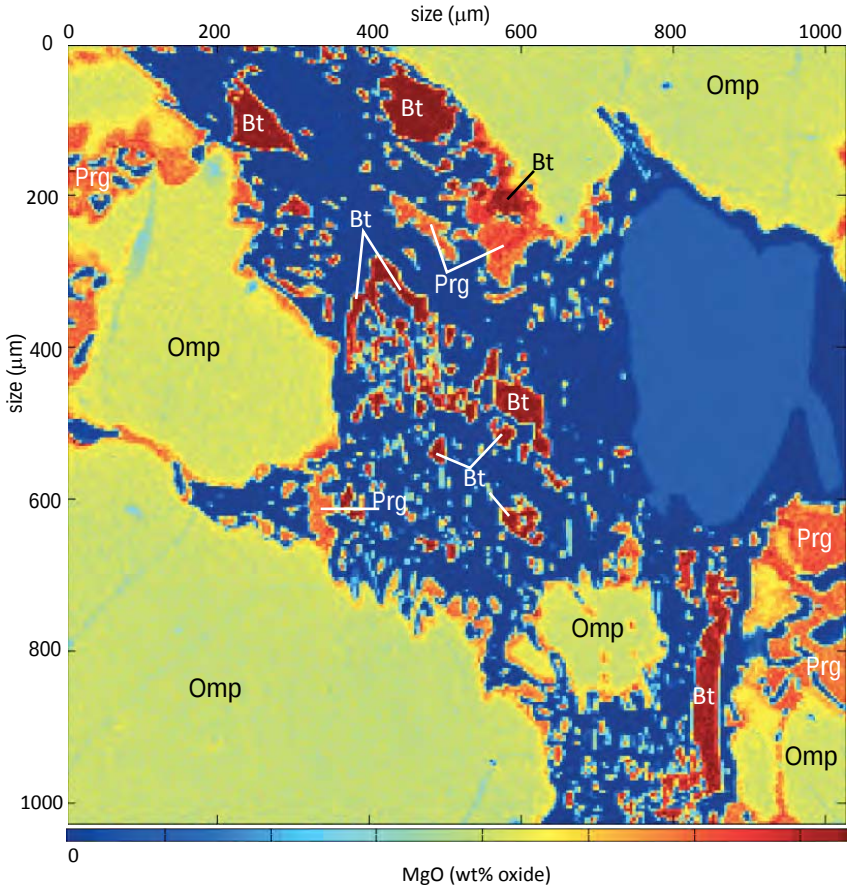

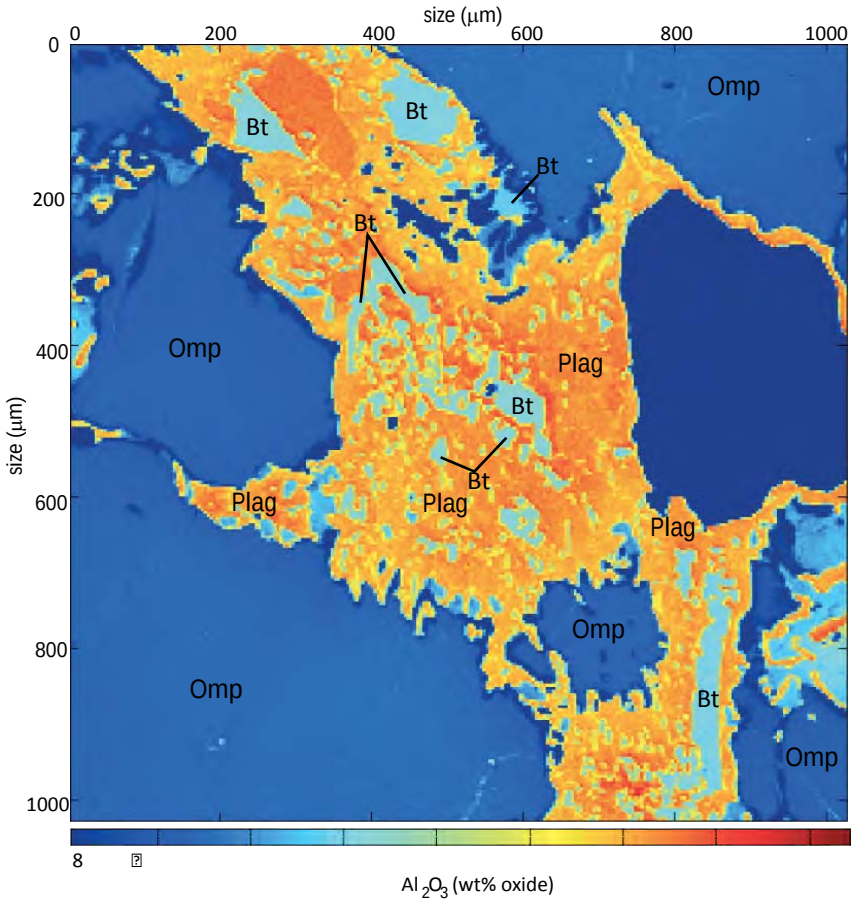

Fig 6.54 0904C. Element mapping image showing MgO concentration. shows omphacite breakdown into biotite and pargasite symplectite.

Fig 6.55 0904C. Element mapping image showing Al_2O_3 concentration, shows plagioclase development in symplectite. Both images are 1.024mm across.

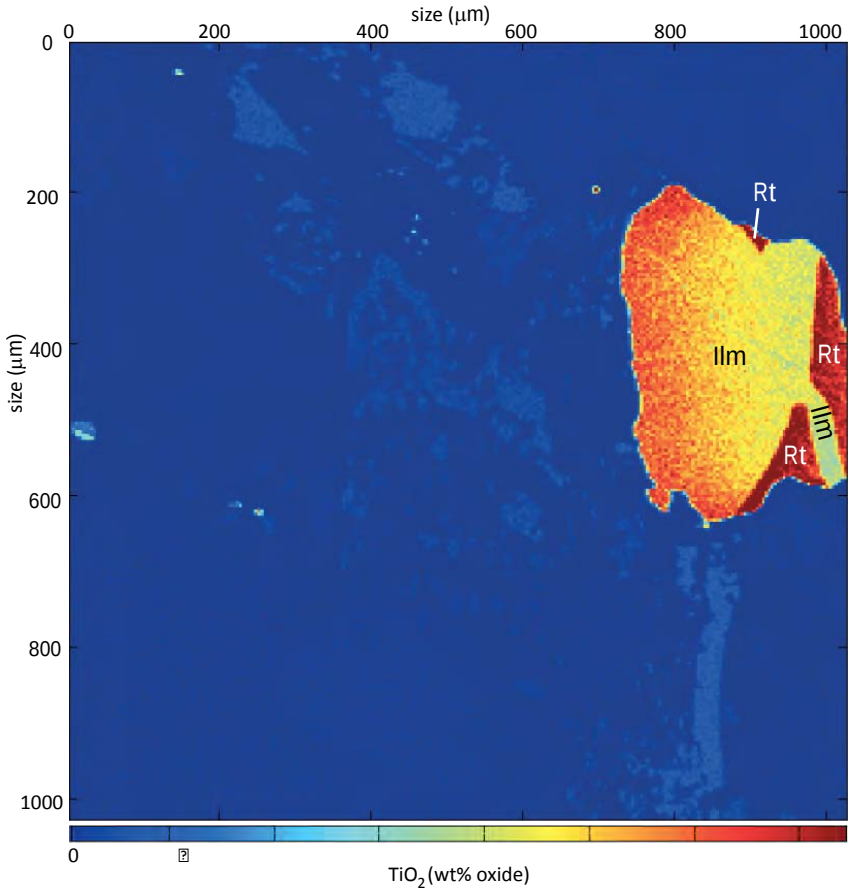

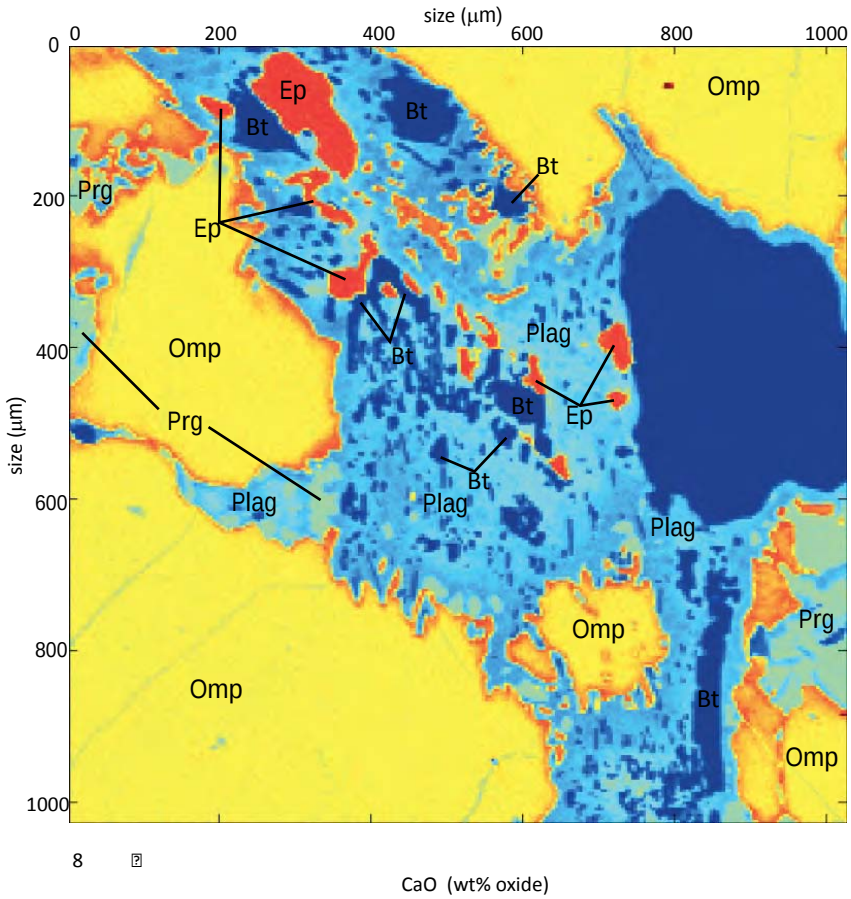

Fig 6.56 0904C. Element mapping image showing TiO_2 concentration. Shows ilmenite – rutile exsolution.

Fig 6.57 0904C. Element mapping image showing CaO concentration, shows the extent of zoning in omphacite and also shows pargasite and biotite in symplectite. Also shows epidote within symplectite.Both images are 1.024mm across.

Layered Garnetite – Pyroxenite

The layered rocks show little evidence of symplectite development and as such sample 0906B (garnetite) was selected for mapping to show zoning in garnet and diopside. Ca from 0 – 20wt% shows apatite, diopside, garnet and pargasite forming at the pyroxene/garnet boundary (Fig. 6.58). Al from 3-13wt% shows the extent of zoning in diopside as well as confirming the presence of pargasite (Fig. 6.59). Mg from 5 – 12wt% shows zoning in diopside and garnet, highlights pargasite at grain boundaries (Fig. 6.60). A euhedral garnet grain can also be observed in all figures.

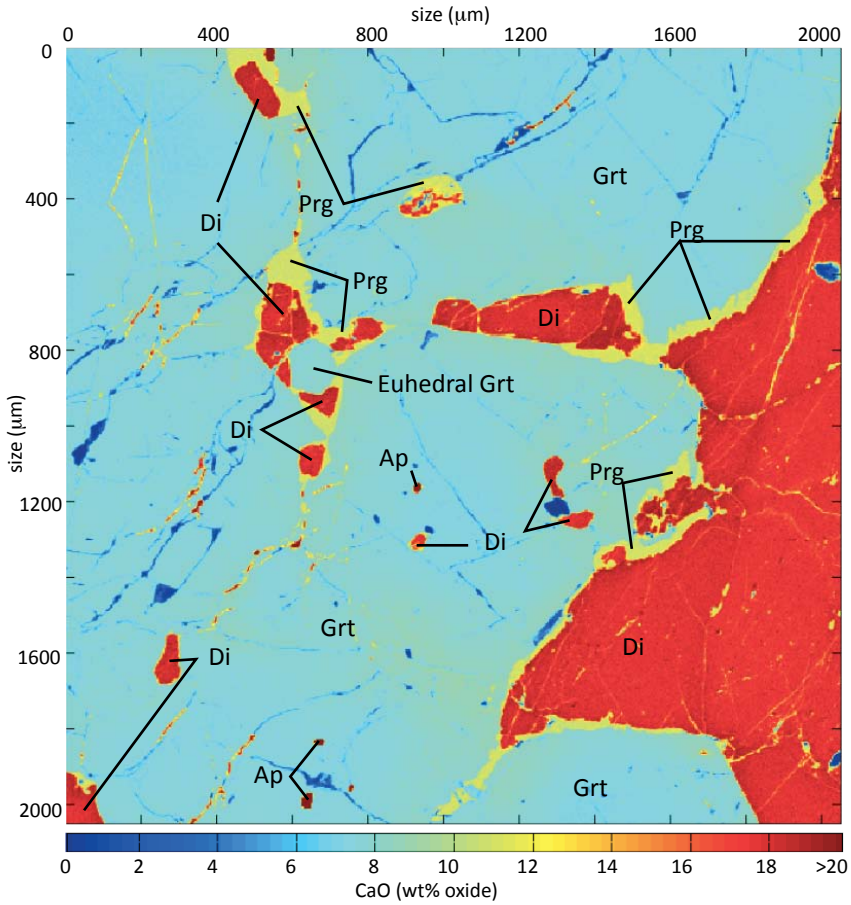

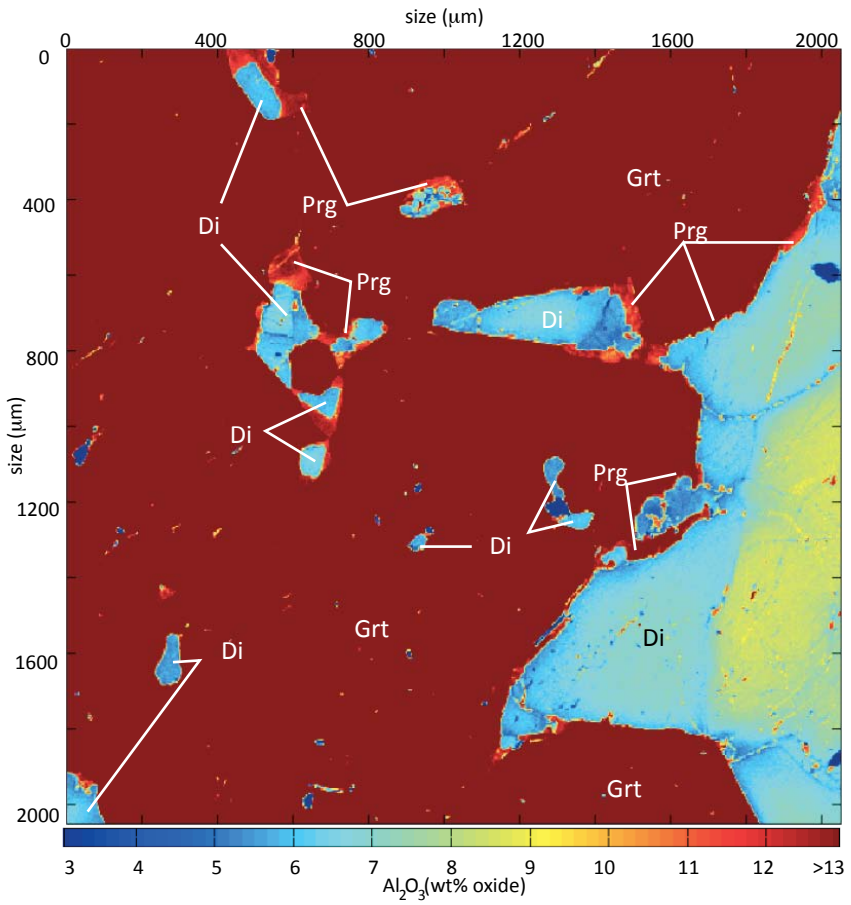

Fig 6.58 0906B. Element mapping image showing CaO concentration. Shows apatite, diopside, garnet and pargasite forming at the pyroxene/garnet boundary. Euhedral garnet is also visible.

Fig 6.59 0906B. Element mapping image showing Al_2O_3concentration. Shows the extent of zoning in diopside as well as confirming the presence of pargasite Both images are 2.048mm across.

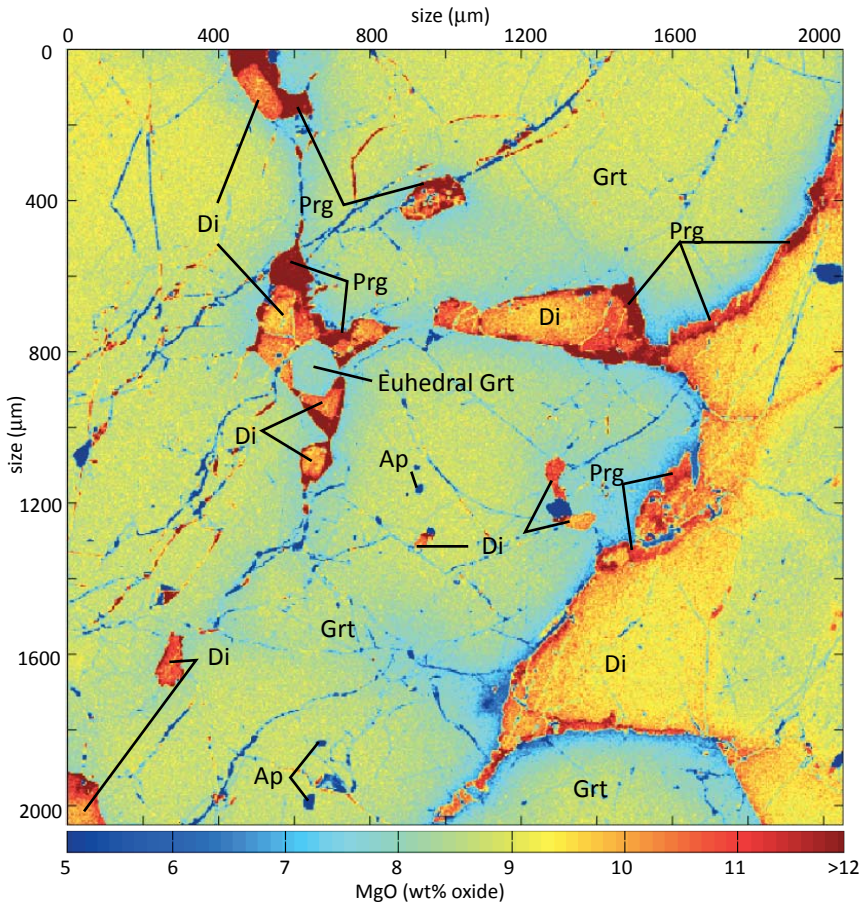

Fig 6.60 0906B. Element mapping image showing MgO concentration. Shows zoning in diopside and garnet, highlights pargasite at grain boundaries. Euhedral garnet also visible. Image is 2.048mm across.

Hornblende Peridotite

The hornblende peridotite symplectite can be seen in PPL in Fig. 6.61. Fe from 0 – 25wt% shows the extent of almandine zonation in garnet and allows enstatite to be seen as small interstitial grains (Fig. 6.62). Fe also allows ilmenite within the symplectite to be identified, along with hornblende and diopside. Mg from 0 – 20wt% shows insterstitial enstatite well, along with pyrope garnet zonation (Fig 6.63). Na from 0 – 1 wt% shows the extent of zoning within diopside, and clearly delineates pargasite (Fig 6.64).

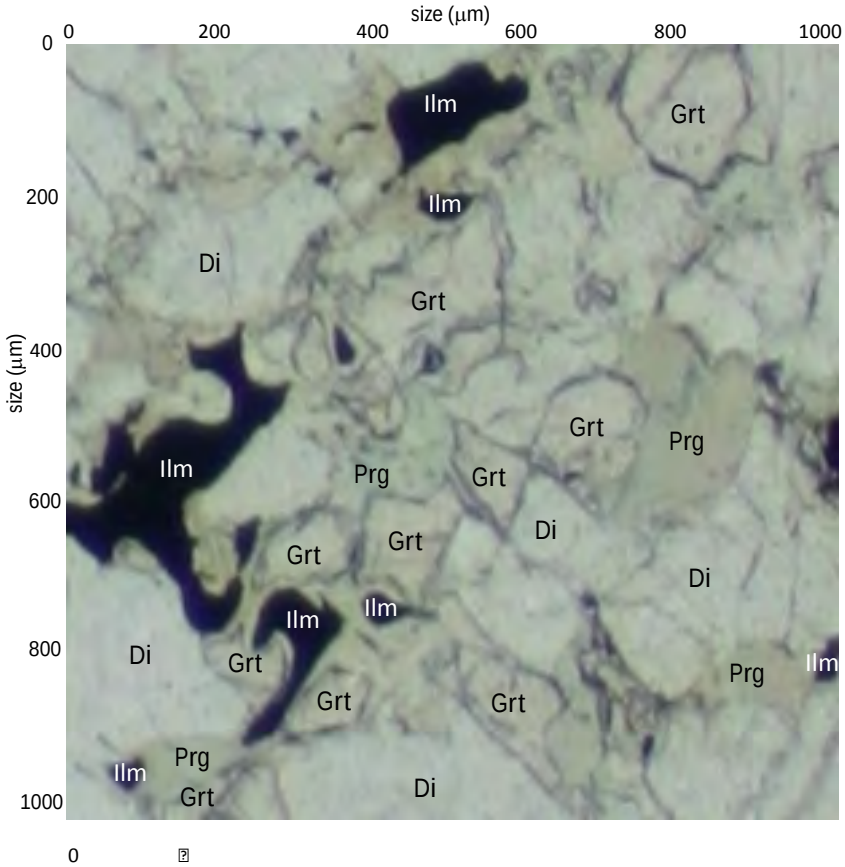

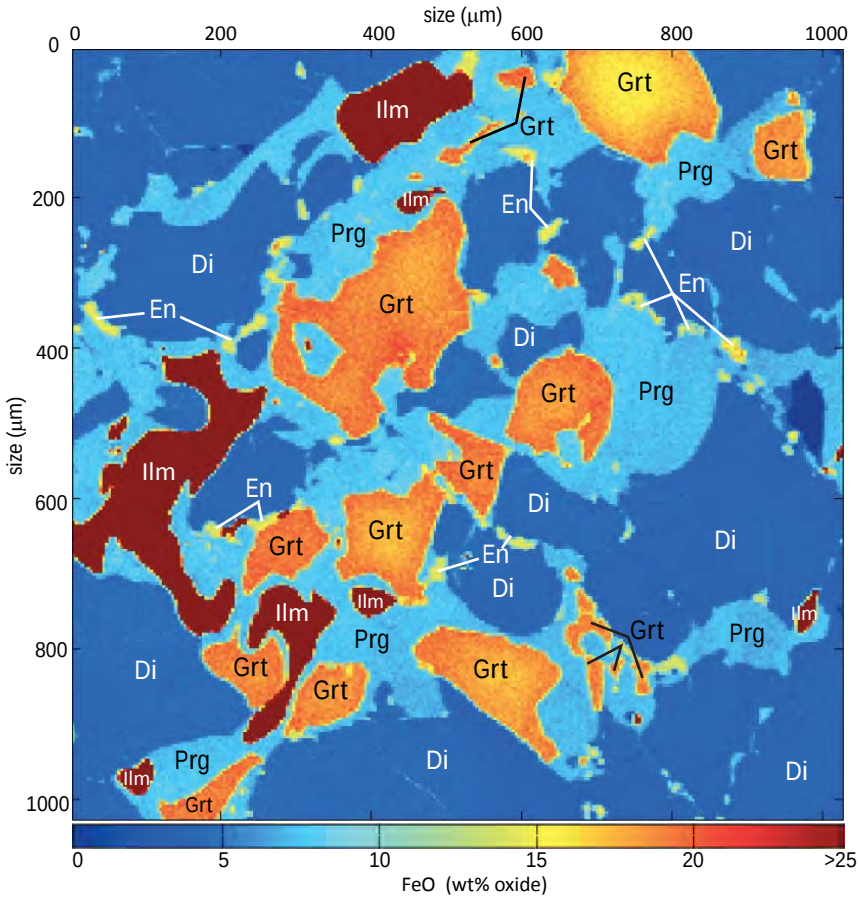

Fig 6.61 0903B. PPL photomicrograph of 0903B element mapping area.

Fig 6.62 0903B. Element mapping image showing FeO concentration, shows the extent of almandine zonation in garnet and allows enstatite to be seen as small interstitial grains. Ilmenite, diopside and pargasite can also be seen. Both images are 1.024mm across.

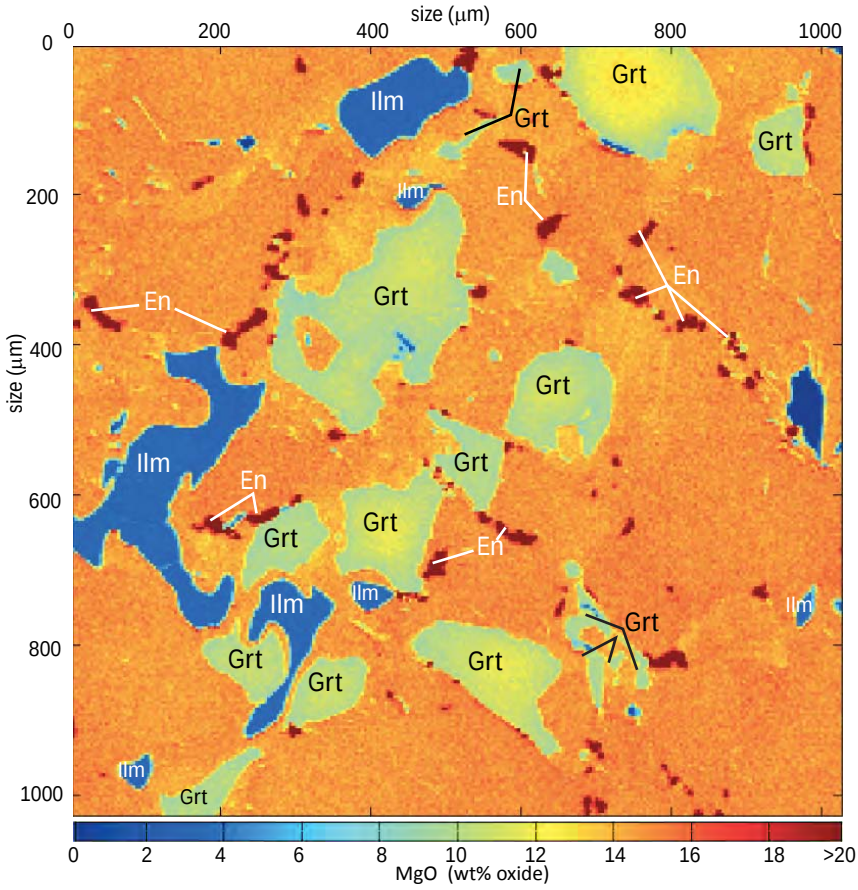

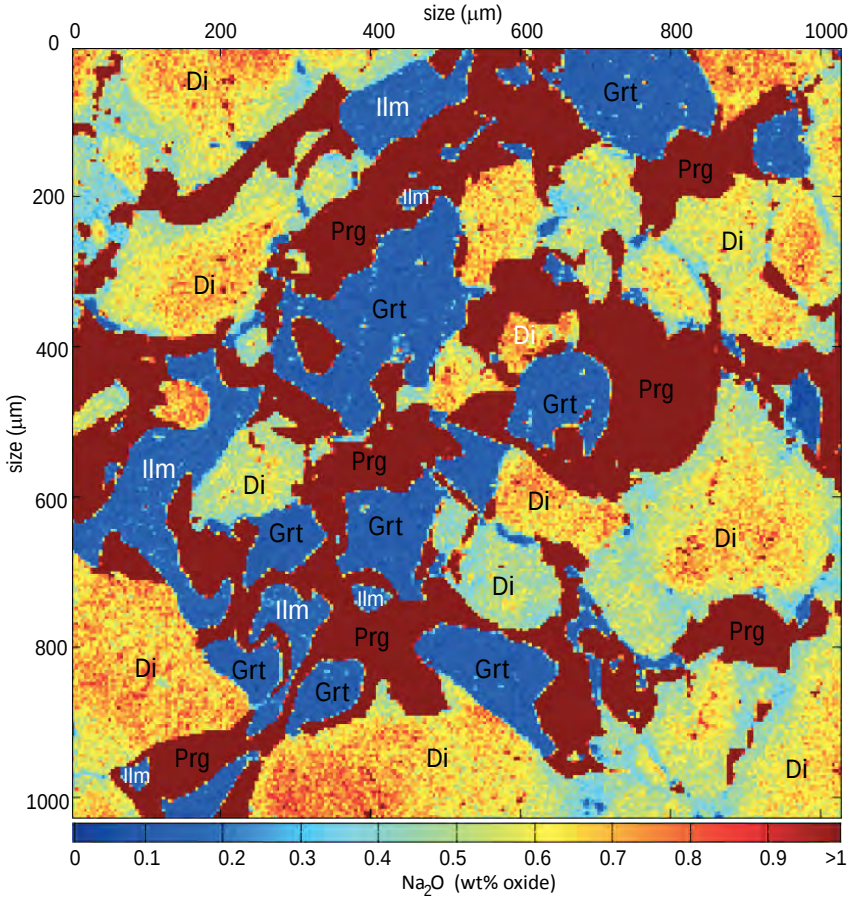

Fig 6.63 0903B. Element mapping image showing MgO concentration, showing insterstitial enstatite, along with pyrope garnet zonation.

Fig 6.64 0903B. Element mapping image showing Na_2O concentration, showing pargasite and diopside zoning. Both images are 1.024mm across.

7. Discussion

By combining data from different geochemical methods further insights can be gained in order to provide explanation for many of the features and trends exhibited thus far. An in depth examination of geochemical results also points to igneous crystallisation of garnet, diopside and omphacite.

Harker diagrams of SiO_2 vs. Al_2O_3 and SiO_2 vs. MgO (Figs. 7.01 & 7.02) show that the hornblende peridotite sampled (0903B) shows similar characteristics to the hornblende peridotite units of the Hawes Head Ultramafics (HHU) (Fig. 2.03) (Emami, S. 2008) and that the BOG shows similar chemical characteristics to the main concentration of points from the WFO database (Appendix 5.A). The SiO_2 vs. MgO Harker diagram is also useful as it indicates that the BE sampled is not metamorphosed HHU; if this were the case the BE would have comparable bulk rock MgO values to those of the HHU (Fig 7.02). Published 'characteristic' WFO chemical signatures from McCulloch et al., (1987) and Muir et al., (1998) have been added to XRF plots; the BOG (both from this study and from the WFO database) does not plot within the geochemical 'definition' from McCulloch et al., (1987) and Muir et al., (1998), only c. half of the WFO database plots within prescribed values; with most of these coming from the Worsley Pluton and Mckerr Intrusives (east) with small amounts from the Misty and Malaspina Plutons. McCulloch et al., (1987) sample locations were almost solely located within the Worsley Pluton; so the 'characteristic' WFO chemical signature given amounts to a characteristic Worsley Pluton signature as opposed to a single definition that will encompass the entire WFO suite. Visible trends have been marked on the diagrams (Figs. 7.01 – 7.02) which for Al_2O_3 show an increasing trend within the HHU, hornblende peridotite, eclogite and layered garnetite – pyroxenite and a decreasing trend through the BOG and WFO suite database. MgO shows a steeply decreasing trend line from the HHU through to the layered units and BE, with a distinct 'gap' between these low silica rocks and the higher silica rocks of the WFO suite (Fig. 7.02); with the exception of the layered pyroxenite, all samples with $SiO_2 > 48$wt% show MgO <7.5wt%.

EMP data for garnet, pyroxene and plagioclase grains has been averaged and added to Harker diagrams (Figs. 7.01 – 7.02) to demonstrate that variation within the BOG and the entire WFO suite is a function of modal proportion – another reason why definition from McCulloch et al., (1987) do not fit the BOG is because the Worsley Pluton is a two pyroxene plagioclase gneiss – indicated by higher silica and lower Al and Mg than other rocks. The dashed lines joining the EMP average data points are theoretical mixing lines along which only two mineral components are a part (e.g. the dashed line joining garnet and omphacite assumes zero plagioclase, any movement perpendicular to this line indicates plagioclase above zero).

Garnetite and pyroxenite plot near the garnet and pyroxene mineral averages but not on them; due to the fact that they are not 100% monomineralic.

Harker diagrams of SiO_2 vs. Na_2O and SiO_2 vs. Sr also give various insights into the nature of rocks from the study area. For the BOG, and entire WFO suite, higher Na_2O and Sr are consistent with higher plagioclase contents while comparatively low values are found in the plagioclase absent rocks (Figs. 7.03 & 7.04). A chemical boundary between plagioclase bearing and non plagioclase bearing samples can be drawn on the Harker diagrams for Na_2O and Sr. Plotting SiO_2 against Na_2O and Sr also shows that the BE is not a metamorphosed plagioclase bearing rock as Na and Sr a lower than what would be observed if the protolith to the BE was plagioclase bearing.

Most WFO data points fall outside the defined WFO chemical signature outline by McCulloch et al., (1987) shows as a grey field on the Harker plots (Figs. 7.03 & 7.04) with only some samples from the Worsley, Malaspina and Misty Plutons as well as some McKerr Intrusive (west) rocks falling inside the prescribed values. The garnet bearing BOG (from further south in Fiordland than the Worsley and Misty Plutons (Fig. 2.03) falls well outside the values of McCulloch et al., (1987). SiO_2 vs. Sr clearly separates WFO plutons from each other (Fig. 7.04) with different trends evident for the Worsley Pluton compared to the BOG and Malaspina Pluton.

EMP mineral data averages are also added to these Harker diagrams and show that, moving from south to north the plutons of the WFO increase in plagioclase content (Figs 7.03 & 7.04).

Harker diagrams of SiO_2 vs. MnO and SiO_2 vs. Y show opposite trends to those observed in Na_2O and Sr; the result of these trends being largely controlled by garnet rather than plagioclase (Figs. 7.05 & 7.06). Samples with higher garnet contents (from EMP averages) also have correspondingly higher MnO – the spessartine end member in garnet and Y – a heavy rare earth element (REE), both MnO and Y partition preferentially into garnet (Jiang & Palmer, 1996). Separation of WFO plutons can again be seen, with predominantly the Worsley and Misty Plutons, along with McKerr Intrusives (west) being the main units that fit into prescribed regions of McCulloch et al., (1987) (Figs. 7.05 & 7.06).

TAS plots of XRF derived data (Fig. 7.07) shows that the WFO suite plots fairly concordantly; similar to Harker diagram plots, with the BOG showing generally lower alkalis and SiO_2 than other WFO plutons. The WFO plutons show a trend along the line separating alkaline from sub-alkaline/tholeiitic, moving south to north there is an increase in SiO_2 and total alkalis (Fig. 7.07). The TAS diagram also shows that the BE, garnetite and hornblende peridotite all have <45% SiO_2 and plot below the TAS plot boundaries. The large variation observed in both the total alkalis and $Na_2)/K_2O$ for the BE is due to varying amounts (down to zero) of K (Appendix 6.D).

Large chemical differences between the BOG and all other rock units in the study area suggests that they are not produced from the same source, a finding supported by the field observation of straight, unmixed contacts between the various inclusions/rafts and the BOG.

By comparison, the BOG is similar to, but generally just below the 'characteristic' WFO signatures from McCulloch et al., (1987) and Muir et al., (1998) outlined in Chapter 2, as samples used for the development of prescribed WFO values in McCulloch et al., (1987) and used by Muir et al., (1998) are from the Worsley Pluton.

This is testament to the statement of Allibone et al., (2009) that the WFO must be regarded by its individual constituent plutons rather than a single large batholith, highlighted conclusively through the variety of chemical variation within and between the plutons that make up the WFO.

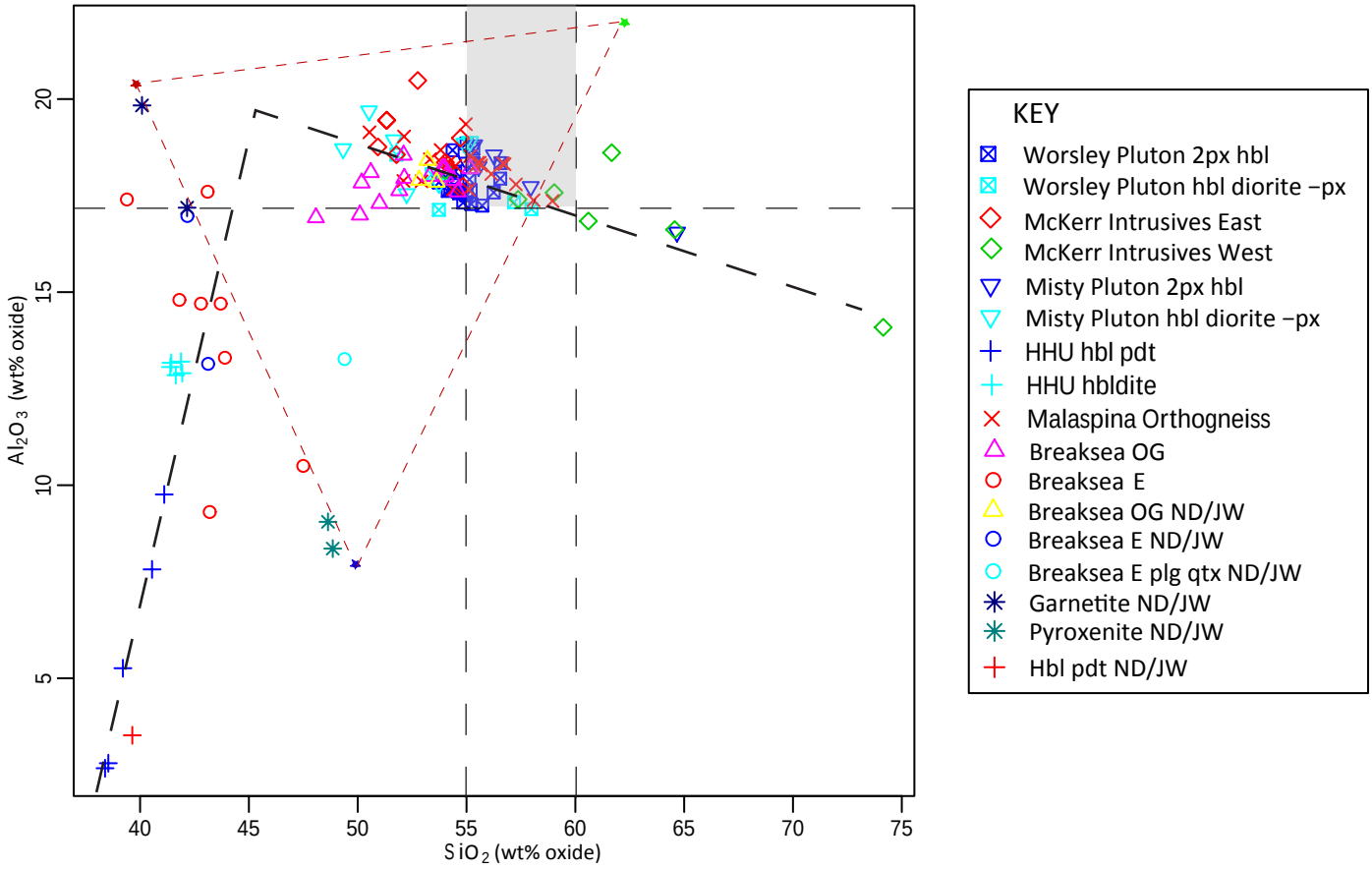

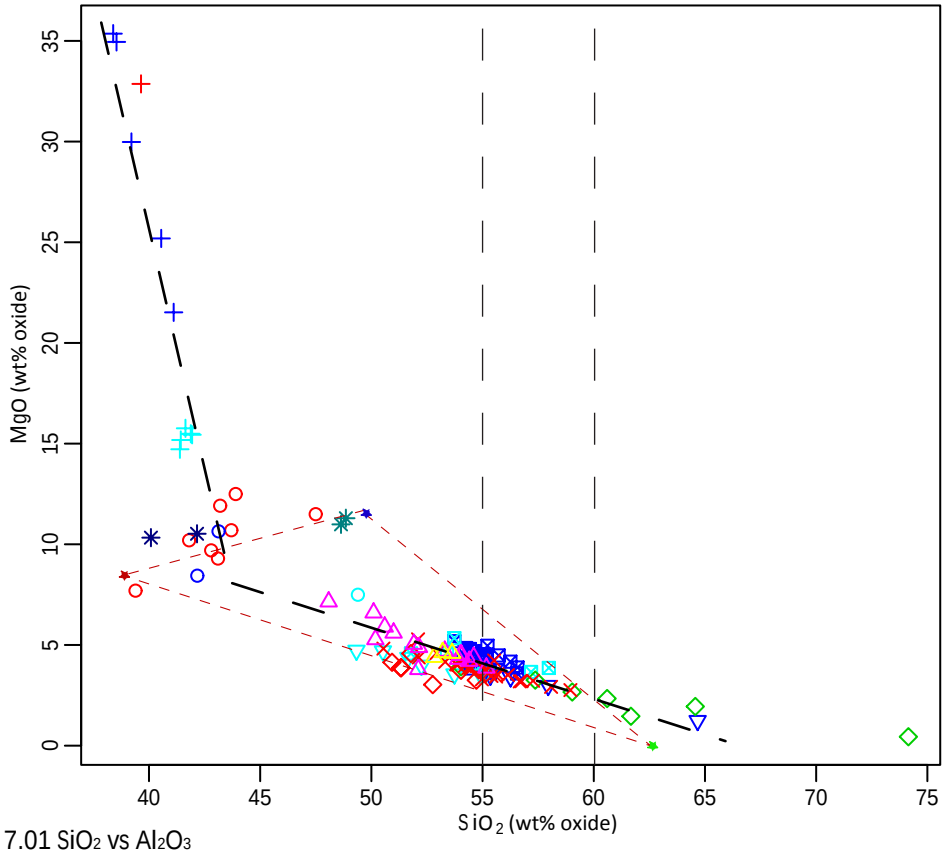

Fig 7.01 SiO_2 vs Al_2O_3
Fig 7.02 SiO_2 vs MgO

Amounts are wt% oxide. Samples with suffix ND/JW correspond to sample groups in row one of Table 5.07. Other data is listed North to South from WFO database given in Appendix 5.A. Field and dashed lines in grey show 'characteristic' WFO chemical signature (McCulloch et al., 1987; Muir et al.,1998). Red star shows av. garnet composition; blue star shows av. omp composition; green star shows av. plag composition (from EMP). Trends are shown in dashed black line.

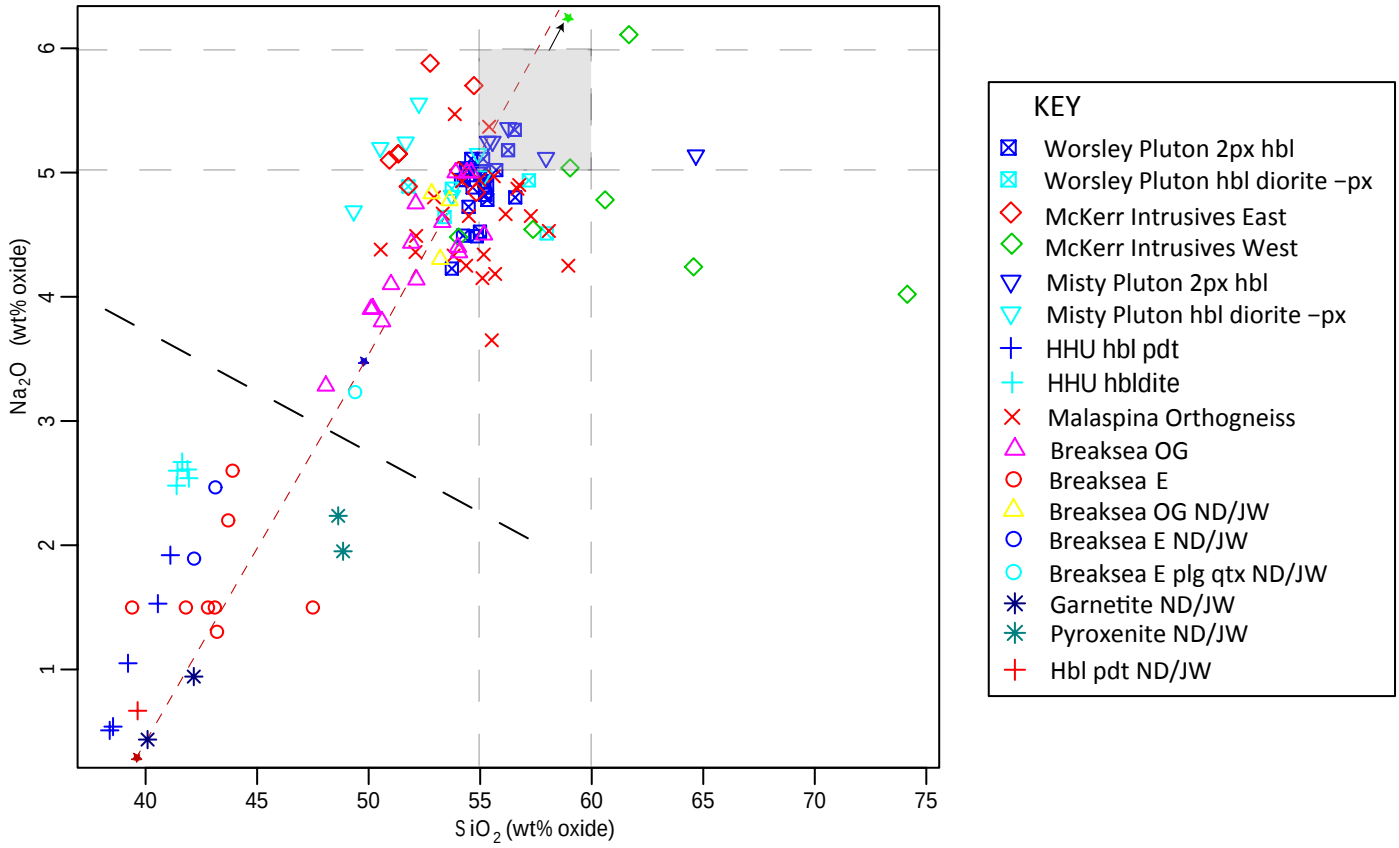

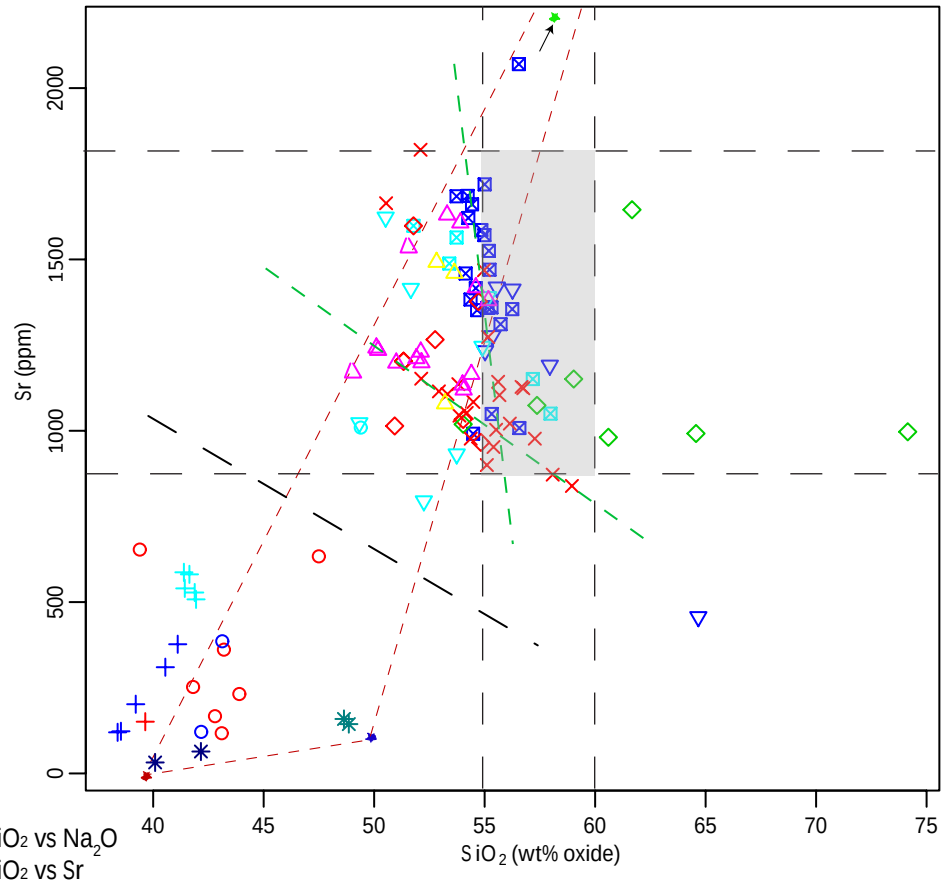

Fig 7.03 SiO_2 vs Na_2O
Fig 7.04 SiO_2 vs Sr

Amounts are wt% oxide (Na_2O, SiO_2) and ppm (Sr). Samples with suffix ND/JW correspond to sample groups in row one of Table 5.07. Other data is listed North to South from WFO database given in Appendix 5.A. Field and dashed lines in grey show 'characteristic' WFO chemical signature (McCulloch et al., 1987; Muir et al.,1998). Red star shows av. garnet composition; blue star shows av. omp composition; green star shows av. plag composition (from EMP). Dashed black line marks the compositional boundary between plagioclase bearing and absent rocks. Green dashed lines show Sr trends among single plutons.

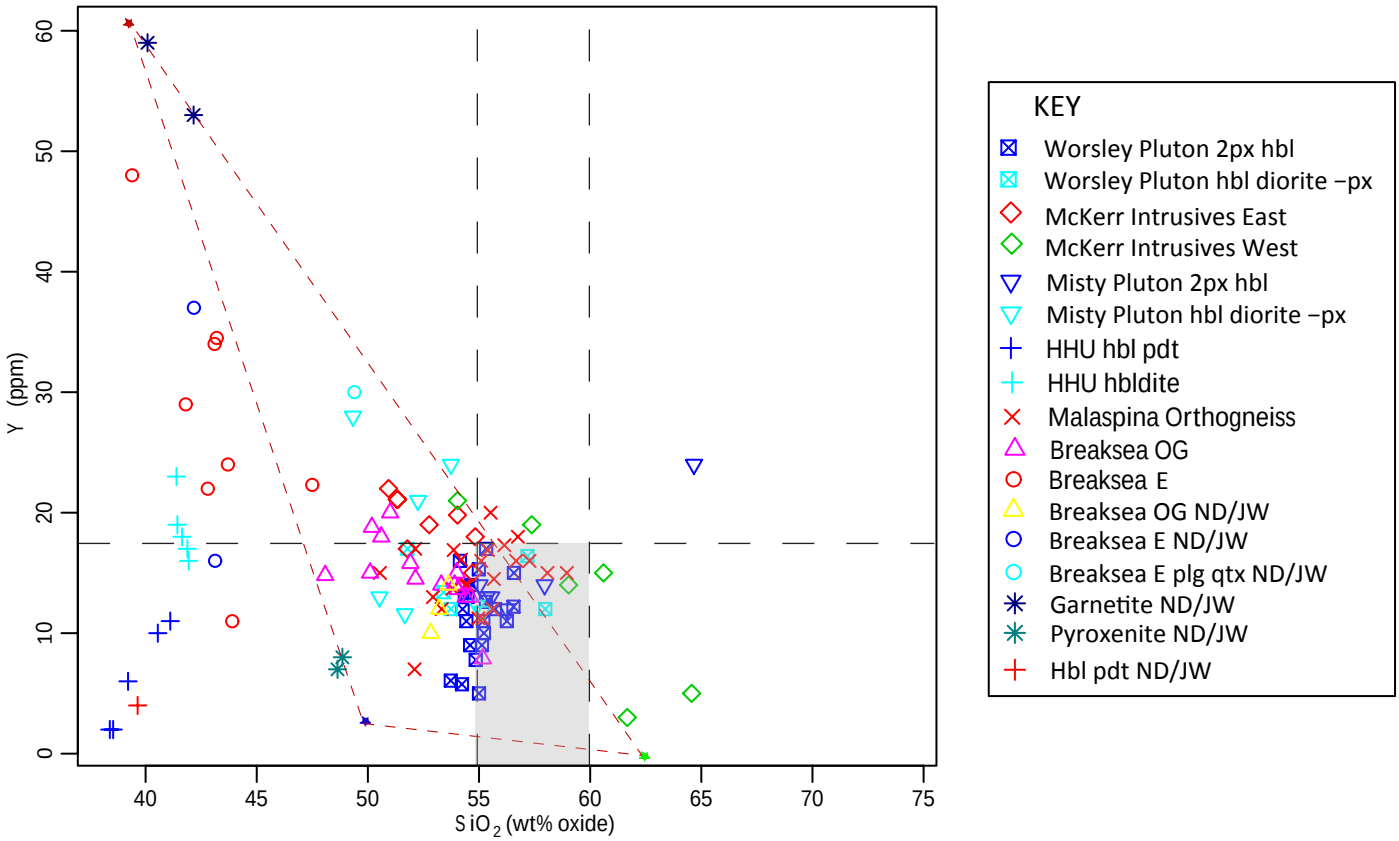

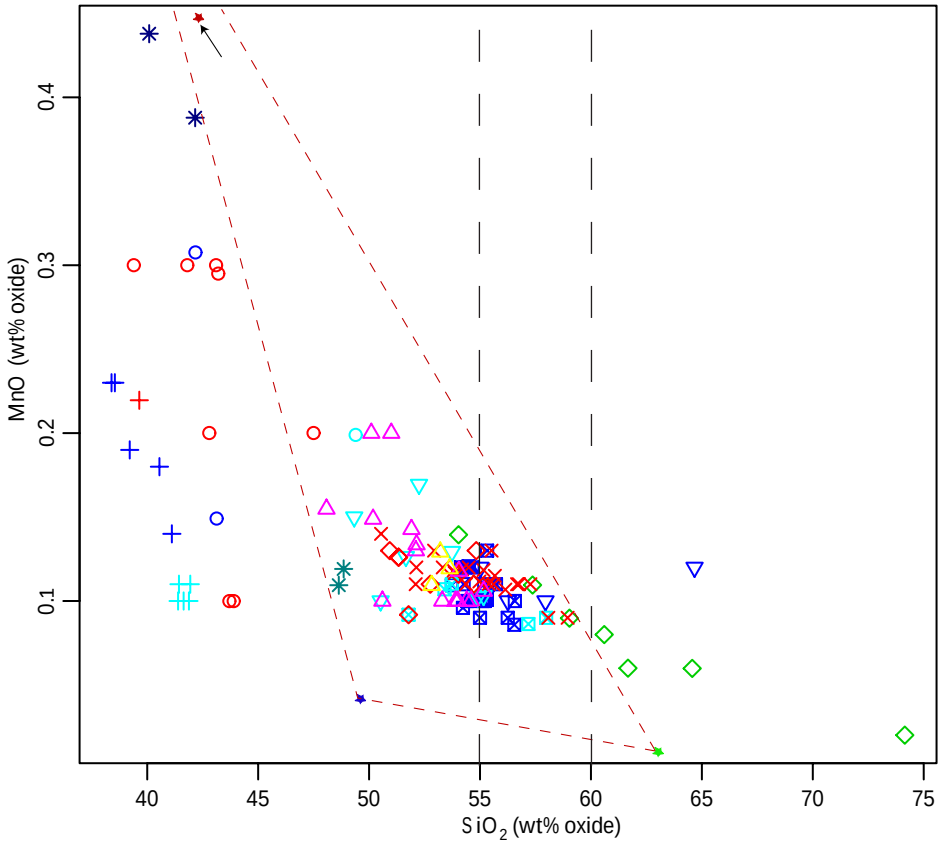

Fig 7.05 SiO_2 vs Y
Fig 7.06 SiO_2 vs MnO

Amounts are wt% oxide (MnO, SiO_2) and ppm (Y). Samples with suffix ND/JW correspond to sample groups in row one of Table 5.07. Other data is listed North to South from WFO database given in Appendix 5.A. Field and dashed lines in grey show 'characteristic' WFO chemical signature (McCulloch et al., 1987; Muir et al.,1998). Red star shows av. garnet composition; blue star shows av. omp composition; green star shows av. plag composition (from EMP)

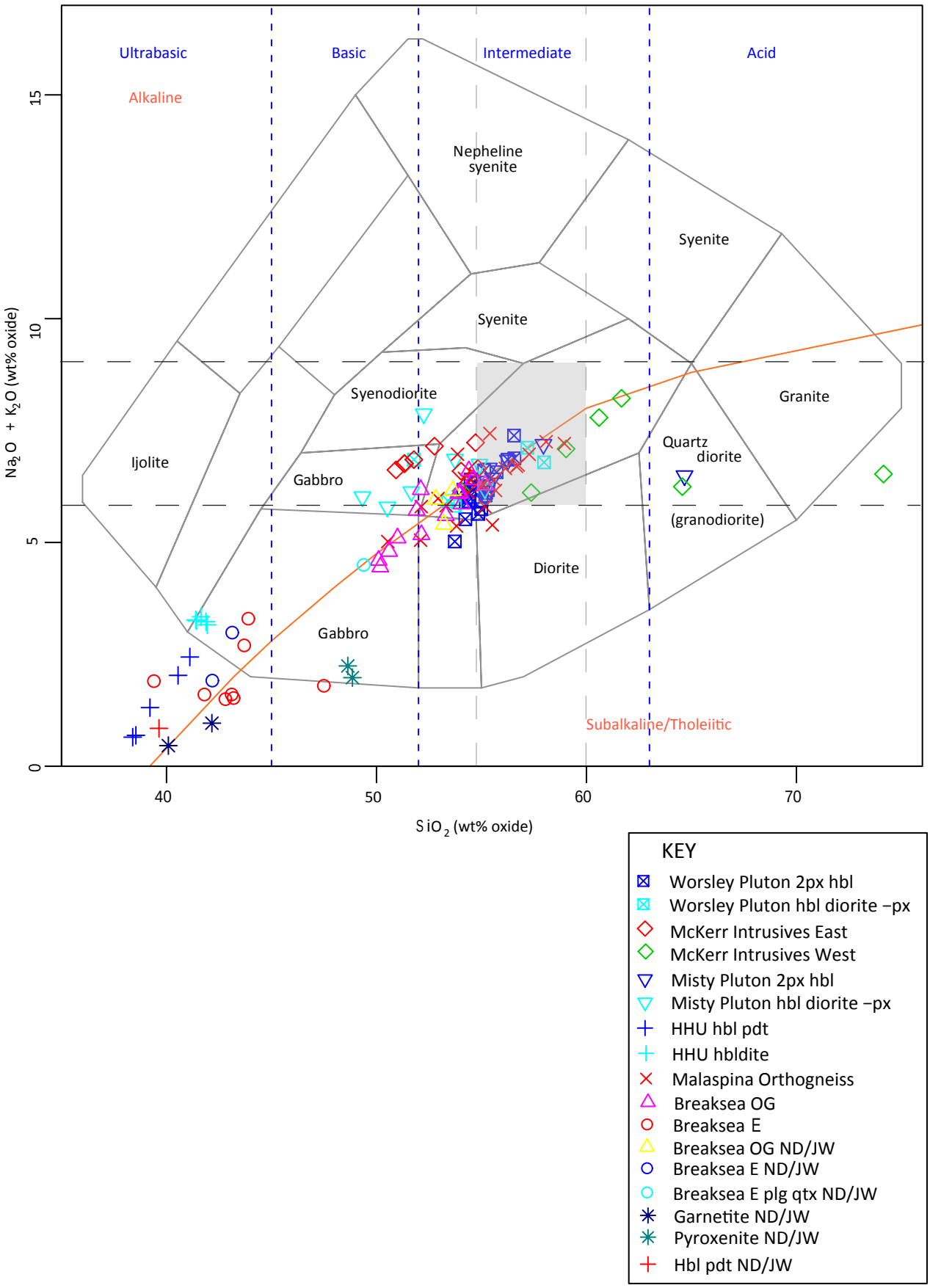

Fig 7.07 TAS diagram after Cox et al., (1979).
Amounts are wt% oxide. Samples with suffix ND/JW correspond to sample groups in row one of Table 5.07. Other data is listed North to South from WFO database given in Appendix 5.A. Field and dashed lines in grey show 'characteristic' WFO chemical signature (McCulloch et al., 1987; Muir et al.,1998).

CIPW norms give idealised mineralogical modes in an attempt to recognise similarities between rock units, leading to the inference that they formed from the same protolith. This is not the case with the units of this study (Table 5.08), which show similar values within units but large amounts of variation between different units. Problems with CIPW norms calculations can be caused by the differing oxidations states of Fe ($^{3+}$ and $^{2+}$) causing errors in magnetite and hematite values; this seems to have affected this dataset to a degree as hematite values are often much higher than observed values (Table 5.08), keeping in mind that CIPW norm calculations are not designed to predict the mineralogy of metamorphic rocks, nominally they will indicate a common protolith. The BOG exhibited fairly constrained CIPW ranges – indicative of all three BOG samples tested coming from the same source. The BE however shows a large amount of variation in both hydrous and anhydrous CIPW norm calculations which could be indicative of a chemically variable protolith for the different eclogite inclusions sampled. Sample 0901C of the BE (plagioclase and quartz bearing) has vastly different CIPW norms again (Table 5.08) due to its different chemical make up, influencing results of the calculation. Garnetite samples show constrained values and are regarded as having a similar source (Table 5.08). Pyroxenite also shows constrained values, although the higher calculated plagioclase of this sample should not be misinterpreted for a higher plagioclase bearing protolith or an indication of metamorphic garnet (from a plagioclase bearing source) within the pyroxenite; garnet only comprises 5% modal proportion of the pyroxenite and XRF results (Na and Sr) show that this rock is not and has not been plagioclase bearing (Figs. 7.03 & 7.04), the higher plagioclase is likely the result of higher aluminium, calcium and silica in the pyroxenite due to mineral cores having an elevated Ca-Tschermak component (element mapping).

Further examples of the CIPW normative mode calculations producing erroneous results can be seen in the 20wt% wollastonite content for pyroxenite (Table 5.08) – due to higher bulk calcium in the rock (Table 5.07). The same can be said of the calculated hematite content of 18.25wt% in hornblende peridotite sample 0903B – due to high iron content (Table 5.07). Hydrous CIPS norm calculations often show lower totals than anhydrous CIPW norm calculations (Table 5.08), notably in the

garnetite and hornblende peridotite samples. These samples have low silica, zero plagioclase, low hornblende (for garnetite) and high iron and magnesium (hornblende peridotite) which in conjunction typically make up large portions of the hydrous CIPW mineral modes of other rock groups examined (Table 5.08).

There is no indication that idealised mineralogy is similar between different rock types, for anhydrous or hydrous CIPW norm calculations, further evidence that the BE is not a metamorphosed product of the HHU. This also indicates that the garnetite and pyroxenite layers are not calculated to be similar to any other rock units observed.

The WFO typically has a Sr/Y ratio 50.00<x<108.82, using McCulloch et al., (1987) and Muir et al., (1998) Sr values of 850 – 1850 and Y < 17. The BOG has an average Sr/Y ratio of 66.74 and two Misty Pluton samples from (Emami, S. 2008) show an average Sr/Y ratio of 97.57; both the BOG and Misty Pluton samples fit within defined boundaries. Multi element spider diagrams and REE plots compare the BOG trace element patterns to those of the two Misty Pluton samples (Figs. 7.08 & 7.09) and show that the Misty Pluton samples have (compared to the BOG) lower Cs, Rb, Th and U as well as a more pronounced Zr negative anomaly and lower HREE's, while Eu plots on the bottom edge of BOG values (Figs. 7.08 & 7.09). Th and U relative depletion could be due the Misty Pluton having less or no accessory zircon present while Cs, Rb and Eu could be due to the Misty Pluton source having more plagioclase present (indicated by XRF with EMP averages). HREE depletion relative to the BOG is explained by the BOG containing higher levels of garnet (indicated by XRF with EMP averages).

Trace element variation between within units, and between the BOG and BE, layered garnetite – pyroxenite and hornblende peridotite is a function of changing chemical composition and is better understood in conjunction with laser ablation data.

Eu variation in the BOG is due to differences in amounts of plagioclase (recorded with field data) and is not indicative of changing processes; BOG samples with higher

plagioclase show a positive anomaly while plagioclase poor samples showed negative or no anomaly (Figs. 5.08 & 5.09). High Cs, Ba, Pb and Sr are influenced heavily by plagioclase (Fig. 7.10) while the HREE trend is the average of garnet and omphacite mineral trends (Figs. 7.10 & 7.11).

Negative anomalies and overall lower values, especially in the LREE's of the BE relative to the BOG are caused primarily by a lack of plagioclase. Near matching HREE's for the BOG and BE are due to the fact that plagioclase does not influence the HREE's (evident in laser ablation data), a result of which is the HREE patterns seen for all bulk rock ICP-MS data are the average of garnet and omphacite/diopside values (Figs 7.12 & 7.13). Elevated bulk rock LREE's compared to garnet and omphacite values for the BE are attributed by the affects of symplectite development adding plagioclase and biotite REE trends (elevated LREE) to the bulk rock trend (Figs. 7.12 & 7.13).

Garnetite relative negative values (to BOG) are due to a lack of plagioclase. The depleted LREE's (relative to BOG) are attributed to a lack of symplectite development and associated compatible elements. Garnetite shows an ascending REE pattern due to high garnet content bringing bulk rock REE closer to garnet mineral HREE (Figs. 7.14 & 7.15). The slightly depleted LREE pattern is attributed to pyroxene. HREE values for bulk rock garnetite can be seen to lie much closer to garnet values rather than an average of garnet and diopside/omphacite (for garnetite, omphacite only for BE) (Figs. 7.14 & 7.15), this is due to the much higher modal proportions of garnet in the garnetite layer, enriching the HREE's to levels approaching garnet minerals abundances.

Pyroxenite shows a similar spider plot to garnetite, except for a negative Nb anomaly and depleted HREE's. Relative to the BOG, pyroxenite exhibits a much lower spider plot and overall depleted REE plot – this is due to the lack of garnet in the pyroxenite (only 5%) causing a HREE depletion (the opposite effect to what is observed in garnetite) and due to a lack of plagioclase and symplectite development. Pyroxenite spider plots match the trace element abundances almost perfectly for diopside up

until the HREE's, where they are only slightly more enriched than diopside mineral values (Figs. 7.16 and 7.17) due to a slight enrichment from the minor garnet in the rock.

Hornblende peridotite shows a similar spider plot pattern at much lower abundances than the BOG (Fig. 5.16). This is due mainly to highly depleted enstatite bringing the bulk rock values for hornblende peridotite down to well below BOG averages (Figs. 7. 18 & 7.19). The positive Ba anomaly in hornblende peridotite is attributed to pargasite (Fig. 7.18). The REE plot shows a humped patter similar to those observed, though at lower abundances (Fig. 7.19). Laser ablation data shows that the LREE and MREE are an averaged value of pargasite and enstatite, while the HREE's are influenced by pargasite and garnet (Fig. 7.19), the high HREE abundances in garnet bringing the HREE's up to a level similar to those seen in other rock units, with the effect of flattening the overall humped pattern slightly.

Spider plot patterns are heavily influenced by plagioclase, omphacite and diopside, with input from garnet in the HREE's, while REE plots see the LREE's controlled by the pyroxenes and pargasite, with garnet causing elevation in the HREE's. Plagioclase only affects the Eu abundance of REE patterns, which is only observed in plagioclase bearing samples (BOG) and only then to a small degree.

To compare isotope data rocks must be plotted at the same initial ages, namely rocks from this study at 120Ma and rocks of the Darran Suite (168 – 131Ma), argued by Muir et al., (1998) as a potential source rock for the WFO and the Separation Point Suite (115Ma) argued by Muir et al., (1998) as the deep crustal equivalent of the WFO, a theory challenged by Allibone et al., (2009). However, the Darran Suite did partially melt to form the WFO and the WFO is the deep crustal equivalent of the SPS, then at similar ages, εNd and Sr_i values for the Darran Suite rocks and rocks of this study, or the SPS and rocks from this study should coincide.

As ages for the BOG are increased (Fig. 5.18) they are observed to trend upwards, with Sr_i decreasing slightly and εNd increasing, bringing BOG values closer to the

field occupied by the Darran Suite, with only one sample reaching the field of the Darran Suite rocks at T=160Ma (i.e. BOG plotted 40Ma older than real values). This leads to the finding that the BOG is not isotopically similar to the Darran Suite rocks.

The SPS are recalculated from published data of McCulloch et al., (1987) for ages of 120Ma and plotted with the rocks of this study (Fig 5.18). The BE and garnetite do not overlap SPS data, all BOG except for one sample (0907) plot separately to the SPS. Pyroxenite plots with a higher Sri than the SPS. This suggests that the rocks of this study, namely the BOG (main country rock) is not isotopically homogenous with the SPS.

Within the rocks of this study, BOG all show an identical upward trend (Fig. 5.18). Most BE samples show the same trend except for one sample (0904C) which trends in an opposite direction to the other BE samples and the BOG data. Garnetite shows a pattern similar to the BE of sample 0904C, decreasing along a near vertical plane (Fig. 5.18) while pyroxenite shows no variation even at ages up to 200Ma (Fig. 5.18).

The different trends observed suggests that rocks of this study are not related to one another, Garnetite and pyroxenite are interlayered (spatially related) and inferred to be coeval, but show vastly different time progressions (Fig. 5.18), suggesting that initial Rb and Sm were not identical between samples. This implies that bulk rock modal proportions of minerals, for e.g. plagioclase and garnet, control initial Rb/Sr and Sm/Nd abundances, which in turn affects the calculated εNd and Sr_i values as for e.g. a higher initial Rb will over time lead to a higher concentration of Sr in a sample, through radioactive decay.

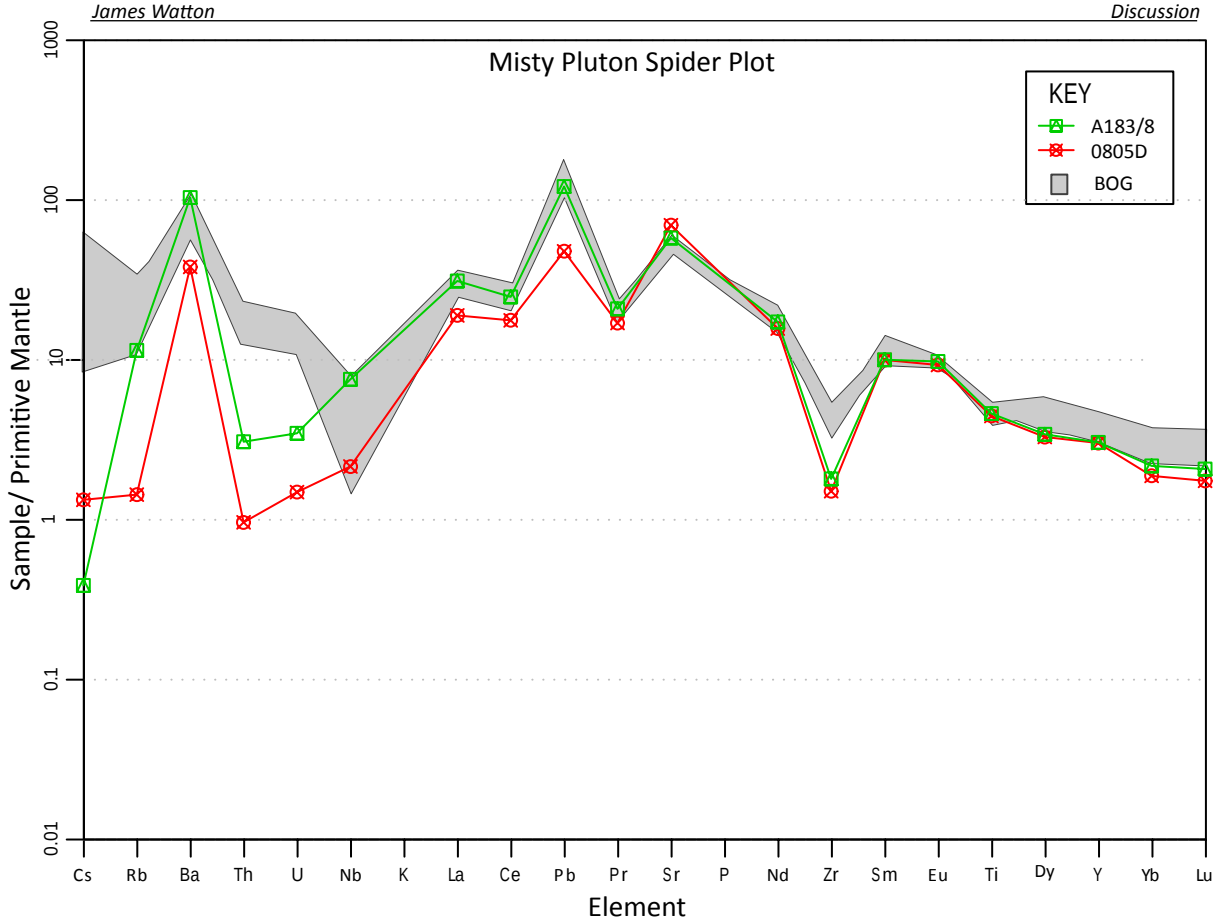

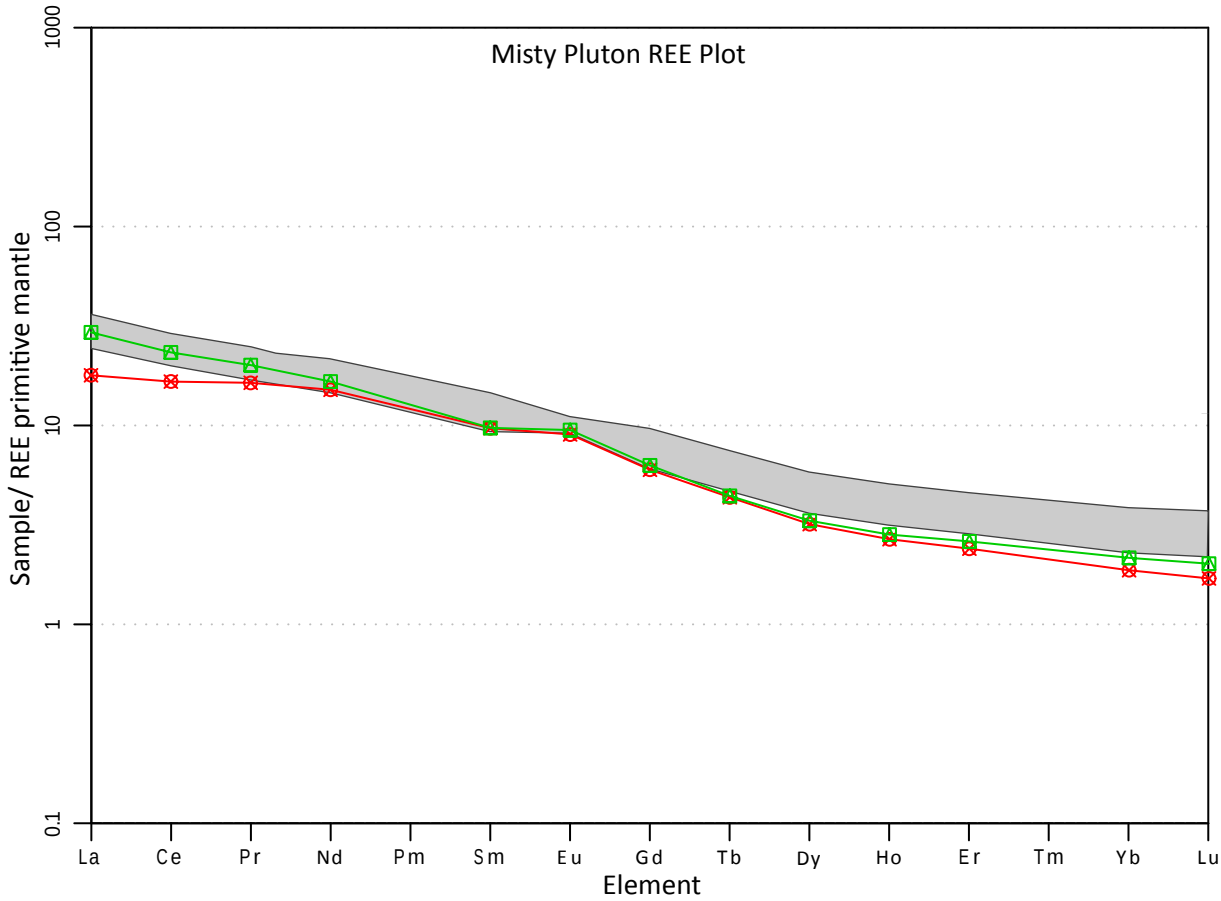

Fig 7.10 Spider diagram of WFO normalised to primitive mantle values of Sun & McDonough (1989).
Fig 7.11 REE plot of WFO normalised to primitive mantle values of McDonough et al., (1991). Shown in grey is the Spider and REE pattern for BOG. WFO data from Emami, S. (2008).

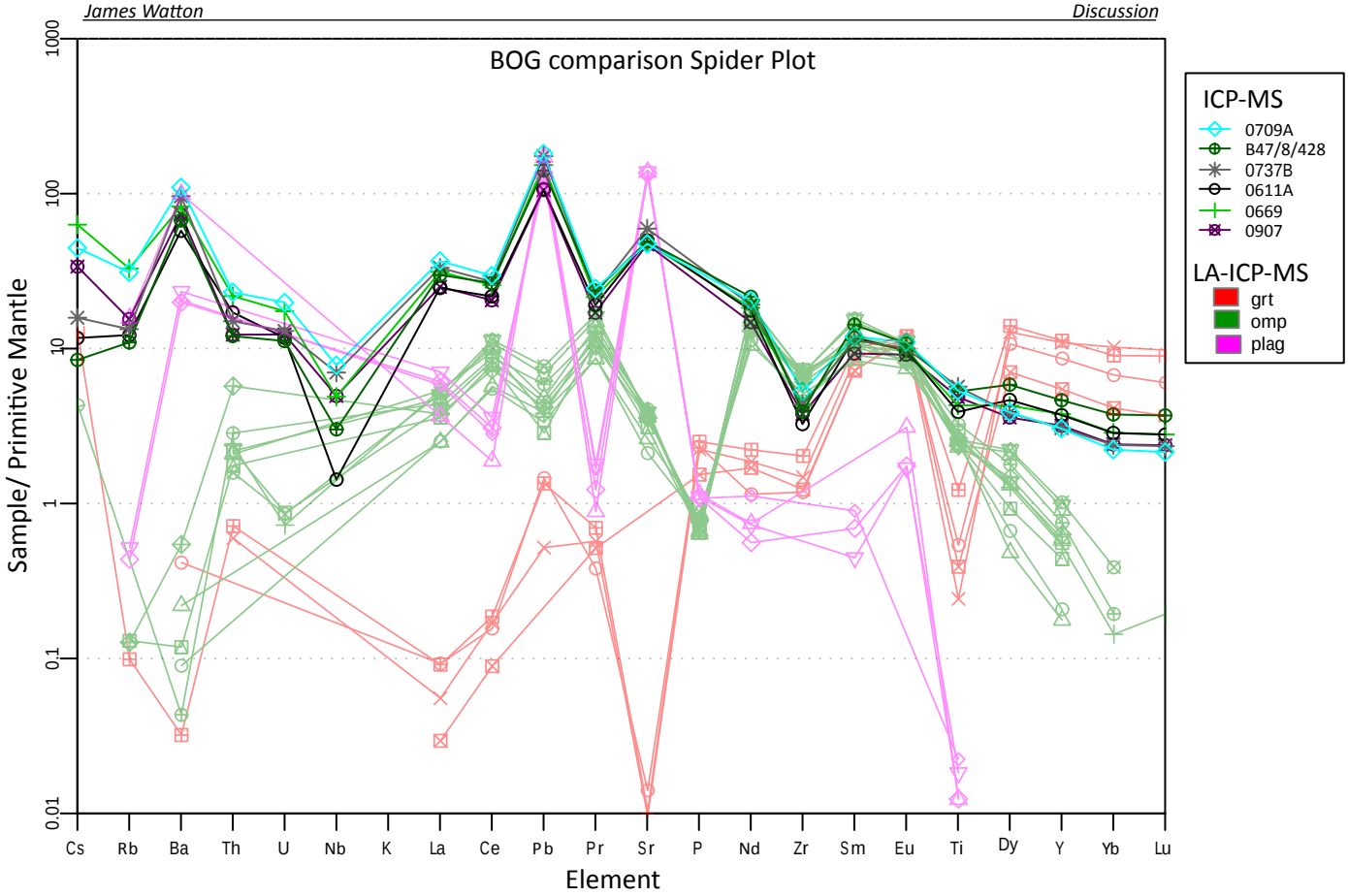

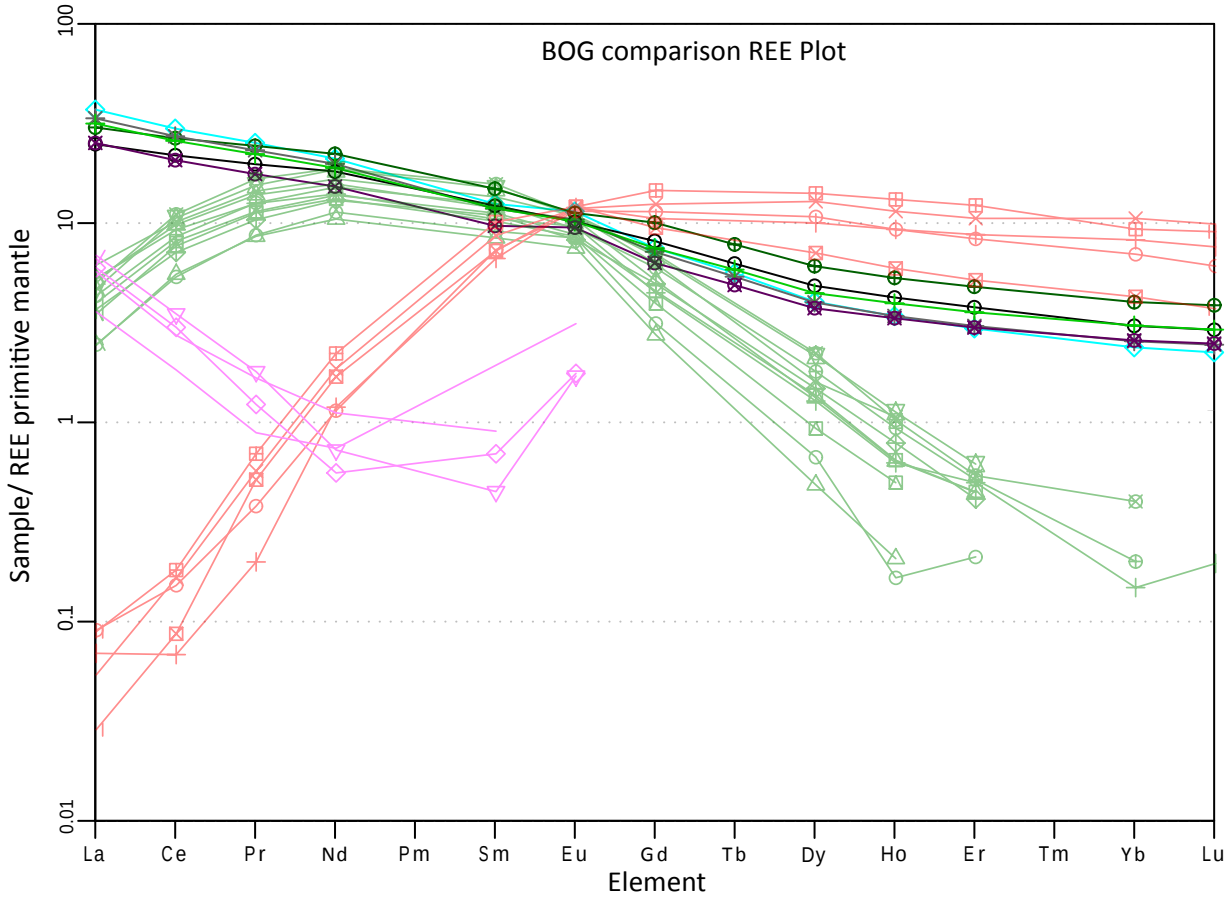

Fig 7.10 Spider diagram comparing ICP-MS to LA-ICP-MS for BOG normalised to primitive mantle values of Sun & McDonough (1989).

Fig 7.11 REE plot comparing ICP-MS to LA-ICP-MS for BOG normalised to primitive mantle values of McDonough et al., (1991).

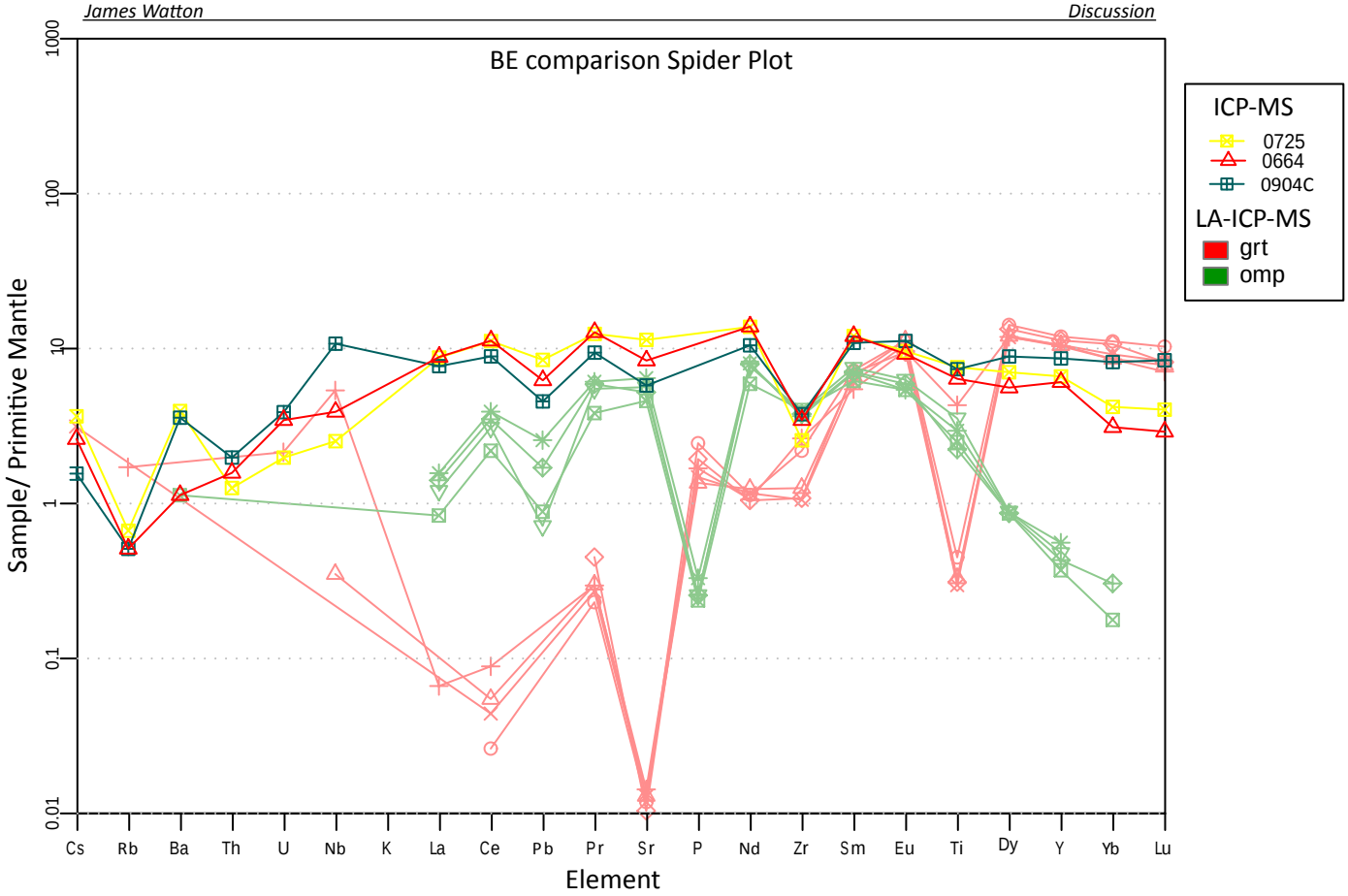

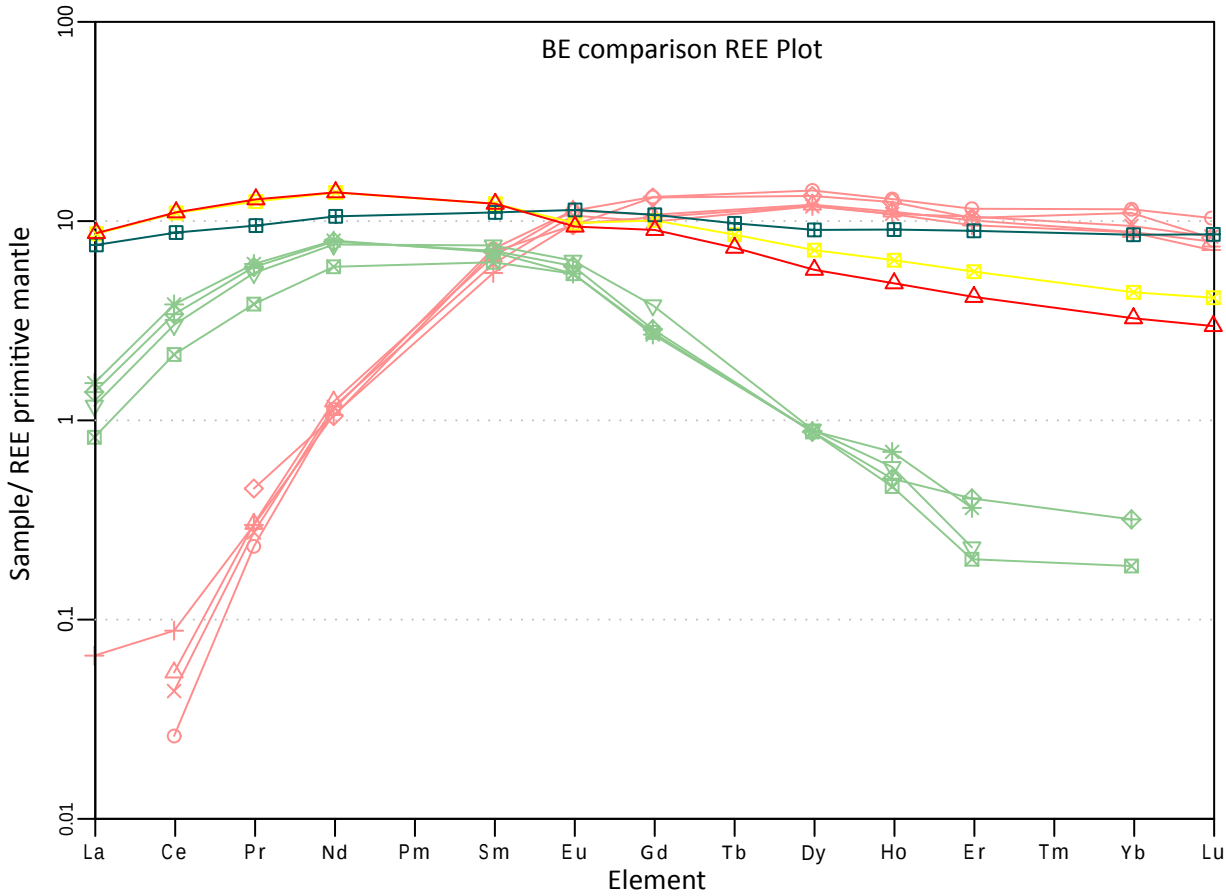

Fig 7.12 Spider diagram comparing ICP-MS to LA-ICP-MS for BE normalised to primitive mantle values of Sun & McDonough (1989).

Fig 7.13 REE plot comparing ICP-MS to LA-ICP-MS for BE normalised to primitive mantle values of McDonough et al., (1991).

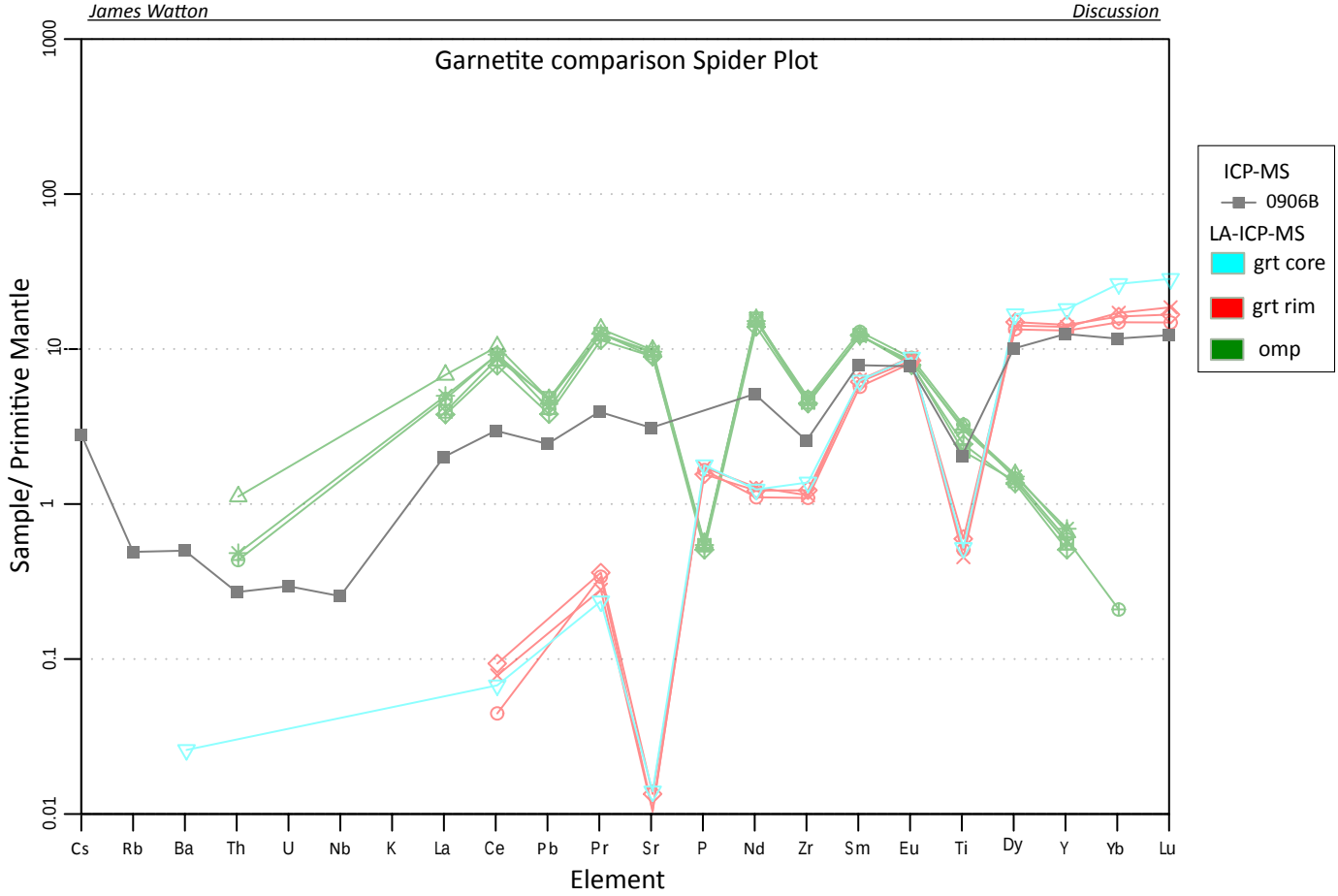

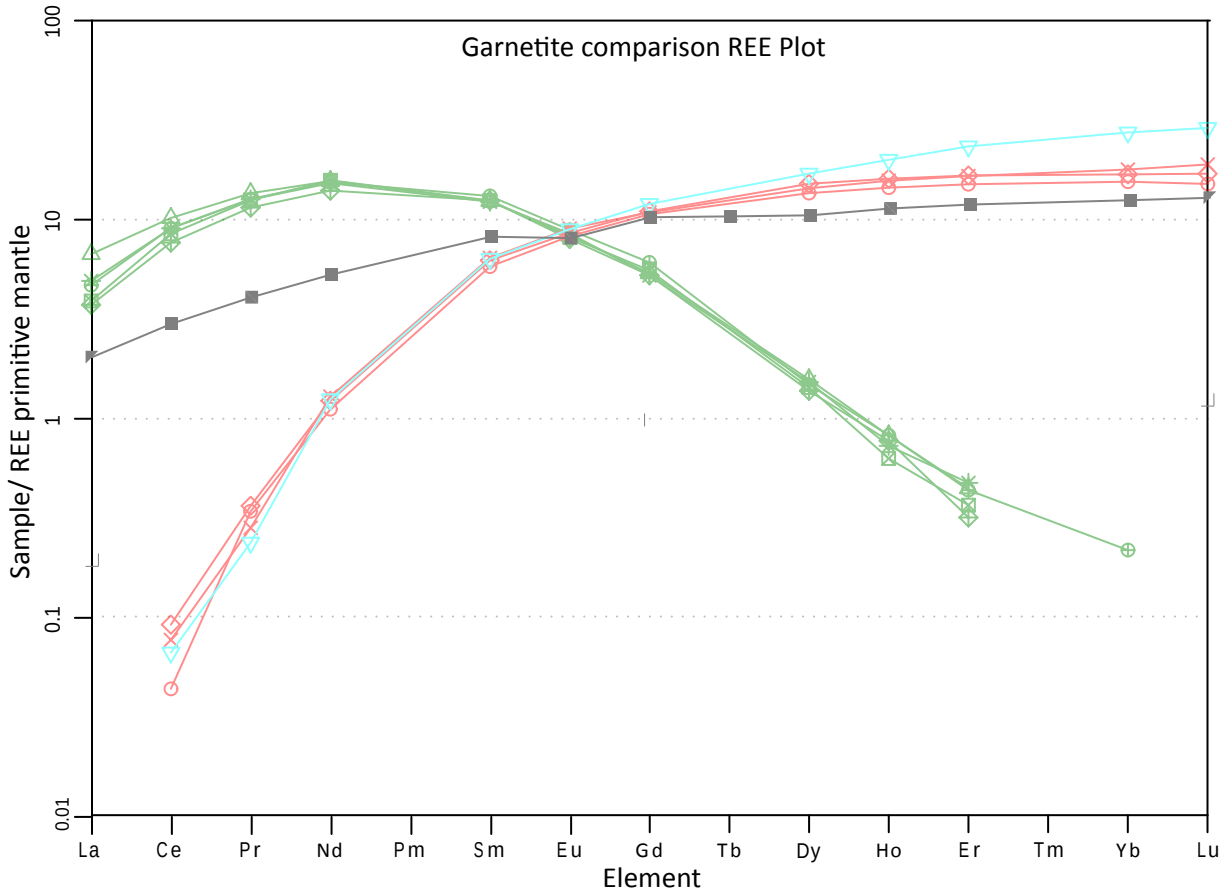

Fig 7.14 Spider diagram comparing ICP-MS to LA-ICP-MS for garnetite normalised to primitive mantle values of Sun & McDonough (1989).

Fig 7.15 REE plot comparing ICP-MS to LA-ICP-MS for garnetite normalised to primitive mantle values of McDonough et al., (1991).

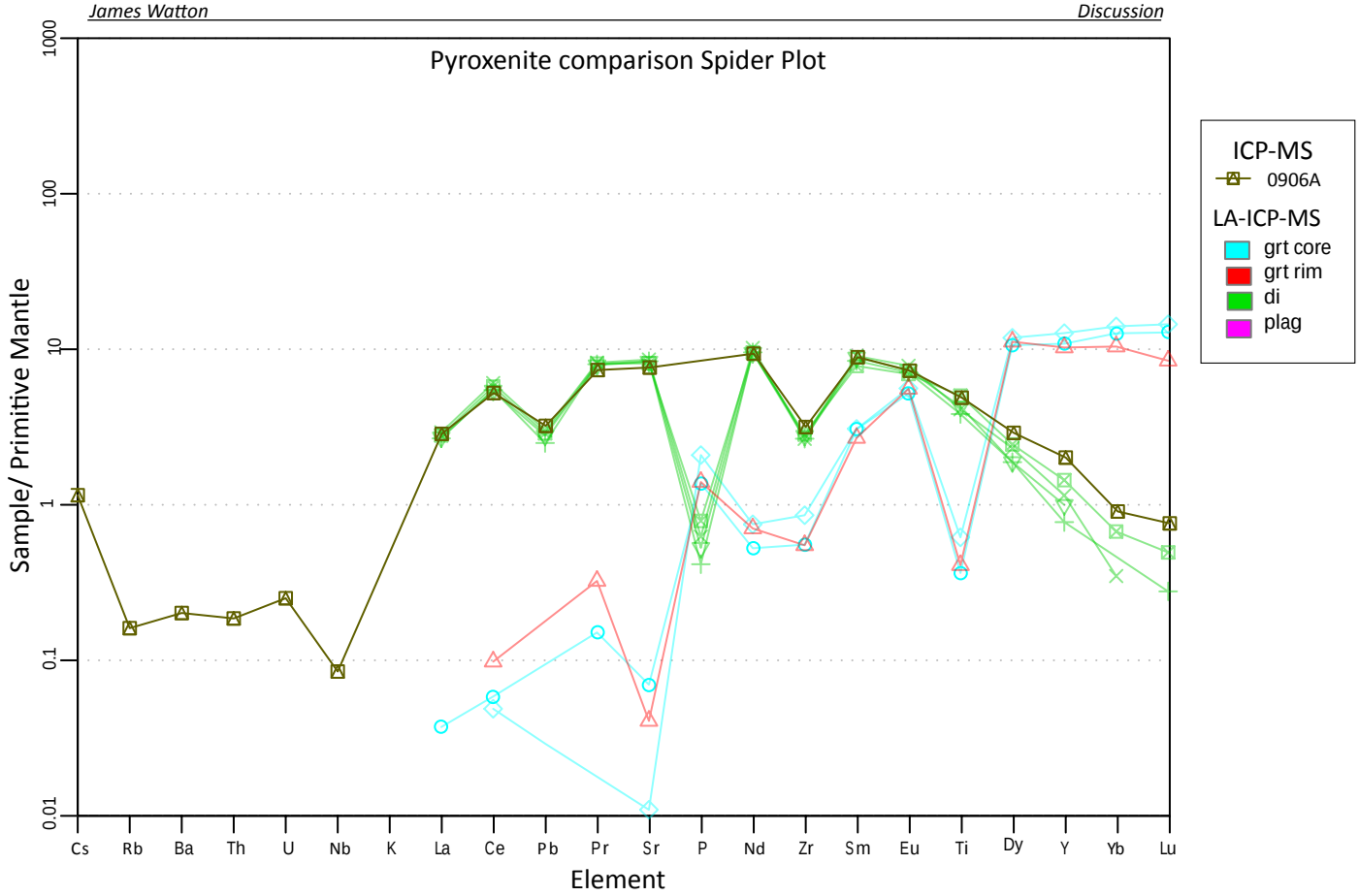

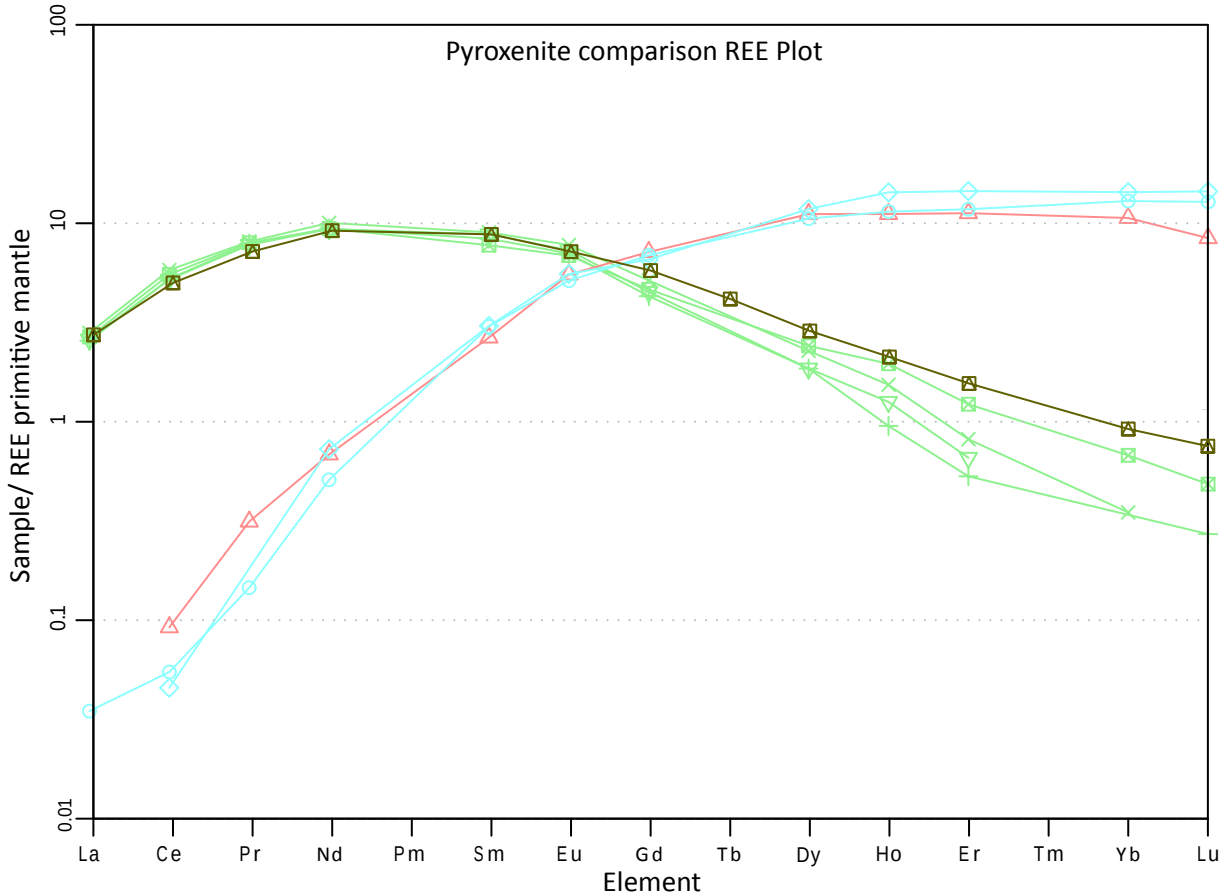

Fig 7.16 Spider diagram comparing ICP-MS to LA-ICP-MS for pyroxenite normalised to primitive mantle values of Sun & McDonough (1989).

Fig 7.17 REE plot comparing ICP-MS to LA-ICP-MS for pyroxenite normalised to primitive mantle values of McDonough et al., (1991).

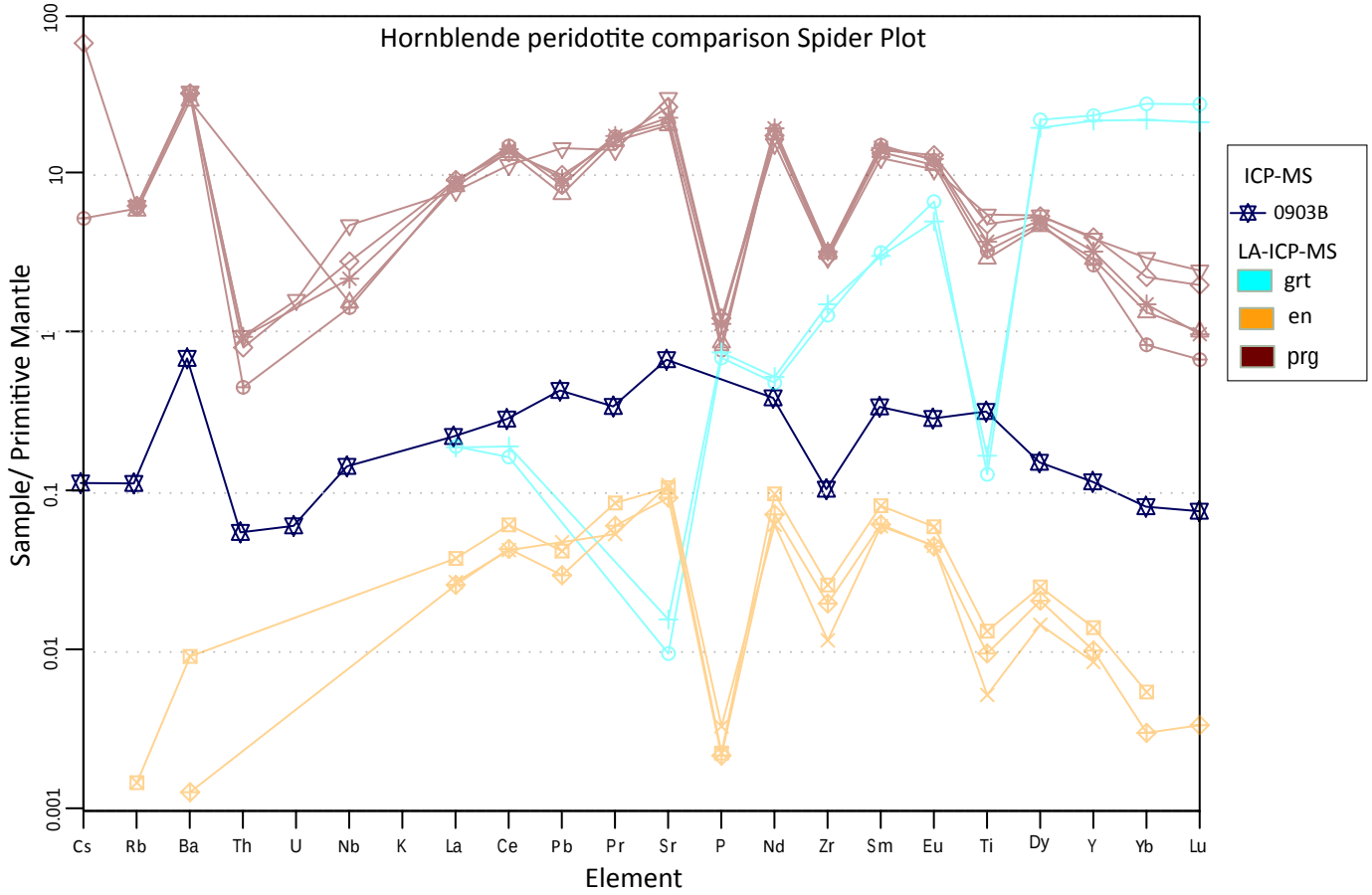

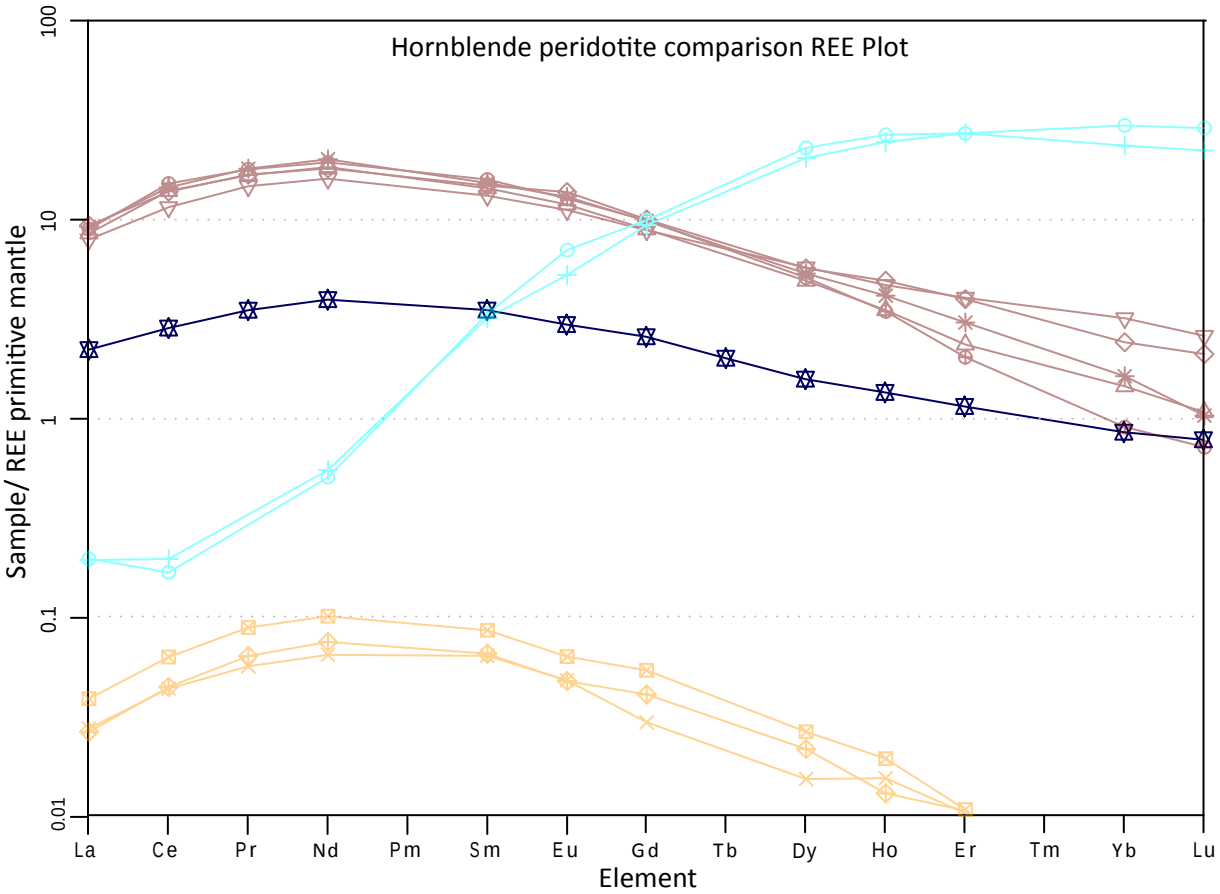

Fig 7.18 Spider diagram comparing ICP-MS to LA-ICP-MS for hornblende peridotite normalised to primitive mantle values of Sun & McDonough (1989).

Fig 7.19 REE plot comparing ICP-MS to LA-ICP-MS for hornblende peridotite normalised to primitive mantle values of McDonough et al., (1991).

EMP garnet zoning traverses in the BOG show that zoning affects the almandine, pyrope and grossular end members, while being constrained to within ~200μm of grain boundaries; almandine and grossular (Fe and Ca) content increases at garnet rims while pyrope (Mg) content decreases (Figs 6.01 & 6.02). For this reason zoning was set as a target of element mapping, as narrow grain boundary zoning in garnet and omphacite/diopside is seen as being the result of diffusion driven thermal re-equilibration (O'Brien, P. 2008), a retrograde feature seen during cooling from high temperatures (O'Brien, P. 2008). Garnet zoning in the BE is of the same nature though shows less pronounced zoning in the grossular (Ca) end member, being controlled by almandine (Fe) and pyrope (Mg) (Fig. 6.10). While traverses were not conducted for garnetite, pyroxenite and hornblende peridotite EMP analysis noted core and rim data points and these show similar zoning trends to the BOG (higher almandine and grossular and lower pyrope). Garnetite generally has less almandine while pyroxenite generally has more almandine. Garnet in hornblende peridotite is more Mg rich (pyrope) due to its precursor mineral composition (olivine, enstatite, pargasite, and diopside). Garnet in hornblende peridotite is not zoned in grossular at all, with zoning controlled by the Fe and Mg end members (Fig. 6.22).

With no plagioclase to provide Na, omphacite in garnetite and pyroxenite show lower jadeite content than the BOG (Fig. 6.20 & 6.21). BE omphacite is similar to BOG, with some omphacite (within symplectites) showing a higher jadeite content (Fig. 6.13). Generally, jadeite content increases as plagioclase increases. Diopside in the hornblende peridotite is more Mg and Fe poor than diopsides of the BOG and layered units (Fig. 6.22), due to the high bulk rock magnesium content. Diopside in garnetite and pyroxenite generally becomes more Mg rich when moving from core to rim, also viewed in element mapping (Fig. 6.60) and viewed as the effects of thermal re-equilibration from a high Tschermak's diopside to a diopside (O'Brien, P. 2008). This observed pyroxene zoning in EMP data was set as another target for element mapping.

Pargasite observed in BOG, BE and garnetite are all of similar chemical composition and texture (symplectite), implying that all experienced the same retrogressive

event. Pargasite in hornblende peridotite is identical to HHU hornblende and is more Mg rich and Fe poor than pargasite found in the BOG, BE and garnetite symplectites, showing similar trends to the pyroxenes observed in 0903B (Mg rich, Fe poor). The complete overlap of pargasite from the hornblende peridotite with pargasite of the HHU (Fig. 6.09) is further chemical evidence for the hornblende peridotite observed at site 0903B being the same rock seen at Hawes Head. Olivine and enstatite in hornblende peridotite follow the same Mg enrichment as pargasite and diopside.

To improve element mapping accuracy, different α (and resultant β) factors were found and tested in an attempt to achieve closer results to Pouchou & Pichoir (1984) (PAP) matrix corrected probe data. Refer to Table 6.07 (α- and β-factors) and 6.08 (results of testing). The α-factors of Love & Scott (1984) and Kato (2005) were tested; α-factors of Kato (2005) were also transposed in an attempt to achieve element map results that were closer to PAP matrix corrected values, seen in the *BenceAlbee_Kato_Transposed.m* script as the line with reads: *alpha = alpha.'* (Appendix 6.A). .' is the MATLAB transpose matrix command. Testing (Table 6.08) uses non-transposed α-factors. Background correction was also tested (*BackgroundCorrection_grt.m* & *BackgroundCorrection_cpx.m* scripts) (Table 6.08) (Appendix 6.C), calculated from EMP probe data on garnet and omphacite averaged background readings and converted to 100nA. Data masking was also attempted *(filter0905B.m & filter0906B.m* scripts) by not allowing small accessory minerals to be included which were believed to be altering totals (Appendix 6.C).

Testing (Table 6.08) compares PAP matrix corrections done by CAMECA software on raw (pk-bkg) data (column B) to Bence-Albee matrix corrections on raw (pk–bkg) data, using α-factors from Love & Scott (column C) and Kato (column D). For 'Pk-bkg Bence-Albee' values blue text shows the value with lower relative deviation from PAP matrix corrected values.

Testing then compared totals derived by running the full element mapping procedure on the same raw test data, using a non corrected and a background

corrected Bence-Albee matrix correction script for both Love & Scott (columns E & F) and Kato (columns G & H) α-factors (Appendix 6.C).

Peak – Background data using the Bence-Albee matrix correction and α-factors from Love & Scott (1984) shows lower %relative deviation from PAP matrix corrected values than Kato (2005) α-factors for all elements except Fe. This stage of testing concluded (see Table 6.08) that output from the Bence-Albee matrix correction procedure was heavily dependant on the variables (α- and β-factors) chosen.

Background correction effectiveness depended heavily on how close background averages taken were to the mineral being corrected (i.e. a garnet background correction will perform poorly on a clinopyroxene grain and vice versa). In the same sense a bulk rock background correction is not useful, as for example background Ti counts on a rutile grain will be much higher than background Ti counts on an omphacite grain. Masking scripts were attempted to remove this affect (Appendix 6.C); although the outcome was identical to background corrections - where one elements' %relative deviation (from PAP values) may improve, another will deteriorate. In Table 6.08, for all 'Map total' values green text indicates the value with the lowest %relative deviation from PAP values, comparing the Love & Scott and Kato uncorrected and background corrected values. Within each set of alpha factors, background correction itself is measured relative to that α- factor set. Here, blue values show that %relative deviation has decreased while red values show that %relative deviation has increased (relative to PAP values). If the value in the background corrected column is green this indicates that %relative deviation has decreased and this value is the closest to PAP values. In cases where mineral concentration was low to begin with i.e. K, Na in garnet, Mn in clinopyroxene; background correction removed the element concentration completely.

Count times input were all less than the actual time of 150μs (to achieve the best results) – this is believed to be due to dead time while the EMP moves to a new step.

PTS no. used for testing	Known PAP corr. From probe	Pk-Bkg Bence-Albee correction of raw EMP data (Love & Scott)		Pk-Bkg Bence-Albee correction of raw EMP data (Kato)		Map total 0906B (Love & Scott)				Map total 0906B (Kato)			
		t=1s Iterations=10	%Relative Deviation	t=.995s Iterations=10	%Relative Deviation	t=0.133s Iterations=3	%Relative Deviation	t=0.125s Iterations=3	%Relative Deviation	t=0.132s Iterations=3	%Relative Deviation	t=0.125s Iterations=3	%Relative Deviation
0906B grt core						No corr.		Bkg corr. t=0.150s		No corr.		Bkg corr. t=0.150s	
SiO2	39.43	40.30	2.21	35.90	8.95	39.30	0.33	41.49	5.23	35.15	10.85	36.79	6.69
TiO2	0.04	0.04	2.20	0.04	2.20	0.03	26.65	0.00	97.56	0.04	2.20	0.00	100.00
Al2O3	22.25	22.52	1.20	22.61	1.60	21.48	3.48	22.35	0.43	21.20	4.74	22.19	0.29
Cr2O3	0.02	-		-		-		-		-		-	
Fe2O3	0.00	-		-		-		-		-		-	
FeO	19.96	18.58	6.91	20.49	2.66	21.03	5.36	19.37	2.96	23.26	16.53	21.31	6.76
MnO	0.58	0.59	1.10	0.61	4.52	0.77	31.94	0.30	48.59	0.80	37.08	0.31	46.88
MgO	10.12	10.16	0.44	11.28	11.52	11.21	10.82	11.49	13.59	12.13	19.92	12.64	24.96
CaO	8.18	8.13	0.62	8.54	4.39	8.21	0.36	8.66	5.86	8.65	5.74	9.05	10.63
Na2O	0.03	0.03	7.14	0.02	28.57	0.13	364.29	0.02	28.57	0.10	257.14	0.02	28.57
K2O	0.00	0.00	0.00	0.00	0.00	0.10	100.00	0.00	0.00	0.10	100.00	0.00	0.00
NiO2	0.02	-		-		-		-		-		-	
Total	100.61	100.35	0.26	99.49	1.11	102.26	1.64	103.68	3.05	101.43	0.81	102.31	1.69
FeO	19.96	18.58	6.91	20.49	2.66								
omp core													
SiO2	50.71	51.64	1.84	49.40	2.57	48.07	5.20	50.83	0.25	45.95	9.38	48.25	4.84
TiO2	0.67	0.66	1.11	0.66	1.11	0.11	83.52	0.00	100.00	0.11	83.52	0.00	100.00
Al2O3	7.87	7.95	1.00	8.52	8.24	8.54	8.50	8.67	10.15	9.04	14.85	9.30	18.15
Cr2O3	0.01	-		-		-				-			
Fe2O3	0.00	-		-		-				-			
FeO	7.65	7.12	6.93	7.75	1.31	7.79	1.83	6.38	16.60	8.57	12.03	6.94	9.28
MnO	0.04	0.04	7.41	0.04	7.41	0.19	339.81	0.00	100.00	0.20	362.96	0.00	100.00
MgO	10.74	10.76	0.16	11.87	10.49	10.81	0.62	11.22	4.44	11.82	10.03	12.36	15.05
CaO	19.34	19.23	0.55	19.77	2.24	19.70	1.88	20.99	8.55	20.38	5.40	21.43	10.83
Na2O	3.09	3.14	1.67	2.76	10.63	3.35	8.47	3.24	4.91	2.92	5.45	2.90	6.10
K2O	0.00	0.00	0.00	0.00	0.00	0.09	4900.00	0.00	0.00	0.09	4900.00	0.00	0.00
NiO2	0.02	-											
Total	100.13	100.54	0.41	100.77	0.64	98.65	1.48	101.33	1.20	99.08	1.05	101.18	1.05
FeO	7.65	7.12	6.95	7.75	1.28								

Table 6.08 Comparative matrix correction results on PTS 0906B. %Relative Deviation = ABS[{1-(result/PAP value)}*100].
Grt core bkg corrections are based on average garnet bkg counts. Omp core bkg corrections are based on average omphacite bkg counts. See in text (Chapter 7) for explanation of colours.

As a general rule, background corrections on element map derived data increase the %relative deviation from PAP matrix corrected values (Table 6.08). Element map data from uncorrected Love & Scott (1984) α-factors produces the most values that have the lowest %relative deviation out of all tests.

As a result of testing on Pk-Bkg Bence-Albee matrix corrected data and element mapping derived data, the α-factors of Love & Scott (1984) produce a better matrix correction than the α-factors of Kato (2005) and the transposed α-factors of Kato (2005). Background correction on element mapping derived data was generally detrimental to %relative deviation and therefore lowered accuracy to real known values. Masking also produced poor results, lowering totals and not improving error.

Bence-Albee matrix corrections (and thus element mapping as a whole) show %relative deviation from PAP matrix corrected values that is too great to allow the use of element mapping as an accurate quantitative indicator, although as shown in Chapter 6 (and below) it is an excellent qualitative indicator and was used as such.

Element mapping, by contrasting the elemental concentration of different minerals using colour, is an excellent indicator of mineral zoning as well as highlighting the interstitial nature and composition of symplectite development. In the BOG, narrow Al zoning in omphacite and Ca and Mg zoning in garnet can be observed to extend only 100 - 150μm into the grain.

Mineral zoning on a scale such as this is the result of garnet and omphacite undergoing thermal re-equilibration while cooling and is evidence of retrograde metamorphism. The interstitial nature of symplectite development is emphasised through element mapping, showing textures that imply a late growth of symplectite minerals hornblende and plagioclase, further evidence for retrograde metamorphism affecting the BOG.

Zoning is also observed on a sub 100μm in omphacite from the BE (sample 0904C) (Fig. 6.57). This and the interstitial nature of hornblende and biotite in the BE symplectite suggest that both of these features are retrograde in nature; the

omphacite zoning being another example of thermal re-equilibration. The mineral labelled epidote was arrived at by a process of elimination; based on Ca content the mineral could potentially be a clinopyroxene or a Ca rich plagioclase. It shows no Na or Mg (and thus cannot be omphacite or diopside) it exhibits birefringence too high to render it a high An plagioclase) and thus can only be epidote.

Identical, sub 100µm scale diopside grain boundary zoning can also be observed in the hornblende peridotite (Figs. 6.62 – 6.64

Element maps show Tschermak's diopside (high Al_2O_3, low MgO diopside) content in 0906B diopside cores and diopside at grain rims (Figs. 6.58 – 6.60), interpreted as thermal re-equilibration (O'Brien, P. 2008) from Ts diopside to diopside and is not thermal re-equilibration from diopside to omphacite as even though Al content decreases, Na is constant while Mg increases from core to rim, if this were an example of thermal re-equilibration from diopside to omphacite, higher Na would be seen at the rim, but this feature is absent (Fig. 7.20) (Appendix 6.D). Na variation is only seen along cracks and is negative, rather than positive Na variation expected for diopside to omphacite re-equilibration.

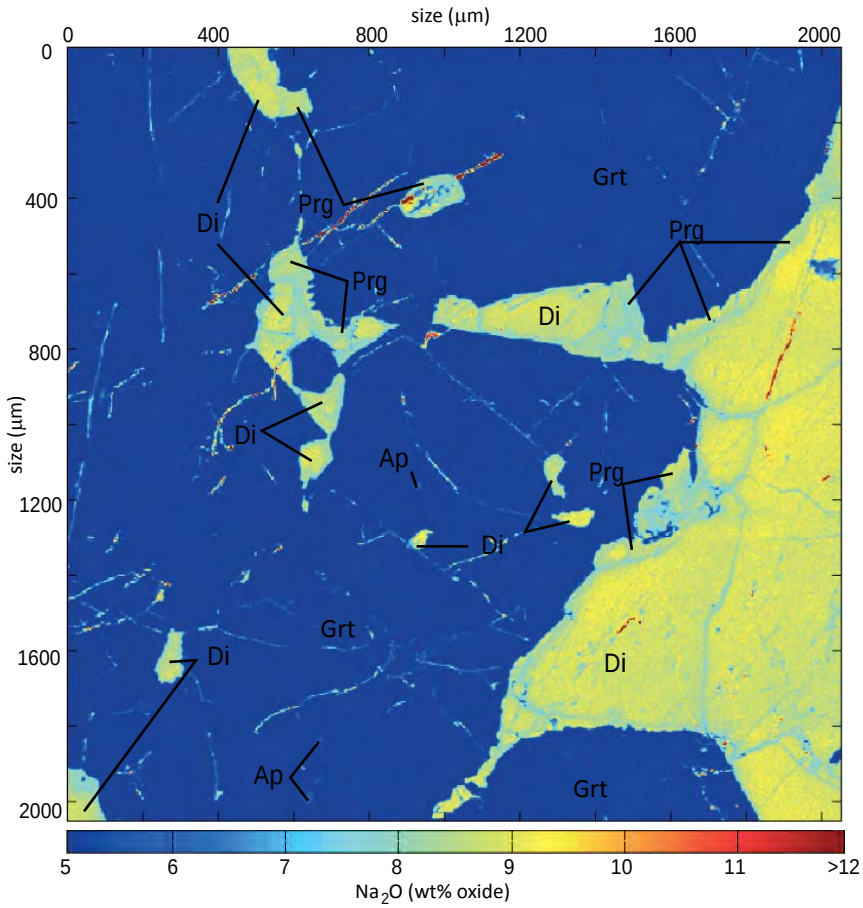

Fig 7.20 0906B. Element mapping image showing Na_2O concentration. Shows a lack of zoning in diopside. Image is 2.048mm across.

An argument for igneous crystallisation of garnet and Tschermak's diopside is presented on an increasingly finer scale; starting from field relationships, petrography and whole rock data to laser ablation and element mapping findings.

Experimental conditions that account for garnet + Tschermak's diopside to crystallise from an igneous liquid (Alonso-Perez et al., 2009) and an explanation of clinopyroxene zoning from Tschermak's diopside (core) to diopside (rim) (garnetite) and Tschermak's diopside (core) (inferred) to omphacite (rim) (BOG) as the effects of diffusion driven thermal re-equilibration (O'Brien, P, 2008) along with laser ablation studies of garnet trace element partitioning in metamorphic and igneous garnet (Schroter et al., 2004) are compared to and supported by the results of laser ablation and element mapping from this study. Clinopyroxene zoning from diopside to omphacite can only occur in the presence of available Na, usually from plagioclase.

Field relationships observed were the initial indicator for the preservation of primary igneous textures in layered garnetite and pyroxenite (Figs. 3.06 & 3.07) – by observing what was labelled a primary igneous texture the inference was created that the garnet, diopside and omphacite observed in the layered units must either have crystallised in an igneous setting, or developed as a metamorphic growth of the minerals during the regional granulite facies metamorphism that has affected the area (Chapter 2).

Polished thin sections of pyroxenite produce garnet inclusions that are crystallographically aligned (Figs. 4.18 and 4.19) and are inferred to be coeval with diopside growth.

TAS diagrams (Fig. 5.07 & 7.07) highlight the potential for the hornblende peridotite, eclogite and layered units to be part of a cumulate system, having SiO_2 contents <45wt%. The higher SiO_2 content of pyroxenite is due to its near monomineralic nature and the chemical structure of pyroxene. Harker diagrams of SiO2 vs. Na2O and SiO2 vs. Sr show that the BE, layered units and hornblende peridotite have low Na and Sr – correlating with low to no plagioclase in these rocks. Harker diagrams of SiO2 vs. MnO and SiO2 vs. Y also help build evidence; Mn and Y preferentially

partition into garnet (Jiang & Palmer, 1996). A metamorphic garnet would exhibit MnO and Y values similar to the precursor mineral it grew from, for e.g. the garnet in the BOG which shows metamorphic textures does not have anomalously high MnO or Y abundances, implying garnet growth in an environment with restricted MnO and Y availability, which would be the case during metamorphic growth of garnet, whereas garnet crystallised in an igneous setting will show higher abundances of MnO and Y due to increased availability in a liquid and preferential partitioning. Garnetite shows much higher MnO and Y than any other rocks (Figs. 7.05 & 7.06). Pyroxenite has a very low garnet content (<5%) and so does not mirror garnetite trends for MnO and Y as the low amount of garnet could not raise the whole rock MnO and Y content significantly (Figs. 7.05 & 7.06). At this stage it could still be argued that high MnO and Y is simply an indicator of a high garnet modal percentage.

Laser ablation was conducted to support ICP-MS data and also to determine trace element variation between core and rim values; Schroter et al., (2004) conducted a laser ablation comparison study of garnet reaction zones created within a two pyroxene hornblende granulite as a result of garnet bearing trondhjemitic veins intruding into the granulite host rock, comparing trace element patterns of garnet in the garnet reaction zones to that of garnet in the trondhjemitic veins. The trondhjemitic veins are an igneous feature (partial melting of dioritic gneiss).

The comparison found that garnet trace element patterns from the garnet reaction zones inherit the HREE pattern for their precursor mineral (in this case, hornblende and clinopyroxene), showing a HREE pattern with a slight negative gradient while the igneous garnets show a HREE pattern with an increasing gradient (Schroter et al., 2004).

The BOG and BE show garnet grains with a slightly negative HREE pattern (Figs. 6.25, 6.26, 6.29 & 6.30). Laser ablation of BOG and BE inclusions with the Resolution Orthogneiss (Figs. 6.27 & 6.28) show BOG with a slightly negative HREE pattern and BE with a slightly positive HREE pattern and observable negative Eu anomaly. In the BOG and BE garnet trace elemental abundances did not differ from core to rim and

for all BOG samples and BE sample 0904C garnet exhibits an inherent HREE pattern indicative of metamorphic garnet growth. BE sample 73832 however shows an igneous HREE pattern. Hornblende peridotite shows an increasing HREE trend, although garnet in this sample appears to have in interstitial appearance and this could be an interstitial phase in a cumulate system (Figs. 6.35, 6.36, 6.61 – 6.64). Layered garnetite shows trace elemental abundance variation between garnet cores and rims (Figs. 6.31 & 6.32) with garnet cores having elevated HREE compared to garnet rims, although both an igneous HREE pattern, increasing from Dy to Lu. Pyroxenite shows garnet core values identical to garnetite; a positive HREE slope indicative of an igneous garnet, while garnet rims show an inherent metamorphic texture (Figs. 6.33 & 6.34) inferred to be metamorphic garnet growth around an igneous garnet core, with thermal re-equilibration on cooling creating a zoned feature and not a distinct igneous core/metamorphic rim boundary.

The HREE patterns observed in garnetite cores and rims, pyroxenite cores, hornblende peridotite and one sample of BE imply an igneous origin for garnet growth while pyroxenite rims, BOG and one sample of BE imply a metamorphic origin for garnet growth.

Alonso-Perez et al., (2009) conduct experiments with synthetic andesite at P = 8-12kbar, T = 800 – 1000°C to evaluate the role of garnet fractionation at conditions observed in the roots of island arcs. Alonso-Perez et al., (2009) found that with P=12kbar and T>930°C garnet and Tschermak's diopside will crystallise from a liquid and at T between 930°C and 850°C garnet, Tschermak's diopside and plagioclase (with orthopyroxene and ilmenite accessory minerals) will crystallise. Pyroxene decreases and amphibole increases with increasing H_2O content.

The higher Tschermak's diopside seen in the garnetite layer diopside core during element mapping could therefore potentially have been present as an igneous crystallisation with garnet. Following this, with Tschermak's diopside, having crystallised with garnet (BE) and with garnet and plagioclase (BOG), as well as in the layered units, was then affected by cooling and re-equilibration. In the layered units this Tschermak's diopside equilibrated to form diopside at rims, with some grains

being classified as omphacite due to differing amounts of Na equilibration, although this is concentrated to outer the edges of grains (Appendix 6.D) (O'Brien , P. 2008). Zoning of this nature is supported by EMP data (Figs. 6.18 & 6.19) and element maps (Figs 6.58 – 6.60 and 7.20).

Thermal re-equilibration in the BOG however was from Tschermak's diopside through to omphacite due to the higher amounts of bulk Na on account of plagioclase modal proportions. It thus follows that omphacite in the BOG is the thermally re-equilibrated equivalent (in the presence of higher Na) of the igneous crystallisation of Tschermak's diopside in the layered units. O'Brien (2008) also notes the development of symplectites along with re-equilibration as two examples of retrograde metamorphic textures. Thermal re-equilibration to omphacite as well as symplectite development, in the case of the BOG, served to mask primary igneous textures being sought.

The BE is observed with no plagioclase (and thus no Na source to facilitate the phase transition from diopside → omphacite) and cannot be a thermal re-equilibration of a garnet-diopside eclogite or an eclogite formed from layered garnetite and pyroxenite. Experimental data of Alonso-Perez et al., (2009) shows that omphacite cannot crystallise on liquidus from an igneous system and implies, along with laser ablation data, that BE at site 0904C is metamorphic eclogite. Resolving a protolith for the BE is difficult, although certain rock types can be discounted; garnet-diopside eclogite and an eclogite formed from the layered garnetite and pyroxenite of site 6, as the BE contains omphacite that cannot be formed through thermal re-equilibration from diopside, as a garnet-diopside and the layered units lack the Na necessary to facilitate this phase change. The protolith for the BE is not a metamorphosed plagioclase bearing or ultramafic sample, on the basis of geochemical data.

The assumption that garnet-diopside cannot produce garnet-omphacite through thermal re-equilibration due to lack of available Na is challenged by the garnetite and pyroxenite layers as EMP analysis shows a cluster of very Na poor omphacites, but by definition still omphacite (Fig. 6.20 & 6.21). It is worth noting that there are

very few omphacite grains in the pyroxenite layer (90-95% diopside, 5-10% garnet) but a much larger amount of omphacite grains in the garnetite layer (80-85% garnet, 15-20% diopside).

One possible solution to this problem and a step forward in resolving a protolith for the BE is to have a garnet-diopside eclogite (or garnetite with minor diopside; diopside pyroxenite with minor garnet) present as a podiform raft within the BOG, which is observed in situ at site 6.

The area is subjected to high P T metamorphism up to 18kbar and >750°C (Daczko & Halpin, 2009) and during retrograde cooling from peak metamorphic pressures, Na in the BOG re-equilibrates into the garnet-diopside raft in large enough quantities to facilitate the diopside → omphacite re-equilibration texture.

As such, the relative proportions of diopside to newly re-equilibrated omphacite are a function of relative abundances of initial diopside; in this proposed solution the garnetite and pyroxenite layers receive equal quantities of Na from surrounding plagioclase bearing BOG however Na does not equilibrate into garnet. Thus the smaller amount of diopside in the garnetite (15-20% diopside) layer receives a greater proportion of Na per diopside than the pyroxenite (90-95% diopside) in which the Na is spread evenly amongst the higher abundance of pyroxene, creating a lower overall increase in Na and levels of re-equilibration not sufficient to cause the diopside – omphacite phase transition to occur en masse.

Applying this theory to a garnet-diopside eclogite raft (the equivalent of having garnet and diopside in similar proportions as opposed to near monomineralic proportions seen in the layered rocks), Na re-equilibration from surrounding plagioclase bearing BOG would be proportionately high enough to cause the phase transition from diopside to omphacite.

Element mapping images of sample 0904C show low Na near plagioclase symplectite, moderate Na in omphacite cores and higher Na on omphacite rims that are not in contact with symplectite (Fig 7.21). Symplectite development of late

plagioclase is expected to remove some Na from the omphacite that is breaking down to form the symplectite. Omphacite cores in BE sample 0904C have lower Na than rims; a feature expected of an outcrop scale Na exchange adding Na from mineral rims inwards.

Re-equilibration is consequently found to occur on a grain size scale showing variation between core and rim values and also on an outcrop scale, providing the Na necessary for the diopside – omphacite phase transition even in the absence of Na in the equilibrating pyroxene.

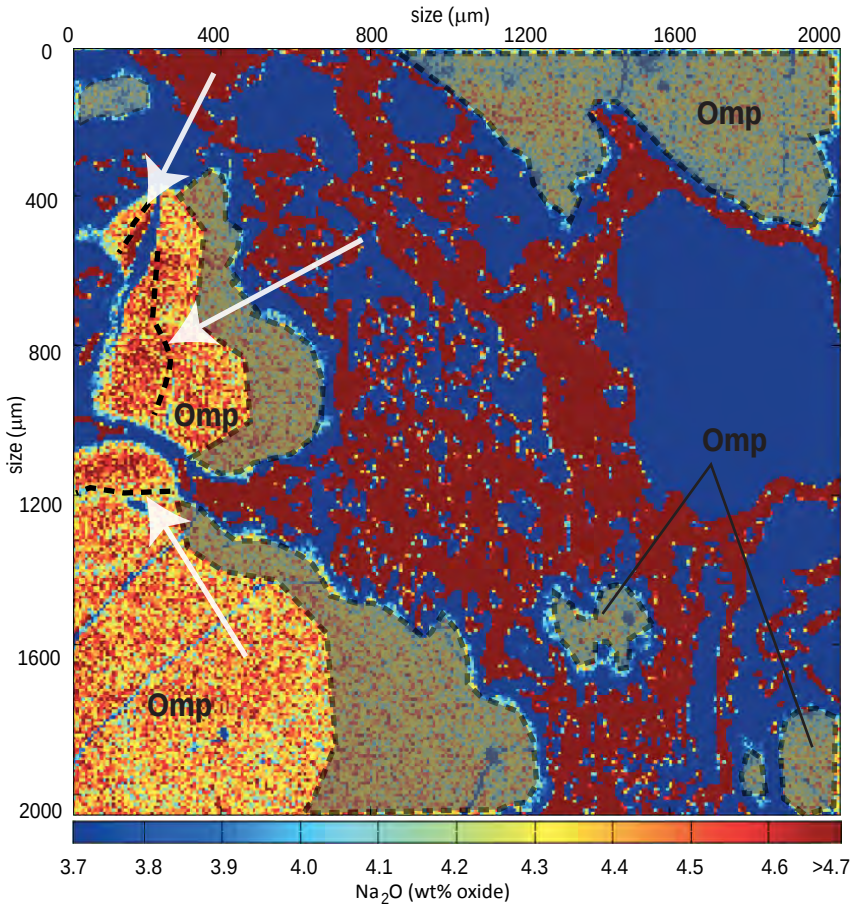

Fig 7.21 0904C. Element mapping image showing Na_2O concentration. Shows slight increase towards omphacite grains with no symplectite development, marked by white arrows and black dashed line. Grey shaded areas so slight Na deficiency due to Na incorporated in plagioclase symplectite. Image is 1.024mm across.

8. Conclusion

The Breaksea Orthogneiss unit has been characterised into four distinct lithologies; the Breaksea Omphacite Granulite, the volumetrically dominant meta-diorite country rock; Breaksea Eclogite, podiform rafts of eclogite bound completely by BOG; spatially associated layered garnetite and pyroxenite, also taking the shape of podiform rafts within the BOG; hornblende peridotite, observed as a single podiform raft within the BOG. Lithological division is based on field relationships and petrological examination and supported by geochemical analysis; showing distinct chemical variation (for example Na and Sr variation between the BOG (plagioclase bearing) and other units (non plagioclase bearing), trace-element partitioning (HREE in garnet, Sr and Pb in plagioclase) and distinct compositional differences (omphacite in plagioclase bearing samples and diopside in non plagioclase bearing samples) and isotope ratios and isotope ratio trends with differing ages.

The BOG is chemically close to the average values for the WFO suite, although is typically outside values prescribed in McCulloch et al., (1987) for the WFO due to a sample bias in the garnet poor Worsley Pluton. Along trends seen in Harker diagrams the BOG can be seen as having the highest 'mafic' characteristics of the BOG, is shown to have been subject to the highest pressure and temperature in the Fiordland arc and represents its deepest exposed part. This shows a trend for increasingly more mafic rocks as depth (and thus P and T) increases. The Hawes Head Ultramafic units are higher in mafic content than neighbouring plutons and show trends identical to those observed in garnet.

By combining field relationships and petrographic observations with whole rock and mineral chemistry it is found that the hornblende peridotite is geochemically analogous to cumulate hornblende peridotite rocks of the Hawes Head Ultramafics.

The layered units of garnetite and pyroxenite represent crystallisation of garnet and Tschermak's diopside in an igneous system. Retrograde diffusion driven thermal re-equilibration is observed in all samples in the form of mineral zoning in garnet, plagioclase and clinopyroxene with accompanying clinopyroxene phase transitions

(Tschermak's diopside → diopside → omphacite [in the presence of Na]) as well as symplectite development in all rock types other than layered garnetite and pyroxenite. On the basis of bulk rock chemistry, the BOG is the product of a magma source region located at depths at which garnet is stable, and has enough available Na (exhibited through Ab content of plagioclase and modal proportion of plagioclase) to facilitate thermal re-equilibration from diopside → omphacite. BE with mineral compositions observed; garnet-omphacite, with elevated Na at omphacite rims i.e. a more diopside rich core, can be produced by outcrop scale Na re-equilibration from plagioclase bearing BOG during retrogression from high PT metamorphism.

References

Allibone, A.H., Jongens, R., Turnbull, I.M., Milan, L.A., Daczko, N.R., DePaoli, M.C., and Tulloch, A.J., (2009) Plutonic rocks of western Fiordland, New Zealand: field relations, geochemistry, correlation and nomenclature. *New Zealand Journal of Geology and Geophysics* v. 52: 101 – 148.

Alonso-Perez, R.,Muntener, O., Ulmer, P., (2009) Igneous garnet and amphibole fractionation in the roots of island arcs: experimental constraints on andesitic liquids. *Contributions to Mineralogy and petrology* v. 157: 541 – 548.

Armstrong JT (1988) Quantitative analysis of silicate and oxide minerals: comparison of Monte Carlo, ZAF and phi–rho-z procedures. *In:* Newbury DE (ed) Microbeam analysis, 1988 San Francisco Press, San Francisco, pp 239–246

Bradshaw, J.Y., (1990) Geology of crystalline rocks of northern Fiordland: details of the granulite facies rock units. *Zealand Journal of Geology and Geophysics* v. 33: 465 – 484.

Bradshaw, J.Y., (1998) Origin and metamorphic history of an Early Cretaceous polybaric granulite terrain, Fiordland, southwest New Zealand. *Contributions to Mineralogy and Petrology* v. 103: 346 – 360.

Brown, E.H., (1996) High-pressure metamorphism caused by magma loading in Fiordland, New Zealand. *Journal of Metamorphic Geology* v. 14: 441 – 452.

Clarke, G.L., Daczko, N.R. and Nockolds, C. (2001) A method for applying matrix corrections to X-ray intensity maps using the Bence-Albee algorithm and Matlab. *Journal of Metamorphic Geology* v. 19: 635 – 644.

Clarke, G.L., Klepeis, K.A., and Daczko, N.R., (2001) Cretaceous granulites at Milford Sound, New Zealand; metamorphic history and emplacement in a convergent margin setting. *Journal of Metamorphic Geology* v. 18: 359 – 374.

Crawford, M.L., Hollister, M.S., and Woodsworth, G.J., (1987) Crustal deformation and regional metamorphism across a terrane boundary, coast plutonic complex, British Columbia. *Tectonics* v. 6: 343 – 361.

Cox, K.G., Bell, J.D., and Pankhurst, R.J., (1979) The interpretation of igneous rocks. *George, Allen & Unwin, London.*

Daczko, N.R., and Halpin, J.A., (2009) Evidence for melt migration enhancing recrystallisation of metastable assemblages at the root of a Cretaceous magmatic arc – Fiordland, New Zealand. *Journal of Metamorphic Petrology* v.27: 233 – 247.

Daczko, N.R., Klepeis, K.A., and Clarke, G.L., (2001) Evidence of Early Cretaceous collisional-style orogenesis in northern Fiordland, New Zealand and its effects on the evolution of the lower crust. *Journal of Structural Geology* v. 23: 693 – 713.

Daczko, N.R., Klepeis, K.A., and Clarke, G.L., (2002) Thermomechanical evolution of the crust during convergence and deep crustal pluton emplacement in the Western Province of Fiordland, New Zealand. *Tectonics* v. 21: 1 – 18.

Davis, D. W., Gray, J. and Cumming, G. L. (1977). Determination of the 87Rb decay constant *Geochimica et Cosmochimica Acta* v. 41: 1745 – 1749.

DeBari, S., and Coleman, R.G., (1989) Examination of the deep levels of an Island Arc: evidence from the Tonsina ultramafic-mafic assemblage, Tonsina Alaska. *Journal of Geophysical Research* v. 94: 4373 – 4391.

DeBari, S.M., and Sleep, N.H., (2009) High-Mg, low-Al bulk composition of the Talkeetna island arc, Alaska: Implications for primary magmas and the nature of arc crust. *Geological Society of America Bulletin* v. 103: 37 – 47.

Deer, W.A., Howie, R.A., and Zussman, J., (1992) An introduction to the rock forming minerals, 2nd edition. *Harlow, Pearson Prentice Hall.*

DePaoli, M.C., Clarke, G.L., Klepeis, K.A., (In Prep). Petrography and thermobarometry of the Breaksea Gneiss and hosted orthopyroxene-bearing eclogite to orthopyroxene-free eclogite, Breaksea Sound, Fiordland, New Zealand. *Journal of Petrology*

El Goresy, A., Chen, M., and Dubrovinsky, L., (2001) An Ultradense Polymorph of Rutile with Seven-Coordinated Titanium from the Ries Crater. *Science* v. 293: 1467

Emami, S (2008) Petrogenisis and geochemical characterisation of ultramafic cumulates from the root of a magmatic arc, Fiordland, New Zealand. Unpublished BSc Honours thesis, Macquarie University.

Gibson, G.M., and Ireland, T.R., (1995) Granulite formation during continental extension in Fiordland, New Zealand. *Nature* v. 375: 479 – 482.

Gibson, G.M., McDougall, I., and Ireland, T.R., (1988) Age constraints on metamorphism and the development of a metamorphic core complex in FIordland, southern New Zealand. *Geology* v. 16: 405 – 408.

Heuberger, S., (2004). The Karakoram-Kohistan suture zone in NW Pakistan - Hindu Kush mountain range*. Verlag der Fachvereine Hochschulverlag AG an der ETH Zurich* 29 -34

Janousek, V., Farrow, C.M., Erban, V., and Smid, J., (2008) Geochemical Data Tookit (GCDKit) v2.3.

Jiang, S.Y and Palmer, M.R., (1996) Mn-rich ilmenite from the Sullivan Pb-Zn-Ag deposit, British Columbia. *Canadian Mineralogist* v. 34: 29 – 36.

Kato, T., (2005) New Accurate Bence-Albee α-Factors for Oxides and Silicates Calculated from the PAP Correction Procedure. *Geostandards and Geoanalytical Research* v. 29: 83 – 94.

Kimbrough, D.L., Tulloch, A.J., Geary, E., Coombs, D.S., and Landis (1993) Isotopic ages from Nelson Region of South Island New Zealand: crustal structure and definition of the Median Tectonic Zone. *Tectonophysics* v.225: 422448.

Klepeis, K.A., and Clarke, G.L., (2004) The evolution of an exposed mid-lower crustal attachment zone in Fiordland, New Zealand. *Geological Society, London, Special Publications* v. 27: 197 – 229.

Leake, B.E., Woolley, A.R., Arps, C.E., Birch, W.D., Gilbert, M.C., Grice, J.D., Hawthorne, F.C., Kato, A., Kisch, H.J., Krivovichev, V.G., Linthout, K., Laird, J., Mandarino, J.A., Maresch, W.V., Nickel, E.H., Rock, N.M., Schumacher, J.C., Smith, D.C., Stephenson, N.C., Ungaretti, L., Whittaker, E.J., and Youzhi, G., (1997) Nomenclature of amphiboles, report of the subcommittee on amphiboles of the international mineralogical association, commission on new minerals and mineral names. *The Canadian Mineralogist* v. 35: 219 – 246.

Lugmair, G. W. and Marti, K. (1978). Lunar initial 143Nd/144Nd: differential evolution of the lunar crust and mantle. *Earth and Planetary Science Letters* v. 39: 349 – 357.

Mattinson, J.M., Kimbrough, D.L., and Bradshaw, J.Y., (1986) WFO: Early Cretaceous arc magmatism and granulite facies metamorphism, New Zealand. *Contributions to Mineralogy and Petrology* v. 92: 383 – 392.

McCulloch, M.T., Bradshaw, J.Y., and Taylor, S.R., (1987) Sm-Nd and Rb-Sr isotopic and geochemical systematics in Phanerozoic granulites from Fiordland, Southwest New Zealand. *Contributions to Mineralogy and Petrology* v. 97: 183 – 195.

McDonough, W.F., Sun, S.S., Ringwood, A.E., Jagoutz, E., and Hofmann, A.W., (1991) Potassium, Rubidium, and cesium in the Earth and Moon and the Evolution of the Mantle of the Earth. *Geochimica et Cosmochimica Acta* v. 56: 1001 – 1012.

Ming, Z., Stephenson P.J., O'Reilly S.Y., McCulloch M.T., and Norman M. (2001) Petrogenesis and geodynamic implications of late Cenozoic basalts in North Queensland, Australia: Trace-element and Sr-Nd-Pb isotope evidence. *Journal of Petrology* v. 42: 685 – 719.

Morimoto, N., (1988) Nomenclature of Pyroxenes. *Mineralogy and Petrology* v. 39: 55 – 76.

Mortimer, N., (2004) New Zealand's Geological Foundations. *Gondwana Research* v. 7: 261 – 272.

Muir, R.J., Ireland, T.R., Weaver, S.D., Bradshaw, S.D., Evans, J.A., Eby, G.N., and Shelley, D. (1998) Geochronology and geochemistry of a Mesozoic magmatic arc system, Fiordland, New Zealand. *Journal of the Geological Society, London* v. 155: 1037 – 1053.

Muir, R.J., Weaver, S.D., Bradshaw, J.D., Eby, G.N., and Evans, J.A., (1995) The Cretaceous Separation Point Batholith, New Zealand: Granitoid Magmas Formed by Melting of Mafic Lithosphere. *Journal of the Geological Society* v. 152: 689 – 701.

Norman M.D., Griffin W.L, Pearson N.J., Garcia M.O., and O'Reilly S.Y., (1998) Quantitative analysis of trace element abundances in glasses and minerals: a comparison of laser ablation inductively coupled plasma mass spectrometry, solution inductively coupled plasma mass spectrometry, proton microprobe and electron microprobe data. *Journal of Analytical Atomic Spectrometry* v. 13: 447 – 482.

Norman M.D., Pearson N.J., Sharma A., and Griffin W.L., (1996) Quantitative analysis of trace elements in geological materials by laser ablation ICPMS: Instrumental operating conditions and calibration values of nist glasses. *Geostandards Newsletter* v. 20: 247 – 261.

Norrish, K. and Hutton, J. T. (1969). *Geochimica et Cosmochimica Acta* v. 33: 431 – 453.

O'Brien, P.J., (2008) Challenges in high-pressure granulite metamorphism in the era of pseudosections: reaction textures, compositional zoning and tectonic interpretation with examples from the Bohemian Massif. *Journal of Metamorphic Geology* v. 26: 235 – 251.

Petterson, M.G., and Treloar, P.J., (2004) Volcanostratigraphy of arc volcanic sequences in the Kohistan arc, North Pakistan: volcanism within island arc, back-arc-basin, and intra-continental tectonic settings. *Journal of Volcanology and Geothermal Research* v. 130: 137 – 148.

Petterson, M.G., and Windley, B.F., (1985) Rb-Sr dating of the Kohistan arc batholith in the Trans Himalaya of N. Pakistan and tectonic implications. *Earth and Planetary Science Letters* v. 74: 54 – 75.

Pouchou, J.L., and Pichoir, F., (1984) A new model for quantitative x-ray microanalysis of homogenous samples. *Recherche Aerospatiale* v. 5: 13 – 38.

Schröter, F.C., Stevenson, J.A., Daczko, N.R., Clarke, G.L., Pearson, N.J. and Klepeis, K.A., (2004) Trace element partitioning during high-P partial melting and melt-rock interaction; an example from northern Fiordland, New Zealand. *Journal of Metamorphic Geology* v. 22: 443 – 457.

Scott, J.M., and Cooper, A.F., (2006) Early Cretaceous extensional exhumation of the lower crust of a magmatic arc: Evidence from the Mount Irene Shear Zone, Fiordland, New Zealand. *Tectonics* v. 25

Stein M., Almogi-Labin A., Goldstein S.L., Hemleben C., and Starinsky A., (2007) Late Quarternary changes in dessert dust inputs to the Red Sea and Gulf of Aden from 87Sr/86Sr ratios in deep-sea cores. *Earth and Planetary Science Letters* v. 261: 104 – 119.

Sun, S.S., and McDonough, W.F., (1989) Chemical and isotopic systematics of oceanic basalts: implications for mantle composition and processes *in* Saunders, A.D., Norry, M.J.S., ed., Magmatism in ocean basins. *Geological Society, London*, *Special Publications* v. 42: 313 – 345.

Treloar, P.J., Petterson, M.G., Jan, M.Q., and Sullivan, M.A., (1996) A re-evaluation of the stratigraphy and evolution of the Kohistan arc sequence, Pakistan Himalaya: implications for magmatic and tectonic arc-building processes. *Journal of the Geological Society, London* v. 153: 681 – 693.

Withers, A.C., Essene, E.J., and Zhang, Y., (2003) Rutile/ TiO_2II phase equilibria. *Contributions to Mineralogy and Petrology* v. 145: 199 – 204.

Wood, D.J., Stowell, H.H., Onstott, T.C., and Hollister, L.S., (2009) $^{39}Ar/^{40}Ar$ constraints on the emplacement, uplift, and cooling of the Coast Plutonic Complex sill, southeastern Alaska. *Geological Society of America Bulletin* v. 103: 849 – 860.

Wu, X., Meng, D., and Han, Y., (2005) α-PbO_2-type nanophase of TiO_2 from coesite-bearing eclogite in the Dabie Mountains, China. *American Mineralogist* v. 90: 1458 – 1461.

Pluton	Data Source	sample no.	Major element (wt% oxide)														
			SiO2	TiO2	Al2O3	Fe2O3	MnO	MgO	CaO	Na2O	K2O	P2O5	LOI (%)	Total	Mg#	Na2O/K2O	Na2O+K2O
Worlsey Pluton 2px hbl	Allibone et al., (2009)	P76569	54.43	1.12	17.77	7.42	0.10	4.80	7.63	5.02	1.00	0.45	0.14	99.88	35.8	5.02	6.02
	Allibone et al., (2009)	P76579	54.60	1.21	17.61	7.79	0.10	4.69	7.22	5.11	1.06	0.42	0.00	99.81	34.2	4.82	6.17
	Allibone et al., (2009)	P76586	54.66	1.22	17.56	8.01	0.12	4.28	7.33	4.88	1.45	0.44	0.10	100.04	31.5	3.37	6.33
	Allibone et al., (2009)	P76587	54.14	1.27	17.62	8.19	0.12	4.38	7.43	4.94	1.24	0.49	0.16	99.97	31.6	3.98	6.18
	Allibone et al., (2009)	P76588	55.72	1.21	17.24	7.55	0.11	4.48	6.62	5.02	1.55	0.44	0.09	100.00	33.8	3.24	6.57
	Allibone et al., (2009)	P76590	55.00	0.83	18.85	6.35	0.09	4.50	7.77	4.99	0.95	0.30	0.04	99.66	37.9	5.25	5.94
	Allibone et al., (2009)	P76597	55.22	1.20	17.28	7.72	0.10	4.96	7.06	4.82	1.29	0.43	-0.09	100.00	35.6	3.74	6.11
	Allibone et al., (2009)	P76601	56.57	0.97	18.34	6.47	0.10	3.88	6.80	4.80	2.08	0.27	-0.09	100.19	34.1	2.31	6.88
	Richard Jongens	P77341	56.25	1.18	17.58	6.80	0.09	4.17	6.52	5.18	1.67	0.41	0.00	99.85	34.6	3.10	6.85
	Richard Jongens	P77342	54.26	1.20	17.64	7.88	0.11	4.85	7.61	4.94	0.98	0.49	0.07	100.03	34.7	5.04	5.92
	Richard Jongens	P77350	55.19	1.09	17.64	7.50	0.11	4.53	7.18	4.93	1.12	0.43	0.13	99.86	34.2	4.40	6.05
	Milan, L. unpub.	LM0490-1	55.13	1.06	17.92	7.06	0.10	4.36	6.78	5.11	1.50	0.40	0.16	99.58	34.7	3.41	6.61
	Daczko, N. (2001)	99-47	55.32	1.07	18.34	7.41	0.13	3.60	6.70	4.78	1.48	0.38		99.21	29.5	3.23	6.26
	Milan, L. unpub.	LM9947	54.48	1.12	18.12	7.53	0.12	3.83	6.59	4.72	1.68	0.41	1.16	99.77	30.5	2.81	6.40
	Milan, L. unpub.	P65326	55.31	1.05	18.71	7.20	0.10	3.70	6.49	4.90	1.27	0.45	0.47	99.66	30.7	3.85	6.17
	Milan, L. unpub.	P65348	56.55	1.10	17.94	6.37	0.09	3.59	5.93	5.34	2.04	0.54	0.20	99.68	32.7	2.62	7.39
	Carroll, S. (2005) unpub.	SC-4050	54.85	1.35	17.32	8.02	0.10	4.40	7.15	4.49	1.15	0.54	0.31	99.68	32.1	3.90	5.64
	Carroll, S. (2005) unpub.	SC-4051	54.23	1.11	18.09	7.42	0.10	4.82	7.63	4.49	1.03	0.45	0.36	99.72	35.9	4.37	5.52
	Carroll, S. (2005) unpub.	SC-4052	53.73	1.17	17.84	8.07	0.11	5.19	7.98	4.23	0.80	0.45	0.17	99.73	35.7	5.32	5.02
	Milan, L. unpub.	P65296	54.99	1.18	17.51	7.77	0.10	4.52	6.93	4.52	1.22	0.52	0.23	99.50	33.4	3.70	5.75
Worsley Pluton hbl diorite -px	Stevenson, J. (2000)	Dan 24	57.98	1.12	17.15	6.66	0.09	3.86	5.32	4.51	2.28	0.31		99.29	33.32	1.98	6.79
	Allibone et al., (2009)	P76570	53.73	1.10	17.13	7.72	0.11	5.34	7.54	4.87	0.95	0.44	1.03	99.95	37.36	5.13	5.82
	Allibone et al., (2009)	P65295	57.18	1.14	17.33	6.73	0.09	3.66	5.56	4.94	2.18	0.43	0.35	99.59	31.91	2.26	7.12
	Allibone et al., (2009)	P65298	53.40	1.23	18.05	8.03	0.11	4.62	7.38	4.64	1.29	0.51	0.60	99.84	33.18	3.61	5.93
	Milan, L. unpub.	LM65306	51.78	1.32	18.56	7.97	0.09	4.58	6.56	4.89	1.96	0.55	1.27	99.51	33.12	2.49	6.85

Appendix 5.A Major element data from WFO database kindly provided by GNS

Pluton	Data Source	sample no.	Major element (wt% oxide)														
			SiO2	TiO2	Al2O3	Fe2O3	MnO	MgO	CaO	Na2O	K2O	P2O5	LOI (%)	Total	Mg#	Na2O/K2O	Na2O+K2O
Mckerr intrusives east	Allibone et al., (2009)	P76604	54.83	1.15	17.74	7.83	0.13	3.76	6.83	4.84	1.81	0.40	0.77	100.08	29.28	2.67	6.65
	Allibone et al., (2009)	P77074	54.72	1.05	18.99	7.08	0.11	3.25	6.35	5.70	1.53	0.43	0.77	99.97	28.36	3.73	7.23
	Degeling, H. (1997)	LM9710D	52.76	1.01	20.48	6.74	0.11	3.03	7.04	5.88	1.27	0.35		98.70	27.93	4.63	7.15
	Degeling, H. (1997)	LM9725	50.93	1.31	18.76	8.60	0.13	4.14	7.69	5.10	1.52	0.45	0.98	99.61	29.33	3.36	6.62
	Milan, L. unpub.	P65307	51.33	1.36	19.45	8.60	0.13	3.87	7.13	5.15	1.61	0.49	0.75	99.88	27.94	3.20	6.76
	Degeling, H. (1997)	LM9719	54.03	1.25	18.36	7.98	0.12	3.74	6.68	5.02	1.58	0.46	0.58	99.80	28.78	3.18	6.59
	Allibone et al., (2009)	P65307	51.33	1.36	19.45	8.60	0.13	3.87	7.13	5.15	1.61	0.49	0.75	99.88	27.94	3.20	6.76
	Allibone et al., (2009)	P65306	51.78	1.32	18.56	7.97	0.09	4.58	6.56	4.89	1.96	0.55	1.27	99.51	33.12	2.49	6.85
Mckerr intrusives west	Allibone et al., (2009)	P77901	59.03	0.86	17.58	6.03	0.09	2.66	5.22	5.04	2.05	0.35	0.55	99.46	27.56	2.45	7.09
	Allibone et al., (2009)	P77069	60.60	0.81	16.84	5.49	0.08	2.34	4.69	4.78	3.01	0.32	0.77	99.74	26.87	1.59	7.79
	Allibone et al., (2009)	P77072	61.67	0.71	18.61	4.08	0.06	1.46	4.40	6.11	2.11	0.31	0.37	99.90	23.58	2.90	8.22
	Allibone et al., (2009)	P77894	54.03	0.97	18.15	8.07	0.14	3.91	7.05	4.48	1.67	0.35	0.68	99.51	29.50	2.68	6.15
	Allibone et al., (2009)	P77910	57.37	0.92	17.40	7.22	0.11	3.26	6.00	4.54	1.57	0.31	0.75	99.44	28.00	2.89	6.11
	Allibone et al., (2009)	P77914	74.15	0.19	14.09	1.32	0.02	0.44	2.08	4.02	2.51	0.05	0.51	99.37	22.46	1.60	6.53
	Allibone et al., (2009)	P77931	64.57	0.74	16.62	4.46	0.06	1.95	3.88	4.24	2.00	0.31	0.75	99.57	27.33	2.12	6.25

Appendix 5.A Major element data from WFO database kindly provided by GNS

Pluton	Data Source	sample no.	Major element (wt% oxide)														
			SiO2	TiO2	Al2O3	Fe2O3	MnO	MgO	CaO	Na2O	K2O	P2O5	LOI (%)	Total	Mg#	Na2O/K2O	Na2O+K2O
Misty pluton 2px hbl	Allibone et al., (2009)	P76709	56.26	1.03	18.55	6.96	0.10	3.41	6.38	5.36	1.48	0.44	-0.05	99.92	29.70	3.62	6.84
	Allibone et al., (2009)	P76713	55.55	1.04	18.25	7.29	0.11	3.82	6.90	5.25	1.19	0.44	0.06	99.89	31.12	4.41	6.44
	Richard Jongens	P77298	55.02	1.04	18.36	7.74	0.12	3.92	7.14	5.02	1.25	0.41	-0.11	99.90	30.40	4.02	6.27
	Allibone et al., (2009)	P77090	57.95	0.92	17.73	6.54	0.10	2.98	5.83	5.12	2.07	0.38	0.32	99.94	28.21	2.47	7.19
	Emami, S. (2008) unpub.	A183/8	55.35	0.93	18.81	7.31	0.11	3.49	6.56	5.25	1.41	0.41	0.00	99.63	29.16	3.72	6.66
Misty pluton hbl diorite - px	Allibone et al., (2009)	P77132	49.33	1.43	18.71	10.00	0.15	4.73	8.34	4.69	1.33	0.45	0.59	99.75	28.97	3.53	6.02
	Milan, L. unpub.	LMMH0270	55.16	0.97	18.90	7.07	0.10	3.63	6.53	4.97	1.23	0.45	0.43	99.44	30.69	4.05	6.20
	Milan, L. unpub.	LM0412	51.66	1.16	18.94	8.54	0.13	4.38	7.58	5.24	0.89	0.50	0.67	99.69	30.63	5.90	6.13
	Milan, L. unpub.	LM0413	54.90	1.03	18.85	7.18	0.10	3.54	6.57	5.15	1.60	0.42	0.43	99.77	29.84	3.23	6.75
	Allibone et al., (2009)	P77630	53.74	1.35	17.81	8.41	0.13	3.55	6.50	4.81	2.04	0.43	0.75	99.53	26.70	2.35	6.86
	Allibone et al., (2009)	P77972	52.25	1.17	17.55	9.15	0.17	3.99	6.22	5.56	2.32	0.52	0.66	99.53	27.31	2.40	7.87
	Emami, S. (2008) unpub.	SE0805D	50.52	1.12	19.69	8.54	0.10	4.70	8.24	5.20	0.59	0.49	0.31	99.50	32.18	8.81	5.79

Appendix 5.A Major element data from WFO database kindly provided by GNS

Pluton	Data Source	sample no.	Major element (wt% oxide)														
			SiO2	TiO2	Al2O3	Fe2O3	MnO	MgO	CaO	Na2O	K2O	P2O5	LOI (%)	Total	Mg#	Na2O/K2O	Na2O+K2O
HHU hbl pdt	Emami, S. (2008) unpub.	A180/8	39.21	1.03	5.26	17.43	0.19	29.98	4.71	1.05	0.26	0.02	0.24	99.36	59.73	4.04	1.31
	Emami, S. (2008) unpub.	SE0801G	38.39	0.57	2.67	19.67	0.23	35.36	2.50	0.51	0.14	0.03	-0.30	99.76	60.78	3.64	0.65
	Emami, S. (2008) unpub.	SE0802F	40.55	1.35	7.82	15.79	0.18	25.19	6.41	1.53	0.50	0.03	-0.03	99.33	57.90	3.06	2.03
	Emami, S. (2008) unpub.	SE0802G	41.11	1.93	9.76	13.49	0.14	21.52	8.56	1.92	0.52	0.02	0.42	99.39	57.90	3.69	2.44
	Emami, S. (2008) unpub.	SE0810B	38.54	0.57	2.80	19.61	0.23	34.95	2.48	0.54	0.15	0.03	-0.67	99.24	60.58	3.60	0.69
HHU hbldite	Emami, S. (2008) unpub.	A1801/8	41.94	2.72	12.90	11.32	0.11	15.44	11.33	2.54	0.62	0.02	0.79	99.74	54.05	4.10	3.16
	Emami, S. (2008) unpub.	SE0804A	41.39	3.03	13.06	12.01	0.10	14.72	11.17	2.48	0.79	0.02	0.52	99.29	51.38	3.14	3.27
	Emami, S. (2008) unpub.	SE0805K	41.88	2.57	13.20	10.94	0.10	15.49	11.40	2.61	0.62	0.02	0.64	99.47	54.97	4.21	3.23
	Emami, S. (2008) unpub.	SE0807E	41.43	2.72	13.17	11.55	0.11	15.18	11.22	2.60	0.65	0.02	0.53	99.20	53.12	4.00	3.25
	Emami, S. (2008) unpub.	SE0810A	41.64	2.88	12.85	11.48	0.10	15.76	11.33	2.67	0.67	0.02	0.48	99.89	54.21	3.99	3.34

Appendix 5.A Major element data from WFO database kindly provided by GNS

Pluton	Data Source	sample no.	Major element (wt% oxide)														
			SiO2	TiO2	Al2O3	Fe2O3	MnO	MgO	CaO	Na2O	K2O	P2O5	LOI (%)	Total	Mg#	Na2O/K2O	Na2O+K2O
Malaspina Orthogneiss	Hollis et al., (2004)	cao10c	55.52	1.10	18.35	7.91	0.13	4.23	7.19	3.65	1.74	0.40		100.20	31.56	2.10	5.39
	Hollis et al., (2004)	cao90a	56.75	0.94	18.31	6.92	0.11	3.20	6.20	4.90	1.83	0.38		99.60	28.51	2.68	6.73
	Hollis et al., (2004)	cao90a-dup	56.67	0.94	18.34	6.92	0.11	3.19	6.19	4.87	1.83	0.37		99.40	28.44	2.66	6.70
	Davids (1999)	ANU960459	57.27	1.02	17.79	6.96	0.11	3.22	5.90	4.65	2.32	0.36		99.83	28.52	2.00	6.97
	Milan, L. unpub.	P71152	55.61	1.01	18.35	7.37	0.11	3.43	6.55	4.97	1.43	0.40	0.57	99.80	28.64	3.48	6.40
	Milan, L. unpub.	P71154	58.08	1.01	17.38	6.59	0.09	2.92	5.43	4.53	2.72	0.38	0.66	99.79	27.64	1.67	7.25
	Milan, L. unpub.	P71155	54.49	1.13	18.27	8.13	0.12	3.86	6.83	4.65	1.74	0.42	0.26	99.89	29.05	2.67	6.39
	Milan, L. unpub.	P71167	55.10	1.04	17.65	7.74	0.11	3.74	6.57	4.15	2.14	0.38	1.13	99.76	29.41	1.94	6.29
	Milan, L. unpub.	P71293	58.95	0.94	17.36	6.38	0.09	2.76	5.05	4.25	2.96	0.36	0.70	99.80	27.17	1.44	7.21
	Milan, L. unpub.	P71307	52.93	1.17	17.87	8.81	0.13	4.60	7.89	4.80	1.18	0.41	0.04	99.82	31.04	4.07	5.98
	Milan, L. unpub.	P71308	50.54	1.46	19.14	9.69	0.14	4.82	8.49	4.38	0.64	0.52	0.03	99.85	30.02	6.84	5.02
	Milan, L. unpub.	P71345	54.37	1.08	17.66	7.72	0.11	3.86	6.94	4.25	1.87	0.39	1.52	99.79	30.12	2.27	6.12
	Milan, L. unpub.	Grave	52.10	1.51	17.88	9.24	0.11	5.28	8.02	4.36	0.69	0.59	0.04	99.81	33.01	6.32	5.05
	Milan, L. unpub.	LM0409	53.32	1.07	18.44	7.99	0.12	4.16	7.46	4.67	1.15	0.41	1.06	99.85	30.98	4.06	5.82
	Allibone et al., (2009)	P71434	52.13	1.23	19.03	8.57	0.12	4.38	7.21	4.49	1.31	0.46	0.90	99.82	30.59	3.43	5.80
	Allibone et al., (2009)	P73839	54.19	1.13	18.36	8.09	0.12	3.96	7.13	4.93	1.50	0.44	0.06	99.91	29.66	3.28	6.43
	Allibone et al., (2009)	P73845	53.81	0.99	18.68	7.83	0.12	4.04	7.17	4.33	1.04	0.45	1.23	99.68	30.80	4.19	5.37
	Allibone et al., (2009)	P73847	53.86	1.06	18.34	8.11	0.12	4.03	7.07	5.47	1.50	0.43	-0.08	99.90	30.00	3.65	6.97
	Allibone et al., (2009)	P73849	55.40	1.06	18.26	7.42	0.11	3.46	6.24	5.37	2.07	0.40	0.09	99.78	28.66	2.60	7.43
	Allibone et al., (2009)	P71153	54.97	0.98	19.35	7.18	0.11	3.29	6.76	4.94	1.33	0.44	0.36	99.70	28.34	3.71	6.27
	Allibone et al., (2009)	P71160	55.67	1.17	18.28	7.78	0.12	3.55	6.70	4.18	1.98	0.43	-0.10	99.75	28.23	2.12	6.16
	Allibone et al., (2009)	P71164	55.16	1.13	18.52	8.03	0.12	3.71	6.85	4.34	1.46	0.43	-0.01	99.76	28.48	2.97	5.80
	Allibone et al., (2009)	P65367	56.14	1.05	18.06	7.39	0.11	3.51	6.18	4.67	1.99	0.43	0.35	99.86	29.07	2.35	6.65

Appendix 5.A Major element data from WFO database kindly provided by GNS

Pluton	Data Source	sample no.	Major element (wt% oxide)														
			SiO2	TiO2	Al2O3	Fe2O3	MnO	MgO	CaO	Na2O	K2O	P2O5	LOI (%)	Total	Mg#	Na2O/K2O	Na2O+K2O
Breaksea omphacite granulite	Milan, L. unpub.	P71176	47.05	1.39	9.86	9.59	0.12	15.41	13.93	1.62	0.31	< 0.011	0.29	99.60	58.08	5.23	1.93
	Milan, L. unpub.	P71246	52.11	1.47	18.55	9.26	0.13	3.79	7.46	4.75	1.43	0.60	0.26	99.80	26.08	3.32	6.18
	Milan, L. unpub.	P73819	50.18	1.70	17.83	10.52	0.15	5.27	8.94	3.91	0.55	0.70	0.04	99.79	30.18	7.15	4.45
	Milan, L. unpub.	P73824	48.08	1.59	16.93	11.70	0.15	7.15	9.30	3.28	0.49	0.65	0.31	99.64	34.50	6.64	3.78
	Milan, L. unpub.	P73829	52.14	1.63	17.95	9.30	0.13	4.88	8.00	4.14	1.04	0.59	0.01	99.82	31.16	3.99	5.17
	Milan, L. unpub.	P73831	51.91	1.51	17.63	9.71	0.14	5.05	7.48	4.43	1.29	0.61	0.10	99.86	30.94	3.45	5.72
	Milan, L. unpub.	P73832	43.20	2.86	9.31	19.61	0.30	11.91	9.90	1.30	0.22	1.01	-0.06	99.55	34.37	5.87	1.52
	Carroll, S. (2005) unpub.	P71198	55.17	1.24	18.20	7.42	0.11	3.86	7.02	4.50	1.79	0.49	-0.06	99.73	30.99	2.52	6.28
	Carroll, S. (2005) unpub.	P71199	54.05	1.20	17.99	8.30	0.12	4.51	7.46	4.36	1.50	0.41	-0.12	99.77	31.87	2.90	5.86
	Allibone et al., (2009)	MDP0611A	50.10	1.40	17.00	10.90	0.20	6.60	8.90	3.90	0.70	0.40	0.00	100.00	34.30	5.57	4.60
	Allibone et al., (2009)	MDP0709A	54.40	1.30	17.90	8.20	0.10	4.20	6.70	5.00	1.60	0.40	0.10	100.00	30.63	3.13	6.60
	Allibone et al., (2009)	MDP0613	53.30	1.30	18.00	8.60	0.10	4.70	7.80	4.60	1.00	0.50	0.10	100.00	32.03	4.60	5.60
	Allibone et al., (2009)	B47/8/428	51.00	1.40	17.30	10.70	0.20	5.60	7.70	4.10	1.00	0.60	0.30	100.00	31.09	4.10	5.10
	Allibone et al., (2009)	BS716B	53.90	1.10	18.20	7.90	0.10	4.30	7.70	5.00	1.10	0.50	0.10	100.00	31.94	4.55	6.10
	Allibone et al., (2009)	MDP0737B	54.60	1.20	17.60	7.70	0.10	4.40	7.50	5.00	1.40	0.40	0.00	99.90	33.01	3.57	6.40
	Allibone et al., (2009)	MDP0669	54.00	1.20	18.20	7.90	0.10	4.50	7.80	4.40	1.70	0.40	-0.20	99.80	32.94	2.59	6.10
	Allibone et al., (2009)	MDP0705H	50.60	1.50	18.10	9.50	0.10	5.90	8.70	3.80	1.00	0.40	0.20	100.00	34.87	3.80	4.80
Breaksea eclogite	Allibone et al., (2009)	MDP0716	43.70	2.50	14.70	12.10	0.10	10.70	12.50	2.20	0.50	0.60	0.20	99.90	43.26	4.40	2.70
	Allibone et al., (2009)	MDP0664	42.80	2.10	14.70	16.40	0.20	9.70	12.70	1.50	0.00	0.60	-1.00	99.70	33.77		1.50
	Allibone et al., (2009)	MDP0725	41.80	1.80	14.80	16.40	0.30	10.20	12.10	1.50	0.10	0.80	0.10	99.90	34.91	15.00	1.60
	Allibone et al., (2009)	MDP0654E	43.10	0.80	17.60	15.70	0.30	9.30	11.50	1.50	0.10	0.10	0.10	100.00	33.81	15.00	1.60
	Allibone et al., (2009)	MDP0704	43.90	2.00	13.30	12.60	0.10	12.50	11.70	2.60	0.70	0.00	0.50	99.80	46.10	3.71	3.30

Appendix 5.A Major element data from WFO database kindly provided by GNS

Pluton	Data Source	sample no.	Tace elements (ppm)																			
			As	Ba	Ce	Cr	Cu	Ga	La	Nb	Nd	Ni	Pb	Rb	Sc	Sr	Th	U	V	Y	Zn	Zr
Worlsey Pluton 2px hbl	Allibone et al., (2009)	P76569	<1	669	53	108	14	24	32	<1		61	12	10	14	1661	<1	<1	153	11	87	33
	Allibone et al., (2009)	P76579	<1	685	30	76	49	23	<5	<1		57	10	7	17	1416	<1	<1	163	9	90	38
	Allibone et al., (2009)	P76586	<1	682	27	38	59	23	35	5		25	14	14	16	1352	<1	<1	170	14	92	76
	Allibone et al., (2009)	P76587	1	637	49	41	43	25	33	4		29	15	12	13	1459	<1	1	167	16	93	72
	Allibone et al., (2009)	P76588	1	736	42	84	29	23	33	3		50	13	13	10	1311	<1	1	149	12	89	55
	Allibone et al., (2009)	P76590	<1	619	23	117	<1	23	<5	<1		54	10	8	11	1719	<1	<1	125	5	71	22
	Allibone et al., (2009)	P76597	1	668	32	129	33	23	27	<1		61	13	12	13	1470	<1	<1	163	10	89	42
	Allibone et al., (2009)	P76601	1	645	40	79	62	23	26	6		35	16	64	9	1008	<1	2	111	15	65	173
	Richard Jongens	P77341	<1	767	40	70	14	23	29	3		45	16	15	11	1355	<1	<1	132	11	78	53
	Richard Jongens	P77342	1	599	41	75	33	23	34	<1		53	12	8	14	1621	<1	1	168	12	91	40
	Richard Jongens	P77350	1	544	45	52	<1	23	41	<1		39	12	11	12	1525	<1	<1	151	11	89	50
	Milan, L. unpub.	LM0490-1	< 0.5	738	38	75	5	23	18	5		43	14	14		1359	1	< 0.5	140	9	83	68
	Daczko, N. (2001)	99-47		500	38	7	25	21	20	0		10	20	18		1049			145	17	88	144
	Milan, L. unpub.	LM9947	< 0.4	509	40	10	32	21.0	18	7.2		12	11	25		991	0.9	< 0.5	154	13	89	118
	Milan, L. unpub.	P65326	< 0.4	638	34	12	16	22.2	12	8.2		24	14.4	13		1360	2.2	0.8	135	13	94	47
	Milan, L. unpub.	P65348	< 0.5	1038	49	45	48	22.9	18	8.5		38	19.9	23		2070	3.0	1.9	135	12	87	98
	Carroll, S. (2005) unpub.	SC-4050	< 0.4	673	44	103	35	23	20	4.6		43	12	27		1586	4.5	< 0.5	207	7.8	101	42
	Carroll, S. (2005) unpub.	SC-4051	< 0.4	603	33	89	17	23	12	2.4		41	8.0	9.1		1685	0.9	< 0.5	208	5.8	88	32
	Carroll, S. (2005) unpub.	SC-4052	< 0.4	609	31	101	31	22	11	2.5		44	8.1	4.5		1684	0.9	< 0.5	197	6.1	85	28
	Milan, L. unpub.	P65296	< 0.5	620	40	84	35	23.2	17	8.8		44	14.3	23		1571	4.4	4.2	152	15	93	70
Worsley Pluton hbl diorite -px	Stevenson, J. (2000)	Dan 24	1	735	39	82	10	20		8		47	16	65		1050	9	3	150	12	78	176
	Allibone et al., (2009)	P76570	1	503	37	158	<1	22	23	<1		81	11	10	13	1564	<1	<1	178	12	95	31
	Allibone et al., (2009)	P65295	0.9	714	50	86	84	23.7	21	11.4		36	18.9	61		1151	6.2	7.6	148	16	90	212
	Allibone et al., (2009)	P65298	< 0.5	688	42	60	69	22.4	18	6.1		37	13.0	27		1488	2.9	4.1	193	13	95	66
	Milan, L. unpub.	LM65306	< 0.5	721	57	85	76	24.6	24	8.2		52	14.1	50		1598	3.1	1.8	203	17	107	199

Appendix 5.A Trace element data from WFO database kindly provided by GNS

Pluton	Data Source	sample no.	Tace elements (ppm)																			
			As	Ba	Ce	Cr	Cu	Ga	La	Nb	Nd	Ni	Pb	Rb	Sc	Sr	Th	U	V	Y	Zn	Zr
Mckerr intrusives east	Allibone et al., (2009)	P76604	1	534	38	28	68	20	25	8		18	13	39	9	966	<1	1	146	18	90	179
	Allibone et al., (2009)	P77074	1	653	40	9	44	23	27	4		16	12	28	14	1377	<1	<1	123	15	92	205
	Degeling, H. (1997)	LM9710D		449	55	16	36	22	38	0		7	18	27		1266			130	19	81	248
	Degeling, H. (1997)	LM9725	< 0.4	628	53	35	25	23	16	13		20	9	28		1014	< 0.5	< 0.5	169	22	97	243
	Milan, L. unpub.	P65307	< 0.4	707	53	22	90	22.7	19	12.9		15	9.2	34		1203	2.8	3.4	161	21	105	236
	Degeling, H. (1997)	LM9719	< 0.4	599	50	27	32	22.1	19	11.5		16	9.6	22		1033	0.6	< 0.5	153	20	92	256
	Allibone et al., (2009)	P65307	< 0.4	707	53	22	90	22.7	19	12.9		15	9.2	34		1203	2.8	3.4	161	21	105	236
	Allibone et al., (2009)	P65306	< 0.5	721	57	85	76	24.6	24	8.2		52	14.1	50		1598	3.1	1.8	203	17	107	199
Mckerr intrusives west	Allibone et al., (2009)	P77901	1	780	48	11	36	23	32	6		12	16	56	10	1151	5	1	100	14	82	192
	Allibone et al., (2009)	P77069	1	706	50	6	12	21	28	7		10	17	98	9	981	8	2	93	15	72	217
	Allibone et al., (2009)	P77072	<1	1079	31	1	<1	23	32	<1		7	14	31	<2	1645	<1	1	58	3	72	140
	Allibone et al., (2009)	P77894	1	532	45	21	<1	22	25	6		11	12	49	18	1019	2	2	168	21	91	126
	Allibone et al., (2009)	P77910	1	527	50	30	25	20	40	6		14	12	50	9	1074	6	1	130	19	95	207
	Allibone et al., (2009)	P77914	2	3867	<5	<1	<1	13	6	<1		3	11	41	<2	997	3	<1	9	<1	25	93
	Allibone et al., (2009)	P77931	1	960	19	7	19	21	17	5		11	11	74	4	992	<1	<1	75	5	76	111

Appendix 5.A Trace element data from WFO database kindly provided by GNS

Pluton	Data Source	sample no.	Tace elements (ppm)																			
			As	Ba	Ce	Cr	Cu	Ga	La	Nb	Nd	Ni	Pb	Rb	Sc	Sr	Th	U	V	Y	Zn	Zr
Misty pluton 2px hbl	Allibone et al., (2009)	P76709	1	354	48	28	47	23	26	8		16	8	34	20	1023	1	1	206	28	105	315
	Allibone et al., (2009)	P76713	< 0.4	616	36	7.4	4.8	22.3	17	4.4		15	9.2	7.5		1391	0.7	< 0.5	134	12	84	55
	Richard Jongens	P77298	< 0.4	515	47	14	17	24.0	19	4.8		14	8	5		1415	< 0.5	< 0.5	156	12	106	63
	Allibone et al., (2009)	P77090	< 0.4	630	42	8	44	22.8	15	5.8		12	11	23		1246	1.2	< 0.5	123	12	86	187
	Emami, S. (2008) unpub.	A183/8	<1	284	27	16	<5	24	28	<1		22	9	3	12	1623	<1	1	174	13	99	10
Misty pluton hbl diorite - px	Allibone et al., (2009)	P77132	1	354	48	28	47	23	26	8		16	8	34	20	1023	1	1	206	28	105	315
	Milan, L. unpub.	LMMH0270	< 0.4	616	36	7.4	4.8	22.3	17	4.4		15	9.2	7.5		1391	0.7	< 0.5	134	12	84	55
	Milan, L. unpub.	LM0412	< 0.4	515	47	14	17	24.0	19	4.8		14	8	5		1415	< 0.5	< 0.5	156	12	106	63
	Milan, L. unpub.	LM0413	< 0.4	630	42	8	44	22.8	15	5.8		12	11	23		1246	1.2	< 0.5	123	12	86	187
	Allibone et al., (2009)	P77630	1	666	63	22	60	22	36	14		20	13	56	13	932	1	<1	147	24	97	597
	Allibone et al., (2009)	P77972	1	689	52	43	<1	20	38	8		16	20	113	15	795	5	2	177	21	168	178
	Emami, S. (2008) unpub.	SE0805D	<1	284	27	16	<5	24	28	<1		22	9	3	12	1623	<1	1	174	13	99	10

Appendix 5.A Trace element data from WFO database kindly provided by GNS

Pluton	Data Source	sample no.	Tace elements (ppm)																			
			As	Ba	Ce	Cr	Cu	Ga	La	Nb	Nd	Ni	Pb	Rb	Sc	Sr	Th	U	V	Y	Zn	Zr
HHU hbl pdt	Emami, S. (2008) unpub.	A180/8	<1	70	<5	835	7	6	<5	<1		799	5	2	29	202	<1	<1	183	6	120	19
	Emami, S. (2008) unpub.	SE0801G	<1	48	<5	290	6	4	<5	<1		903	5	3	15	120	<1	<1	93	2	153	17
	Emami, S. (2008) unpub.	SE0802F	<1	116	14	231	24	10	<5	<1		519	4	8	36	310	<1	<1	248	10	114	38
	Emami, S. (2008) unpub.	SE0802G	<1	104	<5	1040	9	12	<5	<1		418	4	5	47	377	<1	<1	352	11	81	39
	Emami, S. (2008) unpub.	SE0810B	<1	47	<5	67	9	3	<5	<1		804	3	3	16	123	<1	<1	94	2	147	16
HHU hbldite	Emami, S. (2008) unpub.	A1801/8	1	149	14	476	3	16	<5	<1		260	3	4	56	508	<1	<1	473	16	63	39
	Emami, S. (2008) unpub.	SE0804A	1	185	7	187	5	19	<5	<1		177	3	7	62	587	<1	2	494	23	67	59
	Emami, S. (2008) unpub.	SE0805K	1	146	6	189	2	16	<5	<1		261	3	4	61	528	<1	1	464	17	61	38
	Emami, S. (2008) unpub.	SE0807E	<1	146	7	59	16	18	<5	<1		183	4	4	58	540	<1	<1	476	19	63	41
	Emami, S. (2008) unpub.	SE0810A	<1	152	<5	231	1	17	<5	<1		264	4	5	57	581	<1	<1	461	18	61	45

Appendix 5.A Trace element data from WFO database kindly provided by GNS

Pluton	Data Source	sample no.	Tace elements (ppm)																			
			As	Ba	Ce	Cr	Cu	Ga	La	Nb	Nd	Ni	Pb	Rb	Sc	Sr	Th	U	V	Y	Zn	Zr
Malaspina Orthogneiss	Hollis et al., (2004)	cao10c		491	44	39	11	23	20	0		21	18	25		1003			188	20	89	75
	Hollis et al., (2004)	cao90a		651	37	11	76	24	23	0		5	22	36		1124			124	18	90	125
	Hollis et al., (2004)	cao90a-dup		658	50	13	68	23	19	0		9	23	39		1128			137	16	88	116
	Davids (1999)	ANU960459		685	51	15	50	22	16	9		15	15	79	15	977	4	1	112	16	87	234
	Milan, L. unpub.	P71152	1	643	41	12	38	21	15	6		12	13	31		1143	3	1	133	12	89	115
	Milan, L. unpub.	P71154	1	734	49	15	59	21	21	10		12	15	85		872	5	< 0.5	119	15	77	298
	Milan, L. unpub.	P71155	< 0.4	714	39	12	62	21	15	7		12	12	33		1084	1	< 0.5	151	14	96	157
	Milan, L. unpub.	P71167	2	613	47	33	41	20	17	9		11	12	64		900	4	< 0.5	154	16	90	179
	Milan, L. unpub.	P71293	1	739	49	11	37	21	20	9		9	16	110		839	9	< 0.5	111	15	78	268
	Milan, L. unpub.	P71307	< 0.4	454	37	25	95	21	16	5		19	11	12		1115	1	< 0.5	154	13	94	65
	Milan, L. unpub.	P71308	< 0.4	276	30	51	8	22	10	9		27	9	7		1664	< 0.5	< 0.5	183	15	95	47
	Milan, L. unpub.	P71345	< 0.4	710	41	32	61	20	17	8		19	12	31		977	1	< 0.5	164	14	91	130
	Milan, L. unpub.	Grave	< 0.4	531	41	84	74	23	17	4		54	8	6		1820	1	< 0.5	188	7	114	32
	Milan, L. unpub.	LM0409	< 0.4	502	37	31	22	20	16	5		19	10	10		1107	1	< 0.5	163	12	88	48
	Allibone et al., (2009)	P71434	0.5	551	43	26	54	22.1	16	8.0		15	11.5	34		1152	1.1	2.3	177	17	93	174
	Allibone et al., (2009)	P73839	< 0.4	605	39	36	220	23.5	16	5.8		16	11.9	21		1052	1.5	< 0.5	144	16	89	53
	Allibone et al., (2009)	P73845	0.7	454	34	22	47	22.7	13	4.3		19	9.4	14		1136	2.1	< 0.5	162	14	92	94
	Allibone et al., (2009)	P73847	0.6	541	38	24	185	23.2	15	4.7		12	11.6	22		1044	2.3	< 0.5	157	17	90	103
	Allibone et al., (2009)	P73849	< 0.4	706	40	17	136	22.8	16	8.4		12	12.4	36		953	1.9	3.6	133	17	85	164
	Allibone et al., (2009)	P71153	< 0.8	724	44	21	76	25.2	19	5.7		11	15.1	22		1469	1.2	< 0.5	157	11	94	152
	Allibone et al., (2009)	P71160	< 0.8	721	47	25	13	23.7	20	8.4		8	15.6	36		1104	1.0	< 0.5	155	14	93	142
	Allibone et al., (2009)	P71164	< 0.8	751	67	23	62	24.3	37	5.7		18	13.9	20		1273	0.7	< 0.5	150	11	93	65
	Allibone et al., (2009)	P65367	1.0	648	40	18	77	22.1	16	10.0		15	14.8	47		1021	4.8	7.3	136	17	88	169

Appendix 5.A Trace element data from WFO database kindly provided by GNS

Pluton	Data Source	sample no.	Tace elements (ppm)																			
			As	Ba	Ce	Cr	Cu	Ga	La	Nb	Nd	Ni	Pb	Rb	Sc	Sr	Th	U	V	Y	Zn	Zr
Breaksea omphacite granulite	Milan, L. unpub.	P71176	< 0.3	37	< 3.0	1059	279	14.9	< 2.0	2.3		405	1.7	0.8		217	1.0	0.5	411	11	56	26
	Milan, L. unpub.	P71246	< 0.4	480	47	13	33	24.5	18	10.4		14	9.2	16		1230	1.0	3.6	194	26	101	234
	Milan, L. unpub.	P73819	< 0.4	315	35	60	44	24.6	12	3.3		30	5.1	2.7		1235	0.5	< 0.5	261	19	113	34
	Milan, L. unpub.	P73824	< 0.4	277	37	163	89	22.4	13	4.3		79	4.0	2.0		1169	0.5	1.2	279	15	115	41
	Milan, L. unpub.	P73829	< 0.4	468	32	32	40	23.6	12	5.3		24	8.2	6.6		1199	0.3	< 0.5	239	15	93	47
	Milan, L. unpub.	P73831	< 0.4	552	50	86	36	24.6	22	6.6		46	10.0	15		1211	0.6	< 0.5	215	16	98	111
	Milan, L. unpub.	P73832	< 0.4	109	75	205	235	18.6	28	8.3		117	2.5	3		361	1.0	0.9	486	35	216	124
	Carroll, S. (2005) unpub.	P71198	< 0.4	761	41	51	28	24	16	5.3		22	10	15		1380	< 0.5	< 0.5	178	7.9	81	72
	Carroll, S. (2005) unpub.	P71199	< 0.4	571	36	84	43	21	16	4.3		31	10	21		1119	1.6	< 0.5	191	14	85	64
	Allibone et al., (2009)	MDP0611A	1	497	52	92	178	23	25	<1		60	9	12	17	1242	3	<1	216	15	112	42
	Allibone et al., (2009)	MDP0709A	1	840	62	61	56	23	34	<1		40	15	24	13	1165	<1	<1	156	13	94	91
	Allibone et al., (2009)	MDP0613	<1	639	32	34	5	24	28	<1		33	12	10	13	1630	<1	<1	196	14	100	42
	Allibone et al., (2009)	B47/8/428	2	579	54	66	137	23	33	<1		47	11	9	15	1198	<1	1	199	20	114	50
	Allibone et al., (2009)	BS716B	1	663	58	32	11	24	37	<1		28	11	8	13	1607	<1	<1	170	14	94	40
	Allibone et al., (2009)	MDP0737B	<1	726	43	53	10	24	40	4		35	13	12	14	1418	<1	<1	173	13	89	54
	Allibone et al., (2009)	MDP0669	< 0.3	583	36	56	50	22.6	15	3.6		32	11.9	23		1134	< 0.5	< 0.5	151	15	84	61
	Allibone et al., (2009)	MDP0705H	<1	689	25	89	<1	25	26	<1		58	9	8	21	1534	<1	<1	215	18	90	45
Breaksea eclogite	Allibone et al., (2009)	MDP0716	1	201	53	324	143	23	27	6		128	4	4	42	1117	<1	<1	379	24	95	67
	Allibone et al., (2009)	MDP0664	0.3	5	19	104	7	19.2	5	3.9		71	< 0.8	0.4		167	< 0.5	< 0.5	380	22	127	46
	Allibone et al., (2009)	MDP0725	<1	46	26	124	188	17	<5	<1		87	11	1	36	252	<1	<1	415	29	114	37
	Allibone et al., (2009)	MDP0654E	<1	30	<5	86	12	16	<5	<1		59	4	2	36	117	<1	2	333	34	101	38
	Allibone et al., (2009)	MDP0704	1	122	<5	265	17	19	<5	<1		157	3	4	44	232	<1	<1	518	11	106	32

Appendix 5.A Trace element data from WFO database kindly provided by GNS

Element	STD610-1	STD610-2	BCR-1	BCR-2	0903B-1	0903B-2	0903B-3	0903B-4	0903B-5	0903B-6	0903B-7	0903B-8	0903B-9	0903B-10	STD610-3	STD610-4
Li7	18.48	19.3	0.37	0.37	0.13	0.13	0.0023	0.091	0.11	0.0019	0.078	0.0023	0.088	0.087	24.16	24.63
Be9	37.2	37.54	0.22	0.21	0.47	0.47	0.003	0.13	0.14	0.0012	0.11	0.0011	0.11	0.1	41.43	42.99
B11	24.61	24.45	0.45	0.42	0.71	0.73	0.0047	0.22	0.2	0.002	0.19	0.0018	0.17	0.18	27.3	27.36
Al27	401.61	412.54	2982.25	2963.38	4904.42	4886.31	3.71	3062.55	3263.19	7.65	3062.24	6.12	3152.52	3161.72	475.15	495.99
P31	47.94	45.68	156.26	153.85	11.49	12.07	0.061	16.87	16.68	0.035	15.77	0.034	10.91	12.28	49.57	49.83
Ca42	2613.86	2609.28	1617.1	1617.16	1373.26	1371.94	55.93	2706.65	2707.09	55.86	2706.32	52.02	2706.38	2670.31	2608.9	2606.86
Ca43	2759.9	2808.25	1711.97	1695.31	1480.97	1460.07	59.24	2880.66	2912.17	60.34	2952.64	56.59	3051.71	2990.42	3018.8	3029.89
Sc45	15.04	15.19	1.07	1.05	4.81	4.79	0.015	1.82	1.84	0.02	1.76	0.018	1.67	1.8	15.88	16.2
Ti47	17.94	18.44	514.51	515.01	7.2	9.23	0.27	248.27	289.04	0.7	200.97	0.52	182.3	165.95	21.11	21.47
V51	18.28	17.9	16.67	16.75	4.04	3.49	0.061	14.75	15.13	0.087	16.43	0.075	17.95	16.22	22.53	24.1
Co59	14.41	14.21	1.28	1.29	2.06	2.08	0.012	2.25	2.42	0.013	2.28	0.012	2.39	2.27	16.54	17.29
Ni60	15.95	15.95	0.45	0.45	0.62	0.98	0.047	12.37	12.13	0.049	12.22	0.044	12.54	11.73	18.47	19.36
Ni62	19.55	18.96	0.95	0.96	3.14	3.23	0.066	14.78	14.77	0.061	15.12	0.058	15.87	15.09	24.69	26.14
Ga69	15.44	15.86	1.11	1.08	0.38	0.33	0.002	0.78	0.72	0.0029	0.82	0.0023	0.82	0.73	18.4	19.17
Ga71	14.13	14.36	0.71	0.7	0.37	0.37	0.0022	0.62	0.55	0.0025	0.62	0.0021	0.62	0.54	15.16	15.25
Rb85	13.99	13.93	1.52	1.51	0.097	0.096	0.00061	0.15	0.15	0.00024	0.15	0.00022	0.14	0.14	14.54	14.85
Sr86	18.5	18.95	12.22	12.2	1.52	1.49	0.09	21.01	24.12	0.087	18.68	0.078	17.95	17.43	21.2	21.72
Sr88	16.67	16.8	10.95	10.97	0.051	0.052	0.077	18.38	20.99	0.074	15.86	0.065	14.88	14.36	17.31	17.23
Y89	15.95	16.16	1.07	1.04	3.65	3.39	0.0016	0.63	0.62	0.0023	0.52	0.0017	0.43	0.47	16.63	16.77
Zr90	17.08	17.37	6.42	6.31	0.61	0.7	0.0054	1.27	1.26	0.011	1.41	0.0087	1.45	1.41	18.95	19.57
Nb93	16.94	16.92	0.44	0.44	0.066	0.06	0.00037	0.081	0.13	0.00015	0.065	0.00014	0.047	0.05	17.13	17.34
Cs133	11.68	11.77	0.042	0.044	0.052	0.05	0.00031	0.027	0.014	0.00013	0.011	0.00012	0.011	0.011	12.16	12.38
Ba137	14.96	15.1	22.7	22.6	0.34	0.33	0.0023	7.84	8.08	0.0029	7.96	0.0016	7.87	7.35	15.91	16.26
La139	13.95	14.02	0.79	0.77	0.043	0.041	0.00088	0.22	0.19	0.00095	0.21	0.00067	0.21	0.2	14.07	14.14
Ce140	14.32	14.54	1.69	1.68	0.047	0.049	0.0028	0.82	0.69	0.0038	0.87	0.0027	0.93	0.86	15.13	15.31
Pr141	15.15	15.39	0.23	0.23	0.036	0.036	0.00073	0.16	0.14	0.00088	0.17	0.00066	0.17	0.16	16.12	16.37
Nd146	16.3	16.84	1.09	1.1	0.21	0.21	0.0044	0.96	0.87	0.0056	1.1	0.0044	1.1	1.06	19.27	19.7
Sm152	14.75	14.84	0.23	0.24	0.17	0.18	0.0017	0.23	0.22	0.0015	0.24	0.0012	0.25	0.23	14.97	15.1
Eu153	14.4	14.53	0.075	0.077	0.095	0.089	0.00065	0.087	0.075	0.00048	0.082	0.0004	0.081	0.077	14.85	15.03
Gd158	17.21	17.84	0.26	0.26	0.36	0.35	0.0016	0.27	0.24	0.0016	0.27	0.0013	0.28	0.26	20.96	21.81
Dy161	16.22	16.71	0.25	0.24	0.8	0.72	0.0017	0.19	0.2	0.0011	0.19	0.001	0.18	0.18	18.6	18.9
Ho165	19.95	20.99	0.059	0.059	0.22	0.21	0.00031	0.043	0.043	0.00022	0.038	0.00017	0.034	0.035	25.53	26.6
Er167	18.3	19.11	0.16	0.17	0.67	0.66	0.0011	0.11	0.12	0.00056	0.089	0.00049	0.07	0.078	22.65	23.29
Yb172	16.96	17.45	0.15	0.15	0.67	0.57	0.0012	0.079	0.097	0.00045	0.061	0.00044	0.047	0.062	19.38	19.78
Lu175	18.71	19.57	0.025	0.027	0.12	0.1	0.00025	0.015	0.016	0.00009	0.01	0.00009	0.0086	0.011	23.22	24.01
Hf178	18.04	18.72	0.21	0.21	0.13	0.15	0.0011	0.086	0.09	0.00086	0.092	0.00074	0.095	0.086	21.86	22.8
Ta181	17.59	18.11	0.037	0.038	0.048	0.046	0.0003	0.014	0.02	0.00011	0.013	0.0001	0.0095	0.01	20.1	20.63
Pb208	19.02	20.16	0.45	0.43	0.093	0.09	0.0007	0.051	0.07	0.00031	0.048	0.00027	0.046	0.043	24.67	25.67
Th232	18.72	19.46	0.24	0.24	0.056	0.056	0.00047	0.015	0.017	0.00014	0.012	0.00012	0.012	0.012	22.12	22.61
U238	16.5	16.77	0.071	0.072	0.052	0.054	0.00034	0.014	0.014	0.00014	0.012	0.00012	0.01	0.011	17.34	17.6

Appendix 6.A 1σ error for LAM-ICP-MS data

Element	STD610-1	STD610-2	BCR-1	BCR-2	0903B-1	0903B-2	0903B-3	0903B-4	0903B-5	0903B-6	0903B-7	0903B-8	0903B-9	0903B-10	STD610-3	STD610-4
Li7	0.281	0.235	0.0639	0.054	0.313	0.314	0.00193	0.0713	0.0759	0.00075	0.0718	0.00077	0.0642	0.0656	0.211	0.227
Be9	1.16	0.885	0.249	0.256	1.21	1.24	0.0075	0.333	0.323	0.00281	0.234	0.00233	0.26	0.235	0.943	0.89
B11	2.05	1.58	0.412	0.411	1.89	1.81	0.0121	0.483	0.486	0.00504	0.428	0.00457	0.373	0.428	1.33	1.27
Al27	1.59	1.56	0.393	0.385	1.84	1.83	0.0115	0.424	0.658	0.00668	0.425	0.0288	0.455	0.532	1.73	1.29
P31	15.74	12.04	3.53	3.3	17.43	17.06	0.103	4.03	4.29	0.0412	3.47	0.0385	3.18	3.25	10.65	10.37
Ca42	359.7	255.62	71.69	63.41	307.12	291.69	1.72	65.46	67.29	0.636	56.14	0.672	50.06	50.23	164.3	155.62
Ca43	388.59	299.94	81.34	74.12	371.99	371.23	2.14	84.32	90.15	0.867	71.41	1.01	67.35	66.16	221.75	212.22
Sc45	0.5	0.376	0.0973	0.091	0.457	0.434	0.00267	0.0962	0.102	0.00104	0.0855	0.00115	0.0799	0.0804	0.264	0.265
Ti47	2.51	2.06	0.521	0.592	3.1	3.22	0.0189	0.651	0.889	0.0076	0.68	0.0266	0.595	0.69	2.34	1.86
V51	0.223	0.233	0.0496	0.0495	0.265	0.226	0.00155	0.0551	0.0675	0.00059	0.0525	0.00178	0.0577	0.0522	0.164	0.174
Co59	0.223	0.223	0.0485	0.0459	0.241	0.267	0.00146	0.0606	0.0675	0.0006	0.0549	0.00092	0.0499	0.0497	0.166	0.189
Ni60	0.965	0.726	0.205	0.163	0.963	0.976	0.00558	0.249	0.252	0.00269	0.219	0.00472	0.21	0.233	0.734	0.7
Ni62	5.3	5.18	1.53	1.57	8.2	7.62	0.0454	1.96	2.05	0.0212	1.7	0.02	1.78	1.74	5.71	4.68
Ga69	0.244	0.245	0.0597	0.0482	0.257	0.304	0.00175	0.0618	0.0666	0.00066	0.0578	0.00075	0.0548	0.056	0.174	0.21
Ga71	0.318	0.314	0.0831	0.0693	0.329	0.374	0.00232	0.079	0.0827	0.00085	0.0823	0.00104	0.0681	0.0666	0.239	0.259
Rb85	0.197	0.215	0.0514	0.0471	0.256	0.262	0.00161	0.063	0.0651	0.00061	0.0548	0.0006	0.0494	0.0485	0.172	0.186
Sr86	4.05	3.01	0.845	0.785	4.1	4.05	0.0234	0.967	0.956	0.0092	0.76	0.0101	0.707	0.718	2.41	2.19
Sr88	0.114	0.178	0.0253	0.0271	0.119	0.11	0.00076	0.0287	0.0552	0.00036	0.0359	0.00184	0.0357	0.032	0.0948	0.124
Y89	0.124	0.156	0.0244	0.0244	0.125	0.115	0.00073	0.0302	0.0282	0.00027	0.0272	0.00035	0.0237	0.0194	0.0675	0.129
Zr90	0.232	0.226	0.0551	0.0433	0.256	0.25	0.00184	0.0666	0.0701	0.00068	0.0479	0.00094	0.0524	0.061	0.158	0.212
Nb93	0.143	0.18	0.0355	0.0256	0.178	0.162	0.00099	0.0346	0.0421	0.00039	0.0351	0.00036	0.0289	0.0354	0.109	0.171
Cs133	0.118	0.148	0.0479	0.027	0.142	0.136	0.00077	0.0327	0.0362	0.00034	0.0285	0.00032	0.0248	0.0263	0.0867	0.113
Ba137	0.711	0.647	0.18	0.175	0.905	0.884	0.00634	0.203	0.212	0.00181	0.157	0.00377	0.126	0.164	0.57	0.512
La139	0.114	0.128	0.023	0.0184	0.104	0.0985	0.00067	0.0214	0.0219	0.0002	0.0202	0.00027	0.0204	0.0205	0.0571	0.113
Ce140	0.101	0.127	0.0219	0.0186	0.0983	0.103	0.00064	0.0245	0.025	0.00024	0.0195	0.00045	0.0201	0.022	0.0652	0.101
Pr141	0.0738	0.134	0.0191	0.0161	0.0957	0.0947	0.00054	0.0245	0.0231	0.00021	0.0175	0.00023	0.018	0.0177	0.0633	0.0871
Nd146	0.513	0.426	0.108	0.123	0.5	0.509	0.00311	0.145	0.142	0.00132	0.127	0.00129	0.118	0.118	0.321	0.385
Sm152	0.301	0.32	0.0607	0.0705	0.319	0.376	0.00186	0.0742	0.0878	0.00069	0.078	0.00089	0.0644	0.064	0.197	0.241
Eu153	0.107	0.177	0.0347	0.0337	0.148	0.167	0.00096	0.0379	0.039	0.00036	0.0342	0.00044	0.0301	0.0299	0.101	0.161
Gd158	0.364	0.332	0.0826	0.0811	0.401	0.39	0.00263	0.091	0.101	0.00085	0.0771	0.00078	0.0731	0.0614	0.272	0.28
Dy161	0.494	0.421	0.131	0.108	0.608	0.543	0.00331	0.119	0.138	0.00124	0.122	0.00122	0.107	0.0864	0.292	0.345
Ho165	0.0985	0.136	0.0244	0.0162	0.105	0.105	0.00052	0.0194	0.0316	0.00022	0.0207	0.00023	0.0154	0.0198	0.0575	0.113
Er167	0.4	0.329	0.0857	0.0916	0.488	0.464	0.00241	0.107	0.112	0.00099	0.0763	0.00091	0.0756	0.0795	0.261	0.295
Yb172	0.407	0.349	0.091	0.0993	0.47	0.547	0.00301	0.106	0.121	0.00092	0.0881	0.00106	0.0799	0.102	0.228	0.346
Lu175	0.115	0.136	0.0243	0.02	0.104	0.114	0.00066	0.0272	0.0236	0.00023	0.0204	0.00022	0.0166	0.0194	0.0637	0.102
Hf178	0.268	0.301	0.0749	0.0634	0.29	0.384	0.00211	0.0825	0.0888	0.00085	0.0739	0.00081	0.0704	0.0726	0.223	0.282
Ta181	0.109	0.135	0.0274	0.0237	0.124	0.125	0.00082	0.0242	0.0375	0.00029	0.0262	0.00028	0.0204	0.0216	0.0723	0.128
Pb208	0.22	0.246	0.0512	0.0505	0.243	0.233	0.00152	0.059	0.0587	0.0005	0.0434	0.00051	0.0424	0.042	0.141	0.161
Th232	0.139	0.233	0.0291	0.0284	0.147	0.152	0.00135	0.0331	0.0382	0.00034	0.0247	0.00033	0.0284	0.0303	0.0763	0.148
U238	0.146	0.232	0.0327	0.0291	0.131	0.141	0.00091	0.0372	0.0337	0.00036	0.0312	0.00033	0.026	0.0283	0.0849	0.138

Appendix 6.B LLD (99% confidence) for LAM-ICP-MS data

Element	STD610-7	STD610-8	BCR-4	0904C-1	0904C-2	0904C-3	0904C-4	0904C-5	0904C-6	0904C-7	0904C-8	0904C-9	STD610-9	STD610-10
Li7	18.35	18.67	0.38	0.065	0.039	0.039	0.035	0.11	1.34	1.5	1.18	1.33	22.46	22.3
Be9	36.01	36.47	0.21	0.13	0.1	0.11	0.092	0.39	0.19	0.19	0.16	0.15	40.44	39.53
B11	23.11	22.74	0.43	0.25	0.18	0.2	0.17	0.65	0.24	0.23	0.22	0.19	23.66	23.84
Al27	376.47	376.48	2753.07	5980.8	4763.97	5018.88	4604.35	5132.74	2387.27	2246.16	2289.21	2195.26	394.26	391.66
P31	48.48	46.85	173.34	33	18.54	23.21	20.64	28.07	4.02	3.79	5.12	4.03	57.69	54.42
Ca42	2610.08	2609.57	1617.53	2251.67	2249.8	2249.83	2249.06	2268.57	3646.33	3646.16	3646.3	3644.63	2610.65	2605.4
Ca43	2675.88	2688.23	1648.83	2263.61	2268.43	2281.02	2299.12	2338.32	3739.99	3700.7	3783.99	3744.52	2724.67	2734.17
Sc45	17.45	17.64	1.18	1.82	1.64	1.71	1.64	2.14	0.95	0.93	1.03	1.07	21.67	21.5
Ti47	17.18	17.26	496.32	20.49	15.07	193.77	13.72	15.27	161.69	114.39	136.08	103.86	17.93	18.03
V51	16.51	16.68	15.91	10.25	4.47	5.55	3.97	5.7	17.9	19.42	16.7	17.8	19.37	19.22
Co59	13.63	13.83	1.29	3.49	2.55	2.77	2.43	2.57	0.91	0.9	0.96	0.9	14.37	14.41
Ni60	16.32	16.4	0.51	0.37	0.26	0.3	0.24	0.48	2.95	3.34	2.94	3.09	18.1	17.89
Ni62	18.3	18.34	1.11	1.24	0.94	0.99	0.84	3.18	3.75	3.84	3.63	3.47	19.47	19.26
Ga69	14.4	14.22	1	0.84	0.54	0.56	0.51	0.83	1	1.09	0.92	0.95	15.29	15.36
Ga71	14.06	14.15	0.72	0.85	0.55	0.56	0.52	0.86	1.02	1.06	0.92	0.95	14.94	14.84
Rb85	17.08	17.6	1.99	0.03	0.021	0.062	0.02	0.079	0.022	0.019	0.02	0.017	22.29	22.2
Sr86	23.85	24.38	16.16	0.4	0.29	0.3	0.26	1.11	6.38	5.45	7.68	6.37	32.91	32.39
Sr88	23.86	24.48	16.3	0.025	0.024	0.025	0.022	0.05	6.51	5.48	7.92	6.63	33.6	33.13
Y89	20.89	21.22	1.33	2.43	2.18	2.19	2.28	2.54	0.12	0.096	0.14	0.11	28.27	27.95
Zr90	21.79	22.21	7.85	1.17	0.69	1.46	0.61	0.7	2.35	2.45	2.31	2.45	30.02	29.62
Nb93	18.65	18.85	0.5	0.019	0.025	0.16	0.013	0.061	0.015	0.014	0.013	0.01	21.91	21.77
Cs133	14.19	13.98	0.051	0.015	0.0096	0.011	0.0095	0.043	0.0095	0.016	0.011	0.0076	17.7	17.71
Ba137	17.86	17.71	27.54	0.089	0.065	0.064	0.055	0.28	0.061	0.42	0.064	0.05	22.4	22.23
La139	17.55	17.71	0.98	0.012	0.0079	0.011	0.0078	0.034	0.046	0.035	0.06	0.053	22.69	22.48
Ce140	15.87	15.73	1.9	0.012	0.012	0.015	0.01	0.035	0.22	0.16	0.28	0.26	18.56	18.51
Pr141	17.61	17.47	0.26	0.013	0.011	0.011	0.0092	0.03	0.071	0.052	0.08	0.077	21.64	21.57
Nd146	20.04	20.43	1.32	0.12	0.12	0.11	0.11	0.24	0.58	0.46	0.63	0.63	27.56	27.18
Sm152	18.08	18.12	0.27	0.17	0.15	0.13	0.14	0.24	0.17	0.15	0.17	0.17	23.1	22.92
Eu153	17.59	17.56	0.087	0.094	0.091	0.081	0.087	0.12	0.06	0.053	0.054	0.055	22.3	22.14
Gd158	17.87	18.03	0.25	0.37	0.3	0.3	0.28	0.47	0.13	0.11	0.11	0.1	23.05	22.83
Dy161	20.41	20.5	0.29	0.54	0.46	0.47	0.47	0.65	0.072	0.074	0.074	0.065	28.02	27.61
Ho165	20.83	20.95	0.052	0.11	0.092	0.092	0.093	0.13	0.012	0.011	0.013	0.0096	28.56	28.22
Er167	22.18	22.7	0.18	0.32	0.28	0.27	0.3	0.39	0.042	0.04	0.039	0.033	32.04	31.47
Yb172	17.97	18.06	0.15	0.26	0.2	0.21	0.22	0.37	0.034	0.033	0.04	0.032	22.18	22
Lu175	18.53	18.68	0.026	0.043	0.033	0.031	0.034	0.058	0.0087	0.0084	0.0073	0.0055	23.9	23.68
Hf178	19.02	19.04	0.21	0.052	0.039	0.052	0.036	0.14	0.11	0.11	0.11	0.1	24.94	24.68
Ta181	20.25	20.53	0.039	0.012	0.0091	0.013	0.0084	0.038	0.0099	0.0094	0.0094	0.0061	26.61	26.32
Pb208	18.2	18.2	0.44	0.023	0.016	0.016	0.014	0.069	0.018	0.02	0.023	0.018	24.37	24.08
Th232	21.55	21.97	0.27	0.014	0.0098	0.012	0.0091	0.038	0.01	0.0084	0.011	0.0083	29.68	29.25
U238	17.15	17.23	0.076	0.013	0.011	0.012	0.0082	0.037	0.0098	0.01	0.0096	0.0074	19.87	19.72

Appendix 6.A 1σ error for LAM-ICP-MS data

Element	STD610-7	STD610-8	BCR-4	0904C-1	0904C-2	0904C-3	0904C-4	0904C-5	0904C-6	0904C-7	0904C-8	0904C-9	STD610-9	STD610-10
Li7	0.269	0.224	0.0828	0.0927	0.0737	0.0785	0.0545	0.25	0.0698	0.0713	0.0657	0.0563	0.207	0.253
Be9	0.909	0.718	0.291	0.32	0.264	0.29	0.229	0.97	0.28	0.316	0.224	0.207	0.785	0.831
B11	1.29	1.28	0.431	0.562	0.423	0.485	0.415	1.62	0.43	0.419	0.426	0.324	1.23	1.09
Al27	1.42	0.953	0.387	0.471	2.58	0.411	1.53	7.58	1.56	0.709	0.427	1.5	2.67	1.42
P31	10.88	10.65	3.46	5.29	3.87	4.18	3.43	15.5	3.94	3.79	3.59	2.95	11.02	9.36
Ca42	182.58	177.21	58.13	88.66	64.96	67.1	57.13	252.33	63.93	59.76	57.85	50.76	190.81	149.06
Ca43	208.54	195.61	71.83	104.98	81.41	82.98	71.36	314.88	75.3	70.57	69.89	71.96	228.68	188.29
Sc45	0.287	0.261	0.098	0.136	0.0976	0.102	0.0848	0.365	0.101	0.0888	0.09	0.0697	0.267	0.28
Ti47	2.1	2.24	0.692	0.905	0.956	0.695	0.98	3.4	0.79	0.762	0.732	1.3	2.44	1.47
V51	0.223	0.185	0.0762	0.08	0.106	0.061	0.0646	0.302	0.0672	0.0759	0.0497	0.122	0.276	0.222
Co59	0.267	0.19	0.0852	0.0841	0.0863	0.0648	0.0567	0.306	0.0755	0.0649	0.0553	0.0593	0.191	0.226
Ni60	0.854	0.754	0.265	0.368	0.282	0.283	0.238	1.05	0.215	0.217	0.252	0.211	0.75	0.752
Ni62	5.37	5.4	1.85	2.5	2.05	2.02	1.85	8.09	1.76	2.09	1.77	1.63	7.9	4.57
Ga69	0.232	0.187	0.0689	0.0943	0.0696	0.0595	0.0603	0.205	0.0678	0.0595	0.0517	0.0483	0.178	0.253
Ga71	0.302	0.233	0.0968	0.113	0.0858	0.0814	0.0719	0.259	0.065	0.0769	0.081	0.0666	0.208	0.325
Rb85	0.205	0.163	0.0641	0.077	0.0535	0.0536	0.0513	0.198	0.0566	0.0457	0.0492	0.0431	0.16	0.229
Sr86	2.13	2.16	0.674	1.03	0.721	0.77	0.638	2.87	0.732	0.673	0.711	0.605	2.01	1.79
Sr88	0.162	0.1	0.0488	0.0354	0.0284	0.027	0.0209	0.103	0.0249	0.0322	0.0302	0.054	0.0802	0.184
Y89	0.173	0.111	0.0532	0.0386	0.038	0.0305	0.0329	0.143	0.0299	0.0251	0.0252	0.025	0.0812	0.18
Zr90	0.272	0.184	0.0831	0.0632	0.0644	0.0755	0.0563	0.273	0.0645	0.0625	0.0575	0.0709	0.188	0.282
Nb93	0.176	0.125	0.0591	0.0451	0.0376	0.0392	0.0327	0.151	0.0392	0.0362	0.0328	0.0278	0.0973	0.221
Cs133	0.135	0.101	0.0382	0.0397	0.0244	0.0266	0.022	0.109	0.0248	0.0441	0.0266	0.0199	0.0816	0.141
Ba137	0.556	0.566	0.172	0.218	0.171	0.168	0.147	0.725	0.161	0.149	0.159	0.122	0.51	0.53
La139	0.139	0.0957	0.0448	0.0291	0.0193	0.023	0.0206	0.0861	0.0216	0.0187	0.0219	0.0155	0.0622	0.154
Ce140	0.123	0.0836	0.0429	0.0252	0.0178	0.0241	0.0174	0.0883	0.0203	0.0221	0.0183	0.0183	0.0593	0.141
Pr141	0.134	0.0734	0.0429	0.0258	0.0175	0.02	0.0146	0.0611	0.0212	0.0188	0.0152	0.0158	0.0493	0.143
Nd146	0.465	0.312	0.121	0.126	0.107	0.116	0.0955	0.459	0.107	0.0932	0.101	0.0843	0.326	0.408
Sm152	0.294	0.209	0.0963	0.0865	0.0769	0.0901	0.0474	0.247	0.0543	0.0624	0.0653	0.057	0.176	0.325
Eu153	0.176	0.123	0.0615	0.0367	0.0378	0.0354	0.0246	0.158	0.0333	0.0304	0.0285	0.0239	0.0761	0.194
Gd158	0.337	0.231	0.112	0.119	0.0861	0.0925	0.0722	0.288	0.0632	0.0812	0.0771	0.0574	0.221	0.316
Dy161	0.39	0.285	0.111	0.129	0.103	0.107	0.103	0.341	0.0985	0.111	0.105	0.0875	0.285	0.393
Ho165	0.137	0.0803	0.056	0.0275	0.0204	0.0245	0.0179	0.0771	0.0201	0.0179	0.0182	0.0142	0.0602	0.156
Er167	0.293	0.261	0.12	0.0996	0.0791	0.0788	0.0813	0.293	0.0948	0.0918	0.0747	0.0581	0.225	0.36
Yb172	0.396	0.319	0.0983	0.0963	0.0864	0.0969	0.0867	0.376	0.0784	0.0739	0.0948	0.0643	0.275	0.385
Lu175	0.133	0.078	0.0457	0.0267	0.0184	0.0247	0.019	0.079	0.0227	0.0213	0.0165	0.0142	0.0466	0.155
Hf178	0.287	0.244	0.0938	0.0903	0.0691	0.0898	0.0659	0.355	0.0839	0.054	0.0621	0.0577	0.169	0.308
Ta181	0.161	0.108	0.0506	0.0318	0.0215	0.0235	0.0206	0.101	0.0262	0.0245	0.0233	0.0159	0.0727	0.167
Pb208	0.205	0.13	0.0802	0.0635	0.0368	0.0377	0.0369	0.185	0.0408	0.0451	0.0355	0.0322	0.111	0.225
Th232	0.147	0.105	0.0509	0.0361	0.0232	0.0294	0.0233	0.0937	0.0253	0.0207	0.0282	0.0206	0.0774	0.182
U238	0.135	0.0923	0.0484	0.0311	0.0252	0.0264	0.0203	0.0921	0.0249	0.026	0.0244	0.0199	0.0634	0.156

Appendix 6.B LLD (99% confidence) for LAM-ICP-MS data

Element	STD610-11	STD610-12	STD610-13	BCR-5	73831-1	73831-2	73831-3	73831-4	73831-5	73831-6	STD610-14	STD610-15
Li7	16.96	16.79	17.41	0.34	0.067	0.17	0.13	0.067	0.068	0.087	20.97	21.4
Be9	34.68	35.23	34.3	0.21	0.11	0.12	0.11	0.093	0.12	0.11	38.26	38.22
B11	22.28	21.91	21.9	0.42	0.19	0.2	0.21	0.15	0.17	0.18	24.43	24.81
Al27	386.35	398	389.52	2921.1	5263.82	5133.32	5212.45	4671.44	5378.14	5469.57	443.54	450.86
P31	44.07	42.64	43.17	151.91	30.34	28.59	30.09	23.4	32.03	30.48	45.91	48.21
Ca42	2607.95	2610.72	2605.49	1617.8	1293.92	1293.54	1294.59	1292.75	1293.77	1293.53	2605.03	2608.05
Ca43	2812.75	2894.7	2833.35	1773.74	1411.05	1448.68	1477.52	1498.35	1510.42	1558.9	3205.69	3260.9
Sc45	16.89	17.36	16.89	1.2	1.76	1.65	1.55	1.35	1.79	1.99	20.97	21.2
Ti47	19.08	19.75	18.86	567.34	93.19	41.61	36.86	21.59	56.71	121.21	23.56	24.51
V51	18.24	19.19	18.51	17.67	6.45	6.24	6.8	6.82	7.14	7.67	25.59	26.24
Co59	13.65	13.63	13.55	1.23	3.12	2.7	3.02	2.63	3.05	2.38	14.54	14.52
Ni60	18.21	19.28	18.59	0.55	0.48	0.38	0.58	0.34	0.64	0.32	24.98	25.72
Ni62	18.69	18.93	18.75	1.13	1.11	1.06	1.21	0.87	1.12	0.99	22.87	23.07
Ga69	16.13	16.4	16.63	1.16	0.67	0.71	0.68	0.64	0.71	0.74	21.19	21.19
Ga71	17.59	17.73	17.66	0.88	0.76	0.76	0.8	0.71	0.79	0.84	24.05	23.85
Rb85	17.08	17.35	18.09	1.99	0.023	0.076	0.025	0.021	0.023	0.022	23.8	24.11
Sr86	18.86	19.68	19.12	12.68	0.35	0.31	0.34	0.28	0.31	0.32	23.16	23.97
Sr88	17.66	17.93	17.96	11.76	0.023	0.022	0.016	0.013	0.014	0.016	20.7	20.7
Y89	17.65	18.29	17.89	1.19	2.93	2.64	2.73	2.07	3.17	3.1	21.63	21.91
Zr90	17.29	17.87	17.46	6.49	3.06	2.45	1.83	0.84	2.49	2.86	20.27	20.6
Nb93	18.44	19.04	18.77	0.52	0.018	0.027	0.017	0.013	0.015	0.018	22.02	22.23
Cs133	12.99	13.25	13.22	0.048	0.012	0.015	0.021	0.01	0.011	0.011	16.52	16.5
Ba137	16.75	17.25	17.4	26.77	0.11	0.093	0.083	0.054	0.078	0.072	21.8	21.96
La139	16.66	17.22	17.05	0.97	0.012	0.017	0.014	0.0087	0.011	0.011	21.88	21.91
Ce140	17.53	18.17	18.15	2.17	0.019	0.059	0.031	0.011	0.016	0.016	24.28	24.28
Pr141	17.38	17.97	17.88	0.27	0.019	0.013	0.017	0.0094	0.012	0.012	22.79	22.86
Nd146	16.99	17.64	17.46	1.19	0.14	0.15	0.13	0.11	0.14	0.14	21.89	22.04
Sm152	17.61	18.31	18	0.28	0.19	0.19	0.18	0.15	0.19	0.19	23.07	23.21
Eu153	17.63	18.28	18.3	0.093	0.094	0.087	0.09	0.078	0.091	0.095	23.97	24
Gd158	17.59	18.47	18.27	0.28	0.4	0.38	0.4	0.32	0.42	0.42	23.47	23.8
Dy161	17.54	18.37	18.18	0.29	0.6	0.56	0.56	0.42	0.62	0.65	23.04	23.34
Ho165	20.02	21.23	20.99	0.059	0.14	0.13	0.14	0.1	0.16	0.16	28.09	28.47
Er167	20.47	21.92	21.49	0.18	0.44	0.41	0.43	0.31	0.51	0.5	29.27	29.79
Yb172	20.56	21.87	21.63	0.17	0.42	0.39	0.43	0.3	0.52	0.49	29	29.46
Lu175	18.57	19.6	19.41	0.028	0.06	0.055	0.062	0.042	0.072	0.067	24.94	25.45
Hf178	18.46	19.49	19.21	0.22	0.078	0.071	0.064	0.037	0.071	0.077	24.79	25.2
Ta181	20.08	21.3	20.99	0.041	0.011	0.017	0.011	0.0092	0.0099	0.011	27.2	27.88
Pb208	21.58	23.02	22.44	0.51	0.022	0.033	0.032	0.016	0.02	0.018	33.68	33.15
Th232	21.36	22.92	22.21	0.29	0.016	0.029	0.012	0.01	0.013	0.013	29.98	30.71
U238	20.62	21.81	21.93	0.091	0.012	0.06	0.038	0.0089	0.0097	0.011	29.26	29.79

Appendix 6.A 1σ error for LAM-ICP-MS data

Element	STD610-11	STD610-12	STD610-13	BCR-5	73831-1	73831-2	73831-3	73831-4	73831-5	73831-6	STD610-14	STD610-15
Li7	0.121	0.211	0.214	0.0706	0.0756	0.0691	0.0684	0.0631	0.0728	0.0633	0.16	0.297
Be9	0.544	0.898	0.69	0.271	0.276	0.302	0.283	0.241	0.274	0.261	0.633	0.91
B11	0.981	1.31	1.09	0.404	0.495	0.427	0.477	0.391	0.429	0.46	1.02	1.09
Al27	0.58	1.03	1.2	0.337	0.329	0.762	0.854	0.757	1.07	0.696	1.68	1.81
P31	7.64	12.17	9.51	3.79	4.53	4.11	4.38	3.78	4.26	4.35	9.77	9.29
Ca42	139.28	193.97	148.12	57.22	68.59	61.4	65.57	55.19	62.7	63.89	142.72	142.94
Ca43	163.85	246.96	186.69	71.86	85.21	75.03	80.63	69.67	78.67	82.04	193.07	193.31
Sc45	0.199	0.324	0.268	0.0889	0.0942	0.0962	0.0934	0.0837	0.0952	0.0989	0.2	0.342
Ti47	1.33	2.2	1.68	0.658	0.77	0.672	0.844	0.707	0.721	0.765	1.78	1.84
V51	0.122	0.185	0.205	0.0653	0.0631	0.0645	0.0645	0.0562	0.0593	0.063	0.132	0.277
Co59	0.126	0.218	0.226	0.0749	0.0706	0.0596	0.0646	0.0619	0.0698	0.0679	0.154	0.314
Ni60	0.516	0.894	0.658	0.234	0.306	0.265	0.287	0.281	0.251	0.235	0.666	0.828
Ni62	4.14	5.53	4.45	2.06	1.97	2.11	2.07	1.86	2.14	2.11	5.61	5.41
Ga69	0.136	0.219	0.232	0.0618	0.0605	0.0581	0.0732	0.0591	0.0647	0.0614	0.141	0.307
Ga71	0.161	0.296	0.338	0.0874	0.0828	0.0842	0.0906	0.0837	0.0778	0.0905	0.208	0.374
Rb85	0.118	0.197	0.193	0.0601	0.0591	0.0558	0.0643	0.0516	0.0592	0.0573	0.135	0.285
Sr86	1.72	2.39	1.92	0.75	0.916	0.804	0.847	0.743	0.806	0.838	1.75	1.92
Sr88	0.0604	0.132	0.16	0.0464	0.0283	0.0273	0.0248	0.0247	0.0303	0.0319	0.0631	0.237
Y89	0.069	0.152	0.17	0.0419	0.0355	0.0342	0.0332	0.0322	0.0334	0.0328	0.0766	0.243
Zr90	0.144	0.246	0.266	0.0731	0.0684	0.0664	0.0731	0.0562	0.0698	0.0767	0.138	0.338
Nb93	0.0794	0.175	0.203	0.0456	0.0463	0.0389	0.0423	0.0335	0.0354	0.0415	0.0966	0.3
Cs133	0.0554	0.102	0.121	0.0317	0.0317	0.0287	0.0312	0.0261	0.0282	0.0288	0.0627	0.179
Ba137	0.384	0.643	0.532	0.196	0.183	0.172	0.196	0.129	0.197	0.18	0.425	0.673
La139	0.0537	0.124	0.134	0.032	0.0283	0.0243	0.0272	0.0222	0.0263	0.0246	0.0646	0.195
Ce140	0.0423	0.134	0.131	0.0322	0.0242	0.0239	0.0189	0.019	0.0249	0.021	0.0447	0.188
Pr141	0.0444	0.0847	0.128	0.0321	0.0239	0.0162	0.022	0.0173	0.0204	0.0173	0.0409	0.191
Nd146	0.245	0.452	0.415	0.115	0.136	0.119	0.113	0.11	0.132	0.113	0.24	0.534
Sm152	0.172	0.301	0.336	0.0795	0.0852	0.0755	0.083	0.0663	0.0778	0.058	0.159	0.415
Eu153	0.0763	0.146	0.17	0.041	0.0375	0.0389	0.0392	0.0297	0.0412	0.0358	0.0736	0.241
Gd158	0.203	0.357	0.332	0.108	0.119	0.094	0.0941	0.072	0.108	0.104	0.171	0.404
Dy161	0.271	0.408	0.376	0.0984	0.142	0.102	0.114	0.0857	0.113	0.127	0.236	0.486
Ho165	0.0449	0.109	0.134	0.0346	0.0227	0.0209	0.0234	0.0206	0.021	0.0215	0.0562	0.201
Er167	0.183	0.318	0.391	0.0989	0.0927	0.0924	0.0904	0.0879	0.0911	0.0966	0.23	0.46
Yb172	0.218	0.326	0.369	0.108	0.111	0.0942	0.118	0.0752	0.0891	0.107	0.246	0.439
Lu175	0.0465	0.113	0.145	0.0335	0.0268	0.024	0.0229	0.0199	0.0276	0.0263	0.0432	0.204
Hf178	0.162	0.283	0.339	0.0921	0.0849	0.0818	0.0853	0.0725	0.0792	0.072	0.159	0.425
Ta181	0.0576	0.132	0.166	0.0338	0.0279	0.0279	0.0266	0.0256	0.0252	0.0299	0.0501	0.244
Pb208	0.128	0.207	0.215	0.0614	0.0587	0.0503	0.0468	0.0429	0.0525	0.0441	0.103	0.284
Th232	0.0603	0.122	0.169	0.043	0.0345	0.0336	0.0299	0.0228	0.0287	0.0323	0.0631	0.236
U238	0.0625	0.119	0.164	0.0346	0.0274	0.0286	0.0326	0.0227	0.0245	0.0285	0.0647	0.214

Appendix 6.B LLD (99% confidence) for LAM-ICP-MS data

Element	STD610-16	STD610-17	BCR-6	73832-1	73832-2	73832-3	73832-4	73832-5	STD610-18	STD610-19
Li7	16.97	16.59	0.33	0.069	0.13	0.072	0.11	0.066	19.34	20.08
Be9	35.8	34.65	0.19	0.11	0.12	0.14	0.1	0.088	38.2	38.66
B11	21.79	21.87	0.37	0.19	0.2	0.2	0.16	0.13	22.71	22.59
Al27	392.18	385.66	2880.08	4738.61	5427.15	4942.38	5330.32	5048.7	424.48	440.72
P31	41.08	40.24	139.36	21.07	23.02	22.2	25.68	23.3	43.12	43.16
Ca42	2608.5	2606.12	1616.99	1113.24	1113.21	1113.21	1111.86	1110.85	2610.09	2608.69
Ca43	3019.5	2934.93	1857.4	1304.12	1341.11	1369.65	1415.54	1458.64	3544.03	3684.37
Sc45	15.14	14.95	1.02	2.3	2.29	2.22	2.08	2.3	15.6	15.8
Ti47	17.73	17.61	518.76	14.95	15.07	15.66	34.16	63.04	19.67	20.66
V51	17.1	16.58	16.18	5.74	5.77	6.62	5.96	6.41	20.47	21.53
Co59	14.37	14.09	1.34	2.91	2.66	3.08	2.23	3.05	16.07	16.28
Ni60	17.24	16.78	0.48	0.43	0.23	0.47	0.16	0.4	20.23	21.32
Ni62	21.33	22.46	1.1	1.15	0.98	1.17	0.76	0.97	30.54	31.39
Ga69	14.39	14.27	1.01	0.47	0.52	0.53	0.45	0.45	15.34	15.91
Ga71	14.78	14.49	0.74	0.49	0.58	0.57	0.5	0.49	16.39	16.62
Rb85	14.53	14.33	1.62	0.023	0.076	0.032	0.02	0.018	16.35	16.48
Sr86	16.72	16.65	10.82	0.31	0.32	0.31	0.26	0.22	16.76	16.73
Sr88	16.95	16.7	11.01	0.016	0.014	0.026	0.023	0.012	17.78	17.96
Y89	15.9	15.94	1.01	3.64	3.72	3.99	3.41	3.31	16.47	16.88
Zr90	15.81	15.78	5.56	0.74	0.55	0.65	1.29	1.03	16.03	15.95
Nb93	17.48	17.2	0.47	0.016	0.016	0.032	0.014	0.012	18.44	18.81
Cs133	12.52	12.24	0.044	0.013	0.012	0.037	0.0093	0.0077	14.37	14.63
Ba137	15.46	15.33	23.74	0.062	0.082	0.085	0.062	0.052	17.73	17.74
La139	14.62	14.37	0.79	0.011	0.014	0.021	0.014	0.009	15.64	16.09
Ce140	16.61	16.06	1.95	0.016	0.02	0.022	0.022	0.011	20.1	20.95
Pr141	15.11	14.88	0.22	0.011	0.011	0.021	0.0094	0.0085	15.96	16.07
Nd146	14.5	14.5	0.93	0.11	0.085	0.11	0.094	0.11	15.13	15.05
Sm152	14.54	14.58	0.22	0.15	0.14	0.14	0.14	0.14	14.74	14.9
Eu153	15.18	14.92	0.074	0.063	0.054	0.059	0.057	0.057	16.9	17.02
Gd158	14.57	14.46	0.21	0.36	0.33	0.36	0.33	0.32	15.06	15.42
Dy161	14.78	14.59	0.21	0.62	0.64	0.69	0.58	0.55	15.33	15.64
Ho165	14.95	14.85	0.043	0.14	0.15	0.15	0.13	0.12	15.12	15.09
Er167	14.56	14.55	0.13	0.45	0.47	0.47	0.4	0.37	14.58	14.66
Yb172	15.99	15.82	0.14	0.48	0.51	0.53	0.44	0.43	17.46	17.45
Lu175	14.77	14.66	0.023	0.075	0.084	0.076	0.067	0.065	15.06	15.01
Hf178	14.46	14.37	0.17	0.042	0.043	0.05	0.043	0.036	14.49	14.57
Ta181	16.19	15.99	0.033	0.01	0.011	0.025	0.0088	0.0072	17.11	17.11
Pb208	14.73	14.52	0.34	0.032	0.032	0.032	0.016	0.014	17.05	17.12
Th232	15.43	15.28	0.19	0.013	0.013	0.024	0.011	0.0089	15.5	15.56
U238	17.12	16.84	0.067	0.013	0.033	0.032	0.01	0.0077	19.76	19.86

Appendix 6.A 1σ error for LAM-ICP-MS data

Element	STD610-16	STD610-17	BCR-6	73832-1	73832-2	73832-3	73832-4	73832-5	STD610-18	STD610-19
Li7	0.215	0.2	0.0809	0.0769	0.0842	0.113	0.0655	0.064	0.221	0.225
Be9	0.641	0.756	0.268	0.29	0.307	0.329	0.279	0.248	0.867	0.677
B11	1.37	1.13	0.383	0.481	0.526	0.494	0.406	0.367	1.1	1.14
Al27	0.91	0.886	0.402	0.332	2.01	0.653	0.91	0.343	1.16	1.05
P31	10.17	9.91	3.26	4.29	4.53	4.1	3.57	3.28	10.75	9.61
Ca42	206.04	170.6	53.59	68.95	73.54	68.34	57.7	53.88	173.78	155.79
Ca43	224.81	203.62	68.37	81.26	93.42	94.05	70.74	68.92	210.73	198.92
Sc45	0.286	0.267	0.098	0.103	0.117	0.117	0.0871	0.0853	0.267	0.248
Ti47	2.45	1.94	0.613	0.825	0.938	0.853	0.717	0.555	2.17	1.67
V51	0.182	0.171	0.0842	0.0648	0.0932	0.107	0.0572	0.051	0.174	0.175
Co59	0.204	0.203	0.07	0.0769	0.094	0.118	0.0648	0.0596	0.188	0.222
Ni60	0.803	0.714	0.263	0.258	0.351	0.331	0.249	0.268	0.718	0.62
Ni62	6.85	5.47	1.86	2	2.11	2.15	1.83	1.9	6.07	5.86
Ga69	0.205	0.181	0.0818	0.0716	0.0784	0.103	0.0615	0.0569	0.183	0.176
Ga71	0.253	0.26	0.101	0.0944	0.0897	0.124	0.0849	0.0723	0.227	0.266
Rb85	0.155	0.164	0.0695	0.057	0.188	0.0891	0.0528	0.0499	0.161	0.17
Sr86	2.23	1.95	0.598	0.826	0.86	0.803	0.663	0.585	1.99	1.7
Sr88	0.0823	0.0817	0.0654	0.035	0.033	0.0718	0.0325	0.0182	0.0743	0.136
Y89	0.0881	0.112	0.0496	0.0302	0.0568	0.0687	0.035	0.0255	0.093	0.136
Zr90	0.169	0.209	0.0941	0.0739	0.0792	0.106	0.0613	0.0673	0.216	0.232
Nb93	0.109	0.146	0.0696	0.0403	0.04	0.0867	0.0356	0.0327	0.102	0.155
Cs133	0.0882	0.0854	0.0457	0.0349	0.0288	0.0947	0.0247	0.0206	0.0757	0.106
Ba137	0.514	0.527	0.174	0.153	0.206	0.226	0.169	0.138	0.399	0.582
La139	0.0771	0.0828	0.0465	0.0282	0.0255	0.0599	0.0187	0.0239	0.0724	0.102
Ce140	0.0688	0.0813	0.0476	0.0224	0.0266	0.0608	0.0209	0.0198	0.0654	0.112
Pr141	0.0645	0.0917	0.0407	0.0226	0.0197	0.0606	0.0132	0.0146	0.0443	0.0986
Nd146	0.352	0.42	0.148	0.128	0.139	0.162	0.0969	0.0971	0.323	0.284
Sm152	0.245	0.2	0.0838	0.068	0.0818	0.124	0.0695	0.0499	0.193	0.227
Eu153	0.103	0.102	0.0539	0.0422	0.0381	0.0748	0.0314	0.0263	0.1	0.144
Gd158	0.263	0.256	0.1	0.0834	0.0862	0.141	0.0731	0.0827	0.23	0.303
Dy161	0.307	0.343	0.151	0.124	0.136	0.173	0.11	0.0894	0.247	0.33
Ho165	0.0685	0.0908	0.0455	0.0204	0.025	0.0621	0.0224	0.0193	0.0578	0.114
Er167	0.257	0.282	0.124	0.112	0.089	0.147	0.0672	0.0884	0.212	0.33
Yb172	0.283	0.234	0.111	0.0898	0.118	0.154	0.0944	0.0805	0.284	0.307
Lu175	0.072	0.0879	0.0444	0.015	0.0239	0.0621	0.0196	0.0167	0.0516	0.11
Hf178	0.226	0.209	0.0901	0.0841	0.0874	0.127	0.0726	0.0611	0.204	0.262
Ta181	0.0763	0.0928	0.0498	0.0252	0.0307	0.0721	0.0233	0.0193	0.0506	0.123
Pb208	0.183	0.186	0.0697	0.0507	0.0548	0.0934	0.0419	0.0383	0.124	0.157
Th232	0.0856	0.102	0.0573	0.0348	0.0308	0.0712	0.027	0.0231	0.0608	0.124
U238	0.0775	0.0914	0.0507	0.0376	0.0331	0.0662	0.026	0.0211	0.0731	0.112

Appendix 6.B LLD (99% confidence) for LAM-ICP-MS data

Element	STD610-3	STD610-4	BCR-1	0906A-1	0906A-2	0906A-3	0906A-4	0906A-5	0906A-6	0906A-7	0906A-8	0906A-9	STD610-5	STD610-6
Li7	15.48	15.61	0.32	0.03	0.061	0.25	0.24	0.082	0.24	0.25	0.14	0.43	15.76	15.74
Be9	29.12	29.08	0.19	0.067	0.18	0.11	0.13	0.24	0.13	0.13	0.2	1.49	31.64	31.76
B11	19.32	19.13	0.32	0.12	0.31	0.18	0.19	0.36	0.18	0.2	0.33	2.11	21.74	21.71
Al27	372.79	369.07	2721.71	4489.98	4581.63	1469.28	1606.64	5172.84	1643.82	1731.59	1570.33	621.81	391.42	394.09
P31	42.08	41.58	148.61	15.6	16.27	5.02	7.35	24.13	6.29	9.22	6.33	23.21	41.55	42.91
Ca42	2613.19	2614.37	1619.02	1680.68	1688.01	4469	4469.16	1691	4468.95	4470.17	1703.04	1867.19	2606.12	2604.71
Ca43	2966.83	2969.43	1822.4	1890.24	1939.93	5095.71	5200.85	2003.78	5401.53	5406.32	2107.71	2302.75	3426.18	3410.44
Sc45	15.15	15.13	1.1	2.11	1.98	1.26	1.31	2.25	1.35	1.41	0.95	1.05	15.61	15.84
Ti47	17.59	17.57	499.81	16.61	19.03	176.02	190.05	29.29	201.81	239.4	37.93	79.01	18.74	19.2
V51	15.35	15.24	14.23	4.29	4.75	16.04	15.37	4.53	15.73	15.87	6.26	6.59	16.41	16.35
Co59	15.97	15.54	1.44	2.9	3.21	1.52	1.58	3.84	1.64	1.71	1.61	1.1	19.72	20.36
Ni60	16.83	16.56	0.5	0.23	0.35	5.28	5.25	0.39	5.59	5.4	2.33	4.48	20.43	20.68
Ni62	31.4	29.5	1.35	0.66	1.5	9.96	10.36	1.88	11.16	10.9	5.54	16.12	45.59	49.56
Ga69	16.41	16.05	1.45	0.32	0.39	0.71	0.7	0.4	0.74	0.75	0.38	0.74	19.64	20.39
Ga71	16.43	16.11	0.78	0.33	0.4	0.73	0.72	0.43	0.79	0.78	0.44	0.94	19.63	20.45
Rb85	16.08	15.84	1.82	0.015	0.04	0.021	0.024	0.053	0.022	0.026	0.049	0.33	18.58	19.35
Sr86	17.42	17.28	11.13	0.31	0.81	5.81	5.91	0.96	5.79	5.6	2.2	6.86	18.07	18.07
Sr88	16.38	16.34	10.74	0.054	0.05	5.43	5.56	0.034	5.4	5.26	1.58	2.37	16.37	16.39
Y89	17.69	17.33	1.15	1.77	1.71	0.14	0.21	2.19	0.18	0.27	0.58	0.27	19.96	20.45
Zr90	16.69	16.59	6.1	0.23	0.26	1.04	1.04	0.39	1.1	1.14	0.42	0.93	17.71	18.11
Nb93	18.49	18.14	0.51	0.012	0.03	0.015	0.018	0.039	0.017	0.019	0.034	0.24	20.43	20.82
Cs133	11.58	11.47	0.046	0.0078	0.022	0.01	0.011	0.028	0.011	0.013	0.027	0.17	11.97	11.97
Ba137	15.66	15.41	23.68	0.051	0.16	0.067	0.086	0.17	0.074	0.096	0.16	1.1	17.34	17.47
La139	14.73	14.53	0.81	0.0078	0.019	0.072	0.079	0.022	0.074	0.079	0.046	0.17	15.76	16.04
Ce140	15.68	15.34	1.85	0.011	0.023	0.35	0.39	0.025	0.36	0.39	0.12	0.29	17.63	17.93
Pr141	15.13	15.01	0.23	0.0066	0.018	0.08	0.083	0.019	0.081	0.085	0.045	0.16	15.86	16.12
Nd146	15.95	15.76	1.06	0.058	0.11	0.51	0.55	0.15	0.52	0.54	0.29	0.95	17.82	18.39
Sm152	17.33	16.97	0.27	0.071	0.11	0.17	0.19	0.13	0.19	0.18	0.15	0.51	20.34	21.09
Eu153	14.86	14.68	0.079	0.04	0.06	0.055	0.06	0.064	0.058	0.059	0.058	0.21	15.81	16.09
Gd158	17.44	17.22	0.27	0.18	0.23	0.14	0.16	0.24	0.15	0.16	0.2	0.58	20.9	21.96
Dy161	15.78	15.62	0.26	0.3	0.38	0.096	0.11	0.43	0.1	0.13	0.26	0.69	17.41	17.94
Ho165	15.12	15.02	0.049	0.066	0.077	0.015	0.019	0.098	0.017	0.023	0.052	0.13	15.39	15.51
Er167	14.73	14.68	0.14	0.21	0.25	0.047	0.052	0.32	0.058	0.066	0.18	0.49	14.84	14.94
Yb172	17.93	17.9	0.16	0.26	0.26	0.039	0.047	0.37	0.045	0.059	0.17	0.64	21.14	22.2
Lu175	16.01	15.85	0.026	0.04	0.039	0.0088	0.011	0.062	0.011	0.012	0.031	0.14	17.54	18.05
Hf178	15.76	15.81	0.19	0.027	0.067	0.081	0.084	0.081	0.083	0.087	0.093	0.55	17.39	17.99
Ta181	16.19	16.02	0.038	0.0077	0.019	0.011	0.012	0.025	0.01	0.011	0.024	0.17	16.93	17.17
Pb208	14.22	14.21	0.31	0.013	0.033	0.024	0.026	0.04	0.024	0.028	0.05	0.24	15.48	15.95
Th232	15.99	15.89	0.2	0.0091	0.023	0.011	0.012	0.03	0.012	0.013	0.024	0.16	16.72	17.04
U238	15.94	15.78	0.065	0.0071	0.021	0.0091	0.01	0.025	0.011	0.01	0.023	0.15	16.54	16.77

Appendix 6.A 1σ error for LAM-ICP-MS data

Element	STD610-3	STD610-4	BCR-1	0906A-1	0906A-2	0906A-3	0906A-4	0906A-5	0906A-6	0906A-7	0906A-8	0906A-9	STD610-5	STD610-6
Li7	0.193	0.19	0.0814	0.0439	0.133	0.0634	0.0762	0.169	0.0713	0.0818	0.119	0.876	0.19	0.177
Be9	0.722	0.663	0.264	0.163	0.479	0.244	0.276	0.648	0.296	0.306	0.411	3.54	0.702	0.705
B11	1.34	1.13	0.446	0.287	0.8	0.389	0.475	0.935	0.418	0.457	0.686	5.01	1.05	0.873
Al27	1.09	0.91	0.441	0.24	0.648	0.315	0.353	0.775	0.354	0.4	0.582	6.29	1.1	0.898
P31	12.3	11.37	4.35	3.12	8.83	4.26	4.96	10.27	4.47	4.8	7.46	55.17	10.99	9.37
Ca42	306.09	271.44	102.03	68.42	179.15	81.62	92.24	193.53	79.65	86.23	134.23	963.17	196.42	168.37
Ca43	283.17	255.27	94.82	67.62	187.83	86.42	105.63	225.21	95.83	102.77	156.09	1182.29	245.14	215.96
Sc45	0.411	0.364	0.138	0.0924	0.252	0.111	0.133	0.284	0.117	0.12	0.207	1.52	0.309	0.277
Ti47	2.25	2.16	0.834	0.624	1.55	0.834	0.996	1.94	0.848	1.02	1.5	12.41	2.32	2.09
V51	0.213	0.184	0.0719	0.0444	0.127	0.214	0.0664	0.157	0.0591	0.072	0.103	0.877	0.191	0.161
Co59	0.227	0.16	0.0791	0.0525	0.127	0.0621	0.0586	0.153	0.0692	0.0807	0.131	0.977	0.192	0.16
Ni60	0.788	0.703	0.285	0.188	0.558	0.271	0.253	0.666	0.272	0.309	0.568	4.02	0.846	0.744
Ni62	5.26	4.61	2.07	1.29	3.57	1.79	2.12	4.64	2.17	2.18	3.17	26.91	5.68	4.9
Ga69	0.218	0.18	0.0875	0.0432	0.113	0.0634	0.0716	0.168	0.0733	0.0794	0.118	0.941	0.192	0.191
Ga71	0.257	0.227	0.105	0.0468	0.151	0.088	0.103	0.211	0.0947	0.102	0.167	1.29	0.227	0.231
Rb85	0.165	0.142	0.0746	0.0396	0.103	0.0545	0.0652	0.143	0.056	0.0639	0.112	0.81	0.163	0.153
Sr86	3.21	2.96	1.18	0.805	2.15	1	1.21	2.55	1.06	1.21	1.87	13.49	2.75	2.31
Sr88	0.124	0.0817	0.05	0.0205	0.0622	0.0304	0.0296	0.0692	0.0345	0.0383	0.0572	0.504	0.0945	0.0846
Y89	0.132	0.0968	0.0587	0.0233	0.0692	0.0315	0.0375	0.0914	0.0376	0.0354	0.0614	0.458	0.0936	0.0993
Zr90	0.297	0.196	0.0987	0.0459	0.131	0.0634	0.0708	0.139	0.0769	0.0747	0.145	1.05	0.25	0.187
Nb93	0.182	0.125	0.0643	0.0301	0.0786	0.0364	0.0495	0.101	0.0477	0.0477	0.0735	0.596	0.119	0.131
Cs133	0.121	0.0828	0.0408	0.0196	0.0583	0.0272	0.0297	0.0746	0.0297	0.0327	0.0495	0.398	0.0698	0.0787
Ba137	0.637	0.438	0.189	0.129	0.466	0.163	0.219	0.436	0.194	0.212	0.367	2.54	0.514	0.377
La139	0.108	0.0698	0.0415	0.0178	0.0505	0.0212	0.026	0.0582	0.0237	0.0264	0.0435	0.336	0.0826	0.0969
Ce140	0.103	0.0862	0.0445	0.0186	0.0467	0.0193	0.0228	0.0569	0.0266	0.0288	0.042	0.289	0.0614	0.0793
Pr141	0.0932	0.0657	0.0426	0.013	0.0385	0.0181	0.026	0.0473	0.0249	0.0238	0.033	0.29	0.0636	0.0721
Nd146	0.317	0.317	0.136	0.084	0.19	0.13	0.147	0.303	0.127	0.15	0.231	1.75	0.381	0.296
Sm152	0.251	0.209	0.103	0.0533	0.174	0.0633	0.0688	0.223	0.0716	0.101	0.142	1.09	0.156	0.229
Eu153	0.151	0.107	0.0506	0.0293	0.0807	0.0285	0.0377	0.0771	0.0387	0.0431	0.0705	0.447	0.0913	0.101
Gd158	0.27	0.248	0.114	0.0665	0.168	0.0847	0.0917	0.231	0.0851	0.104	0.145	1.18	0.219	0.267
Dy161	0.377	0.289	0.148	0.0984	0.229	0.0967	0.14	0.314	0.129	0.135	0.214	1.55	0.298	0.33
Ho165	0.107	0.0736	0.0375	0.0185	0.0497	0.0226	0.0266	0.0486	0.0251	0.0274	0.0456	0.282	0.0678	0.0943
Er167	0.298	0.231	0.118	0.0774	0.216	0.0929	0.0941	0.231	0.123	0.106	0.184	1.03	0.261	0.259
Yb172	0.323	0.297	0.129	0.0819	0.165	0.0935	0.104	0.263	0.108	0.113	0.154	1.27	0.291	0.242
Lu175	0.122	0.0719	0.043	0.0185	0.0469	0.0199	0.0271	0.067	0.0315	0.0261	0.0472	0.357	0.0641	0.0862
Hf178	0.247	0.232	0.116	0.0575	0.184	0.087	0.0874	0.2	0.0886	0.0903	0.146	1.32	0.23	0.209
Ta181	0.112	0.0912	0.0536	0.0199	0.0487	0.029	0.032	0.0658	0.0239	0.0261	0.0541	0.38	0.057	0.107
Pb208	0.165	0.0989	0.0615	0.0323	0.0858	0.0435	0.0487	0.0915	0.0413	0.0507	0.0828	0.526	0.119	0.134
Th232	0.106	0.0847	0.0493	0.0235	0.0596	0.0279	0.0328	0.0814	0.0288	0.0361	0.0516	0.366	0.079	0.0926
U238	0.104	0.0872	0.0595	0.0189	0.0592	0.0243	0.0252	0.0676	0.0289	0.0243	0.0467	0.333	0.0754	0.13

Appendix 6.B LLD (99% confidence) for LAM-ICP-MS data

Element	STD610-7	STD610-8	BCR-2	0906B-1	0906B-2	0906B-3	0906B-4	0906B-5	0906B-6	0906B-7	0906B-8	0906B-9	0906B-10	STD610-9	STD610-10
Li7	16.18	16.35	0.34	0.038	0.047	0.036	0.042	0.046	0.33	0.36	0.4	0.4	0.39	18.2	18.92
Be9	30.78	31	0.21	0.089	0.099	0.084	0.091	0.086	0.16	0.14	0.14	0.15	0.14	32.58	32.23
B11	26.64	24.55	0.4	0.14	0.15	0.12	0.13	0.14	0.22	0.27	0.24	0.26	0.25	34.87	36.01
Al27	377.5	381.55	2761.29	4529.21	5159.99	4501.08	4523.43	4841.23	1250.03	1465.64	1461.86	1672.87	1516.37	402.29	399.85
P31	42.25	40.78	148.87	18.84	22.77	19.47	17.61	20.11	6.33	6.34	5.89	6.32	6.46	40.67	41.01
Ca42	2609.36	2608.43	1619.06	1818.54	1818.99	1818.15	1818.41	1818.71	4499.04	4498.36	4497.53	4497.58	4497.85	2609.14	2606.73
Ca43	2661.08	2681.11	1650.77	1826.72	1849.65	1834.84	1830.4	1840.67	4503.37	4581.69	4642.84	4597.09	4613.57	2718.25	2725.97
Sc45	15.31	15.6	1.08	1.75	2.2	1.85	1.8	2.21	1.22	1.18	1.21	1.23	1.22	16.57	16.7
Ti47	16.8	16.97	495.66	22.33	24	20.11	26.44	23.23	97.38	134.8	109.32	146.44	141.68	17.73	17.6
V51	14.93	14.74	14.28	4.13	5.18	4.08	4.14	4.33	18.49	18.7	19.1	18.75	19.53	15.6	15.66
Co59	13.33	13.38	1.26	2.28	2.72	2.25	2.24	2.38	1.17	1.27	1.19	1.18	1.29	13.61	13.72
Ni60	19.28	18.44	0.58	0.28	0.39	0.24	0.24	0.34	6.56	6.6	7.04	6.8	7.55	24.98	25.42
Ni62	18.17	18.45	1.37	0.86	1.03	0.73	0.81	1	6.04	5.73	5.89	5.75	6.14	20.55	20.37
Ga69	14.8	14.78	1.11	0.34	0.5	0.33	0.33	0.32	0.89	0.85	0.91	0.98	0.93	16.91	16.76
Ga71	13.83	13.81	0.72	0.32	0.48	0.3	0.32	0.3	0.81	0.78	0.81	0.86	0.82	14.23	14.12
Rb85	14.43	14.2	1.64	0.021	0.023	0.018	0.019	0.022	0.025	0.024	0.022	0.021	0.023	15.71	16.16
Sr86	16.72	16.74	10.73	0.26	0.29	0.24	0.24	0.27	6.34	6.35	5.91	5.87	6.41	16.74	16.68
Sr88	17.42	17.51	11.56	0.016	0.018	0.016	0.019	0.021	6.88	7.08	6.66	6.74	7.53	19.58	19.42
Y89	18.31	18.4	1.21	2.27	1.93	2.44	2.55	3.28	0.12	0.14	0.11	0.13	0.14	22.59	22.29
Zr90	17.24	17.21	6.34	0.45	0.68	0.47	0.51	0.58	1.89	1.89	1.89	2.09	2.05	19.58	19.36
Nb93	17.78	17.65	0.51	0.013	0.016	0.014	0.012	0.015	0.018	0.016	0.017	0.018	0.016	19.52	19.35
Cs133	15.39	14.63	0.056	0.0097	0.01	0.009	0.0098	0.011	0.012	0.011	0.011	0.0094	0.011	20.06	20.56
Ba137	14.1	14.15	22.12	0.067	0.08	0.053	0.063	0.065	0.08	0.081	0.067	0.073	0.066	14.19	14.21
La139	14.63	14.76	0.84	0.0084	0.0096	0.0077	0.0075	0.008	0.11	0.13	0.1	0.13	0.18	16.25	16.12
Ce140	13.9	13.82	1.71	0.011	0.012	0.011	0.012	0.012	0.49	0.52	0.44	0.52	0.59	14.08	14.02
Pr141	14.88	14.91	0.24	0.0097	0.0097	0.0096	0.0095	0.01	0.12	0.12	0.11	0.12	0.13	15.72	15.59
Nd146	16.19	16.11	1.09	0.094	0.099	0.097	0.097	0.1	0.85	0.83	0.77	0.86	0.89	19.16	18.93
Sm152	16.25	16.48	0.25	0.11	0.13	0.12	0.12	0.13	0.24	0.24	0.24	0.25	0.24	19.21	19.04
Eu153	14.57	14.66	0.084	0.057	0.061	0.059	0.058	0.061	0.062	0.064	0.059	0.064	0.062	15.74	15.61
Gd158	15.97	16.25	0.26	0.25	0.29	0.26	0.26	0.29	0.16	0.16	0.15	0.17	0.16	19.03	18.89
Dy161	16.6	16.89	0.27	0.4	0.38	0.42	0.45	0.51	0.092	0.097	0.086	0.085	0.092	20.21	20.01
Ho165	17.23	17.64	0.054	0.093	0.077	0.1	0.1	0.13	0.014	0.015	0.013	0.013	0.014	21.04	20.92
Er167	16.86	17.02	0.15	0.29	0.21	0.32	0.32	0.45	0.048	0.049	0.042	0.042	0.044	20.29	20.03
Yb172	18.62	18.7	0.17	0.32	0.21	0.36	0.35	0.57	0.046	0.046	0.038	0.036	0.043	23.67	23.28
Lu175	19.68	20.29	0.029	0.054	0.035	0.067	0.062	0.1	0.01	0.009	0.0089	0.0079	0.0091	26.62	26.22
Hf178	17.84	18.23	0.22	0.034	0.045	0.033	0.031	0.036	0.11	0.11	0.11	0.11	0.12	22.78	22.49
Ta181	20.81	21.15	0.044	0.012	0.0093	0.0069	0.0078	0.0098	0.012	0.012	0.01	0.011	0.01	28.05	27.46
Pb208	20.21	19.47	0.45	0.017	0.017	0.014	0.016	0.016	0.034	0.033	0.029	0.03	0.035	28.05	27.47
Th232	20.15	20.74	0.26	0.0095	0.011	0.0083	0.0087	0.01	0.013	0.012	0.011	0.011	0.014	26.91	26.52
U238	18.03	17.48	0.075	0.0081	0.01	0.0076	0.0079	0.0077	0.0091	0.011	0.0094	0.0094	0.0081	21.53	21.63

Appendix 6.A 1σ error for LAM-ICP-MS data

Element	STD610-7	STD610-8	BCR-2	0906B-1	0906B-2	0906B-3	0906B-4	0906B-5	0906B-6	0906B-7	0906B-8	0906B-9	0906B-10	STD610-9	STD610-10
Li7	0.207	0.36	0.0788	0.0576	0.0636	0.0515	0.0552	0.062	0.0715	0.0752	0.0693	0.0644	0.0733	0.209	0.237
Be9	0.853	0.761	0.304	0.247	0.269	0.227	0.252	0.234	0.258	0.29	0.269	0.294	0.28	0.732	0.723
B11	1.43	1.22	0.497	0.382	0.398	0.32	0.329	0.397	0.416	0.401	0.379	0.337	0.398	1.22	1.08
Al27	0.931	1.23	0.355	0.278	0.33	0.357	0.319	0.525	0.926	1.31	1.21	1.11	1.42	3.06	1.38
P31	12.76	12.52	4.52	3.5	3.83	3.09	3.08	3.6	3.82	3.97	3.58	3.48	3.47	10.56	9.34
Ca42	219.46	213.08	78.73	59.38	66.5	53.16	52.92	62.37	65.83	72.55	64.8	64.23	66.1	191.01	171.58
Ca43	256.04	262.12	91.63	73.61	82.25	69.62	64.33	77.97	84.89	99.56	89.27	82.85	97.3	255.25	228.28
Sc45	0.336	0.348	0.13	0.0904	0.0996	0.0842	0.0832	0.0959	0.109	0.119	0.106	0.105	0.106	0.326	0.3
Ti47	2.82	2.84	0.981	0.823	0.952	0.722	0.719	0.875	0.919	1.41	1.38	1.28	1.38	3.78	2.71
V51	0.168	0.248	0.066	0.0473	0.0634	0.0505	0.0449	0.0645	0.0685	0.14	0.124	0.121	0.147	0.321	0.225
Co59	0.247	0.242	0.0884	0.0618	0.0781	0.0688	0.067	0.0819	0.0892	0.0838	0.0801	0.0768	0.0797	0.258	0.249
Ni60	1	1.01	0.365	0.26	0.298	0.26	0.225	0.311	0.288	0.369	0.33	0.345	0.358	0.955	0.899
Ni62	7.98	7.08	2.59	2.08	2.07	1.74	1.91	2.26	2.28	2.67	2.2	2.11	2.53	6.63	6.08
Ga69	0.192	0.273	0.0791	0.0574	0.0653	0.0519	0.0592	0.0727	0.0754	0.0878	0.082	0.0711	0.08	0.219	0.255
Ga71	0.319	0.34	0.119	0.0773	0.102	0.0721	0.0827	0.0906	0.109	0.109	0.0951	0.104	0.108	0.276	0.303
Rb85	0.182	0.227	0.0684	0.0589	0.0626	0.0501	0.0504	0.0607	0.0615	0.0634	0.0601	0.0571	0.0602	0.172	0.192
Sr86	2.71	2.5	0.948	0.712	0.783	0.636	0.654	0.731	0.752	0.838	0.752	0.781	0.801	2.25	2.18
Sr88	0.105	0.165	0.0439	0.0266	0.0304	0.0264	0.0287	0.033	0.0303	0.0646	0.0708	0.0598	0.0662	0.165	0.171
Y89	0.114	0.158	0.0452	0.0379	0.0339	0.0262	0.0317	0.035	0.0374	0.0363	0.0407	0.0318	0.0279	0.107	0.156
Zr90	0.265	0.268	0.1	0.0685	0.0854	0.0604	0.0608	0.0631	0.0833	0.0891	0.0807	0.0768	0.0851	0.218	0.262
Nb93	0.133	0.186	0.053	0.0358	0.0453	0.0381	0.0323	0.0381	0.0432	0.044	0.0469	0.0489	0.0424	0.128	0.168
Cs133	0.0899	0.127	0.0335	0.0262	0.0275	0.0245	0.0266	0.0289	0.0296	0.0276	0.03	0.0241	0.0295	0.0755	0.135
Ba137	0.562	0.613	0.214	0.187	0.226	0.142	0.16	0.164	0.21	0.226	0.177	0.198	0.165	0.568	0.601
La139	0.0813	0.144	0.0304	0.0223	0.0254	0.0205	0.0187	0.0202	0.0291	0.0279	0.0232	0.0272	0.0262	0.079	0.118
Ce140	0.0751	0.125	0.0282	0.0239	0.0265	0.0169	0.0173	0.0245	0.0212	0.0279	0.025	0.0234	0.0289	0.085	0.126
Pr141	0.0655	0.107	0.0289	0.0183	0.0187	0.0203	0.0164	0.0238	0.0188	0.0251	0.0228	0.0231	0.0231	0.0726	0.106
Nd146	0.439	0.458	0.136	0.123	0.12	0.102	0.11	0.128	0.139	0.129	0.116	0.116	0.118	0.35	0.423
Sm152	0.253	0.297	0.0945	0.0727	0.0865	0.0708	0.0701	0.0901	0.0858	0.0845	0.0741	0.0731	0.0855	0.219	0.262
Eu153	0.101	0.187	0.0469	0.0385	0.032	0.0276	0.0324	0.0386	0.0308	0.0411	0.0386	0.0323	0.0397	0.12	0.15
Gd158	0.293	0.337	0.107	0.0868	0.0987	0.0797	0.0835	0.11	0.0891	0.0959	0.0889	0.0943	0.0907	0.268	0.339
Dy161	0.457	0.382	0.0983	0.107	0.126	0.107	0.111	0.111	0.121	0.151	0.131	0.113	0.125	0.406	0.459
Ho165	0.0761	0.132	0.0337	0.0229	0.0222	0.0209	0.0188	0.0258	0.0242	0.027	0.0203	0.0212	0.0248	0.0689	0.109
Er167	0.294	0.402	0.116	0.0908	0.102	0.0887	0.076	0.0985	0.104	0.107	0.0985	0.0898	0.0934	0.286	0.328
Yb172	0.343	0.422	0.113	0.0937	0.115	0.0802	0.0813	0.096	0.116	0.122	0.097	0.085	0.112	0.309	0.363
Lu175	0.0785	0.134	0.0297	0.0255	0.0186	0.0221	0.0193	0.0257	0.0267	0.024	0.0239	0.019	0.0243	0.0669	0.112
Hf178	0.27	0.346	0.102	0.0809	0.0918	0.0707	0.0634	0.0789	0.0796	0.0872	0.0731	0.0698	0.0873	0.263	0.315
Ta181	0.0961	0.122	0.0399	0.0346	0.0242	0.017	0.0209	0.026	0.0305	0.0294	0.0262	0.0307	0.0272	0.0789	0.127
Pb208	0.139	0.209	0.0672	0.0483	0.0441	0.0374	0.0436	0.0461	0.0447	0.0441	0.046	0.042	0.0521	0.128	0.241
Th232	0.108	0.144	0.0355	0.0264	0.0286	0.0222	0.0228	0.0292	0.0301	0.0276	0.0281	0.0257	0.0262	0.0816	0.129
U238	0.0823	0.208	0.0304	0.0217	0.0285	0.0206	0.0215	0.0199	0.0212	0.0308	0.0258	0.0246	0.0205	0.0761	0.127

Appendix 6.B LLD (99% confidence) for LAM-ICP-MS data

Element	STD610-14	STD610-15	BCR-4	0905B-1	0905B-2	0905B-3	0905B-4	0905B-5	0905B-6	0905B-7	0905B-8	0905B-9	0905B-10	0905B-11	0905B-12	STD610-16	STD610-17
Li7	15.53	15.52	0.34	0.064	0.077	0.091	0.15	0.19	3.58	3.08	0.057	0.07	1.35	1.69	0.91	16	16.22
Be9	33.08	32.6	0.19	0.06	0.09	0.086	0.58	0.55	0.25	0.24	0.079	0.089	0.19	0.21	0.27	34.34	33.99
B11	20.34	20.33	0.93	0.091	0.15	0.13	1	1	0.53	0.5	0.12	0.14	0.49	0.46	0.59	20.62	20.74
Al27	381.62	378.18	2722.06	3249.67	4987.07	4410.11	5766.26	5194.6	2452.06	1999.97	4379.23	5353.35	1310.24	1337.2	3245.07	387.7	390.39
P31	44.29	41.87	159.65	17.08	30.04	28.02	15.51	15.15	9.73	10.68	19.43	27.49	7.91	9.84	17.29	45.14	45.76
Ca42	2605.41	2605.98	1617.64	1536.76	1538.47	1538.23	1100.95	1104.45	3817.7	3816.71	1537.99	1539.34	3815.93	3815.86	3822.3	2604.96	2604.48
Ca43	2936.28	2881.67	1792.45	1719.09	1729.45	1754.53	1355.37	1324.19	4413.04	4456.01	1823.23	1840.88	4578.45	4638.25	4757.35	3281.61	3336.53
Sc45	15.07	14.95	0.98	0.58	1.29	1.34	0.21	0.22	0.77	0.9	1.29	1.56	0.84	0.97	0.89	15.3	15.3
Ti47	18.51	18.39	544.5	11.07	60.96	27.11	2.36	2.54	124.15	133.82	9.76	13.19	143.33	142.12	154.16	21.05	21.83
V51	14.93	14.78	14.17	2.89	8.92	7.25	0.2	0.13	19.43	21.28	3.53	5.87	18.32	17.6	14.77	15.47	15.56
Co59	14.28	14.09	1.35	1.92	3.54	2.62	0.17	0.15	1.17	1.23	2.85	3.72	1.29	1.34	1.27	15.5	15.8
Ni60	17.22	16.87	0.52	0.2	0.39	0.2	0.52	0.62	4.63	5.23	0.25	0.42	4.51	4.34	3.68	19.6	19.73
Ni62	29.54	27.82	1.45	0.67	1.09	0.8	4.52	4.09	8.71	10.24	0.85	1.13	8.89	9.43	7.24	42.81	42.73
Ga69	14.74	14.5	1.05	0.34	0.6	0.55	1.21	0.99	1.51	1.36	0.43	0.55	0.86	0.87	1.38	16.1	16.24
Ga71	14.59	14.48	0.74	0.34	0.61	0.56	0.92	0.97	1.5	1.37	0.43	0.57	0.85	0.89	1.33	15.97	15.88
Rb85	14.59	14.35	1.65	0.017	0.022	0.019	0.43	0.12	0.023	0.02	0.016	0.02	0.014	0.014	0.22	16.07	16.21
Sr86	18.44	18.47	11.84	0.81	0.26	0.24	104.75	98.85	1.74	2.15	0.19	0.22	3.17	2.93	42.1	21.14	20.92
Sr88	17.26	17.48	11.22	0.75	0.018	0.02	99.22	93.61	1.53	1.9	0.014	0.012	2.88	2.67	38.31	18.99	18.88
Y89	16.37	16.4	1	0.66	1.73	1.33	0.086	0.065	0.046	0.038	1.43	1.74	0.1	0.094	0.14	17.58	17.42
Zr90	16.1	16.13	5.46	0.32	0.77	0.46	0.14	0.16	1.73	1.92	0.25	0.58	2.56	2.28	2.21	16.59	16.47
Nb93	17.09	16.98	0.46	0.011	0.017	0.014	0.079	0.083	0.017	0.014	0.012	0.014	0.0095	0.0091	0.028	17.52	17.45
Cs133	11.33	11.25	0.043	0.0057	0.013	0.0092	0.053	0.055	0.011	0.0097	0.0074	0.01	0.0077	0.007	0.027	11.47	11.52
Ba137	15.22	14.98	23.19	0.2	0.082	0.16	24.37	5.41	0.1	0.12	0.053	0.056	0.05	0.044	4.86	16.58	16.67
La139	13.75	13.72	0.72	0.0079	0.011	0.011	0.13	0.19	0.065	0.063	0.0086	0.01	0.12	0.12	0.16	13.74	13.72
Ce140	14.86	14.63	1.76	0.018	0.019	0.017	0.16	0.22	0.34	0.35	0.012	0.019	0.63	0.6	0.68	16.16	16.23
Pr141	15.18	15.06	0.22	0.0092	0.013	0.0097	0.05	0.051	0.088	0.086	0.0084	0.013	0.13	0.12	0.15	16.18	16.1
Nd146	14.99	14.82	0.95	0.11	0.14	0.093	0.28	0.28	0.57	0.52	0.089	0.13	0.76	0.68	0.87	15.92	15.9
Sm152	15.67	15.4	0.24	0.13	0.18	0.13	0.16	0.13	0.17	0.15	0.13	0.16	0.21	0.19	0.27	16.94	17.07
Eu153	15.11	14.95	0.073	0.085	0.08	0.076	0.087	0.085	0.063	0.055	0.08	0.083	0.071	0.067	0.09	16.32	16.7
Gd158	15.08	14.84	0.22	0.22	0.32	0.26	0.18	0.16	0.1	0.088	0.24	0.29	0.13	0.12	0.2	16.05	16.18
Dy161	15.97	15.66	0.23	0.2	0.4	0.32	0.19	0.23	0.062	0.047	0.3	0.39	0.068	0.063	0.12	17.75	17.84
Ho165	15.8	15.57	0.045	0.029	0.079	0.058	0.045	0.047	0.011	0.0087	0.058	0.073	0.0099	0.0099	0.02	16.85	16.89
Er167	15.75	15.56	0.13	0.07	0.23	0.17	0.17	0.21	0.037	0.036	0.17	0.22	0.034	0.032	0.071	17.17	17.1
Yb172	15.42	15.3	0.13	0.046	0.18	0.14	0.18	0.17	0.039	0.031	0.16	0.2	0.027	0.027	0.063	15.9	15.85
Lu175	16.31	16.28	0.023	0.0076	0.032	0.023	0.04	0.047	0.0096	0.0068	0.027	0.036	0.0059	0.0052	0.015	18.56	18.35
Hf178	14.71	14.59	0.17	0.021	0.042	0.035	0.13	0.14	0.11	0.11	0.025	0.032	0.11	0.1	0.13	15.09	15.04
Ta181	15.75	15.75	0.034	0.0057	0.0096	0.0095	0.057	0.053	0.011	0.0092	0.0073	0.0097	0.0066	0.0072	0.018	16.17	16.06
Pb208	13.95	13.75	0.34	0.015	0.02	0.018	0.5	0.47	0.026	0.025	0.013	0.015	0.022	0.02	0.16	14.98	15
Th232	16.83	16.7	0.21	0.006	0.012	0.01	0.058	0.048	0.012	0.011	0.0098	0.011	0.013	0.015	0.026	18.79	18.61
U238	16.92	16.84	0.074	0.0049	0.01	0.0092	0.048	0.051	0.0098	0.0081	0.0073	0.0083	0.0065	0.0058	0.016	19.43	19.26

Appendix 6.A 1σ error for LAM-ICP-MS data

Element	STD610-14	STD610-15	BCR-4	0905B-1	0905B-2	0905B-3	0905B-4	0905B-5	0905B-6	0905B-7	0905B-8	0905B-9	0905B-10	0905B-11	0905B-12	STD610-16	STD610-17
Li7	0.255	0.244	0.0542	0.0381	0.072	0.0707	0.307	0.35	0.0704	0.0804	0.0679	0.0584	0.0495	0.0578	0.151	0.2	0.257
Be9	0.966	0.888	0.228	0.162	0.244	0.228	1.46	1.43	0.274	0.244	0.205	0.221	0.224	0.2	0.519	0.706	0.812
B11	1.17	1.25	0.303	0.236	0.402	0.318	1.84	2.03	0.404	0.36	0.289	0.346	0.277	0.274	0.709	1	1.07
Al27	1.32	1.19	0.38	0.392	1.36	0.865	14.27	4.6	1.26	1.96	1.67	2.73	2.17	1.7	4.06	5.09	1.83
P31	10.69	11	3.03	2.08	3.67	3.35	17.56	19.06	3.59	3.19	2.66	3.15	2.47	2.36	6.26	9.11	8.51
Ca42	174.69	179.9	49.29	33.89	58.79	53.97	290.11	301.05	59.16	54.98	48.09	52.22	40.77	45.88	119.76	153.06	143.1
Ca43	245.26	256.77	69.44	50.25	81.47	78.82	423.31	450.72	86.68	87.03	70.26	76.62	59.61	74.15	180.8	230.03	207.64
Sc45	0.34	0.338	0.0941	0.0586	0.104	0.089	0.526	0.544	0.108	0.0914	0.0791	0.0955	0.0763	0.0745	0.188	0.252	0.328
Ti47	2.32	2.24	0.698	0.594	0.737	0.858	5.14	4.04	0.864	1.33	1.26	0.809	0.675	1.37	3.76	4.02	2.31
V51	0.238	0.239	0.052	0.0373	0.0645	0.0616	0.567	0.322	0.0554	0.14	0.133	0.0815	0.0764	0.159	0.386	0.325	0.28
Co59	0.327	0.252	0.0664	0.0497	0.079	0.0764	0.48	0.376	0.0848	0.077	0.0701	0.0928	0.0704	0.0647	0.157	0.211	0.301
Ni60	1.04	0.935	0.262	0.215	0.294	0.309	1.32	1.51	0.277	0.323	0.233	0.274	0.241	0.301	0.634	0.809	0.917
Ni62	7.06	7.41	1.91	1.35	2.36	1.67	12.32	9.89	2.74	2.27	1.71	2.15	1.6	1.64	3.94	6.22	5.76
Ga69	0.285	0.286	0.0618	0.0423	0.0728	0.0625	0.362	0.313	0.0668	0.0707	0.062	0.0658	0.0521	0.0583	0.153	0.203	0.283
Ga71	0.297	0.339	0.0825	0.0583	0.0962	0.0769	0.464	0.437	0.0926	0.095	0.0855	0.082	0.0696	0.0797	0.188	0.245	0.355
Rb85	0.243	0.231	0.0501	0.0363	0.0564	0.0509	0.281	0.292	0.06	0.0508	0.0426	0.0521	0.0379	0.0379	0.1	0.161	0.24
Sr86	1.98	2.25	0.618	0.395	0.726	0.664	3.53	3.7	0.795	0.579	0.508	0.573	0.502	0.475	1.27	1.97	1.74
Sr88	0.166	0.16	0.0328	0.0219	0.035	0.0298	0.144	0.31	0.126	0.0395	0.0342	0.0258	0.0177	0.0515	0.122	0.337	0.212
Y89	0.185	0.176	0.0225	0.017	0.0387	0.0342	0.242	0.171	0.0359	0.0303	0.0228	0.0407	0.0368	0.0269	0.0601	0.0909	0.193
Zr90	0.27	0.289	0.0687	0.0446	0.0626	0.0698	0.358	0.412	0.0678	0.0857	0.0753	0.0646	0.0524	0.0868	0.189	0.229	0.313
Nb93	0.196	0.193	0.0308	0.0269	0.0462	0.0373	0.206	0.218	0.0442	0.0395	0.0312	0.0374	0.0252	0.0229	0.0733	0.0794	0.262
Cs133	0.12	0.155	0.0242	0.0153	0.0304	0.0245	0.137	0.14	0.0293	0.0265	0.0186	0.028	0.0208	0.0189	0.0503	0.0715	0.169
Ba137	0.62	0.663	0.165	0.123	0.211	0.156	0.911	1.1	0.221	0.167	0.144	0.129	0.134	0.113	0.291	0.7	0.655
La139	0.128	0.12	0.0219	0.0152	0.0254	0.0253	0.105	0.155	0.0258	0.0199	0.0187	0.0223	0.0198	0.0194	0.0428	0.0761	0.175
Ce140	0.116	0.131	0.0205	0.0133	0.0265	0.0226	0.115	0.118	0.0235	0.0229	0.0211	0.0201	0.0159	0.026	0.0608	0.0723	0.174
Pr141	0.113	0.13	0.019	0.0128	0.0181	0.0169	0.109	0.0797	0.0179	0.0203	0.018	0.0192	0.0128	0.0164	0.0366	0.0511	0.172
Nd146	0.457	0.458	0.116	0.068	0.11	0.127	0.634	0.573	0.0932	0.107	0.0868	0.107	0.0725	0.0936	0.255	0.331	0.474
Sm152	0.303	0.349	0.0606	0.0499	0.0766	0.0712	0.423	0.299	0.0661	0.062	0.0767	0.0632	0.0529	0.0602	0.132	0.184	0.324
Eu153	0.188	0.189	0.0288	0.0195	0.0298	0.0375	0.176	0.204	0.0364	0.0279	0.0273	0.0372	0.0222	0.0215	0.0487	0.0917	0.203
Gd158	0.294	0.336	0.084	0.0496	0.0958	0.089	0.5	0.406	0.108	0.0937	0.0619	0.0779	0.0546	0.0658	0.139	0.242	0.383
Dy161	0.49	0.43	0.11	0.0723	0.123	0.114	0.469	0.643	0.111	0.0843	0.0769	0.0818	0.0885	0.0668	0.2	0.319	0.496
Ho165	0.127	0.134	0.0188	0.0138	0.0259	0.0199	0.116	0.118	0.0271	0.02	0.0171	0.02	0.0166	0.0174	0.0295	0.0619	0.178
Er167	0.326	0.363	0.0782	0.0625	0.08	0.0987	0.405	0.587	0.0873	0.0994	0.0587	0.0951	0.0694	0.0614	0.171	0.293	0.39
Yb172	0.351	0.36	0.107	0.057	0.106	0.0931	0.484	0.478	0.105	0.0793	0.0813	0.091	0.0656	0.0661	0.15	0.246	0.409
Lu175	0.109	0.116	0.0187	0.0132	0.0266	0.021	0.107	0.115	0.0254	0.0178	0.0169	0.0205	0.0153	0.012	0.0383	0.0593	0.159
Hf178	0.315	0.308	0.0756	0.0497	0.081	0.081	0.321	0.331	0.079	0.0756	0.0662	0.069	0.0492	0.0547	0.16	0.248	0.38
Ta181	0.134	0.151	0.0246	0.0162	0.025	0.0264	0.158	0.13	0.0301	0.0248	0.019	0.0276	0.0175	0.0196	0.0445	0.0717	0.195
Pb208	0.205	0.188	0.0323	0.0306	0.0479	0.0404	0.202	0.249	0.0462	0.0418	0.0325	0.0362	0.0242	0.0278	0.0677	0.107	0.249
Th232	0.124	0.151	0.0264	0.016	0.0265	0.0289	0.15	0.129	0.0315	0.029	0.0194	0.0248	0.0172	0.0204	0.0504	0.0564	0.196
U238	0.14	0.128	0.0175	0.0126	0.0272	0.0256	0.124	0.141	0.0263	0.0222	0.0191	0.0217	0.0174	0.0138	0.0412	0.0613	0.168

Appendix 6.B LLD (99% confidence) for LAM-ICP-MS data

Element	STD610-16	STD610-17	BCR-5	0905B-13	0905B-14	0905B-15	0905B-16	0905B-17	0905B-18	0905B-19	0905B-20	0905B-21	0905B-22	STD610-18	STD610-19
Li7	15.62	15.76	0.35	0.15	0.14	0.049	1.51	1.88	1.31	1.17	1.1	2.19	1.38	16.38	16.68
Be9	33.09	32.65	0.19	0.39	0.29	0.081	0.2	0.2	0.19	0.2	0.2	0.21	0.21	33.82	34.61
B11	20.88	20.98	0.43	0.78	0.7	0.13	0.59	0.58	0.61	0.72	0.65	0.57	0.54	21.5	22
Al27	389.76	392.13	2847.53	5510.62	5608	4306.91	2110.03	1899.12	1314.6	1189.04	1234.89	2309.24	1412.21	417.88	431.27
P31	41.44	41.92	155.36	13.4	13.29	17.8	13.17	9.18	7.84	8.14	8.27	7.76	8.87	43.69	41.92
Ca42	2605.7	2604.14	1618.24	1085.75	1081.84	1538.37	3816.13	3816.9	3816.34	3817.1	3816.38	3816.83	3817.01	2602.36	2603.56
Ca43	2649.83	2656.25	1637.91	1171.07	1161.12	1558.61	3799.86	3822.21	3847	3867.76	3843.63	3828.55	3825.46	2675.44	2670
Sc45	14.75	14.73	0.98	0.14	0.11	0.75	0.69	0.88	0.75	0.93	0.89	0.77	0.72	14.73	14.8
Ti47	18.59	19.01	566.29	2.11	1.67	20.23	106.86	124.97	174.84	131.64	145.53	140.43	168.91	22.19	23.27
V51	14.58	14.64	14.39	0.12	0.059	3.97	25.36	20.7	18.16	17.73	18.03	23.08	18.74	14.8	14.77
Co59	13.42	13.48	1.29	0.099	0.083	2.6	1.4	1.14	1.15	1.12	1.15	0.98	1.15	13.54	13.56
Ni60	16.2	16.12	0.53	0.44	0.34	0.25	5.12	4.69	3.98	3.76	3.73	5.02	4.58	17.17	17.05
Ni62	20.92	19.91	1.32	3.03	2.1	0.9	6.48	6.22	5.42	5.27	5.15	6.78	6.75	24.47	25.66
Ga69	13.67	13.61	1.03	0.79	0.79	0.42	0.9	0.91	0.75	0.73	0.76	1.07	0.81	13.66	13.65
Ga71	14.83	14.59	0.78	0.75	0.79	0.46	1.01	1.01	0.87	0.85	0.89	1.27	0.96	16.59	16.56
Rb85	13.58	13.55	1.63	0.086	0.071	0.019	0.021	0.02	0.016	0.018	0.018	0.02	0.018	13.78	13.96
Sr86	20.57	20.15	13.22	111.65	115.34	0.23	3.85	3.16	3.63	3.49	3.63	3.01	3.79	25.02	26.66
Sr88	17.96	17.71	11.69	99.23	100.81	0.039	3.22	2.66	3.07	2.87	2.91	2.45	3.04	19.99	20.79
Y89	15.9	15.71	0.97	0.051	0.034	0.82	0.21	0.1	0.12	0.15	0.16	0.077	0.096	16.32	16.5
Zr90	16.28	16.15	5.61	0.1	0.07	0.48	3.45	2.61	2.5	2.68	2.66	2.82	2.53	16.92	17.3
Nb93	17.1	17.03	0.46	0.054	0.039	0.013	0.013	0.013	0.011	0.013	0.012	0.014	0.012	17.62	17.96
Cs133	12.12	12.2	0.046	0.035	0.031	0.0087	0.0078	0.0096	0.0093	0.0087	0.0086	0.0094	0.0093	13.55	14.1
Ba137	14.45	14.41	22.07	4.73	5.46	0.062	0.41	0.19	0.059	0.059	0.052	0.086	0.055	15.03	15.39
La139	14.32	14.32	0.77	0.17	0.19	0.0073	0.16	0.095	0.11	0.12	0.13	0.093	0.11	15.2	15.63
Ce140	15.14	15.11	1.83	0.22	0.24	0.013	0.76	0.47	0.56	0.71	0.75	0.53	0.57	17.04	17.8
Pr141	15.61	15.45	0.23	0.037	0.036	0.01	0.16	0.11	0.13	0.16	0.17	0.12	0.12	17.05	17.66
Nd146	14.61	14.5	0.96	0.18	0.18	0.11	0.88	0.61	0.7	0.87	0.87	0.63	0.66	15.14	15.47
Sm152	14.37	14.41	0.22	0.074	0.074	0.12	0.23	0.18	0.19	0.24	0.24	0.17	0.18	14.45	14.55
Eu153	14.19	14.38	0.074	0.056	0.042	0.076	0.074	0.057	0.062	0.072	0.071	0.06	0.061	14.88	15.01
Gd158	14.83	14.87	0.23	0.11	0.089	0.21	0.16	0.13	0.15	0.17	0.17	0.11	0.13	15.96	16.47
Dy161	14.86	14.8	0.23	0.16	0.11	0.21	0.089	0.075	0.078	0.093	0.091	0.063	0.074	15.73	16.18
Ho165	14.99	14.93	0.044	0.029	0.024	0.038	0.014	0.012	0.011	0.014	0.013	0.01	0.011	15.28	15.5
Er167	15.18	15	0.14	0.13	0.093	0.11	0.047	0.036	0.034	0.041	0.038	0.036	0.034	15.99	16.38
Yb172	15.23	15.12	0.14	0.12	0.093	0.095	0.043	0.037	0.029	0.037	0.031	0.036	0.034	15.5	15.72
Lu175	16.15	15.79	0.025	0.033	0.025	0.017	0.0089	0.008	0.0073	0.0067	0.0066	0.0074	0.0075	18.01	18.62
Hf178	14.3	14.22	0.16	0.092	0.08	0.028	0.11	0.11	0.11	0.12	0.11	0.12	0.11	14.28	14.3
Ta181	15.86	15.67	0.035	0.034	0.028	0.0065	0.0074	0.0082	0.0075	0.0081	0.008	0.0087	0.0083	16.34	16.56
Pb208	13.35	13.23	0.3	0.35	0.34	0.013	0.028	0.023	0.026	0.03	0.03	0.022	0.026	13.68	13.9
Th232	17.3	16.94	0.2	0.039	0.029	0.0077	0.02	0.027	0.017	0.015	0.013	0.014	0.015	19.82	20.71
U238	17	16.64	0.072	0.029	0.024	0.0075	0.0071	0.0096	0.0084	0.0086	0.0061	0.0073	0.0068	19.16	19.89

Appendix 6.A 1σ error for LAM-ICP-MS data

Element	STD610-16	STD610-17	BCR-5	0905B-13	0905B-14	0905B-15	0905B-16	0905B-17	0905B-18	0905B-19	0905B-20	0905B-21	0905B-22	STD610-18	STD610-19
Li7	0.203	0.255	0.0857	0.233	0.181	0.0563	0.0604	0.0754	0.0684	0.0803	0.0689	0.0758	0.0804	0.182	0.284
Be9	0.716	0.804	0.301	0.993	0.688	0.215	0.249	0.28	0.181	0.209	0.215	0.259	0.228	0.601	0.853
B11	1.02	1.06	0.342	1.33	0.962	0.313	0.322	0.395	0.278	0.327	0.32	0.345	0.357	0.868	1.05
Al27	5.17	1.81	0.5	3.36	4.09	1.4	2.23	1.92	1.77	1.9	1.61	1.89	2.02	4.29	2.39
P31	9.28	8.44	3.32	11.47	9.26	2.86	3.02	3.23	2.7	2.94	2.77	3.18	3.01	7.33	8.64
Ca42	155.65	141.86	54.72	191.44	154.3	46.4	48.79	55.91	48.11	56.57	52.73	59.31	55.96	137.34	144.32
Ca43	233.8	205.77	80.52	263.53	211.54	64.92	71.38	86.81	77.93	96.47	83.86	96.92	85.03	216.58	210.92
Sc45	0.256	0.325	0.113	0.34	0.252	0.0833	0.0798	0.0954	0.0787	0.0928	0.0843	0.0953	0.0926	0.21	0.315
Ti47	4.09	2.29	0.66	4.84	2.52	0.591	0.814	1.43	1.41	1.85	1.54	1.84	1.48	4.41	2.75
V51	0.33	0.277	0.085	0.294	0.148	0.0442	0.0732	0.161	0.158	0.199	0.179	0.19	0.18	0.433	0.311
Co59	0.215	0.298	0.0914	0.259	0.219	0.0656	0.0847	0.0861	0.0735	0.088	0.0755	0.0839	0.0813	0.192	0.35
Ni60	0.823	0.908	0.311	1.2	0.941	0.284	0.249	0.297	0.286	0.304	0.308	0.34	0.305	0.836	0.989
Ni62	6.33	5.7	2.58	8.43	5.44	2.34	2.03	2.45	2.09	2.15	1.96	2.26	1.93	5.24	6.13
Ga69	0.207	0.28	0.101	0.26	0.178	0.0612	0.0646	0.0697	0.0691	0.0717	0.0673	0.0773	0.0727	0.2	0.265
Ga71	0.248	0.352	0.108	0.298	0.248	0.074	0.0798	0.0861	0.0751	0.0798	0.0897	0.103	0.0974	0.202	0.338
Rb85	0.164	0.238	0.0782	0.216	0.171	0.0528	0.0559	0.0474	0.0418	0.0466	0.0487	0.0486	0.0478	0.113	0.258
Sr86	1.99	1.72	0.703	2.29	2.06	0.606	0.523	0.643	0.536	0.603	0.556	0.578	0.609	1.52	1.73
Sr88	0.342	0.21	0.0603	0.166	0.307	0.107	0.0365	0.0518	0.0523	0.0638	0.0528	0.0606	0.0617	0.142	0.213
Y89	0.0923	0.191	0.0581	0.143	0.0934	0.0295	0.0318	0.0338	0.0259	0.0282	0.0244	0.0278	0.0327	0.0737	0.203
Zr90	0.233	0.311	0.103	0.273	0.194	0.0532	0.0654	0.0984	0.0877	0.103	0.0942	0.107	0.0965	0.275	0.314
Nb93	0.0806	0.259	0.0707	0.146	0.101	0.0357	0.0372	0.0343	0.0288	0.0334	0.0317	0.0386	0.0304	0.0821	0.253
Cs133	0.0727	0.168	0.0508	0.0908	0.0859	0.0236	0.0208	0.0251	0.0222	0.0223	0.024	0.0245	0.0254	0.053	0.161
Ba137	0.711	0.649	0.237	0.962	0.529	0.164	0.179	0.157	0.127	0.153	0.134	0.148	0.142	0.417	0.629
La139	0.0772	0.173	0.048	0.0931	0.0801	0.0174	0.0213	0.0209	0.0188	0.0241	0.0235	0.0251	0.0185	0.0545	0.168
Ce140	0.0735	0.172	0.0449	0.0915	0.059	0.0218	0.019	0.0301	0.0214	0.0283	0.0291	0.0297	0.0277	0.0662	0.162
Pr141	0.0519	0.171	0.0418	0.0681	0.0471	0.0125	0.0173	0.0186	0.016	0.0201	0.0168	0.019	0.0195	0.0404	0.156
Nd146	0.336	0.471	0.146	0.423	0.392	0.105	0.0969	0.0935	0.0892	0.12	0.124	0.123	0.101	0.304	0.439
Sm152	0.187	0.322	0.101	0.157	0.175	0.0615	0.0744	0.056	0.0553	0.0716	0.0598	0.0571	0.0639	0.157	0.316
Eu153	0.0931	0.202	0.0628	0.124	0.0826	0.0265	0.0288	0.0363	0.0288	0.0301	0.0287	0.0356	0.0255	0.0711	0.229
Gd158	0.245	0.38	0.115	0.296	0.238	0.0624	0.0819	0.0795	0.0653	0.0782	0.0719	0.0704	0.0706	0.155	0.34
Dy161	0.324	0.492	0.152	0.432	0.28	0.103	0.0976	0.0968	0.0814	0.0866	0.0898	0.105	0.0996	0.2	0.474
Ho165	0.0628	0.177	0.0502	0.0772	0.0679	0.0193	0.0157	0.0203	0.0129	0.0179	0.0199	0.0202	0.0196	0.0437	0.152
Er167	0.297	0.387	0.125	0.365	0.235	0.0707	0.0902	0.0775	0.0653	0.0758	0.0764	0.0913	0.0652	0.222	0.383
Yb172	0.25	0.406	0.136	0.328	0.254	0.0598	0.0845	0.0991	0.0677	0.0893	0.0628	0.0902	0.0877	0.226	0.396
Lu175	0.0602	0.158	0.0447	0.0911	0.0727	0.0205	0.0166	0.02	0.0193	0.0164	0.0177	0.0199	0.0189	0.0515	0.174
Hf178	0.251	0.377	0.112	0.241	0.224	0.0596	0.0648	0.0669	0.0527	0.0626	0.0595	0.0682	0.0724	0.18	0.305
Ta181	0.0728	0.194	0.0573	0.0891	0.0766	0.0163	0.0198	0.0203	0.0207	0.0205	0.0212	0.0238	0.0206	0.0567	0.188
Pb208	0.109	0.247	0.0761	0.158	0.121	0.0344	0.038	0.0339	0.0302	0.033	0.032	0.0413	0.0411	0.0789	0.231
Th232	0.0572	0.194	0.0594	0.112	0.0793	0.0195	0.0216	0.0233	0.0213	0.02	0.0219	0.0201	0.0196	0.0639	0.18
U238	0.0624	0.167	0.0429	0.083	0.0635	0.02	0.0174	0.0273	0.0224	0.0237	0.0144	0.018	0.016	0.0504	0.19

Appendix 6.B LLD (99% confidence) for LAM-ICP-MS data

Appendix 6.C – MATLAB element mapping scripts.

elmap_incl_Ti.m

```
%Step one in element mapping process - takes the ASCII format data and builds an XxXx9 matrix

function [answer] = elmap(numrows,numcols,fname);

% The function elmap takes three arguments.
% They are
% 1) numrows {integer}
%        the number of rows in the element maps
%        usually 256, 512 or 1024
%
% 2) numcols {integer}
%        the number of columns in the element maps
%        usually 256, 512 or 1024
%
% 3) fname {string}
%        the first part of the file names (XX in part 1),
%        e.g. jww0905B would be entered for files
%        called jww0905BAl.txt jww0905BCa.txt jww0905BFe.txt etc
%
% The function elmap must be invoked by:
% elmap(numrows,numcols,'fname');
%        e.g elmap(256,512,'jww0905B');
%
% The following protocol must be followed:
% The user must delete the header manually from each txt file before running
% this script.
% THE USER MUST TYPE save fname fname (e.g. save jww0905B jww0905B); after the function has finished!
%
% Nathan Daczko 15-4-09. James Watton 20-4-09

for h = 1:9,
   switch h,
      case 1,
         element = 'Si';
      case 2,
         element = 'Ti';
      case 3,
         element = 'Al';
      case 4,
         element = 'Fe';
      case 5,
         element = 'Mn';
      case 6,
         element = 'Mg';
      case 7,
         element = 'Ca';
      case 8,
         element = 'Na';
      case 9,
         element = 'K';
   end

   % Open and load the txt data file into data

   command = ['load -ASCII ',fname,element,'.txt'];
```

```
    eval(command);
    command = ['data=',fname,element,';'];
    eval(command);

    % Place the data into element variables

    switch h
        case 1,
            Si = data;
        case 2,
            Ti = data;
        case 3,
            Al = data;
        case 4,
            Fe = data;
        case 5,
            Mn = data;
        case 6,
            Mg = data;
        case 7,
            Ca = data;
        case 8,
            Na = data;
        case 9,
            K = data;
    end

        % plot a figure to make sure that all is ok

        figure, imagesc(data), axis image, colorbar;
end

clear data numcols numrows element command;

% Place the data as a n x m x 9 matrix called fname in the workspace

answer = Si;
answer(:,:,2) = Ti;
answer(:,:,3) = Al;
answer(:,:,4) = Fe;
answer(:,:,5) = Mn;
answer(:,:,6) = Mg;
answer(:,:,7) = Ca;
answer(:,:,8) = Na;
answer(:,:,9) = K;


assignin('caller',fname,answer);

'Reminder: Type save fname fname (e.g. save jww0904c jww0904c;)'
```

BackgroundCorrection_cpx.m

```
% Peak minus background correction for omphacite
% Ask for the name of the .mat file to have the background subtracted.

[thefile,pname] = uigetfile('*.mat','Please choose the n x m x 9 matrix to correct');
if thefile == 0 & pname == 0,
   msgbox('Without data, this program will exit','ERROR');
   return;
else
   thefile = thefile(:,1:(length(thefile)-4));
   thefile = cellstr(thefile);
   thefile = thefile{1};
   pname = strcat(pname,thefile);
   load(pname);
end

% Open the .mat file into a variable called data
% Subtract the background from data

data=eval(thefile);
[numrows,numcol,numvars]=size(data);

% Ask for the count time and the current it was collected
% at

prompt   = {'Enter the time (in seconds, e.g. 0.15 for 150 milliseconds) that x-rays were counted for at each step'};
title    = 'Data count time';
lines = 1;
counttime = inputdlg(prompt,title,lines);
counttime = cellstr(counttime);
counttime = str2num(counttime{1});

prompt   = {'Enter the current (nA) used to collect the element map (e.g. 100)'};
title    = 'Current';
lines = 1;
current = inputdlg(prompt,title,lines);
current = cellstr(current);
current = str2num(current{1});

%comment below is for iron collected on LIF (for running testing scripts on raw EMP data)

bkg = ones(numrows,numcol,9);
bkg(:,:,1) = bkg(:,:,1)*1.336957209*counttime*current;
bkg(:,:,2) = bkg(:,:,2)*1.552641279*counttime*current;
bkg(:,:,3) = bkg(:,:,3)*3.886243605*counttime*current;
bkg(:,:,4) = bkg(:,:,4)*6.389486047*counttime*current;
%bkg(:,:,4) = bkg(:,:,4)*1.277897209*counttime*current;
bkg(:,:,5) = bkg(:,:,5)*2.928797674*counttime*current;
bkg(:,:,6) = bkg(:,:,6)*1.395613140*counttime*current;
bkg(:,:,7) = bkg(:,:,7)*1.140997093*counttime*current;
bkg(:,:,8) = bkg(:,:,8)*2.118233953*counttime*current;
bkg(:,:,9) = bkg(:,:,9)*2.728440814*counttime*current;

data=data-bkg;

% Save the answer into a file called bkgfname.mat where fname.mat was the input file

savefile = strcat(thefile, 'bkgcpx');
assignin('base',savefile,data);
save(savefile,savefile);
```

BackgroundCorrection_grt.m

```
% Peak minus background correction for garnet
% Ask for the name of the .mat file to have the background subtracted.

[thefile,pname] = uigetfile('*.mat','Please choose the n x m x 9 matrix to correct');
if thefile == 0 & pname == 0,
   msgbox('Without data, this program will exit','ERROR');
   return;
else
   thefile = thefile(:,1:(length(thefile)-4));
   thefile = cellstr(thefile);
   thefile = thefile{1};
   pname = strcat(pname,thefile);
   load(pname);
end

% Open the .mat file into a variable called data
% Subtract the background from data

data=eval(thefile);
[numrows,numcol,numvars]=size(data);

% Ask for the count time and the current it was collected
% at

prompt   = {'Enter the time (in seconds, e.g. 0.15 for 150 milliseconds) that x-rays were counted for at each step'};
title    = 'Data count time';
lines = 1;
counttime = inputdlg(prompt,title,lines);
counttime = cellstr(counttime);
counttime = str2num(counttime{1});

prompt   = {'Enter the current (nA) used to collect the element map (e.g. 100)'};
title    = 'Current';
lines = 1;
current = inputdlg(prompt,title,lines);
current = cellstr(current);
current = str2num(current{1});

%comment below is for iron collected on LIF (for running testing scripts on raw EMP data)

bkg = ones(numrows,numcol,9);
bkg(:,:,1) = bkg(:,:,1)*1.484802639*counttime*current;
bkg(:,:,2) = bkg(:,:,2)*2.226104907*counttime*current;
bkg(:,:,3) = bkg(:,:,3)*5.637643657*counttime*current;
bkg(:,:,4) = bkg(:,:,4)*10.03962352*counttime*current;
$bkg(:,:,4) = bkg(:,:,4)*2.007924704*counttime*current;
bkg(:,:,5) = bkg(:,:,5)*2.272357083*counttime*current;
bkg(:,:,6) = bkg(:,:,6)*1.412778657*counttime*current;
bkg(:,:,7) = bkg(:,:,7)*1.183247222*counttime*current;
bkg(:,:,8) = bkg(:,:,8)*0.989139676*counttime*current;
bkg(:,:,9) = bkg(:,:,9)*2.623990278*counttime*current;

data=data-bkg;

% Save the answer into a file called bkgfname.mat where fname.mat was the input file

savefile = strcat(thefile, 'bkggrt');
assignin('base',savefile,data);
save(savefile,savefile);
```

BenceAlbee_Love_Scott.m

```
% Bence-Albee matrix correction of x-ray maps from the GEMOC SX-100
% using the alpha-factors of Love and Scott (from Armstrong, 1984 Microbeam Analysis)
% Nathan Daczko & James Watton 20-4-09

disp(' ');
disp('  ************************************************************************');
disp('Bence-Albee matrix correction procedure for X-Ray maps from the GEMOC SX-100');
disp('                  Nathan Daczko and James Watton');
disp('             Department of Earth and Planetary Sciences');
disp('                     Macquarie University');
disp('  ************************************************************************');
disp(' ');
disp(' ');

% Ask for the name of the .mat file to be analysed.

[thefile,pname] = uigetfile('*.mat','Please choose the n x m x 8 matrix to correct');
if thefile == 0 & pname == 0,
   msgbox('Without data, this program will exit','ERROR');
   return;
else
   thefile = thefile(:,1:(length(thefile)-4));
   thefile = cellstr(thefile);
   thefile = thefile{1};
   pname = strcat(pname,thefile);
   load(pname);
end

% Ask for the count time and iteration number

prompt   = {'Enter the time (in seconds, e.g. 0.15 for 150 milliseconds) that x-rays were counted for at each step'};
title    = 'Data count time';
lines = 1;
counttime = inputdlg(prompt,title,lines);
counttime = cellstr(counttime);
counttime = str2num(counttime{1});

prompt   = {'Enter the number of times you wish the Bence-Albee to iterate (3 or greater)'};
title    = 'Iterate';
lines = 1;
iterate = inputdlg(prompt,title,lines);
iterate = cellstr(iterate);
iterate = str2num(iterate{1});

% Open the .mat file into a variable called data
% Convert the data to a counts/second format

data=eval(thefile);
data=data.*(1/counttime);

% Declare alpha-factors (Love & Scott alpha-factors (from Armstrong, 1984 Microbeam Analysis))
% alpha=[SiO2   TiO2   Al2O3          FeO      MnO      MgO      CaO      Na2O     K2O
%     Si   1.000  1.083  1.494          1.279    1.211    1.431    1.048    1.356    0.987
%     Ti   1.111  1.000  1.089          0.894    0.846    1.099    1.161    1.071    1.132
%     Al   0.999  1.220  1.000          1.556    1.451    1.756    1.149    1.645    1.072
%     Fe   1.148  1.087  1.128          1.000    0.987    1.141    1.124    1.114    1.093
%     Mn   1.161  1.113  1.140          1.014    1.000    1.153    1.149    1.125    1.117
%     Mg   1.086  1.440  1.009          2.013    1.846    1.000    1.302    2.134    1.196
%     Ca   1.091  0.863  1.068          0.932    0.902    1.073    1.000    1.044    1.197
%     Na   1.352  2.021  1.242          3.066    2.778    1.130    1.741    1.000    1.564
%     K    1.144  0.935  1.118          0.987    0.959    1.120    0.858    1.088    1.000
```

```
alpha=[   1.000    1.083    1.494    1.279    1.211    1.431    1.048    1.356    0.987
      1.111  1.000  1.089    0.894    0.846    1.099    1.161    1.071    1.132
      0.999  1.220  1.000    1.556    1.451    1.756    1.149    1.645    1.072
      1.148  1.087  1.128    1.000    0.987    1.141    1.124    1.114    1.093
      1.161  1.113  1.140    1.014    1.000    1.153    1.149    1.125    1.117
      1.086  1.440  1.009    2.013    1.846    1.000    1.302    2.134    1.196
      1.091  0.863  1.068    0.932    0.902    1.073    1.000    1.044    1.197
      1.352  2.021  1.242    3.066    2.778    1.130    1.741    1.000    1.564
      1.144  0.935  1.118    0.987    0.959    1.120    0.858    1.088    1.000 ];

% Declare beta-factors for the standards (taken from excel spreadsheet BetaFactors.xls)
%         Si                  Ti                  Al                  Fe                  Mn                  Mg                  Ca                  Na
                    K

beta = [1.023153047         1.000439969         0.999554086         1.128935799         1.084905728         1.109841781         1.047044051
          1.29164622        1.111077012];

% Declare standards information (peak-background in counts/second; concentration is wt% oxide)
%                   Si        Ti        Al        Fe        Mn        Mg        Ca        Na        K

stdconc = [    0.5172         1.0000    0.6270    0.0762    0.4071    0.5078    0.4827    0.1146    0.1540    ];

% 20nA Fe = LLIF for EMP!  Si=TAP Ti=LPET Al=LTAP Fe=LLIF Mn=LLIF Mg=TAP Ca=LPET Na=LTAP K=LPET
% stdcounts = [   9685.4  29728   37636   851.56   4386   8318    13793   3195.4  4142.6  ];

% for Element Mapping Session One (includes testing)
% 100 nA Fe = LIF for mapping! Si=TAP Ti=LLIF Al=LTAP Fe=LIF Mn=LLIF Mg=TAP Ca=LPET Na=LTAP K=LPET
% stdcounts = [      48427     17837     188180    584.5     21930     41590     68965   15977       20713     ];

% for Element Mapping Session Two
% 100 nA Fe = LLIF for mapping! Ti = LIF!   Si=TAP Ti=LIF Al=LTAP Fe=LLIF Mn=LLIF Mg=TAP Ca=LPET Na=LTAP K=LPET
stdcounts = [          48427     3520      188180    4258      21930     41590     68965   15977       20713     ];

% Perform the matrix correction for each point in the matrix

[m,n,o] = size(data);
answer = zeros(m,n,o);
g = waitbar(0,'Please wait for the Bence-Albee procedure to finish');
for h = 1:m,
  for i = 1:n,

    % Make the first approximation of the chemical composition of the unknown
                    % For each element k[E,U] = (I[E,U]/I[E,STD])*(C[E,STD]/B[E,STD])
                    % where  k[E,U] is wt% oxide for element E in unknown
                    %        I[E,U] is intensity of counts of element E in unknown          {get from element maps}
                    %        I[E,STD] is intensity of counts of element E in standard       {get from standards variable}
                    %        C[E,STD] is wt% oxide concentration of element E in standard   {get from concentration variable}
                    %        B[E,STD] is beta-factor for element E in standard              {get from beta variable}

    conc1 = zeros(1,o);
    for j = 1:o,
      conc1(1,j) = (data(h,i,j)/stdcounts(1,j))*(stdconc(1,j)/beta(1,j));
    end

    conc2 = conc1;

    for iteratenum = 1:iterate,

          % Make the first iteration
          % The first approximation of the chemical composition is used to determine
          % the correction factors (beta) using the relation:
          % B[E,U] = (k[E1,U]*a[E,E1] + k[E2,U]*a[E,E2] + ... k[En,U]*a[E,En])/(SUM(k(E1)...k(En)))
```

```
            % where  B[E,U]      is beta correction-factor for element E in the unknown
            %        k[E1,U] ... k[En,U] are estimates of concentration made in the first approximation
            %        a(E,E1] ... a[E,En] are the alpha-factors for element E1...n on element E

            sumconc = sum(conc2);
            beta1 = zeros(1,o);
            for j = 1:o,
            ka = 0;
            for k = 1:o,
            ka = ka + (conc2(1,k)*alpha(j,k));
            end
            beta1(1,j) = (1/sumconc)*ka;
            end

            % These new beta-factors are used to determine the next estimate of the chemical composition
            % of the unknown: for each element the new k[E,U] = B[E,U]* old k[E,U]

            conc2 = zeros(1,o);
            for j = 1:o,
            conc2(1,j) = (beta1(1,j))*(conc1(1,j));
            end
    end

    % Put the result into the answer matrix

    answer(h,i,:) = reshape(conc2,1,1,o);
  end
  waitbar((h*i)/(n*m));
end
close(g);

% Save the answer into a file called bafname.mat where fname.mat was the input file

savefile = strcat(thefile, 'ba_LS');
assignin('base',savefile,answer);
save(savefile,savefile);
```

BenceAlbee_Kato_Transposed.m

```
% Bence-Albee matrix correction of x-ray maps from the GEMOC SX-100
% using the alpha-factors of Kato (2005) and transposed alpha-factors from Kato (2005)
% Nathan Daczko & James Watton 20-4-09

disp(' ');
disp('  ************************************************************************');
disp('Bence-Albee matrix correction procedure for X-Ray maps from the GEMOC SX-100');
disp('                    Nathan Daczko and James Watton');
disp('              Department of Earth and Planetary Sciences');
disp('                      Macquarie University');
disp('  ************************************************************************');
disp(' ');
disp(' ');

clear

% Ask for the name of the .mat file to be analysed.

[thefile,pname] = uigetfile('*.mat','Please choose the n x m x 9 matrix to correct');
if thefile == 0 & pname == 0,
   msgbox('Without data, this program will exit','ERROR');
   return;
else
   thefile = thefile(:,1:(length(thefile)-4));
   thefile = cellstr(thefile);
   thefile = thefile{1};
   pname = strcat(pname,thefile);
   load(pname);
end

% Ask for the count time and iteration number

prompt   = {'Enter the time (in seconds, e.g. 0.15 for 150 milliseconds) that x-rays were counted for at each step'};
title    = 'Data count time';
lines = 1;
counttime = inputdlg(prompt,title,lines);
counttime = cellstr(counttime);
counttime = str2num(counttime{1});

prompt   = {'Enter the number of times you wish the Bence-Albee to iterate (3 or greater)'};
title    = 'Iterate';
lines = 1;
iterate = inputdlg(prompt,title,lines);
iterate = cellstr(iterate);
iterate = str2num(iterate{1});

% Open the .mat file into a variable called data
% Convert the data to a counts/second format

data=eval(thefile);
data=data.*(1/counttime);

% Declare alpha-factors (Love & Scott alpha-factors (from Armstrong, 1984 Microbeam Analysis))
% alpha=[SiO2   TiO2        Al2O3    FeO      MnO      MgO      CaO      Na2O     K2O
%     Si   1.000  1.083  1.494       1.279    1.211    1.431    1.048    1.356    0.987
%     Ti   1.111     1.000    1.089    0.894    0.846    1.099    1.161    1.071    1.132
%     Al   0.999  1.220       1.000    1.556    1.451    1.756    1.149    1.645    1.072
%     Fe   1.148  1.087  1.128       1.000    0.987    1.141    1.124    1.114    1.093
%     Mn 1.161  1.113  1.140       1.014    1.000    1.153    1.149    1.125    1.117
%     Mg 1.086  1.440  1.009       2.013    1.846    1.000    1.302    2.134    1.196
```

```
%     Ca  1.091  0.863  1.068          0.932     0.902     1.073     1.000     1.044     1.197
%     Na  1.352  2.021  1.242          3.066     2.778     1.130     1.741     1.000     1.564
%     K   1.144  0.935  1.118          0.987     0.959     1.120     0.858     1.088     1.000
%
%alpha=[ 1.000  1.083  1.494          1.279     1.211     1.431     1.048     1.356     0.987
%     1.111          1.000     1.089     0.894     0.846     1.099     1.161     1.071     1.132
%     0.999  1.220 1.000     1.556     1.451     1.756     1.149     1.645     1.072
%     1.148  1.087  1.128     1.000     0.987     1.141     1.124     1.114     1.093
%     1.161  1.113  1.140     1.014     1.000     1.153     1.149     1.125     1.117
%     1.086  1.440  1.009     2.013     1.846     1.000     1.302     2.134     1.196
%     1.091  0.863  1.068     0.932     0.902     1.073     1.000     1.044     1.197
%     1.352  2.021  1.242     3.066     2.778     1.130     1.741     1.000     1.564
%     1.144  0.935  1.118     0.987     0.959     1.120     0.858     1.088     1.000 ];

%from Kato 2005 (TRANSPOSED)
alpha=[ 1.000  1.055  1.448  1.202     1.138     1.450     1.032     1.357     0.969
     1.127          1.000     1.103     0.880     0.836     1.114     1.171     1.083     1.140
     1.028  1.180  1.000     1.417     1.325     1.741     1.136     1.618     1.054
     1.173  1.102  1.151     1.000     0.988     1.165     1.140     1.136     1.104
     1.186  1.127  1.164     0.979     1.000     1.177     1.166     1.148     1.130
     1.113  1.368  1.035     1.745     1.606     1.000     1.283     2.044     1.177
     1.114  0.877  1.087     0.919     0.888     1.096     1.000     1.062     1.218
     1.416  1.889  1.294     2.541     2.313     1.182     1.724     1.000     1.548
     1.175  0.948  1.144     0.978     0.949     1.152     0.900     1.112  1.000 ];

alpha = alpha.'
% NB: the above command transposes these values BACK to normal Kato alpha-factors.
% to use transposed values, comment out the above command.

% Declare beta-factors for the standards (taken from excel spreadsheet BetaFactors.xls)
%          Si                    Ti                    Al                    Fe                    Mn                    Mg                    Ca                    Na
                    K

% Based on Love & Scott
%beta = [1.023153047          1.000439969          0.999554086          1.128935799          1.084905728          1.109841781          1.047044051
          1.29164622           1.111077012];
% Based on Kato 2005
beta = [1.015428491.00043997          1.01005139           1.15141127           1.09837143           1.10030315           1.05893952           1.34538081
          1.13562344];

% Declare standards information (peak-background in counts/second; concentration is wt% oxide)
%                    Si        Ti        Al        Fe        Mn        Mg        Ca        Na        K

stdconc = [0.5172   1.0000    0.6270    0.0762    0.4071    0.5078    0.4827    0.1146    0.1540    ];

% 20nA Fe = LLIF for EMP!  Si=TAP Ti=LPET Al=LTAP Fe=LLIF Mn=LLIF Mg=TAP Ca=LPET Na=LTAP K=LPET
% stdcounts = [   9685.4  29728   37636   851.56   4386   8318    13793   3195.4  4142.6  ];

% for Element Mapping Session One (includes testing)
% 100 nA Fe = LIF for mapping! Si=TAP Ti=LLIF Al=LTAP Fe=LIF Mn=LLIF Mg=TAP Ca=LPET Na=LTAP K=LPET
% stdcounts = [       48427     17837     188180    584.5     21930     41590     68965   15977         20713     ];

% for Element Mapping Session Two
% 100 nA Fe = LLIF for mapping! Ti = LIF!   Si=TAP Ti=LIF Al=LTAP Fe=LLIF Mn=LLIF Mg=TAP Ca=LPET Na=LTAP K=LPET
stdcounts = [          48427     3520      188180    4258      21930     41590     68965   15977         20713     ];

% Perform the matrix correction for each point in the matrix

[m,n,o] = size(data);
answer = zeros(m,n,o);
g = waitbar(0,'Please wait for the Bence-Albee procedure to finish');
for h = 1:m,
  for i = 1:n,
```

```
    % Make the first approximation of the chemical composition of the unknown
                    % For each element k[E,U] = (I[E,U]/I[E,STD])*(C[E,STD]/B[E,STD])
                    % where  k[E,U] is wt% oxide for element E in unknown
                    %        I[E,U] is intensity of counts of element E in unknown          {get from element maps}
                    %        I[E,STD] is intensity of counts of element E in standard       {get from standards variable}
                    %        C[E,STD] is wt% oxide concentration of element E in standard   {get from concentration variable}
                    %        B[E,STD] is beta-factor for element E in standard        {get from beta variable}

    conc1 = zeros(1,o);
    for j = 1:o,
      conc1(1,j) = (data(h,i,j)/stdcounts(1,j))*(stdconc(1,j)/beta(1,j));
    end

    conc2 = conc1;

    for iteratenum = 1:iterate,

          % Make the first iteration
          % The first approximation of the chemical composition is used to determine
          % the correction factors (beta) using the relation:
          % B[E,U] = (k[E1,U]*a[E,E1] + k[E2,U]*a[E,E2] + ... k[En,U]*a[E,En])/(SUM(k(E1)...k(En)))
          % where  B[E,U]     is beta correction-factor for element E in the unknown
          %        k[E1,U] ... k[En,U] are estimates of concentration made in the first approximation
          %        a(E,E1] ... a[E,En] are the alpha-factors for element E1...n on element E

          sumconc = sum(conc2);
          beta1 = zeros(1,o);
          for j = 1:o,
          ka = 0;
          for k = 1:o,
          ka = ka + (conc2(1,k)*alpha(j,k));
          end
          beta1(1,j) = (1/sumconc)*ka;
          end

          % These new beta-factors are used to determine the next estimate of the chemical composition
          % of the unknown: for each element the new k[E,U] = B[E,U]* old k[E,U]

          conc2 = zeros(1,o);
          for j = 1:o,
          conc2(1,j) = (beta1(1,j))*(conc1(1,j));
          end
    end

    % Put the result into the answer matrix

    answer(h,i,:) = reshape(conc2,1,1,o);
  end
  waitbar((h*i)/(n*m));
end
close(g);

% Save the answer into a file called bafname.mat where fname.mat was the input file

savefile = strcat(thefile, 'ba_K_Tr');
assignin('base',savefile,answer);
save(savefile,savefile);
```

filter0906B.m

```
% Filter garnet, cpx, plag
% Nathan Daczko & James Watton 20-4-2009
load jww0906Bba;

maskgrt = jww0905Bba(:,:,1)>0.3&jww0906Bba(:,:,3)>0.15&jww0906Bba(:,:,4)>0.15;
   Sigrt = mean(nonzeros(maskgrt.*jww0906Bba(:,:,1)));
   Tigrt = mean(nonzeros(maskgrt.*jww0906Bba(:,:,2)));
   Algrt = mean(nonzeros(maskgrt.*jww0906Bba(:,:,3)));
   Fegrt = mean(nonzeros(maskgrt.*jww0906Bba(:,:,4)));
   Mngrt = mean(nonzeros(maskgrt.*jww0906Bba(:,:,5)));
   Mggrt = mean(nonzeros(maskgrt.*jww0906Bba(:,:,6)));
   Cagrt = mean(nonzeros(maskgrt.*jww0906Bba(:,:,7)));
   Nagrt = mean(nonzeros(maskgrt.*jww0906Bba(:,:,8)));
   Kgrt = mean(nonzeros(maskgrt.*jww0906Bba(:,:,9)));
totalgrt = Sigrt+Tigrt+Algrt+Fegrt+Mngrt+Mggrt+Cagrt+Nagrt+Kgrt;

grt = [Sigrt,Tigrt,Algrt,Fegrt,Mngrt,Mggrt,Cagrt,Nagrt,Kgrt,totalgrt];

maskcpx = jww0906Bba(:,:,1)>0.4&jww0906Bba(:,:,7)>0.15&jww0906Bba(:,:,3)<0.2;
   Sicpx = mean(nonzeros(maskcpx.*jww0906Bba(:,:,1)));
   Ticpx = mean(nonzeros(maskcpx.*jww0906Bba(:,:,2)));
   Alcpx = mean(nonzeros(maskcpx.*jww0906Bba(:,:,3)));
   Fecpx = mean(nonzeros(maskcpx.*jww0906Bba(:,:,4)));
   Mncpx = mean(nonzeros(maskcpx.*jww0906Bba(:,:,5)));
   Mgcpx = mean(nonzeros(maskcpx.*jww0906Bba(:,:,6)));
   Cacpx = mean(nonzeros(maskcpx.*jww0906Bba(:,:,7)));
   Nacpx = mean(nonzeros(maskcpx.*jww0906Bba(:,:,8)));
   Kcpx = mean(nonzeros(maskcpx.*jww0906Bba(:,:,9)));
totalcpx = Sicpx+Ticpx+Alcpx+Fecpx+Mncpx+Mgcpx+Cacpx+Nacpx+Kcpx;

cpx = [Sicpx,Ticpx,Alcpx,Fecpx,Mncpx,Mgcpx,Cacpx,Nacpx,Kcpx,totalcpx];

maskplg = jww0906Bba(:,:,1)>0.55&jww0906Bba(:,:,8)>0.05&jww0906Bba(:,:,6)<0.05;
   Siplg = mean(nonzeros(maskplg.*jww0906Bba(:,:,1)));
   Tiplg = mean(nonzeros(maskplg.*jww0906Bba(:,:,2)));
   Alplg = mean(nonzeros(maskplg.*jww0906Bba(:,:,3)));
   Feplg = mean(nonzeros(maskplg.*jww0906Bba(:,:,4)));
   Mnplg = mean(nonzeros(maskplg.*jww0906Bba(:,:,5)));
   Mgplg = mean(nonzeros(maskplg.*jww0906Bba(:,:,6)));
   Caplg = mean(nonzeros(maskplg.*jww0906Bba(:,:,7)));
   Naplg = mean(nonzeros(maskplg.*jww0906Bba(:,:,8)));
   Kplg = mean(nonzeros(maskplg.*jww0906Bba(:,:,9)));
totalplg = Siplg+Tiplg+Alplg+Feplg+Mnplg+Mgplg+Caplg+Naplg+Kplg;

plg = [Siplg,Tiplg,Alplg,Feplg,Mnplg,Mgplg,Caplg,Naplg,Kplg,totalplg];

grt
cpx
plg
imagesc(maskgrt.*jww0906Bba(:,:,4));
figure
imagesc(maskcpx.*jww0906Bba(:,:,6));
figure
imagesc(maskplg.*jww0906Bba(:,:,8));
```

filter0905B.m

```
% Filter garnet, cpx, plag
% Nathan Daczko & James Watton 20-4-2009
load jww0905Bba;

maskgrt = jww0905Bba(:,:,1)>0.3&jww0905Bba(:,:,3)>0.15&jww0905Bba(:,:,4)>0.15;
   Sigrt = mean(nonzeros(maskgrt.*jww0905Bba(:,:,1)));
   Tigrt = mean(nonzeros(maskgrt.*jww0905Bba(:,:,2)));
   Algrt = mean(nonzeros(maskgrt.*jww0905Bba(:,:,3)));
   Fegrt = mean(nonzeros(maskgrt.*jww0905Bba(:,:,4)));
   Mngrt = mean(nonzeros(maskgrt.*jww0905Bba(:,:,5)));
   Mggrt = mean(nonzeros(maskgrt.*jww0905Bba(:,:,6)));
   Cagrt = mean(nonzeros(maskgrt.*jww0905Bba(:,:,7)));
   Nagrt = mean(nonzeros(maskgrt.*jww0905Bba(:,:,8)));
   Kgrt = mean(nonzeros(maskgrt.*jww0905Bba(:,:,9)));
totalgrt = Sigrt+Tigrt+Algrt+Fegrt+Mngrt+Mggrt+Cagrt+Nagrt+Kgrt;

grt = [Sigrt,Tigrt,Algrt,Fegrt,Mngrt,Mggrt,Cagrt,Nagrt,Kgrt,totalgrt];

maskcpx = jww0905Bba(:,:,1)>0.4&jww0905Bba(:,:,7)>0.15&jww0905Bba(:,:,3)<0.2;
   Sicpx = mean(nonzeros(maskcpx.*jww0905Bba(:,:,1)));
   Ticpx = mean(nonzeros(maskcpx.*jww0905Bba(:,:,2)));
   Alcpx = mean(nonzeros(maskcpx.*jww0905Bba(:,:,3)));
   Fecpx = mean(nonzeros(maskcpx.*jww0905Bba(:,:,4)));
   Mncpx = mean(nonzeros(maskcpx.*jww0905Bba(:,:,5)));
   Mgcpx = mean(nonzeros(maskcpx.*jww0905Bba(:,:,6)));
   Cacpx = mean(nonzeros(maskcpx.*jww0905Bba(:,:,7)));
   Nacpx = mean(nonzeros(maskcpx.*jww0905Bba(:,:,8)));
   Kcpx = mean(nonzeros(maskcpx.*jww0905Bba(:,:,9)));
totalcpx = Sicpx+Ticpx+Alcpx+Fecpx+Mncpx+Mgcpx+Cacpx+Nacpx+Kcpx;

cpx = [Sicpx,Ticpx,Alcpx,Fecpx,Mncpx,Mgcpx,Cacpx,Nacpx,Kcpx,totalcpx];

maskplg = jww0905Bba(:,:,1)>0.55&jww0905Bba(:,:,8)>0.05&jww0905Bba(:,:,6)<0.05;
   Siplg = mean(nonzeros(maskplg.*jww0905Bba(:,:,1)));
   Tiplg = mean(nonzeros(maskplg.*jww0905Bba(:,:,2)));
   Alplg = mean(nonzeros(maskplg.*jww0905Bba(:,:,3)));
   Feplg = mean(nonzeros(maskplg.*jww0905Bba(:,:,4)));
   Mnplg = mean(nonzeros(maskplg.*jww0905Bba(:,:,5)));
   Mgplg = mean(nonzeros(maskplg.*jww0905Bba(:,:,6)));
   Caplg = mean(nonzeros(maskplg.*jww0905Bba(:,:,7)));
   Naplg = mean(nonzeros(maskplg.*jww0905Bba(:,:,8)));
   Kplg = mean(nonzeros(maskplg.*jww0905Bba(:,:,9)));
totalplg = Siplg+Tiplg+Alplg+Feplg+Mnplg+Mgplg+Caplg+Naplg+Kplg;

plg = [Siplg,Tiplg,Alplg,Feplg,Mnplg,Mgplg,Caplg,Naplg,Kplg,totalplg];

grt
cpx
plg
imagesc(maskgrt.*jww0905Bba(:,:,4));
figure
imagesc(maskcpx.*jww0905Bba(:,:,6));
figure
imagesc(maskplg.*jww0905Bba(:,:,8));
```

ELMAPGUI.m

```
function elmapgui(action);
%   ELMAPGUI
%   The graphical user interface for element maps
%   It must use an n x m x 9 matrix where each layer represents
%   Si, Ti, Al, Fe, Mn, Mg, Ca, Na, K respectively
%
%   This graphical user interface has the following features:
%   1) change between each of the eight elements
%   2) change between a number of colormaps
%   3) load a new element map {n x m x 8 (9 incl Ti) matrix}
%   4) view the current map with a new lower and upper limit of display
%   5) pick a point from any element map and view its data
%   6) zoom in on a region of an element map by draging a rectangle
%   7) zoom out to full view
%   8) get bulk rock information
%   9) get information of the program
%   10) exit by pressing the close button
%
%   Nathan Daczko, 7-4-09. James Watton 20-4-09

global EM_NAMES EM_DISP EM_PLOTCMD EM_DATA data clim S el thefile pname

if nargin < 1,
   action = 'initialize';
elseif nargin > 1
   disp('Too many arguments');
   return;
end;

if strcmp(action,'initialize')
   oldFigNumber=watchon;

   %==================================================================
   % Set all the global variables
   EM_NAMES = [ 'Si '
      'Ti '
      'Al '
      'Fe '
      'Mn '
      'Mg '
      'Ca '
      'Na '
      'K  ''];

   EM_PLOTCMD = str2mat('imagesc(data), colormap(S), colorbar(''horiz''), axis image;',...
      ['imagesc(data,clim), colormap(S), colorbar(''horiz''), axis image;']);

   EM_DISP = 1;

   S =  jet;
   if (get(0,'ScreenDepth') == 1)
      S = gray(64);
   end

   %==================================================================
   figNumber = figure('colormap',S,'visible','on','NumberTitle','off', ...
      'Name','Element Mapping','pointer','arrow');

   wids = 0.1;
   axes('position', [0.02 .05 .9*(.9-wids) .93], ...
```

```
   'vis','off');

%==================================================================
% Information for all buttons
labelColor=192/255*[1 1 1];
top=0.96;
bottom=0.04;
left=0.75;
yInitLabelPos=0.90;
left=0.78;
labelWid=0.17;
labelHt=0.040;
btnWid=0.17;
btnHt=0.040;
% Spacing between the label and the button for the same command
btnOffset=0.003;
% Spacing between the button and the next command's label
spacing=0.003;

%==================================================================
% The CONSOLE frame
frmBorder=0.02;
yPos=0.05-frmBorder;
frmPos=[left-frmBorder yPos btnWid+2*frmBorder 0.9+2*frmBorder];
h=uicontrol( ...
   'Style','frame', ...
   'Units','normalized', ...
   'Position',frmPos, ...
   'BackgroundColor',[0.5 0.5 0.5]);

%=========================================================================
% The element command popup menu

% Menu label info
btnNumber=1;
yLabelPos=top-(btnNumber-1)*(btnHt+labelHt+spacing);
labelPos=[left yLabelPos-labelHt labelWid labelHt];
h = uicontrol( ...
   'Style','text', ...
   'Units','normalized', ...
   'Position',labelPos, ...
   'BackgroundColor',labelColor, ...
   'HorizontalAlignment','left', ...
   'String',' Element');

% Pop-up menu info
btnPos=[left yLabelPos-labelHt-btnHt-btnOffset btnWid btnHt];

popupStr = str2mat(' Si',' Ti',' Al',' Fe', ...
   ' Mn',' Mg',' Ca',' Na',' K ');

uicontrol('Style','popup',...
   'Units','normalized', ...
   'Position', btnPos, ...
   'String',popupStr, ...
   'Callback','elmapgui(''element'')');

%=========================================================================
% The colormap list

% Menu label info
btnNumber=2;
yLabelPos=top-(btnNumber-1)*(btnHt+labelHt+spacing);
```

```
labelPos=[left yLabelPos-labelHt labelWid labelHt];
uicontrol( ...
   'Style','text', ...
   'Units','normalized', ...
   'Position',labelPos, ...
   'BackgroundColor',labelColor, ...
   'HorizontalAlignment','left', ...
   'String',' Colormap');

% Pop-up menu info
btnPos=[left yLabelPos-labelHt-btnHt-btnOffset btnWid btnHt];

popupStr = str2mat('jet   ','hot   ','pink  ','cool  ','bone  ',...
   'hsv   ','copper','gray  ','winter','ndjet');

uicontrol('Style','popup',...
   'Units','normalized', ...
   'Position', btnPos, ...
   'String',popupStr, ...
   'Callback','elmapgui(''mapcolor'')');

%=========================================================================
% The LOAD button
btnNumber = 3;
yLabelPos=top-(btnNumber-1)*(btnHt+labelHt+spacing);
btnPos=[left yLabelPos-labelHt-btnHt-btnOffset btnWid 1.5*btnHt];
btnHndl=uicontrol( ...
   'Style','pushbutton', ...
   'Units','normalized', ...
   'Position', btnPos, ...
   'String','Load (nxmx9)', ...
   'Callback','elmapgui(''loadmap'')');

%=========================================================================
% The CUTOFF button
btnNumber = 4;
yLabelPos=top-(btnNumber-1)*(btnHt+labelHt+spacing);
btnPos=[left yLabelPos-labelHt-btnHt-btnOffset btnWid 1.5*btnHt];
btnHndl=uicontrol( ...
   'Style','pushbutton', ...
   'Units','normalized', ...
   'Position', btnPos, ...
   'String','Pick a cutoff', ...
   'Callback','elmapgui(''cutoff'')');

%=========================================================================
% The PICK A POINT button
btnNumber = 5;
yLabelPos=top-(btnNumber-1)*(btnHt+labelHt+spacing);
btnPos=[left yLabelPos-labelHt-btnHt-btnOffset btnWid 1.5*btnHt];
btnHndl=uicontrol( ...
   'Style','pushbutton', ...
   'Units','normalized', ...
   'Position', btnPos, ...
   'String','Pick a point', ...
   'Callback','elmapgui(''pick'')');

%=========================================================================
% The PICK A REGION OF INTEREST button
btnNumber = 6;
yLabelPos=top-(btnNumber-1)*(btnHt+labelHt+spacing);
btnPos=[left yLabelPos-labelHt-btnHt-btnOffset btnWid 1.5*btnHt];
btnHndl=uicontrol( ...
```

```
   'Style','pushbutton', ...
   'Units','normalized', ...
   'Position', btnPos, ...
   'String','Pick a region', ...
   'Callback','elmapgui(''region'')');

%=========================================================================
% The ZOOM OUT button
btnNumber = 7;
yLabelPos=top-(btnNumber-1)*(btnHt+labelHt+spacing);
btnPos=[left yLabelPos-labelHt-btnHt-btnOffset btnWid 1.5*btnHt];
btnHndl=uicontrol( ...
   'Style','pushbutton', ...
   'Units','normalized', ...
   'Position', btnPos, ...
   'String','Zoom out', ...
   'Callback','elmapgui(''zoomout'')');

%=========================================================================
% The BULK ROCK button
btnNumber = 8;
yLabelPos=top-(btnNumber-1)*(btnHt+labelHt+spacing);
btnPos=[left yLabelPos-labelHt-btnHt-btnOffset btnWid 1.5*btnHt];
btnHndl=uicontrol( ...
   'Style','pushbutton', ...
   'Units','normalized', ...
   'Position', btnPos, ...
   'String','Bulk Rock', ...
   'Callback','elmapgui(''bulk'')');


%=========================================================================
% The INFO button
btnNumber = 9;
yLabelPos=top-(btnNumber-1)*(btnHt+labelHt+spacing);
uicontrol( ...
   'Style','pushbutton', ...
   'Units','normalized', ...
   'Position',[left yLabelPos-labelHt-btnHt-btnOffset btnWid 1.5*btnHt], ...
   'String','Info', ...
   'Callback','elmapgui(''info'')');

%=========================================================================
% The CLOSE button
uicontrol( ...
   'Style','pushbutton', ...
   'Units','normalized', ...
   'Position',[left bottom btnWid 1.5*btnHt], ...
   'String','Close', ...
   'Callback','elmapgui(''close'')');

%=========================================================================
% Initialize with load a file

close(1);
[thefile,pname] = uigetfile('*.mat','Load a element map matrix');
if thefile == 0 & pname == 0,
   msgbox('Without a map, this program will exit','ERROR');
   close(2);
   return;
else
   thefile = thefile(:,1:(length(thefile)-4));
   thefile = cellstr(thefile);
```

```
      thefile = thefile{1};
      pname = strcat(pname,thefile);
      load(pname);
      [n,m,o] = size(eval(thefile));
      if o == 9,
         EM_DATA = eval(thefile);
         el=1;
         data = EM_DATA(:,:,el);
         set(gcf,'UserData',1);
         n = EM_DISP;
         eval([EM_PLOTCMD(n,:)]);
         drawnow;
         set(gcf,'pointer','arrow');
      else
         msgbox('The file you load must be n x m x 8!','ERROR!');
         close(2);
         return;
      end
   end

   %=====================================================================
   watchoff(oldFigNumber);

   % END of INITIALIZE section
   %=====================================================================
   % Element callback.

elseif strcmp(action,'element')
   hndl=gco;
   popStr=get(hndl,'String');
   el=get(hndl,'Value');
   selectStr=deblank(popStr(el,:));
   drawnow;

   data = EM_DATA(:,:,el);
   n = EM_DISP;
   eval([EM_PLOTCMD(n,:)]);
   drawnow;
   set(gcf,'pointer','arrow');

   %=====================================================================
   % Mapcolor callback.

elseif strcmp(action,'mapcolor')
   hndl=gco;
   popStr=get(hndl,'String');
   value=get(hndl,'Value');
   selectStr=deblank(popStr(value,:));
   drawnow;

   % Load file, if available. Otherwise, use FUNCS to do a fnct evaluation
   S = popStr(value,:);
   S = deblank(S);
   n = EM_DISP;
   eval([EM_PLOTCMD(n,:)]);
   drawnow;
   set(gcf,'pointer','arrow');

   %=====================================================================
   % Load a map callback.

elseif strcmp(action,'loadmap')
   [thefile,pname] = uigetfile('*.mat','Load a element map matrix');
```

```
   if thefile == 0 & pname == 0,
      % don't do anything
   else
      thefile = thefile(:,1:(length(thefile)-4));
      thefile = cellstr(thefile);
      thefile = thefile{1};
      pname = strcat(pname,thefile);
      load(pname);
      [n,m,o] = size(eval(thefile));
      if o == 9,
         EM_DATA = eval(thefile);
         data = EM_DATA(:,:,el);
         n = EM_DISP;
         eval([EM_PLOTCMD(n,:)]);
         drawnow;
         set(gcf,'pointer','arrow');
      else
         msgbox('The file you load must be n x m x 8!','ERROR!');
      end
   end


   %=====================================================================
   % Pick a cut off callback.

elseif strcmp(action,'cutoff')
   prompt   = {'Enter the matrix [clow,chigh] for the lower and upper cutoffs:'};
   title    = 'Limit display range for the element map';
   lines = 1;
   clim = inputdlg(prompt,title,lines);
   try,
      clim = eval(clim{1});
      eval([EM_PLOTCMD(2,:)]);
      drawnow;
      set(gcf,'pointer','arrow');
   catch,
      msgbox('Enter the lower and upper limit as [lolim,hilim] e.g [0,120]','ERROR!');
   end

   %=====================================================================
   % Pick a point callback.

elseif strcmp(action,'pick')
   [n,m] = size(data);
   [x,y] = ginput(1);
   if x > 0 & y > 0 & x < m & y < n,
      x = round(x);
      y = round(y);
      message = {['X =  ',num2str(x),'  Y =  ',num2str(y)];...
         ['Si =  ',num2str((EM_DATA(y,x,1)*100),'%1.2f')];...
         ['Ti =  ',num2str((EM_DATA(y,x,2)*100),'%1.2f')];...
         ['Al =  ',num2str((EM_DATA(y,x,3)*100),'%1.2f')];...
         ['Fe =  ',num2str((EM_DATA(y,x,4)*100),'%1.2f')];...
         ['Mn =  ',num2str((EM_DATA(y,x,5)*100),'%1.2f')];...
         ['Mg =  ',num2str((EM_DATA(y,x,6)*100),'%1.2f')];...
         ['Ca =  ',num2str((EM_DATA(y,x,7)*100),'%1.2f')];...
         ['Na =  ',num2str((EM_DATA(y,x,8)*100),'%1.2f')];...
                                 ['K  =  ',num2str((EM_DATA(y,x,9)*100),'%1.2f')];...
                                          ['Total =  ',num2str((EM_DATA(y,x,1)+EM_DATA(y,x,2)+...
                                          EM_DATA(y,x,3)+EM_DATA(y,x,4)+EM_DATA(y,x,5)+EM_DATA(y,x,6)+...
                                          EM_DATA(y,x,7)+EM_DATA(y,x,8)+EM_DATA(y,x,9))*100)];...
         ['   ']    };
      msgbox(message,'Wt% data');
```

```
    set(gcf,'pointer','arrow');
  else,
    msgbox('Don''t press outside the regions of the map!','ERROR');
  end

  %=========================================================================
  % Region of interest

elseif strcmp(action,'region')
  waitforbuttonpress;
  point1 = get(gca,'CurrentPoint');    % button down detected
  finalRect = rbbox;                   % return figure units
  point2 = get(gca,'CurrentPoint');    % button up detected
  point1 = point1(1,1:2);              % extract x and y
  point2 = point2(1,1:2);
  p1 = min(point1,point2);             % calculate locations
  offset = abs(point1-point2);         % and dimensions

  [n,m] = size(data);
  if round(p1(2)) > 0 & round(p1(2)+offset(2)) < n & p1(1) > 0 & round(p1(1)+offset(1)) < m,
    EM_DATA = EM_DATA(round(p1(2)):round(p1(2)+offset(2)),round(p1(1)):round(p1(1)+offset(1)),:);
    data = EM_DATA(:,:,el);
    n = EM_DISP;
    eval([EM_PLOTCMD(n,:)]);
    drawnow;
    set(gcf,'pointer','arrow');
  else
    msgbox('Don''t press outside the regions of the map!','ERROR');
  end


  %=========================================================================
  % Zoom out

elseif strcmp(action,'zoomout')
  load(pname);
  EM_DATA = eval(thefile);
  data = EM_DATA(:,:,el);
  n = EM_DISP;
  eval([EM_PLOTCMD(n,:)]);
  drawnow;
  set(gcf,'pointer','arrow');

            %=============================================================================
  % Calculate bulk rock.

elseif strcmp(action,'bulk')
   Si=mean2(EM_DATA(:,:,1))*100;
   Ti=mean2(EM_DATA(:,:,2))*100;
            Al=mean2(EM_DATA(:,:,3))*100;
            Fe=mean2(EM_DATA(:,:,4))*100;
            Mn=mean2(EM_DATA(:,:,5))*100;
            Mg=mean2(EM_DATA(:,:,6))*100;
            Ca=mean2(EM_DATA(:,:,7))*100;
            Na=mean2(EM_DATA(:,:,8))*100;
            K=mean2(EM_DATA(:,:,9))*100;
            message = {['Si =  ',num2str(Si,'%1.2f')];...
          ['Ti =  ',num2str(Ti,'%1.2f')];...
          ['Al =  ',num2str(Al,'%1.2f')];...
          ['Fe =  ',num2str(Fe,'%1.2f')];...
          ['Mn =  ',num2str(Mn,'%1.2f')];...
          ['Mg =  ',num2str(Mg,'%1.2f')];...
          ['Ca =  ',num2str(Ca,'%1.2f')];...
```

```
            ['Na =  ',num2str(Na,'%1.2f')];...
                                                ['K  =  ',num2str(K,'%1.2f')];...
                                                ['Total =  ',num2str(Si+Ti+Al+Fe+Mn+Mg+Ca+Na+K)];...
            ['   ']     };
      msgbox(message,'Bulk Rock Wt% data');
      set(gcf,'pointer','arrow');

elseif strcmp(action,'info'),
   helpwin(mfilename)

elseif strcmp(action,'close'),
   close(gcf);
   clear global EM_NAMES EM_DISP EM_PLOTCMD EM_DATA data clim S el;

end;
```

Comment	0906A 1.1+ g trav	0906A 1.1+ g trav	0906A 1.1+ g trav	0906A 1.1+ g trav	0906A 1.1+ g trav	0906A 1.1+ g trav	0906A 1.1+ g trav	0906A 1.2 g r	0906A 1.3 g c	0906A 1.5 g r	0906A 1.6 g c
X	9093	9089	9069	9038	9028	9013	9002	8636	8614	8422	8448
Y	27099	27093	27079	27051	27041	27025	27007	27072	27024	27104	27137
Z	73	73	73	73	73	73	73	73	73	73	73
SiO2	40.86	39.01	38.82	38.85	38.88	38.82	38.98	38.70	38.81	38.73	39.03
TiO2	0.06	0.08	0.09	0.08	0.09	0.10	0.05	0.04	0.13	0.07	0.09
Al2O3	19.71	22.18	22.06	22.05	22.14	22.11	22.09	22.05	22.15	21.95	22.03
Cr2O3	0.07	0.09	0.12	0.07	0.07	0.12	0.07	0.08	0.08	0.05	0.03
Fe2O3	2.68	2.26	2.85	2.45	2.49	2.23	2.23	2.42	2.81	2.03	1.90
FeO	18.00	20.50	20.50	20.50	20.50	20.50	20.50	20.20	20.50	20.50	20.90
MnO	0.62	0.79	0.73	0.75	0.77	0.76	0.75	0.74	0.77	0.73	0.73
MgO	10.01	9.15	9.34	9.45	9.36	9.21	9.06	9.27	9.38	8.43	8.66
CaO	8.60	7.15	6.76	6.64	6.67	6.78	7.24	6.97	6.50	7.85	7.42
Na2O	0.30	0.01	0.02	0.02	0.02	0.02	0.01	0.02	0.02	0.03	0.02
K2O	0.00	0.00	0.00	0.00	0.00	0.00	0.00	0.00	0.00	0.00	0.00
NiO	0.07	0.01	0.04	0.00	0.00	0.03	0.00	0.00	0.00	0.02	0.00
Total	100.72	101.00	101.04	100.62	100.74	100.46	100.75	100.23	100.87	100.18	100.62
FeO	20.41	22.54	23.06	22.70	22.74	22.51	22.51	22.38	23.03	22.33	22.61
Num ox	12	12	12	12	12	12	12	12	12	12	12
Si	3.07	2.94	2.93	2.94	2.94	2.94	2.95	2.94	2.93	2.95	2.96
Ti	0.00	0.00	0.01	0.00	0.01	0.01	0.00	0.00	0.01	0.00	0.00
Al	1.74	1.97	1.96	1.97	1.97	1.98	1.97	1.97	1.97	1.97	1.97
Cr	0.00	0.01	0.01	0.00	0.00	0.01	0.00	0.00	0.00	0.00	0.00
Fe3+	0.15	0.13	0.16	0.14	0.14	0.13	0.13	0.14	0.16	0.12	0.11
Fe2+	1.13	1.29	1.29	1.30	1.30	1.30	1.30	1.28	1.29	1.31	1.32
Mn	0.04	0.05	0.05	0.05	0.05	0.05	0.05	0.05	0.05	0.05	0.05
Mg	1.12	1.03	1.05	1.06	1.05	1.04	1.02	1.05	1.05	0.96	0.98
Ca	0.69	0.58	0.55	0.54	0.54	0.55	0.59	0.57	0.53	0.64	0.60
Na	0.04	0.00	0.00	0.00	0.00	0.00	0.00	0.00	0.00	0.00	0.00
K	0.00	0.00	0.00	0.00	0.00	0.00	0.00	0.00	0.00	0.00	0.00
Ni	0.00	0.00	0.00	0.00	0.00	0.00	0.00	0.00	0.00	0.00	0.00
Total	8.00	8.00	8.00	8.00	8.00	8.00	8.00	8.00	8.00	8.00	8.00
Tetrahedral (Si)	3.07	2.94	2.93	2.94	2.94	2.94	2.95	2.94	2.93	2.95	2.96
Tetrahedral (Al)	-0.07	0.06	0.07	0.06	0.06	0.06	0.05	0.06	0.07	0.05	0.04
Tetrahedral (3)	3.00	3.00	3.00	3.00	3.00	3.00	3.00	3.00	3.00	3.00	3.00
Octahedral (2)	1.97	2.05	2.06	2.05	2.06	2.06	2.05	2.06	2.07	2.05	2.04
Cavities (3)	2.98	2.95	2.94	2.95	2.94	2.94	2.95	2.94	2.92	2.95	2.95
XAlm	0.38	0.44	0.44	0.44	0.44	0.44	0.44	0.44	0.44	0.44	0.45
XPyp	0.38	0.35	0.36	0.36	0.36	0.35	0.35	0.36	0.36	0.32	0.33
XGrs	0.23	0.20	0.19	0.18	0.18	0.19	0.20	0.19	0.18	0.22	0.20
XSps	0.01	0.02	0.02	0.02	0.02	0.02	0.02	0.02	0.02	0.02	0.02

Appendix 6.D EMP data for garnet with calculated end member proportions. XAlm = $Fe^{2+}/(Fe^{2+}+Mn+Mg+Ca)$. XPyp = $Mg/(Fe^{2+}+Mn+Mg+Ca)$, XGrs = $Ca/(Fe^{2+}+Mn+Mg+Ca)$, XSps = $Mn/(Fe^{2+}+Mn+Mg+Ca)$

Comment	0906A 1.7 g r	0906A 1.8 g c	0906A 1.9 g trav	0906A 1.9 g trav	0906A 1.9 g trav	0906A 1.9 g trav	0906A 1.9 g trav	0909 1.1 g trav	0909 1.1 g trav	0909 1.1 g trav	0909 1.1 g trav
X	8406	8426	8047	8048	8053	8053	8053	13494	13494	13494	13494
Y	27261	27281	27498	27490	27484	27476	27465	-17995	-17982	-17960	-17937
Z	73	73	73	73	73	73	73	82	82	82	82
SiO2	38.48	38.65	38.55	38.61	38.32	38.68	38.34	38.73	39.01	39.31	39.32
TiO2	0.09	0.06	0.09	0.10	0.09	0.09	0.05	0.10	0.09	0.07	0.12
Al2O3	21.94	22.10	22.04	22.17	22.17	22.07	22.39	21.76	21.84	21.97	21.86
Cr2O3	0.11	0.03	0.09	0.09	0.06	0.10	0.09	0.01	0.00	0.01	0.00
Fe2O3	2.36	2.59	3.21	2.61	3.36	2.58	3.04	2.00	1.99	1.85	2.46
FeO	20.30	20.30	19.00	19.50	19.00	19.50	19.00	21.00	21.00	20.50	19.50
MnO	0.71	0.74	0.63	0.63	0.71	0.67	0.64	1.01	0.71	0.55	0.54
MgO	7.96	8.33	9.14	9.01	9.08	9.05	9.02	7.71	8.38	9.05	9.69
CaO	8.46	8.25	7.79	7.57	7.58	7.62	7.71	8.09	7.82	7.53	7.31
Na2O	0.03	0.01	0.02	0.03	0.02	0.02	0.03	0.03	0.04	0.03	0.05
K2O	0.00	0.00	0.02	0.02	0.00	0.00	0.01	0.01	0.00	0.01	0.00
NiO	0.01	0.02	0.00	0.00	0.00	0.00	0.00	0.01	0.02	0.01	0.01
Total	100.21	100.84	100.27	100.09	100.05	100.11	100.02	100.26	100.70	100.71	100.60
FeO	22.42	22.63	21.89	21.84	22.02	21.82	21.74	22.80	22.79	22.17	21.71
Num ox	12	12	12	12	12	12	12	12	12	12	12
Si	2.94	2.93	2.92	2.93	2.91	2.94	2.91	2.96	2.96	2.97	2.96
Ti	0.00	0.00	0.01	0.01	0.01	0.01	0.00	0.01	0.01	0.00	0.01
Al	1.97	1.97	1.97	1.98	1.98	1.98	2.00	1.96	1.95	1.96	1.94
Cr	0.01	0.00	0.01	0.01	0.00	0.01	0.01	0.00	0.00	0.00	0.00
Fe3+	0.14	0.15	0.18	0.15	0.19	0.15	0.17	0.12	0.11	0.11	0.14
Fe2+	1.30	1.29	1.20	1.24	1.21	1.24	1.21	1.34	1.33	1.29	1.23
Mn	0.05	0.05	0.04	0.04	0.05	0.04	0.04	0.07	0.05	0.04	0.03
Mg	0.91	0.94	1.03	1.02	1.03	1.02	1.02	0.88	0.95	1.02	1.09
Ca	0.69	0.67	0.63	0.62	0.62	0.62	0.63	0.66	0.64	0.61	0.59
Na	0.00	0.00	0.00	0.01	0.00	0.00	0.00	0.00	0.01	0.00	0.01
K	0.00	0.00	0.00	0.00	0.00	0.00	0.00	0.00	0.00	0.00	0.00
Ni	0.00	0.00	0.00	0.00	0.00	0.00	0.00	0.00	0.00	0.00	0.00
Total	8.00	8.00	8.00	8.00	8.00	8.00	8.00	8.00	8.00	8.00	8.00
Tetrahedral (Si)	2.94	2.93	2.92	2.93	2.91	2.94	2.91	2.96	2.96	2.97	2.96
Tetrahedral (Al)	0.06	0.07	0.08	0.07	0.09	0.06	0.09	0.04	0.04	0.03	0.04
Tetrahedral (3)	3.00	3.00	3.00	3.00	3.00	3.00	3.00	3.00	3.00	3.00	3.00
Octahedral (2)	2.06	2.06	2.08	2.08	2.10	2.07	2.10	2.04	2.03	2.03	2.05
Cavities (3)	2.94	2.95	2.91	2.91	2.90	2.92	2.90	2.95	2.96	2.96	2.94
XAlm	0.44	0.44	0.41	0.42	0.42	0.42	0.42	0.46	0.45	0.44	0.42
XPyp	0.31	0.32	0.35	0.35	0.35	0.35	0.35	0.30	0.32	0.34	0.37
XGrs	0.24	0.23	0.22	0.21	0.21	0.21	0.22	0.22	0.21	0.21	0.20
XSps	0.02	0.02	0.01	0.01	0.02	0.01	0.01	0.02	0.02	0.01	0.01

Appendix 6.D EMP data for garnet with calculated end member proportions. XAlm = $Fe^{2+}/(Fe^{2+}+Mn+Mg+Ca)$. XPyp = $Mg/(Fe^{2+}+Mn+Mg+Ca)$, XGrs = $Ca/(Fe^{2+}+Mn+Mg+Ca)$, XSps = $Mn/(Fe^{2+}+Mn+Mg+Ca)$

Comment	0909 1.1 g trav	0909 1.1 g trav	0909 1.1 g trav	0909 1.1 g trav	0909 1.1 g trav	0909 1.1 g trav	0909 1.1 g trav	0909 1.1 g trav	0909 1.1 g trav	0909 1.1 g trav	0909 1.1 g trav
X	13494	13494	13494	13494	13494	13494	13494	13494	13494	13494	13494
Y	-17897	-17858	-17797	-17743	-17624	-17548	-17374	-17298	-17203	-17082	-16978
Z	82	82	82	82	82	82	82	82	82	82	82
SiO2	39.43	39.56	39.74	39.28	39.71	39.52	39.61	39.47	39.29	39.49	39.21
TiO2	0.07	0.09	0.11	0.17	0.09	0.12	0.13	0.11	0.08	0.13	0.08
Al2O3	22.10	22.15	22.02	21.94	22.11	21.98	21.94	21.97	22.12	21.88	22.00
Cr2O3	0.01	0.00	0.01	0.00	0.01	0.02	0.03	0.03	0.02	0.01	0.02
Fe2O3	2.31	1.95	2.59	2.22	1.72	2.71	2.01	2.50	2.74	1.92	2.64
FeO	19.50	19.50	19.50	19.50	20.00	19.50	20.00	19.50	19.50	20.00	19.50
MnO	0.52	0.53	0.55	0.57	0.58	0.61	0.56	0.58	0.58	0.51	0.56
MgO	10.27	10.48	10.64	10.43	10.51	10.60	10.41	10.61	10.58	10.43	10.51
CaO	6.72	6.65	6.53	6.34	6.30	6.36	6.31	6.36	6.14	6.20	6.28
Na2O	0.03	0.03	0.03	0.06	0.03	0.04	0.01	0.05	0.04	0.04	0.04
K2O	0.00	0.00	0.01	0.01	0.00	0.00	0.01	0.00	0.01	0.02	0.00
NiO	0.01	0.01	0.04	0.00	0.01	0.01	0.03	0.02	0.04	0.02	0.00
Total	100.74	100.76	101.50	100.28	100.88	101.19	100.85	100.94	100.86	100.45	100.57
FeO	21.58	21.26	21.83	21.50	21.55	21.94	21.81	21.75	21.96	21.73	21.88
Num ox	12	12	12	12	12	12	12	12	12	12	12
Si	2.96	2.96	2.96	2.96	2.97	2.95	2.97	2.95	2.94	2.97	2.95
Ti	0.00	0.01	0.01	0.01	0.00	0.01	0.01	0.01	0.00	0.01	0.00
Al	1.95	1.96	1.93	1.95	1.95	1.94	1.94	1.94	1.95	1.94	1.95
Cr	0.00	0.00	0.00	0.00	0.00	0.00	0.00	0.00	0.00	0.00	0.00
Fe3+	0.13	0.11	0.15	0.13	0.10	0.15	0.11	0.14	0.15	0.11	0.15
Fe2+	1.22	1.22	1.21	1.23	1.25	1.22	1.25	1.22	1.22	1.26	1.23
Mn	0.03	0.03	0.03	0.04	0.04	0.04	0.04	0.04	0.04	0.03	0.04
Mg	1.15	1.17	1.18	1.17	1.17	1.18	1.16	1.18	1.18	1.17	1.18
Ca	0.54	0.53	0.52	0.51	0.51	0.51	0.51	0.51	0.49	0.50	0.51
Na	0.00	0.00	0.00	0.01	0.00	0.01	0.00	0.01	0.01	0.01	0.01
K	0.00	0.00	0.00	0.00	0.00	0.00	0.00	0.00	0.00	0.00	0.00
Ni	0.00	0.00	0.00	0.00	0.00	0.00	0.00	0.00	0.00	0.00	0.00
Total	8.00	8.00	8.00	8.00	8.00	8.00	8.00	8.00	8.00	8.00	8.00
Tetrahedral (Si)	2.96	2.96	2.96	2.96	2.97	2.95	2.97	2.95	2.94	2.97	2.95
Tetrahedral (Al)	0.04	0.04	0.04	0.04	0.03	0.05	0.03	0.05	0.06	0.03	0.05
Tetrahedral (3)	3.00	3.00	3.00	3.00	3.00	3.00	3.00	3.00	3.00	3.00	3.00
Octahedral (2)	2.05	2.04	2.04	2.04	2.03	2.05	2.03	2.04	2.06	2.03	2.05
Cavities (3)	2.95	2.96	2.95	2.95	2.97	2.94	2.96	2.95	2.93	2.96	2.94
XAlm	0.42	0.41	0.41	0.42	0.42	0.41	0.42	0.41	0.42	0.43	0.42
XPyp	0.39	0.40	0.40	0.40	0.40	0.40	0.39	0.40	0.40	0.40	0.40
XGrs	0.18	0.18	0.18	0.17	0.17	0.17	0.17	0.17	0.17	0.17	0.17
XSps	0.01	0.01	0.01	0.01	0.01	0.01	0.01	0.01	0.01	0.01	0.01

Table 6.xx EMP data for garnet with calculated end member proportions. XAlm = $Fe^{2+}/(Fe^{2+}+Mn+Mg+Ca)$. XPyp = $Mg/(Fe^{2+}+Mn+Mg+Ca)$, XGrs = $Ca/(Fe^{2+}+Mn+Mg+Ca)$, XSps = $Mn/(Fe^{2+}+Mn+Mg+Ca)$

Comment	0909 1.1 g trav	0909 1.1 g trav	0909 1.1 g trav	0909 1.1 g trav	0909 1.1 g trav	0909 1.1 g trav	0909 1.1 g trav	0909 1.1 g trav	0909 1.1 g trav	0909 1.1 g trav	0909 1.1 g trav
X	13494	13494	13494	13494	13494	13494	13494	13494	13494	13494	13494
Y	-16860	-16753	-16668	-16563	-16455	-16354	-16203	-16160	-16053	-15989	-15929
Z	82	82	82	82	82	80	80	80	80	80	80
SiO2	39.20	39.42	39.48	39.24	39.62	38.99	39.16	39.42	39.22	39.32	39.26
TiO2	0.07	0.09	0.07	0.13	0.12	0.04	0.07	0.06	0.08	0.08	0.07
Al2O3	22.08	22.08	21.99	22.08	22.00	22.16	22.06	22.03	22.08	22.10	21.98
Cr2O3	0.05	0.03	0.00	0.03	0.02	0.02	0.00	0.03	0.02	0.04	0.02
Fe2O3	2.59	2.98	2.01	2.63	1.73	3.11	2.07	2.14	2.23	2.16	2.46
FeO	19.50	19.50	20.00	19.50	20.00	19.50	20.00	19.50	19.00	19.50	19.00
MnO	0.55	0.54	0.53	0.62	0.60	0.57	0.53	0.55	0.49	0.57	0.57
MgO	10.56	10.57	10.39	10.45	10.37	10.22	9.87	9.98	9.55	9.43	9.62
CaO	6.15	6.39	6.15	6.33	6.31	6.48	6.70	7.14	8.06	7.64	8.03
Na2O	0.05	0.05	0.05	0.05	0.04	0.03	0.02	0.03	0.03	0.05	0.04
K2O	0.00	0.01	0.02	0.01	0.00	0.01	0.00	0.00	0.00	0.01	0.00
NiO	0.04	0.00	0.04	0.04	0.00	0.00	0.00	0.00	0.00	0.00	0.00
Total	100.58	101.35	100.54	100.85	100.64	100.82	100.27	100.67	100.53	100.68	100.80
FeO	21.83	22.18	21.81	21.87	21.56	22.30	21.86	21.43	21.01	21.45	21.21
Num ox	12	12	12	12	12	12	12	12	12	12	12
Si	2.95	2.94	2.97	2.94	2.98	2.93	2.96	2.96	2.95	2.96	2.95
Ti	0.00	0.00	0.00	0.01	0.01	0.00	0.00	0.00	0.00	0.00	0.00
Al	1.96	1.94	1.95	1.95	1.95	1.96	1.96	1.95	1.96	1.96	1.95
Cr	0.00	0.00	0.00	0.00	0.00	0.00	0.00	0.00	0.00	0.00	0.00
Fe3+	0.15	0.17	0.11	0.15	0.10	0.18	0.12	0.12	0.13	0.12	0.14
Fe2+	1.23	1.22	1.26	1.22	1.26	1.22	1.26	1.23	1.20	1.23	1.19
Mn	0.03	0.03	0.03	0.04	0.04	0.04	0.03	0.03	0.03	0.04	0.04
Mg	1.18	1.18	1.16	1.17	1.16	1.14	1.11	1.12	1.07	1.06	1.08
Ca	0.49	0.51	0.50	0.51	0.51	0.52	0.54	0.58	0.65	0.62	0.65
Na	0.01	0.01	0.01	0.01	0.01	0.00	0.00	0.00	0.00	0.01	0.01
K	0.00	0.00	0.00	0.00	0.00	0.00	0.00	0.00	0.00	0.00	0.00
Ni	0.00	0.00	0.00	0.00	0.00	0.00	0.00	0.00	0.00	0.00	0.00
Total	8.00	8.00	8.00	8.00	8.00	8.00	8.00	8.00	8.00	8.00	8.00
Tetrahedral (Si)	2.95	2.94	2.97	2.94	2.98	2.93	2.96	2.96	2.95	2.96	2.95
Tetrahedral (Al)	0.05	0.06	0.03	0.06	0.02	0.07	0.04	0.04	0.05	0.04	0.05
Tetrahedral (3)	3.00	3.00	3.00	3.00	3.00	3.00	3.00	3.00	3.00	3.00	3.00
Octahedral (2)	2.05	2.06	2.04	2.05	2.03	2.07	2.04	2.04	2.05	2.05	2.04
Cavities (3)	2.94	2.94	2.95	2.94	2.96	2.93	2.95	2.95	2.95	2.94	2.95
XAlm	0.42	0.41	0.43	0.42	0.42	0.42	0.43	0.41	0.41	0.42	0.40
XPyp	0.40	0.40	0.39	0.40	0.39	0.39	0.38	0.38	0.36	0.36	0.36
XGrs	0.17	0.17	0.17	0.17	0.17	0.18	0.18	0.19	0.22	0.21	0.22
XSps	0.01	0.01	0.01	0.01	0.01	0.01	0.01	0.01	0.01	0.01	0.01

Table 6.xx EMP data for garnet with calculated end member proportions. XAlm = $Fe^{2+}/(Fe^{2+}+Mn+Mg+Ca)$. XPyp = $Mg/(Fe^{2+}+Mn+Mg+Ca)$, XGrs = $Ca/(Fe^{2+}+Mn+Mg+Ca)$, XSps = $Mn/(Fe^{2+}+Mn+Mg+Ca)$

Comment	0909 1.1 g trav	0909 1.1 g trav	0909 1.1 g trav	0909 1.1 g trav	0909 1.1 g trav	0909 1.1 g trav	0909 1.1 g trav	0909 1.1 g trav	0909 1.1 g trav	0909 1.1 g trav	0909 1.1 g trav
X	13494	13494	13494	13494	13494	13494	13494	13494	13494	13494	13494
Y	-15815	-15654	-15421	-15310	-15161	-15065	-14924	-14791	-14678	-14542	-14473
Z	80	80	80	80	80	80	80	80	80	80	80
SiO2	38.94	39.33	39.19	39.41	39.00	39.01	39.12	39.38	39.11	39.16	39.19
TiO2	0.06	0.11	0.10	0.12	0.52	0.09	0.04	0.03	0.05	0.07	0.10
Al2O3	22.01	22.02	22.03	21.96	21.91	22.03	21.99	21.92	22.00	21.90	22.01
Cr2O3	0.00	0.01	0.02	0.02	0.01	0.00	0.00	0.01	0.00	0.00	0.00
Fe2O3	2.85	2.38	2.52	2.33	1.94	2.90	2.52	2.19	2.88	2.84	2.23
FeO	19.00	20.00	20.00	20.00	20.00	19.50	20.00	20.50	19.50	19.50	20.00
MnO	0.55	0.54	0.56	0.52	0.58	0.56	0.54	0.67	0.58	0.57	0.60
MgO	9.63	10.14	10.25	10.17	10.12	10.37	10.12	10.30	9.96	10.04	9.98
CaO	7.63	6.54	6.36	6.41	6.36	6.39	6.27	5.85	6.74	6.79	6.65
Na2O	0.03	0.04	0.03	0.05	0.05	0.04	0.03	0.02	0.03	0.05	0.04
K2O	0.01	0.00	0.01	0.00	0.01	0.01	0.02	0.00	0.00	0.01	0.01
NiO	0.02	0.02	0.03	0.00	0.00	0.00	0.00	0.03	0.00	0.01	0.02
Total	100.44	100.89	100.85	100.75	100.31	100.62	100.41	100.67	100.54	100.67	100.61
FeO	21.56	22.14	22.27	22.09	21.74	22.11	22.27	22.47	22.09	22.06	22.00
Num ox	12	12	12	12	12	12	12	12	12	12	12
Si	2.94	2.95	2.94	2.96	2.95	2.93	2.95	2.96	2.95	2.95	2.95
Ti	0.00	0.01	0.01	0.01	0.03	0.01	0.00	0.00	0.00	0.00	0.01
Al	1.96	1.95	1.95	1.95	1.95	1.95	1.96	1.94	1.95	1.94	1.95
Cr	0.00	0.00	0.00	0.00	0.00	0.00	0.00	0.00	0.00	0.00	0.00
Fe3+	0.16	0.13	0.14	0.13	0.11	0.16	0.14	0.12	0.16	0.16	0.13
Fe2+	1.20	1.26	1.26	1.26	1.26	1.23	1.26	1.29	1.23	1.23	1.26
Mn	0.04	0.03	0.04	0.03	0.04	0.04	0.03	0.04	0.04	0.04	0.04
Mg	1.08	1.13	1.15	1.14	1.14	1.16	1.14	1.15	1.12	1.13	1.12
Ca	0.62	0.53	0.51	0.52	0.51	0.51	0.51	0.47	0.54	0.55	0.54
Na	0.00	0.01	0.00	0.01	0.01	0.01	0.00	0.00	0.00	0.01	0.01
K	0.00	0.00	0.00	0.00	0.00	0.00	0.00	0.00	0.00	0.00	0.00
Ni	0.00	0.00	0.00	0.00	0.00	0.00	0.00	0.00	0.00	0.00	0.00
Total	8.00	8.00	8.00	8.00	8.00	8.00	8.00	8.00	8.00	8.00	8.00
Tetrahedral (Si)	2.94	2.95	2.94	2.96	2.95	2.93	2.95	2.96	2.95	2.95	2.95
Tetrahedral (Al)	0.06	0.05	0.06	0.04	0.05	0.07	0.05	0.04	0.05	0.05	0.05
Tetrahedral (3)	3.00	3.00	3.00	3.00	3.00	3.00	3.00	3.00	3.00	3.00	3.00
Octahedral (2)	2.06	2.04	2.05	2.05	2.04	2.06	2.05	2.04	2.06	2.05	2.04
Cavities (3)	2.93	2.95	2.95	2.94	2.95	2.94	2.94	2.96	2.93	2.94	2.96
XAlm	0.41	0.43	0.43	0.43	0.43	0.42	0.43	0.44	0.42	0.42	0.43
XPyp	0.37	0.38	0.39	0.39	0.39	0.40	0.39	0.39	0.38	0.38	0.38
XGrs	0.21	0.18	0.17	0.18	0.17	0.18	0.17	0.16	0.19	0.19	0.18
XSps	0.01	0.01	0.01	0.01	0.01	0.01	0.01	0.01	0.01	0.01	0.01

Table 6.xx EMP data for garnet with calculated end member proportions. XAlm = $Fe^{2+}/(Fe^{2+}+Mn+Mg+Ca)$. XPyp = $Mg/(Fe^{2+}+Mn+Mg+Ca)$, XGrs = $Ca/(Fe^{2+}+Mn+Mg+Ca)$, XSps = $Mn/(Fe^{2+}+Mn+Mg+Ca)$

Comment	0909 1.1 g trav	0909 1.1 g trav	0909 1.1 g trav	0909 1.1 g trav	0909 1.1 g trav	0909 1.1 g trav	0909 1.1 g trav	0909 1.1 g trav	0909 1.1 g trav	0909 1.1 g trav	0909 1.1 g trav
X	13494	13494	13494	13494	13528	13528	13528	13528	13528	13528	13571
Y	-14354	-14204	-14052	-13914	-13813	-13741	-13698	-13650	-13601	-13501	-13451
Z	80	80	80	80	80	80	80	80	80	80	80
SiO2	39.22	39.15	39.47	39.19	39.17	39.25	39.26	39.34	39.12	39.43	39.17
TiO2	0.06	0.06	0.05	0.41	0.08	0.02	0.06	0.05	0.10	0.10	0.07
Al2O3	21.89	21.81	21.83	21.90	21.80	21.93	21.83	21.93	21.70	21.80	22.00
Cr2O3	0.00	0.02	0.00	0.00	0.01	0.00	0.01	0.00	0.02	0.03	0.03
Fe2O3	2.58	2.03	2.20	2.03	2.18	2.28	2.24	2.08	2.61	2.60	2.75
FeO	20.00	20.00	20.00	20.00	20.00	20.00	20.00	20.00	19.50	19.50	19.50
MnO	0.59	0.58	0.53	0.53	0.50	0.51	0.50	0.55	0.56	0.54	0.52
MgO	10.05	9.90	9.87	9.97	10.02	10.04	10.06	9.98	10.01	10.18	10.22
CaO	6.69	6.75	6.76	6.71	6.74	6.62	6.68	6.68	6.68	6.75	6.72
Na2O	0.01	0.04	0.04	0.03	0.03	0.01	0.02	0.03	0.04	0.06	0.03
K2O	0.01	0.00	0.02	0.00	0.01	0.00	0.02	0.01	0.00	0.01	0.00
NiO	0.00	0.03	0.01	0.00	0.00	0.00	0.04	0.00	0.00	0.03	0.02
Total	100.84	100.18	100.55	100.57	100.30	100.45	100.51	100.44	100.08	100.77	100.77
FeO	22.32	21.82	21.98	21.83	21.96	22.05	22.02	21.87	21.85	21.84	21.98
Num ox	12	12	12	12	12	12	12	12	12	12	12
Si	2.95	2.96	2.97	2.95	2.96	2.96	2.96	2.97	2.96	2.96	2.94
Ti	0.00	0.00	0.00	0.02	0.00	0.00	0.00	0.00	0.01	0.01	0.00
Al	1.94	1.95	1.94	1.95	1.94	1.95	1.94	1.95	1.94	1.93	1.95
Cr	0.00	0.00	0.00	0.00	0.00	0.00	0.00	0.00	0.00	0.00	0.00
Fe3+	0.15	0.12	0.12	0.12	0.12	0.13	0.13	0.12	0.15	0.15	0.16
Fe2+	1.26	1.27	1.26	1.26	1.26	1.26	1.26	1.26	1.23	1.22	1.23
Mn	0.04	0.04	0.03	0.03	0.03	0.03	0.03	0.03	0.04	0.03	0.03
Mg	1.13	1.12	1.11	1.12	1.13	1.13	1.13	1.12	1.13	1.14	1.14
Ca	0.54	0.55	0.55	0.54	0.55	0.54	0.54	0.54	0.54	0.54	0.54
Na	0.00	0.01	0.01	0.00	0.00	0.00	0.00	0.00	0.01	0.01	0.00
K	0.00	0.00	0.00	0.00	0.00	0.00	0.00	0.00	0.00	0.00	0.00
Ni	0.00	0.00	0.00	0.00	0.00	0.00	0.00	0.00	0.00	0.00	0.00
Total	8.00	8.00	8.00	8.00	8.00	8.00	8.00	8.00	8.00	8.00	8.00
Tetrahedral (Si)	2.95	2.96	2.97	2.95	2.96	2.96	2.96	2.97	2.96	2.96	2.94
Tetrahedral (Al)	0.05	0.04	0.03	0.05	0.04	0.04	0.04	0.03	0.04	0.04	0.06
Tetrahedral (3)	3.00	3.00	3.00	3.00	3.00	3.00	3.00	3.00	3.00	3.00	3.00
Octahedral (2)	2.04	2.03	2.04	2.04	2.03	2.04	2.03	2.04	2.05	2.05	2.05
Cavities (3)	2.96	2.97	2.95	2.96	2.97	2.96	2.96	2.96	2.94	2.94	2.94
XAlm	0.42	0.43	0.43	0.43	0.43	0.43	0.43	0.43	0.42	0.42	0.42
XPyp	0.38	0.38	0.38	0.38	0.38	0.38	0.38	0.38	0.38	0.39	0.39
XGrs	0.18	0.18	0.19	0.18	0.18	0.18	0.18	0.18	0.18	0.18	0.18
XSps	0.01	0.01	0.01	0.01	0.01	0.01	0.01	0.01	0.01	0.01	0.01

Table 6.xx EMP data for garnet with calculated end member proportions. XAlm = $Fe^{2+}/(Fe^{2+}+Mn+Mg+Ca)$. XPyp = $Mg/(Fe^{2+}+Mn+Mg+Ca)$, XGrs = $Ca/(Fe^{2+}+Mn+Mg+Ca)$, XSps = $Mn/(Fe^{2+}+Mn+Mg+Ca)$

Comment	0909 1.1 g trav	0909 1.1 g trav	0909 1.1 g trav	0909 1.1 g trav	0909 1.1 g trav	0909 1.1 g trav	0909 1.1 g trav	0909 1.1 g trav	0909 1.1 g trav	0909 1.1 g trav	0909 1.1 g trav
X	13519	13519	13551	13551	13551	13551	13551	13551	13551	13551	13551
Y	-13336	-13262	-13239	-12774	-12642	-12606	-12560	-12495	-12442	-12398	-12352
Z	80	80	78	78	78	77	77	77	77	77	77
SiO2	39.51	39.37	39.00	39.14	39.31	38.69	38.96	39.25	39.13	39.27	38.91
TiO2	0.09	0.09	0.11	0.12	0.10	0.12	0.12	0.14	0.15	0.16	0.15
Al2O3	21.82	21.88	21.93	22.10	21.93	21.89	22.20	22.08	22.10	21.96	22.02
Cr2O3	0.04	0.02	0.04	0.04	0.00	0.01	0.04	0.02	0.03	0.01	0.02
Fe2O3	2.63	2.57	2.66	2.94	1.91	3.02	3.24	2.47	2.91	2.55	3.11
FeO	19.50	19.50	19.00	19.00	20.00	19.00	19.00	19.50	19.00	19.50	19.00
MnO	0.52	0.55	0.53	0.55	0.52	0.56	0.51	0.52	0.51	0.57	0.48
MgO	10.21	10.17	10.07	10.38	10.24	10.27	10.45	10.42	10.63	10.50	10.53
CaO	6.76	6.94	6.95	6.74	6.44	6.31	6.38	6.31	6.28	6.40	6.38
Na2O	0.06	0.06	0.04	0.04	0.05	0.06	0.05	0.08	0.06	0.04	0.05
K2O	0.00	0.01	0.00	0.02	0.01	0.01	0.01	0.00	0.01	0.00	0.01
NiO	0.01	0.00	0.00	0.04	0.05	0.00	0.00	0.02	0.00	0.00	0.03
Total	100.88	100.90	100.06	100.82	100.36	99.64	100.65	100.58	100.52	100.70	100.39
FeO	21.86	21.82	21.40	21.65	21.72	21.71	21.92	21.72	21.61	21.79	21.80
Num ox	12	12	12	12	12	12	12	12	12	12	12
Si	2.96	2.95	2.95	2.93	2.96	2.93	2.92	2.95	2.94	2.95	2.93
Ti	0.01	0.01	0.01	0.01	0.01	0.01	0.01	0.01	0.01	0.01	0.01
Al	1.93	1.94	1.95	1.95	1.95	1.96	1.96	1.96	1.96	1.94	1.95
Cr	0.00	0.00	0.00	0.00	0.00	0.00	0.00	0.00	0.00	0.00	0.00
Fe3+	0.15	0.15	0.15	0.17	0.11	0.17	0.18	0.14	0.16	0.14	0.18
Fe2+	1.22	1.22	1.20	1.19	1.26	1.21	1.19	1.23	1.19	1.22	1.20
Mn	0.03	0.04	0.03	0.04	0.03	0.04	0.03	0.03	0.03	0.04	0.03
Mg	1.14	1.14	1.13	1.16	1.15	1.16	1.17	1.17	1.19	1.17	1.18
Ca	0.54	0.56	0.56	0.54	0.52	0.51	0.51	0.51	0.50	0.51	0.51
Na	0.01	0.01	0.01	0.01	0.01	0.01	0.01	0.01	0.01	0.01	0.01
K	0.00	0.00	0.00	0.00	0.00	0.00	0.00	0.00	0.00	0.00	0.00
Ni	0.00	0.00	0.00	0.00	0.00	0.00	0.00	0.00	0.00	0.00	0.00
Total	8.00	8.00	8.00	8.00	8.00	8.00	8.00	8.00	8.00	8.00	8.00
Tetrahedral (Si)	2.96	2.95	2.95	2.93	2.96	2.93	2.92	2.95	2.94	2.95	2.93
Tetrahedral (Al)	0.04	0.05	0.05	0.07	0.04	0.07	0.08	0.05	0.06	0.05	0.07
Tetrahedral (3)	3.00	3.00	3.00	3.00	3.00	3.00	3.00	3.00	3.00	3.00	3.00
Octahedral (2)	2.05	2.04	2.06	2.06	2.03	2.07	2.08	2.05	2.07	2.05	2.07
Cavities (3)	2.94	2.95	2.93	2.93	2.97	2.92	2.91	2.93	2.92	2.95	2.92
XAlm	0.42	0.41	0.41	0.41	0.43	0.41	0.41	0.42	0.41	0.42	0.41
XPyp	0.39	0.38	0.39	0.40	0.39	0.40	0.40	0.40	0.41	0.40	0.40
XGrs	0.18	0.19	0.19	0.19	0.18	0.18	0.18	0.17	0.17	0.17	0.18
XSps	0.01	0.01	0.01	0.01	0.01	0.01	0.01	0.01	0.01	0.01	0.01

Appendix 6.D EMP data for garnet with calculated end member proportions. XAlm = $Fe^{2+}/(Fe^{2+}+Mn+Mg+Ca)$. XPyp = $Mg/(Fe^{2+}+Mn+Mg+Ca)$, XGrs = $Ca/(Fe^{2+}+Mn+Mg+Ca)$, XSps = $Mn/(Fe^{2+}+Mn+Mg+Ca)$

Comment	0909 1.1 g trav	0909 1.1 g trav	0909 1.1 g trav	0909 1.1 g trav	0909 1.1 g trav	0909 1.1 g trav	0909 1.1 g trav	0909 1.1 g trav	0909 1.1 g trav	0909 1.1 g trav	0909 1.1 g trav
X	13551	13551	13551	13551	13551	13551	13551	13551	13551	13551	13551
Y	-12331	-12318	-12274	-12253	-12235	-12214	-12196	-12176	-12153	-12137	-12119
Z	77	77	77	77	77	77	77	77	77	77	77
SiO2	39.01	39.16	39.22	39.15	39.02	39.25	39.56	39.02	38.87	39.23	39.34
TiO2	0.13	0.12	0.15	0.14	0.13	0.10	0.12	0.10	0.08	0.05	0.09
Al2O3	22.04	22.00	22.02	22.15	22.13	22.10	21.94	21.97	22.13	21.98	21.90
Cr2O3	0.01	0.00	0.04	0.02	0.01	0.02	0.04	0.01	0.00	0.04	0.02
Fe2O3	3.16	2.24	2.85	3.21	2.82	2.96	1.92	2.98	3.29	2.27	2.17
FeO	19.00	19.50	19.00	19.00	19.00	19.00	19.75	19.00	18.50	19.00	19.00
MnO	0.56	0.53	0.48	0.58	0.56	0.55	0.53	0.48	0.50	0.50	0.56
MgO	10.44	10.45	10.49	10.43	10.51	10.43	10.20	10.16	9.92	9.61	9.27
CaO	6.44	6.45	6.67	6.63	6.62	6.77	6.88	7.08	7.66	7.98	8.37
Na2O	0.05	0.06	0.05	0.05	0.04	0.05	0.03	0.05	0.03	0.03	0.03
K2O	0.00	0.01	0.01	0.00	0.00	0.00	0.00	0.00	0.00	0.01	0.01
NiO	0.00	0.03	0.00	0.00	0.01	0.00	0.00	0.00	0.01	0.00	0.00
Total	100.53	100.32	100.68	101.04	100.56	100.93	100.76	100.54	100.67	100.48	100.54
FeO	21.84	21.51	21.57	21.89	21.54	21.67	21.48	21.68	21.46	21.04	20.95
Num ox	12	12	12	12	12	12	12	12	12	12	12
Si	2.93	2.95	2.94	2.93	2.93	2.94	2.97	2.94	2.92	2.96	2.97
Ti	0.01	0.01	0.01	0.01	0.01	0.01	0.01	0.01	0.00	0.00	0.00
Al	1.95	1.95	1.95	1.95	1.96	1.95	1.94	1.95	1.96	1.95	1.95
Cr	0.00	0.00	0.00	0.00	0.00	0.00	0.00	0.00	0.00	0.00	0.00
Fe3+	0.18	0.13	0.16	0.18	0.16	0.17	0.11	0.17	0.19	0.13	0.12
Fe2+	1.19	1.23	1.19	1.19	1.19	1.19	1.24	1.20	1.16	1.20	1.20
Mn	0.04	0.03	0.03	0.04	0.04	0.03	0.03	0.03	0.03	0.03	0.04
Mg	1.17	1.17	1.17	1.16	1.18	1.16	1.14	1.14	1.11	1.08	1.04
Ca	0.52	0.52	0.54	0.53	0.53	0.54	0.55	0.57	0.62	0.64	0.68
Na	0.01	0.01	0.01	0.01	0.01	0.01	0.00	0.01	0.00	0.00	0.01
K	0.00	0.00	0.00	0.00	0.00	0.00	0.00	0.00	0.00	0.00	0.00
Ni	0.00	0.00	0.00	0.00	0.00	0.00	0.00	0.00	0.00	0.00	0.00
Total	8.00	8.00	8.00	8.00	8.00	8.00	8.00	8.00	8.00	8.00	8.00
Tetrahedral (Si)	2.93	2.95	2.94	2.93	2.93	2.94	2.97	2.94	2.92	2.96	2.97
Tetrahedral (Al)	0.07	0.05	0.06	0.07	0.07	0.06	0.03	0.06	0.08	0.04	0.03
Tetrahedral (3)	3.00	3.00	3.00	3.00	3.00	3.00	3.00	3.00	3.00	3.00	3.00
Octahedral (2)	2.07	2.04	2.06	2.07	2.06	2.06	2.03	2.06	2.07	2.04	2.04
Cavities (3)	2.92	2.96	2.93	2.92	2.94	2.93	2.97	2.94	2.92	2.95	2.95
XAlm	0.41	0.42	0.41	0.41	0.41	0.41	0.42	0.41	0.40	0.41	0.41
XPyp	0.40	0.40	0.40	0.40	0.40	0.40	0.38	0.39	0.38	0.37	0.35
XGrs	0.18	0.18	0.18	0.18	0.18	0.19	0.19	0.19	0.21	0.22	0.23
XSps	0.01	0.01	0.01	0.01	0.01	0.01	0.01	0.01	0.01	0.01	0.01

Appendix 6.D EMP data for garnet with calculated end member proportions. XAlm = $Fe^{2+}/(Fe^{2+}+Mn+Mg+Ca)$. XPyp = $Mg/(Fe^{2+}+Mn+Mg+Ca)$, XGrs = $Ca/(Fe^{2+}+Mn+Mg+Ca)$, XSps = $Mn/(Fe^{2+}+Mn+Mg+Ca)$

Comment	0909 1.1 g trav	0909 1.1 g trav	0909 1.1 g trav	0909 1.1 g trav	0909 1.5 g	)909 1.12+ g-cpx-pla	)909 1.12+ g-cpx-pla	0909 2.1 g trav	0909 2.1 g trav	0909 2.1 g trav	0909 2.1 g trav
X	13551	13530	13530	13530	13233	15108	15125	14627	14691	14731	14794
Y	-12099	-12081	-12072	-12060	-13222	-14863	-14860	-23112	-23112	-23112	-23112
Z	77	77	77	77	77	75	75	79	79	79	79
SiO2	38.97	39.03	38.86	38.74	38.93	38.92	38.83	38.42	38.48	38.34	38.36
TiO2	0.07	0.06	0.06	0.05	0.05	0.02	0.07	0.01	0.06	0.04	0.09
Al2O3	22.06	22.03	21.91	21.76	22.32	22.28	22.11	22.08	22.20	22.36	22.22
Cr2O3	0.03	0.00	0.02	0.01	0.00	0.03	0.03	0.03	0.02	0.05	0.01
Fe2O3	2.30	1.92	1.99	1.84	3.04	3.15	2.27	3.67	3.25	3.82	4.22
FeO	19.00	20.00	20.50	21.00	18.00	18.50	19.00	18.50	18.00	17.50	17.50
MnO	0.47	0.49	0.60	0.63	0.57	0.53	0.52	0.61	0.54	0.58	0.54
MgO	9.00	8.27	7.77	7.37	9.51	9.35	9.23	8.58	9.57	9.90	10.38
CaO	8.69	8.92	8.99	9.08	8.57	8.27	8.40	8.97	8.29	7.80	7.08
Na2O	0.02	0.03	0.03	0.03	0.01	0.03	0.01	0.01	0.00	0.03	0.04
K2O	0.00	0.03	0.00	0.01	0.00	0.01	0.01	0.00	0.00	0.00	0.00
NiO	0.00	0.04	0.00	0.01	0.02	0.06	0.05	0.01	0.00	0.01	0.02
Total	100.38	100.62	100.53	100.34	100.73	100.83	100.30	100.52	100.10	100.05	100.03
FeO	21.07	21.72	22.29	22.66	20.73	21.33	21.04	21.80	20.93	20.94	21.30
Num ox	12	12	12	12	12	12	12	12	12	12	12
Si	2.95	2.96	2.96	2.96	2.92	2.93	2.94	2.91	2.91	2.90	2.89
Ti	0.00	0.00	0.00	0.00	0.00	0.00	0.00	0.00	0.00	0.00	0.01
Al	1.97	1.97	1.97	1.96	1.98	1.97	1.97	1.97	1.98	1.99	1.98
Cr	0.00	0.00	0.00	0.00	0.00	0.00	0.00	0.00	0.00	0.00	0.00
Fe3+	0.13	0.11	0.11	0.11	0.17	0.18	0.13	0.21	0.19	0.22	0.24
Fe2+	1.20	1.27	1.30	1.34	1.13	1.16	1.20	1.17	1.14	1.11	1.10
Mn	0.03	0.03	0.04	0.04	0.04	0.03	0.03	0.04	0.03	0.04	0.03
Mg	1.01	0.93	0.88	0.84	1.06	1.05	1.04	0.97	1.08	1.11	1.17
Ca	0.70	0.72	0.73	0.74	0.69	0.67	0.68	0.73	0.67	0.63	0.57
Na	0.00	0.00	0.00	0.00	0.00	0.00	0.00	0.00	0.00	0.00	0.01
K	0.00	0.00	0.00	0.00	0.00	0.00	0.00	0.00	0.00	0.00	0.00
Ni	0.00	0.00	0.00	0.00	0.00	0.00	0.00	0.00	0.00	0.00	0.00
Total	8.00	8.00	8.00	8.00	8.00	8.00	8.00	8.00	8.00	8.00	8.00
Tetrahedral (Si)	2.95	2.96	2.96	2.96	2.92	2.93	2.94	2.91	2.91	2.90	2.89
Tetrahedral (Al)	0.05	0.04	0.04	0.04	0.08	0.07	0.06	0.09	0.09	0.10	0.11
Tetrahedral (3)	3.00	3.00	3.00	3.00	3.00	3.00	3.00	3.00	3.00	3.00	3.00
Octahedral (2)	2.05	2.04	2.04	2.03	2.08	2.08	2.05	2.09	2.08	2.11	2.11
Cavities (3)	2.95	2.96	2.96	2.97	2.92	2.91	2.96	2.91	2.92	2.89	2.88
XAlm	0.41	0.43	0.44	0.45	0.39	0.40	0.41	0.40	0.39	0.38	0.38
XPyp	0.34	0.32	0.30	0.28	0.36	0.36	0.35	0.33	0.37	0.39	0.41
XGrs	0.24	0.24	0.25	0.25	0.24	0.23	0.23	0.25	0.23	0.22	0.20
XSps	0.01	0.01	0.01	0.01	0.01	0.01	0.01	0.01	0.01	0.01	0.01

Appendix 6.D EMP data for garnet with calculated end member proportions. XAlm = $Fe^{2+}/(Fe^{2+}+Mn+Mg+Ca)$. XPyp = $Mg/(Fe^{2+}+Mn+Mg+Ca)$, XGrs = $Ca/(Fe^{2+}+Mn+Mg+Ca)$, XSps = $Mn/(Fe^{2+}+Mn+Mg+Ca)$

Comment	0909 2.1 g trav	0909 2.1 g trav	0909 2.1 g trav	0909 2.1 g trav	0909 2.1 g trav	0909 2.1 g trav	0909 2.1 g trav	0909 2.1 g trav	0909 2.1 g trav	0909 2.1 g trav	0909 2.2 g trav
X	14886	14912	15009	15049	15126	15167	15228	15283	15318	15366	11474
Y	-23112	-23112	-23112	-23112	-23112	-23112	-23112	-23112	-23099	-23094	-25923
Z	79	79	79	79	79	79	79	79	79	79	87
SiO2	38.47	38.82	38.87	38.71	38.69	38.55	39.18	39.17	38.45	37.62	39.17
TiO2	0.06	0.04	0.07	0.05	0.06	0.08	0.04	0.04	0.08	0.05	0.07
Al2O3	22.32	22.30	22.25	22.27	22.34	22.23	22.36	22.09	22.19	21.81	22.13
Cr2O3	0.04	0.01	0.00	0.05	0.00	0.00	0.03	0.00	0.02	0.00	0.01
Fe2O3	3.84	3.16	3.15	3.78	3.80	3.43	2.89	2.86	3.57	4.34	1.81
FeO	18.00	18.50	18.50	18.00	18.00	18.00	18.50	18.50	18.00	17.75	19.00
MnO	0.54	0.56	0.54	0.55	0.53	0.47	0.52	0.54	0.50	0.67	0.49
MgO	10.75	10.80	10.70	10.77	10.61	10.53	10.46	9.80	9.26	9.03	8.56
CaO	6.54	6.27	6.37	6.44	6.76	6.84	7.22	7.83	8.35	8.20	9.42
Na2O	0.04	0.02	0.04	0.04	0.02	0.04	0.03	0.04	0.03	0.01	0.03
K2O	0.02	0.00	0.00	0.01	0.00	0.00	0.00	0.01	0.00	0.00	0.02
NiO	0.04	0.02	0.00	0.00	0.00	0.00	0.03	0.02	0.00	0.02	0.00
Total	100.27	100.18	100.18	100.30	100.43	99.83	100.96	100.60	100.09	99.07	100.52
FeO	21.45	21.34	21.34	21.40	21.42	21.09	21.10	21.07	21.21	21.66	20.63
Num ox	12	12	12	12	12	12	12	12	12	12	12
Si	2.89	2.92	2.92	2.91	2.90	2.91	2.93	2.94	2.91	2.88	2.96
Ti	0.00	0.00	0.00	0.00	0.00	0.00	0.00	0.00	0.00	0.00	0.00
Al	1.98	1.98	1.97	1.97	1.98	1.98	1.97	1.96	1.98	1.97	1.97
Cr	0.00	0.00	0.00	0.00	0.00	0.00	0.00	0.00	0.00	0.00	0.00
Fe3+	0.22	0.18	0.18	0.21	0.21	0.20	0.16	0.16	0.20	0.25	0.10
Fe2+	1.13	1.16	1.16	1.13	1.13	1.14	1.16	1.16	1.14	1.14	1.20
Mn	0.03	0.04	0.03	0.04	0.03	0.03	0.03	0.03	0.03	0.04	0.03
Mg	1.20	1.21	1.20	1.21	1.19	1.19	1.17	1.10	1.04	1.03	0.96
Ca	0.53	0.51	0.51	0.52	0.54	0.55	0.58	0.63	0.68	0.67	0.76
Na	0.01	0.00	0.01	0.01	0.00	0.01	0.00	0.01	0.00	0.00	0.00
K	0.00	0.00	0.00	0.00	0.00	0.00	0.00	0.00	0.00	0.00	0.00
Ni	0.00	0.00	0.00	0.00	0.00	0.00	0.00	0.00	0.00	0.00	0.00
Total	8.00	8.00	8.00	8.00	8.00	8.00	8.00	8.00	8.00	8.00	8.00
Tetrahedral (Si)	2.89	2.92	2.92	2.91	2.90	2.91	2.93	2.94	2.91	2.88	2.96
Tetrahedral (Al)	0.11	0.08	0.08	0.09	0.10	0.09	0.07	0.06	0.09	0.12	0.04
Tetrahedral (3)	3.00	3.00	3.00	3.00	3.00	3.00	3.00	3.00	3.00	3.00	3.00
Octahedral (2)	2.10	2.08	2.08	2.10	2.10	2.09	2.07	2.07	2.10	2.11	2.04
Cavities (3)	2.90	2.92	2.91	2.89	2.90	2.91	2.93	2.93	2.89	2.89	2.96
XAlm	0.39	0.40	0.40	0.39	0.39	0.39	0.39	0.40	0.39	0.39	0.41
XPyp	0.42	0.42	0.41	0.42	0.41	0.41	0.40	0.38	0.36	0.36	0.33
XGrs	0.18	0.17	0.18	0.18	0.19	0.19	0.20	0.22	0.23	0.23	0.26
XSps	0.01	0.01	0.01	0.01	0.01	0.01	0.01	0.01	0.01	0.02	0.01

Appendix 6.D EMP data for garnet with calculated end member proportions. XAlm = $Fe^{2+}/(Fe^{2+}+Mn+Mg+Ca)$. XPyp = $Mg/(Fe^{2+}+Mn+Mg+Ca)$, XGrs = $Ca/(Fe^{2+}+Mn+Mg+Ca)$, XSps = $Mn/(Fe^{2+}+Mn+Mg+Ca)$

Comment	0909 2.2 g trav	0909 2.2 g trav	0909 2.2 g trav	0909 2.2 g trav	0909 2.2 g trav	0909 2.2 g trav	0909 2.2 g trav	0909 2.2 g trav	0909 2.2 g trav	0909 2.2 g trav	0909 2.2 g trav
X	11489	11517	11555	11567	11589	11607	11620	11642	11679	11735	11769
Y	-25915	-25901	-25884	-25862	-25843	-25824	-25799	-25774	-25747	-25713	-25683
Z	87	87	87	87	87	87	87	87	87	87	87
SiO2	38.92	39.05	39.30	39.62	39.35	39.41	39.09	39.29	39.69	39.15	39.29
TiO2	0.09	0.12	0.11	0.12	0.18	0.11	0.14	0.11	0.11	0.11	0.12
Al2O3	22.08	22.20	22.17	22.38	22.09	22.30	22.17	22.21	22.44	22.16	22.14
Cr2O3	0.04	0.03	0.03	0.02	0.02	0.00	0.00	0.00	0.01	0.00	0.04
Fe2O3	2.62	2.38	2.21	2.46	2.35	2.22	2.55	2.14	2.37	2.99	2.83
FeO	18.00	18.50	19.00	19.00	19.00	19.00	19.00	19.00	19.00	18.50	18.50
MnO	0.52	0.49	0.43	0.52	0.51	0.53	0.49	0.52	0.55	0.53	0.51
MgO	9.23	9.73	10.12	10.44	10.62	10.64	10.62	10.61	10.89	10.61	10.55
CaO	8.93	8.04	7.42	7.13	6.67	6.64	6.63	6.57	6.63	6.67	6.94
Na2O	0.03	0.04	0.05	0.05	0.07	0.06	0.04	0.05	0.06	0.04	0.04
K2O	0.00	0.01	0.00	0.00	0.04	0.01	0.00	0.01	0.01	0.00	0.00
NiO	0.01	0.00	0.01	0.00	0.02	0.03	0.03	0.00	0.00	0.00	0.02
Total	100.22	100.36	100.62	101.49	100.68	100.72	100.51	100.30	101.53	100.46	100.70
FeO	20.36	20.64	20.99	21.21	21.12	21.00	21.30	20.93	21.13	21.19	21.05
Num ox	12	12	12	12	12	12	12	12	12	12	12
Si	2.94	2.94	2.95	2.95	2.95	2.95	2.94	2.95	2.95	2.94	2.94
Ti	0.01	0.01	0.01	0.01	0.01	0.01	0.01	0.01	0.01	0.01	0.01
Al	1.97	1.97	1.96	1.96	1.95	1.97	1.96	1.97	1.96	1.96	1.95
Cr	0.00	0.00	0.00	0.00	0.00	0.00	0.00	0.00	0.00	0.00	0.00
Fe3+	0.15	0.13	0.12	0.14	0.13	0.12	0.14	0.12	0.13	0.17	0.16
Fe2+	1.14	1.17	1.19	1.18	1.19	1.19	1.19	1.19	1.18	1.16	1.16
Mn	0.03	0.03	0.03	0.03	0.03	0.03	0.03	0.03	0.03	0.03	0.03
Mg	1.04	1.09	1.13	1.16	1.19	1.19	1.19	1.19	1.20	1.19	1.18
Ca	0.72	0.65	0.60	0.57	0.54	0.53	0.53	0.53	0.53	0.54	0.56
Na	0.00	0.01	0.01	0.01	0.01	0.01	0.01	0.01	0.01	0.01	0.01
K	0.00	0.00	0.00	0.00	0.00	0.00	0.00	0.00	0.00	0.00	0.00
Ni	0.00	0.00	0.00	0.00	0.00	0.00	0.00	0.00	0.00	0.00	0.00
Total	8.00	8.00	8.00	8.00	8.00	8.00	8.00	8.00	8.00	8.00	8.00
Tetrahedral (Si)	2.94	2.94	2.95	2.95	2.95	2.95	2.94	2.95	2.95	2.94	2.94
Tetrahedral (Al)	0.06	0.06	0.05	0.05	0.05	0.05	0.06	0.05	0.05	0.06	0.06
Tetrahedral (3)	3.00	3.00	3.00	3.00	3.00	3.00	3.00	3.00	3.00	3.00	3.00
Octahedral (2)	2.06	2.06	2.05	2.05	2.05	2.05	2.05	2.05	2.05	2.07	2.06
Cavities (3)	2.93	2.94	2.95	2.94	2.94	2.94	2.95	2.94	2.95	2.92	2.93
XAlm	0.39	0.40	0.40	0.40	0.40	0.40	0.41	0.41	0.40	0.40	0.40
XPyp	0.35	0.37	0.38	0.39	0.40	0.40	0.40	0.40	0.41	0.41	0.40
XGrs	0.25	0.22	0.20	0.19	0.18	0.18	0.18	0.18	0.18	0.18	0.19
XSps	0.01	0.01	0.01	0.01	0.01	0.01	0.01	0.01	0.01	0.01	0.01

Appendix 6.D EMP data for garnet with calculated end member proportions. XAlm = $Fe^{2+}/(Fe^{2+}+Mn+Mg+Ca)$. XPyp = $Mg/(Fe^{2+}+Mn+Mg+Ca)$, XGrs = $Ca/(Fe^{2+}+Mn+Mg+Ca)$, XSps = $Mn/(Fe^{2+}+Mn+Mg+Ca)$

Comment	0909 2.2 g trav	0909 2.2 g trav	0909 2.2 g trav	0909 2.2 g trav	0909 2.2 g trav	0909 2.2 g trav	0909 2.2 g trav	0909 2.2 g trav	0909 2.2 g trav	0909 2.2 g trav	0909 2.3 g trav
X	11826	11871	11893	11914	11937	12167	12193	12233	12250	12268	9289
Y	-25661	-25640	-25615	-25594	-25580	-25390	-25371	-25373	-25335	-25320	-5114
Z	87	87	87	87	87	87	87	87	87	87	75
SiO2	39.23	39.02	39.03	38.76	38.76	39.04	39.34	39.32	39.28	39.29	38.15
TiO2	0.08	0.08	0.03	0.07	0.05	0.25	0.08	0.05	0.06	0.04	0.12
Al2O3	22.07	22.10	22.02	21.93	22.00	21.87	21.98	21.99	21.96	21.91	20.54
Cr2O3	0.00	0.02	0.01	0.04	0.03	0.00	0.01	0.02	0.02	0.01	0.00
Fe2O3	2.38	3.19	2.61	2.55	1.98	1.93	1.63	2.41	1.69	1.77	3.69
FeO	19.00	18.00	18.50	19.00	19.75	19.00	19.50	18.50	19.00	19.50	17.50
MnO	0.52	0.49	0.47	0.54	0.58	0.60	0.51	0.51	0.49	0.51	0.65
MgO	10.23	9.62	8.77	7.91	7.49	7.89	8.00	8.49	8.21	7.82	6.66
CaO	7.12	8.35	9.45	9.76	9.90	10.18	10.00	9.93	10.08	10.12	12.18
Na2O	0.04	0.03	0.01	0.02	0.01	0.03	0.02	0.02	0.02	0.02	0.01
K2O	0.01	0.01	0.00	0.00	0.00	0.01	0.01	0.00	0.02	0.00	0.07
NiO	0.04	0.00	0.01	0.00	0.01	0.00	0.01	0.01	0.01	0.00	0.00
Total	100.48	100.61	100.66	100.33	100.37	100.60	100.91	101.01	100.66	100.82	99.20
FeO	21.14	20.87	20.85	21.30	21.53	20.74	20.97	20.67	20.52	21.10	20.82
Num ox	12	12	12	12	12	12	12	12	12	12	12
Si	2.95	2.93	2.94	2.94	2.95	2.96	2.97	2.96	2.97	2.97	2.95
Ti	0.00	0.00	0.00	0.00	0.00	0.01	0.00	0.00	0.00	0.00	0.01
Al	1.96	1.96	1.96	1.96	1.97	1.95	1.96	1.95	1.96	1.95	1.87
Cr	0.00	0.00	0.00	0.00	0.00	0.00	0.00	0.00	0.00	0.00	0.00
Fe3+	0.13	0.18	0.15	0.15	0.11	0.11	0.09	0.14	0.10	0.10	0.21
Fe2+	1.19	1.13	1.17	1.21	1.26	1.20	1.23	1.16	1.20	1.23	1.13
Mn	0.03	0.03	0.03	0.03	0.04	0.04	0.03	0.03	0.03	0.03	0.04
Mg	1.15	1.08	0.99	0.90	0.85	0.89	0.90	0.95	0.92	0.88	0.77
Ca	0.57	0.67	0.76	0.79	0.81	0.83	0.81	0.80	0.82	0.82	1.01
Na	0.01	0.00	0.00	0.00	0.00	0.00	0.00	0.00	0.00	0.00	0.00
K	0.00	0.00	0.00	0.00	0.00	0.00	0.00	0.00	0.00	0.00	0.01
Ni	0.00	0.00	0.00	0.00	0.00	0.00	0.00	0.00	0.00	0.00	0.00
Total	8.00	8.00	8.00	8.00	8.00	8.00	8.00	8.00	8.00	8.00	8.00
Tetrahedral (Si)	2.95	2.93	2.94	2.94	2.95	2.96	2.97	2.96	2.97	2.97	2.95
Tetrahedral (Al)	0.05	0.07	0.06	0.06	0.05	0.04	0.03	0.04	0.03	0.03	0.05
Tetrahedral (3)	3.00	3.00	3.00	3.00	3.00	3.00	3.00	3.00	3.00	3.00	3.00
Octahedral (2)	2.05	2.08	2.05	2.06	2.04	2.04	2.02	2.05	2.03	2.03	2.04
Cavities (3)	2.95	2.91	2.95	2.93	2.95	2.96	2.97	2.95	2.97	2.97	2.95
XAlm	0.41	0.39	0.40	0.41	0.43	0.41	0.41	0.39	0.40	0.42	0.38
XPyp	0.39	0.37	0.33	0.31	0.29	0.30	0.30	0.32	0.31	0.30	0.26
XGrs	0.19	0.23	0.26	0.27	0.27	0.28	0.27	0.27	0.27	0.28	0.34
XSps	0.01	0.01	0.01	0.01	0.01	0.01	0.01	0.01	0.01	0.01	0.01

Appendix 6.D EMP data for garnet with calculated end member proportions. XAlm = $Fe^{2+}/(Fe^{2+}+Mn+Mg+Ca)$. XPyp = $Mg/(Fe^{2+}+Mn+Mg+Ca)$, XGrs = $Ca/(Fe^{2+}+Mn+Mg+Ca)$, XSps = $Mn/(Fe^{2+}+Mn+Mg+Ca)$

Comment	0909 2.3 g trav	0909 2.3 g trav	0909 2.3 g trav	0909 2.3 g trav	0909 2.3 g trav	0909 2.3 g trav	0909 2.3 g trav	0909 2.3 g trav	0909 2.3 g trav	0909 2.3 g trav	0909 2.3 g trav
X	9303	9325	9351	9374	9407	9453	9494	9611	9671	9987	10036
Y	-5107	-5081	-5073	-5055	-5035	-5012	-4992	-4902	-4916	-4939	-4939
Z	75	75	75	75	75	75	75	75	75	75	75
SiO2	38.90	39.18	39.37	39.51	39.42	39.29	39.21	39.04	39.17	38.71	39.01
TiO2	0.08	0.07	0.06	0.07	0.12	0.10	0.08	0.08	0.05	0.13	0.08
Al2O3	21.98	22.02	22.15	22.14	22.05	22.16	21.98	22.09	21.99	21.92	21.95
Cr2O3	0.00	0.02	0.01	0.02	0.03	0.03	0.00	0.00	0.02	0.06	0.04
Fe2O3	2.56	2.05	1.93	2.17	1.84	2.56	2.26	2.15	1.94	2.48	3.32
FeO	19.00	19.00	19.00	19.00	19.50	19.00	19.00	19.00	19.50	19.00	18.00
MnO	0.53	0.44	0.44	0.50	0.45	0.51	0.44	0.47	0.57	0.57	0.47
MgO	8.25	8.74	9.12	9.80	10.14	10.39	10.16	9.86	7.96	7.83	9.37
CaO	9.50	9.07	8.96	7.98	7.17	7.07	7.27	7.42	9.61	10.04	8.66
Na2O	0.04	0.02	0.02	0.04	0.03	0.04	0.03	0.06	0.02	0.04	0.04
K2O	0.01	0.00	0.02	0.01	0.02	0.01	0.00	0.01	0.02	0.01	0.03
NiO	0.00	0.00	0.00	0.00	0.00	0.04	0.00	0.01	0.00	0.00	0.00
Total	100.59	100.40	100.87	101.01	100.58	100.95	100.20	99.97	100.66	100.54	100.63
FeO	21.30	20.85	20.73	20.95	21.15	21.30	21.04	20.93	21.24	21.23	20.99
Num ox	12	12	12	12	12	12	12	12	12	12	12
Si	2.94	2.96	2.96	2.96	2.96	2.94	2.96	2.95	2.97	2.94	2.94
Ti	0.00	0.00	0.00	0.00	0.01	0.01	0.00	0.00	0.00	0.01	0.00
Al	1.96	1.96	1.96	1.95	1.95	1.96	1.95	1.97	1.96	1.96	1.95
Cr	0.00	0.00	0.00	0.00	0.00	0.00	0.00	0.00	0.00	0.00	0.00
Fe3+	0.15	0.12	0.11	0.12	0.10	0.14	0.13	0.12	0.11	0.14	0.19
Fe2+	1.20	1.20	1.19	1.19	1.23	1.19	1.20	1.20	1.23	1.21	1.13
Mn	0.03	0.03	0.03	0.03	0.03	0.03	0.03	0.03	0.04	0.04	0.03
Mg	0.93	0.98	1.02	1.09	1.14	1.16	1.14	1.11	0.90	0.89	1.05
Ca	0.77	0.73	0.72	0.64	0.58	0.57	0.59	0.60	0.78	0.82	0.70
Na	0.01	0.00	0.00	0.01	0.00	0.01	0.00	0.01	0.00	0.01	0.01
K	0.00	0.00	0.00	0.00	0.00	0.00	0.00	0.00	0.00	0.00	0.00
Ni	0.00	0.00	0.00	0.00	0.00	0.00	0.00	0.00	0.00	0.00	0.00
Total	8.00	8.00	8.00	8.00	8.00	8.00	8.00	8.00	8.00	8.00	8.00
Tetrahedral (Si)	2.94	2.96	2.96	2.96	2.96	2.94	2.96	2.95	2.97	2.94	2.94
Tetrahedral (Al)	0.06	0.04	0.04	0.04	0.04	0.06	0.04	0.05	0.03	0.06	0.06
Tetrahedral (3)	3.00	3.00	3.00	3.00	3.00	3.00	3.00	3.00	3.00	3.00	3.00
Octahedral (2)	2.06	2.04	2.03	2.04	2.03	2.05	2.04	2.05	2.04	2.05	2.08
Cavities (3)	2.94	2.95	2.96	2.96	2.97	2.95	2.95	2.94	2.95	2.95	2.91
XAlm	0.41	0.41	0.40	0.40	0.41	0.40	0.41	0.41	0.42	0.41	0.39
XPyp	0.32	0.33	0.34	0.37	0.38	0.39	0.39	0.38	0.30	0.30	0.36
XGrs	0.26	0.25	0.24	0.22	0.19	0.19	0.20	0.20	0.26	0.28	0.24
XSps	0.01	0.01	0.01	0.01	0.01	0.01	0.01	0.01	0.01	0.01	0.01

Appendix 6.D EMP data for garnet with calculated end member proportions. XAlm = $Fe^{2+}/(Fe^{2+}+Mn+Mg+Ca)$. XPyp = $Mg/(Fe^{2+}+Mn+Mg+Ca)$, XGrs = $Ca/(Fe^{2+}+Mn+Mg+Ca)$, XSps = $Mn/(Fe^{2+}+Mn+Mg+Ca)$

Comment	0909 2.3 g trav	0909 2.3 g trav	0909 2.3 g trav	0909 2.3 g trav	0909 2.3 g trav	0909 2.3 g trav	0909 2.3 g trav	0909 2.3 g trav	0909 2.3 g trav	0909 2.3 g trav	0910B 1.3+ g trav
X	10127	10176	10247	10289	10447	10498	10554	10628	10684	10705	-14133
Y	-4933	-4911	-4903	-4903	-4819	-4812	-4782	-4777	-4740	-4756	-29980
Z	75	75	75	75	75	75	75	75	75	75	81
SiO2	39.45	39.35	39.05	39.23	38.96	39.79	39.45	39.49	39.50	39.65	38.60
TiO2	0.08	0.02	0.05	0.05	0.07	0.11	0.15	0.12	0.08	0.08	0.04
Al2O3	22.14	22.38	22.40	22.38	22.04	22.24	22.16	22.21	22.25	22.30	21.71
Cr2O3	0.03	0.03	0.01	0.01	0.03	0.00	0.01	0.02	0.02	0.00	0.02
Fe2O3	2.51	2.38	2.75	2.83	2.44	1.69	2.77	1.92	1.95	1.64	2.06
FeO	18.00	18.50	18.00	17.50	17.50	19.00	18.50	19.00	18.50	18.50	20.00
MnO	0.50	0.47	0.50	0.44	0.46	0.45	0.46	0.47	0.44	0.45	0.63
MgO	10.02	10.29	10.47	10.21	9.19	10.45	10.73	10.37	10.11	9.26	7.64
CaO	8.15	7.69	7.51	8.25	9.61	7.36	6.83	7.28	8.09	9.19	9.50
Na2O	0.04	0.02	0.03	0.02	0.03	0.05	0.05	0.04	0.04	0.05	0.00
K2O	0.01	0.01	0.00	0.00	0.02	0.01	0.01	0.00	0.01	0.02	0.00
NiO	0.01	0.03	0.02	0.02	0.02	0.00	0.00	0.01	0.00	0.04	0.05
Total	100.69	100.93	100.52	100.67	100.12	100.99	100.86	100.74	100.79	101.02	100.06
FeO	20.26	20.64	20.48	20.04	19.70	20.52	20.99	20.72	20.26	19.98	21.86
Num ox	12	12	12	12	12	12	12	12	12	12	12
Si	2.95	2.94	2.93	2.93	2.94	2.97	2.95	2.96	2.96	2.97	2.95
Ti	0.00	0.00	0.00	0.00	0.00	0.01	0.01	0.01	0.00	0.00	0.00
Al	1.95	1.97	1.98	1.97	1.96	1.96	1.95	1.96	1.96	1.97	1.96
Cr	0.00	0.00	0.00	0.00	0.00	0.00	0.00	0.00	0.00	0.00	0.00
Fe3+	0.14	0.13	0.16	0.16	0.14	0.09	0.16	0.11	0.11	0.09	0.12
Fe2+	1.13	1.16	1.13	1.09	1.11	1.19	1.16	1.19	1.16	1.16	1.28
Mn	0.03	0.03	0.03	0.03	0.03	0.03	0.03	0.03	0.03	0.03	0.04
Mg	1.12	1.15	1.17	1.14	1.03	1.16	1.19	1.16	1.13	1.03	0.87
Ca	0.65	0.62	0.60	0.66	0.78	0.59	0.55	0.58	0.65	0.74	0.78
Na	0.01	0.00	0.00	0.00	0.00	0.01	0.01	0.01	0.01	0.01	0.00
K	0.00	0.00	0.00	0.00	0.00	0.00	0.00	0.00	0.00	0.00	0.00
Ni	0.00	0.00	0.00	0.00	0.00	0.00	0.00	0.00	0.00	0.00	0.00
Total	8.00	8.00	8.00	8.00	8.00	8.00	8.00	8.00	8.00	8.00	8.00
Tetrahedral (Si)	2.95	2.94	2.93	2.93	2.94	2.97	2.95	2.96	2.96	2.97	2.95
Tetrahedral (Al)	0.05	0.06	0.07	0.07	0.06	0.03	0.05	0.04	0.04	0.03	0.05
Tetrahedral (3)	3.00	3.00	3.00	3.00	3.00	3.00	3.00	3.00	3.00	3.00	3.00
Octahedral (2)	2.06	2.05	2.07	2.07	2.05	2.03	2.06	2.03	2.04	2.03	2.03
Cavities (3)	2.93	2.95	2.93	2.92	2.95	2.97	2.93	2.96	2.96	2.96	2.97
XAlm	0.38	0.39	0.38	0.37	0.38	0.40	0.39	0.40	0.39	0.39	0.43
XPyp	0.38	0.39	0.40	0.39	0.35	0.39	0.41	0.39	0.38	0.35	0.29
XGrs	0.22	0.21	0.21	0.23	0.26	0.20	0.19	0.20	0.22	0.25	0.26
XSps	0.01	0.01	0.01	0.01	0.01	0.01	0.01	0.01	0.01	0.01	0.01

Appendix 6.D EMP data for garnet with calculated end member proportions. XAlm = $Fe^{2+}/(Fe^{2+}+Mn+Mg+Ca)$. XPyp = $Mg/(Fe^{2+}+Mn+Mg+Ca)$, XGrs = $Ca/(Fe^{2+}+Mn+Mg+Ca)$, XSps = $Mn/(Fe^{2+}+Mn+Mg+Ca)$

Comment	0910B 1.3+ g trav	0910B 1.3+ g trav	0910B 1.3+ g trav	0910B 1.3+ g trav	0910B 1.3+ g trav	0910B 1.3+ g trav	0910B 1.3+ g trav	0910B 1.3+ g trav	0910B 1.3+ g trav	0910B 1.3+ g trav	0910B 1.3+ g trav
X	-14133	-14133	-14133	-14133	-14133	-14133	-14133	-14133	-14133	-14133	-14133
Y	-29996	-30021	-30059	-30091	-30294	-30374	-30508	-30729	-30830	-30936	-31064
Z	81	81	81	81	81	81	81	81	81	81	81
SiO2	39.16	39.36	39.03	39.37	39.05	39.33	39.08	39.04	39.51	39.26	38.77
TiO2	0.03	0.06	0.04	0.04	0.06	0.03	0.06	0.04	0.03	0.04	0.06
Al2O3	21.84	21.97	21.98	22.12	21.94	22.02	22.15	22.13	22.08	22.04	21.93
Cr2O3	0.00	0.02	0.05	0.00	0.02	0.00	0.00	0.02	0.02	0.00	0.02
Fe2O3	2.10	1.79	3.12	2.61	2.59	2.89	2.95	2.85	1.65	2.53	2.79
FeO	19.00	18.50	17.00	17.50	17.00	17.00	17.00	17.00	18.00	17.50	17.00
MnO	0.56	0.52	0.53	0.51	0.50	0.52	0.54	0.52	0.53	0.56	0.52
MgO	8.39	8.98	9.56	9.72	9.81	9.86	9.93	9.92	9.49	9.80	9.67
CaO	9.56	9.47	9.36	9.36	9.08	9.09	9.02	8.95	9.33	8.89	9.09
Na2O	0.01	0.03	0.03	0.00	0.02	0.02	0.01	0.01	0.02	0.00	0.01
K2O	0.00	0.00	0.00	0.00	0.00	0.02	0.00	0.00	0.00	0.02	0.00
NiO	0.00	0.00	0.01	0.01	0.00	0.00	0.00	0.01	0.00	0.00	0.00
Total	100.45	100.52	100.41	100.97	99.80	100.48	100.44	100.21	100.51	100.39	99.58
FeO	20.89	20.11	19.81	19.85	19.33	19.60	19.65	19.57	19.49	19.78	19.51
Num ox	12	12	12	12	12	12	12	12	12	12	12
Si	2.96	2.97	2.94	2.94	2.95	2.95	2.93	2.94	2.97	2.95	2.94
Ti	0.00	0.00	0.00	0.00	0.00	0.00	0.00	0.00	0.00	0.00	0.00
Al	1.95	1.95	1.95	1.95	1.95	1.95	1.96	1.96	1.96	1.95	1.96
Cr	0.00	0.00	0.00	0.00	0.00	0.00	0.00	0.00	0.00	0.00	0.00
Fe3+	0.12	0.10	0.18	0.15	0.15	0.16	0.17	0.16	0.09	0.14	0.16
Fe2+	1.20	1.17	1.07	1.09	1.07	1.07	1.07	1.07	1.13	1.10	1.08
Mn	0.04	0.03	0.03	0.03	0.03	0.03	0.03	0.03	0.03	0.04	0.03
Mg	0.95	1.01	1.07	1.08	1.10	1.10	1.11	1.11	1.06	1.10	1.09
Ca	0.78	0.77	0.75	0.75	0.73	0.73	0.73	0.72	0.75	0.72	0.74
Na	0.00	0.00	0.00	0.00	0.00	0.00	0.00	0.00	0.00	0.00	0.00
K	0.00	0.00	0.00	0.00	0.00	0.00	0.00	0.00	0.00	0.00	0.00
Ni	0.00	0.00	0.00	0.00	0.00	0.00	0.00	0.00	0.00	0.00	0.00
Total	8.00	8.00	8.00	8.00	8.00	8.00	8.00	8.00	8.00	8.00	8.00
Tetrahedral (Si)	2.96	2.97	2.94	2.94	2.95	2.95	2.93	2.94	2.97	2.95	2.94
Tetrahedral (Al)	0.04	0.03	0.06	0.06	0.05	0.05	0.07	0.06	0.03	0.05	0.06
Tetrahedral (3)	3.00	3.00	3.00	3.00	3.00	3.00	3.00	3.00	3.00	3.00	3.00
Octahedral (2)	2.04	2.03	2.07	2.04	2.05	2.06	2.06	2.06	2.02	2.05	2.06
Cavities (3)	2.96	2.97	2.93	2.96	2.94	2.93	2.94	2.93	2.98	2.95	2.94
XAlm	0.41	0.39	0.37	0.37	0.36	0.36	0.36	0.36	0.38	0.37	0.37
XPyp	0.32	0.34	0.37	0.37	0.37	0.38	0.38	0.38	0.36	0.37	0.37
XGrs	0.26	0.26	0.26	0.25	0.25	0.25	0.25	0.25	0.25	0.24	0.25
XSps	0.01	0.01	0.01	0.01	0.01	0.01	0.01	0.01	0.01	0.01	0.01

Appendix 6.D EMP data for garnet with calculated end member proportions. XAlm = $Fe^{2+}/(Fe^{2+}+Mn+Mg+Ca)$. XPyp = $Mg/(Fe^{2+}+Mn+Mg+Ca)$, XGrs = $Ca/(Fe^{2+}+Mn+Mg+Ca)$, XSps = $Mn/(Fe^{2+}+Mn+Mg+Ca)$

Comment	0910B 1.3+ g trav	0910B 1.3+ g trav	0910B 1.3+ g trav	0910B 1.3+ g trav	0910B 1.3+ g trav	0910B 1.3+ g trav	0910B 1.3+ g trav	0910B 1.3+ g trav	0910B 1.3+ g trav	0910B 1.3+ g trav	0910B 1.3+ g trav
X	-14133	-14133	-14133	-14133	-14133	-14133	-14133	-14133	-14133	-14133	-14133
Y	-31192	-31786	-32133	-32504	-32861	-33134	-33674	-34011	-34422	-34717	-34934
Z	81	81	81	81	81	81	81	81	81	81	81
SiO2	39.26	39.29	39.26	39.23	39.01	39.43	38.98	39.18	39.33	39.31	39.31
TiO2	0.05	0.11	0.04	0.02	0.02	0.02	0.07	0.08	0.02	0.03	0.05
Al2O3	22.13	22.17	22.22	22.18	22.14	22.47	22.32	22.38	22.19	22.28	22.04
Cr2O3	0.02	0.00	0.03	0.00	0.00	0.02	0.00	0.00	0.00	0.00	0.00
Fe2O3	2.06	2.37	2.39	2.25	3.28	2.21	2.75	2.45	3.00	2.10	2.46
FeO	18.00	17.50	17.50	17.50	17.00	18.00	17.00	17.50	17.50	18.50	17.50
MnO	0.50	0.52	0.51	0.53	0.54	0.51	0.46	0.51	0.57	0.56	0.50
MgO	10.07	10.40	10.10	10.23	10.37	10.59	10.51	10.29	10.43	9.78	10.49
CaO	8.34	8.18	8.59	8.15	8.39	7.61	8.18	8.27	8.02	8.32	8.24
Na2O	0.01	0.02	0.00	0.01	0.02	0.02	0.01	0.03	0.00	0.01	0.00
K2O	0.00	0.00	0.01	0.00	0.00	0.01	0.01	0.01	0.01	0.00	0.01
NiO	0.00	0.00	0.00	0.01	0.02	0.04	0.00	0.02	0.01	0.00	0.00
Total	100.24	100.33	100.42	99.89	100.46	100.69	100.00	100.46	100.78	100.69	100.36
FeO	19.85	19.63	19.65	19.52	19.95	19.99	19.47	19.70	20.20	20.39	19.72
Num ox	12	12	12	12	12	12	12	12	12	12	12
Si	2.95	2.95	2.95	2.95	2.92	2.95	2.93	2.94	2.94	2.95	2.95
Ti	0.00	0.01	0.00	0.00	0.00	0.00	0.00	0.00	0.00	0.00	0.00
Al	1.96	1.96	1.97	1.97	1.96	1.98	1.98	1.98	1.95	1.97	1.95
Cr	0.00	0.00	0.00	0.00	0.00	0.00	0.00	0.00	0.00	0.00	0.00
Fe3+	0.12	0.13	0.14	0.13	0.19	0.12	0.16	0.14	0.17	0.12	0.14
Fe2+	1.13	1.10	1.10	1.10	1.07	1.12	1.07	1.10	1.09	1.16	1.10
Mn	0.03	0.03	0.03	0.03	0.03	0.03	0.03	0.03	0.04	0.04	0.03
Mg	1.13	1.16	1.13	1.15	1.16	1.18	1.18	1.15	1.16	1.09	1.17
Ca	0.67	0.66	0.69	0.66	0.67	0.61	0.66	0.66	0.64	0.67	0.66
Na	0.00	0.00	0.00	0.00	0.00	0.00	0.00	0.00	0.00	0.00	0.00
K	0.00	0.00	0.00	0.00	0.00	0.00	0.00	0.00	0.00	0.00	0.00
Ni	0.00	0.00	0.00	0.00	0.00	0.00	0.00	0.00	0.00	0.00	0.00
Total	8.00	8.00	8.00	8.00	8.00	8.00	8.00	8.00	8.00	8.00	8.00
Tetrahedral (Si)	2.95	2.95	2.95	2.95	2.92	2.95	2.93	2.94	2.94	2.95	2.95
Tetrahedral (Al)	0.05	0.05	0.05	0.05	0.08	0.05	0.07	0.06	0.06	0.05	0.05
Tetrahedral (3)	3.00	3.00	3.00	3.00	3.00	3.00	3.00	3.00	3.00	3.00	3.00
Octahedral (2)	2.04	2.05	2.05	2.05	2.07	2.05	2.07	2.06	2.06	2.04	2.04
Cavities (3)	2.97	2.95	2.95	2.94	2.93	2.95	2.93	2.94	2.93	2.96	2.96
XAlm	0.38	0.37	0.37	0.37	0.36	0.38	0.36	0.37	0.37	0.39	0.37
XPyp	0.38	0.39	0.38	0.39	0.40	0.40	0.40	0.39	0.40	0.37	0.40
XGrs	0.23	0.22	0.23	0.22	0.23	0.21	0.22	0.23	0.22	0.23	0.22
XSps	0.01	0.01	0.01	0.01	0.01	0.01	0.01	0.01	0.01	0.01	0.01

Appendix 6.D EMP data for garnet with calculated end member proportions. XAlm = $Fe^{2+}/(Fe^{2+}+Mn+Mg+Ca)$. XPyp = $Mg/(Fe^{2+}+Mn+Mg+Ca)$, XGrs = $Ca/(Fe^{2+}+Mn+Mg+Ca)$, XSps = $Mn/(Fe^{2+}+Mn+Mg+Ca)$

Comment	0910B 1.3+ g trav	0910B 1.3+ g trav	0910B 1.3+ g trav	0910B 1.3+ g trav	0910B 1.3+ g trav	0910B 1.3+ g trav	0910B 1.3+ g trav	0910B 1.3+ g trav	0910B 1.3+ g trav	0910B 1.3+ g trav	0910B 1.3+ g trav
X	-14133	-14133	-14133	-14133	-14133	-14133	-14133	-14133	-14178	-14178	-14178
Y	-35538	-35653	-35793	-35919	-35960	-36180	-36538	-37115	-37332	-37558	-38138
Z	81	81	81	81	81	81	81	81	81	81	81
SiO2	39.16	39.14	39.26	39.56	39.20	39.37	39.27	39.24	38.90	38.91	39.28
TiO2	0.04	0.03	0.02	0.03	0.06	0.02	0.20	0.03	0.02	0.04	0.04
Al2O3	22.13	22.19	22.28	22.29	22.23	22.35	22.16	22.16	22.11	22.19	22.23
Cr2O3	0.01	0.00	0.01	0.02	0.01	0.00	0.00	0.03	0.00	0.01	0.00
Fe2O3	2.85	2.85	3.23	2.55	2.71	2.46	2.43	2.62	3.31	3.20	2.02
FeO	17.50	17.50	17.00	17.50	17.25	17.50	17.50	17.50	17.00	17.00	18.00
MnO	0.55	0.59	0.53	0.53	0.52	0.49	0.51	0.50	0.52	0.55	0.53
MgO	10.66	10.43	10.60	10.39	10.36	10.46	10.54	10.46	10.29	10.43	10.20
CaO	7.79	8.01	8.03	8.18	8.32	8.12	8.10	8.00	8.28	8.02	8.12
Na2O	0.00	0.00	0.01	0.01	0.00	0.00	0.02	0.01	0.02	0.02	0.02
K2O	0.00	0.00	0.00	0.01	0.00	0.01	0.00	0.00	0.00	0.00	0.01
NiO	0.00	0.04	0.00	0.00	0.00	0.00	0.01	0.01	0.01	0.02	0.02
Total	100.41	100.49	100.64	100.82	100.40	100.53	100.50	100.28	100.14	100.08	100.27
FeO	20.07	20.06	19.91	19.80	19.69	19.71	19.68	19.86	19.98	19.88	19.82
Num ox	12	12	12	12	12	12	12	12	12	12	12
Si	2.94	2.93	2.93	2.95	2.94	2.94	2.94	2.94	2.93	2.93	2.95
Ti	0.00	0.00	0.00	0.00	0.00	0.00	0.01	0.00	0.00	0.00	0.00
Al	1.96	1.96	1.96	1.96	1.96	1.97	1.96	1.96	1.96	1.97	1.97
Cr	0.00	0.00	0.00	0.00	0.00	0.00	0.00	0.00	0.00	0.00	0.00
Fe3+	0.16	0.16	0.18	0.14	0.15	0.14	0.14	0.15	0.19	0.18	0.11
Fe2+	1.10	1.10	1.06	1.09	1.08	1.09	1.10	1.10	1.07	1.07	1.13
Mn	0.04	0.04	0.03	0.03	0.03	0.03	0.03	0.03	0.03	0.04	0.03
Mg	1.19	1.17	1.18	1.16	1.16	1.17	1.18	1.17	1.15	1.17	1.14
Ca	0.63	0.64	0.64	0.65	0.67	0.65	0.65	0.64	0.67	0.65	0.65
Na	0.00	0.00	0.00	0.00	0.00	0.00	0.00	0.00	0.00	0.00	0.00
K	0.00	0.00	0.00	0.00	0.00	0.00	0.00	0.00	0.00	0.00	0.00
Ni	0.00	0.00	0.00	0.00	0.00	0.00	0.00	0.00	0.00	0.00	0.00
Total	8.00	8.00	8.00	8.00	8.00	8.00	8.00	8.00	8.00	8.00	8.00
Tetrahedral (Si)	2.94	2.93	2.93	2.95	2.94	2.94	2.94	2.94	2.93	2.93	2.95
Tetrahedral (Al)	0.06	0.07	0.07	0.05	0.06	0.06	0.06	0.06	0.07	0.07	0.05
Tetrahedral (3)	3.00	3.00	3.00	3.00	3.00	3.00	3.00	3.00	3.00	3.00	3.00
Octahedral (2)	2.05	2.06	2.08	2.06	2.06	2.06	2.04	2.06	2.07	2.08	2.04
Cavities (3)	2.95	2.94	2.92	2.94	2.94	2.94	2.95	2.94	2.92	2.92	2.96
XAlm	0.37	0.37	0.36	0.37	0.37	0.37	0.37	0.37	0.37	0.37	0.38
XPyp	0.40	0.40	0.40	0.39	0.39	0.40	0.40	0.40	0.39	0.40	0.39
XGrs	0.21	0.22	0.22	0.22	0.23	0.22	0.22	0.22	0.23	0.22	0.22
XSps	0.01	0.01	0.01	0.01	0.01	0.01	0.01	0.01	0.01	0.01	0.01

Appendix 6.D EMP data for garnet with calculated end member proportions. XAlm = $Fe^{2+}/(Fe^{2+}+Mn+Mg+Ca)$. XPyp = $Mg/(Fe^{2+}+Mn+Mg+Ca)$, XGrs = $Ca/(Fe^{2+}+Mn+Mg+Ca)$, XSps = $Mn/(Fe^{2+}+Mn+Mg+Ca)$

Comment	0910B 1.3+ g trav	0910B 1.3+ g trav	0910B 1.3+ g trav	0905B 2.1+ g trav	0905B 2.1+ g trav	0905B 2.1+ g trav	0905B 2.1+ g trav	0905B 2.1+ g trav	0905B 2.1+ g trav	0905B 2.1+ g trav	0905B 2.1+ g trav
X	-14178	-14178	-14178	15934	15908	15868	15814	15746	15665	15485	15313
Y	-38700	-39139	-39393	11899	11899	11867	11867	11867	11867	11867	11867
Z	81	81	81	65	65	65	65	65	65	65	65
SiO2	39.38	39.20	39.43	40.01	40.25	40.08	39.82	39.86	40.23	39.93	39.94
TiO2	0.05	0.03	0.05	0.08	0.08	0.14	0.12	0.17	0.09	0.19	0.15
Al2O3	22.19	22.23	22.33	22.07	22.14	21.90	22.03	21.98	21.94	21.95	21.97
Cr2O3	0.00	0.04	0.04	0.00	0.00	0.05	0.02	0.02	0.06	0.01	0.04
Fe2O3	2.81	2.78	2.68	0.00	0.86	1.16	1.70	1.15	1.19	1.17	1.50
FeO	17.50	17.50	17.50	20.40	20.50	21.00	20.50	21.00	21.00	21.00	21.00
MnO	0.50	0.52	0.54	0.70	0.52	0.49	0.53	0.55	0.48	0.50	0.52
MgO	10.40	10.39	10.53	7.99	9.49	9.78	10.04	9.95	10.15	10.18	10.09
CaO	8.11	7.97	8.03	9.91	7.81	6.90	6.63	6.42	6.39	6.28	6.26
Na2O	0.02	0.00	0.02	0.02	0.05	0.06	0.05	0.06	0.06	0.07	0.06
K2O	0.00	0.00	0.00	0.01	0.02	0.01	0.00	0.00	0.01	0.00	0.00
NiO	0.00	0.00	0.00	0.00	0.00	0.00	0.00	0.00	0.00	0.00	0.02
Total	100.67	100.39	100.88	101.18	101.62	101.46	101.27	101.05	101.49	101.16	101.40
FeO	20.03	20.00	19.92	20.40	21.27	22.05	22.03	22.04	22.07	22.05	22.35
Num ox	12	12	12	12	12	12	12	12	12	12	12
Si	2.94	2.94	2.94	3.01	3.00	3.00	2.98	2.99	3.00	2.99	2.99
Ti	0.00	0.00	0.00	0.00	0.00	0.01	0.01	0.01	0.01	0.01	0.01
Al	1.96	1.97	1.96	1.96	1.95	1.93	1.94	1.94	1.93	1.94	1.94
Cr	0.00	0.00	0.00	0.00	0.00	0.00	0.00	0.00	0.00	0.00	0.00
Fe3+	0.16	0.16	0.15	0.00	0.05	0.07	0.10	0.07	0.07	0.07	0.08
Fe2+	1.09	1.10	1.09	1.28	1.28	1.31	1.28	1.32	1.31	1.32	1.31
Mn	0.03	0.03	0.03	0.04	0.03	0.03	0.03	0.04	0.03	0.03	0.03
Mg	1.16	1.16	1.17	0.90	1.06	1.09	1.12	1.11	1.13	1.14	1.12
Ca	0.65	0.64	0.64	0.80	0.62	0.55	0.53	0.52	0.51	0.50	0.50
Na	0.00	0.00	0.00	0.00	0.01	0.01	0.01	0.01	0.01	0.01	0.01
K	0.00	0.00	0.00	0.00	0.00	0.00	0.00	0.00	0.00	0.00	0.00
Ni	0.00	0.00	0.00	0.00	0.00	0.00	0.00	0.00	0.00	0.00	0.00
Total	8.00	8.00	8.00	8.00	8.00	8.00	8.00	8.00	8.00	8.00	8.00
Tetrahedral (Si)	2.94	2.94	2.94	3.01	3.00	3.00	2.98	2.99	3.00	2.99	2.99
Tetrahedral (Al)	0.06	0.06	0.06	-0.01	0.00	0.00	0.02	0.01	0.00	0.01	0.01
Tetrahedral (3)	3.00	3.00	3.00	3.00	3.00	3.00	3.00	3.00	3.00	3.00	3.00
Octahedral (2)	2.06	2.06	2.06	1.98	2.00	2.00	2.02	2.01	2.01	2.00	2.02
Cavities (3)	2.93	2.93	2.94	3.03	2.99	2.99	2.97	2.98	2.98	2.99	2.97
XAlm	0.37	0.37	0.37	0.42	0.43	0.44	0.43	0.44	0.44	0.44	0.44
XPyp	0.39	0.40	0.40	0.30	0.35	0.36	0.38	0.37	0.38	0.38	0.38
XGrs	0.22	0.22	0.22	0.26	0.21	0.19	0.18	0.17	0.17	0.17	0.17
XSps	0.01	0.01	0.01	0.01	0.01	0.01	0.01	0.01	0.01	0.01	0.01

Appendix 6.D EMP data for garnet with calculated end member proportions. XAlm = $Fe^{2+}/(Fe^{2+}+Mn+Mg+Ca)$. XPyp = $Mg/(Fe^{2+}+Mn+Mg+Ca)$, XGrs = $Ca/(Fe^{2+}+Mn+Mg+Ca)$, XSps = $Mn/(Fe^{2+}+Mn+Mg+Ca)$

Comment	0905B 2.1+ g trav	0905B 2.1+ g trav	0905B 2.1+ g trav	0905B 2.1+ g trav	0905B 2.1+ g trav	0905B 2.1+ g trav	0905B 2.1+ g trav	0905B 2.1+ g trav	0905B 2.1+ g trav	0905B 2.1+ g trav	0905B 2.1+ g trav
X	15077	14852	14535	14370	14237	14006	13856	13707	13226	12939	12717
Y	11867	11867	11867	11867	11842	11842	11853	11911	11911	11911	11911
Z	65	65	65	65	65	65	65	65	65	65	65
SiO2	39.85	39.91	40.13	39.95	40.10	40.00	39.95	39.73	39.85	40.04	40.08
TiO2	0.21	0.12	0.11	0.10	0.13	0.10	0.08	0.03	0.07	0.19	0.11
Al2O3	21.83	22.07	22.10	21.95	21.99	22.01	22.11	22.03	21.97	22.08	21.92
Cr2O3	0.00	0.00	0.01	0.00	0.02	0.04	0.03	0.00	0.00	0.00	0.00
Fe2O3	1.47	1.70	1.07	1.12	1.16	1.00	1.49	1.48	0.81	0.96	1.22
FeO	20.50	20.50	21.00	21.00	21.00	21.00	20.50	20.50	20.50	21.00	21.00
MnO	0.54	0.50	0.51	0.48	0.52	0.50	0.52	0.54	0.56	0.47	0.50
MgO	10.31	10.35	10.30	10.24	10.43	10.23	10.39	9.86	9.52	10.31	10.28
CaO	6.17	6.18	6.17	6.19	6.17	6.12	6.14	6.89	7.51	6.20	6.27
Na2O	0.07	0.07	0.04	0.04	0.06	0.05	0.06	0.04	0.04	0.08	0.07
K2O	0.01	0.01	0.00	0.00	0.00	0.00	0.00	0.01	0.00	0.00	0.00
NiO	0.00	0.00	0.01	0.04	0.00	0.00	0.02	0.00	0.00	0.02	0.00
Total	100.82	101.25	101.33	100.98	101.46	100.94	101.14	100.97	100.75	101.25	101.32
FeO	21.82	22.03	21.96	22.01	22.04	21.90	21.84	21.83	21.23	21.86	22.10
Num ox	12	12	12	12	12	12	12	12	12	12	12
Si	2.99	2.98	3.00	3.00	2.99	3.00	2.99	2.98	3.00	2.99	3.00
Ti	0.01	0.01	0.01	0.01	0.01	0.01	0.00	0.00	0.00	0.01	0.01
Al	1.93	1.94	1.95	1.94	1.93	1.95	1.95	1.95	1.95	1.95	1.93
Cr	0.00	0.00	0.00	0.00	0.00	0.00	0.00	0.00	0.00	0.00	0.00
Fe3+	0.08	0.10	0.06	0.06	0.07	0.06	0.08	0.08	0.05	0.05	0.07
Fe2+	1.29	1.28	1.31	1.32	1.31	1.32	1.28	1.29	1.29	1.31	1.31
Mn	0.03	0.03	0.03	0.03	0.03	0.03	0.03	0.03	0.04	0.03	0.03
Mg	1.15	1.15	1.15	1.14	1.16	1.14	1.16	1.10	1.07	1.15	1.15
Ca	0.50	0.49	0.49	0.50	0.49	0.49	0.49	0.55	0.61	0.50	0.50
Na	0.01	0.01	0.01	0.01	0.01	0.01	0.01	0.01	0.01	0.01	0.01
K	0.00	0.00	0.00	0.00	0.00	0.00	0.00	0.00	0.00	0.00	0.00
Ni	0.00	0.00	0.00	0.00	0.00	0.00	0.00	0.00	0.00	0.00	0.00
Total	8.00	8.00	8.00	8.00	8.00	8.00	8.00	8.00	8.00	8.00	8.00
Tetrahedral (Si)	2.99	2.98	3.00	3.00	2.99	3.00	2.99	2.98	3.00	2.99	3.00
Tetrahedral (Al)	0.01	0.02	0.00	0.00	0.01	0.00	0.01	0.02	0.00	0.01	0.00
Tetrahedral (3)	3.00	3.00	3.00	3.00	3.00	3.00	3.00	3.00	3.00	3.00	3.00
Octahedral (2)	2.02	2.03	2.01	2.00	2.00	2.01	2.02	2.02	2.00	2.00	2.00
Cavities (3)	2.97	2.96	2.98	2.99	3.00	2.98	2.96	2.98	3.00	2.99	2.99
XAlm	0.43	0.43	0.44	0.44	0.44	0.44	0.43	0.43	0.43	0.44	0.44
XPyp	0.39	0.39	0.38	0.38	0.39	0.38	0.39	0.37	0.36	0.38	0.38
XGrs	0.17	0.17	0.17	0.17	0.16	0.16	0.17	0.19	0.20	0.17	0.17
XSps	0.01	0.01	0.01	0.01	0.01	0.01	0.01	0.01	0.01	0.01	0.01

Appendix 6.D EMP data for garnet with calculated end member proportions. XAlm = $Fe^{2+}/(Fe^{2+}+Mn+Mg+Ca)$. XPyp = $Mg/(Fe^{2+}+Mn+Mg+Ca)$, XGrs = $Ca/(Fe^{2+}+Mn+Mg+Ca)$, XSps = $Mn/(Fe^{2+}+Mn+Mg+Ca)$

Comment	0905B 2.1+ g trav	0905B 2.1+ g trav	0905B 2.1+ g trav	0905B 2.1+ g trav	0905B 2.1+ g trav	0905B 2.1+ g trav	0905B 2.1+ g trav	0905B 2.1+ g trav	0905B 2.1+ g trav	0905B 2.1+ g trav
X	12452	12295	12116	11890	11734	11609	11578	11546	11523	11476
Y	11911	11903	11903	11903	11903	11903	11948	11948	11948	11941
Z	65	65	65	65	65	65	65	65	65	65
SiO2	39.82	39.87	39.96	39.74	39.78	39.80	39.95	39.91	39.81	39.60
TiO2	0.11	0.14	0.13	0.20	0.18	0.14	0.12	0.14	0.15	0.18
Al2O3	21.94	22.05	21.97	21.93	21.82	22.04	21.96	21.90	21.93	21.89
Cr2O3	0.02	0.00	0.03	0.00	0.01	0.01	0.00	0.01	0.02	0.00
Fe2O3	1.28	1.66	1.40	1.71	1.51	1.68	1.23	0.98	1.75	0.83
FeO	20.50	20.50	20.50	20.50	20.50	20.50	20.75	21.00	20.50	20.50
MnO	0.55	0.51	0.55	0.47	0.53	0.45	0.50	0.46	0.53	0.76
MgO	10.34	10.37	10.34	10.19	10.06	10.22	10.10	10.01	9.87	8.65
CaO	6.22	6.22	6.31	6.29	6.52	6.44	6.56	6.59	6.77	8.43
Na2O	0.04	0.05	0.06	0.07	0.06	0.08	0.05	0.03	0.06	0.03
K2O	0.01	0.02	0.02	0.00	0.01	0.00	0.01	0.01	0.02	0.00
NiO	0.00	0.00	0.05	0.00	0.00	0.00	0.01	0.00	0.00	0.01
Total	100.70	101.23	101.20	100.94	100.84	101.18	101.10	100.94	101.23	100.80
FeO	21.65	22.00	21.76	22.04	21.86	22.01	21.85	21.88	22.08	21.24
Num ox	12	12	12	12	12	12	12	12	12	12
Si	2.99	2.98	2.99	2.98	2.99	2.98	2.99	3.00	2.98	2.99
Ti	0.01	0.01	0.01	0.01	0.01	0.01	0.01	0.01	0.01	0.01
Al	1.94	1.94	1.94	1.94	1.93	1.94	1.94	1.94	1.94	1.95
Cr	0.00	0.00	0.00	0.00	0.00	0.00	0.00	0.00	0.00	0.00
Fe3+	0.07	0.09	0.08	0.10	0.09	0.09	0.07	0.06	0.10	0.05
Fe2+	1.29	1.28	1.28	1.29	1.29	1.28	1.30	1.32	1.28	1.30
Mn	0.04	0.03	0.03	0.03	0.03	0.03	0.03	0.03	0.03	0.05
Mg	1.16	1.16	1.15	1.14	1.13	1.14	1.13	1.12	1.10	0.97
Ca	0.50	0.50	0.51	0.51	0.52	0.52	0.53	0.53	0.54	0.68
Na	0.01	0.01	0.01	0.01	0.01	0.01	0.01	0.01	0.01	0.00
K	0.00	0.00	0.00	0.00	0.00	0.00	0.00	0.00	0.00	0.00
Ni	0.00	0.00	0.00	0.00	0.00	0.00	0.00	0.00	0.00	0.00
Total	8.00	8.00	8.00	8.00	8.00	8.00	8.00	8.00	8.00	8.00
Tetrahedral (Si)	2.99	2.98	2.99	2.98	2.99	2.98	2.99	3.00	2.98	2.99
Tetrahedral (Al)	0.01	0.02	0.01	0.02	0.01	0.02	0.01	0.00	0.02	0.01
Tetrahedral (3)	3.00	3.00	3.00	3.00	3.00	3.00	3.00	3.00	3.00	3.00
Octahedral (2)	2.01	2.02	2.01	2.03	2.02	2.02	2.01	2.00	2.03	2.00
Cavities (3)	2.98	2.97	2.98	2.96	2.97	2.97	2.99	3.00	2.96	3.00
XAlm	0.43	0.43	0.43	0.43	0.43	0.43	0.44	0.44	0.43	0.43
XPyp	0.39	0.39	0.39	0.38	0.38	0.38	0.38	0.37	0.37	0.32
XGrs	0.17	0.17	0.17	0.17	0.18	0.17	0.18	0.18	0.18	0.23
XSps	0.01	0.01	0.01	0.01	0.01	0.01	0.01	0.01	0.01	0.02

Appendix 6.D EMP data for garnet with calculated end member proportions. XAlm = $Fe^{2+}/(Fe^{2+}+Mn+Mg+Ca)$. XPyp = $Mg/(Fe^{2+}+Mn+Mg+Ca)$, XGrs = $Ca/(Fe^{2+}+Mn+Mg+Ca)$, XSps = $Mn/(Fe^{2+}+Mn+Mg+Ca)$

Comment	0905B 2.2 g	0906B 1.2 g r	0906B 1.14 g r	0906B 1.16 ?	0906B 1.17 ?	0906B 1.18 ?	0906B 1.19 g c	0906B 1.21 g r	0906B 1.22 g r	0906B 1.23 g r	0906B 1.26 g r
X	11918	-14093	-13856	-12741	-17433	-16633	-16645	-16480	-14029	-14012	-13603
Y	12668	25287	25799	27535	27130	29051	29157	28057	27285	27418	28068
Z	65	60	57	55	55	55	55	55	54	54	54
SiO2	39.71	40.47	40.11	39.77	40.29	40.64	40.33	40.45	39.89	39.64	40.10
TiO2	0.06	0.05	0.13	0.06	0.07	0.09	0.10	0.07	0.12	0.05	0.07
Al2O3	21.86	22.29	22.08	22.00	22.14	21.99	21.97	22.11	22.07	21.86	22.09
Cr2O3	0.00	0.04	0.05	0.03	0.03	0.04	0.02	0.00	0.05	0.00	0.02
Fe2O3	1.14	0.62	0.67	2.26	1.17	0.23	1.22	0.87	1.67	0.89	0.80
FeO	20.00	19.50	20.50	19.00	19.00	20.00	19.00	19.50	19.50	20.50	20.00
MnO	0.50	0.57	0.61	0.56	0.60	0.59	0.55	0.57	0.61	0.67	0.57
MgO	9.37	10.61	9.54	9.24	10.51	10.44	10.64	10.59	9.69	8.25	9.53
CaO	7.93	7.27	7.83	8.78	7.49	7.34	7.54	7.31	7.91	9.04	8.34
Na2O	0.04	0.03	0.02	0.02	0.03	0.04	0.03	0.02	0.03	0.02	0.00
K2O	0.01	0.01	0.00	0.00	0.01	0.00	0.00	0.00	0.02	0.00	0.00
NiO	0.02	0.00	0.00	0.00	0.01	0.00	0.00	0.02	0.00	0.02	0.01
Total	100.53	101.40	101.48	101.50	101.24	101.38	101.28	101.43	101.40	100.86	101.45
FeO	21.03	20.06	21.10	21.03	20.05	20.21	20.10	20.29	21.00	21.30	20.72
Num ox	12	12	12	12	12	12	12	12	12	12	12
Si	2.99	3.01	3.00	2.97	3.00	3.02	3.00	3.00	2.98	3.00	3.00
Ti	0.00	0.00	0.01	0.00	0.00	0.00	0.01	0.00	0.01	0.00	0.00
Al	1.94	1.95	1.95	1.94	1.94	1.93	1.93	1.94	1.94	1.95	1.95
Cr	0.00	0.00	0.00	0.00	0.00	0.00	0.00	0.00	0.00	0.00	0.00
Fe3+	0.06	0.03	0.04	0.13	0.07	0.01	0.07	0.05	0.09	0.05	0.04
Fe2+	1.26	1.21	1.28	1.19	1.18	1.24	1.18	1.21	1.22	1.30	1.25
Mn	0.03	0.04	0.04	0.04	0.04	0.04	0.03	0.04	0.04	0.04	0.04
Mg	1.05	1.17	1.06	1.03	1.17	1.16	1.18	1.17	1.08	0.93	1.06
Ca	0.64	0.58	0.63	0.70	0.60	0.59	0.60	0.58	0.63	0.73	0.67
Na	0.01	0.00	0.00	0.00	0.00	0.01	0.00	0.00	0.01	0.00	0.00
K	0.00	0.00	0.00	0.00	0.00	0.00	0.00	0.00	0.00	0.00	0.00
Ni	0.00	0.00	0.00	0.00	0.00	0.00	0.00	0.00	0.00	0.00	0.00
Total	8.00	8.00	8.00	8.00	8.00	8.00	8.00	8.00	8.00	8.00	8.00
Tetrahedral (Si)	2.99	3.01	3.00	2.97	3.00	3.02	3.00	3.00	2.98	3.00	3.00
Tetrahedral (Al)	0.01	-0.01	0.00	0.03	0.00	-0.02	0.00	0.00	0.02	0.00	0.00
Tetrahedral (3)	3.00	3.00	3.00	3.00	3.00	3.00	3.00	3.00	3.00	3.00	3.00
Octahedral (2)	2.01	2.00	1.99	2.04	2.01	1.97	2.00	1.99	2.02	2.00	1.99
Cavities (3)	2.99	3.00	3.01	2.95	2.98	3.02	3.00	3.00	2.97	3.00	3.01
XAlm	0.42	0.40	0.43	0.40	0.40	0.41	0.39	0.40	0.41	0.43	0.41
XPyp	0.35	0.39	0.35	0.35	0.39	0.38	0.39	0.39	0.36	0.31	0.35
XGrs	0.21	0.19	0.21	0.24	0.20	0.19	0.20	0.19	0.21	0.24	0.22
XSps	0.01	0.01	0.01	0.01	0.01	0.01	0.01	0.01	0.01	0.01	0.01

Appendix 6.D EMP data for garnet with calculated end member proportions. XAlm = $Fe^{2+}/(Fe^{2+}+Mn+Mg+Ca)$. XPyp = $Mg/(Fe^{2+}+Mn+Mg+Ca)$, XGrs = $Ca/(Fe^{2+}+Mn+Mg+Ca)$, XSps = $Mn/(Fe^{2+}+Mn+Mg+Ca)$

Comment	0904C 1.1+ g trav	0904C 1.1+ g trav	0904C 1.1+ g trav	0904C 1.1+ g trav	0904C 1.1+ g trav	0904C 1.1+ g trav	0904C 1.1+ g trav	0904C 1.1+ g trav	0904C 1.1+ g trav	0904C 1.1+ g trav	0904C 1.1+ g trav
X	-17025	-16994	-16949	-16876	-16702	-16610	-16493	-16369	-16246	-16148	-16004
Y	-7937	-7937	-7937	-7937	-7937	-7937	-7946	-7946	-7946	-7946	-7946
Z	64	64	64	64	64	64	64	64	64	64	64
SiO2	39.23	39.72	40.06	39.76	39.94	39.82	39.85	39.49	39.67	39.70	39.37
TiO2	0.06	0.03	0.05	0.04	0.05	0.08	0.04	0.06	0.08	0.07	0.08
Al2O3	21.66	21.84	21.89	22.05	21.93	21.98	22.04	22.33	22.00	22.06	22.11
Cr2O3	0.03	0.04	0.06	0.05	0.03	0.03	0.01	0.00	0.00	0.03	0.02
Fe2O3	0.91	1.07	1.36	1.47	0.96	1.10	0.81	1.28	1.86	1.88	2.46
FeO	20.80	19.00	18.50	18.00	18.50	18.50	18.50	18.00	18.00	18.00	17.50
MnO	0.96	0.57	0.56	0.57	0.56	0.47	0.51	0.57	0.49	0.54	0.51
MgO	7.09	8.41	8.89	9.02	9.05	8.95	9.01	8.92	8.83	9.04	9.06
CaO	9.90	10.17	10.02	10.07	9.86	9.79	9.92	9.93	10.26	10.19	9.99
Na2O	0.02	0.01	0.01	0.02	0.02	0.03	0.02	0.02	0.04	0.02	0.01
K2O	0.00	0.00	0.00	0.01	0.00	0.00	0.01	0.00	0.01	0.00	0.01
NiO	0.00	0.00	0.00	0.00	0.01	0.00	0.00	0.01	0.00	0.04	0.00
Total	100.56	100.77	101.26	100.90	100.81	100.64	100.64	100.49	101.04	101.37	100.89
FeO	21.62	19.97	19.72	19.32	19.36	19.49	19.23	19.15	19.68	19.69	19.71
Num ox	12	12	12	12	12	12	12	12	12	12	12
Si	2.99	2.99	3.00	2.98	3.00	2.99	3.00	2.97	2.97	2.97	2.95
Ti	0.00	0.00	0.00	0.00	0.00	0.00	0.00	0.00	0.00	0.00	0.00
Al	1.95	1.94	1.93	1.95	1.94	1.95	1.95	1.98	1.94	1.94	1.95
Cr	0.00	0.00	0.00	0.00	0.00	0.00	0.00	0.00	0.00	0.00	0.00
Fe3+	0.05	0.06	0.08	0.08	0.05	0.06	0.05	0.07	0.11	0.11	0.14
Fe2+	1.33	1.20	1.16	1.13	1.16	1.16	1.16	1.13	1.13	1.12	1.10
Mn	0.06	0.04	0.04	0.04	0.04	0.03	0.03	0.04	0.03	0.03	0.03
Mg	0.81	0.95	0.99	1.01	1.01	1.00	1.01	1.00	0.99	1.01	1.01
Ca	0.81	0.82	0.80	0.81	0.79	0.79	0.80	0.80	0.82	0.82	0.80
Na	0.00	0.00	0.00	0.00	0.00	0.00	0.00	0.00	0.01	0.00	0.00
K	0.00	0.00	0.00	0.00	0.00	0.00	0.00	0.00	0.00	0.00	0.00
Ni	0.00	0.00	0.00	0.00	0.00	0.00	0.00	0.00	0.00	0.00	0.00
Total	8.00	8.00	8.00	8.00	8.00	8.00	8.00	8.00	8.00	8.00	8.00
Tetrahedral (Si)	2.99	2.99	3.00	2.98	3.00	2.99	3.00	2.97	2.97	2.97	2.95
Tetrahedral (Al)	0.01	0.01	0.00	0.02	0.00	0.01	0.00	0.03	0.03	0.03	0.05
Tetrahedral (3)	3.00	3.00	3.00	3.00	3.00	3.00	3.00	3.00	3.00	3.00	3.00
Octahedral (2)	2.00	2.00	2.01	2.02	2.00	2.01	2.00	2.03	2.03	2.02	2.05
Cavities (3)	3.00	3.00	2.99	2.98	3.00	2.98	3.00	2.97	2.97	2.98	2.94
XAlm	0.44	0.40	0.39	0.38	0.39	0.39	0.39	0.38	0.38	0.38	0.37
XPyp	0.27	0.31	0.33	0.34	0.34	0.34	0.34	0.34	0.33	0.34	0.34
XGrs	0.27	0.27	0.27	0.27	0.26	0.26	0.27	0.27	0.28	0.27	0.27
XSps	0.02	0.01	0.01	0.01	0.01	0.01	0.01	0.01	0.01	0.01	0.01

Appendix 6.D EMP data for garnet with calculated end member proportions. XAlm = $Fe^{2+}/(Fe^{2+}+Mn+Mg+Ca)$. XPyp = $Mg/(Fe^{2+}+Mn+Mg+Ca)$, XGrs = $Ca/(Fe^{2+}+Mn+Mg+Ca)$, XSps = $Mn/(Fe^{2+}+Mn+Mg+Ca)$

Comment	0904C 1.1+ g trav	0904C 1.1+ g trav	0904C 1.1+ g trav	0904C 1.1+ g trav	0904C 1.1+ g trav	0904C 1.1+ g trav	0903B 2.6 g	0903B 2.7 g r	73831 1.1 g c	73831 1.2 g r	73831 1.3 g c
X	-15779	-15632	-15453	-15352	-15320	-15297	7092	7169	16660	16174	12586
Y	-7946	-7946	-7946	-7947	-7933	-7933	-17104	-17135	24595	25053	26525
Z	64	64	64	64	64	64	81	81	101	101	97
SiO2	39.61	39.60	39.35	39.56	39.23	38.74	40.66	40.19	40.03	39.85	40.04
TiO2	0.05	0.07	0.04	0.05	0.03	0.04	0.03	0.03	0.14	0.10	0.09
Al2O3	21.90	22.00	22.03	21.99	22.24	21.88	22.47	22.15	22.26	22.15	22.38
Cr2O3	0.00	0.00	0.02	0.02	0.00	0.04	0.14	0.16	0.04	0.03	0.00
Fe2O3	1.29	2.09	2.46	1.75	2.01	2.16	0.94	0.92	1.33	1.34	0.99
FeO	18.75	18.00	17.50	18.00	18.00	19.50	18.50	20.00	22.50	23.25	22.00
MnO	0.57	0.57	0.54	0.51	0.57	0.96	0.85	0.98	0.54	0.64	0.50
MgO	9.22	9.70	9.21	8.89	8.59	7.26	12.12	10.88	10.22	9.24	10.09
CaO	9.00	8.91	9.70	10.06	10.12	9.94	6.02	6.06	5.24	5.69	5.72
Na2O	0.03	0.01	0.03	0.01	0.01	0.01	0.00	0.00	0.05	0.02	0.01
K2O	0.01	0.01	0.00	0.01	0.01	0.00	0.00	0.00	0.00	0.00	0.01
NiO	0.01	0.00	0.00	0.03	0.00	0.00	0.00	0.01	0.04	0.01	0.01
Total	100.30	100.76	100.62	100.69	100.60	100.32	101.64	101.29	102.39	102.32	101.85
FeO	19.91	19.88	19.71	19.57	19.81	21.45	19.35	20.83	23.70	24.46	22.89
Num ox	12	12	12	12	12	12	12	12	12	12	12
Si	2.99	2.97	2.96	2.97	2.96	2.95	2.99	2.99	2.98	2.98	2.99
Ti	0.00	0.00	0.00	0.00	0.00	0.00	0.00	0.00	0.01	0.01	0.01
Al	1.95	1.94	1.95	1.95	1.98	1.97	1.95	1.94	1.95	1.95	1.97
Cr	0.00	0.00	0.00	0.00	0.00	0.00	0.01	0.01	0.00	0.00	0.00
Fe3+	0.07	0.12	0.14	0.10	0.11	0.12	0.05	0.05	0.07	0.08	0.06
Fe2+	1.18	1.13	1.10	1.13	1.13	1.24	1.14	1.25	1.40	1.45	1.37
Mn	0.04	0.04	0.03	0.03	0.04	0.06	0.05	0.06	0.03	0.04	0.03
Mg	1.04	1.08	1.03	1.00	0.96	0.83	1.33	1.21	1.13	1.03	1.12
Ca	0.73	0.72	0.78	0.81	0.82	0.81	0.47	0.48	0.42	0.46	0.46
Na	0.00	0.00	0.00	0.00	0.00	0.00	0.00	0.00	0.01	0.00	0.00
K	0.00	0.00	0.00	0.00	0.00	0.00	0.00	0.00	0.00	0.00	0.00
Ni	0.00	0.00	0.00	0.00	0.00	0.00	0.00	0.00	0.00	0.00	0.00
Total	8.00	8.00	8.00	8.00	8.00	8.00	8.00	8.00	8.00	8.00	8.00
Tetrahedral (Si)	2.99	2.97	2.96	2.97	2.96	2.95	2.99	2.99	2.98	2.98	2.99
Tetrahedral (Al)	0.01	0.03	0.04	0.03	0.04	0.05	0.01	0.01	0.02	0.02	0.01
Tetrahedral (3)	3.00	3.00	3.00	3.00	3.00	3.00	3.00	3.00	3.00	3.00	3.00
Octahedral (2)	2.01	2.03	2.05	2.03	2.05	2.05	2.00	2.00	2.01	2.02	2.01
Cavities (3)	2.98	2.96	2.95	2.97	2.95	2.94	3.00	3.00	2.98	2.98	2.98
XAlm	0.40	0.38	0.37	0.38	0.38	0.42	0.38	0.42	0.47	0.49	0.46
XPyp	0.35	0.37	0.35	0.34	0.33	0.28	0.44	0.40	0.38	0.35	0.38
XGrs	0.24	0.24	0.27	0.27	0.28	0.28	0.16	0.16	0.14	0.15	0.15
XSps	0.01	0.01	0.01	0.01	0.01	0.02	0.02	0.02	0.01	0.01	0.01

Appendix 6.D EMP data for garnet with calculated end member proportions. XAlm = $Fe^{2+}/(Fe^{2+}+Mn+Mg+Ca)$. XPyp = $Mg/(Fe^{2+}+Mn+Mg+Ca)$, XGrs = $Ca/(Fe^{2+}+Mn+Mg+Ca)$, XSps = $Mn/(Fe^{2+}+Mn+Mg+Ca)$

Comment	73831 1.4 g r	73831 1.5 g c	73831 1.6 g r	73832 1.5 g c	73832 1.4 g r	73832 1.3 g c	73832 1.2 g r	73832 1.1 g c	0910B 1.3+ g trav	0910B 1.3+ g trav	0910B 1.3+ g trav
X	12308	11756	11533	-737	-801	-13925	-13854	-13524	-14133	-14133	-14133
Y	25968	28134	28542	-21000	-22456	-13478	-14176	-12097	-30508	-30729	-30830
Z	97	92	89	230	227	199	199	202	81	81	81
SiO2	39.84	40.03	39.22	40.24	39.17	40.24	39.57	40.18	39.08	39.04	39.51
TiO2	0.06	0.16	0.09	0.04	0.09	0.06	0.05	0.09	0.06	0.04	0.03
Al2O3	22.31	22.14	21.75	22.41	21.83	22.29	21.93	22.41	22.15	22.13	22.08
Cr2O3	0.03	0.01	0.02	0.02	0.00	0.00	0.01	0.05	0.00	0.02	0.02
Fe2O3	1.51	1.27	1.02	1.35	0.90	1.21	0.56	0.78	2.95	2.85	1.65
FeO	22.00	22.00	26.00	22.00	26.50	22.00	25.50	22.00	17.00	17.00	18.00
MnO	0.47	0.52	1.40	0.64	1.36	0.70	1.41	0.71	0.54	0.52	0.53
MgO	9.63	10.03	6.80	10.47	7.38	10.48	8.16	10.52	9.93	9.92	9.49
CaO	6.15	5.76	5.64	5.10	4.63	5.06	4.56	5.15	9.02	8.95	9.33
Na2O	0.01	0.05	0.02	0.02	0.00	0.01	0.03	0.01	0.01	0.01	0.02
K2O	0.01	0.00	0.01	0.01	0.00	0.01	0.00	0.00	0.00	0.00	0.00
NiO	0.00	0.01	0.00	0.01	0.00	0.00	0.00	0.07	0.00	0.01	0.00
Total	102.02	101.98	101.96	102.30	101.87	102.04	101.77	101.98	100.44	100.21	100.51
FeO	23.36	23.15	26.92	23.22	27.31	23.09	26.01	22.70	19.65	19.57	19.49
Num ox	12	12	12	12	12	12	12	12	12	12	12
Si	2.97	2.99	2.99	2.99	2.99	2.99	3.00	2.99	2.93	2.94	2.97
Ti	0.00	0.01	0.01	0.00	0.01	0.00	0.00	0.01	0.00	0.00	0.00
Al	1.96	1.95	1.96	1.96	1.96	1.95	1.96	1.97	1.96	1.96	1.96
Cr	0.00	0.00	0.00	0.00	0.00	0.00	0.00	0.00	0.00	0.00	0.00
Fe3+	0.08	0.07	0.06	0.08	0.05	0.07	0.03	0.04	0.17	0.16	0.09
Fe2+	1.37	1.37	1.66	1.37	1.69	1.37	1.62	1.37	1.07	1.07	1.13
Mn	0.03	0.03	0.09	0.04	0.09	0.04	0.09	0.04	0.03	0.03	0.03
Mg	1.07	1.11	0.77	1.16	0.84	1.16	0.92	1.17	1.11	1.11	1.06
Ca	0.49	0.46	0.46	0.41	0.38	0.40	0.37	0.41	0.73	0.72	0.75
Na	0.00	0.01	0.00	0.00	0.00	0.00	0.00	0.00	0.00	0.00	0.00
K	0.00	0.00	0.00	0.00	0.00	0.00	0.00	0.00	0.00	0.00	0.00
Ni	0.00	0.00	0.00	0.00	0.00	0.00	0.00	0.00	0.00	0.00	0.00
Total	8.00	8.00	8.00	8.00	8.00	8.00	8.00	8.00	8.00	8.00	8.00
Tetrahedral (Si)	2.97	2.99	2.99	2.99	2.99	2.99	3.00	2.99	2.93	2.94	2.97
Tetrahedral (Al)	0.03	0.01	0.01	0.01	0.01	0.01	0.00	0.01	0.07	0.06	0.03
Tetrahedral (3)	3.00	3.00	3.00	3.00	3.00	3.00	3.00	3.00	3.00	3.00	3.00
Octahedral (2)	2.03	2.01	2.01	2.02	2.01	2.02	2.00	2.01	2.06	2.06	2.02
Cavities (3)	2.97	2.98	2.98	2.97	2.99	2.98	3.00	2.99	2.94	2.93	2.98
XAlm	0.46	0.46	0.56	0.46	0.56	0.46	0.54	0.46	0.36	0.36	0.38
XPyp	0.36	0.37	0.26	0.39	0.28	0.39	0.31	0.39	0.38	0.38	0.36
XGrs	0.17	0.15	0.15	0.14	0.13	0.14	0.12	0.14	0.25	0.25	0.25
XSps	0.01	0.01	0.03	0.01	0.03	0.01	0.03	0.01	0.01	0.01	0.01

Table 6.xx EMP data for garnet with calculated end member proportions. XAlm = $Fe^{2+}/(Fe^{2+}+Mn+Mg+Ca)$. XPyp = $Mg/(Fe^{2+}+Mn+Mg+Ca)$, XGrs = $Ca/(Fe^{2+}+Mn+Mg+Ca)$, XSps = $Mn/(Fe^{2+}+Mn+Mg+Ca)$

Comment	0910B 1.3+ g trav	0910B 1.3+ g trav	0910B 1.3+ g trav	0910B 1.3+ g trav	0910B 1.3+ g trav	0910B 1.3+ g trav	0910B 1.3+ g trav	0910B 1.3+ g trav	0910B 1.3+ g trav	0910B 1.3+ g trav	0910B 1.3+ g trav
X	-14133	-14133	-14133	-14133	-14133	-14133	-14133	-14133	-14133	-14133	-14133
Y	-30936	-31064	-31192	-31786	-32133	-32504	-32861	-33134	-33674	-34011	-34422
Z	81	81	81	81	81	81	81	81	81	81	81
SiO2	39.26	38.77	39.26	39.29	39.26	39.23	39.01	39.43	38.98	39.18	39.33
TiO2	0.04	0.06	0.05	0.11	0.04	0.02	0.02	0.02	0.07	0.08	0.02
Al2O3	22.04	21.93	22.13	22.17	22.22	22.18	22.14	22.47	22.32	22.38	22.19
Cr2O3	0.00	0.02	0.02	0.00	0.03	0.00	0.00	0.02	0.00	0.00	0.00
Fe2O3	2.53	2.79	2.06	2.37	2.39	2.25	3.28	2.21	2.75	2.45	3.00
FeO	17.50	17.00	18.00	17.50	17.50	17.50	17.00	18.00	17.00	17.50	17.50
MnO	0.56	0.52	0.50	0.52	0.51	0.53	0.54	0.51	0.46	0.51	0.57
MgO	9.80	9.67	10.07	10.40	10.10	10.23	10.37	10.59	10.51	10.29	10.43
CaO	8.89	9.09	8.34	8.18	8.59	8.15	8.39	7.61	8.18	8.27	8.02
Na2O	0.00	0.01	0.01	0.02	0.00	0.01	0.02	0.02	0.01	0.03	0.00
K2O	0.02	0.00	0.00	0.00	0.01	0.00	0.00	0.01	0.01	0.01	0.01
NiO	0.00	0.00	0.00	0.00	0.00	0.01	0.02	0.04	0.00	0.02	0.01
Total	100.39	99.58	100.24	100.33	100.42	99.89	100.46	100.69	100.00	100.46	100.78
FeO	19.78	19.51	19.85	19.63	19.65	19.52	19.95	19.99	19.47	19.70	20.20
Num ox	12	12	12	12	12	12	12	12	12	12	12
Si	2.95	2.94	2.95	2.95	2.95	2.95	2.92	2.95	2.93	2.94	2.94
Ti	0.00	0.00	0.00	0.01	0.00	0.00	0.00	0.00	0.00	0.00	0.00
Al	1.95	1.96	1.96	1.96	1.97	1.97	1.96	1.98	1.98	1.98	1.95
Cr	0.00	0.00	0.00	0.00	0.00	0.00	0.00	0.00	0.00	0.00	0.00
Fe3+	0.14	0.16	0.12	0.13	0.14	0.13	0.19	0.12	0.16	0.14	0.17
Fe2+	1.10	1.08	1.13	1.10	1.10	1.10	1.07	1.12	1.07	1.10	1.09
Mn	0.04	0.03	0.03	0.03	0.03	0.03	0.03	0.03	0.03	0.03	0.04
Mg	1.10	1.09	1.13	1.16	1.13	1.15	1.16	1.18	1.18	1.15	1.16
Ca	0.72	0.74	0.67	0.66	0.69	0.66	0.67	0.61	0.66	0.66	0.64
Na	0.00	0.00	0.00	0.00	0.00	0.00	0.00	0.00	0.00	0.00	0.00
K	0.00	0.00	0.00	0.00	0.00	0.00	0.00	0.00	0.00	0.00	0.00
Ni	0.00	0.00	0.00	0.00	0.00	0.00	0.00	0.00	0.00	0.00	0.00
Total	8.00	8.00	8.00	8.00	8.00	8.00	8.00	8.00	8.00	8.00	8.00
Tetrahedral (Si)	2.95	2.94	2.95	2.95	2.95	2.95	2.92	2.95	2.93	2.94	2.94
Tetrahedral (Al)	0.05	0.06	0.05	0.05	0.05	0.05	0.08	0.05	0.07	0.06	0.06
Tetrahedral (3)	3.00	3.00	3.00	3.00	3.00	3.00	3.00	3.00	3.00	3.00	3.00
Octahedral (2)	2.05	2.06	2.04	2.05	2.05	2.05	2.07	2.05	2.07	2.06	2.06
Cavities (3)	2.95	2.94	2.97	2.95	2.95	2.94	2.93	2.95	2.93	2.94	2.93
XAlm	0.37	0.37	0.38	0.37	0.37	0.37	0.36	0.38	0.36	0.37	0.37
XPyp	0.37	0.37	0.38	0.39	0.38	0.39	0.40	0.40	0.40	0.39	0.40
XGrs	0.24	0.25	0.23	0.22	0.23	0.22	0.23	0.21	0.22	0.23	0.22
XSps	0.01	0.01	0.01	0.01	0.01	0.01	0.01	0.01	0.01	0.01	0.01

Table 6.xx EMP data for garnet with calculated end member proportions. XAlm = $Fe^{2+}/(Fe^{2+}+Mn+Mg+Ca)$. XPyp = $Mg/(Fe^{2+}+Mn+Mg+Ca)$, XGrs = $Ca/(Fe^{2+}+Mn+Mg+Ca)$, XSps = $Mn/(Fe^{2+}+Mn+Mg+Ca)$

Comment	0910B 1.3+ g trav	0910B 1.3+ g trav	0910B 1.3+ g trav	0910B 1.3+ g trav	0910B 1.3+ g trav	0910B 1.3+ g trav	0910B 1.3+ g trav	0910B 1.3+ g trav	0910B 1.3+ g trav	0910B 1.3+ g trav	0910B 1.3+ g trav
X	-14133	-14133	-14133	-14133	-14133	-14133	-14133	-14133	-14133	-14178	-14178
Y	-34934	-35538	-35653	-35793	-35919	-35960	-36180	-36538	-37115	-37332	-37558
Z	81	81	81	81	81	81	81	81	81	81	81
SiO2	39.31	39.16	39.14	39.26	39.56	39.20	39.37	39.27	39.24	38.90	38.91
TiO2	0.05	0.04	0.03	0.02	0.03	0.06	0.02	0.20	0.03	0.02	0.04
Al2O3	22.04	22.13	22.19	22.28	22.29	22.23	22.35	22.16	22.16	22.11	22.19
Cr2O3	0.00	0.01	0.00	0.01	0.02	0.01	0.00	0.00	0.03	0.00	0.01
Fe2O3	2.46	2.85	2.85	3.23	2.55	2.71	2.46	2.43	2.62	3.31	3.20
FeO	17.50	17.50	17.50	17.00	17.50	17.25	17.50	17.50	17.50	17.00	17.00
MnO	0.50	0.55	0.59	0.53	0.53	0.52	0.49	0.51	0.50	0.52	0.55
MgO	10.49	10.66	10.43	10.60	10.39	10.36	10.46	10.54	10.46	10.29	10.43
CaO	8.24	7.79	8.01	8.03	8.18	8.32	8.12	8.10	8.00	8.28	8.02
Na2O	0.00	0.00	0.00	0.01	0.01	0.00	0.00	0.02	0.01	0.02	0.02
K2O	0.01	0.00	0.00	0.00	0.01	0.00	0.01	0.00	0.00	0.00	0.00
NiO	0.00	0.00	0.04	0.00	0.00	0.00	0.00	0.01	0.01	0.01	0.02
Total	100.36	100.41	100.49	100.64	100.82	100.40	100.53	100.50	100.28	100.14	100.08
FeO	19.72	20.07	20.06	19.91	19.80	19.69	19.71	19.68	19.86	19.98	19.88
Num ox	12	12	12	12	12	12	12	12	12	12	12
Si	2.95	2.94	2.93	2.93	2.95	2.94	2.94	2.94	2.94	2.93	2.93
Ti	0.00	0.00	0.00	0.00	0.00	0.00	0.00	0.01	0.00	0.00	0.00
Al	1.95	1.96	1.96	1.96	1.96	1.96	1.97	1.96	1.96	1.96	1.97
Cr	0.00	0.00	0.00	0.00	0.00	0.00	0.00	0.00	0.00	0.00	0.00
Fe3+	0.14	0.16	0.16	0.18	0.14	0.15	0.14	0.14	0.15	0.19	0.18
Fe2+	1.10	1.10	1.10	1.06	1.09	1.08	1.09	1.10	1.10	1.07	1.07
Mn	0.03	0.04	0.04	0.03	0.03	0.03	0.03	0.03	0.03	0.03	0.04
Mg	1.17	1.19	1.17	1.18	1.16	1.16	1.17	1.18	1.17	1.15	1.17
Ca	0.66	0.63	0.64	0.64	0.65	0.67	0.65	0.65	0.64	0.67	0.65
Na	0.00	0.00	0.00	0.00	0.00	0.00	0.00	0.00	0.00	0.00	0.00
K	0.00	0.00	0.00	0.00	0.00	0.00	0.00	0.00	0.00	0.00	0.00
Ni	0.00	0.00	0.00	0.00	0.00	0.00	0.00	0.00	0.00	0.00	0.00
Total	8.00	8.00	8.00	8.00	8.00	8.00	8.00	8.00	8.00	8.00	8.00
Tetrahedral (Si)	2.95	2.94	2.93	2.93	2.95	2.94	2.94	2.94	2.94	2.93	2.93
Tetrahedral (Al)	0.05	0.06	0.07	0.07	0.05	0.06	0.06	0.06	0.06	0.07	0.07
Tetrahedral (3)	3.00	3.00	3.00	3.00	3.00	3.00	3.00	3.00	3.00	3.00	3.00
Octahedral (2)	2.04	2.05	2.06	2.08	2.06	2.06	2.06	2.04	2.06	2.07	2.08
Cavities (3)	2.96	2.95	2.94	2.92	2.94	2.94	2.94	2.95	2.94	2.92	2.92
XAlm	0.37	0.37	0.37	0.36	0.37	0.37	0.37	0.37	0.37	0.37	0.37
XPyp	0.40	0.40	0.40	0.40	0.39	0.39	0.40	0.40	0.40	0.39	0.40
XGrs	0.22	0.21	0.22	0.22	0.22	0.23	0.22	0.22	0.22	0.23	0.22
XSps	0.01	0.01	0.01	0.01	0.01	0.01	0.01	0.01	0.01	0.01	0.01

Table 6.xx EMP data for garnet with calculated end member proportions. XAlm = $Fe^{2+}/(Fe^{2+}+Mn+Mg+Ca)$. XPyp = $Mg/(Fe^{2+}+Mn+Mg+Ca)$, XGrs = $Ca/(Fe^{2+}+Mn+Mg+Ca)$, XSps = $Mn/(Fe^{2+}+Mn+Mg+Ca)$

Comment	0910B 1.3+ g trav	0910B 1.3+ g trav	0910B 1.3+ g trav	0910B 1.3+ g trav	0905B 2.1+ g trav	0905B 2.1+ g trav	0905B 2.1+ g trav	0905B 2.1+ g trav	0905B 2.1+ g trav	0905B 2.1+ g trav	0905B 2.1+ g trav
X	-14178	-14178	-14178	-14178	15934	15908	15868	15814	15746	15665	15485
Y	-38138	-38700	-39139	-39393	11899	11899	11867	11867	11867	11867	11867
Z	81	81	81	81	65	65	65	65	65	65	65
SiO2	39.28	39.38	39.20	39.43	40.01	40.25	40.08	39.82	39.86	40.23	39.93
TiO2	0.04	0.05	0.03	0.05	0.08	0.08	0.14	0.12	0.17	0.09	0.19
Al2O3	22.23	22.19	22.23	22.33	22.07	22.14	21.90	22.03	21.98	21.94	21.95
Cr2O3	0.00	0.00	0.04	0.04	0.00	0.00	0.05	0.02	0.02	0.06	0.01
Fe2O3	2.02	2.81	2.78	2.68	0.00	0.86	1.16	1.70	1.15	1.19	1.17
FeO	18.00	17.50	17.50	17.50	20.40	20.50	21.00	20.50	21.00	21.00	21.00
MnO	0.53	0.50	0.52	0.54	0.70	0.52	0.49	0.53	0.55	0.48	0.50
MgO	10.20	10.40	10.39	10.53	7.99	9.49	9.78	10.04	9.95	10.15	10.18
CaO	8.12	8.11	7.97	8.03	9.91	7.81	6.90	6.63	6.42	6.39	6.28
Na2O	0.02	0.02	0.00	0.02	0.02	0.05	0.06	0.05	0.06	0.06	0.07
K2O	0.01	0.00	0.00	0.00	0.01	0.02	0.01	0.00	0.00	0.01	0.00
NiO	0.02	0.00	0.00	0.00	0.00	0.00	0.00	0.00	0.00	0.00	0.00
Total	100.27	100.67	100.39	100.88	101.18	101.62	101.46	101.27	101.05	101.49	101.16
FeO	19.82	20.03	20.00	19.92	20.40	21.27	22.05	22.03	22.04	22.07	22.05
Num ox	12	12	12	12	12	12	12	12	12	12	12
Si	2.95	2.94	2.94	2.94	3.01	3.00	3.00	2.98	2.99	3.00	2.99
Ti	0.00	0.00	0.00	0.00	0.00	0.00	0.01	0.01	0.01	0.01	0.01
Al	1.97	1.96	1.97	1.96	1.96	1.95	1.93	1.94	1.94	1.93	1.94
Cr	0.00	0.00	0.00	0.00	0.00	0.00	0.00	0.00	0.00	0.00	0.00
Fe3+	0.11	0.16	0.16	0.15	0.00	0.05	0.07	0.10	0.07	0.07	0.07
Fe2+	1.13	1.09	1.10	1.09	1.28	1.28	1.31	1.28	1.32	1.31	1.32
Mn	0.03	0.03	0.03	0.03	0.04	0.03	0.03	0.03	0.04	0.03	0.03
Mg	1.14	1.16	1.16	1.17	0.90	1.06	1.09	1.12	1.11	1.13	1.14
Ca	0.65	0.65	0.64	0.64	0.80	0.62	0.55	0.53	0.52	0.51	0.50
Na	0.00	0.00	0.00	0.00	0.00	0.01	0.01	0.01	0.01	0.01	0.01
K	0.00	0.00	0.00	0.00	0.00	0.00	0.00	0.00	0.00	0.00	0.00
Ni	0.00	0.00	0.00	0.00	0.00	0.00	0.00	0.00	0.00	0.00	0.00
Total	8.00	8.00	8.00	8.00	8.00	8.00	8.00	8.00	8.00	8.00	8.00
Tetrahedral (Si)	2.95	2.94	2.94	2.94	3.01	3.00	3.00	2.98	2.99	3.00	2.99
Tetrahedral (Al)	0.05	0.06	0.06	0.06	-0.01	0.00	0.00	0.02	0.01	0.00	0.01
Tetrahedral (3)	3.00	3.00	3.00	3.00	3.00	3.00	3.00	3.00	3.00	3.00	3.00
Octahedral (2)	2.04	2.06	2.06	2.06	1.98	2.00	2.00	2.02	2.01	2.01	2.00
Cavities (3)	2.96	2.93	2.93	2.94	3.03	2.99	2.99	2.97	2.98	2.98	2.99
XAlm	0.38	0.37	0.37	0.37	0.42	0.43	0.44	0.43	0.44	0.44	0.44
XPyp	0.39	0.39	0.40	0.40	0.30	0.35	0.36	0.38	0.37	0.38	0.38
XGrs	0.22	0.22	0.22	0.22	0.26	0.21	0.19	0.18	0.17	0.17	0.17
XSps	0.01	0.01	0.01	0.01	0.01	0.01	0.01	0.01	0.01	0.01	0.01

Table 6.xx EMP data for garnet with calculated end member proportions. XAlm = $Fe^{2+}/(Fe^{2+}+Mn+Mg+Ca)$. XPyp = $Mg/(Fe^{2+}+Mn+Mg+Ca)$, XGrs = $Ca/(Fe^{2+}+Mn+Mg+Ca)$, XSps = $Mn/(Fe^{2+}+Mn+Mg+Ca)$

Comment	0905B 2.1+ g trav	0905B 2.1+ g trav	0905B 2.1+ g trav	0905B 2.1+ g trav	0905B 2.1+ g trav	0905B 2.1+ g trav	0905B 2.1+ g trav	0905B 2.1+ g trav	0905B 2.1+ g trav	0905B 2.1+ g trav	0905B 2.1+ g trav
X	15313	15077	14852	14535	14370	14237	14006	13856	13707	13226	12939
Y	11867	11867	11867	11867	11867	11842	11842	11853	11911	11911	11911
Z	65	65	65	65	65	65	65	65	65	65	65
SiO2	39.94	39.85	39.91	40.13	39.95	40.10	40.00	39.95	39.73	39.85	40.04
TiO2	0.15	0.21	0.12	0.11	0.10	0.13	0.10	0.08	0.03	0.07	0.19
Al2O3	21.97	21.83	22.07	22.10	21.95	21.99	22.01	22.11	22.03	21.97	22.08
Cr2O3	0.04	0.00	0.00	0.01	0.00	0.02	0.04	0.03	0.00	0.00	0.00
Fe2O3	1.50	1.47	1.70	1.07	1.12	1.16	1.00	1.49	1.48	0.81	0.96
FeO	21.00	20.50	20.50	21.00	21.00	21.00	21.00	20.50	20.50	20.50	21.00
MnO	0.52	0.54	0.50	0.51	0.48	0.52	0.50	0.52	0.54	0.56	0.47
MgO	10.09	10.31	10.35	10.30	10.24	10.43	10.23	10.39	9.86	9.52	10.31
CaO	6.26	6.17	6.18	6.17	6.19	6.17	6.12	6.14	6.89	7.51	6.20
Na2O	0.06	0.07	0.07	0.04	0.04	0.06	0.05	0.06	0.04	0.04	0.08
K2O	0.00	0.01	0.01	0.00	0.00	0.00	0.00	0.00	0.01	0.00	0.00
NiO	0.02	0.00	0.00	0.01	0.04	0.00	0.00	0.02	0.00	0.00	0.02
Total	101.40	100.82	101.25	101.33	100.98	101.46	100.94	101.14	100.97	100.75	101.25
FeO	22.35	21.82	22.03	21.96	22.01	22.04	21.90	21.84	21.83	21.23	21.86
Num ox	12	12	12	12	12	12	12	12	12	12	12
Si	2.99	2.99	2.98	3.00	3.00	2.99	3.00	2.99	2.98	3.00	2.99
Ti	0.01	0.01	0.01	0.01	0.01	0.01	0.01	0.00	0.00	0.00	0.01
Al	1.94	1.93	1.94	1.95	1.94	1.93	1.95	1.95	1.95	1.95	1.95
Cr	0.00	0.00	0.00	0.00	0.00	0.00	0.00	0.00	0.00	0.00	0.00
Fe3+	0.08	0.08	0.10	0.06	0.06	0.07	0.06	0.08	0.08	0.05	0.05
Fe2+	1.31	1.29	1.28	1.31	1.32	1.31	1.32	1.28	1.29	1.29	1.31
Mn	0.03	0.03	0.03	0.03	0.03	0.03	0.03	0.03	0.03	0.04	0.03
Mg	1.12	1.15	1.15	1.15	1.14	1.16	1.14	1.16	1.10	1.07	1.15
Ca	0.50	0.50	0.49	0.49	0.50	0.49	0.49	0.49	0.55	0.61	0.50
Na	0.01	0.01	0.01	0.01	0.01	0.01	0.01	0.01	0.01	0.01	0.01
K	0.00	0.00	0.00	0.00	0.00	0.00	0.00	0.00	0.00	0.00	0.00
Ni	0.00	0.00	0.00	0.00	0.00	0.00	0.00	0.00	0.00	0.00	0.00
Total	8.00	8.00	8.00	8.00	8.00	8.00	8.00	8.00	8.00	8.00	8.00
Tetrahedral (Si)	2.99	2.99	2.98	3.00	3.00	2.99	3.00	2.99	2.98	3.00	2.99
Tetrahedral (Al)	0.01	0.01	0.02	0.00	0.00	0.01	0.00	0.01	0.02	0.00	0.01
Tetrahedral (3)	3.00	3.00	3.00	3.00	3.00	3.00	3.00	3.00	3.00	3.00	3.00
Octahedral (2)	2.02	2.02	2.03	2.01	2.00	2.00	2.01	2.02	2.02	2.00	2.00
Cavities (3)	2.97	2.97	2.96	2.98	2.99	3.00	2.98	2.96	2.98	3.00	2.99
XAlm	0.44	0.43	0.43	0.44	0.44	0.44	0.44	0.43	0.43	0.43	0.44
XPyp	0.38	0.39	0.39	0.38	0.38	0.39	0.38	0.39	0.37	0.36	0.38
XGrs	0.17	0.17	0.17	0.17	0.17	0.16	0.16	0.17	0.19	0.20	0.17
XSps	0.01	0.01	0.01	0.01	0.01	0.01	0.01	0.01	0.01	0.01	0.01

Appendix 6.D EMP data for garnet with calculated end member proportions. XAlm = $Fe^{2+}/(Fe^{2+}+Mn+Mg+Ca)$. XPyp = $Mg/(Fe^{2+}+Mn+Mg+Ca)$, XGrs = $Ca/(Fe^{2+}+Mn+Mg+Ca)$, XSps = $Mn/(Fe^{2+}+Mn+Mg+Ca)$

Comment	0905B 2.1+ g trav	0905B 2.1+ g trav	0905B 2.1+ g trav	0905B 2.1+ g trav	0905B 2.1+ g trav	0905B 2.1+ g trav	0905B 2.1+ g trav	0905B 2.1+ g trav	0905B 2.1+ g trav	0905B 2.1+ g trav	0905B 2.2 g
X	12717	12452	12116	11890	11734	11609	11578	11546	11523	11476	11918
Y	11911	11911	11903	11903	11903	11903	11948	11948	11948	11941	12668
Z	65	65	65	65	65	65	65	65	65	65	65
SiO2	40.08	39.82	39.96	39.74	39.78	39.80	39.95	39.91	39.81	39.60	39.71
TiO2	0.11	0.11	0.13	0.20	0.18	0.14	0.12	0.14	0.15	0.18	0.06
Al2O3	21.92	21.94	21.97	21.93	21.82	22.04	21.96	21.90	21.93	21.89	21.86
Cr2O3	0.00	0.02	0.03	0.00	0.01	0.01	0.00	0.01	0.02	0.00	0.00
Fe2O3	1.22	1.28	1.40	1.71	1.51	1.68	1.23	0.98	1.75	0.83	1.14
FeO	21.00	20.50	20.50	20.50	20.50	20.50	20.75	21.00	20.50	20.50	20.00
MnO	0.50	0.55	0.55	0.47	0.53	0.45	0.50	0.46	0.53	0.76	0.50
MgO	10.28	10.34	10.34	10.19	10.06	10.22	10.10	10.01	9.87	8.65	9.37
CaO	6.27	6.22	6.31	6.29	6.52	6.44	6.56	6.59	6.77	8.43	7.93
Na2O	0.07	0.04	0.06	0.07	0.06	0.08	0.05	0.03	0.06	0.03	0.04
K2O	0.00	0.01	0.02	0.00	0.01	0.00	0.01	0.01	0.02	0.00	0.01
NiO	0.00	0.00	0.05	0.00	0.00	0.00	0.01	0.00	0.00	0.01	0.02
Total	101.32	100.70	101.20	100.94	100.84	101.18	101.10	100.94	101.23	100.80	100.53
FeO	22.10	21.65	21.76	22.04	21.86	22.01	21.85	21.88	22.08	21.24	21.03
Num ox	12	12	12	12	12	12	12	12	12	12	12
Si	3.00	2.99	2.99	2.98	2.99	2.98	2.99	3.00	2.98	2.99	2.99
Ti	0.01	0.01	0.01	0.01	0.01	0.01	0.01	0.01	0.01	0.01	0.00
Al	1.93	1.94	1.94	1.94	1.93	1.94	1.94	1.94	1.94	1.95	1.94
Cr	0.00	0.00	0.00	0.00	0.00	0.00	0.00	0.00	0.00	0.00	0.00
Fe3+	0.07	0.07	0.08	0.10	0.09	0.09	0.07	0.06	0.10	0.05	0.06
Fe2+	1.31	1.29	1.28	1.29	1.29	1.28	1.30	1.32	1.28	1.30	1.26
Mn	0.03	0.04	0.03	0.03	0.03	0.03	0.03	0.03	0.03	0.05	0.03
Mg	1.15	1.16	1.15	1.14	1.13	1.14	1.13	1.12	1.10	0.97	1.05
Ca	0.50	0.50	0.51	0.51	0.52	0.52	0.53	0.53	0.54	0.68	0.64
Na	0.01	0.01	0.01	0.01	0.01	0.01	0.01	0.01	0.01	0.00	0.01
K	0.00	0.00	0.00	0.00	0.00	0.00	0.00	0.00	0.00	0.00	0.00
Ni	0.00	0.00	0.00	0.00	0.00	0.00	0.00	0.00	0.00	0.00	0.00
Total	8.00	8.00	8.00	8.00	8.00	8.00	8.00	8.00	8.00	8.00	8.00
Tetrahedral (Si)	3.00	2.99	2.99	2.98	2.99	2.98	2.99	3.00	2.98	2.99	2.99
Tetrahedral (Al)	0.00	0.01	0.01	0.02	0.01	0.02	0.01	0.00	0.02	0.01	0.01
Tetrahedral (3)	3.00	3.00	3.00	3.00	3.00	3.00	3.00	3.00	3.00	3.00	3.00
Octahedral (2)	2.00	2.01	2.01	2.03	2.02	2.02	2.01	2.00	2.03	2.00	2.01
Cavities (3)	2.99	2.98	2.98	2.96	2.97	2.97	2.99	3.00	2.96	3.00	2.99
XAlm	0.44	0.43	0.43	0.43	0.43	0.43	0.44	0.44	0.43	0.43	0.42
XPyp	0.38	0.39	0.39	0.38	0.38	0.38	0.38	0.37	0.37	0.32	0.35
XGrs	0.17	0.17	0.17	0.17	0.18	0.17	0.18	0.18	0.18	0.23	0.21
XSps	0.01	0.01	0.01	0.01	0.01	0.01	0.01	0.01	0.01	0.02	0.01

Appendix 6.D EMP data for garnet with calculated end member proportions. XAlm = $Fe^{2+}/(Fe^{2+}+Mn+Mg+Ca)$. XPyp = $Mg/(Fe^{2+}+Mn+Mg+Ca)$, XGrs = $Ca/(Fe^{2+}+Mn+Mg+Ca)$, XSps = $Mn/(Fe^{2+}+Mn+Mg+Ca)$

Comment	0906B 1.1 g	0906B 1.2 g r	0906B 1.14 g r	0906B 1.16 ?	0906B 1.17 ?	0906B 1.18 ?	0906B 1.19 g c	0906B 1.21 g r	0906B 1.22 g r	0906B 1.23 g r	0906B 1.26 g r
X	-14093	-13856	-12741	-17433	-16633	-16645	-16480	-14029	-14012	-14234	-13603
Y	25287	25799	27535	27130	29051	29157	28057	27285	27418	27476	28068
Z	60	57	55	55	55	55	55	54	54	54	54
SiO2	40.47	40.11	39.77	40.29	40.64	40.33	40.45	39.89	39.64	39.71	40.10
TiO2	0.05	0.13	0.06	0.07	0.09	0.10	0.07	0.12	0.05	0.06	0.07
Al2O3	22.29	22.08	22.00	22.14	21.99	21.97	22.11	22.07	21.86	22.01	22.09
Cr2O3	0.04	0.05	0.03	0.03	0.04	0.02	0.00	0.05	0.00	0.00	0.02
Fe2O3	0.62	0.67	2.26	1.17	0.23	1.22	0.87	1.67	0.89	1.29	0.80
FeO	19.50	20.50	19.00	19.00	20.00	19.00	19.50	19.50	20.50	20.00	20.00
MnO	0.57	0.61	0.56	0.60	0.59	0.55	0.57	0.61	0.67	0.63	0.57
MgO	10.61	9.54	9.24	10.51	10.44	10.64	10.59	9.69	8.25	8.98	9.53
CaO	7.27	7.83	8.78	7.49	7.34	7.54	7.31	7.91	9.04	8.48	8.34
Na2O	0.03	0.02	0.02	0.03	0.04	0.03	0.02	0.03	0.02	0.03	0.00
K2O	0.01	0.00	0.00	0.01	0.00	0.00	0.00	0.02	0.00	0.00	0.00
NiO	0.00	0.00	0.00	0.01	0.00	0.00	0.02	0.00	0.02	0.00	0.01
Total	101.40	101.48	101.50	101.24	101.38	101.28	101.43	101.40	100.86	101.06	101.45
FeO	20.06	21.10	21.03	20.05	20.21	20.10	20.29	21.00	21.30	21.16	20.72
Num ox	12	12	12	12	12	12	12	12	12	12	12
Si	3.01	3.00	2.97	3.00	3.02	3.00	3.00	2.98	3.00	2.99	3.00
Ti	0.00	0.01	0.00	0.00	0.00	0.01	0.00	0.01	0.00	0.00	0.00
Al	1.95	1.95	1.94	1.94	1.93	1.93	1.94	1.94	1.95	1.95	1.95
Cr	0.00	0.00	0.00	0.00	0.00	0.00	0.00	0.00	0.00	0.00	0.00
Fe3+	0.03	0.04	0.13	0.07	0.01	0.07	0.05	0.09	0.05	0.07	0.04
Fe2+	1.21	1.28	1.19	1.18	1.24	1.18	1.21	1.22	1.30	1.26	1.25
Mn	0.04	0.04	0.04	0.04	0.04	0.03	0.04	0.04	0.04	0.04	0.04
Mg	1.17	1.06	1.03	1.17	1.16	1.18	1.17	1.08	0.93	1.01	1.06
Ca	0.58	0.63	0.70	0.60	0.59	0.60	0.58	0.63	0.73	0.68	0.67
Na	0.00	0.00	0.00	0.00	0.01	0.00	0.00	0.01	0.00	0.00	0.00
K	0.00	0.00	0.00	0.00	0.00	0.00	0.00	0.00	0.00	0.00	0.00
Ni	0.00	0.00	0.00	0.00	0.00	0.00	0.00	0.00	0.00	0.00	0.00
Total	8.00	8.00	8.00	8.00	8.00	8.00	8.00	8.00	8.00	8.00	8.00
Tetrahedral (Si)	3.01	3.00	2.97	3.00	3.02	3.00	3.00	2.98	3.00	2.99	3.00
Tetrahedral (Al)	-0.01	0.00	0.03	0.00	-0.02	0.00	0.00	0.02	0.00	0.01	0.00
Tetrahedral (3)	3.00	3.00	3.00	3.00	3.00	3.00	3.00	3.00	3.00	3.00	3.00
Octahedral (2)	2.00	1.99	2.04	2.01	1.97	2.00	1.99	2.02	2.00	2.01	1.99
Cavities (3)	3.00	3.01	2.95	2.98	3.02	3.00	3.00	2.97	3.00	2.99	3.01
XAlm	0.40	0.43	0.40	0.40	0.41	0.39	0.40	0.41	0.43	0.42	0.41
XPyp	0.39	0.35	0.35	0.39	0.38	0.39	0.39	0.36	0.31	0.34	0.35
XGrs	0.19	0.21	0.24	0.20	0.19	0.20	0.19	0.21	0.24	0.23	0.22
XSps	0.01	0.01	0.01	0.01	0.01	0.01	0.01	0.01	0.01	0.01	0.01

Appendix 6.D EMP data for garnet with calculated end member proportions. XAlm = $Fe^{2+}/(Fe^{2+}+Mn+Mg+Ca)$. XPyp = $Mg/(Fe^{2+}+Mn+Mg+Ca)$, XGrs = $Ca/(Fe^{2+}+Mn+Mg+Ca)$, XSps = $Mn/(Fe^{2+}+Mn+Mg+Ca)$

Comment	0906B random	0906B random	0906B random	0906B random	0906B random	0906B random	0906B random	0906B random	0906B random
X	-9094	-9094	-9094	-9094	-9094	-9094	-9027	-9027	-9027
Y	24960	27765	26946	24249	23640	22966	22163	21707	21307
Z	62	57	57	62	62	62	62	62	62
SiO2	40.03	39.89	39.91	40.09	40.09	40.25	39.86	39.85	39.16
TiO2	0.08	0.00	0.02	0.04	0.04	0.07	0.06	0.07	0.10
Al2O3	22.08	21.99	22.29	22.24	22.14	22.24	22.22	22.13	22.23
Cr2O3	0.01	0.03	0.01	0.01	0.01	0.00	0.02	0.03	0.02
Fe2O3	0.90	1.27	1.60	0.95	1.55	1.62	1.70	1.53	2.28
FeO	19.50	19.50	18.50	19.50	19.00	19.00	18.50	18.50	19.00
MnO	0.56	0.61	0.58	0.61	0.53	0.59	0.56	0.56	0.63
MgO	9.63	9.27	10.36	9.94	10.46	10.50	10.16	10.42	9.42
CaO	8.15	8.64	8.02	8.04	7.63	7.49	8.26	7.70	8.00
Na2O	0.02	0.01	0.02	0.00	0.02	0.03	0.02	0.00	0.02
K2O	0.00	0.00	0.00	0.01	0.01	0.00	0.00	0.00	0.00
NiO	0.00	0.01	0.00	0.00	0.04	0.00	0.00	0.00	0.00
Total	100.87	101.09	101.15	101.34	101.37	101.62	101.19	100.64	100.64
FeO	20.31	20.64	19.94	20.36	20.40	20.45	20.03	19.87	21.05
Num ox	12	12	12	12	12	12	12	12	12
Si	3.00	2.99	2.97	2.99	2.98	2.98	2.97	2.98	2.95
Ti	0.00	0.00	0.00	0.00	0.00	0.00	0.00	0.00	0.01
Al	1.95	1.94	1.96	1.96	1.94	1.94	1.95	1.95	1.97
Cr	0.00	0.00	0.00	0.00	0.00	0.00	0.00	0.00	0.00
Fe3+	0.05	0.07	0.09	0.05	0.09	0.09	0.10	0.09	0.13
Fe2+	1.22	1.22	1.15	1.22	1.18	1.18	1.15	1.16	1.20
Mn	0.04	0.04	0.04	0.04	0.03	0.04	0.04	0.04	0.04
Mg	1.08	1.04	1.15	1.10	1.16	1.16	1.13	1.16	1.06
Ca	0.65	0.69	0.64	0.64	0.61	0.59	0.66	0.62	0.65
Na	0.00	0.00	0.00	0.00	0.00	0.00	0.00	0.00	0.00
K	0.00	0.00	0.00	0.00	0.00	0.00	0.00	0.00	0.00
Ni	0.00	0.00	0.00	0.00	0.00	0.00	0.00	0.00	0.00
Total	8.00	8.00	8.00	8.00	8.00	8.00	8.00	8.00	8.00
Tetrahedral (Si)	3.00	2.99	2.97	2.99	2.98	2.98	2.97	2.98	2.95
Tetrahedral (Al)	0.00	0.01	0.03	0.01	0.02	0.02	0.03	0.02	0.05
Tetrahedral (3)	3.00	3.00	3.00	3.00	3.00	3.00	3.00	3.00	3.00
Octahedral (2)	2.01	2.01	2.02	2.00	2.01	2.02	2.02	2.02	2.06
Cavities (3)	2.99	2.99	2.98	3.00	2.98	2.97	2.98	2.97	2.94
XAlm	0.41	0.41	0.39	0.41	0.40	0.40	0.39	0.39	0.41
XPyp	0.36	0.35	0.39	0.37	0.39	0.39	0.38	0.39	0.36
XGrs	0.22	0.23	0.21	0.21	0.20	0.20	0.22	0.21	0.22
XSps	0.01	0.01	0.01	0.01	0.01	0.01	0.01	0.01	0.01

Appendix 6.D EMP data for garnet with calculated end member proportions. XAlm = $Fe^{2+}/(Fe^{2+}+Mn+Mg+Ca)$. XPyp = $Mg/(Fe^{2+}+Mn+Mg+Ca)$, XGrs = $Ca/(Fe^{2+}+Mn+Mg+Ca)$, XSps = $Mn/(Fe^{2+}+Mn+Mg+Ca)$

sample	0905C 1	0905C 1.5+ opx trav	0905C 1.5+ opx trav	0905C 1.5+ opx trav	0905C 1.5+ opx trav	0905C 1.5+ opx trav	0905C 1.5+ opx trav	0905C 1.5+ opx trav	0905C 1.5+ opx trav	0905C 1.5+ opx trav	0905C 1.5+ opx trav	0905C 1.5+ opx trav	0905C 1.5+ opx trav	0905C 1.5+ opx trav
x	-10227.00	-10223.00	-10226.00	-10215.00	-10215.00	-10223.00	-10212.00	-10189.00	-10172.00	-10165.00	-10160.00	-10160.00	-10152.00	-10152.00
y	8768.00	8765.00	8755.00	8741.00	8723.00	8705.00	8683.00	8666.00	8661.00	8644.00	8622.00	8594.00	8569.00	8549.00
z	70.00	70.00	70.00	70.00	70.00	70.00	70.00	70.00	70.00	70.00	70.00	70.00	70.00	70.00
SiO2	51.65	51.87	51.20	50.74	48.61	49.46	49.02	49.12	48.82	48.89	48.78	49.14	48.83	48.63
TiO2	0.06	0.06	0.03	0.05	0.03	0.03	0.03	0.06	0.04	0.04	0.04	0.03	0.07	0.06
Al2O3	2.74	2.66	3.31	4.27	6.26	6.14	6.50	7.36	7.48	7.44	7.62	7.51	7.51	7.35
FeO	19.22	19.27	19.37	19.65	19.21	19.68	19.88	19.47	19.67	19.16	19.26	19.20	19.51	19.45
MnO	0.82	0.78	0.78	0.83	0.79	0.71	0.63	0.66	0.60	0.62	0.60	0.64	0.61	0.58
MgO	24.54	24.47	24.34	23.88	22.23	23.26	23.10	22.85	22.99	22.88	23.00	22.86	22.98	22.99
CaO	0.25	0.22	0.22	0.18	0.42	0.20	0.20	0.26	0.21	0.23	0.19	0.15	0.19	0.18
K2O	0.01	0.01	0.01	0.01	0.06	0.00	0.00	0.02	0.00	0.00	0.02	0.00	0.00	0.01
Na2O	0.01	0.01	0.03	0.01	0.02	0.00	0.01	0.05	0.02	0.04	0.02	0.02	0.03	0.06
Li2O	0.00													
ZnO	0.00													
NiO	0.00	0.03	0.00	0.00	0.00	0.04	0.05	0.08	0.00	0.00	0.04	0.00	0.04	0.02
Cr2O3	0.00	0.03	0.02	0.00	0.05	0.00	0.01	0.00	0.02	0.02	0.00	0.01	0.01	0.00
Sc2O3	0.00													
Total	99.31	99.40	99.31	99.62	97.66	99.53	99.45	99.93	99.85	99.31	99.57	99.54	99.79	99.32
Fe3+ model	Droop 1987	Droop 1987	Droop 1987	Droop 1987	Droop 1987	Droop 1987	Droop 1987	Droop 1987	Droop 1987	Droop 1987	Droop 1987	Droop 1987	Droop 1987	Droop 1987
Si Calc	1.91	1.92	1.90	1.88	1.84	1.83	1.82	1.81	1.80	1.81	1.80	1.81	1.80	1.81
Ti Calc	0.00	0.00	0.00	0.00	0.00	0.00	0.00	0.00	0.00	0.00	0.00	0.00	0.00	0.00
Al Calc	0.12	0.12	0.14	0.19	0.28	0.27	0.28	0.32	0.33	0.32	0.33	0.33	0.33	0.32
Fe Calc	0.60	0.60	0.60	0.61	0.61	0.61	0.62	0.60	0.61	0.59	0.60	0.59	0.60	0.60
Mn Calc	0.03	0.02	0.02	0.03	0.03	0.02	0.02	0.02	0.02	0.02	0.02	0.02	0.02	0.02
Mg Calc	1.36	1.35	1.35	1.32	1.25	1.29	1.28	1.26	1.27	1.26	1.27	1.26	1.27	1.27
Ca Calc	0.01	0.01	0.01	0.01	0.02	0.01	0.01	0.01	0.01	0.01	0.01	0.01	0.01	0.01
K Calc	0.00	0.00	0.00	0.00	0.00	0.00	0.00	0.00	0.00	0.00	0.00	0.00	0.00	0.00
Na Calc	0.00	0.00	0.00	0.00	0.00	0.00	0.00	0.00	0.00	0.00	0.00	0.00	0.00	0.00
Li Calc														
Zn Calc														
Ni Calc	0.00	0.00	0.00	0.00	0.00	0.00	0.00	0.00	0.00	0.00	0.00	0.00	0.00	0.00
Cr Calc	0.00	0.00	0.00	0.00	0.00	0.00	0.00	0.00	0.00	0.00	0.00	0.00	0.00	0.00
Sc Calc														
Fe 3+ Droop	0.07	0.06	0.08	0.08	0.07	0.09	0.11	0.08	0.10	0.08	0.09	0.06	0.09	0.10
Total Calc	4.02	4.02	4.03	4.03	4.02	4.03	4.04	4.03	4.03	4.03	4.03	4.02	4.03	4.03
Si	1.90	1.91	1.89	1.87	1.83	1.82	1.81	1.80	1.79	1.80	1.79	1.81	1.79	1.79
Ti	0.00	0.00	0.00	0.00	0.00	0.00	0.00	0.00	0.00	0.00	0.00	0.00	0.00	0.00
Al (T)	0.10	0.09	0.11	0.13	0.17	0.18	0.19	0.20	0.21	0.20	0.21	0.19	0.21	0.21
Al (M1)	0.02	0.03	0.03	0.05	0.10	0.09	0.09	0.12	0.11	0.12	0.12	0.13	0.11	0.11
Fe3+ (T)	0.00	0.00	0.00	0.00	0.00	0.00	0.00	0.00	0.00	0.00	0.00	0.00	0.00	0.00
Fe3+ (M1)	0.07	0.06	0.08	0.08	0.07	0.09	0.11	0.08	0.10	0.08	0.09	0.06	0.09	0.10
Fe2+	0.52	0.53	0.51	0.52	0.53	0.51	0.51	0.51	0.50	0.51	0.50	0.53	0.50	0.49
Mn	0.03	0.02	0.02	0.03	0.03	0.02	0.02	0.02	0.02	0.02	0.02	0.02	0.02	0.02
Mg	1.35	1.34	1.34	1.31	1.24	1.28	1.27	1.25	1.26	1.26	1.26	1.25	1.26	1.26
Ca	0.01	0.01	0.01	0.01	0.02	0.01	0.01	0.01	0.01	0.01	0.01	0.01	0.01	0.01
K	0.00	0.00	0.00	0.00	0.00	0.00	0.00	0.00	0.00	0.00	0.00	0.00	0.00	0.00
Na	0.00	0.00	0.00	0.00	0.00	0.00	0.00	0.00	0.00	0.00	0.00	0.00	0.00	0.00
Li	0.00	0.00	0.00	0.00	0.00	0.00	0.00	0.00	0.00	0.00	0.00	0.00	0.00	0.00
Zn	0.00	0.00	0.00	0.00	0.00	0.00	0.00	0.00	0.00	0.00	0.00	0.00	0.00	0.00
Ni	0.00	0.00	0.00	0.00	0.00	0.00	0.00	0.00	0.00	0.00	0.00	0.00	0.00	0.00
Cr	0.00	0.00	0.00	0.00	0.00	0.00	0.00	0.00	0.00	0.00	0.00	0.00	0.00	0.00
Sc	0.00	0.00	0.00	0.00	0.00	0.00	0.00	0.00	0.00	0.00	0.00	0.00	0.00	0.00
Total	4.00	4.00	4.00	4.00	4.00	4.00	4.00	4.00	4.00	4.00	4.00	4.00	4.00	4.00
J	0.00	0.00	0.00	0.00	0.00	0.00	0.00	0.01	0.00	0.01	0.00	0.00	0.00	0.01
Q	1.88	1.88	1.86	1.84	1.79	1.80	1.78	1.77	1.77	1.78	1.77	1.78	1.77	1.76
group	Quad	Quad	Quad	Quad	Quad	Quad	Quad	Quad	Quad	Quad	Quad	Quad	Quad	Quad
adjective	aluminian	aluminian	aluminian	aluminian	aluminian	aluminian	aluminian ferrian	aluminian	aluminian	aluminian	aluminian	aluminian	aluminian	aluminian ferrian
pyroxene	(clino)enstatite	(clino)enstatite	(clino)enstatite	(clino)enstatite	(clino)enstatite	(clino)enstatite	(clino)enstatite	(clino)enstatite	(clino)enstatite	(clino)enstatite	(clino)enstatite	(clino)enstatite	(clino)enstatite	(clino)enstatite
enstatite	68.23	68.20	67.98	67.25	65.86	66.75	66.47	66.56	66.62	67.01	67.09	67.04	66.78	66.91
ferrosillite	31.28	31.36	31.58	32.37	33.26	32.83	33.12	32.90	32.95	32.51	32.51	32.64	32.83	32.72
wollastonite	0.49	0.44	0.44	0.37	0.88	0.41	0.41	0.54	0.43	0.49	0.40	0.32	0.39	0.37
jadeite	----------	----------	----------	----------	----------	----------	----------	----------	----------	----------	----------	----------	----------	----------
aegirine	----------	----------	----------	----------	----------	----------	----------	----------	----------	----------	----------	----------	----------	----------
Quad	----------	----------	----------	----------	----------	----------	----------	----------	----------	----------	----------	----------	----------	----------

Appendix 6.D EMP data for pyroxene modified from PX-NOM (Sturm, R. 2002)

sample	0905C 1.5+ opx trav	0905C 1.5+ opx trav	0905C 1.5+ opx trav	0905C 1.5+ opx trav	0905C 1.5+ opx trav	0905C 1.5+ opx trav	0905C 1.5+ opx trav	0905C 1.6+ cpx trav	0905C 1.6+ cpx trav	0905C 1.6+ cpx trav	0905C 1.6+ cpx trav	0905C 1.6+ cpx trav	0905C 1.6+ cpx trav
x	-10155.00	-10159.00	-10165.00	-10165.00	-10165.00	-10163.00	-10152.00	-9868.00	-9866.00	-9868.00	-9870.00	-9870.00	-9870.00
y	8538.00	8505.00	8503.00	8498.00	8487.00	8480.00	8472.00	9327.00	9319.00	9308.00	9302.00	9289.00	9281.00
z	70.00	70.00	70.00	70.00	70.00	70.00	70.00	70.00	70.00	70.00	70.00	70.00	70.00
SiO2	48.25	48.97	48.97	49.21	49.79	50.44	51.62	49.20	48.67	49.24	49.81	49.35	49.14
TiO2	0.05	0.05	0.01	0.07	0.04	0.06	0.02	0.47	0.72	0.44	0.53	0.60	0.58
Al2O3	7.26	6.79	6.35	5.76	4.97	4.38	5.33	6.44	6.41	9.46	10.78	10.44	10.83
FeO	19.64	19.65	19.74	19.71	19.82	19.71	18.60	7.69	8.56	7.82	8.31	8.56	8.75
MnO	0.63	0.66	0.69	0.63	0.73	0.76	0.68	0.28	0.22	0.28	0.29	0.27	0.23
MgO	22.78	22.80	22.90	23.41	23.57	23.71	22.46	11.73	12.40	9.81	9.18	9.82	8.47
CaO	0.16	0.19	0.21	0.22	0.20	0.20	0.53	21.67	19.54	19.07	17.22	16.79	16.11
K2O	0.00	0.01	0.00	0.00	0.00	0.01	0.02	0.02	0.33	0.00	0.00	0.04	0.00
Na2O	0.02	0.03	0.01	0.02	0.01	0.01	0.64	1.68	1.59	2.91	3.46	3.30	4.20
Li2O													
ZnO													
NiO	0.05	0.03	0.00	0.03	0.02	0.05	0.07	0.05	0.00	0.01	0.00	0.05	0.01
Cr2O3	0.00	0.00	0.01	0.03	0.00	0.00	0.01	0.03	0.02	0.00	0.00	0.00	0.00
Sc2O3													
Total	98.85	99.18	98.88	99.08	99.15	99.32	99.97	99.26	98.47	99.04	99.58	99.22	98.33
Fe3+ model	Droop 1987	Droop 1987	Droop 1987	Droop 1987	Droop 1987	Droop 1987	Droop 1987	Droop 1987	Droop 1987	Droop 1987	Droop 1987	Droop 1987	Droop 1987
Si Calc	1.80	1.82	1.83	1.83	1.86	1.87	1.89	1.85	1.84	1.84	1.84	1.84	1.85
Ti Calc	0.00	0.00	0.00	0.00	0.00	0.00	0.00	0.01	0.02	0.01	0.01	0.02	0.02
Al Calc	0.32	0.30	0.28	0.25	0.22	0.19	0.23	0.29	0.29	0.42	0.47	0.46	0.48
Fe Calc	0.61	0.61	0.62	0.61	0.62	0.61	0.57	0.24	0.27	0.24	0.26	0.27	0.27
Mn Calc	0.02	0.02	0.02	0.02	0.02	0.02	0.02	0.01	0.01	0.01	0.01	0.01	0.01
Mg Calc	1.27	1.26	1.27	1.30	1.31	1.31	1.23	0.66	0.70	0.55	0.51	0.54	0.47
Ca Calc	0.01	0.01	0.01	0.01	0.01	0.01	0.02	0.87	0.79	0.76	0.68	0.67	0.65
K Calc	0.00	0.00	0.00	0.00	0.00	0.00	0.00	0.00	0.02	0.00	0.00	0.00	0.00
Na Calc	0.00	0.00	0.00	0.00	0.00	0.00	0.05	0.12	0.12	0.21	0.25	0.24	0.31
Li Calc													
Zn Calc													
Ni Calc	0.00	0.00	0.00	0.00	0.00	0.00	0.00	0.00	0.00	0.00	0.00	0.00	0.00
Cr Calc	0.00	0.00	0.00	0.00	0.00	0.00	0.00	0.00	0.00	0.00	0.00	0.00	0.00
Sc Calc													
Fe 3+ Droop	0.11	0.09	0.09	0.11	0.10	0.08	0.04	0.16	0.17	0.13	0.09	0.12	0.15
Total Calc	4.04	4.03	4.03	4.04	4.03	4.03	4.01	4.06	4.06	4.04	4.03	4.04	4.05
Si	1.79	1.81	1.81	1.82	1.84	1.86	1.89	1.82	1.82	1.82	1.83	1.82	1.82
Ti	0.00	0.00	0.00	0.00	0.00	0.00	0.00	0.01	0.02	0.01	0.01	0.02	0.02
Al (T)	0.21	0.19	0.19	0.18	0.16	0.14	0.11	0.18	0.18	0.18	0.17	0.18	0.18
Al (M1)	0.10	0.10	0.09	0.07	0.06	0.05	0.12	0.11	0.10	0.23	0.30	0.27	0.29
Fe3+ (T)	0.00	0.00	0.00	0.00	0.00	0.00	0.00	0.00	0.00	0.00	0.00	0.00	0.00
Fe3+ (M1)	0.11	0.09	0.09	0.11	0.10	0.08	0.04	0.16	0.17	0.13	0.09	0.12	0.15
Fe2+	0.50	0.52	0.52	0.50	0.51	0.52	0.53	0.07	0.10	0.11	0.16	0.15	0.12
Mn	0.02	0.02	0.02	0.02	0.02	0.02	0.02	0.01	0.01	0.01	0.01	0.01	0.01
Mg	1.26	1.26	1.27	1.29	1.30	1.30	1.22	0.65	0.69	0.54	0.50	0.54	0.47
Ca	0.01	0.01	0.01	0.01	0.01	0.01	0.02	0.86	0.78	0.76	0.68	0.66	0.64
K	0.00	0.00	0.00	0.00	0.00	0.00	0.00	0.00	0.02	0.00	0.00	0.00	0.00
Na	0.00	0.00	0.00	0.00	0.00	0.00	0.05	0.12	0.12	0.21	0.25	0.24	0.30
Li	0.00	0.00	0.00	0.00	0.00	0.00	0.00	0.00	0.00	0.00	0.00	0.00	0.00
Zn	0.00	0.00	0.00	0.00	0.00	0.00	0.00	0.00	0.00	0.00	0.00	0.00	0.00
Ni	0.00	0.00	0.00	0.00	0.00	0.00	0.00	0.00	0.00	0.00	0.00	0.00	0.00
Cr	0.00	0.00	0.00	0.00	0.00	0.00	0.00	0.00	0.00	0.00	0.00	0.00	0.00
Sc	0.00	0.00	0.00	0.00	0.00	0.00	0.00	0.00	0.00	0.00	0.00	0.00	0.00
Total	4.00	4.00	4.00	4.00	4.00	4.00	4.00	4.00	4.00	4.00	4.00	4.00	4.00
J	0.00	0.00	0.00	0.00	0.00	0.00	0.09	0.24	0.23	0.42	0.49	0.47	0.60
Q	1.76	1.78	1.79	1.80	1.82	1.84	1.77	1.58	1.57	1.41	1.34	1.35	1.23
group	Quad	Quad	Quad	Quad	Quad	Quad	Quad	Quad	Quad	Ca-Na	Ca-Na	Ca-Na	Ca-Na
adjective	aluminian ferrian	aluminian	aluminian	aluminian ferrian	aluminian ferrian	aluminian	aluminian	uminian ferrian sodian	aluminian ferrian sodian				
pyroxene	(clino)enstatite	(clino)enstatite	(clino)enstatite	(clino)enstatite	(clino)enstatite	(clino)enstatite	(clino)enstatite	diopside	augite	omphacite	omphacite	omphacite	omphacite
enstatite	66.47	66.40	66.35	66.92	66.87	67.09	66.74	36.91	39.53	----------	----------	----------	----------
ferrosillite	33.19	33.19	33.22	32.62	32.72	32.50	32.14	14.07	15.70	----------	----------	----------	----------
wollastonite	0.33	0.41	0.43	0.46	0.42	0.41	1.13	49.02	44.76	----------	----------	----------	----------
jadeite	----------	----------	----------	----------	----------	----------	----------	----------	----------	14.60	20.39	18.12	21.70
aegirine	----------	----------	----------	----------	----------	----------	----------	----------	----------	8.25	6.46	7.74	11.29
Quad	----------	----------	----------	----------	----------	----------	----------	----------	----------	77.15	73.15	74.14	67.01

Appendix 6.D EMP data for pyroxene modified from PX-NOM (Sturm, R. 2002)

sample	0905C 1.6+ cpx trav	0905C 1.6+ cpx trav	0905C 1.6+ cpx trav	0905C 1.6+ cpx trav	0905C 1.6+ cpx trav	0905C 1.6+ cpx trav	0905C 1.6+ cpx trav	0905C 1.6+ cpx trav	0905C 1.6+ cpx trav	0905C 1.6+ cpx trav	0905C 1.6+ cpx trav	0905C 1.6+ cpx trav	0905C 1.6+ cpx trav	0905C 1.6+ cpx trav
x	-9870.00	-9870.00	-9870.00	-9870.00	-9870.00	-9870.00	-9870.00	-9870.00	-9870.00	-9870.00	-9870.00	-9870.00	-9870.00	-9870.00
y	9272.00	9266.00	9261.00	9249.00	9227.00	9203.00	9186.00	9158.00	9129.00	9118.00	9101.00	9084.00	9066.00	9043.00
z	70.00	70.00	70.00	70.00	70.00	70.00	70.00	70.00	70.00	70.00	70.00	70.00	70.00	70.00
SiO2	49.21	49.63	49.24	49.26	48.81	48.72	48.56	48.60	48.45	48.62	48.93	48.35	48.42	50.71
TiO2	0.58	0.59	0.63	0.64	0.69	0.74	0.69	0.70	0.71	0.74	0.72	0.68	0.71	0.99
Al2O3	10.93	10.85	10.77	10.75	10.83	10.76	10.71	10.67	10.57	10.51	10.81	10.57	10.59	12.20
FeO	8.45	8.66	8.88	8.97	8.87	9.12	8.85	8.63	9.09	8.56	8.97	8.87	8.56	10.15
MnO	0.22	0.26	0.23	0.28	0.25	0.22	0.23	0.26	0.25	0.25	0.30	0.28	0.22	0.17
MgO	8.33	8.53	8.64	8.58	8.41	8.49	8.53	8.81	8.79	8.77	8.62	8.92	9.10	8.85
CaO	16.49	16.44	16.45	16.62	16.85	17.10	17.20	17.46	16.93	17.51	17.13	17.47	17.83	12.35
K2O	0.01	0.01	0.00	0.01	0.01	0.00	0.01	0.01	0.01	0.01	0.00	0.02	0.01	0.02
Na2O	4.28	4.14	4.04	3.93	3.89	3.76	3.74	3.56	3.59	3.47	3.68	3.57	3.37	2.50
Li2O														
ZnO														
NiO	0.00	0.05	0.00	0.02	0.04	0.02	0.00	0.00	0.00	0.00	0.04	0.02	0.00	0.00
Cr2O3	0.02	0.02	0.01	0.02	0.00	0.07	0.01	0.00	0.02	0.01	0.01	0.00	0.00	0.04
Sc2O3														
Total	98.53	99.18	98.89	99.08	98.65	99.00	98.52	98.71	98.42	98.45	99.21	98.74	98.81	97.97
Fe3+ model	Droop 1987	Droop 1987	Droop 1987	Droop 1987	Droop 1987	Droop 1987	Droop 1987	Droop 1987	Droop 1987	Droop 1987	Droop 1987	Droop 1987	Droop 1987	Droop 1987
Si Calc	1.84	1.85	1.84	1.84	1.83	1.83	1.83	1.82	1.83	1.83	1.83	1.82	1.82	1.88
Ti Calc	0.02	0.02	0.02	0.02	0.02	0.02	0.02	0.02	0.02	0.02	0.02	0.02	0.02	0.03
Al Calc	0.48	0.48	0.47	0.47	0.48	0.48	0.47	0.47	0.47	0.47	0.48	0.47	0.47	0.53
Fe Calc	0.26	0.27	0.28	0.28	0.28	0.29	0.28	0.27	0.29	0.27	0.28	0.28	0.27	0.31
Mn Calc	0.01	0.01	0.01	0.01	0.01	0.01	0.01	0.01	0.01	0.01	0.01	0.01	0.01	0.01
Mg Calc	0.47	0.47	0.48	0.48	0.47	0.47	0.48	0.49	0.49	0.49	0.48	0.50	0.51	0.49
Ca Calc	0.66	0.66	0.66	0.66	0.68	0.69	0.69	0.70	0.68	0.71	0.69	0.70	0.72	0.49
K Calc	0.00	0.00	0.00	0.00	0.00	0.00	0.00	0.00	0.00	0.00	0.00	0.00	0.00	0.00
Na Calc	0.31	0.30	0.29	0.28	0.28	0.27	0.27	0.26	0.26	0.25	0.27	0.26	0.24	0.18
Li Calc														
Zn Calc														
Ni Calc	0.00	0.00	0.00	0.00	0.00	0.00	0.00	0.00	0.00	0.00	0.00	0.00	0.00	0.00
Cr Calc	0.00	0.00	0.00	0.00	0.00	0.00	0.00	0.00	0.00	0.00	0.00	0.00	0.00	0.00
Sc Calc														
Fe 3+ Droop	0.16	0.14	0.15	0.14	0.15	0.15	0.15	0.15	0.15	0.13	0.14	0.17	0.15	0.00
Total Calc	4.05	4.05	4.05	4.05	4.05	4.05	4.05	4.05	4.05	4.04	4.05	4.06	4.05	3.92
Si	1.82	1.83	1.82	1.82	1.81	1.80	1.80	1.80	1.80	1.81	1.81	1.79	1.79	1.92
Ti	0.02	0.02	0.02	0.02	0.02	0.02	0.02	0.02	0.02	0.02	0.02	0.02	0.02	0.03
Al (T)	0.18	0.17	0.18	0.18	0.19	0.20	0.20	0.20	0.20	0.19	0.19	0.21	0.21	0.08
Al (M1)	0.30	0.30	0.29	0.29	0.28	0.27	0.27	0.27	0.27	0.27	0.28	0.25	0.26	0.46
Fe3+ (T)	0.00	0.00	0.00	0.00	0.00	0.00	0.00	0.00	0.00	0.00	0.00	0.00	0.00	0.00
Fe3+ (M1)	0.16	0.14	0.15	0.14	0.15	0.15	0.15	0.15	0.15	0.13	0.14	0.17	0.15	0.00
Fe2+	0.10	0.12	0.12	0.13	0.12	0.13	0.12	0.12	0.13	0.14	0.14	0.10	0.11	0.32
Mn	0.01	0.01	0.01	0.01	0.01	0.01	0.01	0.01	0.01	0.01	0.01	0.01	0.01	0.01
Mg	0.46	0.47	0.48	0.47	0.46	0.47	0.47	0.49	0.49	0.49	0.47	0.49	0.50	0.50
Ca	0.65	0.65	0.65	0.66	0.67	0.68	0.68	0.69	0.68	0.70	0.68	0.69	0.71	0.50
K	0.00	0.00	0.00	0.00	0.00	0.00	0.00	0.00	0.00	0.00	0.00	0.00	0.00	0.00
Na	0.31	0.30	0.29	0.28	0.28	0.27	0.27	0.26	0.26	0.25	0.26	0.26	0.24	0.18
Li	0.00	0.00	0.00	0.00	0.00	0.00	0.00	0.00	0.00	0.00	0.00	0.00	0.00	0.00
Zn	0.00	0.00	0.00	0.00	0.00	0.00	0.00	0.00	0.00	0.00	0.00	0.00	0.00	0.00
Ni	0.00	0.00	0.00	0.00	0.00	0.00	0.00	0.00	0.00	0.00	0.00	0.00	0.00	0.00
Cr	0.00	0.00	0.00	0.00	0.00	0.00	0.00	0.00	0.00	0.00	0.00	0.00	0.00	0.00
Sc	0.00	0.00	0.00	0.00	0.00	0.00	0.00	0.00	0.00	0.00	0.00	0.00	0.00	0.00
Total	4.00	4.00	4.00	4.00	4.00	4.00	4.00	4.00	4.00	4.00	4.00	4.00	4.00	4.00
J	0.61	0.59	0.58	0.56	0.56	0.54	0.54	0.51	0.52	0.50	0.53	0.51	0.48	0.37
Q	1.21	1.24	1.25	1.26	1.26	1.28	1.28	1.30	1.30	1.32	1.29	1.29	1.32	1.32
group	Ca-Na	Ca-Na	Ca-Na	Ca-Na	Ca-Na	Ca-Na	Ca-Na	Ca-Na	Ca-Na	Ca-Na	Ca-Na	Ca-Na	Ca-Na	Ca-Na
adjective pyroxene	omphacite	omphacite	omphacite	omphacite	omphacite	omphacite	omphacite	omphacite	omphacite	omphacite	omphacite	omphacite	omphacite	omphacite
enstatite	----------	----------	----------	----------	----------	----------	----------	----------	----------	----------	----------	----------	----------	----------
ferrosillite	----------	----------	----------	----------	----------	----------	----------	----------	----------	----------	----------	----------	----------	----------
wollastonite	----------	----------	----------	----------	----------	----------	----------	----------	----------	----------	----------	----------	----------	----------
jadeite	21.80	21.82	20.73	20.55	20.08	19.04	18.91	18.21	18.27	18.53	19.28	16.88	16.73	21.76
aegirine	11.79	10.43	10.94	10.23	10.69	10.68	10.76	10.01	10.27	8.94	9.76	11.60	10.07	0.00
Quad	66.42	67.74	68.33	69.22	69.23	70.28	70.34	71.77	71.46	72.53	70.96	71.52	73.21	78.24

Appendix 6.D EMP data for pyroxene modified from PX-NOM (Sturm, R. 2002)

sample	0905C 1.6+ cpx trav	0905C 1.6+ cpx trav	0905C 1.6+ cpx trav	0905C 1.6+ cpx trav	0905C 1.6+ cpx trav	0905C 1.6+ cpx trav	0905C 1.6+ cpx trav	0905C 1.6+ cpx trav	0905C 1.6+ cpx trav	0905C 1.6+ cpx trav	0905C 1.6+ cpx trav	0905C 1.6+ cpx trav	0905C 1.6+ cpx trav	0905C 1.6+ cpx trav
x	-9870.00	-9870.00	-9870.00	-9870.00	-9870.00	-9870.00	-9870.00	-9870.00	-9870.00	-9870.00	-9870.00	-9870.00	-9870.00	-9870.00
y	9028.00	9017.00	9004.00	8980.00	8937.00	8921.00	8903.00	8885.00	8865.00	8858.00	8849.00	8843.00	8838.00	8830.00
z	70.00	70.00	70.00	70.00	70.00	70.00	70.00	70.00	70.00	70.00	70.00	70.00	70.00	70.00
SiO2	48.19	48.70	48.39	48.42	48.55	48.53	48.56	48.71	47.65	48.89	48.52	48.72	49.10	48.25
TiO2	0.71	0.71	0.75	0.73	0.70	0.70	0.68	0.69	0.79	0.70	0.69	0.68	0.60	0.62
Al2O3	10.58	10.58	10.67	10.58	10.34	10.42	10.40	10.54	10.84	10.71	10.52	10.69	10.35	10.66
FeO	8.60	8.90	8.81	8.74	8.99	9.03	9.80	8.97	9.53	8.62	9.20	9.28	9.47	9.59
MnO	0.28	0.27	0.28	0.29	0.30	0.32	0.30	0.26	0.25	0.26	0.32	0.27	0.28	0.29
MgO	8.64	8.69	8.81	8.67	9.24	8.73	9.65	8.81	9.33	8.73	8.76	9.18	9.20	9.03
CaO	17.57	17.30	17.36	17.46	16.84	17.21	16.34	17.04	16.18	17.49	16.73	16.26	16.08	16.06
K2O	0.02	0.00	0.00	0.01	0.01	0.00	0.01	0.00	0.00	0.01	0.00	0.01	0.01	0.00
Na2O	3.70	3.61	3.65	3.76	3.54	3.63	3.35	3.64	3.45	3.72	3.65	3.69	3.68	3.57
Li2O														
ZnO														
NiO	0.03	0.02	0.00	0.05	0.01	0.00	0.00	0.00	0.02	0.01	0.00	0.01	0.00	0.01
Cr2O3	0.00	0.03	0.03	0.01	0.02	0.02	0.03	0.03	0.02	0.01	0.00	0.00	0.03	0.01
Sc2O3														
Total	98.30	98.79	98.77	98.71	98.54	98.59	99.11	98.69	98.08	99.16	98.37	98.79	98.80	98.09
Fe3+ model	Droop 1987	Droop 1987	Droop 1987	Droop 1987	Droop 1987	Droop 1987	Droop 1987	Droop 1987	Droop 1987	Droop 1987	Droop 1987	Droop 1987	Droop 1987	Droop 1987
Si Calc	1.82	1.83	1.82	1.82	1.83	1.83	1.82	1.83	1.80	1.83	1.83	1.83	1.84	1.82
Ti Calc	0.02	0.02	0.02	0.02	0.02	0.02	0.02	0.02	0.02	0.02	0.02	0.02	0.02	0.02
Al Calc	0.47	0.47	0.47	0.47	0.46	0.46	0.46	0.47	0.48	0.47	0.47	0.47	0.46	0.48
Fe Calc	0.27	0.28	0.28	0.27	0.28	0.28	0.31	0.28	0.30	0.27	0.29	0.29	0.30	0.30
Mn Calc	0.01	0.01	0.01	0.01	0.01	0.01	0.01	0.01	0.01	0.01	0.01	0.01	0.01	0.01
Mg Calc	0.49	0.49	0.49	0.49	0.52	0.49	0.54	0.49	0.53	0.49	0.49	0.51	0.51	0.51
Ca Calc	0.71	0.70	0.70	0.70	0.68	0.69	0.66	0.69	0.66	0.70	0.68	0.65	0.65	0.65
K Calc	0.00	0.00	0.00	0.00	0.00	0.00	0.00	0.00	0.00	0.00	0.00	0.00	0.00	0.00
Na Calc	0.27	0.26	0.27	0.27	0.26	0.26	0.24	0.27	0.25	0.27	0.27	0.27	0.27	0.26
Li Calc														
Zn Calc														
Ni Calc	0.00	0.00	0.00	0.00	0.00	0.00	0.00	0.00	0.00	0.00	0.00	0.00	0.00	0.00
Cr Calc	0.00	0.00	0.00	0.00	0.00	0.00	0.00	0.00	0.00	0.00	0.00	0.00	0.00	0.00
Sc Calc														
Fe 3+ Droop	0.18	0.15	0.17	0.18	0.16	0.16	0.16	0.15	0.17	0.16	0.15	0.16	0.14	0.15
Total Calc	4.06	4.05	4.06	4.06	4.05	4.05	4.05	4.05	4.06	4.05	4.05	4.05	4.05	4.05
Si	1.79	1.81	1.79	1.79	1.80	1.80	1.80	1.81	1.78	1.80	1.81	1.80	1.82	1.80
Ti	0.02	0.02	0.02	0.02	0.02	0.02	0.02	0.02	0.02	0.02	0.02	0.02	0.02	0.02
Al (T)	0.21	0.19	0.21	0.21	0.20	0.20	0.20	0.19	0.22	0.20	0.19	0.20	0.18	0.20
Al (M1)	0.26	0.27	0.26	0.26	0.25	0.26	0.25	0.27	0.25	0.27	0.27	0.27	0.27	0.27
Fe3+ (T)	0.00	0.00	0.00	0.00	0.00	0.00	0.00	0.00	0.00	0.00	0.00	0.00	0.00	0.00
Fe3+ (M1)	0.18	0.15	0.17	0.18	0.16	0.16	0.16	0.15	0.17	0.16	0.15	0.16	0.14	0.15
Fe2+	0.09	0.13	0.10	0.09	0.12	0.12	0.14	0.13	0.13	0.11	0.14	0.13	0.15	0.15
Mn	0.01	0.01	0.01	0.01	0.01	0.01	0.01	0.01	0.01	0.01	0.01	0.01	0.01	0.01
Mg	0.48	0.48	0.49	0.48	0.51	0.48	0.53	0.49	0.52	0.48	0.49	0.51	0.51	0.50
Ca	0.70	0.69	0.69	0.69	0.67	0.69	0.65	0.68	0.65	0.69	0.67	0.64	0.64	0.64
K	0.00	0.00	0.00	0.00	0.00	0.00	0.00	0.00	0.00	0.00	0.00	0.00	0.00	0.00
Na	0.27	0.26	0.26	0.27	0.25	0.26	0.24	0.26	0.25	0.27	0.26	0.26	0.26	0.26
Li	0.00	0.00	0.00	0.00	0.00	0.00	0.00	0.00	0.00	0.00	0.00	0.00	0.00	0.00
Zn	0.00	0.00	0.00	0.00	0.00	0.00	0.00	0.00	0.00	0.00	0.00	0.00	0.00	0.00
Ni	0.00	0.00	0.00	0.00	0.00	0.00	0.00	0.00	0.00	0.00	0.00	0.00	0.00	0.00
Cr	0.00	0.00	0.00	0.00	0.00	0.00	0.00	0.00	0.00	0.00	0.00	0.00	0.00	0.00
Sc	0.00	0.00	0.00	0.00	0.00	0.00	0.00	0.00	0.00	0.00	0.00	0.00	0.00	0.00
Total	4.00	4.00	4.00	4.00	4.00	4.00	4.00	4.00	4.00	4.00	4.00	4.00	4.00	4.00
J	0.53	0.52	0.52	0.54	0.51	0.52	0.48	0.52	0.50	0.53	0.53	0.53	0.53	0.52
Q	1.27	1.30	1.28	1.26	1.30	1.29	1.32	1.29	1.29	1.28	1.29	1.28	1.30	1.29
group	Ca-Na	Ca-Na	Ca-Na	Ca-Na	Ca-Na	Ca-Na	Ca-Na	Ca-Na	Ca-Na	Ca-Na	Ca-Na	Ca-Na	Ca-Na	Ca-Na
adjective														
pyroxene	omphacite	omphacite	omphacite	omphacite	omphacite	omphacite	omphacite	omphacite	omphacite	omphacite	omphacite	omphacite	omphacite	omphacite
enstatite	----------	----------	----------	----------	----------	----------	----------	----------	----------	----------	----------	----------	----------	----------
ferrosillite	----------	----------	----------	----------	----------	----------	----------	----------	----------	----------	----------	----------	----------	----------
wollastonite	----------	----------	----------	----------	----------	----------	----------	----------	----------	----------	----------	----------	----------	----------
jadeite	17.44	18.48	17.59	17.60	17.34	17.85	16.25	18.53	16.66	18.56	18.56	18.48	18.98	18.30
aegirine	12.21	10.09	11.47	12.35	10.81	10.97	10.39	10.29	11.23	10.82	10.43	10.72	9.95	10.25
Quad	70.36	71.42	70.94	70.05	71.85	71.18	73.36	71.18	72.11	70.62	71.00	70.80	71.07	71.45

Appendix 6.D EMP data for pyroxene modified from PX-NOM (Sturm, R. 2002)

Sample	0906A 1.10 cpx trav	0906A 1.10 cpx trav	0906A 1.10 cpx trav	0906A 1.10 cpx trav	0906A 1.10 cpx trav	0906A 1.10 cpx trav	0906A 1.10 cpx trav	0906A 1.10 cpx trav	0906A 1.10 cpx trav	0906A 1.10 cpx trav	0906A 1.10 cpx trav	0906A 1.10 cpx trav	0906A 1.10 cpx trav	0906A 1.10 cpx trav	0906A 1.10 cpx trav	0906A 1.10 cpx trav
x	7844.00	7844.00	7844.00	7844.00	7844.00	7844.00	7844.00	7844.00	7844.00	7844.00	7844.00	7844.00	7844.00	7844.00	7844.00	7844.00
y	27384.00	27406.00	27422.00	27454.00	27472.00	27501.00	27537.00	27549.00	27579.00	27599.00	27644.00	27676.00	27704.00	27755.00	27822.00	27851.00
z	73.00	73.00	73.00	73.00	73.00	73.00	73.00	73.00	73.00	73.00	73.00	73.00	73.00	73.00	73.00	73.00
SiO2	51.96	51.11	50.72	49.35	49.16	48.66	48.41	49.20	49.39	48.57	48.45	48.45	48.38	48.88	48.47	48.45
TiO2	0.33	0.42	0.55	0.78	0.86	0.92	0.99	0.88	0.75	1.00	1.05	0.95	0.94	0.76	0.91	0.90
Al2O3	4.08	5.57	6.46	8.02	8.41	8.61	8.74	8.58	8.33	8.96	9.03	9.12	9.10	9.15	9.35	9.03
FeO	6.12	6.58	6.65	7.03	6.96	7.33	7.24	7.29	7.30	7.39	7.42	7.39	7.77	7.60	7.54	7.56
MnO	0.05	0.05	0.00	0.03	0.06	0.07	0.05	0.07	0.07	0.06	0.06	0.07	0.09	0.06	0.07	0.09
MgO	13.25	12.29	11.88	11.06	10.89	10.70	10.55	10.67	10.84	10.51	10.48	10.44	10.71	10.34	10.65	10.14
CaO	21.18	20.46	20.31	20.04	20.09	20.03	19.85	19.93	20.05	19.82	19.88	19.87	19.82	19.95	19.48	19.83
K2O	0.01	0.00	0.00	0.00	0.00	0.00	0.00	0.00	0.00	0.00	0.00	0.01	0.00	0.02	0.00	0.00
Na2O	1.86	2.29	2.41	2.55	2.46	2.49	2.48	2.50	2.47	2.49	2.53	2.53	2.51	2.53	2.52	2.41
Li2O																
ZnO																
NiO	0.02	0.02	0.00	0.00	0.00	0.02	0.08	0.07	0.00	0.04	0.03	0.00	0.06	0.03	0.03	0.00
Cr2O3	0.07	0.11	0.09	0.08	0.09	0.06	0.06	0.08	0.07	0.10	0.06	0.10	0.05	0.10	0.07	0.09
Sc2O3																
Total	98.94	98.91	99.07	98.94	98.98	98.90	98.46	99.28	99.29	98.94	99.01	98.93	99.43	99.42	99.09	98.50
Fe3+ model	Droop 1987	Droop 1987	Droop 1987	Droop 1987	Droop 1987	Droop 1987	Droop 1987	Droop 1987	Droop 1987	Droop 1987	Droop 1987	Droop 1987	Droop 1987	Droop 1987	Droop 1987	Droop 1987
Si Calc	1.93	1.91	1.89	1.85	1.84	1.82	1.82	1.83	1.84	1.82	1.81	1.82	1.81	1.82	1.81	1.82
Ti Calc	0.01	0.01	0.02	0.02	0.02	0.03	0.03	0.02	0.02	0.03	0.03	0.03	0.03	0.02	0.03	0.03
Al Calc	0.18	0.24	0.28	0.35	0.37	0.38	0.39	0.38	0.37	0.40	0.40	0.40	0.40	0.40	0.41	0.40
Fe Calc	0.19	0.21	0.21	0.22	0.22	0.23	0.23	0.23	0.23	0.23	0.23	0.23	0.24	0.24	0.24	0.24
Mn Calc	0.00	0.00	0.00	0.00	0.00	0.00	0.00	0.00	0.00	0.00	0.00	0.00	0.00	0.00	0.00	0.00
Mg Calc	0.74	0.68	0.66	0.62	0.61	0.60	0.59	0.59	0.60	0.59	0.58	0.58	0.60	0.58	0.59	0.57
Ca Calc	0.85	0.82	0.81	0.80	0.80	0.80	0.80	0.80	0.80	0.80	0.80	0.80	0.79	0.80	0.78	0.80
K Calc	0.00	0.00	0.00	0.00	0.00	0.00	0.00	0.00	0.00	0.00	0.00	0.00	0.00	0.00	0.00	0.00
Na Calc	0.13	0.17	0.17	0.19	0.18	0.18	0.18	0.18	0.18	0.18	0.18	0.18	0.18	0.18	0.18	0.18
Li Calc																
Zn Calc																
Ni Calc	0.00	0.00	0.00	0.00	0.00	0.00	0.00	0.00	0.00	0.00	0.00	0.00	0.00	0.00	0.00	0.00
Cr Calc	0.00	0.00	0.00	0.00	0.00	0.00	0.00	0.00	0.00	0.00	0.00	0.00	0.00	0.00	0.00	0.00
Sc Calc																
Fe 3+ Droop	0.10	0.12	0.12	0.14	0.12	0.15	0.14	0.12	0.13	0.13	0.14	0.14	0.17	0.13	0.14	0.11
Total Calc	4.03	4.04	4.04	4.05	4.04	4.05	4.05	4.04	4.04	4.04	4.05	4.05	4.06	4.04	4.05	4.04
Si	1.92	1.89	1.87	1.82	1.82	1.80	1.80	1.82	1.82	1.80	1.79	1.79	1.78	1.80	1.79	1.81
Ti	0.01	0.01	0.02	0.02	0.02	0.03	0.03	0.02	0.02	0.03	0.03	0.03	0.03	0.02	0.03	0.03
Al (T)	0.08	0.11	0.13	0.18	0.18	0.20	0.20	0.18	0.18	0.20	0.21	0.21	0.22	0.20	0.21	0.19
Al (M1)	0.10	0.13	0.15	0.17	0.18	0.18	0.18	0.19	0.18	0.19	0.19	0.19	0.18	0.20	0.20	0.20
Fe3+ (T)	0.00	0.00	0.00	0.00	0.00	0.00	0.00	0.00	0.00	0.00	0.00	0.00	0.00	0.00	0.00	0.00
Fe3+ (M1)	0.10	0.12	0.12	0.14	0.12	0.15	0.14	0.12	0.13	0.13	0.14	0.14	0.17	0.13	0.14	0.11
Fe2+	0.09	0.08	0.09	0.08	0.09	0.08	0.09	0.10	0.10	0.10	0.09	0.09	0.07	0.10	0.09	0.12
Mn	0.00	0.00	0.00	0.00	0.00	0.00	0.00	0.00	0.00	0.00	0.00	0.00	0.00	0.00	0.00	0.00
Mg	0.73	0.68	0.65	0.61	0.60	0.59	0.59	0.59	0.60	0.58	0.58	0.58	0.59	0.57	0.59	0.56
Ca	0.84	0.81	0.80	0.79	0.80	0.79	0.79	0.79	0.79	0.79	0.79	0.79	0.78	0.79	0.77	0.79
K	0.00	0.00	0.00	0.00	0.00	0.00	0.00	0.00	0.00	0.00	0.00	0.00	0.00	0.00	0.00	0.00
Na	0.13	0.16	0.17	0.18	0.18	0.18	0.18	0.18	0.18	0.18	0.18	0.18	0.18	0.18	0.18	0.17
Li	0.00	0.00	0.00	0.00	0.00	0.00	0.00	0.00	0.00	0.00	0.00	0.00	0.00	0.00	0.00	0.00
Zn	0.00	0.00	0.00	0.00	0.00	0.00	0.00	0.00	0.00	0.00	0.00	0.00	0.00	0.00	0.00	0.00
Ni	0.00	0.00	0.00	0.00	0.00	0.00	0.00	0.00	0.00	0.00	0.00	0.00	0.00	0.00	0.00	0.00
Cr	0.00	0.00	0.00	0.00	0.00	0.00	0.00	0.00	0.00	0.00	0.00	0.00	0.00	0.00	0.00	0.00
Sc	0.00	0.00	0.00	0.00	0.00	0.00	0.00	0.00	0.00	0.00	0.00	0.00	0.00	0.00	0.00	0.00
Total	4.00	4.00	4.00	4.00	4.00	4.00	4.00	4.00	4.00	4.00	4.00	4.00	4.00	4.00	4.00	4.00
J	0.27	0.33	0.34	0.37	0.35	0.36	0.36	0.36	0.35	0.36	0.36	0.36	0.36	0.36	0.36	0.35
Q	1.66	1.57	1.54	1.48	1.49	1.47	1.47	1.48	1.49	1.47	1.46	1.45	1.45	1.46	1.45	1.48
group	Quad	Quad	Quad	Quad	Quad	Quad	Quad	Quad	Quad	Quad	Quad	Ca-Na	Quad	Quad	Quad	Quad
adjective	aluminian sodian	aluminian ferrian sodian	aluminian ferrian sodian	aluminian ferrian sodian	aluminian ferrian sodian	aluminian ferrian sodian	aluminian ferrian sodian	aluminian ferrian sodian	aluminian ferrian sodian	aluminian ferrian sodian	aluminian ferrian sodian		aluminian ferrian sodian	aluminian ferrian sodian	aluminian ferrian sodian	aluminian ferrian sodian
pyroxene	diopside	diopside	diopside	diopside	diopside	diopside	diopside	diopside	diopside	diopside	diopside	omphacite	diopside	diopside	diopside	diopside
enstatite	41.49	40.01	39.33	37.59	37.22	36.59	36.50	36.62	36.88	36.34	36.16	----------	36.47	35.69	36.82	35.35
ferrosillite	10.84	12.11	12.35	13.46	13.46	14.20	14.15	14.19	14.08	14.44	14.50	----------	15.02	14.84	14.76	14.96
wollastonite	47.67	47.87	48.32	48.95	49.32	49.21	49.35	49.18	49.04	49.22	49.33	----------	48.51	49.47	48.43	49.70
jadeite	----------	----------	----------	----------	----------	----------	----------	----------	----------	----------	----------	11.59	----------	----------	----------	----------
aegirine	----------	----------	----------	----------	----------	----------	----------	----------	----------	----------	----------	8.43	----------	----------	----------	----------
Quad	----------	----------	----------	----------	----------	----------	----------	----------	----------	----------	----------	79.98	----------	----------	----------	----------

Appendix 6.D EMP data for pyroxene modified from PX-NOM (Sturm, R. 2002)

Sample	0906A 1.10 cpx trav	0906A 1.10 cpx trav	0906A 1.10 cpx trav	0906A 1.10 cpx trav	0906A 1.10 cpx trav	0906A 1.10 cpx trav	0906A 1.10 cpx trav	0906A 1.10 cpx trav	0906A 1.10 cpx trav	0906A 1.10 cpx trav	0906A 1.10 cpx trav	0906A 1.10 cpx trav	0906A 1.10 cpx trav	0906A 1.10 cpx trav	0906A 1.10 cpx trav	0906A 1.10 cpx trav
x	7844.00	7844.00	7844.00	7844.00	7844.00	7844.00	7844.00	7844.00	7844.00	7844.00	7844.00	7844.00	7844.00	7844.00	7844.00	7844.00
y	27868.00	27925.00	27942.00	27978.00	28039.00	28102.00	28167.00	28238.00	28267.00	28304.00	28396.00	28500.00	28555.00	28601.00	28685.00	28774.00
z	73.00	73.00	73.00	73.00	73.00	73.00	73.00	73.00	73.00	73.00	73.00	73.00	73.00	73.00	73.00	73.00
SiO2	48.63	48.53	49.05	49.18	47.60	49.21	46.17	48.61	48.93	48.16	48.28	48.45	48.82	48.77	48.64	48.31
TiO2	0.94	0.86	0.75	0.89	0.78	0.55	1.39	0.78	0.78	2.30	0.77	0.91	0.80	0.74	0.94	0.93
Al2O3	9.20	9.18	8.77	9.00	10.16	8.49	11.26	9.35	9.18	8.26	9.21	9.26	9.24	9.07	9.32	9.23
FeO	7.61	7.63	7.60	7.56	8.81	7.96	10.31	7.76	7.66	8.28	7.76	7.62	7.86	7.88	7.89	7.55
MnO	0.10	0.12	0.09	0.12	0.11	0.13	0.13	0.07	0.14	0.13	0.11	0.09	0.10	0.12	0.11	0.10
MgO	10.50	10.54	10.60	10.19	11.45	11.09	12.21	10.38	10.22	11.11	10.16	10.31	10.58	10.85	10.56	10.37
CaO	19.52	19.80	19.73	19.72	17.29	19.11	13.71	19.41	19.84	18.44	20.08	19.63	19.63	19.17	19.02	19.68
K2O	0.00	0.00	0.00	0.01	0.06	0.03	0.00	0.00	0.00	0.00	0.01	0.00	0.01	0.00	0.00	0.02
Na2O	2.54	2.40	2.42	2.50	2.46	2.41	2.33	2.39	2.46	2.29	2.33	2.47	2.41	2.35	2.47	2.41
Li2O																
ZnO																
NiO	0.00	0.02	0.03	0.03	0.03	0.00	0.07	0.01	0.02	0.02	0.02	0.01	0.04	0.02	0.00	0.07
Cr2O3	0.09	0.10	0.08	0.08	0.09	0.05	0.10	0.07	0.07	0.10	0.08	0.06	0.09	0.08	0.09	0.08
Sc2O3																
Total	99.11	99.18	99.13	99.27	98.85	99.03	97.68	98.84	99.29	99.07	98.80	98.83	99.57	99.06	99.05	98.73
Fe3+ model	Droop 1987	Droop 1987	Droop 1987	Droop 1987	Droop 1987	Droop 1987	Droop 1987	Droop 1987	Droop 1987	Droop 1987	Droop 1987	Droop 1987	Droop 1987	Droop 1987	Droop 1987	Droop 1987
Si Calc	1.82	1.81	1.83	1.83	1.79	1.84	1.75	1.82	1.83	1.81	1.81	1.82	1.82	1.82	1.82	1.81
Ti Calc	0.03	0.02	0.02	0.03	0.02	0.02	0.04	0.02	0.02	0.06	0.02	0.03	0.02	0.02	0.03	0.03
Al Calc	0.41	0.40	0.39	0.40	0.45	0.37	0.50	0.41	0.40	0.36	0.41	0.41	0.41	0.40	0.41	0.41
Fe Calc	0.24	0.24	0.24	0.24	0.28	0.25	0.33	0.24	0.24	0.26	0.24	0.24	0.24	0.25	0.25	0.24
Mn Calc	0.00	0.00	0.00	0.00	0.00	0.00	0.00	0.00	0.00	0.00	0.00	0.00	0.00	0.00	0.00	0.00
Mg Calc	0.58	0.59	0.59	0.57	0.64	0.62	0.69	0.58	0.57	0.62	0.57	0.58	0.59	0.60	0.59	0.58
Ca Calc	0.78	0.79	0.79	0.79	0.69	0.77	0.56	0.78	0.79	0.74	0.81	0.79	0.78	0.77	0.76	0.79
K Calc	0.00	0.00	0.00	0.00	0.00	0.00	0.00	0.00	0.00	0.00	0.00	0.00	0.00	0.00	0.00	0.00
Na Calc	0.18	0.17	0.18	0.18	0.18	0.17	0.17	0.17	0.18	0.17	0.17	0.18	0.17	0.17	0.18	0.18
Li Calc																
Zn Calc																
Ni Calc	0.00	0.00	0.00	0.00	0.00	0.00	0.00	0.00	0.00	0.00	0.00	0.00	0.00	0.00	0.00	0.00
Cr Calc	0.00	0.00	0.00	0.00	0.00	0.00	0.00	0.00	0.00	0.00	0.00	0.00	0.00	0.00	0.00	0.00
Sc Calc																
Fe 3+ Droop	0.13	0.13	0.12	0.10	0.17	0.13	0.13	0.11	0.11	0.09	0.13	0.12	0.13	0.12	0.11	0.13
Total Calc	4.04	4.04	4.04	4.03	4.06	4.04	4.04	4.04	4.04	4.03	4.04	4.04	4.04	4.04	4.04	4.04
Si	1.80	1.79	1.81	1.82	1.76	1.82	1.73	1.80	1.81	1.79	1.80	1.80	1.80	1.80	1.80	1.80
Ti	0.03	0.02	0.02	0.02	0.02	0.02	0.04	0.02	0.02	0.06	0.02	0.03	0.02	0.02	0.03	0.03
Al (T)	0.20	0.21	0.19	0.18	0.24	0.18	0.27	0.20	0.19	0.21	0.20	0.20	0.20	0.20	0.20	0.20
Al (M1)	0.20	0.19	0.20	0.21	0.20	0.19	0.23	0.21	0.21	0.15	0.20	0.20	0.20	0.20	0.21	0.20
Fe3+ (T)	0.00	0.00	0.00	0.00	0.00	0.00	0.00	0.00	0.00	0.00	0.00	0.00	0.00	0.00	0.00	0.00
Fe3+ (M1)	0.13	0.13	0.12	0.10	0.17	0.13	0.13	0.11	0.11	0.09	0.13	0.12	0.13	0.12	0.11	0.13
Fe2+	0.10	0.10	0.12	0.14	0.10	0.11	0.19	0.13	0.12	0.17	0.11	0.11	0.12	0.12	0.13	0.11
Mn	0.00	0.00	0.00	0.00	0.00	0.00	0.00	0.00	0.00	0.00	0.00	0.00	0.00	0.00	0.00	0.00
Mg	0.58	0.58	0.58	0.56	0.63	0.61	0.68	0.57	0.56	0.62	0.56	0.57	0.58	0.60	0.58	0.57
Ca	0.77	0.78	0.78	0.78	0.68	0.76	0.55	0.77	0.79	0.73	0.80	0.78	0.78	0.76	0.75	0.78
K	0.00	0.00	0.00	0.00	0.00	0.00	0.00	0.00	0.00	0.00	0.00	0.00	0.00	0.00	0.00	0.00
Na	0.18	0.17	0.17	0.18	0.18	0.17	0.17	0.17	0.18	0.17	0.17	0.18	0.17	0.17	0.18	0.17
Li	0.00	0.00	0.00	0.00	0.00	0.00	0.00	0.00	0.00	0.00	0.00	0.00	0.00	0.00	0.00	0.00
Zn	0.00	0.00	0.00	0.00	0.00	0.00	0.00	0.00	0.00	0.00	0.00	0.00	0.00	0.00	0.00	0.00
Ni	0.00	0.00	0.00	0.00	0.00	0.00	0.00	0.00	0.00	0.00	0.00	0.00	0.00	0.00	0.00	0.00
Cr	0.00	0.00	0.00	0.00	0.00	0.00	0.00	0.00	0.00	0.00	0.00	0.00	0.00	0.00	0.00	0.00
Sc	0.00	0.00	0.00	0.00	0.00	0.00	0.00	0.00	0.00	0.00	0.00	0.00	0.00	0.00	0.00	0.00
Total	4.00	4.00	4.00	4.00	4.00	4.00	4.00	4.00	4.00	4.00	4.00	4.00	4.00	4.00	4.00	4.00
J	0.36	0.34	0.35	0.36	0.35	0.35	0.34	0.34	0.35	0.33	0.34	0.36	0.34	0.34	0.35	0.35
Q	1.46	1.47	1.49	1.48	1.42	1.48	1.42	1.48	1.47	1.52	1.48	1.46	1.47	1.48	1.47	1.47
group	Quad	Quad	Quad	Quad	Quad	Quad	Quad	Quad	Quad	Quad	Quad	Quad	Quad	Quad	Quad	Quad
adjective	aluminian ferrian sodian	aluminian ferrian sodian	aluminian ferrian sodian	aluminian sodian	aluminian ferrian sodian	aluminian ferrian sodian	aluminian ferrian sodian subsilicic	aluminian ferrian sodian	aluminian ferrian sodian	aluminian sodian	aluminian ferrian sodian	aluminian ferrian sodian	aluminian ferrian sodian	aluminian ferrian sodian	aluminian ferrian sodian	aluminian ferrian sodian
pyroxene	diopside	diopside	diopside	diopside	augite	diopside	augite	diopside	diopside	diopside	diopside	diopside	diopside	diopside	diopside	diopside
enstatite	36.38	36.20	36.42	35.54	39.63	37.77	43.73	36.14	35.43	38.21	35.03	35.86	36.28	37.27	36.76	36.00
ferrosillite	15.00	14.93	14.83	15.03	17.35	15.47	20.97	15.30	15.17	16.22	15.22	15.06	15.32	15.41	15.65	14.89
wollastonite	48.63	48.87	48.74	49.43	43.02	46.76	35.29	48.56	49.41	45.58	49.76	49.08	48.40	47.32	47.60	49.11
jadeite	----------	----------	----------	----------	----------	----------	----------	----------	----------	----------	----------	----------	----------	----------	----------	----------
aegirine	----------	----------	----------	----------	----------	----------	----------	----------	----------	----------	----------	----------	----------	----------	----------	----------
Quad	----------	----------	----------	----------	----------	----------	----------	----------	----------	----------	----------	----------	----------	----------	----------	----------

Appendix 6.D EMP data for pyroxene modified from PX-NOM (Sturm, R. 2002)

Sample	0906A 1.10 cpx trav	0906A 1.10 cpx trav	0906A 1.10 cpx trav	0906A 1.10 cpx trav	0906A 1.10 cpx trav	0906A 1.10 cpx trav	0906A 1.10 cpx trav	0906A 1.10 cpx trav	0906A 1.10 cpx trav	0906A 1.10 cpx trav	0906A 1.10 cpx trav	0906A 1.10 cpx trav	0906A 1.10 cpx trav	0906A 1.10 cpx trav	0906A 1.10 cpx trav	0906A 1.10 cpx trav
x	7844.00	7844.00	7844.00	7844.00	7844.00	7844.00	7844.00	7844.00	7844.00	7844.00	7844.00	7844.00	7844.00	7844.00	7844.00	7844.00
y	28803.00	28815.00	28846.00	28901.00	28955.00	29050.00	29109.00	29176.00	29238.00	29301.00	29347.00	29365.00	29398.00	29438.00	29449.00	29463.00
z	73.00	73.00	73.00	73.00	73.00	73.00	73.00	73.00	73.00	73.00	73.00	73.00	73.00	73.00	73.00	73.00
SiO2	48.70	49.14	48.50	48.84	48.05	48.89	48.91	48.96	49.11	49.04	49.05	49.30	48.91	49.07	48.47	49.17
TiO2	0.91	0.97	0.86	0.81	0.90	0.86	0.92	0.91	0.78	0.83	0.99	0.97	0.96	0.98	0.94	1.00
Al2O3	9.02	9.04	9.17	8.93	9.41	9.03	9.03	9.18	8.82	8.98	9.16	9.03	8.98	8.78	8.56	8.76
FeO	7.58	7.69	7.78	7.52	8.00	7.45	7.32	7.50	7.37	7.25	7.30	7.32	7.13	7.36	7.10	7.32
MnO	0.11	0.09	0.10	0.11	0.08	0.07	0.09	0.08	0.08	0.08	0.04	0.07	0.06	0.05	0.04	0.06
MgO	10.49	10.49	10.51	10.35	10.69	10.56	10.45	10.45	10.48	10.36	10.41	10.46	10.35	10.51	10.23	10.67
CaO	19.38	19.29	19.19	19.77	18.61	19.71	19.81	19.52	19.69	19.93	19.93	19.90	19.77	19.75	19.70	19.72
K2O	0.00	0.00	0.00	0.00	0.00	0.00	0.00	0.00	0.00	0.00	0.00	0.01	0.00	0.00	0.00	0.00
Na2O	2.48	2.47	2.51	2.46	2.47	2.41	2.46	2.51	2.48	2.58	2.54	2.56	2.58	2.50	2.48	2.46
Li2O																
ZnO																
NiO	0.03	0.01	0.05	0.04	0.02	0.00	0.01	0.07	0.00	0.03	0.02	0.07	0.02	0.00	0.00	0.05
Cr2O3	0.06	0.06	0.05	0.08	0.08	0.07	0.11	0.11	0.12	0.11	0.09	0.11	0.11	0.12	0.12	0.12
Sc2O3																
Total	98.76	99.27	98.72	98.92	98.31	99.03	99.11	99.30	98.94	99.19	99.53	99.78	98.87	99.14	97.65	99.33
Fe3+ model	Droop 1987	Droop 1987	Droop 1987	Droop 1987	Droop 1987	Droop 1987	Droop 1987	Droop 1987	Droop 1987	Droop 1987	Droop 1987	Droop 1987	Droop 1987	Droop 1987	Droop 1987	Droop 1987
Si Calc	1.83	1.83	1.82	1.83	1.81	1.83	1.83	1.83	1.84	1.83	1.82	1.83	1.83	1.83	1.84	1.83
Ti Calc	0.03	0.03	0.02	0.02	0.03	0.02	0.03	0.03	0.02	0.02	0.03	0.03	0.03	0.03	0.03	0.03
Al Calc	0.40	0.40	0.41	0.39	0.42	0.40	0.40	0.40	0.39	0.39	0.40	0.39	0.40	0.39	0.38	0.38
Fe Calc	0.24	0.24	0.24	0.24	0.25	0.23	0.23	0.23	0.23	0.23	0.23	0.23	0.22	0.23	0.22	0.23
Mn Calc	0.00	0.00	0.00	0.00	0.00	0.00	0.00	0.00	0.00	0.00	0.00	0.00	0.00	0.00	0.00	0.00
Mg Calc	0.59	0.58	0.59	0.58	0.60	0.59	0.58	0.58	0.58	0.58	0.58	0.58	0.58	0.58	0.58	0.59
Ca Calc	0.78	0.77	0.77	0.79	0.75	0.79	0.79	0.78	0.79	0.80	0.79	0.79	0.79	0.79	0.80	0.79
K Calc	0.00	0.00	0.00	0.00	0.00	0.00	0.00	0.00	0.00	0.00	0.00	0.00	0.00	0.00	0.00	0.00
Na Calc	0.18	0.18	0.18	0.18	0.18	0.17	0.18	0.18	0.18	0.19	0.18	0.18	0.19	0.18	0.18	0.18
Li Calc																
Zn Calc																
Ni Calc	0.00	0.00	0.00	0.00	0.00	0.00	0.00	0.00	0.00	0.00	0.00	0.00	0.00	0.00	0.00	0.00
Cr Calc	0.00	0.00	0.00	0.00	0.00	0.00	0.00	0.00	0.00	0.00	0.00	0.00	0.00	0.00	0.00	0.00
Sc Calc																
Fe 3+ Droop	0.11	0.09	0.13	0.12	0.13	0.11	0.11	0.11	0.11	0.12	0.11	0.11	0.11	0.11	0.10	0.11
Total Calc	4.04	4.03	4.04	4.04	4.04	4.04	4.04	4.04	4.04	4.04	4.04	4.04	4.04	4.04	4.03	4.04
Si	1.81	1.82	1.80	1.81	1.79	1.81	1.81	1.81	1.82	1.81	1.81	1.81	1.81	1.82	1.82	1.82
Ti	0.03	0.03	0.02	0.02	0.03	0.02	0.03	0.03	0.02	0.02	0.03	0.03	0.03	0.03	0.03	0.03
Al (T)	0.19	0.18	0.20	0.19	0.21	0.19	0.19	0.19	0.18	0.19	0.19	0.19	0.19	0.18	0.18	0.18
Al (M1)	0.20	0.21	0.20	0.20	0.20	0.20	0.20	0.21	0.20	0.20	0.20	0.20	0.20	0.20	0.20	0.20
Fe3+ (T)	0.00	0.00	0.00	0.00	0.00	0.00	0.00	0.00	0.00	0.00	0.00	0.00	0.00	0.00	0.00	0.00
Fe3+ (M1)	0.11	0.09	0.13	0.12	0.13	0.11	0.11	0.11	0.11	0.12	0.11	0.11	0.11	0.11	0.10	0.11
Fe2+	0.12	0.14	0.11	0.12	0.12	0.12	0.12	0.12	0.12	0.10	0.11	0.11	0.11	0.12	0.12	0.12
Mn	0.00	0.00	0.00	0.00	0.00	0.00	0.00	0.00	0.00	0.00	0.00	0.00	0.00	0.00	0.00	0.00
Mg	0.58	0.58	0.58	0.57	0.59	0.58	0.58	0.58	0.58	0.57	0.57	0.57	0.57	0.58	0.57	0.59
Ca	0.77	0.76	0.76	0.79	0.74	0.78	0.79	0.77	0.78	0.79	0.79	0.78	0.78	0.78	0.79	0.78
K	0.00	0.00	0.00	0.00	0.00	0.00	0.00	0.00	0.00	0.00	0.00	0.00	0.00	0.00	0.00	0.00
Na	0.18	0.18	0.18	0.18	0.18	0.17	0.18	0.18	0.18	0.18	0.18	0.18	0.19	0.18	0.18	0.18
Li	0.00	0.00	0.00	0.00	0.00	0.00	0.00	0.00	0.00	0.00	0.00	0.00	0.00	0.00	0.00	0.00
Zn	0.00	0.00	0.00	0.00	0.00	0.00	0.00	0.00	0.00	0.00	0.00	0.00	0.00	0.00	0.00	0.00
Ni	0.00	0.00	0.00	0.00	0.00	0.00	0.00	0.00	0.00	0.00	0.00	0.00	0.00	0.00	0.00	0.00
Cr	0.00	0.00	0.00	0.00	0.00	0.00	0.00	0.00	0.00	0.00	0.00	0.00	0.00	0.00	0.00	0.00
Sc	0.00	0.00	0.00	0.00	0.00	0.00	0.00	0.00	0.00	0.00	0.00	0.00	0.00	0.00	0.00	0.00
Total	4.00	4.00	4.00	4.00	4.00	4.00	4.00	4.00	4.00	4.00	4.00	4.00	4.00	4.00	4.00	4.00
J	0.36	0.35	0.36	0.35	0.36	0.35	0.35	0.36	0.36	0.37	0.36	0.36	0.37	0.36	0.36	0.35
Q	1.47	1.49	1.46	1.48	1.46	1.49	1.48	1.47	1.48	1.46	1.47	1.47	1.47	1.48	1.48	1.49
group	Quad	Quad	Quad	Quad	Quad	Quad	Quad	Quad	Quad	Ca-Na	Quad	Quad	Ca-Na	Quad	Quad	Quad
adjective	aluminian ferrian sodian	aluminian sodian	aluminian ferrian sodian	aluminian ferrian sodian	aluminian ferrian sodian	aluminian ferrian sodian	aluminian ferrian sodian	aluminian ferrian sodian	aluminian ferrian sodian		aluminian ferrian sodian	aluminian ferrian sodian		aluminian ferrian sodian	aluminian ferrian sodian	aluminian ferrian sodian
pyroxene	diopside	diopside	diopside	diopside	diopside	diopside	diopside	diopside	diopside	omphacite	diopside	diopside	omphacite	diopside	diopside	diopside
enstatite	36.50	36.52	36.59	35.88	37.36	36.48	36.24	36.36	36.38	----------	36.09	36.18	----------	36.42	36.03	36.81
ferrosillite	15.02	15.21	15.40	14.86	15.86	14.57	14.40	14.82	14.50	----------	14.28	14.34	----------	14.41	14.11	14.29
wollastonite	48.48	48.27	48.01	49.26	46.78	48.95	49.35	48.83	49.11	----------	49.64	49.48	----------	49.17	49.86	48.91
jadeite	----------	----------	----------	----------	----------	----------	----------	----------	----------	12.61	----------	----------	13.06	----------	----------	----------
aegirine	----------	----------	----------	----------	----------	----------	----------	----------	----------	7.55	----------	----------	7.11	----------	----------	----------
Quad	----------	----------	----------	----------	----------	----------	----------	----------	----------	79.83	----------	----------	79.83	----------	----------	----------

Appendix 6.D EMP data for pyroxene modified from PX-NOM (Sturm, R. 2002)

Sample	0906A 1.10 cpx trav	0906A 1.10 cpx trav	0906A 1.10 cpx trav	0906A 1.10 cpx trav	0906A 1.10 cpx trav
x	7844.00	7844.00	7844.00	7844.00	7844.00
y	29479.00	29518.00	29543.00	29578.00	29601.00
z	73.00	73.00	73.00	73.00	73.00
SiO2	49.57	49.85	50.59	50.35	51.74
TiO2	0.89	0.79	0.64	0.66	0.29
Al2O3	8.32	7.62	6.85	6.79	4.51
FeO	7.09	6.95	6.87	6.90	6.42
MnO	0.07	0.08	0.06	0.06	0.08
MgO	10.77	11.30	11.49	11.38	13.12
CaO	20.12	20.28	20.30	20.16	20.94
K2O	0.00	0.00	0.00	0.01	0.02
Na2O	2.48	2.49	2.34	2.42	1.89
Li2O					
ZnO					
NiO	0.01	0.02	0.00	0.00	0.04
Cr2O3	0.10	0.14	0.11	0.11	0.14
Sc2O3					
Total	99.43	99.53	99.26	98.85	99.18
Fe3+ model	Droop 1987	Droop 1987	Droop 1987	Droop 1987	Droop 1987
Si Calc	1.84	1.85	1.88	1.88	1.92
Ti Calc	0.02	0.02	0.02	0.02	0.01
Al Calc	0.36	0.33	0.30	0.30	0.20
Fe Calc	0.22	0.22	0.21	0.22	0.20
Mn Calc	0.00	0.00	0.00	0.00	0.00
Mg Calc	0.60	0.63	0.64	0.63	0.73
Ca Calc	0.80	0.81	0.81	0.81	0.83
K Calc	0.00	0.00	0.00	0.00	0.00
Na Calc	0.18	0.18	0.17	0.18	0.14
Li Calc					
Zn Calc					
Ni Calc	0.00	0.00	0.00	0.00	0.00
Cr Calc	0.00	0.00	0.00	0.00	0.00
Sc Calc					
Fe 3+ Droop	0.11	0.14	0.10	0.11	0.11
Total Calc	4.04	4.05	4.03	4.04	4.04
Si	1.83	1.83	1.87	1.86	1.91
Ti	0.02	0.02	0.02	0.02	0.01
Al (T)	0.17	0.17	0.13	0.14	0.09
Al (M1)	0.19	0.16	0.16	0.16	0.10
Fe3+ (T)	0.00	0.00	0.00	0.00	0.00
Fe3+ (M1)	0.11	0.14	0.10	0.11	0.11
Fe2+	0.11	0.08	0.11	0.10	0.09
Mn	0.00	0.00	0.00	0.00	0.00
Mg	0.59	0.62	0.63	0.63	0.72
Ca	0.79	0.80	0.80	0.80	0.83
K	0.00	0.00	0.00	0.00	0.00
Na	0.18	0.18	0.17	0.17	0.14
Li	0.00	0.00	0.00	0.00	0.00
Zn	0.00	0.00	0.00	0.00	0.00
Ni	0.00	0.00	0.00	0.00	0.00
Cr	0.00	0.00	0.00	0.00	0.00
Sc	0.00	0.00	0.00	0.00	0.00
Total	4.00	4.00	4.00	4.00	4.00
J	0.36	0.36	0.33	0.35	0.27
Q	1.49	1.49	1.55	1.53	1.64
group	Quad	Quad	Quad	Quad	Quad
adjective	aluminian ferrian sodian	aluminian ferrian sodian	aluminian sodian	aluminian ferrian sodian	aluminian ferrian sodian
pyroxene	diopside	diopside	diopside	diopside	diopside
enstatite	36.82	37.88	38.33	38.23	41.24
ferrosillite	13.73	13.23	12.97	13.11	11.46
wollastonite	49.46	48.89	48.70	48.66	47.30
jadeite	----------	----------	----------	----------	----------
aegirine	----------	----------	----------	----------	----------
Quad	----------	----------	----------	----------	----------

Appendix 6.D EMP data for pyroxene modified from PX-NOM (Sturm, R. 2002)

Sample	0909 1.8 cpx r	0909 1.9 cpx r	0909 1.10 cpx c	0909 1.11 cpx c	0909 2.4 cpx	0909 2.4 cpx	0909 2.4 cpx	0909 2.4 cpx	0909 2.4 cpx	0909 2.4 cpx	0909 2.4 cpx	0909 2.4 cpx
X	14113.00	14057.00	14069.00	14138.00	12806.00	12814.00	12705.00	12670.00	12674.00	12568.00	12429.00	12428.00
Y	-14645.00	-14785.00	-14719.00	-14693.00	-24912.00	-24739.00	-24690.00	-24580.00	-24431.00	-24400.00	-24400.00	-24201.00
Z	77.00	77.00	77.00	77.00	87.00	87.00	87.00	87.00	87.00	87.00	87.00	87.00
SiO2	51.39	51.17	51.47	50.86	51.08	51.17	51.44	51.99	50.82	51.43	51.11	52.12
TiO2	0.48	0.48	0.46	0.55	0.57	0.48	0.51	0.52	0.49	0.43	0.47	0.48
Al2O3	10.33	9.54	10.14	10.37	10.10	9.61	9.50	9.18	8.90	8.95	9.55	9.15
FeO	7.73	8.61	7.57	8.32	8.18	8.64	8.36	8.60	8.88	8.65	8.57	8.26
MnO	0.02	0.03	0.04	0.02	0.02	0.04	0.04	0.04	0.07	0.03	0.00	0.04
MgO	8.46	8.54	8.42	8.18	8.48	8.83	8.77	8.86	9.23	8.94	9.01	8.94
CaO	15.85	16.16	15.80	15.89	16.84	16.77	17.04	16.77	17.30	16.72	16.98	16.82
K2O	0.01	0.00	0.00	0.00	0.00	0.00	0.01	0.02	0.00	0.01	0.02	0.02
Na2O	5.02	4.88	4.99	5.00	4.27	4.16	4.12	4.26	3.64	4.16	3.99	4.27
Li2O												
ZnO												
NiO	0.00	0.00	0.04	0.00	0.01	0.02	0.00	0.04	0.00	0.00	0.00	0.01
Cr2O3	0.03	0.01	0.00	0.01	0.00	0.01	0.04	0.01	0.02	0.02	0.02	0.06
Sc2O3												
Total	99.33	99.42	98.94	99.20	99.55	99.72	99.85	100.29	99.34	99.35	99.72	100.16
Fe3+ model	Droop 1987	Droop 1987	Droop 1987	Droop 1987	Droop 1987	Droop 1987	Droop 1987	Droop 1987	Droop 1987	Droop 1987	Droop 1987	Droop 1987
Si Calc	1.89	1.90	1.90	1.88	1.89	1.89	1.89	1.91	1.89	1.91	1.89	1.91
Ti Calc	0.01	0.01	0.01	0.02	0.02	0.01	0.01	0.01	0.01	0.01	0.01	0.01
Al Calc	0.45	0.42	0.44	0.45	0.44	0.42	0.41	0.40	0.39	0.39	0.42	0.40
Fe Calc	0.24	0.27	0.23	0.26	0.25	0.27	0.26	0.26	0.28	0.27	0.26	0.25
Mn Calc	0.00	0.00	0.00	0.00	0.00	0.00	0.00	0.00	0.00	0.00	0.00	0.00
Mg Calc	0.47	0.47	0.46	0.45	0.47	0.49	0.48	0.48	0.51	0.49	0.50	0.49
Ca Calc	0.63	0.64	0.63	0.63	0.67	0.66	0.67	0.66	0.69	0.66	0.67	0.66
K Calc	0.00	0.00	0.00	0.00	0.00	0.00	0.00	0.00	0.00	0.00	0.00	0.00
Na Calc	0.36	0.35	0.36	0.36	0.31	0.30	0.29	0.30	0.26	0.30	0.29	0.30
Li Calc												
Zn Calc												
Ni Calc	0.00	0.00	0.00	0.00	0.00	0.00	0.00	0.00	0.00	0.00	0.00	0.00
Cr Calc	0.00	0.00	0.00	0.00	0.00	0.00	0.00	0.00	0.00	0.00	0.00	0.00
Sc Calc												
Fe 3+ Droop	0.14	0.17	0.13	0.16	0.10	0.11	0.09	0.09	0.10	0.11	0.10	0.09
Total Calc	4.05	4.06	4.04	4.05	4.03	4.04	4.03	4.03	4.03	4.04	4.03	4.03
Si	1.87	1.87	1.88	1.86	1.87	1.87	1.88	1.89	1.87	1.89	1.87	1.90
Ti	0.01	0.01	0.01	0.02	0.02	0.01	0.01	0.01	0.01	0.01	0.01	0.01
Al (T)	0.13	0.13	0.12	0.14	0.13	0.13	0.12	0.11	0.13	0.11	0.13	0.10
Al (M1)	0.32	0.28	0.32	0.31	0.31	0.29	0.29	0.29	0.26	0.28	0.28	0.29
Fe3+ (T)	0.00	0.00	0.00	0.00	0.00	0.00	0.00	0.00	0.00	0.00	0.00	0.00
Fe3+ (M1)	0.14	0.17	0.13	0.16	0.10	0.11	0.09	0.09	0.10	0.11	0.10	0.09
Fe2+	0.10	0.09	0.11	0.10	0.16	0.15	0.16	0.17	0.17	0.16	0.16	0.16
Mn	0.00	0.00	0.00	0.00	0.00	0.00	0.00	0.00	0.00	0.00	0.00	0.00
Mg	0.46	0.47	0.46	0.45	0.46	0.48	0.48	0.48	0.51	0.49	0.49	0.49
Ca	0.62	0.63	0.62	0.62	0.66	0.66	0.67	0.65	0.68	0.66	0.67	0.66
K	0.00	0.00	0.00	0.00	0.00	0.00	0.00	0.00	0.00	0.00	0.00	0.00
Na	0.35	0.35	0.35	0.35	0.30	0.30	0.29	0.30	0.26	0.30	0.28	0.30
Li	0.00	0.00	0.00	0.00	0.00	0.00	0.00	0.00	0.00	0.00	0.00	0.00
Zn	0.00	0.00	0.00	0.00	0.00	0.00	0.00	0.00	0.00	0.00	0.00	0.00
Ni	0.00	0.00	0.00	0.00	0.00	0.00	0.00	0.00	0.00	0.00	0.00	0.00
Cr	0.00	0.00	0.00	0.00	0.00	0.00	0.00	0.00	0.00	0.00	0.00	0.00
Sc	0.00	0.00	0.00	0.00	0.00	0.00	0.00	0.00	0.00	0.00	0.00	0.00
Total	4.00	4.00	4.00	4.00	4.00	4.00	4.00	4.00	4.00	4.00	4.00	4.00
J	0.71	0.69	0.71	0.71	0.61	0.59	0.58	0.60	0.52	0.59	0.57	0.60
Q	1.17	1.19	1.18	1.16	1.28	1.29	1.31	1.30	1.36	1.31	1.32	1.30
group	Ca-Na	Ca-Na	Ca-Na	Ca-Na	Ca-Na	Ca-Na	Ca-Na	Ca-Na	Ca-Na	Ca-Na	Ca-Na	Ca-Na
adjective pyroxene	omphacite	omphacite	omphacite	omphacite	omphacite	omphacite	omphacite	omphacite	omphacite	omphacite	omphacite	omphacite
enstatite	----------	----------	----------	----------	----------	----------	----------	----------	----------	----------	----------	----------
ferrosillite	----------	----------	----------	----------	----------	----------	----------	----------	----------	----------	----------	----------
wollastonite	----------	----------	----------	----------	----------	----------	----------	----------	----------	----------	----------	----------
jadeite	26.14	22.82	26.89	25.00	24.54	22.59	23.36	23.74	19.96	22.52	22.02	24.24
aegirine	11.52	13.91	10.53	12.84	7.63	8.79	7.51	7.85	7.64	8.69	8.05	7.34
Quad	62.34	63.27	62.58	62.16	67.83	68.62	69.13	68.41	72.41	68.79	69.93	68.42

Appendix 6.D EMP data for pyroxene modified from PX-NOM (Sturm, R. 2002)

Sample	0910B 1.1+ cpx random	0910B 1.1+ cpx random	0910B 1.1+ cpx random	0910B 1.1+ cpx random	0910B 1.1+ cpx random	0910B 1.1+ cpx random	0910B 1.1+ cpx random	0910B 1.1+ cpx random	0910B 1.1+ cpx random
X	-19388.00	-19454.00	-19609.00	-19546.00	-19169.00	-19209.00	-19223.00	-19421.00	-19532.00
Y	-19398.00	-19526.00	-19415.00	-19372.00	-19637.00	-19757.00	-19862.00	-19874.00	-19976.00
Z	68.00	68.00	68.00	68.00	68.00	68.00	68.00	68.00	68.00
SiO2	48.62	48.38	48.58	48.58	48.24	47.95	48.04	48.71	48.06
TiO2	0.65	0.61	0.67	0.70	0.71	0.72	0.78	0.72	0.73
Al2O3	8.87	8.20	8.99	8.93	9.42	9.56	9.35	8.71	8.90
FeO	7.28	7.73	7.40	7.37	7.25	7.51	7.66	7.40	7.77
MnO	0.05	0.03	0.01	0.05	0.00	0.03	0.04	0.04	0.03
MgO	10.05	10.36	9.91	10.03	9.82	9.72	9.90	10.17	10.04
CaO	20.30	20.86	20.31	20.40	20.21	20.41	20.86	20.55	20.93
K2O	0.01	0.01	0.01	0.00	0.00	0.00	0.00	0.01	0.01
Na2O	2.75	2.43	2.71	2.67	2.76	2.70	2.47	2.57	2.49
Li2O									
ZnO									
NiO	0.00	0.09	0.02	0.03	0.00	0.03	0.00	0.01	0.02
Cr2O3	0.03	0.03	0.02	0.00	0.00	0.01	0.02	0.02	0.01
Sc2O3									
Total	98.60	98.74	98.62	98.74	98.40	98.65	99.12	98.91	98.98
Fe3+ model	Droop 1987	Droop 1987	Droop 1987	Droop 1987	Droop 1987	Droop 1987	Droop 1987	Droop 1987	Droop 1987
Si Calc	1.83	1.83	1.83	1.83	1.82	1.81	1.80	1.83	1.81
Ti Calc	0.02	0.02	0.02	0.02	0.02	0.02	0.02	0.02	0.02
Al Calc	0.39	0.36	0.40	0.40	0.42	0.42	0.41	0.39	0.40
Fe Calc	0.23	0.24	0.23	0.23	0.23	0.24	0.24	0.23	0.24
Mn Calc	0.00	0.00	0.00	0.00	0.00	0.00	0.00	0.00	0.00
Mg Calc	0.56	0.58	0.56	0.56	0.55	0.55	0.55	0.57	0.56
Ca Calc	0.82	0.84	0.82	0.82	0.82	0.82	0.84	0.83	0.84
K Calc	0.00	0.00	0.00	0.00	0.00	0.00	0.00	0.00	0.00
Na Calc	0.20	0.18	0.20	0.19	0.20	0.20	0.18	0.19	0.18
Li Calc									
Zn Calc									
Ni Calc	0.00	0.00	0.00	0.00	0.00	0.00	0.00	0.00	0.00
Cr Calc	0.00	0.00	0.00	0.00	0.00	0.00	0.00	0.00	0.00
Sc Calc									
Fe 3+ Droop	0.16	0.19	0.16	0.16	0.16	0.17	0.17	0.15	0.18
Total Calc	4.06	4.06	4.05	4.05	4.05	4.06	4.06	4.05	4.06
Si	1.80	1.80	1.80	1.80	1.79	1.78	1.78	1.81	1.78
Ti	0.02	0.02	0.02	0.02	0.02	0.02	0.02	0.02	0.02
Al (T)	0.20	0.20	0.20	0.20	0.21	0.22	0.22	0.19	0.22
Al (M1)	0.19	0.16	0.20	0.19	0.21	0.20	0.19	0.19	0.17
Fe3+ (T)	0.00	0.00	0.00	0.00	0.00	0.00	0.00	0.00	0.00
Fe3+ (M1)	0.16	0.19	0.16	0.16	0.16	0.17	0.17	0.15	0.18
Fe2+	0.06	0.05	0.07	0.07	0.07	0.06	0.07	0.08	0.06
Mn	0.00	0.00	0.00	0.00	0.00	0.00	0.00	0.00	0.00
Mg	0.56	0.57	0.55	0.55	0.54	0.54	0.55	0.56	0.56
Ca	0.81	0.83	0.81	0.81	0.81	0.81	0.83	0.82	0.83
K	0.00	0.00	0.00	0.00	0.00	0.00	0.00	0.00	0.00
Na	0.20	0.18	0.20	0.19	0.20	0.19	0.18	0.18	0.18
Li	0.00	0.00	0.00	0.00	0.00	0.00	0.00	0.00	0.00
Zn	0.00	0.00	0.00	0.00	0.00	0.00	0.00	0.00	0.00
Ni	0.00	0.00	0.00	0.00	0.00	0.00	0.00	0.00	0.00
Cr	0.00	0.00	0.00	0.00	0.00	0.00	0.00	0.00	0.00
Sc	0.00	0.00	0.00	0.00	0.00	0.00	0.00	0.00	0.00
Total	4.00	4.00	4.00	4.00	4.00	4.00	4.00	4.00	4.00
J	0.40	0.35	0.39	0.38	0.40	0.39	0.35	0.37	0.36
Q	1.42	1.46	1.43	1.44	1.42	1.41	1.44	1.45	1.44
group	Ca-Na	Quad	Ca-Na	Ca-Na	Ca-Na	Ca-Na	Quad	Ca-Na	Quad
adjective		aluminian ferrian sodian					aluminian ferrian sodian		aluminian ferrian sodian
pyroxene	omphacite	wollastonite	omphacite	omphacite	omphacite	omphacite	wollastonite	omphacite	wollastonite
enstatite	----------	34.88	----------	----------	----------	----------	33.90	----------	34.08
ferrosillite	----------	14.66	----------	----------	----------	----------	14.77	----------	14.85
wollastonite	----------	50.46	----------	----------	----------	----------	51.33	----------	51.06
jadeite	11.71	----------	11.99	11.57	12.39	11.55	----------	11.08	----------
aegirine	10.04	----------	9.46	9.51	9.57	10.06	----------	9.17	----------
Quad	78.24	----------	78.56	78.92	78.05	78.39	----------	79.74	----------

Appendix 6.D EMP data for pyroxene modified from PX-NOM (Sturm, R. 2002)

Sample	0910B 1.1+ cpx random	0910B 1.1+ cpx random	0910B 1.1+ cpx random	0910B 1.1+ cpx random	0910B 1.1+ cpx random	0910B 1.1+ cpx random	0910B 1.1+ cpx random	0910B 1.1+ cpx random	0910B 1.1+ cpx random	0910B 1.1+ cpx random
X	-19632.00	-19445.00	-19254.00	-19307.00	-19072.00	-19127.00	-19101.00	-18993.00	-18826.00	-19416.00
Y	-19976.00	-20150.00	-20162.00	-20239.00	-20352.00	-20590.00	-20540.00	-20622.00	-20631.00	-20773.00
Z	68.00	68.00	68.00	68.00	68.00	68.00	68.00	68.00	68.00	68.00
SiO2	48.44	48.70	47.88	47.99	47.00	48.26	48.56	48.93	48.59	48.48
TiO2	0.54	0.61	0.83	0.82	0.90	0.59	0.61	0.56	0.65	0.71
Al2O3	7.56	8.25	9.70	9.81	9.99	9.09	9.02	8.75	8.46	9.23
FeO	7.54	7.30	7.84	7.35	7.73	7.27	7.49	7.17	7.54	7.44
MnO	0.04	0.06	0.01	0.02	0.04	0.04	0.01	0.03	0.03	0.03
MgO	10.31	10.38	9.73	9.73	9.69	9.95	9.93	10.19	10.39	10.07
CaO	20.36	20.42	20.49	20.37	20.55	20.15	20.46	20.07	20.49	20.34
K2O	0.01	0.01	0.00	0.00	0.00	0.01	0.00	0.00	0.00	0.00
Na2O	2.43	2.54	2.51	2.69	2.60	2.72	2.71	2.87	2.64	2.75
Li2O										
ZnO										
NiO	0.05	0.01	0.00	0.02	0.01	0.04	0.05	0.02	0.00	0.03
Cr2O3	0.00	0.01	0.01	0.03	0.02	0.00	0.03	0.03	0.01	0.01
Sc2O3										
Total	97.26	98.30	98.99	98.83	98.53	98.12	98.86	98.64	98.81	99.09
Fe3+ model	Droop 1987	Droop 1987	Droop 1987	Droop 1987	Droop 1987	Droop 1987	Droop 1987	Droop 1987	Droop 1987	Droop 1987
Si Calc	1.85	1.84	1.80	1.80	1.78	1.82	1.82	1.84	1.83	1.82
Ti Calc	0.02	0.02	0.02	0.02	0.03	0.02	0.02	0.02	0.02	0.02
Al Calc	0.34	0.37	0.43	0.43	0.45	0.41	0.40	0.39	0.38	0.41
Fe Calc	0.24	0.23	0.25	0.23	0.24	0.23	0.24	0.23	0.24	0.23
Mn Calc	0.00	0.00	0.00	0.00	0.00	0.00	0.00	0.00	0.00	0.00
Mg Calc	0.59	0.58	0.55	0.54	0.55	0.56	0.56	0.57	0.58	0.56
Ca Calc	0.83	0.83	0.83	0.82	0.83	0.82	0.82	0.81	0.83	0.82
K Calc	0.00	0.00	0.00	0.00	0.00	0.00	0.00	0.00	0.00	0.00
Na Calc	0.18	0.19	0.18	0.20	0.19	0.20	0.20	0.21	0.19	0.20
Li Calc										
Zn Calc										
Ni Calc	0.00	0.00	0.00	0.00	0.00	0.00	0.00	0.00	0.00	0.00
Cr Calc	0.00	0.00	0.00	0.00	0.00	0.00	0.00	0.00	0.00	0.00
Sc Calc										
Fe 3+ Droop	0.16	0.16	0.16	0.16	0.20	0.17	0.17	0.17	0.18	0.17
Total Calc	4.05	4.05	4.05	4.05	4.07	4.06	4.06	4.06	4.06	4.06
Si	1.83	1.81	1.78	1.78	1.75	1.80	1.80	1.81	1.80	1.79
Ti	0.02	0.02	0.02	0.02	0.03	0.02	0.02	0.02	0.02	0.02
Al (T)	0.17	0.19	0.22	0.22	0.25	0.20	0.20	0.19	0.20	0.21
Al (M1)	0.16	0.18	0.20	0.21	0.19	0.20	0.19	0.19	0.17	0.19
Fe3+ (T)	0.00	0.00	0.00	0.00	0.00	0.00	0.00	0.00	0.00	0.00
Fe3+ (M1)	0.16	0.16	0.16	0.16	0.20	0.17	0.17	0.17	0.18	0.17
Fe2+	0.08	0.07	0.09	0.07	0.04	0.06	0.07	0.05	0.05	0.06
Mn	0.00	0.00	0.00	0.00	0.00	0.00	0.00	0.00	0.00	0.00
Mg	0.58	0.58	0.54	0.54	0.54	0.55	0.55	0.56	0.57	0.55
Ca	0.82	0.82	0.81	0.81	0.82	0.80	0.81	0.80	0.81	0.80
K	0.00	0.00	0.00	0.00	0.00	0.00	0.00	0.00	0.00	0.00
Na	0.18	0.18	0.18	0.19	0.19	0.20	0.19	0.21	0.19	0.20
Li	0.00	0.00	0.00	0.00	0.00	0.00	0.00	0.00	0.00	0.00
Zn	0.00	0.00	0.00	0.00	0.00	0.00	0.00	0.00	0.00	0.00
Ni	0.00	0.00	0.00	0.00	0.00	0.00	0.00	0.00	0.00	0.00
Cr	0.00	0.00	0.00	0.00	0.00	0.00	0.00	0.00	0.00	0.00
Sc	0.00	0.00	0.00	0.00	0.00	0.00	0.00	0.00	0.00	0.00
Total	4.00	4.00	4.00	4.00	4.00	4.00	4.00	4.00	4.00	4.00
J	0.36	0.37	0.36	0.39	0.38	0.39	0.39	0.41	0.38	0.39
Q	1.48	1.46	1.44	1.41	1.40	1.42	1.43	1.41	1.44	1.41
group	Quad	Ca-Na	Ca-Na	Ca-Na	Ca-Na	Ca-Na	Ca-Na	Ca-Na	Ca-Na	Ca-Na
adjective	luminian ferrian sodian				subsilicic					
pyroxene	wollastonite	omphacite	omphacite	omphacite	aegirine-augite	omphacite	omphacite	omphacite	aegirine-augite	omphacite
enstatite	35.32	----------	----------	----------	----------	----------	----------	----------	----------	----------
ferrosillite	14.56	----------	----------	----------	----------	----------	----------	----------	----------	----------
wollastonite	50.12	----------	----------	----------	----------	----------	----------	----------	----------	----------
jadeite	----------	10.60	11.24	12.11	10.24	11.84	11.50	12.11	10.06	11.40
aegirine	----------	9.45	8.81	9.37	10.92	9.82	9.93	10.48	10.80	10.35
Quad	----------	79.95	79.96	78.53	78.83	78.33	78.58	77.41	79.15	78.25

Appendix 6.D EMP data for pyroxene modified from PX-NOM (Sturm, R. 2002)

Sample	0910B 1.1+ cpx random	0910B 1.1+ cpx random	0910B 1.1+ cpx random	0910B 1.1+ cpx random	0910B 1.1+ cpx random	0910B 1.1+ cpx random	0910B 1.1+ cpx random	0910B 1.1+ cpx random	0910B 1.1+ cpx random
X	-19416.00	-19587.00	-19732.00	-19843.00	-19771.00	-19207.00	-19072.00	-18964.00	-18826.00
Y	-20954.00	-20915.00	-20975.00	-21056.00	-21332.00	-21511.00	-21761.00	-22031.00	-22121.00
Z	68.00	68.00	68.00	68.00	68.00	68.00	68.00	70.00	70.00
SiO2	48.25	48.04	47.97	47.93	48.23	48.31	49.92	48.92	48.29
TiO2	0.67	0.77	0.74	0.74	0.75	0.81	0.31	0.70	0.78
Al2O3	9.07	9.41	9.04	9.14	9.19	8.94	6.45	9.00	9.25
FeO	7.61	7.70	7.51	7.80	7.62	7.32	7.32	7.45	7.47
MnO	0.03	0.01	0.03	0.03	0.04	0.03	0.05	0.03	0.01
MgO	10.05	9.85	10.10	10.12	10.11	10.13	11.06	10.14	10.09
CaO	20.60	20.48	20.61	20.84	20.43	20.75	20.85	20.50	20.46
K2O	0.00	0.00	0.00	0.00	0.00	0.00	0.00	0.00	0.00
Na2O	2.55	2.63	2.56	2.54	2.61	2.55	2.43	2.56	2.64
Li2O									
ZnO									
NiO	0.00	0.01	0.02	0.04	0.08	0.04	0.04	0.02	0.00
Cr2O3	0.02	0.02	0.01	0.01	0.00	0.02	0.02	0.01	0.03
Sc2O3									
Total	98.85	98.93	98.59	99.18	99.06	98.90	98.46	99.34	99.01
Fe3+ model	Droop 1987	Droop 1987	Droop 1987	Droop 1987	Droop 1987	Droop 1987	Droop 1987	Droop 1987	Droop 1987
Si Calc	1.82	1.81	1.81	1.80	1.81	1.82	1.88	1.83	1.81
Ti Calc	0.02	0.02	0.02	0.02	0.02	0.02	0.01	0.02	0.02
Al Calc	0.40	0.42	0.40	0.40	0.41	0.40	0.29	0.40	0.41
Fe Calc	0.24	0.24	0.24	0.25	0.24	0.23	0.23	0.23	0.23
Mn Calc	0.00	0.00	0.00	0.00	0.00	0.00	0.00	0.00	0.00
Mg Calc	0.56	0.55	0.57	0.57	0.57	0.57	0.62	0.56	0.56
Ca Calc	0.83	0.83	0.83	0.84	0.82	0.84	0.84	0.82	0.82
K Calc	0.00	0.00	0.00	0.00	0.00	0.00	0.00	0.00	0.00
Na Calc	0.19	0.19	0.19	0.18	0.19	0.19	0.18	0.19	0.19
Li Calc									
Zn Calc									
Ni Calc	0.00	0.00	0.00	0.00	0.00	0.00	0.00	0.00	0.00
Cr Calc	0.00	0.00	0.00	0.00	0.00	0.00	0.00	0.00	0.00
Sc Calc									
Fe 3+ Droop	0.17	0.17	0.18	0.20	0.18	0.17	0.16	0.14	0.17
Total Calc	4.06	4.06	4.06	4.07	4.06	4.06	4.05	4.05	4.06
Si	1.79	1.78	1.78	1.77	1.78	1.79	1.86	1.81	1.79
Ti	0.02	0.02	0.02	0.02	0.02	0.02	0.01	0.02	0.02
Al (T)	0.21	0.22	0.22	0.23	0.22	0.21	0.14	0.19	0.21
Al (M1)	0.19	0.19	0.18	0.17	0.18	0.18	0.14	0.20	0.19
Fe3+ (T)	0.00	0.00	0.00	0.00	0.00	0.00	0.00	0.00	0.00
Fe3+ (M1)	0.17	0.17	0.18	0.20	0.18	0.17	0.16	0.14	0.17
Fe2+	0.07	0.07	0.05	0.04	0.06	0.06	0.07	0.09	0.06
Mn	0.00	0.00	0.00	0.00	0.00	0.00	0.00	0.00	0.00
Mg	0.56	0.54	0.56	0.56	0.56	0.56	0.61	0.56	0.56
Ca	0.82	0.81	0.82	0.83	0.81	0.82	0.83	0.81	0.81
K	0.00	0.00	0.00	0.00	0.00	0.00	0.00	0.00	0.00
Na	0.18	0.19	0.18	0.18	0.19	0.18	0.18	0.18	0.19
Li	0.00	0.00	0.00	0.00	0.00	0.00	0.00	0.00	0.00
Zn	0.00	0.00	0.00	0.00	0.00	0.00	0.00	0.00	0.00
Ni	0.00	0.00	0.00	0.00	0.00	0.00	0.00	0.00	0.00
Cr	0.00	0.00	0.00	0.00	0.00	0.00	0.00	0.00	0.00
Sc	0.00	0.00	0.00	0.00	0.00	0.00	0.00	0.00	0.00
Total	4.00	4.00	4.00	4.00	4.00	4.00	4.00	4.00	4.00
J	0.37	0.38	0.37	0.36	0.37	0.37	0.35	0.37	0.38
Q	1.44	1.42	1.43	1.43	1.43	1.44	1.51	1.46	1.43
group	Ca-Na	Ca-Na	Ca-Na	Ca-Na	Ca-Na	Ca-Na	Quad	Ca-Na	Ca-Na
adjective							aluminian ferrian sodian		
pyroxene	omphacite	omphacite	aegirine-augite	aegirine-augite	omphacite	omphacite	diopside	omphacite	omphacite
enstatite	----------	----------	----------	----------	----------	----------	36.66	----------	----------
ferrosillite	----------	----------	----------	----------	----------	----------	13.69	----------	----------
wollastonite	----------	----------	----------	----------	----------	----------	49.65	----------	----------
jadeite	10.63	11.04	10.20	9.41	10.64	10.55	----------	11.69	11.06
aegirine	9.66	9.93	10.27	10.89	10.17	9.70	----------	8.40	9.88
Quad	79.71	79.03	79.53	79.70	79.18	79.75	----------	79.91	79.06

Appendix 6.D EMP data for pyroxene modified from PX-NOM (Sturm, R. 2002)

Sample	0910B 1.1+ cpx random	0910B 1.1+ cpx random	0910B 1.1+ cpx random	0910B 1.1+ cpx random	0910B 1.1+ cpx random	0910B 1.1+ cpx random	0910B 1.1+ cpx random	0910B 1.1+ cpx random	0910B 1.1+ cpx random
X	-19150.00	-19424.00	-19428.00	-19556.00	-19371.00	-19976.00	-19976.00	-19747.00	-19933.00
Y	-22313.00	-22336.00	-22415.00	-22539.00	-22658.00	-20585.00	-20514.00	-20379.00	-20341.00
Z	70.00	70.00	70.00	70.00	70.00	70.00	70.00	70.00	70.00
SiO2	48.37	40.06	48.14	48.34	48.34	49.02	49.00	48.46	49.32
TiO2	0.82	1.42	0.77	0.65	0.80	0.79	0.85	0.85	0.72
Al2O3	9.79	16.63	9.89	9.59	9.75	8.78	8.97	9.20	8.58
FeO	7.54	12.89	7.70	7.56	7.50	7.49	7.45	7.45	7.53
MnO	0.02	0.05	0.03	0.02	0.04	0.00	0.01	0.05	0.03
MgO	9.90	10.77	9.61	9.74	9.79	10.18	10.13	10.07	10.40
CaO	20.56	11.68	20.63	20.43	20.39	20.56	20.58	20.58	20.66
K2O	0.00	0.43	0.00	0.00	0.00	0.00	0.00	0.00	0.00
Na2O	2.51	3.04	2.53	2.60	2.67	2.68	2.61	2.65	2.67
Li2O									
ZnO									
NiO	0.00	0.09	0.00	0.00	0.02	0.04	0.00	0.03	0.00
Cr2O3	0.02	0.04	0.02	0.02	0.01	0.01	0.01	0.00	0.00
Sc2O3									
Total	99.53	97.09	99.33	98.97	99.30	99.54	99.60	99.33	99.91
Fe3+ model	Droop 1987	Droop 1987	Droop 1987	Droop 1987	Droop 1987	Droop 1987	Droop 1987	Droop 1987	Droop 1987
Si Calc	1.80	1.56	1.80	1.81	1.81	1.83	1.83	1.81	1.83
Ti Calc	0.02	0.04	0.02	0.02	0.02	0.02	0.02	0.02	0.02
Al Calc	0.43	0.76	0.44	0.42	0.43	0.39	0.39	0.41	0.38
Fe Calc	0.24	0.42	0.24	0.24	0.23	0.23	0.23	0.23	0.23
Mn Calc	0.00	0.00	0.00	0.00	0.00	0.00	0.00	0.00	0.00
Mg Calc	0.55	0.62	0.54	0.54	0.55	0.57	0.56	0.56	0.58
Ca Calc	0.82	0.49	0.83	0.82	0.82	0.82	0.82	0.82	0.82
K Calc	0.00	0.02	0.00	0.00	0.00	0.00	0.00	0.00	0.00
Na Calc	0.18	0.23	0.18	0.19	0.19	0.19	0.19	0.19	0.19
Li Calc									
Zn Calc									
Ni Calc	0.00	0.00	0.00	0.00	0.00	0.00	0.00	0.00	0.00
Cr Calc	0.00	0.00	0.00	0.00	0.00	0.00	0.00	0.00	0.00
Sc Calc									
Fe 3+ Droop	0.14	0.42	0.15	0.15	0.15	0.16	0.14	0.17	0.16
Total Calc	4.05	4.14	4.05	4.05	4.05	4.05	4.05	4.06	4.06
Si	1.78	1.50	1.78	1.79	1.78	1.80	1.80	1.79	1.81
Ti	0.02	0.04	0.02	0.02	0.02	0.02	0.02	0.02	0.02
Al (T)	0.22	0.50	0.22	0.21	0.22	0.20	0.20	0.21	0.19
Al (M1)	0.21	0.24	0.21	0.21	0.21	0.19	0.19	0.19	0.18
Fe3+ (T)	0.00	0.00	0.00	0.00	0.00	0.00	0.00	0.00	0.00
Fe3+ (M1)	0.14	0.42	0.15	0.15	0.15	0.16	0.14	0.17	0.16
Fe2+	0.09	0.00	0.09	0.09	0.08	0.07	0.09	0.06	0.07
Mn	0.00	0.00	0.00	0.00	0.00	0.00	0.00	0.00	0.00
Mg	0.54	0.60	0.53	0.54	0.54	0.56	0.56	0.55	0.57
Ca	0.81	0.47	0.82	0.81	0.81	0.81	0.81	0.81	0.81
K	0.00	0.02	0.00	0.00	0.00	0.00	0.00	0.00	0.00
Na	0.18	0.22	0.18	0.19	0.19	0.19	0.19	0.19	0.19
Li	0.00	0.00	0.00	0.00	0.00	0.00	0.00	0.00	0.00
Zn	0.00	0.00	0.00	0.00	0.00	0.00	0.00	0.00	0.00
Ni	0.00	0.00	0.00	0.00	0.00	0.00	0.00	0.00	0.00
Cr	0.00	0.00	0.00	0.00	0.00	0.00	0.00	0.00	0.00
Sc	0.00	0.00	0.00	0.00	0.00	0.00	0.00	0.00	0.00
Total	4.00	4.01	4.00	4.00	4.00	4.00	4.00	4.00	4.00
J	0.36	0.44	0.36	0.37	0.38	0.38	0.37	0.38	0.38
Q	1.45	1.07	1.44	1.44	1.42	1.44	1.46	1.43	1.45
group	Quad	Ca-Na	Ca-Na	Ca-Na	Ca-Na	Ca-Na	Ca-Na	Ca-Na	Ca-Na
adjective	luminian ferrian sodian	subsilicic							
pyroxene	wollastonite	aegirine-augite	omphacite	omphacite	omphacite	omphacite	omphacite	omphacite	omphacite
enstatite	34.24	----------	----------	----------	----------	----------	----------	----------	----------
ferrosillite	14.67	----------	----------	----------	----------	----------	----------	----------	----------
wollastonite	51.09	----------	----------	----------	----------	----------	----------	----------	----------
jadeite	----------	10.57	11.86	12.12	12.18	11.33	11.73	11.08	10.86
aegirine	----------	18.62	8.30	8.51	8.97	9.62	8.63	9.86	9.92
Quad	----------	70.81	79.84	79.37	78.85	79.05	79.64	79.06	79.23

Appendix 6.D EMP data for pyroxene modified from PX-NOM (Sturm, R. 2002)

Sample	0910B 1.1+ cpx random	0910B 1.1+ cpx random	0910B 1.1+ cpx random	0910B 1.1+ cpx random	0910B 1.1+ cpx random	0910B 1.1+ cpx random	0910B 1.1+ cpx random	0910B 1.1+ cpx random
X	-20084.00	-20168.00	-20168.00	-19963.00	-20024.00	-20072.00	-20049.00	-19908.00
Y	-20356.00	-20311.00	-20145.00	-20145.00	-20133.00	-20114.00	-20022.00	-20021.00
Z	70.00	70.00	70.00	70.00	70.00	70.00	70.00	70.00
SiO2	50.31	50.12	49.00	50.77	50.80	50.49	50.24	50.24
TiO2	0.33	0.52	0.69	0.28	0.27	0.36	0.35	0.49
Al2O3	6.66	7.28	7.99	6.33	6.07	6.42	6.66	7.48
FeO	7.35	7.33	7.98	7.19	7.33	7.67	7.62	7.55
MnO	0.02	0.06	0.06	0.05	0.02	0.05	0.03	0.03
MgO	10.91	10.88	10.80	11.28	11.42	11.24	11.08	10.76
CaO	20.93	20.85	21.03	21.03	20.99	21.18	21.00	20.62
K2O	0.01	0.00	0.00	0.00	0.00	0.00	0.00	0.00
Na2O	2.48	2.44	2.19	2.48	2.31	2.29	2.38	2.50
Li2O								
ZnO								
NiO	0.02	0.00	0.07	0.02	0.02	0.00	0.00	0.05
Cr2O3	0.00	0.01	0.02	0.01	0.02	0.00	0.01	0.00
Sc2O3								
Total	99.03	99.49	99.82	99.45	99.24	99.71	99.38	99.72
Fe3+ model	Droop 1987	Droop 1987	Droop 1987	Droop 1987	Droop 1987	Droop 1987	Droop 1987	Droop 1987
Si Calc	1.88	1.87	1.83	1.89	1.90	1.88	1.88	1.87
Ti Calc	0.01	0.01	0.02	0.01	0.01	0.01	0.01	0.01
Al Calc	0.29	0.32	0.35	0.28	0.27	0.28	0.29	0.33
Fe Calc	0.23	0.23	0.25	0.22	0.23	0.24	0.24	0.23
Mn Calc	0.00	0.00	0.00	0.00	0.00	0.00	0.00	0.00
Mg Calc	0.61	0.60	0.60	0.63	0.64	0.62	0.62	0.60
Ca Calc	0.84	0.83	0.84	0.84	0.84	0.85	0.84	0.82
K Calc	0.00	0.00	0.00	0.00	0.00	0.00	0.00	0.00
Na Calc	0.18	0.18	0.16	0.18	0.17	0.17	0.17	0.18
Li Calc								
Zn Calc								
Ni Calc	0.00	0.00	0.00	0.00	0.00	0.00	0.00	0.00
Cr Calc	0.00	0.00	0.00	0.00	0.00	0.00	0.00	0.00
Sc Calc								
Fe 3+ Droop	0.15	0.14	0.16	0.15	0.13	0.15	0.15	0.13
Total Calc	4.05	4.05	4.05	4.05	4.05	4.05	4.05	4.04
Si	1.86	1.85	1.80	1.87	1.88	1.86	1.85	1.85
Ti	0.01	0.01	0.02	0.01	0.01	0.01	0.01	0.01
Al (T)	0.14	0.15	0.20	0.13	0.12	0.14	0.15	0.15
Al (M1)	0.15	0.16	0.15	0.14	0.14	0.14	0.14	0.17
Fe3+ (T)	0.00	0.00	0.00	0.00	0.00	0.00	0.00	0.00
Fe3+ (M1)	0.15	0.14	0.16	0.15	0.13	0.15	0.15	0.13
Fe2+	0.08	0.09	0.08	0.07	0.09	0.09	0.08	0.10
Mn	0.00	0.00	0.00	0.00	0.00	0.00	0.00	0.00
Mg	0.60	0.60	0.59	0.62	0.63	0.62	0.61	0.59
Ca	0.83	0.82	0.83	0.83	0.83	0.84	0.83	0.81
K	0.00	0.00	0.00	0.00	0.00	0.00	0.00	0.00
Na	0.18	0.17	0.16	0.18	0.17	0.16	0.17	0.18
Li	0.00	0.00	0.00	0.00	0.00	0.00	0.00	0.00
Zn	0.00	0.00	0.00	0.00	0.00	0.00	0.00	0.00
Ni	0.00	0.00	0.00	0.00	0.00	0.00	0.00	0.00
Cr	0.00	0.00	0.00	0.00	0.00	0.00	0.00	0.00
Sc	0.00	0.00	0.00	0.00	0.00	0.00	0.00	0.00
Total	4.00	4.00	4.00	4.00	4.00	4.00	4.00	4.00
J	0.36	0.35	0.31	0.35	0.33	0.33	0.34	0.36
Q	1.51	1.51	1.51	1.52	1.55	1.54	1.52	1.50
group	Quad	Quad	Quad	Quad	Quad	Quad	Quad	Quad
adjective	aluminian ferrian sodian	aluminian ferrian sodian	aluminian ferrian sodian	aluminian ferrian sodian	aluminian ferrian sodian	aluminian ferrian sodian	aluminian ferrian sodian	aluminian ferrian sodian
pyroxene	diopside	diopside	diopside	diopside	diopside	diopside	diopside	diopside
enstatite	36.27	36.26	35.50	37.04	37.27	36.51	36.37	36.07
ferrosillite	13.75	13.81	14.83	13.34	13.46	14.06	14.10	14.25
wollastonite	49.98	49.92	49.68	49.62	49.26	49.43	49.54	49.67
jadeite	----------	----------	----------	----------	----------	----------	----------	----------
aegirine	----------	----------	----------	----------	----------	----------	----------	----------
Quad	----------	----------	----------	----------	----------	----------	----------	----------

Appendix 6.D EMP data for pyroxene modified from PX-NOM (Sturm, R. 2002)

Sample	0910B 1.1+ cpx random	0910B 1.1+ cpx random	0910B 1.1+ cpx random	0910B 1.1+ cpx random	0910B 1.1+ cpx random	0910B 1.1+ cpx random	0910B 1.1+ cpx random
X	-19888.00	-19637.00	-19408.00	-19394.00	-19467.00	-19485.00	-19272.00
Y	-19939.00	-19933.00	-19877.00	-19763.00	-19624.00	-19552.00	-19394.00
Z	70.00	70.00	70.00	70.00	70.00	70.00	70.00
SiO2	49.82	49.59	49.29	49.21	49.68	49.28	49.15
TiO2	0.56	0.60	0.66	0.69	0.52	0.59	0.66
Al2O3	7.10	7.81	8.73	8.63	7.75	8.25	9.03
FeO	7.67	7.57	7.36	7.72	7.54	7.61	7.49
MnO	0.05	0.04	0.02	0.02	0.01	0.06	0.04
MgO	10.95	10.53	10.18	10.32	10.69	10.42	10.04
CaO	21.11	20.87	20.26	20.69	20.74	20.48	20.58
K2O	0.01	0.00	0.00	0.00	0.01	0.00	0.00
Na2O	2.24	2.52	2.64	2.51	2.55	2.61	2.48
Li2O							
ZnO							
NiO	0.03	0.04	0.00	0.01	0.07	0.00	0.04
Cr2O3	0.04	0.02	0.05	0.00	0.04	0.00	0.06
Sc2O3							
Total	99.58	99.59	99.19	99.81	99.60	99.29	99.56
Fe3+ model	Droop 1987	Droop 1987	Droop 1987	Droop 1987	Droop 1987	Droop 1987	Droop 1987
Si Calc	1.86	1.85	1.84	1.83	1.85	1.84	1.83
Ti Calc	0.02	0.02	0.02	0.02	0.01	0.02	0.02
Al Calc	0.31	0.34	0.38	0.38	0.34	0.36	0.40
Fe Calc	0.24	0.24	0.23	0.24	0.24	0.24	0.23
Mn Calc	0.00	0.00	0.00	0.00	0.00	0.00	0.00
Mg Calc	0.61	0.59	0.57	0.57	0.59	0.58	0.56
Ca Calc	0.84	0.83	0.81	0.83	0.83	0.82	0.82
K Calc	0.00	0.00	0.00	0.00	0.00	0.00	0.00
Na Calc	0.16	0.18	0.19	0.18	0.18	0.19	0.18
Li Calc							
Zn Calc							
Ni Calc	0.00	0.00	0.00	0.00	0.00	0.00	0.00
Cr Calc	0.00	0.00	0.00	0.00	0.00	0.00	0.00
Sc Calc							
Fe 3+ Droop	0.14	0.15	0.13	0.15	0.16	0.16	0.12
Total Calc	4.05	4.05	4.04	4.05	4.05	4.05	4.04
Si	1.84	1.83	1.82	1.81	1.83	1.82	1.81
Ti	0.02	0.02	0.02	0.02	0.01	0.02	0.02
Al (T)	0.16	0.17	0.18	0.19	0.17	0.18	0.19
Al (M1)	0.15	0.17	0.20	0.18	0.16	0.18	0.20
Fe3+ (T)	0.00	0.00	0.00	0.00	0.00	0.00	0.00
Fe3+ (M1)	0.14	0.15	0.13	0.15	0.16	0.16	0.12
Fe2+	0.09	0.08	0.10	0.09	0.07	0.08	0.11
Mn	0.00	0.00	0.00	0.00	0.00	0.00	0.00
Mg	0.60	0.58	0.56	0.57	0.59	0.57	0.55
Ca	0.83	0.82	0.80	0.81	0.82	0.81	0.81
K	0.00	0.00	0.00	0.00	0.00	0.00	0.00
Na	0.16	0.18	0.19	0.18	0.18	0.19	0.18
Li	0.00	0.00	0.00	0.00	0.00	0.00	0.00
Zn	0.00	0.00	0.00	0.00	0.00	0.00	0.00
Ni	0.00	0.00	0.00	0.00	0.00	0.00	0.00
Cr	0.00	0.00	0.00	0.00	0.00	0.00	0.00
Sc	0.00	0.00	0.00	0.00	0.00	0.00	0.00
Total	4.00	4.00	4.00	4.00	4.00	4.00	4.00
J	0.32	0.36	0.38	0.36	0.36	0.37	0.35
Q	1.53	1.48	1.46	1.47	1.48	1.46	1.47
group	Quad	Quad	Ca-Na	Quad	Quad	Ca-Na	Quad
adjective	aluminian ferrian sodian	aluminian ferrian sodian		aluminian ferrian sodian	aluminian ferrian sodian		aluminian ferrian sodian
pyroxene	diopside	wollastonite	omphacite	wollastonite	diopside	omphacite	wollastonite
enstatite	35.95	35.34	----------	34.94	35.85	----------	34.57
ferrosillite	14.21	14.33	----------	14.70	14.19	----------	14.52
wollastonite	49.84	50.33	----------	50.36	49.96	----------	50.91
jadeite	----------	----------	12.50	----------	----------	10.78	----------
aegirine	----------	----------	8.10	----------	----------	9.61	----------
Quad	----------	----------	79.40	----------	----------	79.60	----------

Appendix 6.D EMP data for pyroxene modified from PX-NOM (Sturm, R. 2002)

Sample	0905B 1.4 cpx r	0905B 1.5 cpx c	0905B 1.6 cpx r	0905B 1.9 cpx c	0905B 2.3 cpx	0905B 2.4 cpx	0905B 2.5 cpx	0905B 2.8 cpx c	0905B random	0905B random
X	5659.00	5497.00	6032.00	3454.00	11975.00	12382.00	12476.00	14430.00	12396.00	12454.00
Y	14504.00	14457.00	12702.00	10266.00	12668.00	12668.00	12599.00	10674.00	24386.00	24428.00
Z	57.00	57.00	60.00	60.00	65.00	65.00	65.00	65.00	57.00	57.00
SiO2	51.03	51.57	50.48	52.23	51.88	51.52	51.77	51.90	51.19	51.65
TiO2	0.66	0.69	0.43	0.48	0.53	0.67	0.54	0.64	0.05	0.38
Al2O3	12.44	10.00	10.16	7.32	10.67	9.09	11.11	9.49	2.92	10.00
FeO	7.59	8.11	8.42	8.36	7.00	8.79	7.51	8.24	6.53	6.41
MnO	0.01	0.04	0.08	0.06	0.04	0.03	0.04	0.02	0.06	0.07
MgO	7.80	8.65	10.04	9.87	9.05	8.86	8.45	8.56	13.36	10.32
CaO	16.08	16.70	17.81	17.74	16.89	16.82	16.32	16.61	22.34	18.66
K2O	0.01	0.02	0.03	0.01	0.00	0.00	0.01	0.00	0.03	0.11
Na2O	4.50	4.27	2.74	3.79	4.09	4.41	4.52	4.49	0.78	2.48
Li2O										
ZnO										
NiO	0.00	0.00	0.01	0.03	0.02	0.02	0.02	0.01	0.00	0.02
Cr2O3	0.01	0.00	0.00	0.02	0.04	0.04	0.01	0.04	0.01	0.00
Sc2O3										
Total	100.12	100.06	100.19	99.90	100.23	100.26	100.29	99.99	97.27	100.10
Fe3+ model	Droop 1987	Droop 1987	Droop 1987	Droop 1987	Droop 1987	Droop 1987	Droop 1987	Droop 1987	Droop 1987	Droop 1987
Si Calc	1.86	1.89	1.85	1.93	1.89	1.90	1.88	1.91	1.95	1.88
Ti Calc	0.02	0.02	0.01	0.01	0.01	0.02	0.01	0.02	0.00	0.01
Al Calc	0.53	0.43	0.44	0.32	0.46	0.39	0.48	0.41	0.13	0.43
Fe Calc	0.23	0.25	0.26	0.26	0.21	0.27	0.23	0.25	0.21	0.20
Mn Calc	0.00	0.00	0.00	0.00	0.00	0.00	0.00	0.00	0.00	0.00
Mg Calc	0.42	0.47	0.55	0.54	0.49	0.49	0.46	0.47	0.76	0.56
Ca Calc	0.63	0.66	0.70	0.70	0.66	0.66	0.64	0.65	0.91	0.73
K Calc	0.00	0.00	0.00	0.00	0.00	0.00	0.00	0.00	0.00	0.01
Na Calc	0.32	0.30	0.20	0.27	0.29	0.31	0.32	0.32	0.06	0.17
Li Calc										
Zn Calc										
Ni Calc	0.00	0.00	0.00	0.00	0.00	0.00	0.00	0.00	0.00	0.00
Cr Calc	0.00	0.00	0.00	0.00	0.00	0.00	0.00	0.00	0.00	0.00
Sc Calc										
Fe 3+ Droop	0.04	0.08	0.04	0.11	0.04	0.13	0.06	0.09	0.05	0.00
Total Calc	4.01	4.03	4.01	4.04	4.01	4.05	4.02	4.03	4.02	3.99
Si	1.85	1.88	1.85	1.91	1.88	1.87	1.87	1.89	1.94	1.89
Ti	0.02	0.02	0.01	0.01	0.01	0.02	0.01	0.02	0.00	0.01
Al (T)	0.15	0.12	0.15	0.09	0.12	0.13	0.13	0.11	0.06	0.11
Al (M1)	0.39	0.31	0.29	0.23	0.34	0.26	0.35	0.30	0.07	0.32
Fe3+ (T)	0.00	0.00	0.00	0.00	0.00	0.00	0.00	0.00	0.00	0.00
Fe3+ (M1)	0.04	0.08	0.04	0.11	0.04	0.13	0.06	0.09	0.05	0.00
Fe2+	0.19	0.17	0.22	0.15	0.17	0.13	0.16	0.16	0.16	0.20
Mn	0.00	0.00	0.00	0.00	0.00	0.00	0.00	0.00	0.00	0.00
Mg	0.42	0.47	0.55	0.54	0.49	0.48	0.46	0.47	0.75	0.56
Ca	0.63	0.65	0.70	0.70	0.66	0.66	0.63	0.65	0.91	0.73
K	0.00	0.00	0.00	0.00	0.00	0.00	0.00	0.00	0.00	0.01
Na	0.32	0.30	0.19	0.27	0.29	0.31	0.32	0.32	0.06	0.18
Li	0.00	0.00	0.00	0.00	0.00	0.00	0.00	0.00	0.00	0.00
Zn	0.00	0.00	0.00	0.00	0.00	0.00	0.00	0.00	0.00	0.00
Ni	0.00	0.00	0.00	0.00	0.00	0.00	0.00	0.00	0.00	0.00
Cr	0.00	0.00	0.00	0.00	0.00	0.00	0.00	0.00	0.00	0.00
Sc	0.00	0.00	0.00	0.00	0.00	0.00	0.00	0.00	0.00	0.00
Total	4.00	4.00	4.00	4.00	4.00	4.00	4.00	4.00	4.00	4.00
J	0.63	0.60	0.39	0.54	0.58	0.62	0.63	0.63	0.11	0.35
Q	1.24	1.29	1.47	1.38	1.32	1.27	1.25	1.27	1.82	1.49
group	Ca-Na	Ca-Na	Ca-Na	Ca-Na	Ca-Na	Ca-Na	Ca-Na	Ca-Na	Quad	Quad
adjective									aluminian	aluminian sodian
pyroxene	omphacite	omphacite	omphacite	omphacite	omphacite	omphacite	omphacite	omphacite	diopside	diopside
enstatite	----------	----------	----------	----------	----------	----------	----------	----------	40.34	37.70
ferrosillite	----------	----------	----------	----------	----------	----------	----------	----------	11.16	13.29
wollastonite	----------	----------	----------	----------	----------	----------	----------	----------	48.50	49.01
jadeite	30.58	25.45	18.50	19.00	27.22	21.76	28.41	25.49	----------	----------
aegirine	3.30	6.42	2.48	9.00	3.15	11.12	5.20	7.74	----------	----------
Quad	66.12	68.13	79.02	71.99	69.63	67.12	66.39	66.77	----------	----------

Appendix 6.D EMP data for pyroxene modified from PX-NOM (Sturm, R. 2002)

Sample	0906B 1.3 opx c	0906B 1.4 opx r	0906B 1.5 opx r	0906B 1.6 opx c	0906B 1.7 opx r	0906B 1.8 opx r	0906B 1.9 opx r	0906B 1.10 opx c	0906B 1.11 opx c	0906B 1.12 opx r	0906B 1.24 cpx c	0906B 1.25 cpx r	0906B 1.27 cpx r
X	-13526.00	-13592.00	-13631.00	-14130.00	-14611.00	-13932.00	-13894.00	-13397.00	-13251.00	-12786.00	-14555.00	-14555.00	-13370.00
Y	25666.00	25461.00	25878.00	26348.00	26267.00	26276.00	26269.00	26626.00	27823.00	27774.00	27666.00	27566.00	28449.00
Z	60.00	60.00	60.00	57.00	55.00	55.00	55.00	55.00	55.00	55.00	54.00	54.00	54.00
SiO2	51.32	52.63	52.62	51.46	52.29	51.58	52.04	50.18	51.63	52.04	51.92	52.52	51.90
TiO2	0.64	0.32	0.40	0.61	0.22	0.46	0.46	0.85	0.58	0.47	0.59	0.41	0.46
Al2O3	7.75	5.74	6.63	7.49	5.62	7.09	7.15	9.04	7.34	6.57	7.11	6.05	6.36
FeO	7.44	6.41	7.07	7.50	7.00	7.19	7.21	7.60	7.60	7.03	7.40	6.61	7.23
MnO	0.02	0.06	0.06	0.00	0.04	0.04	0.04	0.03	0.03	0.02	0.01	0.04	0.04
MgO	10.61	12.42	11.27	10.71	12.23	11.02	11.07	10.37	10.76	11.58	10.99	12.10	11.54
CaO	19.46	20.70	19.49	19.37	21.01	19.71	19.78	19.04	19.41	20.23	19.44	20.51	20.30
K2O	0.00	0.00	0.01	0.00	0.00	0.01	0.00	0.00	0.01	0.00	0.00	0.00	0.00
Na2O	2.92	2.29	2.92	2.90	2.16	2.83	2.80	2.99	2.92	2.53	2.87	2.41	2.48
Li2O													
ZnO													
NiO	0.04	0.04	0.01	0.04	0.03	0.00	0.04	0.02	0.03	0.04	0.03	0.06	0.01
Cr2O3	0.02	0.01	0.06	0.03	0.02	0.03	0.01	0.04	0.01	0.05	0.03	0.02	0.02
Sc2O3													
Total	100.21	100.64	100.53	100.10	100.62	99.98	100.61	100.16	100.33	100.55	100.40	100.73	100.35
Fe3+ model	Droop 1987	Droop 1987	Droop 1987	Droop 1987	Droop 1987	Droop 1987	Droop 1987	Droop 1987	Droop 1987	Droop 1987	Droop 1987	Droop 1987	Droop 1987
Si Calc	1.89	1.92	1.92	1.90	1.92	1.90	1.90	1.85	1.90	1.91	1.90	1.92	1.91
Ti Calc	0.02	0.01	0.01	0.02	0.01	0.01	0.01	0.02	0.02	0.01	0.02	0.01	0.01
Al Calc	0.34	0.25	0.29	0.33	0.24	0.31	0.31	0.39	0.32	0.28	0.31	0.26	0.28
Fe Calc	0.23	0.20	0.22	0.23	0.21	0.22	0.22	0.23	0.23	0.22	0.23	0.20	0.22
Mn Calc	0.00	0.00	0.00	0.00	0.00	0.00	0.00	0.00	0.00	0.00	0.00	0.00	0.00
Mg Calc	0.58	0.68	0.61	0.59	0.67	0.61	0.60	0.57	0.59	0.63	0.60	0.66	0.63
Ca Calc	0.77	0.81	0.76	0.76	0.83	0.78	0.78	0.75	0.76	0.79	0.76	0.80	0.80
K Calc	0.00	0.00	0.00	0.00	0.00	0.00	0.00	0.00	0.00	0.00	0.00	0.00	0.00
Na Calc	0.21	0.16	0.21	0.21	0.15	0.20	0.20	0.21	0.21	0.18	0.20	0.17	0.18
Li Calc													
Zn Calc													
Ni Calc	0.00	0.00	0.00	0.00	0.00	0.00	0.00	0.00	0.00	0.00	0.00	0.00	0.00
Cr Calc	0.00	0.00	0.00	0.00	0.00	0.00	0.00	0.00	0.00	0.00	0.00	0.00	0.00
Sc Calc													
Fe 3+ Droop	0.09	0.08	0.07	0.09	0.09	0.10	0.08	0.11	0.09	0.08	0.08	0.08	0.09
Total Calc	4.03	4.03	4.03	4.03	4.03	4.03	4.03	4.04	4.03	4.03	4.03	4.03	4.03
Si	1.87	1.91	1.91	1.88	1.90	1.89	1.89	1.83	1.88	1.89	1.89	1.91	1.89
Ti	0.02	0.01	0.01	0.02	0.01	0.01	0.01	0.02	0.02	0.01	0.02	0.01	0.01
Al (T)	0.13	0.09	0.09	0.12	0.10	0.11	0.11	0.17	0.12	0.11	0.11	0.09	0.11
Al (M1)	0.21	0.16	0.20	0.20	0.14	0.19	0.20	0.22	0.20	0.18	0.20	0.16	0.17
Fe3+ (T)	0.00	0.00	0.00	0.00	0.00	0.00	0.00	0.00	0.00	0.00	0.00	0.00	0.00
Fe3+ (M1)	0.09	0.08	0.07	0.09	0.09	0.10	0.08	0.11	0.09	0.08	0.08	0.08	0.09
Fe2+	0.14	0.12	0.14	0.14	0.12	0.12	0.14	0.12	0.14	0.13	0.15	0.12	0.13
Mn	0.00	0.00	0.00	0.00	0.00	0.00	0.00	0.00	0.00	0.00	0.00	0.00	0.00
Mg	0.58	0.67	0.61	0.58	0.66	0.60	0.60	0.56	0.59	0.63	0.60	0.65	0.63
Ca	0.76	0.80	0.76	0.76	0.82	0.77	0.77	0.74	0.76	0.79	0.76	0.80	0.79
K	0.00	0.00	0.00	0.00	0.00	0.00	0.00	0.00	0.00	0.00	0.00	0.00	0.00
Na	0.21	0.16	0.21	0.21	0.15	0.20	0.20	0.21	0.21	0.18	0.20	0.17	0.18
Li	0.00	0.00	0.00	0.00	0.00	0.00	0.00	0.00	0.00	0.00	0.00	0.00	0.00
Zn	0.00	0.00	0.00	0.00	0.00	0.00	0.00	0.00	0.00	0.00	0.00	0.00	0.00
Ni	0.00	0.00	0.00	0.00	0.00	0.00	0.00	0.00	0.00	0.00	0.00	0.00	0.00
Cr	0.00	0.00	0.00	0.00	0.00	0.00	0.00	0.00	0.00	0.00	0.00	0.00	0.00
Sc	0.00	0.00	0.00	0.00	0.00	0.00	0.00	0.00	0.00	0.00	0.00	0.00	0.00
Total	4.00	4.00	4.00	4.00	4.00	4.00	4.00	4.00	4.00	4.00	4.00	4.00	4.00
J	0.41	0.32	0.41	0.41	0.30	0.40	0.39	0.42	0.41	0.36	0.41	0.34	0.35
Q	1.48	1.59	1.51	1.49	1.60	1.49	1.51	1.43	1.48	1.55	1.50	1.57	1.55
group	Ca-Na	Quad	Ca-Na	Ca-Na	Quad	Ca-Na	Ca-Na	Ca-Na	Ca-Na	Quad	Ca-Na	Quad	Quad
adjective		aluminian sodian			aluminian sodian					aluminian sodian		aluminian sodian	aluminian sodian
pyroxene	omphacite	diopside	omphacite	omphacite	diopside	omphacite	omphacite	omphacite	omphacite	diopside	omphacite	diopside	diopside
enstatite	----------	40.16	----------	----------	39.09	----------	----------	----------	----------	38.52	----------	39.57	38.19
ferrosillite	----------	11.75	----------	----------	12.64	----------	----------	----------	----------	13.15	----------	12.20	13.50
wollastonite	----------	48.09	----------	----------	48.28	----------	----------	----------	----------	48.34	----------	48.22	48.30
jadeite	15.27	----------	15.48	15.28	----------	13.99	14.64	15.21	14.91	----------	15.15	----------	----------
aegirine	6.59	----------	5.92	6.37	----------	7.19	6.13	7.66	6.88	----------	6.13	----------	----------
Quad	78.14	----------	78.60	78.35	----------	78.82	79.23	77.13	78.21	----------	78.72	----------	----------

Appendix 6.D EMP data for pyroxene modified from PX-NOM (Sturm, R. 2002)

Sample	0906B random	0906B random	0906B random	0906B random	0906B random	0906B random	0906B random	0906B random
X	-9094.00	-9027.00	-9029.00	-8946.00	-8946.00	-8946.00	-8946.00	-8948.00
Y	25955.00	21229.00	20071.00	19054.00	18499.00	17961.00	17581.00	16642.00
Z	57.00	62.00	66.00	66.00	66.00	66.00	66.00	66.00
SiO2	51.18	51.85	51.71	52.20	51.17	50.27	51.03	50.90
TiO2	0.64	0.36	0.42	0.46	0.58	0.80	0.64	0.61
Al2O3	7.54	5.89	6.26	6.16	7.28	8.67	8.17	8.00
FeO	7.53	6.35	7.16	6.86	7.32	7.46	7.23	7.14
MnO	0.03	0.03	0.06	0.08	0.06	0.00	0.00	0.01
MgO	10.93	12.15	11.73	11.86	10.94	10.24	10.51	10.68
CaO	19.47	20.61	20.74	20.21	19.56	19.52	19.42	19.54
K2O	0.00	0.00	0.01	0.01	0.00	0.01	0.00	0.02
Na2O	2.95	2.37	2.31	2.57	2.89	2.97	2.93	2.88
Li2O								
ZnO								
NiO	0.04	0.05	0.01	0.03	0.04	0.00	0.03	0.00
Cr2O3	0.01	0.01	0.00	0.05	0.02	0.00	0.02	0.03
Sc2O3								
Total	100.32	99.69	100.42	100.49	99.85	99.95	99.98	99.82
Fe3+ model	Droop 1987	Droop 1987	Droop 1987	Droop 1987	Droop 1987	Droop 1987	Droop 1987	Droop 1987
Si Calc	1.88	1.91	1.90	1.91	1.89	1.86	1.88	1.88
Ti Calc	0.02	0.01	0.01	0.01	0.02	0.02	0.02	0.02
Al Calc	0.33	0.26	0.27	0.27	0.32	0.38	0.35	0.35
Fe Calc	0.23	0.20	0.22	0.21	0.23	0.23	0.22	0.22
Mn Calc	0.00	0.00	0.00	0.00	0.00	0.00	0.00	0.00
Mg Calc	0.60	0.67	0.64	0.65	0.60	0.56	0.58	0.59
Ca Calc	0.77	0.82	0.82	0.79	0.77	0.77	0.77	0.77
K Calc	0.00	0.00	0.00	0.00	0.00	0.00	0.00	0.00
Na Calc	0.21	0.17	0.17	0.18	0.21	0.21	0.21	0.21
Li Calc								
Zn Calc								
Ni Calc	0.00	0.00	0.00	0.00	0.00	0.00	0.00	0.00
Cr Calc	0.00	0.00	0.00	0.00	0.00	0.00	0.00	0.00
Sc Calc								
Fe 3+ Droop	0.12	0.10	0.10	0.10	0.11	0.11	0.09	0.10
Total Calc	4.04	4.03	4.03	4.03	4.04	4.04	4.03	4.03
Si	1.86	1.90	1.89	1.90	1.87	1.84	1.87	1.86
Ti	0.02	0.01	0.01	0.01	0.02	0.02	0.02	0.02
Al (T)	0.14	0.10	0.11	0.10	0.13	0.16	0.13	0.14
Al (M1)	0.19	0.15	0.16	0.16	0.19	0.21	0.22	0.21
Fe3+ (T)	0.00	0.00	0.00	0.00	0.00	0.00	0.00	0.00
Fe3+ (M1)	0.12	0.10	0.10	0.10	0.11	0.11	0.09	0.10
Fe2+	0.11	0.10	0.12	0.11	0.11	0.12	0.13	0.12
Mn	0.00	0.00	0.00	0.00	0.00	0.00	0.00	0.00
Mg	0.59	0.66	0.64	0.64	0.60	0.56	0.57	0.58
Ca	0.76	0.81	0.81	0.79	0.77	0.77	0.76	0.77
K	0.00	0.00	0.00	0.00	0.00	0.00	0.00	0.00
Na	0.21	0.17	0.16	0.18	0.20	0.21	0.21	0.20
Li	0.00	0.00	0.00	0.00	0.00	0.00	0.00	0.00
Zn	0.00	0.00	0.00	0.00	0.00	0.00	0.00	0.00
Ni	0.00	0.00	0.00	0.00	0.00	0.00	0.00	0.00
Cr	0.00	0.00	0.00	0.00	0.00	0.00	0.00	0.00
Sc	0.00	0.00	0.00	0.00	0.00	0.00	0.00	0.00
Total	4.00	4.00	4.00	4.00	4.00	4.00	4.00	4.00
J	0.42	0.34	0.33	0.36	0.41	0.42	0.42	0.41
Q	1.46	1.57	1.57	1.54	1.48	1.44	1.47	1.47
group	Ca-Na	Quad	Quad	Quad	Ca-Na	Ca-Na	Ca-Na	Ca-Na
adjective		aluminian sodian	aluminian sodian	aluminian sodian				
pyroxene	omphacite	diopside	diopside	diopside	omphacite	omphacite	omphacite	omphacite
enstatite	----------	39.78	38.22	39.18	----------	----------	----------	----------
ferrosillite	----------	11.72	13.20	12.86	----------	----------	----------	----------
wollastonite	----------	48.50	48.58	47.97	----------	----------	----------	----------
jadeite	13.56	----------	----------	----------	13.59	14.84	15.74	14.79
aegirine	8.58	----------	----------	----------	8.14	7.81	6.32	6.97
Quad	77.86	----------	----------	----------	78.27	77.35	77.95	78.24

Appendix 6.D EMP data for pyroxene modified from PX-NOM (Sturm, R. 2002)

Sample	904C 1.2+ cpx tra	0904C 1.2+ cpx trav	904C 1.2+ cpx tra	904C 1.2+ cpx tra	0904C 1.2+ cpx trav	904C 1.2+ cpx tra	904C 1.2+ cpx tra	0904C 1.2+ cpx trav	0904C random	0904C random	0904C random	0904C random	0904C random	0904C random	0904C random	0904C random
X	-15795.00	-15795.00	-15795.00	-15795.00	-15795.00	-15795.00	-15795.00	-15795.00	-8549.00	-8612.00	-8549.00	-8734.00	-8710.00	-8549.00	-9003.00	-8906.00
Y	-9673.00	-9638.00	-9499.00	-9336.00	-9160.00	-9076.00	-8902.00	-8811.00	-13641.00	-14052.00	-11303.00	-9465.00	-9398.00	-9398.00	-5172.00	-7553.00
Z	64.00	66.00	66.00	66.00	66.00	66.00	66.00	66.00	81.00	80.00	81.00	81.00	81.00	81.00	78.00	81.00
SiO2	50.64	51.50	50.93	50.65	50.41	51.13	50.80	51.32	51.70	50.37	49.11	42.30	42.80	42.24	51.43	45.01
TiO2	0.32	0.42	0.58	0.67	0.64	0.60	0.54	0.35	0.42	0.63	0.41	0.46	0.31	0.48	0.45	0.75
Al2O3	10.47	11.19	11.66	11.90	11.77	11.68	11.42	9.86	11.21	11.53	10.05	14.94	15.06	14.34	11.08	12.19
FeO	9.32	7.52	7.73	7.88	7.88	7.94	7.89	7.94	7.94	8.01	7.59	10.39	10.50	11.52	8.03	10.22
MnO	0.08	0.05	0.02	0.04	0.00	0.04	0.03	0.03	0.05	0.02	0.03	0.09	0.03	0.09	0.06	0.05
MgO	9.22	8.08	8.02	7.87	7.90	7.96	8.02	8.96	8.21	7.93	8.45	14.24	13.91	13.64	8.22	14.33
CaO	15.55	15.68	16.10	15.95	15.95	16.09	16.11	16.82	15.92	16.34	16.77	12.01	11.88	11.78	16.09	12.60
K2O	0.02	0.00	0.00	0.00	0.00	0.00	0.00	0.00	0.01	0.01	0.01	0.23	0.21	0.24	0.01	0.06
Na2O	3.81	4.91	4.76	4.69	4.62	4.62	4.67	4.17	4.80	4.54	3.67	2.77	2.74	2.80	4.61	2.40
Li2O																
ZnO																
NiO	0.04	0.01	0.00	0.01	0.02	0.00	0.04	0.00	0.01	0.00	0.00	0.04	0.00	0.00	0.03	0.05
Cr2O3	0.01	0.02	0.04	0.02	0.00	0.01	0.00	0.03	0.01	0.05	0.04	0.02	0.02	0.00	0.06	0.03
Sc2O3																
Total	99.48	99.37	99.83	99.67	99.18	100.08	99.52	99.50	100.28	99.44	96.12	97.48	97.46	97.14	100.07	97.68
Fe3+ model	Droop 1987	Droop 1987	Droop 1987	Droop 1987	Droop 1987	Droop 1987	Droop 1987	Droop 1987	Droop 1987	Droop 1987	Droop 1987	Droop 1987	Droop 1987	Droop 1987	Droop 1987	Droop 1987
Si Calc	1.87	1.89	1.87	1.86	1.86	1.87	1.87	1.89	1.89	1.86	1.87	1.61	1.63	1.62	1.88	1.70
Ti Calc	0.01	0.01	0.02	0.02	0.02	0.02	0.01	0.01	0.01	0.02	0.01	0.01	0.01	0.01	0.01	0.02
Al Calc	0.46	0.48	0.50	0.51	0.51	0.50	0.50	0.43	0.48	0.50	0.45	0.67	0.67	0.65	0.48	0.54
Fe Calc	0.29	0.23	0.24	0.24	0.24	0.24	0.24	0.24	0.24	0.25	0.24	0.33	0.33	0.37	0.25	0.32
Mn Calc	0.00	0.00	0.00	0.00	0.00	0.00	0.00	0.00	0.00	0.00	0.00	0.00	0.00	0.00	0.00	0.00
Mg Calc	0.51	0.44	0.44	0.43	0.43	0.43	0.44	0.49	0.45	0.44	0.48	0.81	0.79	0.78	0.45	0.81
Ca Calc	0.62	0.62	0.63	0.63	0.63	0.63	0.64	0.66	0.62	0.65	0.69	0.49	0.48	0.49	0.63	0.51
K Calc	0.00	0.00	0.00	0.00	0.00	0.00	0.00	0.00	0.00	0.00	0.00	0.01	0.01	0.01	0.00	0.00
Na Calc	0.27	0.35	0.34	0.33	0.33	0.33	0.33	0.30	0.34	0.32	0.27	0.20	0.20	0.21	0.33	0.18
Li Calc																
Zn Calc																
Ni Calc	0.00	0.00	0.00	0.00	0.00	0.00	0.00	0.00	0.00	0.00	0.00	0.00	0.00	0.00	0.00	0.00
Cr Calc	0.00	0.00	0.00	0.00	0.00	0.00	0.00	0.00	0.00	0.00	0.00	0.00	0.00	0.00	0.00	0.00
Sc Calc																
Fe 3+ Droop	0.08	0.09	0.10	0.09	0.09	0.08	0.10	0.10	0.09	0.10	0.07	0.33	0.33	0.37	0.09	0.27
Total Calc	4.03	4.03	4.03	4.03	4.03	4.03	4.03	4.03	4.03	4.03	4.02	4.15	4.13	4.15	4.03	4.09
Si	1.86	1.88	1.85	1.85	1.85	1.86	1.85	1.88	1.87	1.84	1.86	1.55	1.58	1.57	1.87	1.66
Ti	0.01	0.01	0.02	0.02	0.02	0.02	0.01	0.01	0.01	0.02	0.01	0.01	0.01	0.01	0.01	0.02
Al (T)	0.14	0.12	0.15	0.15	0.15	0.14	0.15	0.12	0.13	0.16	0.14	0.45	0.42	0.43	0.13	0.34
Al (M1)	0.31	0.36	0.35	0.36	0.35	0.36	0.35	0.30	0.35	0.34	0.31	0.20	0.23	0.19	0.34	0.20
Fe3+ (T)	0.00	0.00	0.00	0.00	0.00	0.00	0.00	0.00	0.00	0.00	0.00	0.00	0.00	0.00	0.00	0.00
Fe3+ (M1)	0.08	0.09	0.10	0.09	0.09	0.08	0.10	0.10	0.09	0.10	0.07	0.33	0.33	0.37	0.09	0.27
Fe2+	0.20	0.14	0.13	0.15	0.15	0.16	0.14	0.15	0.15	0.14	0.17	0.00	0.00	0.00	0.15	0.04
Mn	0.00	0.00	0.00	0.00	0.00	0.00	0.00	0.00	0.00	0.00	0.00	0.00	0.00	0.00	0.00	0.00
Mg	0.50	0.44	0.43	0.43	0.43	0.43	0.44	0.49	0.44	0.43	0.48	0.78	0.76	0.75	0.45	0.79
Ca	0.61	0.61	0.63	0.62	0.63	0.63	0.63	0.66	0.62	0.64	0.68	0.47	0.47	0.47	0.63	0.50
K	0.00	0.00	0.00	0.00	0.00	0.00	0.00	0.00	0.00	0.00	0.00	0.01	0.01	0.01	0.00	0.00
Na	0.27	0.35	0.34	0.33	0.33	0.33	0.33	0.30	0.34	0.32	0.27	0.20	0.20	0.20	0.33	0.17
Li	0.00	0.00	0.00	0.00	0.00	0.00	0.00	0.00	0.00	0.00	0.00	0.00	0.00	0.00	0.00	0.00
Zn	0.00	0.00	0.00	0.00	0.00	0.00	0.00	0.00	0.00	0.00	0.00	0.00	0.00	0.00	0.00	0.00
Ni	0.00	0.00	0.00	0.00	0.00	0.00	0.00	0.00	0.00	0.00	0.00	0.00	0.00	0.00	0.00	0.00
Cr	0.00	0.00	0.00	0.00	0.00	0.00	0.00	0.00	0.00	0.00	0.00	0.00	0.00	0.00	0.00	0.00
Sc	0.00	0.00	0.00	0.00	0.00	0.00	0.00	0.00	0.00	0.00	0.00	0.00	0.00	0.00	0.00	0.00
Total	4.00	4.00	4.00	4.00	4.00	4.00	4.00	4.00	4.00	4.00	4.00	4.01	4.01	4.01	4.00	4.00
J	0.54	0.69	0.67	0.66	0.66	0.65	0.66	0.59	0.67	0.64	0.54	0.39	0.39	0.40	0.65	0.34
Q	1.32	1.19	1.20	1.20	1.21	1.22	1.21	1.29	1.21	1.21	1.33	1.25	1.23	1.22	1.23	1.33
group	Ca-Na	Ca-Na	Ca-Na	Ca-Na	Ca-Na	Ca-Na	Ca-Na	Ca-Na	Ca-Na	Ca-Na	Ca-Na	Ca-Na	Ca-Na	Ca-Na	Ca-Na	Ca-Na
adjective												subsilicic	subsilicic	subsilicic		subsilicic
pyroxene	omphacite	omphacite	omphacite	omphacite	omphacite	omphacite	omphacite	omphacite	omphacite	omphacite	omphacite	aegirine-augite	aegirine-augite	aegirine-augite	omphacite	aegirine-augite
enstatite	----------	----------	----------	----------	----------	----------	----------	----------	----------	----------	----------	----------	----------	----------	----------	----------
ferrosillite	----------	----------	----------	----------	----------	----------	----------	----------	----------	----------	----------	----------	----------	----------	----------	----------
wollastonite	----------	----------	----------	----------	----------	----------	----------	----------	----------	----------	----------	----------	----------	----------	----------	----------
jadeite	23.04	29.51	27.93	28.40	27.99	28.63	27.37	23.74	28.19	26.57	23.75	9.07	9.80	8.47	27.49	8.58
aegirine	6.09	7.31	7.98	7.18	7.20	6.13	8.03	7.66	7.63	8.07	5.04	14.88	14.29	16.34	7.15	11.95
Quad	70.87	63.18	64.09	64.42	64.81	65.23	64.60	68.60	64.18	65.36	71.21	76.05	75.90	75.19	65.36	79.46

Appendix 6.D EMP data for pyroxene modified from PX-NOM (Sturm, R. 2002)

Sample	0903B 1.7 opx	0903B 1.8 ?	0903B 1.8 ?	0903B 2.2 hb	0903B 2.3 opx	0903B 2.4 opx	0903B 2.5 opx	0903B random	0903B random	0903B random	0903B random	0903B random
X	13688.00	14795.00	14880.00	5692.00	7102.00	7131.00	7220.00	11347.00	11446.00	11416.00	11416.00	11354.00
Y	-17973.00	-17743.00	-17634.00	-16218.00	-18873.00	-18240.00	-17998.00	-24553.00	-24942.00	-14655.00	-14939.00	-15695.00
Z	72.00	68.00	68.00	81.00	81.00	81.00	81.00	77.00	77.00	74.00	74.00	74.00
SiO2	55.21	56.01	55.92	53.86	53.27	53.32	54.40	55.91	55.60	55.69	53.93	53.93
TiO2	0.08	0.03	0.04	0.18	0.28	0.18	0.06	0.03	0.04	0.05	0.14	0.15
Al2O3	2.50	1.18	1.20	2.06	3.02	1.96	1.33	1.04	1.16	1.26	1.74	1.82
FeO	13.50	13.73	13.66	4.37	4.45	4.83	3.98	14.13	14.16	14.15	4.07	4.49
MnO	0.23	0.27	0.31	0.12	0.10	0.07	0.12	0.25	0.26	0.25	0.10	0.08
MgO	29.15	29.52	29.60	15.82	15.67	15.92	16.24	28.94	29.07	29.21	16.06	15.87
CaO	0.25	0.22	0.24	24.07	23.14	22.91	23.70	0.29	0.21	0.27	23.78	23.17
K2O	0.00	0.00	0.01	0.01	0.01	0.00	0.00	0.01	0.00	0.00	0.01	0.00
Na2O	0.02	0.00	0.00	0.52	0.62	0.44	0.42	0.01	0.04	0.01	0.54	0.55
Li2O												
ZnO												
NiO	0.00	0.01	0.03	0.02	0.00	0.03	0.02	0.05	0.02	0.02	0.03	0.04
Cr2O3	0.04	0.00	0.00	0.09	0.06	0.09	0.04	0.01	0.06	0.05	0.06	0.08
Sc2O3												
Total	100.98	100.97	101.00	101.12	100.64	99.75	100.31	100.69	100.63	100.96	100.46	100.18
Fe3+ model	Droop 1987	Droop 1987	Droop 1987	Droop 1987	Droop 1987	Droop 1987	Droop 1987	Droop 1987	Droop 1987	Droop 1987	Droop 1987	Droop 1987
Si Calc	1.95	1.98	1.97	1.95	1.94	1.96	1.98	1.98	1.97	1.97	1.96	1.97
Ti Calc	0.00	0.00	0.00	0.01	0.01	0.01	0.00	0.00	0.00	0.00	0.00	0.00
Al Calc	0.10	0.05	0.05	0.09	0.13	0.08	0.06	0.04	0.05	0.05	0.07	0.08
Fe Calc	0.40	0.41	0.40	0.13	0.14	0.15	0.12	0.42	0.42	0.42	0.12	0.14
Mn Calc	0.01	0.01	0.01	0.00	0.00	0.00	0.00	0.01	0.01	0.01	0.00	0.00
Mg Calc	1.53	1.55	1.56	0.86	0.85	0.87	0.88	1.53	1.54	1.54	0.87	0.86
Ca Calc	0.01	0.01	0.01	0.94	0.90	0.90	0.92	0.01	0.01	0.01	0.93	0.91
K Calc	0.00	0.00	0.00	0.00	0.00	0.00	0.00	0.00	0.00	0.00	0.00	0.00
Na Calc	0.00	0.00	0.00	0.04	0.04	0.03	0.03	0.00	0.00	0.00	0.04	0.04
Li Calc												
Zn Calc												
Ni Calc	0.00	0.00	0.00	0.00	0.00	0.00	0.00	0.00	0.00	0.00	0.00	0.00
Cr Calc	0.00	0.00	0.00	0.00	0.00	0.00	0.00	0.00	0.00	0.00	0.00	0.00
Sc Calc												
Fe 3+ Droop	0.00	0.00	0.01	0.04	0.03	0.02	0.01	0.00	0.01	0.01	0.04	0.01
Total Calc	4.00	4.00	4.00	4.01	4.01	4.01	4.00	4.00	4.00	4.00	4.01	4.00
Si	1.95	1.98	1.97	1.95	1.93	1.95	1.98	1.98	1.97	1.97	1.96	1.97
Ti	0.00	0.00	0.00	0.01	0.01	0.01	0.00	0.00	0.00	0.00	0.00	0.00
Al (T)	0.05	0.02	0.03	0.05	0.07	0.05	0.02	0.02	0.03	0.03	0.04	0.03
Al (M1)	0.05	0.02	0.02	0.03	0.06	0.04	0.04	0.03	0.02	0.02	0.03	0.05
Fe3+ (T)	0.00	0.00	0.00	0.00	0.00	0.00	0.00	0.00	0.00	0.00	0.00	0.00
Fe3+ (M1)	0.00	0.00	0.01	0.04	0.03	0.02	0.01	0.00	0.01	0.01	0.04	0.01
Fe2+	0.40	0.41	0.40	0.09	0.10	0.12	0.11	0.42	0.41	0.41	0.09	0.12
Mn	0.01	0.01	0.01	0.00	0.00	0.00	0.00	0.01	0.01	0.01	0.00	0.00
Mg	1.53	1.55	1.56	0.85	0.85	0.87	0.88	1.53	1.54	1.54	0.87	0.86
Ca	0.01	0.01	0.01	0.93	0.90	0.90	0.92	0.01	0.01	0.01	0.93	0.91
K	0.00	0.00	0.00	0.00	0.00	0.00	0.00	0.00	0.00	0.00	0.00	0.00
Na	0.00	0.00	0.00	0.04	0.04	0.03	0.03	0.00	0.00	0.00	0.04	0.04
Li	0.00	0.00	0.00	0.00	0.00	0.00	0.00	0.00	0.00	0.00	0.00	0.00
Zn	0.00	0.00	0.00	0.00	0.00	0.00	0.00	0.00	0.00	0.00	0.00	0.00
Ni	0.00	0.00	0.00	0.00	0.00	0.00	0.00	0.00	0.00	0.00	0.00	0.00
Cr	0.00	0.00	0.00	0.00	0.00	0.00	0.00	0.00	0.00	0.00	0.00	0.00
Sc	0.00	0.00	0.00	0.00	0.00	0.00	0.00	0.00	0.00	0.00	0.00	0.00
Total	4.00	4.00	4.00	4.00	4.00	4.00	4.00	4.00	4.00	4.00	4.00	4.00
J	0.00	0.00	0.00	0.07	0.09	0.06	0.06	0.00	0.01	0.00	0.08	0.08
Q	1.94	1.97	1.96	1.87	1.85	1.89	1.92	1.96	1.96	1.96	1.88	1.89
group	Quad	Quad	Quad	Quad	Quad	Quad	Quad	Quad	Quad	Quad	Quad	Quad
adjective	aluminian				aluminian							
pyroxene	(clino)enstatite	(clino)enstatite	(clino)enstatite	diopside	diopside	diopside	diopside	(clino)enstatite	(clino)enstatite	(clino)enstatite	diopside	diopside
enstatite	78.72	78.65	78.69	44.40	44.95	45.32	45.64	77.76	77.90	77.93	45.24	45.23
ferrosillite	20.80	20.93	20.85	7.07	7.33	7.82	6.46	21.68	21.69	21.55	6.60	7.30
wollastonite	0.48	0.42	0.46	48.53	47.72	46.86	47.89	0.57	0.41	0.52	48.16	47.47
jadeite	----------	----------	----------	----------	----------	----------	----------	----------	----------	----------	----------	----------
aegirine	----------	----------	----------	----------	----------	----------	----------	----------	----------	----------	----------	----------
Quad	----------	----------	----------	----------	----------	----------	----------	----------	----------	----------	----------	----------

Appendix 6.D EMP data for pyroxene modified from PX-NOM (Sturm, R. 2002)

Comment	0910B 1.2+ hb r	0910B 1.2+ hb r	0910B 1.2+ hb c	0910B 1.2+ hb c	0910B 1.2+ hb r	0910B 1.2+ hb r	0910B 1.2+ hb c
X	-18115.00	-17963.00	-18045.00	-18093.00	-18872.00	-18713.00	-18829.00
Y	-28880.00	-28773.00	-28752.00	-28772.00	-29313.00	-29302.00	-29418.00
Z	70.00	70.00	70.00	70.00	70.00	70.00	70.00
SiO2	40.84	41.86	41.50	41.04	43.11	42.48	42.40
TiO2	0.61	0.61	0.88	0.83	0.82	1.31	0.93
Al2O3	17.86	15.34	15.65	15.65	14.36	14.82	14.66
Cr2O3	0.02	0.00	0.01	0.05	0.01	0.00	0.00
Fe2O3	1.06	1.57	0.95	1.02	0.95	0.85	0.89
FeO	8.80	9.35	9.55	9.50	10.15	10.55	10.25
MnO	0.01	0.08	0.04	0.00	0.02	0.06	0.06
MgO	13.16	13.08	13.21	13.29	13.37	12.79	13.19
CaO	11.81	11.05	11.69	11.75	11.66	11.47	11.73
Na2O	3.00	2.51	2.75	2.84	2.69	2.82	2.81
K2O	0.22	0.22	0.40	0.38	0.24	0.24	0.25
NiO	0.00	0.04	0.02	0.02	0.05	0.02	0.02
Total	97.28	95.57	96.55	96.29	97.34	97.32	97.09
FeO	9.76	10.76	10.41	10.42	11.01	11.32	11.05
num ox	23.00	23.00	23.00	23.00	23.00	23.00	23.00
Si	5.94	6.20	6.11	6.07	6.29	6.22	6.22
Ti	0.07	0.07	0.10	0.09	0.09	0.14	0.10
Al	3.06	2.68	2.72	2.73	2.47	2.56	2.53
Cr	0.00	0.00	0.00	0.01	0.00	0.00	0.00
Fe3+	0.12	0.18	0.11	0.11	0.10	0.09	0.10
Fe2+	1.07	1.16	1.18	1.17	1.24	1.29	1.26
Mn	0.00	0.01	0.00	0.00	0.00	0.01	0.01
Mg	2.85	2.89	2.90	2.93	2.91	2.79	2.88
Ca	1.84	1.75	1.84	1.86	1.82	1.80	1.84
Na	0.85	0.72	0.79	0.81	0.76	0.80	0.80
K	0.04	0.04	0.07	0.07	0.04	0.04	0.05
Total	15.84	15.69	15.81	15.86	15.73	15.74	15.79
(Si+Al+Cr+Ti+Fe+Mg+Mn)	13.00	13.00	13.00	13.00	13.00	13.00	13.00
c	1.36	1.39	1.38	1.37	1.43	1.41	1.41
a	0.02	0.02	0.02	0.02	0.02	0.03	0.02
l	0.53	0.45	0.46	0.46	0.42	0.44	0.43
c	0.00	0.00	0.00	0.00	0.00	0.00	0.00
u	0.02	0.03	0.02	0.02	0.02	0.02	0.02
l	0.12	0.13	0.13	0.13	0.14	0.15	0.14
a	0.00	0.00	0.00	0.00	0.00	0.00	0.00
t	0.33	0.32	0.33	0.33	0.33	0.32	0.33
i	0.21	0.20	0.21	0.21	0.21	0.20	0.21
o	0.05	0.04	0.04	0.05	0.04	0.05	0.05
n	0.00	0.00	0.00	0.00	0.00	0.00	0.00
s	8.74	8.90	8.85	8.88	8.77	8.79	8.81
Fe3+ check (=0?)	0.00	0.00	0.00	0.00	0.00	0.00	0.00
SUM T to 8 (Si, Al, Ti)							
Si	5.94	6.20	6.11	6.07	6.29	6.22	6.22
Al	2.06	1.80	1.89	1.93	1.71	1.78	1.78
Ti	0.00	0.00	0.00	0.00	0.00	0.00	0.00
TOTAL T	8.00	8.00	8.00	8.00	8.00	8.00	8.00
Sum C to 5 (Al, Ti, Fe3+, Cr, Mg, Fe, Mn)							
Al	1.01	0.88	0.83	0.80	0.76	0.77	0.75
Ti	0.07	0.07	0.10	0.09	0.09	0.14	0.10
Fe3+	0.12	0.18	0.11	0.11	0.10	0.09	0.10
Cr	0.00	0.00	0.00	0.01	0.00	0.00	0.00
Mg	2.85	2.89	2.90	2.93	2.91	2.79	2.88
Fe	0.96	1.00	1.08	1.06	1.14	1.20	1.17
Mn	0.00	0.00	0.00	0.00	0.00	0.00	0.00
TOTAL C (2 M1, 2 M2, 1 M3)	5.00	5.00	5.00	5.00	5.00	5.00	5.00
Sum B to 2 (Fe, Mn, Ca, Na)							
Mg	0.00	0.00	0.00	0.00	0.00	0.00	0.00
Fe	0.11	0.16	0.10	0.11	0.10	0.09	0.09
Mn	0.00	0.01	0.00	0.00	0.00	0.01	0.01
Ca	1.84	1.75	1.84	1.86	1.82	1.80	1.84
Na	0.05	0.08	0.05	0.03	0.07	0.11	0.06
TOTAL B (2 M4)	2.00	2.00	2.00	2.00	2.00	2.00	2.00
Sum A (Excess B + K)							
Ca	0.00	0.00	0.00	0.00	0.00	0.00	0.00
Na	0.80	0.64	0.74	0.79	0.69	0.70	0.74
K	0.04	0.04	0.07	0.07	0.04	0.04	0.05
TOTAL A	0.84	0.69	0.81	0.86	0.73	0.74	0.79
B(Mg, Fe, Mn, Li)	0.11	0.17	0.10	0.11	0.10	0.10	0.10
B(Ca, Na)	1.89	1.83	1.90	1.89	1.90	1.90	1.90
B(Na)	0.05	0.08	0.05	0.03	0.07	0.11	0.06
(Ca+Na) B >= 1.00	1.89	1.83	1.90	1.89	1.90	1.90	1.90
Na B is 0.50 to 1.50	0.05	0.08	0.05	0.03	0.07	0.11	0.06
(Na+K) A < 0.50	0.84	0.69	0.81	0.86	0.73	0.74	0.79
Mg/(Mg+Fe)	0.73	0.71	0.71	0.71	0.70	0.68	0.70
Si in formula	5.94	6.20	6.11	6.07	6.29	6.22	6.22
Amphibole Type	calcic	calcic	calcic	calcic	calcic	calcic	calcic
Name	pargasite	pargasite	pargasite	pargasite	pargasite	pargasite	pargasite

Appendix 6.D Amphibole classification from EMP data

Comment	0910B 1.2+ hb c	0910B 1.2+ hb r	0910B 1.2+ hb r	0910B 1.2+ hb c	0910B 1.2+ hb c
X	-18829.00	-19611.00	-19904.00	-19809.00	-19635.00
Y	-29497.00	-29001.00	-28902.00	-28902.00	-28896.00
Z	70.00	70.00	70.00	70.00	70.00
SiO2	42.89	41.39	41.40	42.22	41.76
TiO2	0.81	0.63	0.82	0.61	0.59
Al2O3	14.37	16.87	17.44	15.72	16.21
Cr2O3	0.00	0.01	0.01	0.01	0.01
Fe2O3	1.02	1.00	0.80	0.94	0.91
FeO	10.00	10.70	11.50	10.85	10.50
MnO	0.08	0.09	0.03	0.02	0.03
MgO	13.30	12.14	11.04	12.45	12.38
CaO	11.55	11.60	11.38	11.72	11.60
Na2O	2.69	3.01	2.85	2.86	2.94
K2O	0.18	0.15	0.09	0.09	0.13
NiO	0.03	0.04	0.05	0.00	0.03
Total	96.81	97.53	97.32	97.39	96.99
FeO	10.92	11.60	12.22	11.70	11.32
num ox	23.00	23.00	23.00	23.00	23.00
Si	6.29	6.05	6.07	6.18	6.13
Ti	0.09	0.07	0.09	0.07	0.07
Al	2.48	2.91	3.01	2.71	2.80
Cr	0.00	0.00	0.00	0.00	0.00
Fe3+	0.11	0.11	0.09	0.10	0.10
Fe2+	1.23	1.31	1.41	1.33	1.29
Mn	0.01	0.01	0.00	0.00	0.00
Mg	2.91	2.65	2.41	2.71	2.71
Ca	1.81	1.82	1.79	1.84	1.82
Na	0.76	0.85	0.81	0.81	0.84
K	0.03	0.03	0.02	0.02	0.02
Total	15.72	15.81	15.70	15.76	15.78
(Si+Al+Cr+Ti+Fe+Mg+Mn)	13.00	13.00	13.00	13.00	13.00
c	1.43	1.38	1.38	1.41	1.39
a	0.02	0.02	0.02	0.02	0.01
l	0.42	0.50	0.51	0.46	0.48
c	0.00	0.00	0.00	0.00	0.00
u	0.02	0.02	0.02	0.02	0.02
l	0.14	0.15	0.16	0.15	0.15
a	0.00	0.00	0.00	0.00	0.00
t	0.33	0.30	0.27	0.31	0.31
i	0.21	0.21	0.20	0.21	0.21
o	0.04	0.05	0.05	0.05	0.05
n	0.00	0.00	0.00	0.00	0.00
s	8.81	8.79	8.81	8.79	8.82
Fe3+ check (=0?)	0.00	0.00	0.00	0.00	0.00
SUM T to 8 (Si, Al, Ti)					
Si	6.29	6.05	6.07	6.18	6.13
Al	1.71	1.95	1.93	1.82	1.87
Ti	0.00	0.00	0.00	0.00	0.00
TOTAL T	8.00	8.00	8.00	8.00	8.00
Sum C to 5 (Al, Ti, Fe3+, Cr, Mg, Fe, Mn)					
Al	0.77	0.96	1.08	0.89	0.93
Ti	0.09	0.07	0.09	0.07	0.07
Fe3+	0.11	0.11	0.09	0.10	0.10
Cr	0.00	0.00	0.00	0.00	0.00
Mg	2.91	2.65	2.41	2.71	2.71
Fe	1.13	1.21	1.33	1.23	1.19
Mn	0.00	0.00	0.00	0.00	0.00
TOTAL C (2 M1, 2 M2, 1 M3)	5.00	5.00	5.00	5.00	5.00
Sum B to 2 (Fe, Mn, Ca, Na)					
Mg	0.00	0.00	0.00	0.00	0.00
Fe	0.10	0.10	0.08	0.10	0.10
Mn	0.01	0.01	0.00	0.00	0.00
Ca	1.81	1.82	1.79	1.84	1.82
Na	0.08	0.07	0.13	0.06	0.07
TOTAL B (2 M4)	2.00	2.00	2.00	2.00	2.00
Sum A (Excess B + K)					
Ca	0.00	0.00	0.00	0.00	0.00
Na	0.69	0.78	0.68	0.75	0.76
K	0.03	0.03	0.02	0.02	0.02
TOTAL A	0.72	0.81	0.70	0.77	0.79
B(Mg, Fe, Mn, Li)	0.11	0.11	0.08	0.10	0.10
B(Ca, Na)	1.89	1.89	1.92	1.90	1.90
B(Na)	0.08	0.07	0.13	0.06	0.07
(Ca+Na) B >= 1.00	1.89	1.89	1.92	1.90	1.90
Na B is 0.50 to 1.50	0.08	0.07	0.13	0.06	0.07
(Na+K) A < 0.50	0.72	0.81	0.70	0.77	0.79
Mg/(Mg+Fe)	0.70	0.67	0.63	0.67	0.68
Si in formula	6.29	6.05	6.07	6.18	6.13
Amphibole Type	calcic	calcic	calcic	calcic	calcic
Name	pargasite	pargasite	pargasite	pargasite	pargasite

Appendix 6.D Amphibole classification from EMP data

Comment	0905B random	0905B random	0905B random	0905B random	0905B random	0905B random
X	12395.00	12467.00	12447.00	12457.00	12633.00	12516.00
Y	24200.00	24238.00	24272.00	24547.00	24604.00	24685.00
Z	57.00	57.00	57.00	57.00	57.00	57.00
SiO2	46.79	42.33	41.26	42.55	43.16	43.38
TiO2	0.43	0.62	0.72	0.67	0.49	1.67
Al2O3	15.47	13.93	14.59	13.37	13.73	13.00
Cr2O3	0.00	0.01	0.00	0.01	0.00	0.00
Fe2O3	0.00	1.08	1.10	1.17	1.35	0.85
FeO	8.95	10.80	11.60	11.50	10.85	10.40
MnO	0.02	0.03	0.03	0.01	0.04	0.03
MgO	10.62	13.21	12.48	13.14	13.38	13.63
CaO	11.05	11.94	11.87	12.00	11.99	12.07
Na2O	2.80	1.67	1.82	1.71	1.49	1.42
K2O	1.08	1.53	1.67	1.52	1.41	1.46
NiO	0.00	0.01	0.00	0.01	0.02	0.05
Total	97.22	97.06	97.03	97.54	97.77	97.87
FeO	8.95	11.77	12.59	12.55	12.06	11.16
num ox	23.00	23.00	23.00	23.00	23.00	23.00
Si	6.72	6.26	6.14	6.28	6.32	6.34
Ti	0.05	0.07	0.08	0.07	0.05	0.18
Al	2.62	2.43	2.56	2.33	2.37	2.24
Cr	0.00	0.00	0.00	0.00	0.00	0.00
Fe3+	0.00	0.12	0.12	0.13	0.15	0.09
Fe2+	1.07	1.34	1.44	1.42	1.33	1.27
Mn	0.00	0.00	0.00	0.00	0.00	0.00
Mg	2.27	2.91	2.77	2.89	2.92	2.97
Ca	1.70	1.89	1.89	1.90	1.88	1.89
Na	0.78	0.48	0.52	0.49	0.42	0.40
K	0.20	0.29	0.32	0.29	0.26	0.27
Total	15.41	15.78	15.86	15.80	15.71	15.65
(Si+Al+Cr+Ti+Fe+Mg+Mn)	12.73	13.00	13.00	13.00	13.00	13.00
c	1.56	1.41	1.37	1.42	1.44	1.44
a	0.01	0.02	0.02	0.02	0.01	0.04
l	0.46	0.41	0.43	0.39	0.40	0.38
c	0.00	0.00	0.00	0.00	0.00	0.00
u	0.00	0.02	0.02	0.02	0.03	0.02
l	0.12	0.15	0.16	0.16	0.15	0.14
a	0.00	0.00	0.00	0.00	0.00	0.00
t	0.26	0.33	0.31	0.33	0.33	0.34
i	0.20	0.21	0.21	0.21	0.21	0.22
o	0.05	0.03	0.03	0.03	0.02	0.02
n	0.01	0.02	0.02	0.02	0.01	0.02
s	8.63	8.88	8.94	8.87	8.80	8.78
Fe3+ check (=0?)	0.27	0.00	0.00	0.00	0.00	0.00
SUM T to 8 (Si, Al, Ti)						
Si	6.72	6.26	6.14	6.28	6.32	6.34
Al	1.28	1.74	1.86	1.72	1.68	1.66
Ti	0.00	0.00	0.00	0.00	0.00	0.00
TOTAL T	8.00	8.00	8.00	8.00	8.00	8.00
Sum C to 5 (Al, Ti, Fe3+, Cr, Mg, Fe, Mn)						
Al	1.34	0.68	0.70	0.61	0.69	0.57
Ti	0.05	0.07	0.08	0.07	0.05	0.18
Fe3+	0.00	0.12	0.12	0.13	0.15	0.09
Cr	0.00	0.00	0.00	0.00	0.00	0.00
Mg	2.27	2.91	2.77	2.89	2.92	2.97
Fe	1.07	1.22	1.32	1.29	1.19	1.18
Mn	0.00	0.00	0.00	0.00	0.00	0.00
TOTAL C (2 M1, 2 M2, 1 M3)	4.73	5.00	5.00	5.00	5.00	5.00
Sum B to 2 (Fe, Mn, Ca, Na)						
Mg	0.00	0.00	0.00	0.00	0.00	0.00
Fe	0.00	0.12	0.12	0.13	0.14	0.09
Mn	0.00	0.00	0.00	0.00	0.00	0.00
Ca	1.70	1.89	1.89	1.90	1.88	1.89
Na	0.30	-0.02	-0.02	-0.03	-0.03	0.02
TOTAL B (2 M4)	2.00	2.00	2.00	2.00	2.00	2.00
Sum A (Excess B + K)						
Ca	0.00	0.00	0.00	0.00	0.00	0.00
Na	0.48	0.49	0.54	0.52	0.45	0.38
K	0.20	0.29	0.32	0.29	0.26	0.27
TOTAL A	0.68	0.78	0.86	0.81	0.71	0.65
B(Mg, Fe, Mn, Li)	0.00	0.12	0.12	0.13	0.14	0.09
B(Ca, Na)	2.00	1.88	1.88	1.87	1.86	1.91
B(Na)	0.30	-0.02	-0.02	-0.03	-0.03	0.02
(Ca+Na) B >= 1.00	2.00	1.88	1.88	1.87	1.86	1.91
Na B is 0.50 to 1.50	0.30	-0.02	-0.02	-0.03	-0.03	0.02
(Na+K) A < 0.50	0.68	0.78	0.86	0.81	0.71	0.65
Mg/(Mg+Fe)	0.68	0.69	0.66	0.67	0.69	0.70
Si in formula	6.72	6.26	6.14	6.28	6.32	6.34
Amphibole Type	calcic	calcic	calcic	calcic	calcic	calcic
Name	edenite	pargasite	pargasite	pargasite	pargasite	pargasite

Appendix 6.D Amphibole classification from EMP data

Comment	0904C 1.3 hb	0904C 1.4 hb
X	-17100.00	-17232.00
Y	-8012.00	-8318.00
Z	66.00	66.00
SiO2	42.59	42.76
TiO2	0.93	1.01
Al2O3	13.83	13.94
Cr2O3	0.07	0.03
Fe2O3	1.46	1.25
FeO	11.10	10.75
MnO	0.07	0.06
MgO	13.37	13.35
CaO	11.63	11.73
Na2O	2.82	2.74
K2O	0.12	0.07
NiO	0.02	0.02
Total	97.87	97.58
FeO	12.42	11.87
num ox	23.00	23.00
Si	6.23	6.25
Ti	0.10	0.11
Al	2.38	2.40
Cr	0.01	0.00
Fe3+	0.16	0.14
Fe2+	1.36	1.31
Mn	0.01	0.01
Mg	2.91	2.91
Ca	1.82	1.84
Na	0.80	0.78
K	0.02	0.01
Total	15.81	15.76
(Si+Al+Cr+Ti+Fe+Mg+Mn)	13.00	13.00
c	1.42	1.42
a	0.02	0.03
l	0.41	0.41
c	0.00	0.00
u	0.03	0.02
l	0.15	0.15
a	0.00	0.00
t	0.33	0.33
i	0.21	0.21
o	0.05	0.04
n	0.00	0.00
s	8.79	8.78
Fe3+ check (=0?)	0.00	0.00
SUM T to 8 (Si, Al, Ti)		
Si	6.23	6.25
Al	1.77	1.75
Ti	0.00	0.00
TOTAL T	8.00	8.00
Sum C to 5 (Al, Ti, Fe3+, Cr, Mg, Fe, Mn)		
Al	0.61	0.65
Ti	0.10	0.11
Fe3+	0.16	0.14
Cr	0.01	0.00
Mg	2.91	2.91
Fe	1.21	1.18
Mn	0.00	0.00
TOTAL C (2 M1, 2 M2, 1 M3)	5.00	5.00
Sum B to 2 (Fe, Mn, Ca, Na)		
Mg	0.00	0.00
Fe	0.15	0.13
Mn	0.01	0.01
Ca	1.82	1.84
Na	0.02	0.03
TOTAL B (2 M4)	2.00	2.00
Sum A (Excess B + K)		
Ca	0.00	0.00
Na	0.78	0.75
K	0.02	0.01
TOTAL A	0.80	0.76
B(Mg, Fe, Mn, Li)	0.16	0.14
B(Ca, Na)	1.84	1.86
B(Na)	0.02	0.03
(Ca+Na) B >= 1.00	1.84	1.86
Na B is 0.50 to 1.50	0.02	0.03
(Na+K) A < 0.50	0.80	0.76
Mg/(Mg+Fe)	0.68	0.69
Si in formula	6.23	6.25
Amphibole Type	calcic	calcic
Name	pargasite	pargasite

Appendix 6.D Amphibole classification from EMP data

Comment	0903B 1.1 hb c	0903B 1.2 hb r	0903B 1.3 hb c	0903B 1.4 hb r	0903B 1.8 ?	0903B 1.11+ hb trav
X	17626.00	15590.00	14438.00	15029.00	14811.00	13537.00
Y	-17741.00	-17722.00	-16829.00	-16755.00	-17634.00	-16482.00
Z	63.00	68.00	70.00	70.00	68.00	71.00
SiO2	43.67	44.36	43.19	43.53	43.99	44.08
TiO2	1.08	0.66	1.05	0.61	0.61	0.67
Al2O3	13.73	13.88	13.73	14.68	13.88	13.22
Cr2O3	0.13	0.22	0.18	0.22	0.21	0.08
Fe2O3	1.03	0.86	1.14	0.84	1.02	0.82
FeO	6.60	6.10	6.70	6.55	6.25	6.60
MnO	0.10	0.09	0.06	0.10	0.09	0.06
MgO	16.43	16.52	16.30	16.02	16.49	16.67
CaO	11.81	12.06	11.87	12.12	12.08	12.28
Na2O	2.94	2.73	2.76	2.89	2.73	2.77
K2O	0.96	0.77	0.98	0.72	0.71	0.86
NiO	0.06	0.02	0.03	0.04	0.05	0.01
Total	98.45	98.19	97.88	98.22	98.01	98.04
FeO	7.53	6.88	7.73	7.31	7.17	7.34
num ox	23.00	23.00	23.00	23.00	23.00	23.00
Si	6.25	6.32	6.22	6.23	6.29	6.32
Ti	0.12	0.07	0.11	0.07	0.07	0.07
Al	2.32	2.33	2.33	2.47	2.34	2.23
Cr	0.01	0.02	0.02	0.02	0.02	0.01
Fe3+	0.11	0.09	0.12	0.09	0.11	0.09
Fe2+	0.79	0.73	0.81	0.78	0.75	0.79
Mn	0.01	0.01	0.01	0.01	0.01	0.01
Mg	3.50	3.51	3.50	3.41	3.52	3.56
Ca	1.81	1.84	1.83	1.86	1.85	1.89
Na	0.82	0.75	0.77	0.80	0.76	0.77
K	0.18	0.14	0.18	0.13	0.13	0.16
Total	15.91	15.83	15.90	15.88	15.85	15.90
(Si+Al+Cr+Ti+Fe+Mg+Mn)	13.00	13.00	13.00	13.00	13.00	13.00
c	1.45	1.48	1.44	1.45	1.46	1.47
a	0.03	0.02	0.03	0.02	0.02	0.02
l	0.40	0.41	0.40	0.43	0.41	0.39
c	0.00	0.00	0.00	0.00	0.00	0.00
u	0.02	0.02	0.02	0.02	0.02	0.02
l	0.09	0.08	0.09	0.09	0.09	0.09
a	0.00	0.00	0.00	0.00	0.00	0.00
t	0.41	0.41	0.40	0.40	0.41	0.41
i	0.21	0.22	0.21	0.22	0.22	0.22
o	0.05	0.04	0.04	0.05	0.04	0.04
n	0.01	0.01	0.01	0.01	0.01	0.01
s	8.60	8.56	8.65	8.59	8.60	8.62
Fe3+ check (=0?)	0.00	0.00	0.00	0.00	0.00	0.00
SUM T to 8 (Si, Al, Ti)						
Si	6.25	6.32	6.22	6.23	6.29	6.32
Al	1.75	1.68	1.78	1.77	1.71	1.68
Ti	0.00	0.00	0.00	0.00	0.00	0.00
TOTAL T	8.00	8.00	8.00	8.00	8.00	8.00
Sum C to 5 (Al, Ti, Fe3+, Cr, Mg, Fe, Mn)						
Al	0.56	0.66	0.55	0.70	0.64	0.56
Ti	0.12	0.07	0.11	0.07	0.07	0.07
Fe3+	0.11	0.09	0.12	0.09	0.11	0.09
Cr	0.01	0.02	0.02	0.02	0.02	0.01
Mg	3.50	3.51	3.50	3.41	3.52	3.56
Fe	0.69	0.65	0.70	0.70	0.65	0.71
Mn	0.00	0.00	0.00	0.00	0.00	0.00
TOTAL C (2 M1, 2 M2, 1 M3)	5.00	5.00	5.00	5.00	5.00	5.00
Sum B to 2 (Fe, Mn, Ca, Na)						
Mg	0.00	0.00	0.00	0.00	0.00	0.00
Fe	0.10	0.08	0.11	0.08	0.10	0.08
Mn	0.01	0.01	0.01	0.01	0.01	0.01
Ca	1.81	1.84	1.83	1.86	1.85	1.89
Na	0.08	0.07	0.05	0.05	0.04	0.02
TOTAL B (2 M4)	2.00	2.00	2.00	2.00	2.00	2.00
Sum A (Excess B + K)						
Ca	0.00	0.00	0.00	0.00	0.00	0.00
Na	0.74	0.69	0.72	0.75	0.72	0.75
K	0.18	0.14	0.18	0.13	0.13	0.16
TOTAL A	0.91	0.83	0.90	0.88	0.85	0.90
B(Mg, Fe, Mn, Li)	0.11	0.09	0.12	0.09	0.11	0.09
B(Ca, Na)	1.89	1.91	1.88	1.91	1.89	1.91
B(Na)	0.08	0.07	0.05	0.05	0.04	0.02
(Ca+Na) B >= 1.00	1.89	1.91	1.88	1.91	1.89	1.91
Na B is 0.50 to 1.50	0.08	0.07	0.05	0.05	0.04	0.02
(Na+K) A < 0.50	0.91	0.83	0.90	0.88	0.85	0.90
Mg/(Mg+Fe)	0.82	0.83	0.81	0.81	0.82	0.82
Si in formula	6.25	6.32	6.22	6.23	6.29	6.32
Amphibole Type	calcic	calcic	calcic	calcic	calcic	calcic
Name	pargasite	pargasite	pargasite	pargasite	pargasite	pargasite

Appendix 6.D Amphibole classification from EMP data

Comment	0903B 1.11+ hb trav	0903B 1.11+ hb trav	0903B 1.11+ hb trav	0903B 1.11+ hb trav	0903B 1.11+ hb trav
X	13611.00	13745.00	13912.00	14032.00	14204.00
Y	-16482.00	-16482.00	-16482.00	-16482.00	-16482.00
Z	71.00	71.00	71.00	71.00	71.00
SiO2	44.12	43.57	43.41	43.05	43.32
TiO2	0.69	0.92	1.10	1.13	1.07
Al2O3	13.29	13.58	13.76	13.87	13.78
Cr2O3	0.13	0.18	0.17	0.15	0.15
Fe2O3	0.84	1.38	1.09	1.12	1.14
FeO	6.50	6.60	6.85	6.85	6.50
MnO	0.07	0.08	0.06	0.11	0.11
MgO	16.57	16.42	16.13	16.23	16.31
CaO	12.20	11.68	11.75	11.90	11.73
Na2O	2.67	2.72	2.83	2.84	2.77
K2O	0.89	0.95	0.91	0.93	0.90
NiO	0.00	0.07	0.00	0.05	0.04
Total	97.89	98.00	97.94	98.11	97.71
FeO	7.26	7.84	7.83	7.85	7.53
num ox	23.00	23.00	23.00	23.00	23.00
Si	6.33	6.26	6.24	6.19	6.24
Ti	0.07	0.10	0.12	0.12	0.12
Al	2.25	2.30	2.33	2.35	2.34
Cr	0.01	0.02	0.02	0.02	0.02
Fe3+	0.09	0.15	0.12	0.12	0.12
Fe2+	0.78	0.79	0.82	0.82	0.78
Mn	0.01	0.01	0.01	0.01	0.01
Mg	3.54	3.52	3.46	3.48	3.50
Ca	1.88	1.80	1.81	1.83	1.81
Na	0.74	0.76	0.79	0.79	0.77
K	0.16	0.17	0.17	0.17	0.17
Total	15.87	15.87	15.88	15.92	15.88
(Si+Al+Cr+Ti+Fe+Mg+Mn)	13.00	13.00	13.00	13.00	13.00
c	1.47	1.45	1.44	1.43	1.44
a	0.02	0.02	0.03	0.03	0.03
l	0.39	0.40	0.40	0.41	0.41
c	0.00	0.00	0.00	0.00	0.00
u	0.02	0.03	0.02	0.02	0.02
l	0.09	0.09	0.10	0.10	0.09
a	0.00	0.00	0.00	0.00	0.00
t	0.41	0.41	0.40	0.40	0.40
i	0.22	0.21	0.21	0.21	0.21
o	0.04	0.04	0.05	0.05	0.04
n	0.01	0.01	0.01	0.01	0.01
s	8.62	8.63	8.64	8.65	8.65
Fe3+ check (=0?)	0.00	0.00	0.00	0.00	0.00
SUM T to 8 (Si, Al, Ti)					
Si	6.33	6.26	6.24	6.19	6.24
Al	1.67	1.74	1.76	1.81	1.76
Ti	0.00	0.00	0.00	0.00	0.00
TOTAL T	8.00	8.00	8.00	8.00	8.00
Sum C to 5 (Al, Ti, Fe3+, Cr, Mg, Fe, Mn)					
Al	0.58	0.56	0.57	0.55	0.58
Ti	0.07	0.10	0.12	0.12	0.12
Fe3+	0.09	0.15	0.12	0.12	0.12
Cr	0.01	0.02	0.02	0.02	0.02
Mg	3.54	3.52	3.46	3.48	3.50
Fe	0.70	0.65	0.71	0.71	0.67
Mn	0.00	0.00	0.00	0.00	0.00
TOTAL C (2 M1, 2 M2, 1 M3)	5.00	5.00	5.00	5.00	5.00
Sum B to 2 (Fe, Mn, Ca, Na)					
Mg	0.00	0.00	0.00	0.00	0.00
Fe	0.08	0.14	0.11	0.11	0.11
Mn	0.01	0.01	0.01	0.01	0.01
Ca	1.88	1.80	1.81	1.83	1.81
Na	0.04	0.05	0.07	0.04	0.07
TOTAL B (2 M4)	2.00	2.00	2.00	2.00	2.00
Sum A (Excess B + K)					
Ca	0.00	0.00	0.00	0.00	0.00
Na	0.71	0.70	0.72	0.75	0.71
K	0.16	0.17	0.17	0.17	0.17
TOTAL A	0.87	0.88	0.88	0.92	0.87
B(Mg, Fe, Mn, Li)	0.09	0.15	0.12	0.12	0.12
B(Ca, Na)	1.91	1.85	1.88	1.88	1.88
B(Na)	0.04	0.05	0.07	0.04	0.07
(Ca+Na) B >= 1.00	1.91	1.85	1.88	1.88	1.88
Na B is 0.50 to 1.50	0.04	0.05	0.07	0.04	0.07
(Na+K) A < 0.50	0.87	0.88	0.88	0.92	0.87
Mg/(Mg+Fe)	0.82	0.82	0.81	0.81	0.82
Si in formula	6.33	6.26	6.24	6.19	6.24
Amphibole Type	calcic	calcic	calcic	calcic	calcic
Name	pargasite	pargasite	pargasite	pargasite	pargasite

Appendix 6.D Amphibole classification from EMP data

Comment	0903B 1.11+ hb trav	0903B 1.11+ hb trav	0903B 1.11+ hb trav	0903B 1.11+ hb trav	0903B 1.11+ hb trav
X	14395.00	14528.00	14696.00	14843.00	14996.00
Y	-16482.00	-16482.00	-16482.00	-16482.00	-16482.00
Z	71.00	71.00	71.00	71.00	71.00
SiO2	43.24	43.48	43.61	43.58	43.93
TiO2	1.09	1.04	1.00	0.90	0.75
Al2O3	13.95	13.85	13.71	13.36	13.23
Cr2O3	0.17	0.15	0.13	0.17	0.14
Fe2O3	1.28	1.35	1.15	1.02	1.33
FeO	6.70	6.75	6.65	6.70	6.55
MnO	0.08	0.08	0.10	0.07	0.06
MgO	16.20	16.36	16.30	16.41	16.87
CaO	11.70	11.72	11.74	11.93	11.91
Na2O	2.78	2.83	2.77	2.67	2.61
K2O	0.91	0.95	0.92	1.09	1.12
NiO	0.01	0.04	0.06	0.03	0.01
Total	97.98	98.47	98.03	97.82	98.37
FeO	7.85	7.96	7.68	7.62	7.75
num ox	23.00	23.00	23.00	23.00	23.00
Si	6.21	6.22	6.26	6.28	6.29
Ti	0.12	0.11	0.11	0.10	0.08
Al	2.36	2.34	2.32	2.27	2.23
Cr	0.02	0.02	0.02	0.02	0.02
Fe3+	0.14	0.14	0.12	0.11	0.14
Fe2+	0.81	0.81	0.80	0.81	0.78
Mn	0.01	0.01	0.01	0.01	0.01
Mg	3.47	3.49	3.49	3.52	3.60
Ca	1.80	1.80	1.81	1.84	1.83
Na	0.77	0.79	0.77	0.75	0.73
K	0.17	0.17	0.17	0.20	0.21
Total	15.88	15.90	15.87	15.90	15.90
(Si+Al+Cr+Ti+Fe+Mg+Mn)	13.00	13.00	13.00	13.00	13.00
c	1.44	1.45	1.45	1.45	1.46
a	0.03	0.03	0.02	0.02	0.02
l	0.41	0.41	0.40	0.39	0.39
c	0.00	0.00	0.00	0.00	0.00
u	0.02	0.03	0.02	0.02	0.02
l	0.09	0.09	0.09	0.09	0.09
a	0.00	0.00	0.00	0.00	0.00
t	0.40	0.41	0.40	0.41	0.42
i	0.21	0.21	0.21	0.21	0.21
o	0.04	0.05	0.04	0.04	0.04
n	0.01	0.01	0.01	0.01	0.01
s	8.63	8.60	8.63	8.66	8.60
Fe3+ check (=0?)	0.00	0.00	0.00	0.00	0.00
SUM T to 8 (Si, Al, Ti)					
Si	6.21	6.22	6.26	6.28	6.29
Al	1.79	1.78	1.74	1.72	1.71
Ti	0.00	0.00	0.00	0.00	0.00
TOTAL T	8.00	8.00	8.00	8.00	8.00
Sum C to 5 (Al, Ti, Fe3+, Cr, Mg, Fe, Mn)					
Al	0.58	0.56	0.58	0.55	0.52
Ti	0.12	0.11	0.11	0.10	0.08
Fe3+	0.14	0.14	0.12	0.11	0.14
Cr	0.02	0.02	0.02	0.02	0.02
Mg	3.47	3.49	3.49	3.52	3.60
Fe	0.68	0.68	0.69	0.71	0.64
Mn	0.00	0.00	0.00	0.00	0.00
TOTAL C (2 M1, 2 M2, 1 M3)	5.00	5.00	5.00	5.00	5.00
Sum B to 2 (Fe, Mn, Ca, Na)					
Mg	0.00	0.00	0.00	0.00	0.00
Fe	0.13	0.13	0.11	0.10	0.14
Mn	0.01	0.01	0.01	0.01	0.01
Ca	1.80	1.80	1.81	1.84	1.83
Na	0.06	0.06	0.07	0.05	0.03
TOTAL B (2 M4)	2.00	2.00	2.00	2.00	2.00
Sum A (Excess B + K)					
Ca	0.00	0.00	0.00	0.00	0.00
Na	0.72	0.72	0.70	0.70	0.70
K	0.17	0.17	0.17	0.20	0.21
TOTAL A	0.88	0.90	0.87	0.90	0.90
B(Mg, Fe, Mn, Li)	0.14	0.14	0.12	0.11	0.15
B(Ca, Na)	1.86	1.86	1.88	1.89	1.85
B(Na)	0.06	0.06	0.07	0.05	0.03
(Ca+Na) B >= 1.00	1.86	1.86	1.88	1.89	1.85
Na B is 0.50 to 1.50	0.06	0.06	0.07	0.05	0.03
(Na+K) A < 0.50	0.88	0.90	0.87	0.90	0.90
Mg/(Mg+Fe)	0.81	0.81	0.81	0.81	0.82
Si in formula	6.21	6.22	6.26	6.28	6.29
Amphibole Type	calcic	calcic	calcic	calcic	calcic
Name	pargasite	pargasite	pargasite	pargasite	pargasite

Appendix 6.D Amphibole classification from EMP data

Comment	0903B 1.11+ hb trav	0903B 1.11+ hb trav	0903B 2.8 opx r	0903B 2.9 hb	0903B 2.10 hb	0903B random	0903B random
X	15068.00	15149.00	7192.00	7144.00	7337.00	11416.00	11354.00
Y	-16483.00	-16483.00	-17127.00	-15178.00	-15178.00	-15171.00	-15197.00
Z	71.00	71.00	81.00	81.00	81.00	74.00	74.00
SiO2	42.85	43.69	42.89	44.31	44.03	44.39	43.90
TiO2	0.74	0.51	0.37	0.87	0.73	0.82	0.94
Al2O3	15.33	15.25	15.56	12.76	12.68	12.92	13.14
Cr2O3	0.16	0.17	0.16	0.18	0.09	0.12	0.15
Fe2O3	0.74	1.04	1.12	0.85	0.95	1.00	0.96
FeO	6.80	6.05	6.55	7.40	7.45	6.65	6.75
MnO	0.06	0.12	0.08	0.05	0.06	0.08	0.08
MgO	15.64	16.17	15.88	16.26	16.18	16.82	16.39
CaO	12.07	11.92	12.19	12.12	12.16	12.23	12.05
Na2O	2.81	2.96	3.17	2.93	2.84	2.76	2.64
K2O	1.05	0.65	0.18	0.47	0.52	0.71	0.84
NiO	0.05	0.02	0.00	0.02	0.01	0.06	0.05
Total	98.24	98.45	98.03	98.14	97.60	98.45	97.78
FeO	7.46	6.99	7.56	8.17	8.31	7.55	7.61
num ox	23.00	23.00	23.00	23.00	23.00	23.00	23.00
Si	6.15	6.21	6.14	6.36	6.36	6.34	6.32
Ti	0.08	0.05	0.04	0.09	0.08	0.09	0.10
Al	2.59	2.56	2.62	2.16	2.16	2.17	2.23
Cr	0.02	0.02	0.02	0.02	0.01	0.01	0.02
Fe3+	0.08	0.11	0.12	0.09	0.10	0.11	0.10
Fe2+	0.82	0.72	0.78	0.89	0.90	0.79	0.81
Mn	0.01	0.02	0.01	0.01	0.01	0.01	0.01
Mg	3.34	3.42	3.39	3.48	3.48	3.58	3.51
Ca	1.86	1.82	1.87	1.86	1.88	1.87	1.86
Na	0.78	0.82	0.88	0.82	0.80	0.76	0.74
K	0.19	0.12	0.03	0.09	0.10	0.13	0.15
Total	15.92	15.86	15.90	15.86	15.87	15.87	15.85
(Si+Al+Cr+Ti+Fe+Mg+Mn)	13.00	13.00	13.00	13.00	13.00	13.00	13.00
c	1.43	1.45	1.43	1.47	1.47	1.48	1.46
a	0.02	0.01	0.01	0.02	0.02	0.02	0.02
l	0.45	0.45	0.46	0.38	0.37	0.38	0.39
c	0.00	0.00	0.00	0.00	0.00	0.00	0.00
u	0.01	0.02	0.02	0.02	0.02	0.02	0.02
l	0.09	0.08	0.09	0.10	0.10	0.09	0.09
a	0.00	0.00	0.00	0.00	0.00	0.00	0.00
t	0.39	0.40	0.39	0.40	0.40	0.42	0.41
i	0.22	0.21	0.22	0.22	0.22	0.22	0.21
o	0.05	0.05	0.05	0.05	0.05	0.04	0.04
n	0.01	0.01	0.00	0.01	0.01	0.01	0.01
s	8.62	8.54	8.60	8.62	8.68	8.58	8.65
Fe3+ check (=0?)	0.00	0.00	0.00	0.00	0.00	0.00	0.00
SUM T to 8 (Si, Al, Ti)							
Si	6.15	6.21	6.14	6.36	6.36	6.34	6.32
Al	1.85	1.79	1.86	1.64	1.64	1.66	1.68
Ti	0.00	0.00	0.00	0.00	0.00	0.00	0.00
TOTAL T	8.00	8.00	8.00	8.00	8.00	8.00	8.00
Sum C to 5 (Al, Ti, Fe3+, Cr, Mg, Fe, Mn)							
Al	0.74	0.77	0.76	0.52	0.52	0.51	0.55
Ti	0.08	0.05	0.04	0.09	0.08	0.09	0.10
Fe3+	0.08	0.11	0.12	0.09	0.10	0.11	0.10
Cr	0.02	0.02	0.02	0.02	0.01	0.01	0.02
Mg	3.34	3.42	3.39	3.48	3.48	3.58	3.51
Fe	0.74	0.63	0.67	0.80	0.81	0.69	0.72
Mn	0.00	0.00	0.00	0.00	0.00	0.00	0.00
TOTAL C (2 M1, 2 M2, 1 M3)	5.00	5.00	5.00	5.00	5.00	5.00	5.00
Sum B to 2 (Fe, Mn, Ca, Na)							
Mg	0.00	0.00	0.00	0.00	0.00	0.00	0.00
Fe	0.08	0.09	0.11	0.09	0.09	0.10	0.09
Mn	0.01	0.02	0.01	0.01	0.01	0.01	0.01
Ca	1.86	1.82	1.87	1.86	1.88	1.87	1.86
Na	0.06	0.08	0.01	0.04	0.02	0.02	0.04
TOTAL B (2 M4)	2.00	2.00	2.00	2.00	2.00	2.00	2.00
Sum A (Excess B + K)							
Ca	0.00	0.00	0.00	0.00	0.00	0.00	0.00
Na	0.73	0.74	0.87	0.78	0.78	0.74	0.69
K	0.19	0.12	0.03	0.09	0.10	0.13	0.15
TOTAL A	0.92	0.85	0.90	0.86	0.87	0.87	0.85
B(Mg, Fe, Mn, Li)	0.09	0.11	0.12	0.10	0.10	0.11	0.10
B(Ca, Na)	1.91	1.89	1.88	1.90	1.90	1.89	1.90
B(Na)	0.06	0.08	0.01	0.04	0.02	0.02	0.04
(Ca+Na) B >= 1.00	1.91	1.89	1.88	1.90	1.90	1.89	1.90
Na B is 0.50 to 1.50	0.06	0.08	0.01	0.04	0.02	0.02	0.04
(Na+K) A < 0.50	0.92	0.85	0.90	0.86	0.87	0.87	0.85
Mg/(Mg+Fe)	0.80	0.83	0.81	0.80	0.79	0.82	0.81
Si in formula	6.15	6.21	6.14	6.36	6.36	6.34	6.32
Amphibole Type	calcic	calcic	calcic	calcic	calcic	calcic	calcic
Name	pargasite	pargasite	pargasite	pargasite	pargasite	pargasite	pargasite

Appendix 6.D Amphibole classification from EMP data

Comment	0903B random	0903B random	0903B random	0903B random	0903B random	0903B random	0903B random
X	11354.00	11351.00	11349.00	11360.00	11514.00	11514.00	11546.00
Y	-15951.00	-18532.00	-19725.00	-20362.00	-20821.00	-21404.00	-23062.00
Z	74.00	74.00	75.00	75.00	75.00	75.00	75.00
SiO2	44.00	43.78	43.95	41.96	43.42	42.91	43.46
TiO2	0.67	0.69	0.75	0.74	0.89	1.11	0.87
Al2O3	13.16	13.62	13.86	15.37	13.47	13.73	12.94
Cr2O3	0.13	0.16	0.18	0.16	0.16	0.15	0.15
Fe2O3	0.89	0.91	1.11	0.87	1.21	1.37	1.16
FeO	6.90	6.45	6.75	7.10	6.75	6.80	6.60
MnO	0.10	0.10	0.08	0.08	0.03	0.11	0.10
MgO	16.52	16.46	16.33	15.50	16.51	16.28	16.54
CaO	12.34	12.02	11.89	12.28	11.78	11.61	11.86
Na2O	2.65	2.85	2.75	2.91	2.91	2.87	2.84
K2O	0.96	0.82	0.96	0.89	0.95	0.91	0.78
NiO	0.02	0.01	0.04	0.00	0.05	0.02	0.07
Total	98.24	97.78	98.53	97.76	98.01	97.72	97.24
FeO	7.70	7.27	7.75	7.88	7.84	8.04	7.64
num ox	23.00	23.00	23.00	23.00	23.00	23.00	23.00
Si	6.31	6.29	6.28	6.07	6.25	6.19	6.29
Ti	0.07	0.07	0.08	0.08	0.10	0.12	0.09
Al	2.23	2.31	2.33	2.62	2.28	2.34	2.21
Cr	0.01	0.02	0.02	0.02	0.02	0.02	0.02
Fe3+	0.10	0.10	0.12	0.09	0.13	0.15	0.13
Fe2+	0.83	0.78	0.81	0.86	0.81	0.82	0.80
Mn	0.01	0.01	0.01	0.01	0.00	0.01	0.01
Mg	3.53	3.52	3.48	3.34	3.54	3.50	3.57
Ca	1.90	1.85	1.82	1.90	1.82	1.80	1.84
Na	0.74	0.79	0.76	0.82	0.81	0.80	0.80
K	0.18	0.15	0.17	0.16	0.17	0.17	0.14
Total	15.90	15.89	15.87	15.97	15.93	15.92	15.91
(Si+Al+Cr+Ti+Fe+Mg+Mn)	13.00	13.00	13.00	13.00	13.00	13.00	13.00
c	1.46	1.46	1.46	1.40	1.45	1.43	1.45
a	0.02	0.02	0.02	0.02	0.02	0.03	0.02
l	0.39	0.40	0.41	0.45	0.40	0.40	0.38
c	0.00	0.00	0.00	0.00	0.00	0.00	0.00
u	0.02	0.02	0.02	0.02	0.02	0.03	0.02
l	0.10	0.09	0.09	0.10	0.09	0.09	0.09
a	0.00	0.00	0.00	0.00	0.00	0.00	0.00
t	0.41	0.41	0.41	0.38	0.41	0.40	0.41
i	0.22	0.21	0.21	0.22	0.21	0.21	0.21
o	0.04	0.05	0.04	0.05	0.05	0.05	0.05
n	0.01	0.01	0.01	0.01	0.01	0.01	0.01
s	8.62	8.63	8.58	8.69	8.65	8.67	8.70
Fe3+ check (=0?)	0.00	0.00	0.00	0.00	0.00	0.00	0.00
SUM T to 8 (Si, Al, Ti)							
Si	6.31	6.29	6.28	6.07	6.25	6.19	6.29
Al	1.69	1.71	1.72	1.93	1.75	1.81	1.71
Ti	0.00	0.00	0.00	0.00	0.00	0.00	0.00
TOTAL T	8.00	8.00	8.00	8.00	8.00	8.00	8.00
Sum C to 5 (Al, Ti, Fe3+, Cr, Mg, Fe, Mn)							
Al	0.54	0.60	0.61	0.69	0.53	0.53	0.50
Ti	0.07	0.07	0.08	0.08	0.10	0.12	0.09
Fe3+	0.10	0.10	0.12	0.09	0.13	0.15	0.13
Cr	0.01	0.02	0.02	0.02	0.02	0.02	0.02
Mg	3.53	3.52	3.48	3.34	3.54	3.50	3.57
Fe	0.75	0.69	0.70	0.78	0.68	0.68	0.69
Mn	0.00	0.00	0.00	0.00	0.00	0.00	0.00
TOTAL C (2 M1, 2 M2, 1 M3)	5.00	5.00	5.00	5.00	5.00	5.00	5.00
Sum B to 2 (Fe, Mn, Ca, Na)							
Mg	0.00	0.00	0.00	0.00	0.00	0.00	0.00
Fe	0.08	0.09	0.11	0.08	0.13	0.14	0.11
Mn	0.01	0.01	0.01	0.01	0.00	0.01	0.01
Ca	1.90	1.85	1.82	1.90	1.82	1.80	1.84
Na	0.01	0.05	0.06	0.01	0.05	0.05	0.04
TOTAL B (2 M4)	2.00	2.00	2.00	2.00	2.00	2.00	2.00
Sum A (Excess B + K)							
Ca	0.00	0.00	0.00	0.00	0.00	0.00	0.00
Na	0.73	0.75	0.70	0.81	0.76	0.75	0.76
K	0.18	0.15	0.17	0.16	0.17	0.17	0.14
TOTAL A	0.90	0.90	0.87	0.97	0.94	0.92	0.91
B(Mg, Fe, Mn, Li)	0.09	0.10	0.12	0.09	0.13	0.15	0.12
B(Ca, Na)	1.91	1.90	1.88	1.91	1.87	1.85	1.88
B(Na)	0.01	0.05	0.06	0.01	0.05	0.05	0.04
(Ca+Na) B >= 1.00	1.91	1.90	1.88	1.91	1.87	1.85	1.88
Na B is 0.50 to 1.50	0.01	0.05	0.06	0.01	0.05	0.05	0.04
(Na+K) A < 0.50	0.90	0.90	0.87	0.97	0.94	0.92	0.91
Mg/(Mg+Fe)	0.81	0.82	0.81	0.80	0.81	0.81	0.82
Si in formula	6.31	6.29	6.28	6.07	6.25	6.19	6.29
Amphibole Type	calcic	calcic	calcic	calcic	calcic	calcic	calcic
Name	pargasite	pargasite	pargasite	pargasite	pargasite	pargasite	pargasite

Appendix 6.D Amphibole classification from EMP data

Comment	0903B random	0903B random	0903B random	0903B random	0903B random	0903B random	0903B random
X	11546.00	11546.00	11426.00	11451.00	11448.00	11347.00	11446.00
Y	-23879.00	-24293.00	-24293.00	-24366.00	-24516.00	-24648.00	-25055.00
Z	75.00	75.00	77.00	77.00	77.00	77.00	77.00
SiO2	40.43	43.11	43.53	42.69	42.76	43.48	43.65
TiO2	0.39	0.81	1.03	1.08	1.13	0.72	0.64
Al2O3	18.08	14.13	13.79	14.43	14.16	13.70	13.30
Cr2O3	0.13	0.08	0.12	0.12	0.20	0.21	0.16
Fe2O3	2.57	1.07	0.94	1.02	0.88	0.83	0.00
FeO	6.10	6.75	7.10	6.85	7.10	6.75	4.60
MnO	0.12	0.04	0.09	0.07	0.08	0.09	0.06
MgO	15.68	16.08	15.95	15.93	15.93	16.21	16.59
CaO	11.33	11.91	11.93	11.97	12.18	12.12	12.01
Na2O	3.06	3.04	2.92	3.03	2.96	2.97	2.74
K2O	0.46	0.48	0.66	0.57	0.65	0.64	0.96
NiO	0.00	0.05	0.04	0.03	0.01	0.04	0.06
Total	98.11	97.44	98.00	97.69	97.96	97.69	97.80
FeO	8.42	7.71	7.95	7.77	7.89	7.50	7.63
num ox	23.00	23.00	23.00	23.00	23.00	23.00	23.00
Si	5.80	6.22	6.26	6.16	6.16	6.27	6.41
Ti	0.04	0.09	0.11	0.12	0.12	0.08	0.07
Al	3.05	2.40	2.34	2.45	2.41	2.33	2.30
Cr	0.01	0.01	0.01	0.01	0.02	0.02	0.02
Fe3+	0.28	0.12	0.10	0.11	0.10	0.09	0.00
Fe2+	0.73	0.81	0.85	0.83	0.86	0.81	0.56
Mn	0.01	0.01	0.01	0.01	0.01	0.01	0.01
Mg	3.35	3.46	3.42	3.42	3.42	3.48	3.63
Ca	1.74	1.84	1.84	1.85	1.88	1.87	1.89
Na	0.85	0.85	0.81	0.85	0.83	0.83	0.78
K	0.08	0.09	0.12	0.10	0.12	0.12	0.18
Total	15.96	15.90	15.87	15.91	15.93	15.91	15.84
(Si+Al+Cr+Ti+Fe+Mg+Mn)	13.00	13.00	13.00	13.00	13.00	13.00	13.00
c	1.35	1.43	1.45	1.42	1.42	1.45	1.45
a	0.01	0.02	0.03	0.03	0.03	0.02	0.02
l	0.53	0.42	0.41	0.42	0.42	0.40	0.39
c	0.00	0.00	0.00	0.00	0.00	0.00	0.00
u	0.05	0.02	0.02	0.02	0.02	0.02	0.00
l	0.08	0.09	0.10	0.10	0.10	0.09	0.06
a	0.00	0.00	0.00	0.00	0.00	0.00	0.00
t	0.39	0.40	0.40	0.40	0.40	0.40	0.41
i	0.20	0.21	0.21	0.21	0.22	0.22	0.21
o	0.05	0.05	0.05	0.05	0.05	0.05	0.04
n	0.00	0.01	0.01	0.01	0.01	0.01	0.01
s	8.61	8.67	8.64	8.67	8.66	8.66	8.82
Fe3+ check (=0?)	0.00	0.00	0.00	0.00	0.00	0.00	0.00
SUM T to 8 (Si, Al, Ti)							
Si	5.80	6.22	6.26	6.16	6.16	6.27	6.41
Al	2.20	1.78	1.74	1.84	1.84	1.73	1.59
Ti	0.00	0.00	0.00	0.00	0.00	0.00	0.00
TOTAL T	8.00	8.00	8.00	8.00	8.00	8.00	8.00
Sum C to 5 (Al, Ti, Fe3+, Cr, Mg, Fe, Mn)							
Al	0.85	0.62	0.59	0.61	0.57	0.59	0.71
Ti	0.04	0.09	0.11	0.12	0.12	0.08	0.07
Fe3+	0.28	0.12	0.10	0.11	0.10	0.09	0.00
Cr	0.01	0.01	0.01	0.01	0.02	0.02	0.02
Mg	3.35	3.46	3.42	3.42	3.42	3.48	3.63
Fe	0.46	0.70	0.76	0.73	0.77	0.73	0.56
Mn	0.00	0.00	0.00	0.00	0.00	0.00	0.01
TOTAL C (2 M1, 2 M2, 1 M3)	5.00	5.00	5.00	5.00	5.00	5.00	5.00
Sum B to 2 (Fe, Mn, Ca, Na)							
Mg	0.00	0.00	0.00	0.00	0.00	0.00	0.00
Fe	0.27	0.11	0.09	0.10	0.09	0.08	0.00
Mn	0.01	0.01	0.01	0.01	0.01	0.01	0.00
Ca	1.74	1.84	1.84	1.85	1.88	1.87	1.89
Na	-0.03	0.04	0.06	0.04	0.02	0.04	0.11
TOTAL B (2 M4)	2.00	2.00	2.00	2.00	2.00	2.00	2.00
Sum A (Excess B + K)							
Ca	0.00	0.00	0.00	0.00	0.00	0.00	0.00
Na	0.88	0.81	0.75	0.81	0.81	0.79	0.67
K	0.08	0.09	0.12	0.10	0.12	0.12	0.18
TOTAL A	0.96	0.90	0.87	0.91	0.93	0.91	0.85
B(Mg, Fe, Mn, Li)	0.28	0.12	0.10	0.11	0.10	0.09	0.00
B(Ca, Na)	1.72	1.88	1.90	1.89	1.90	1.91	2.00
B(Na)	-0.03	0.04	0.06	0.04	0.02	0.04	0.11
(Ca+Na) B >= 1.00	1.72	1.88	1.90	1.89	1.90	1.91	2.00
Na B is 0.50 to 1.50	-0.03	0.04	0.06	0.04	0.02	0.04	0.11
(Na+K) A < 0.50	0.96	0.90	0.87	0.91	0.93	0.91	0.85
Mg/(Mg+Fe)	0.82	0.81	0.80	0.81	0.80	0.81	0.87
Si in formula	5.80	6.22	6.26	6.16	6.16	6.27	6.41
Amphibole Type	calcic	calcic	calcic	calcic	calcic	calcic	calcic
Name	pargasite	pargasite	pargasite	pargasite	pargasite	pargasite	pargasite

Appendix 6.D Amphibole classification from EMP data

Comment	0905C 1.7+ plag trav domain	0905C 1.7+ plag trav domain	0905C 1.7+ plag trav domain	0905C 1.7+ plag trav domain	0905C 1.7+ plag trav domain	0905C 1.7+ plag trav domain	0905C 1.7+ plag trav domain	0905C 1.7+ plag trav domain	0905C 1.7+ plag trav domain	0905C 1.7+ plag trav domain	0905C 1.7+ plag trav domain
X	-8417	-8363	-8325	-8273	-8192	-8116	-8053	-7988	-7925	-7889	-7840
Y	8924	8924	8924	8924	8924	8921	8921	8921	8921	8921	8921
Z	70	70	70	70	70	70	70	70	70	70	70
SiO2	61.40	61.71	61.48	60.55	59.78	60.59	59.96	58.52	60.42	59.04	59.65
TiO2	0.00	0.01	0.00	0.01	0.04	0.00	0.02	0.02	0.03	0.01	0.02
Al2O3	23.07	23.16	23.36	24.04	24.41	24.00	24.26	23.67	23.97	24.87	24.59
Cr2O3	0.00	0.00	0.02	0.02	0.00	0.01	0.02	0.00	0.00	0.01	0.00
Fe2O3	0.03	0.00	0.00	0.00	0.00	0.00	0.00	0.00	0.00	0.00	0.00
FeO	0.05	0.07	0.07	0.07	0.08	0.06	0.10	0.09	0.05	0.05	0.06
MnO	0.00	0.00	0.02	0.00	0.00	0.00	0.00	0.01	0.01	0.00	0.00
MgO	0.00	0.00	0.00	0.00	0.00	0.00	0.00	0.00	0.00	0.00	0.00
CaO	4.19	4.36	4.60	5.40	5.86	5.33	5.55	5.27	5.46	5.95	6.05
Na2O	8.70	8.59	8.34	8.13	7.98	8.20	8.18	7.86	8.19	8.09	7.82
K2O	0.49	0.53	0.63	0.41	0.45	0.38	0.33	0.43	0.45	0.45	0.45
NiO	0.01	0.01	0.00	0.00	0.00	0.00	0.00	0.01	0.00	0.00	0.00
Total	97.94	98.45	98.50	98.65	98.60	98.57	98.41	95.89	98.59	98.48	98.62
FeO	0.08	0.07	0.07	0.07	0.08	0.06	0.10	0.09	0.05	0.05	0.06
Num ox	8	8	8	8	8	8	8	8	8	8	8
Si	2.78	2.78	2.77	2.73	2.70	2.73	2.71	2.71	2.72	2.67	2.69
Ti	0.00	0.00	0.00	0.00	0.00	0.00	0.00	0.00	0.00	0.00	0.00
Al	1.23	1.23	1.24	1.28	1.30	1.27	1.29	1.29	1.27	1.33	1.31
Cr	0.00	0.00	0.00	0.00	0.00	0.00	0.00	0.00	0.00	0.00	0.00
Fe3+	0.00	0.00	0.00	0.00	0.00	0.00	0.00	0.00	0.00	0.00	0.00
Fe2+	0.00	0.00	0.00	0.00	0.00	0.00	0.00	0.00	0.00	0.00	0.00
Mn	0.00	0.00	0.00	0.00	0.00	0.00	0.00	0.00	0.00	0.00	0.00
Mg	0.00	0.00	0.00	0.00	0.00	0.00	0.00	0.00	0.00	0.00	0.00
Ca	0.20	0.21	0.22	0.26	0.28	0.26	0.27	0.26	0.26	0.29	0.29
Na	0.76	0.75	0.73	0.71	0.70	0.72	0.72	0.71	0.72	0.71	0.68
K	0.03	0.03	0.04	0.02	0.03	0.02	0.02	0.03	0.03	0.03	0.03
Ni	0.00	0.00	0.00	0.00	0.00	0.00	0.00	0.00	0.00	0.00	0.00
Total	5.00	5.00	5.00	5.00	5.01	5.00	5.01	5.01	5.01	5.03	5.01
XAn	0.20	0.21	0.22	0.26	0.28	0.26	0.27	0.26	0.26	0.28	0.29
XAb	0.77	0.76	0.74	0.71	0.69	0.72	0.71	0.71	0.71	0.69	0.68
XOr	0.03	0.03	0.04	0.02	0.03	0.02	0.02	0.03	0.03	0.03	0.03

Appendix 6.D EMP data for plagioclase with calculated end member proportions. XAn = Ca/(Ca+Na+K), XAb = Na/(Ca+Na+K), XOr = K/(Ca+Na+K)

Comment	0905C 1.7+ plag trav domain	0905C 1.7+ plag trav domain	0905C 1.7+ plag trav domain	0905C 1.7+ plag trav domain	0905C 1.7+ plag trav domain	0905C 1.7+ plag trav domain	0905C 1.7+ plag trav domain
X	-7778	-7748	-7706	-7634	-7564	-7527	-7364
Y	8921	8921	8921	8921	8929	8929	8930
Z	70	70	70	70	70	70	70
SiO2	59.95	59.66	59.44	60.28	61.62	61.87	62.07
TiO2	0.00	0.00	0.00	0.00	0.00	0.00	0.00
Al2O3	24.52	24.26	24.42	23.80	22.88	22.99	22.69
Cr2O3	0.00	0.01	0.00	0.02	0.00	0.03	0.00
Fe2O3	0.00	0.00	0.00	0.00	0.00	0.00	0.00
FeO	0.10	0.10	0.06	0.08	0.07	0.08	0.09
MnO	0.00	0.00	0.00	0.00	0.00	0.01	0.00
MgO	0.00	0.00	0.00	0.00	0.00	0.00	0.00
CaO	5.87	5.54	5.66	5.20	3.86	4.20	3.91
Na2O	8.07	8.11	8.07	8.23	8.74	8.82	8.95
K2O	0.46	0.53	0.36	0.49	0.59	0.50	0.50
NiO	0.03	0.03	0.04	0.00	0.00	0.00	0.01
Total	99.00	98.24	98.05	98.09	97.76	98.51	98.23
FeO	0.10	0.10	0.06	0.08	0.07	0.08	0.09
Num ox	8	8	8	8	8	8	8
Si	2.70	2.70	2.70	2.73	2.79	2.78	2.80
Ti	0.00	0.00	0.00	0.00	0.00	0.00	0.00
Al	1.30	1.30	1.31	1.27	1.22	1.22	1.21
Cr	0.00	0.00	0.00	0.00	0.00	0.00	0.00
Fe3+	0.00	0.00	0.00	0.00	0.00	0.00	0.00
Fe2+	0.00	0.00	0.00	0.00	0.00	0.00	0.00
Mn	0.00	0.00	0.00	0.00	0.00	0.00	0.00
Mg	0.00	0.00	0.00	0.00	0.00	0.00	0.00
Ca	0.28	0.27	0.28	0.25	0.19	0.20	0.19
Na	0.70	0.71	0.71	0.72	0.77	0.77	0.78
K	0.03	0.03	0.02	0.03	0.03	0.03	0.03
Ni	0.00	0.00	0.00	0.00	0.00	0.00	0.00
Total	5.02	5.02	5.01	5.01	5.00	5.01	5.01
XAn	0.28	0.27	0.27	0.25	0.19	0.20	0.19
XAb	0.69	0.70	0.71	0.72	0.78	0.77	0.78
XOr	0.03	0.03	0.02	0.03	0.03	0.03	0.03

Appendix 6.D EMP data for plagioclase with calculated end member proportions. XAn = Ca/(Ca+Na+K), XAb = Na/(Ca+Na+K), XOr = K/(Ca+Na+K)

Comment	0909 1.2 plag r	0909 1.3 plag r	0909 1.6 plag c	0909 1.7 plag c	0909 3.1 plag trav domain	0909 3.1 plag trav domain	0909 3.1 plag trav domain	0909 3.1 plag trav domain	0909 3.1 plag trav domain	0909 3.1 plag trav domain	0909 3.1 plag trav domain
X	13335	13177	13494	13398	9351	9333	9215	9158	9054	8966	8874
Y	-13094	-13201	-13003	-13011	-4717	-4700	-4700	-4700	-4700	-4710	-4733
Z	77	77	77	77	75	70	70	70	70	70	70
SiO2	63.86	63.25	63.74	63.73	54.11	55.97	60.82	60.97	61.00	61.11	60.47
TiO2	0.00	0.00	0.01	0.01	0.03	0.00	0.01	0.00	0.00	0.00	0.00
Al2O3	19.07	19.26	22.79	21.03	28.90	26.42	23.48	23.17	23.43	23.37	23.41
Cr2O3	0.01	0.01	0.00	0.02	0.00	0.00	0.01	0.00	0.00	0.01	0.00
Fe2O3	0.00	0.00	0.00	0.00	0.00	0.00	0.00	0.00	0.00	0.00	0.00
FeO	0.14	0.14	0.06	0.05	0.75	0.20	0.07	0.09	0.07	0.07	0.06
MnO	0.00	0.01	0.03	0.00	0.03	0.01	0.00	0.01	0.02	0.00	0.01
MgO	0.03	0.01	0.00	0.00	0.08	0.00	0.00	0.00	0.00	0.00	0.00
CaO	0.11	0.13	3.65	2.10	10.61	8.28	4.54	4.43	4.56	4.62	4.68
Na2O	1.45	2.10	9.54	5.93	5.64	6.67	8.59	8.74	8.52	8.63	8.59
K2O	14.31	13.21	0.14	6.86	0.16	0.20	0.50	0.41	0.83	0.59	0.50
NiO	0.00	0.00	0.00	0.02	0.00	0.01	0.01	0.01	0.02	0.00	0.02
Total	98.99	98.13	99.97	99.75	100.31	97.78	98.03	97.81	98.45	98.40	97.74
FeO	0.14	0.14	0.06	0.05	0.75	0.20	0.07	0.09	0.07	0.07	0.06
Num ox	8	8	8	8	8	8	8	8	8	8	8
Si	2.97	2.95	2.82	2.88	2.44	2.57	2.75	2.76	2.75	2.76	2.75
Ti	0.00	0.00	0.00	0.00	0.00	0.00	0.00	0.00	0.00	0.00	0.00
Al	1.04	1.06	1.19	1.12	1.54	1.43	1.25	1.24	1.25	1.24	1.25
Cr	0.00	0.00	0.00	0.00	0.00	0.00	0.00	0.00	0.00	0.00	0.00
Fe3+	0.00	0.00	0.00	0.00	0.00	0.00	0.00	0.00	0.00	0.00	0.00
Fe2+	0.01	0.01	0.00	0.00	0.03	0.01	0.00	0.00	0.00	0.00	0.00
Mn	0.00	0.00	0.00	0.00	0.00	0.00	0.00	0.00	0.00	0.00	0.00
Mg	0.00	0.00	0.00	0.00	0.01	0.00	0.00	0.00	0.00	0.00	0.00
Ca	0.01	0.01	0.17	0.10	0.51	0.41	0.22	0.22	0.22	0.22	0.23
Na	0.13	0.19	0.82	0.52	0.49	0.59	0.75	0.77	0.75	0.76	0.76
K	0.85	0.79	0.01	0.40	0.01	0.01	0.03	0.02	0.05	0.03	0.03
Ni	0.00	0.00	0.00	0.00	0.00	0.00	0.00	0.00	0.00	0.00	0.00
Total	5.00	5.00	5.00	5.02	5.04	5.02	5.01	5.01	5.02	5.02	5.02
XAn	0.01	0.01	0.17	0.10	0.50	0.40	0.22	0.21	0.22	0.22	0.22
XAb	0.13	0.19	0.82	0.51	0.49	0.59	0.75	0.76	0.74	0.75	0.75
XOr	0.86	0.80	0.01	0.39	0.01	0.01	0.03	0.02	0.05	0.03	0.03

Appendix 6.D EMP data for plagioclase with calculated end member proportions. XAn = Ca/(Ca+Na+K), XAb = Na/(Ca+Na+K), XOr = K/(Ca+Na+K)

Comment	0909 3.1 plag trav domain	0909 3.1 plag trav domain	0909 3.1 plag trav domain	0909 3.1 plag trav domain	0909 3.1 plag trav domain	0909 3.1 plag trav domain	0909 3.1 plag trav domain	0909 3.1 plag trav domain	0909 3.1 plag trav domain
X	8794	8718	8633	8573	8432	8371	8290	8211	8091
Y	-4733	-4733	-4733	-4699	-4697	-4675	-4619	-4576	-4617
Z	70	70	70	70	70	70	70	70	70
SiO2	60.52	60.60	60.35	59.78	59.95	60.03	59.98	60.41	60.39
TiO2	0.00	0.00	0.00	0.00	0.01	0.00	0.00	0.00	0.00
Al2O3	23.58	23.57	23.75	24.03	23.92	23.76	23.70	23.65	23.45
Cr2O3	0.00	0.00	0.00	0.01	0.00	0.00	0.01	0.00	0.00
Fe2O3	0.00	0.00	0.00	0.00	0.00	0.00	0.00	0.00	0.00
FeO	0.06	0.05	0.03	0.06	0.07	0.06	0.04	0.05	0.07
MnO	0.00	0.00	0.00	0.03	0.03	0.00	0.00	0.00	0.00
MgO	0.00	0.00	0.00	0.00	0.00	0.00	0.00	0.00	0.00
CaO	4.81	4.81	5.03	5.25	5.10	5.15	5.03	4.92	4.75
Na2O	8.44	8.40	8.28	8.28	8.38	8.26	8.14	8.33	8.46
K2O	0.54	0.54	0.55	0.58	0.55	0.53	0.56	0.58	0.59
NiO	0.00	0.02	0.00	0.00	0.01	0.00	0.00	0.03	0.03
Total	97.95	97.99	97.99	98.01	98.02	97.79	97.47	97.98	97.75
FeO	0.06	0.05	0.03	0.06	0.07	0.06	0.04	0.05	0.07
Num ox	8	8	8	8	8	8	8	8	8
Si	2.74	2.75	2.74	2.71	2.72	2.73	2.73	2.74	2.74
Ti	0.00	0.00	0.00	0.00	0.00	0.00	0.00	0.00	0.00
Al	1.26	1.26	1.27	1.29	1.28	1.27	1.27	1.26	1.26
Cr	0.00	0.00	0.00	0.00	0.00	0.00	0.00	0.00	0.00
Fe3+	0.00	0.00	0.00	0.00	0.00	0.00	0.00	0.00	0.00
Fe2+	0.00	0.00	0.00	0.00	0.00	0.00	0.00	0.00	0.00
Mn	0.00	0.00	0.00	0.00	0.00	0.00	0.00	0.00	0.00
Mg	0.00	0.00	0.00	0.00	0.00	0.00	0.00	0.00	0.00
Ca	0.23	0.23	0.24	0.26	0.25	0.25	0.25	0.24	0.23
Na	0.74	0.74	0.73	0.73	0.74	0.73	0.72	0.73	0.75
K	0.03	0.03	0.03	0.03	0.03	0.03	0.03	0.03	0.03
Ni	0.00	0.00	0.00	0.00	0.00	0.00	0.00	0.00	0.00
Total	5.01	5.01	5.01	5.02	5.02	5.01	5.01	5.01	5.02
XAn	0.23	0.23	0.24	0.25	0.24	0.25	0.25	0.24	0.23
XAb	0.74	0.74	0.72	0.72	0.72	0.72	0.72	0.73	0.74
XOr	0.03	0.03	0.03	0.03	0.03	0.03	0.03	0.03	0.03

Appendix 6.D EMP data for plagioclase with calculated end member proportions. XAn = Ca/(Ca+Na+K), XAb = Na/(Ca+Na+K), XOr = K/(Ca+Na+K)

Comment	0905B 1.1 pl	0905B 1.2 pl	0905B 1.3 pl	0905B 2.6 plag	0905B 2.6 plag	0905B 2.6 plag	0905B 2.7 plag	0905B random	0905B random	0905B random	0905B random	0905B random
X	6070	7071	5713	12513	12651	12651	13074	12894	12894	12894	12894	12949
Y	9739	12008	14484	12599	12666	12878	12878	18625	18774	19278	19567	20064
Z	61	64	57	65	65	65	65	57	59	59	59	59
SiO2	64.04	62.79	62.70	63.91	64.71	64.32	63.96	62.27	62.48	62.73	62.99	62.90
TiO2	0.00	0.00	0.00	0.01	0.05	0.00	0.01	0.00	0.00	0.00	0.00	0.00
Al2O3	23.13	23.69	23.44	22.63	18.79	22.77	22.97	23.48	23.35	23.50	23.54	23.48
Cr2O3	0.03	0.01	0.00	0.00	0.00	0.00	0.00	0.01	0.03	0.00	0.00	0.00
Fe2O3	0.00	0.00	0.00	0.00	0.00	0.00	0.00	0.00	0.00	0.00	0.00	0.00
FeO	0.16	0.06	0.10	0.11	0.10	0.20	0.23	0.03	0.05	0.05	0.07	0.07
MnO	0.02	0.00	0.00	0.01	0.00	0.01	0.01	0.00	0.00	0.01	0.02	0.00
MgO	0.00	0.00	0.00	0.00	0.00	0.00	0.00	0.00	0.00	0.00	0.00	0.00
CaO	4.22	5.11	4.83	4.05	0.10	4.08	4.25	4.94	4.84	4.94	4.91	4.89
Na2O	9.44	7.99	8.16	8.84	1.33	8.78	8.81	8.30	8.20	8.15	8.29	8.29
K2O	0.54	0.55	0.59	0.32	14.70	0.49	0.47	0.52	0.64	0.61	0.58	0.53
NiO	0.02	0.00	0.02	0.01	0.02	0.01	0.00	0.02	0.00	0.01	0.00	0.00
Total	101.61	100.19	99.84	99.88	99.80	100.65	100.72	99.59	99.58	99.99	100.41	100.17
FeO	0.16	0.06	0.10	0.11	0.10	0.20	0.23	0.03	0.05	0.05	0.07	0.07
Num ox	8	8	8	8	8	8	8	8	8	8	8	8
Si	2.80	2.77	2.78	2.82	2.98	2.82	2.81	2.77	2.78	2.78	2.78	2.78
Ti	0.00	0.00	0.00	0.00	0.00	0.00	0.00	0.00	0.00	0.00	0.00	0.00
Al	1.19	1.23	1.23	1.18	1.02	1.18	1.19	1.23	1.22	1.23	1.22	1.22
Cr	0.00	0.00	0.00	0.00	0.00	0.00	0.00	0.00	0.00	0.00	0.00	0.00
Fe3+	0.00	0.00	0.00	0.00	0.00	0.00	0.00	0.00	0.00	0.00	0.00	0.00
Fe2+	0.01	0.00	0.00	0.00	0.00	0.01	0.01	0.00	0.00	0.00	0.00	0.00
Mn	0.00	0.00	0.00	0.00	0.00	0.00	0.00	0.00	0.00	0.00	0.00	0.00
Mg	0.00	0.00	0.00	0.00	0.00	0.00	0.00	0.00	0.00	0.00	0.00	0.00
Ca	0.20	0.24	0.23	0.19	0.00	0.19	0.20	0.24	0.23	0.23	0.23	0.23
Na	0.80	0.68	0.70	0.76	0.12	0.75	0.75	0.72	0.71	0.70	0.71	0.71
K	0.03	0.03	0.03	0.02	0.86	0.03	0.03	0.03	0.04	0.03	0.03	0.03
Ni	0.00	0.00	0.00	0.00	0.00	0.00	0.00	0.00	0.00	0.00	0.00	0.00
Total	5.02	4.97	4.97	4.97	5.00	4.97	4.98	4.99	4.98	4.98	4.98	4.98
XAn	0.19	0.25	0.24	0.20	0.00	0.20	0.20	0.24	0.24	0.24	0.24	0.24
XAb	0.78	0.71	0.73	0.78	0.12	0.77	0.77	0.73	0.73	0.72	0.73	0.73
XOr	0.03	0.03	0.03	0.02	0.87	0.03	0.03	0.03	0.04	0.04	0.03	0.03

Appendix 6.D EMP data for plagioclase with calculated end member proportions. XAn = Ca/(Ca+Na+K), XAb = Na/(Ca+Na+K), XOr = K/(Ca+Na+K)

Comment	0905B random	0905B random	0905B random	0905B random	0905B random	0905B random	0905B random	0905B random
X	12949	12953	12352	12352	12372	12389	12389	12389
Y	20676	21282	21905	22424	22606	23303	23771	24082
Z	59	59	58	58	58	57	57	57
SiO2	63.00	60.02	62.21	62.38	62.66	62.74	63.27	64.35
TiO2	0.01	0.00	0.00	0.00	0.01	0.00	0.01	0.01
Al2O3	23.46	21.18	23.92	23.75	23.68	23.25	23.08	18.86
Cr2O3	0.00	0.01	0.00	0.00	0.00	0.00	0.02	0.01
Fe2O3	0.00	0.00	0.00	0.00	0.00	0.00	0.00	0.00
FeO	0.03	0.02	0.06	0.07	0.06	0.08	0.05	0.01
MnO	0.00	0.01	0.01	0.01	0.01	0.00	0.00	0.02
MgO	0.00	0.00	0.00	0.00	0.00	0.00	0.00	0.00
CaO	4.72	2.92	5.22	5.20	5.14	4.61	4.39	0.06
Na2O	8.46	5.37	8.07	8.13	8.27	8.35	8.72	1.43
K2O	0.58	6.24	0.50	0.52	0.53	0.60	0.34	14.41
NiO	0.01	0.01	0.02	0.01	0.00	0.01	0.00	0.01
Total	100.27	95.78	100.00	100.07	100.37	99.64	99.88	99.17
FeO	0.03	0.02	0.06	0.07	0.06	0.08	0.05	0.01
Num ox	8	8	8	8	8	8	8	8
Si	2.78	2.83	2.76	2.76	2.77	2.79	2.80	2.98
Ti	0.00	0.00	0.00	0.00	0.00	0.00	0.00	0.00
Al	1.22	1.18	1.25	1.24	1.23	1.22	1.20	1.03
Cr	0.00	0.00	0.00	0.00	0.00	0.00	0.00	0.00
Fe3+	0.00	0.00	0.00	0.00	0.00	0.00	0.00	0.00
Fe2+	0.00	0.00	0.00	0.00	0.00	0.00	0.00	0.00
Mn	0.00	0.00	0.00	0.00	0.00	0.00	0.00	0.00
Mg	0.00	0.00	0.00	0.00	0.00	0.00	0.00	0.00
Ca	0.22	0.15	0.25	0.25	0.24	0.22	0.21	0.00
Na	0.72	0.49	0.69	0.70	0.71	0.72	0.75	0.13
K	0.03	0.38	0.03	0.03	0.03	0.03	0.02	0.85
Ni	0.00	0.00	0.00	0.00	0.00	0.00	0.00	0.00
Total	4.98	5.02	4.98	4.98	4.98	4.98	4.98	4.99
XAn	0.23	0.15	0.26	0.25	0.25	0.23	0.21	0.00
XAb	0.74	0.48	0.72	0.72	0.72	0.74	0.77	0.13
XOr	0.03	0.37	0.03	0.03	0.03	0.04	0.02	0.87

Appendix 6.D EMP data for plagioclase with calculated end member proportions. XAn = Ca/(Ca+Na+K), XAb = Na/(Ca+Na+K), XOr = K/(Ca+Na+K)

	0905C						0906A	0909	
Comment	apatite	apatite	apatite	apatite	ilmenite	ilmenite	rutile	quartz	quartz
X	-9474.00	-9524.00	-9571.00	-9487.00	-9367.00	-9384.00	8666.00	15111.00	15121.00
Y	8308.00	8460.00	8460.00	8263.00	6918.00	7114.00	26979.00	-14822.00	-14790.00
Z	70.00	70.00	70.00	70.00	70.00	70.00	73.00	75.00	75.00
SiO2	0.06	0.04	0.04	0.03	0.00	0.00	0.02	98.15	98.28
TiO2	0.00	0.00	0.01	0.01	17.97	19.81	98.68	0.01	0.00
Al2O3	0.00	0.01	0.02	0.01	0.08	0.08	0.00	0.03	0.00
Cr2O3	0.00	0.00	0.01	0.00	0.03	0.06	0.17	0.01	0.01
Fe2O3	0.00	0.00	0.00	0.00	65.64	61.59	0.00	0.00	0.00
FeO	0.08	0.08	0.09	0.22	15.00	17.00	0.54	0.39	0.21
MnO	0.04	0.08	0.06	0.07	0.08	0.07	0.00	0.00	0.00
MgO	0.00	0.00	0.00	0.00	0.28	0.34	0.00	0.00	0.00
CaO	54.63	54.79	54.59	54.61	0.00	0.01	0.30	0.03	0.03
Na2O	0.09	0.14	0.15	0.08	0.04	0.02	0.00	0.01	0.01
K2O	0.00	0.00	0.00	0.00	0.01	0.00	0.00	0.00	0.01
NiO	0.00	0.00	0.00	0.02	0.00	0.01	0.00	0.00	0.01
Total	54.90	55.14	54.96	55.06	92.55	92.80	99.72	98.63	98.56
FeO	0.08	0.08	0.09	0.22	74.07	72.42	0.54	0.39	0.21
Num ox	13.00	13.00	13.00	13.00	3.00	3.00	2.00	2.00	2.00
Si	0.01	0.01	0.01	0.01	0.00	0.00	0.00	1.00	1.00
Ti	0.00	0.00	0.00	0.00	0.35	0.39	0.99	0.00	0.00
Al	0.00	0.00	0.00	0.00	0.00	0.00	0.00	0.00	0.00
Cr	0.00	0.00	0.00	0.00	0.00	0.00	0.00	0.00	0.00
Fe3+	0.00	0.00	0.00	0.00	1.30	1.22	0.00	0.00	0.00
Fe2+	0.02	0.01	0.02	0.04	0.33	0.37	0.01	0.00	0.00
Mn	0.01	0.01	0.01	0.01	0.00	0.00	0.00	0.00	0.00
Mg	0.00	0.00	0.00	0.00	0.01	0.01	0.00	0.00	0.00
Ca	12.93	12.92	12.91	12.90	0.00	0.00	0.00	0.00	0.00
Na	0.04	0.06	0.06	0.04	0.00	0.00	0.00	0.00	0.00
K	0.00	0.00	0.00	0.00	0.00	0.00	0.00	0.00	0.00
Ni	0.00	0.00	0.00	0.00	0.00	0.00	0.00	0.00	0.00
Total	13.01	13.02	13.02	13.00	2.00	2.00	1.01	1.00	1.00

Appendix 6.D accessory minerals separated by thin section analysed by EMP

	0905B		0906B			0904C					
Comment	rutile	rutile	rutile	rutile	rutile	rutile	rutile	rutile	rutile	ilmenite	ilmenite
X	3876.00	3751.00	-12691.00	-14503.00	-8946.00	-17489.00	-15487.00	-8870.00	-8612.00	-15431.00	-8612.00
Y	13827.00	13483.00	27724.00	26907.00	20048.00	-8352.00	-8473.00	-8583.00	-14621.00	-8523.00	-14534.00
Z	55.00	55.00	55.00	55.00	66.00	66.00	66.00	81.00	83.00	66.00	80.00
SiO2	0.01	0.00	0.00	0.00	0.02	0.03	0.03	0.10	0.07	0.04	2.63
TiO2	99.15	99.29	99.17	98.72	98.87	98.83	97.65	98.17	98.61	52.27	48.42
Al2O3	0.00	0.00	0.00	0.00	0.00	0.00	0.00	0.00	0.00	0.00	1.87
Cr2O3	0.02	0.03	0.01	0.04	0.02	0.04	0.05	0.04	0.07	0.04	0.03
Fe2O3	0.00	0.00	0.00	0.00	0.00	0.00	0.00	0.00	0.00	2.14	0.00
FeO	0.35	0.36	0.49	0.48	0.89	0.33	0.43	0.86	0.52	42.00	42.42
MnO	0.00	0.01	0.03	0.00	0.02	0.00	0.01	0.00	0.02	0.35	0.24
MgO	0.00	0.00	0.00	0.00	0.00	0.00	0.00	0.00	0.00	2.75	3.43
CaO	0.03	0.03	0.02	0.03	0.21	0.01	1.59	0.25	0.09	0.01	0.54
Na2O	0.00	0.00	0.01	0.01	0.00	0.00	0.01	0.00	0.02	0.00	0.01
K2O	0.00	0.02	0.00	0.00	0.00	0.00	0.00	0.01	0.00	0.01	0.01
NiO	0.00	0.02	0.01	0.00	0.00	0.01	0.01	0.00	0.00	0.09	0.01
Total	99.57	99.75	99.75	99.28	100.04	99.25	99.79	99.43	99.40	99.49	99.61
FeO	0.35	0.36	0.49	0.48	0.89	0.33	0.43	0.86	0.52	43.93	42.42
Num ox	2.00	2.00	2.00	2.00	2.00	2.00	2.00	2.00	2.00	3.00	3.00
Si	0.00	0.00	0.00	0.00	0.00	0.00	0.00	0.00	0.00	0.00	0.06
Ti	1.00	1.00	1.00	1.00	0.99	1.00	0.99	0.99	0.99	0.98	0.89
Al	0.00	0.00	0.00	0.00	0.00	0.00	0.00	0.00	0.00	0.00	0.05
Cr	0.00	0.00	0.00	0.00	0.00	0.00	0.00	0.00	0.00	0.00	0.00
Fe3+	0.00	0.00	0.00	0.00	0.00	0.00	0.00	0.00	0.00	0.04	0.00
Fe2+	0.00	0.00	0.01	0.01	0.01	0.00	0.00	0.01	0.01	0.87	0.87
Mn	0.00	0.00	0.00	0.00	0.00	0.00	0.00	0.00	0.00	0.01	0.00
Mg	0.00	0.00	0.00	0.00	0.00	0.00	0.00	0.00	0.00	0.10	0.12
Ca	0.00	0.00	0.00	0.00	0.00	0.00	0.02	0.00	0.00	0.00	0.01
Na	0.00	0.00	0.00	0.00	0.00	0.00	0.00	0.00	0.00	0.00	0.00
K	0.00	0.00	0.00	0.00	0.00	0.00	0.00	0.00	0.00	0.00	0.00
Ni	0.00	0.00	0.00	0.00	0.00	0.00	0.00	0.00	0.00	0.00	0.00
Total	1.00	1.00	1.00	1.00	1.01	1.00	1.01	1.01	1.00	2.00	2.02

Appendix 6.D accessory minerals separated by thin section analysed by EMP

	0903B				
Comment	olivine	olivine	spinel	spinel	ilmenite
X	13338.00	13928.00	16731.00	16759.00	11351.00
Y	-15821.00	-15477.00	-18681.00	-18681.00	-18412.00
Z	70.00	69.00	68.00	68.00	74.00
SiO2	39.17	39.00	0.01	0.01	1.15
TiO2	0.00	0.01	0.11	0.15	49.49
Al2O3	0.00	0.00	53.34	53.80	0.00
Cr2O3	0.00	0.00	6.51	6.22	0.12
Fe2O3	0.00	0.00	0.00	0.00	0.00
FeO	22.36	22.46	22.82	22.53	44.15
MnO	0.24	0.22	0.06	0.07	0.56
MgO	39.09	39.29	13.02	13.33	3.20
CaO	0.01	0.00	0.00	0.01	0.13
Na2O	0.00	0.01	0.04	0.05	0.00
K2O	0.01	0.00	0.00	0.00	0.00
NiO	0.06	0.15	0.13	0.18	0.00
Total	100.94	101.14	96.04	96.37	98.80
FeO	22.36	22.46	22.82	22.53	44.15
Num ox	4.00	4.00	4.00	4.00	3.00
Si	1.01	1.00	0.00	0.00	0.03
Ti	0.00	0.00	0.00	0.00	0.94
Al	0.00	0.00	1.78	1.79	0.00
Cr	0.00	0.00	0.15	0.14	0.00
Fe3+	0.00	0.00	0.00	0.00	0.00
Fe2+	0.48	0.48	0.54	0.53	0.93
Mn	0.01	0.00	0.00	0.00	0.01
Mg	1.50	1.50	0.55	0.56	0.12
Ca	0.00	0.00	0.00	0.00	0.00
Na	0.00	0.00	0.00	0.00	0.00
K	0.00	0.00	0.00	0.00	0.00
Ni	0.00	0.00	0.00	0.00	0.00
Total	2.99	2.99	3.03	3.03	2.03

Appendix 6.D accessory minerals separated by thin section analysed by EMP

	Breaksea Omphacite Granulite 0905B					Breaksea Eclogite 0904C				
Element	core	rim	core	rim	rim	core	rim	core	rim	-
Li7	1.936	2.382	1.652	1.285	1.052	0.958	0.359	0.331	0.436	0.63
Be9	<0.244	<0.228	<0.221	<0.205	<0.215	<0.32	<0.26	<0.29	<0.229	<0.97
B11	<0.40	0.67	<0.35	0.36	0.35	1.15	0.43	0.67	0.47	<1.62
Al27	131835.97	116467.82	139990.05	114779.3	109520.84	159158.02	126487.54	132870.41	121520.87	134582.47
P31	238.78	222.2	213.18	151.28	146.5	232.84	129.23	160.19	140.75	184.07
Ca42	48528.18	48528.18	48528.18	48528.18	48528.2	70969.8	70969.79	70969.79	70969.79	70969.79
Sc45	38.3	40.02	46.04	38.07	22.65	45.01	40.22	41.38	39.14	48.86
Ti47	1597.85	702.67	316.43	237.22	510.26	586.01	429.56	5596.51	388.17	406.08
V51	266.14	215.62	171.47	103.35	120.66	270.16	116.38	143.07	101.2	141.82
Co59	95.86	70.39	96.05	74.18	74.74	98	71.34	77.27	67.67	69.03
Ni60	7.49	2.78	7.57	4.19	4.13	6.07	3.93	4.85	3.71	1.9
Ga69	17.04	15.63	14.96	11.59	12.83	24.45	15.41	15.98	14.6	21.75
Ga71	17.29	15.92	15.22	11.73	12.72	24.77	15.65	16.09	14.75	22.01
Rb85	0.063	<0.051	<0.052	<0.043	<0.053	<0.077	<0.053	1.09	<0.051	<0.198
Sr88	0.204	0.298	0.067	0.047	<0.107	0.253	0.277	0.305	0.275	0.222
Y89	51.37	39.36	49.86	41.38	24.95	54.18	47.69	47.01	47.87	51.15
Zr90	22.81	13.34	16.62	6.79	13.85	24.52	14.1	29.47	11.87	12.14
Nb93	<0.046	<0.037	<0.037	<0.031	<0.036	<0.045	0.251	3.82	<0.033	<0.151
Cs133	0.1	<0.0245	<0.028	<0.0186	<0.0236	<0.040	<0.0244	<0.027	0.0248	<0.109
Ba137	0.225	2.92	<0.129	<0.144	<0.164	<0.218	<0.171	<0.168	<0.147	<0.72
La139	0.063	0.064	0.0382	0.049	0.0203	<0.029	<0.0193	0.046	<0.0206	<0.086
Ce140	0.332	0.278	0.303	0.125	0.159	0.047	0.098	0.159	0.079	<0.088
Pr141	0.193	0.1054	0.158	0.0553	0.143	0.064	0.083	0.082	0.0752	0.125
Nd146	3.02	1.559	2.53	1.624	2.31	1.54	1.68	1.44	1.58	1.42
Sm152	4.48	3.25	3.83	2.94	3.21	3.2	2.93	2.42	2.69	3.09
Eu153	2.024	1.92	1.981	2.006	2.02	1.885	1.884	1.617	1.781	1.59
Gd158	8.65	6.77	7.38	6.25	5.62	7.82	6.36	6.18	5.87	7.77
Dy161	10.36	7.9	9.43	7.36	5.2	10.44	8.86	8.73	8.69	9.8
Ho165	2.135	1.509	1.862	1.51	0.962	2.09	1.809	1.756	1.761	2.02
Er167	5.86	3.98	5.04	4.18	2.47	5.49	4.8	4.54	5.01	4.94
Yb172	4.46	3.34	5.05	3.94	2.042	5.47	4.21	4.19	4.51	5.24
Lu175	0.665	0.447	0.726	0.558	0.273	0.759	0.578	0.524	0.612	0.603
Hf178	0.41	0.178	0.132	<0.066	0.146	0.367	0.258	0.443	0.224	<0.35
Ta181	<0.0250	<0.0264	<0.0276	<0.0190	<0.0163	<0.032	<0.0215	0.078	<0.0206	<0.101
Pb208	0.096	0.104	0.037	<0.032	<0.034	<0.064	<0.037	<0.038	<0.037	<0.185
Th232	0.061	<0.029	0.051	0.0687	<0.0195	<0.036	<0.0232	<0.029	<0.0233	<0.094
U238	<0.027	<0.0256	<0.0217	<0.0191	<0.0200	<0.031	<0.025	0.045	<0.0203	<0.092

Appendix 6.E Garnet trace element analysis from LAM-ICP-MS

	Garnetite 0906B					Pyroxenite 0906A			Hornblende Peridotite 0903B	
Element	rim	core	rim	core	rim	core	rim	-	-	-
Li7	0.67	0.905	0.663	0.905	0.83	0.496	0.528	0.83	0.66	0.9
Be9	<0.247	<0.269	<0.227	<0.234	<0.252	<0.163	<0.48	<0.65	<1.21	<1.24
B11	<0.38	<0.40	<0.32	<0.40	<0.33	0.6	<0.80	<0.94	<1.89	2.48
Al27	119812.27	136166.08	118451.61	126438.46	118621.38	121075.79	122896.59	136835.33	118680.62	117236.94
P31	157.36	190.68	163.39	169.05	147.84	128.7	131.37	195.85	68.43	74.04
Ca42	57390.47	57390.48	57390.48	57390.48	57390.48	53030.79	53030.8	53030.8	42667.64	42667.64
Sc45	50.79	63.55	53.39	62.93	51.57	62.52	57.92	64.92	140.84	139.93
Ti47	658.22	705.95	590.22	677.18	774.69	466.26	523.71	790.76	173.28	226.68
V51	123.57	154.55	121.39	128.08	122.9	124.05	136.1	127.46	95.84	81.67
Co59	66.07	78.83	65.01	68.68	64.58	69.6	75.3	84.91	53.56	53.67
Ni60	4.57	6.78	3.68	5.52	3.66	4.2	4.14	3.96	7.9	17.66
Ga69	9.32	14.09	8.98	8.62	9.09	8.09	9.19	8.87	8.3	6.94
Ga71	9.34	14.09	8.83	8.74	9.26	8.25	9.13	8.96	8.04	7.65
Rb85	<0.059	<0.063	<0.050	<0.061	<0.050	<0.040	<0.103	<0.143	<0.256	<0.262
Sr88	0.191	0.21	0.202	0.295	0.284	1.445	0.844	0.226	0.209	0.343
Y89	59.85	50.5	63.2	82.49	65.19	48.88	46.23	57.22	109.9	101.85
Zr90	12.25	18.54	12.75	15.43	13.74	6.12	6.06	9.46	14.97	17.52
Nb93	<0.036	<0.045	<0.038	<0.038	<0.032	<0.030	<0.079	<0.101	<0.178	<0.162
Cs133	<0.0262	<0.027	<0.0245	<0.029	<0.0266	<0.0196	<0.058	<0.075	<0.142	<0.136
Ba137	<0.187	<0.226	<0.142	0.181	<0.160	<0.129	<0.47	<0.44	<0.90	<0.88
La139	<0.0223	<0.0254	<0.0205	<0.0202	<0.0187	0.0251	<0.050	<0.058	0.137	0.135
Ce140	0.079	0.08	0.139	0.12	0.166	0.102	0.171	0.085	0.303	0.354
Pr141	0.0935	0.0835	0.0772	0.065	0.0996	0.041	0.088	<0.047	<0.096	<0.095
Nd146	1.497	1.595	1.734	1.68	1.652	0.701	0.94	1	0.68	0.74
Sm152	2.54	2.85	2.81	2.78	2.73	1.341	1.18	1.35	1.47	1.4
Eu153	1.366	1.477	1.494	1.481	1.418	0.862	0.925	0.931	1.164	0.873
Gd158	6.24	7.31	6.37	7.03	6.45	4.09	4.25	3.9	5.84	5.51
Dy161	9.87	9.21	10.44	12.37	11	7.74	8.16	8.65	16.71	14.86
Ho165	2.325	1.854	2.52	3.21	2.58	1.856	1.806	2.32	4.3	3.96
Er167	7.11	4.86	7.82	11.02	7.87	5.61	5.36	6.92	12.86	12.86
Yb172	7.34	4.44	8.45	12.98	7.99	6.18	5.08	6.85	14.1	11.16
Lu175	1.098	0.645	1.376	2.1	1.236	0.94	0.618	1.061	2.1	1.62
Hf178	0.148	0.336	0.225	0.212	0.193	0.118	<0.184	<0.200	0.51	<0.38
Ta181	<0.035	<0.0242	<0.0170	<0.0260	<0.0209	<0.0199	<0.049	<0.066	<0.124	<0.125
Pb208	<0.048	<0.044	<0.037	<0.046	<0.044	<0.032	<0.086	0.13	<0.243	<0.233
Th232	<0.0264	<0.029	<0.0222	<0.029	<0.0228	<0.0235	<0.060	<0.081	<0.147	<0.152
U238	<0.0217	<0.029	<0.0206	<0.0199	<0.0215	<0.0189	<0.059	<0.068	<0.131	<0.141

Appendix 6.E Garnet trace element analysis from LAM-ICP-MS

	Breaksea Omphacite Granulite within Resolution Orthogneiss 73831						Breaksea Eclogite within Resolution Orthogneiss 73832					Discarded 0905B	
Element	core	rim	core	rim	core	rim	core	core	rim	core	rim	rim crack	core crack
Li7	1.286	4.16	2.93	1.314	1.216	1.707	1.351	1.186	3.09	1.372	2.44	1.768	45.91
Be9	<0.28	<0.30	<0.28	<0.241	<0.27	<0.26	<0.29	<0.33	<0.31	<0.248	<0.28	<0.162	2.09
B11	<0.49	1.07	0.81	<0.39	<0.43	<0.46	<0.48	<0.49	<0.53	<0.37	0.43	0.275	9.36
Al27	132714.91	127872.34	127960.45	112861.01	127550.48	127158.33	120849.23	122934.3	136875.27	121333.84	130480.46	86016.68	53397.64
P31	236.47	221.2	230.8	177.85	241.14	227.03	175.32	182.3	190.38	188.81	209.66	136.02	108.06
Ca42	40737.95	40737.96	40737.95	40737.95	40737.95	40737.95	35020.34	35020.34	35020.34	35020.34	35020.34	48528.18	120570.06
Sc45	44.7	41.14	37.47	31.98	41.04	44.34	68.34	65.32	67.5	66.95	60.91	17.09	20.64
Ti47	2309.08	1004.77	864.47	490.98	1253.39	2593.54	406.51	412.83	404.23	1611	891.14	290.56	2677.48
V51	145.3	135.95	142.66	137.27	137.5	141.2	146.67	160.29	143.91	144.61	139.58	86.32	772.29
Co59	87.91	75.59	84.04	72.6	83.55	64.5	77.78	80.03	70.2	76.28	56.87	52.16	40.13
Ni60	8.38	6.19	9.65	5.12	10.46	4.42	8.04	8.44	2.8	7.37	1.81	3.69	130.44
Ga69	16.56	17.14	15.72	14.42	15.41	15.69	13.37	14.71	14.79	12.44	12.62	9.72	28.21
Ga71	16.95	16.64	16.87	14.44	15.5	15.69	13.37	15.23	15.77	12.81	13.13	9.7	28.57
Rb85	<0.059	1.406	<0.064	<0.052	<0.059	<0.057	<0.057	<0.089	<0.188	<0.050	<0.053	0.168	<0.056
Sr88	0.307	0.303	0.137	0.084	0.064	0.097	0.084	<0.072	0.056	0.132	0.359	22.31	92.37
Y89	77.7	68.52	69.36	51.43	76.66	72.78	111.41	121	113.4	98.74	102.65	19.66	6.06
Zr90	83.36	65.64	47.88	21.4	62.98	70.81	22.01	19.16	16.19	31.4	39.44	9.28	103.24
Nb93	<0.046	0.307	<0.042	<0.033	<0.035	0.056	<0.040	<0.087	<0.040	<0.033	<0.036	0.048	<0.037
Cs133	<0.032	0.118	0.235	<0.0261	<0.028	<0.029	<0.035	<0.095	<0.029	<0.0206	<0.0247	<0.0153	<0.0208
Ba137	0.85	0.605	<0.196	<0.129	<0.197	<0.180	<0.153	<0.226	<0.206	<0.138	<0.169	4.73	10.88
La139	0.029	0.172	0.086	<0.0222	0.027	0.046	<0.028	<0.060	0.104	<0.0239	0.18	0.0815	4.52
Ce140	0.222	1.154	0.498	0.094	0.137	0.17	0.167	<0.061	0.272	0.116	0.354	0.418	21.7
Pr141	0.251	0.143	0.187	0.0672	0.1	0.105	0.064	<0.061	0.1	0.0887	0.1029	0.1531	4.65
Nd146	2.12	2.66	1.89	1.62	2.12	2.13	1.71	1.37	0.914	2.16	1.576	2.48	26.29
Sm152	3.95	3.86	3.46	2.93	3.59	3.6	3.75	3.2	3.21	3.79	3.47	3.54	6.62
Eu153	1.905	1.697	1.681	1.456	1.629	1.666	1.357	1.067	1.1	1.299	1.254	2.326	2
Gd158	8.72	8.02	8.11	6.32	8.13	7.99	9.72	9.58	8.86	8.87	8.95	6.02	3.9
Dy161	13.46	12.23	11.7	8.45	12.53	12.7	17.51	19.45	18	15.59	16.28	5	1.618
Ho165	2.85	2.49	2.65	1.87	2.85	2.74	4.21	4.4	4.27	3.66	3.84	0.736	0.245
Er167	8.35	7.58	7.65	5.15	8.49	7.99	12.67	13.42	13.43	10.84	11.76	1.471	0.465
Yb172	8.2	7.28	7.7	5.21	8.86	8.03	12.91	14.16	13.86	11.48	11.83	0.803	0.39
Lu175	1.176	1.052	1.142	0.742	1.295	1.168	2.018	1.933	2.281	1.811	1.829	0.0832	0.0789
Hf178	1.052	0.905	0.655	0.212	0.851	1	0.232	<0.127	0.248	0.406	0.449	0.112	2.88
Ta181	<0.028	0.152	<0.027	<0.0256	<0.0252	<0.030	<0.025	<0.072	<0.031	<0.0193	<0.0233	<0.0162	<0.0198
Pb208	<0.059	0.287	0.257	<0.043	<0.052	<0.044	0.331	<0.093	0.328	<0.038	<0.042	0.135	0.449
Th232	0.067	0.367	<0.030	0.03	0.036	<0.032	<0.035	<0.071	<0.031	<0.0231	0.028	<0.0160	0.343
U238	0.028	1.072	0.553	<0.0227	<0.0245	<0.028	<0.038	0.289	0.599	<0.0211	<0.026	<0.0126	0.0231

Appendix 6.E Garnet trace element analysis from LAM-ICP-MS

	Breaksea Omphacite Granulite 0905B										Breaksea Eclogite 0904C			
Element	core	rim	core	rim	core inclusion in garnet	rim	core inclusion in garnet	rim	core inclusion in garnet	rim	core	rim	core	rim
Li7	94.21	109.75	51.11	40.71	39.35	56.73	32.72	34.88	40.36	64.99	31.54	34.63	26.7	29.44
Be9	2.64	2.6	2.32	1.98	2.03	1.98	2.08	2	2.1	2.14	1.42	1.24	1.1	1.22
B11	7.78	8.02	7.31	7.9	9.6	8.87	10.21	11.28	8.04	8.63	2.01	1.77	1.36	1.72
Al27	52536.43	64514.91	34840.25	34215.75	32831.53	47760.98	30340.89	29463.36	34035.55	56212.56	62560.21	58621.1	59480.64	56780.72
P31	82.95	75.52	75.19	60.56	63.59	74.64	66.73	65.71	70.9	62.07	24.5	22.62	31.48	24.42
Ca42	120570.04	120570.04	120570.05	120570.05	120570.06	120570.07	120570.07	120570.06	120570.08	120570.07	115138.3	115138.3	115138.3	115138.29
Sc45	26.62	22.55	28.49	24.61	22.47	26.62	26.94	27.87	21.41	23.22	21.65	20.77	22.61	22.99
Ti47	3342.29	3135.62	3366.39	3443.41	4235.58	3080.59	3383.78	3125.06	3751.14	3192.35	4605.37	3237.93	3829.85	2905.41
V51	627.68	574.52	511.59	534.75	552.03	629.73	546.69	538.16	566.25	698.61	445.32	475.92	402.85	422.65
Co59	32.11	30.64	33.83	32.95	32.69	32.35	32.68	31.83	32.72	27.86	24.6	24.45	25.86	24.34
Ni60	119.77	106.63	94.95	99.82	100.09	118.53	92.5	93.46	112.01	124.04	70.57	79.43	68.94	72.52
Ga69	38.28	42.46	23.53	23.37	23.39	28.34	23.49	22.52	25.01	33.57	28.67	31.15	26	26.92
Ga71	38.61	42.4	24.19	23.3	23.8	28.02	23.85	23.07	25.07	33.89	29.62	30.82	26.51	27.41
Rb85	<0.051	<0.060	<0.038	<0.038	<0.042	0.081	<0.049	<0.047	<0.048	0.083	<0.057	<0.046	<0.049	<0.043
Sr88	55.44	44.8	75.57	82.4	85.92	75.41	79.23	79.32	80.29	65.81	118.71	96.84	135.68	110.07
Y89	0.807	0.949	2.454	2.72	3.43	2.88	4.65	4.29	2.541	2.007	2.19	1.694	2.55	1.97
Zr90	57.5	51.66	68	76.53	73.98	77.42	77.87	78.85	72.86	81.91	44.11	44.87	40.95	42.3
Nb93	<0.039	<0.044	<0.0229	<0.0252	<0.029	<0.034	<0.032	<0.033	<0.030	<0.039	<0.039	<0.036	<0.033	<0.028
Cs133	<0.0265	<0.029	<0.0189	<0.0208	0.0342	<0.0251	<0.0240	<0.0223	<0.0254	<0.0245	<0.0248	<0.044	<0.027	<0.0199
Ba137	1.54	0.63	<0.113	<0.134	0.304	3.82	<0.134	<0.153	<0.142	0.831	<0.161	7.92	<0.159	<0.122
La139	1.721	1.735	3.73	3.69	3.05	2.606	3.54	3.29	2.81	2.469	0.831	0.576	1.079	0.972
Ce140	10.12	9.81	16.93	17.93	15.63	13.03	20.21	19.4	14.83	14.03	5.48	3.89	6.94	6.2
Pr141	2.38	2.411	3.48	3.84	3.5	2.88	4.62	4.29	3.17	3.12	1.515	1.057	1.682	1.623
Nd146	14.26	15.45	19.06	21.39	20.63	17.72	25.6	25.29	18.79	18.02	10.35	8	10.83	10.7
Sm152	3.73	4.02	4.63	5.27	5.5	4.84	6.94	6.62	4.96	4.52	3.33	2.74	3.08	3.13
Eu153	1.255	1.41	1.615	1.742	1.569	1.38	1.833	1.823	1.464	1.433	1.056	0.908	0.909	0.992
Gd158	1.63	1.86	2.65	3.05	3.53	2.94	4.14	4.03	2.7	2.34	2.23	1.63	1.59	1.69
Dy161	0.357	0.492	0.94	0.976	1.323	1.086	1.633	1.582	1.003	0.685	0.656	0.638	0.646	0.639
Ho165	0.0337	0.027	0.1018	0.104	0.152	0.128	0.167	0.183	0.105	0.081	0.094	0.075	0.112	0.0821
Er167	<0.099	0.101	0.238	0.213	0.246	0.197	0.258	0.295	0.214	<0.091	0.109	0.095	0.172	0.192
Yb172	<0.079	<0.105	0.071	<0.066	0.096	<0.099	0.192	<0.089	<0.088	<0.090	<0.078	0.088	<0.095	0.151
Lu175	<0.0178	<0.0254	0.0144	<0.0153	<0.0193	<0.0200	<0.0177	<0.0164	<0.0189	<0.0199	<0.0227	<0.0213	<0.0165	<0.0142
Hf178	2.45	2.3	2.43	2.8	2.61	2.67	2.66	2.77	2.58	2.84	1.68	1.71	1.69	1.63
Ta181	<0.0248	<0.030	<0.0196	<0.0175	<0.0207	<0.0203	<0.0212	<0.0205	<0.0206	<0.0238	<0.0262	<0.0245	<0.0233	<0.0159
Pb208	0.277	0.238	0.271	0.342	0.419	0.298	0.547	0.486	0.319	0.204	0.051	0.063	0.182	0.121
Th232	<0.029	<0.031	0.202	0.178	0.243	0.488	0.135	0.186	0.188	0.15	<0.025	<0.0207	<0.028	<0.0206
U238	<0.0222	<0.0263	0.0153	<0.0174	<0.0224	<0.0273	0.018	<0.0237	0.0184	<0.0180	<0.0249	<0.0260	<0.0244	<0.0199

Appendix 6.E clinopyroxene trace element analysis from LAM-ICP-MS.

	Garnetite 0906B					Pyroxenite 0906A				Hornblende Peridotite 0903B			Discarded 0905B
Element	rim	core	rim	rim	core	core	rim	core	rim	- opx	- opx	- opx	ablated through two minerals
Li7	8.77	9.69	10.15	10.74	10.66	7	7.31	6.94	7.01	0.0452	0.0411	0.0482	26.61
Be9	1.17	0.8	0.88	0.87	1.04	0.65	0.49	<0.31	0.39	<0.0075	0.0045	0.005	1.73
B11	1.4	2.26	1.85	1.86	2.27	0.7	0.91	0.67	0.96	<0.0121	<0.0050	0.0049	7.58
Al27	32506.54	37922.2	38524.79	37615.28	42782.78	42812.98	39327.54	45422.44	43366.55	88.53	175.37	135.66	84295.65
P31	51.45	51.7	53.17	48.17	51.93	58.4	38.8	73.78	49.48	0.328	0.223	0.215	130.41
Ca42	142082.52	142082.52	142082.53	142082.53	142082.53	141153.42	141153.42	141153.42	141153.42	1765.31	1765.31	1643.81	120570.05
Sc45	34.11	32.96	33.17	33.5	33.69	38.29	36.92	40.45	39.01	0.424	0.585	0.514	25.47
Ti47	2842.27	3921.53	4054.55	3164.09	4216.88	5277.82	4924.46	6468.4	5508.04	7.08	17.85	12.91	3591.1
V51	545.49	549.09	563.8	558.15	544.65	439.47	461.09	444.83	444.37	1.416	1.905	1.573	426.6
Co59	33.07	35.89	36.37	33.83	33.49	35.61	34.91	36.1	35.44	0.303	0.323	0.281	31.07
Ni60	127.74	125.33	131.02	130.08	121.75	121.93	124.72	117.8	125.07	1.152	1.201	1.03	76.84
Ga69	24.3	22.95	24.03	24.14	25.72	17	17.52	17.15	17.29	0.0413	0.0698	0.0535	36.57
Ga71	23.9	23.25	24.41	24.29	25.66	17.34	17.74	17.56	18.35	0.0417	0.0683	0.0551	35.09
Rb85	<0.062	<0.063	<0.060	<0.060	<0.057	<0.065	<0.055	<0.064	<0.056	<0.00161	0.00097	<0.00060	5.25
Sr88	199.05	202.65	207.82	188.71	188.58	179.22	175	169.24	173.96	2.409	2.319	2.003	1078.74
Y89	2.55	3.15	2.98	2.31	2.69	5.16	3.47	6.47	4.48	0.0399	0.0657	0.0471	3.28
Zr90	50.91	50.33	52.5	49.79	54.43	29.36	29.42	31.33	30.74	0.1346	0.3	0.2294	64.54
Nb93	<0.043	<0.044	<0.042	<0.047	<0.049	<0.050	<0.036	<0.048	<0.048	<0.00099	<0.00039	<0.00036	<0.073
Cs133	<0.030	<0.028	<0.030	<0.030	<0.0241	<0.030	<0.027	<0.033	<0.030	<0.00077	<0.00034	<0.00032	0.238
Ba137	<0.210	<0.226	<0.165	<0.177	<0.198	<0.219	<0.163	0.31	<0.194	<0.0063	0.0665	0.0093	130.31
La139	2.72	3.43	4.68	2.6	3.27	1.984	1.813	1.895	1.84	0.01918	0.02705	0.01843	4.35
Ce140	15.33	16.34	18.41	13.85	16.39	10.64	9.61	10.1	9.52	0.0788	0.1136	0.0802	18.53
Pr141	3.43	3.46	3.72	3.15	3.48	2.241	2.187	2.209	2.156	0.01547	0.02426	0.01744	4.01
Nd146	21.24	20.53	21.04	18.85	20.76	13.67	12.8	12.79	12.72	0.0868	0.1358	0.1008	22.67
Sm152	5.46	5.38	5.43	5.46	5.75	3.98	3.7	3.43	3.89	0.0279	0.0375	0.0286	5.98
Eu153	1.35	1.41	1.376	1.322	1.471	1.302	1.18	1.151	1.224	0.00795	0.01046	0.00787	1.817
Gd158	3.26	3.07	3.15	3.08	3.57	3.06	2.55	2.76	2.68	0.0173	0.0316	0.0239	3.71
Dy161	1.039	1.108	1.143	1.001	1.076	1.68	1.368	1.78	1.37	0.0111	0.0192	0.01572	1.17
Ho165	0.101	0.117	0.132	0.124	0.132	0.251	0.156	0.32	0.206	0.00248	0.00311	0.00208	0.173
Er167	0.173	0.224	0.21	0.15	0.206	0.393	0.256	0.589	0.317	0.004	0.00507	0.00422	<0.171
Yb172	<0.116	<0.122	<0.112	<0.097	0.103	0.169	<0.093	0.327	<0.108	<0.0030	0.0028	0.00155	<0.150
Lu175	<0.027	<0.0240	<0.0243	<0.0239	<0.0190	<0.027	0.0202	0.036	<0.031	<0.00066	<0.00023	0.00026	<0.038
Hf178	1.73	1.9	1.89	1.81	1.84	1.321	1.254	1.26	1.296	0.0066	0.01388	0.01109	2.01
Ta181	<0.031	<0.029	<0.027	<0.0262	<0.031	<0.032	<0.029	<0.026	<0.024	<0.00082	<0.00029	<0.00028	<0.045
Pb208	0.342	0.332	0.337	0.27	0.292	0.211	0.175	0.202	0.195	0.00354	0.00311	0.00219	3.72
Th232	<0.030	0.041	0.095	<0.028	0.037	<0.033	<0.028	<0.036	<0.029	<0.00135	<0.00034	<0.00033	0.174
U238	<0.0212	<0.031	<0.0205	<0.0258	<0.0246	<0.025	<0.0243	<0.024	<0.029	<0.00091	<0.00036	<0.00033	<0.041

Appendix 6.E Pyroxene trace element analysis from LAM-ICP-MS. 0904C, 0906B, 0906A are clinopyroxene, 0903B is orthoproxene.

	Breaksea Omphacite Granulite 0905B				Hornblende Peridotite 0903B				
Element	plag				hbl				
	core	rim	core	rim	core	rim	core	core	rim
Li7	2.26	1.34	2.58	2.44	2.19	1.837	1.456	1.549	1.61
Be9	<1.43	<1.46	0.84	<0.99	0.52	<0.33	0.48	0.36	0.33
B11	7.25	8.99	8.38	8.08	0.82	1.37	1.01	0.63	0.97
Al27	135261.22	150522.64	142696.17	140546.25	75867.05	72169.37	69039.71	67498.86	68604.02
P31	103	109.17	105.1	103.92	119.4	121.45	111.93	85.47	76.3
Ca42	33733.88	33733.88	33733.88	33733.88	85478.23	85478.23	85478.23	84334.71	85478.23
Sc45	0.75	0.59	0.99	0.69	53.7	53.26	50.87	50.93	47.59
Ti47	29.2	16.08	23.88	16.18	7462.36	6494.65	5034.7	3941.87	4411.67
V51	<0.32	<0.57	<0.148	0.5	340.26	338.64	353.03	322.4	366.47
Co59	<0.38	<0.48	<0.219	<0.259	61.96	58.36	56.84	53.6	57.49
Ni60	<1.51	<1.32	<0.94	<1.20	300.74	310.86	294.47	267.95	291.94
Ga69	25.03	31.74	23.13	22.57	18.3	20.23	20.32	16.95	19.66
Ga71	22.97	22.2	20.7	19.15	15.82	17.94	17.86	15.13	17.37
Rb85	<0.29	10.02	0.33	0.278	4.14	4.13	4.15	3.86	3.98
Sr88	2729.7	2912.66	2925.66	2891.78	656.02	575.99	492.94	441.41	459.3
Y89	<0.171	<0.242	<0.093	<0.143	18.42	18.8	15.28	13.71	12.58
Zr90	<0.41	<0.36	<0.194	<0.27	34.34	35.02	37.7	36.49	37.94
Nb93	<0.218	<0.206	<0.101	<0.146	3.51	2.077	1.616	1.142	1.066
Cs133	<0.140	<0.137	<0.086	<0.091	<0.036	0.544	<0.029	<0.026	0.043
Ba137	143.48	696	163.5	139.45	238.4	232.79	232.02	209.1	226
La139	4.02	2.53	4.86	4.21	5.55	6.52	6.43	5.95	6.26
Ce140	5	3.35	6.4	5.48	20.88	25	26.27	25.21	27.47
Pr141	0.463	0.246	0.498	0.341	4.04	4.62	4.95	4.59	4.91
Nd146	1.52	1.01	0.99	0.76	21.67	24.4	27.13	24.78	26.18
Sm152	0.4	<0.42	0.199	0.308	5.78	6.49	6.7	6.3	6.97
Eu153	<0.204	0.524	0.286	0.295	1.853	2.282	2.158	1.975	2.114
Gd158	<0.41	<0.50	<0.238	<0.30	5.19	5.88	5.77	5.24	5.81
Dy161	<0.64	<0.47	<0.28	<0.43	4.18	4.13	3.89	3.58	3.71
Ho165	<0.118	<0.116	<0.068	<0.077	0.753	0.792	0.666	0.563	0.555
Er167	<0.59	<0.41	<0.235	<0.37	1.91	1.88	1.434	1.111	0.959
Yb172	<0.48	<0.48	<0.254	<0.33	1.51	1.143	0.771	0.686	0.428
Lu175	<0.115	<0.107	<0.073	<0.091	0.189	0.153	0.075	0.078	0.052
Hf178	<0.33	<0.32	<0.224	<0.241	1.432	1.431	1.575	1.371	1.585
Ta181	<0.130	<0.158	<0.077	<0.089	0.192	0.123	0.109	0.057	0.0453
Pb208	10.81	12.28	9.14	9.11	1.067	0.724	0.683	0.548	0.619
Th232	<0.129	<0.150	<0.079	<0.112	0.084	0.071	0.083	<0.030	0.04
U238	<0.141	<0.124	<0.064	<0.083	0.035	<0.037	<0.031	<0.028	<0.026

Appendix 6.E plagioclase and hornblende trace element analysis from LAM-ICP-MS.